Spring 2109

GROWTH, LIPID PRODUCTION AND BIODIESEL POTENTIAL OF Chromulina freiburgensis Dofl., AN ACIDOPHILIC CHRYSOPHYTE ISOLATED FROM BERKELEY PIT LAKE

June E. Mohler Mitman

GROWTH, LIPID PRODUCTION AND BIODIESEL POTENTIAL OF *Chromulina freiburgensis* Dofl., AN ACIDOPHILIC CHRYSOPHYTE ISOLATED FROM BERKELEY PIT LAKE

by

June E. Mohler Mitman

A thesis submitted in partial fulfillment of the

requirements for the degree of

Interdisciplinary Master of Science

Montana Tech

2019

Abstract

Microalgae remain a promising, but underdeveloped source of lipids for sustainable biodiesel. Some of the obstacles to cost-effective commercial-scale production have been culture contamination and expensive harvest methods. A chrysophyte isolated from Berkeley Pit Lake and identified as *Chromulina freiburgensis*, was found to grow rapidly in a pH 2.5 liquid medium and to amass numerous intracellular lipid bodies. This research addresses the scarcity of published knowledge on the topic of chrysophyte species as potential lipid sources for biodiesel. It investigates how growth phase, culture conditions, and harvest timing influence the quantity and composition of lipids produced by this alga. This research serves as a foundation for optimizing production of lipids that contain the most desirable fatty acid composition for biodiesel. Six experimental treatments, representing six different combinations of nutrient concentrations, were monitored and sampled during a 52-day growth period, while cellular lipid content was tracked by Nile Red fluorescence measurements. Lowering medium nitrogen concentration resulted in increased lipid production, which was further increased by lowering phosphorus concentration and supplementing with CO_2. The combination of lowered nitrogen and phosphorus concentrations resulted in the highest proportion of C18:1 (50.1%) in the composition of fatty acid methyl esters from algal lipids, after approximately 22 days of stationary growth. The alga maintained its growth and favorable fatty acid composition with a modest increase in CO_2. Although *C. freiburgensis* from Berkeley Pit Lake did not clearly demonstrate a high lipid content, its fatty acid composition is favorable for biodiesel production, and it has additional traits which may prove advantageous. Its acidic medium provides protection from culture contamination, and could potentially utilize acid mine drainage water. Fungal-assisted bioflocculation could then provide an economical means of harvest. This unique microalga is well suited for both cost-saving methods, and it has the potential to serve secondary roles in bioremediation or in CO_2 removal from flue gases.

Keywords: biodiesel, algae, chrysophyte, lipids, triglycerides, extremophile

Dedication

I dedicate this work to my husband, Dr. Grant G. Mitman, who discovered fascinatingly hardy algae living in Berkeley Pit Lake, and steadfastly provided support and encouragement. I also dedicate this to my mother, Annemone Mohler and to my grandparents, Donald and Elizabeth Mohler, whose' hard work and loving commitment to their family made it possible for me to pursue knowledge, education, science and art.

Acknowledgements

Dr. Douglas Cameron, as my Graduate Advisor and Committee Chair, provided expert instruction in Chemistry and instrumental analysis. I thank him especially for his patience and persistence in ensuring that I learned and applied important concepts and skills. He was willing to spend extra time developing methods, repairing equipment, and explaining things more than once, whenever necessary. Thanks also to Dr. Grant Mitman and Dr. Martha Apple, who provided advice and expertise in botany and algal culture methods, Dr. Pat Munday, who advised me in Technical Communication and helped improve my writing, and Dr. Kumar Ganesan, who provided a perspective from Environmental Engineering. I also thank Heather Moslander, a recent graduate of Montana Tech, who worked with me for many hours on Nile Red fluorescence and GC/MS methods for the alga.

I would also like to express my sincere gratitude to Dr. Cameron and the Department of Chemistry, and to Dr. Beverly Karplus Hartline and the Research Office, for securing financial assistance to support some of my work to improve and complete this thesis. Their support was very much appreciated.

I also thank Dr. Robert A. Andersen, University of Washington Friday Harbor Laboratories, for his helpful advice and expertise regarding chrysophytes, and Dr. Bill Granath and Dr. Jim Driver at the University of Montana for donating their time preparing SEM images of the alga.

Dr. Stephen O'Leary and Dr. Fabrice Berrue at the National Research Council, Canada, provided an analysis from their laboratory which greatly assisted the interpretation of the results of the experiment, and I thank them for so generously sharing their time and knowledge.

With gratitude, I will never forget my phycological mentors, Dr. Gayle Hansen at Oregon State University, and Dr. Robert Waaland and Dr. Tom Mumford at University of Washington Friday Harbor Marine Laboratories, for the practical skills and experience that they shared, and all of the wonderful collecting trips. I would also like to thank Northwest Algal and Seagrass Symposium for welcoming and encouraging new phycologists, west of the Rockies.

Table of Contents

List of Tables

List of Figures

List of Equations

1. Introduction

1.1. Berkeley Pit Lake and Mining in Butte, Montana

Berkeley Pit Lake, located in Butte, Montana has become symbolic of some of the consequences of Butte's 150-year history as a mining community, and it exemplifies several of the problems associated with acid mine drainage. The Anaconda Mining Company began an open pit mining operation at the Berkeley mine in 1955 to take advantage of the productive ore deposit that had been the target of underground mining almost continuously since the 1860's (Gammons, Metesh, and Duaime, 2006). As the pit expanded, entire neighborhoods, such as Meaderville, Dublin Gulch and McQueen were sacrificed to it (Pit Watch, 2019). The open pit mine operated for 27 years. After the high copper prices that had led to the pit mine's opening began to decline, and the company's operations in Chile were nationalized, the Anaconda company decided to shut down the Berkeley Pit mine (Munday, 2005). The massive, artificial water body that exists today (Figure 1) began to form in 1983. Once mining within the pit had ceased, the dewatering pumps, that had been keeping the pit and surrounding network of tunnels dry, were deactivated. Ground water and a tributary of Silver Bow Creek (Yankee Doodle Creek) began flowing into the abandoned open pit and connected tunnels. Iron pyrite (FeS_2) rich native rock, once exposed to oxygen, water and the activity of iron-oxidizing bacteria and archaea, formed H_2SO_4. The acidified water soon flooded the underground tunnels and began filling the pit lake. This acidic water dissolved an assortment of other metals into solution at high concentrations (Madigan et al., 2015). Mining operations continue to the present in the area near the Berkeley Pit, at times using pit water. In fact, a substantial amount of copper has been recovered from the pit water itself (Pit Watch, 2019).

Figure 1: Berkeley Pit Lake and Butte, Montana, as they appear in satellite photos in 2018, with the water body names and locations added, based on current USGS maps.

1.1.1. Berkeley Pit Lake Chemistry, Past and Current

"An Overview of the Mining History and Geology of Butte, Montana" describes Berkeley Pit Lake as follows, "With over 100 billion liters of pH 2.5 mine water, this man-made body of water is one of the world's largest accumulation of acid mine drainage (measured in

terms of volume of water, total metal load, or total acidity load)". Berkeley Pit Lake is part of the largest contiguous EPA Superfund site in the United States (Gammons, Metesh, and Duaime, 2006). The term, "Superfund" informally refers to the Comprehensive Environmental Response, Compensation and Liability Act (CERCLA), which was passed in 1980 (EPA, 2019). It was intended to enable government agencies, primarily the Environmental Protection Agency (EPA), to hold companies financially responsible for cleaning up environmental disasters that result from their operations. The two responsible parties for Berkeley Pit Lake are Montana Resources and BP-ARCO (Atlantic Richfield).

In 2000, the average pH of surface water (which has tended to remain somewhat less acidic than deeper water) was recorded at pH 2.7, and it contained 136,000 µg/L dissolved copper, and 618,000 µg/L dissolved zinc (Table I) (MBMG GWIC, 2018). For comparison, in reference to pure water, a neutral pH is defined as a pH of 7.0. The normal range for pH in surface water systems is considered to be between 6.5 to 8.5, and the pH of rainwater in Montana ranges from 5.0 to 5.4 (Mesner and John Geiger, 2005, Oram, 2018, USGS, 2018).

Berkeley Pit Lake water has proven to be infamously hazardous to wildlife. An especially unfortunate event occurred on November 28 to 29, 2016, when approximately 10,000 migrating snow geese, caught in a snowstorm, sought refuge there. It is estimated that 3,000 to 4,000 were unable to escape before succumbing to the acidic, metal-laden solution (Dunlap, Montana Standard, 2016 and 2017). A similar incident had occurred in 1995, when 342 snow geese that landed there quickly died. Montana Resources and Atlantic Richfield (ARCO) test and employ a variety of methods to haze birds away from the pit lake (Dunlap, 2017).

Table I: Comparison of concentrations of dissolved metals and nutrients reported in Berkeley Pit Lake in 2000 and 2018 (MBMG GWIC, 2018). Samples were collected between the surface and 150 ft. (45.72 m) depth. Note the large decreases in several metals and metalloids, including iron, copper and arsenic.

Metals (and Metalloids)	**2000 Concentration** (µg/L or **g/L**)	**2018 Concentration** (µg/L or **g/L**)	**US EPA Drinking Water Standards** (µg/L or **g/L**)
Aluminum (Al)	288,000.000 µg/L	322,700.000 µg/L	50-200 µg/L
Arsenic (As)	565.000 µg/L	5.440 µg/L	10 µg/L
Cadmium (Cd)	2,190.000 µg/L	2,176.300 µg/L	5 µg/L
Chromium (Cr)	58.000 µg/L	4.720 J µg/L	100 µg/L
Copper (Cu)	170,000.000 µg/L	65,580.000 µg/L	1,300 µg/L
Iron (Fe)	**993.000 mg/L**	**4.025 mg/L**	**0.3 mg/L**
Lead (Pb)	<20 µg/L	22.360 µg/L	15 µg/L
Manganese (Mn)	**22.200 mg/L**	**275.500 mg/L**	**0.05 mg/L**
Nickel (Ni)	997.000 µg/L	1,319.350 µg/L	NL
Zinc (Zn)	628,000.000 µg/L	603,850.000 µg/L	5,000 µg/L
Macronutrients Required by Plants and Algae			
Nitrogen (as Nitrate, NO3)	**<12.5 mg/L**	Below Detection Limit	**10 mg/L**
Phosphorus (as Phosphate)	0.588 µg/L	Below Detection Limit	NL
Potassium (K)	**8.240 mg/L**	**10.900 mg/L**	NL
Calcium (Ca)	**429.000 mg/L**	**462.370 mg/L**	NL
Magnesium (Mg)	**504.000 mg/L**	**619.610 mg/L**	NL
Sulfur as Sulfate (SO_4)	**8,883.000 mg/L**	**7,210.000 mg/L**	**250 mg/L**
Silicon as Silica (SiO_2)	**109.000 mg/L**	**129.880 mg/L**	NL

NL = Not Currently Listed

Unexpectedly, during the past four to six years, the pH of Berkeley Pit Lake surface water has begun an upward trend, and was recently recorded at 3.8, an order of magnitude above the level where it had remained relatively constant for 28 years (Figure 2, MBMG GWIC, 2018). Dissolved metal concentrations in Berkeley Pit Lake have generally begun to decrease with the increase in pH. The concentration of dissolved iron, for example, has decreased by an order of magnitude (Duaime et al. for MDEQ and EPA, 2017). With the chemical changes, the color of the water has also changed from reddish-brown to greenish-blue (Figure 3). As of January 2017,

the water in the pit lake was approximately 326 m (1070 feet), deep and continuing to fill at an estimated rate of 20 million gallons per day, based on 2016 data (MBMG, 2019).

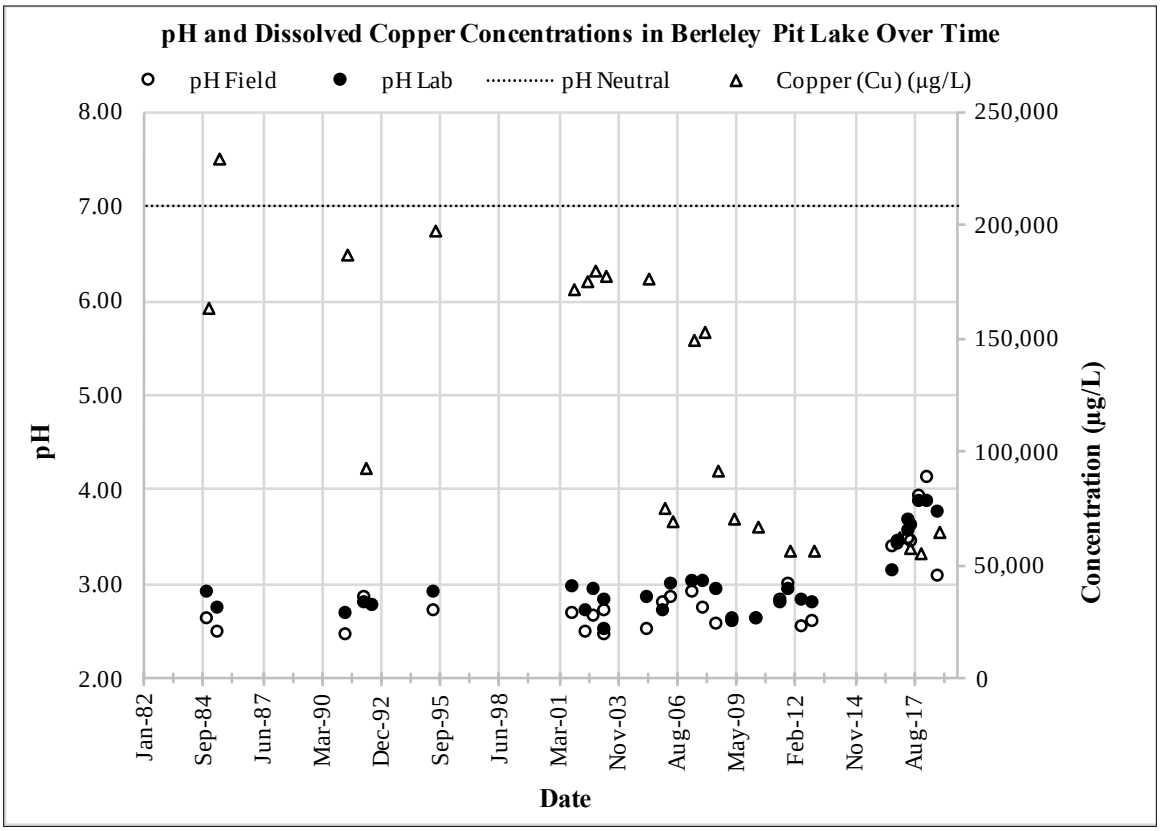

Figure 2: Changes in pH and dissolved metals in Berkeley Pit Lake over 34 years. During the most recent four to six years, the pH has risen by an order of magnitude. As the pH has risen, concentrations of several dissolved metals have decreased. Copper is the example included above.

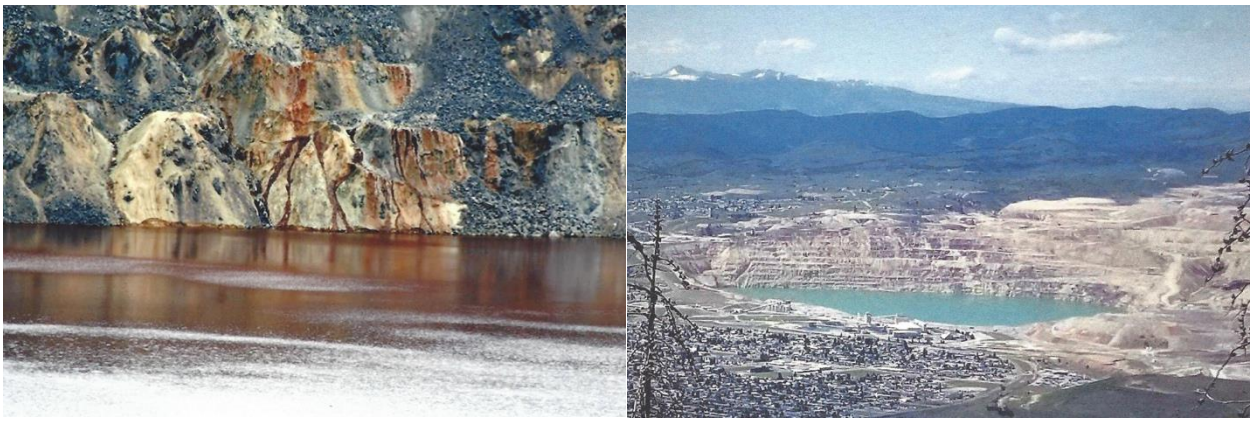

Figure 3: Berkeley Pit Lake as it appeared in 2008 (at Left) and in a 2017 photo by Mike Hogan (Photos from Citizens Technical Environmental Committee, CTEC, Archives, 2019)

While the water body contains high levels of dissolved metal ions, its nutrient levels have been very low (oligotrophic), with nitrogen and phosphorus below detection limits (MBMG GWIC, 2018, Dakel, 2001). Though Berkeley Pit Lake appears lifeless, several extremophiles, microorganisms that are able to survive and grow in environments that would be lethal to most life forms, were found to be living there, including sixteen heterotrophic protists, six species of microalgae, several fungi, numerous bacteria, and one species of moss (Mitman, 1998, Dakel, 2001 and Stierle et al., 2014).

1.1.2. Extremophilic Organisms of Berkeley Pit Lake

At a macroscopic level, Berkeley Pit Lake appears lifeless, nevertheless, several extremophiles, microorganisms that are able to survive and grow in environments that would be lethal to most life forms, were found to be living there, including 16 heterotrophic protists, 6 microalgae, several fungi, bacteria, and one species of moss (Mitman, 1999, Dakel, 2001, Stierle, 2014). Extremophilic microorganisms often produce unique chemical compounds, as adaptations to help them to survive in such environments. For example, six of the fungi found in Berkeley Pit Lake have been found to produce compounds with the potential to lead to improved cancer treatments and antibiotics (Stierle and Stierle, 2005 and 2014).

While algal species composition and diversity are strictly limited by a highly acidic environment, biomass and productivity are not, and under favorable conditions, productivity in such an environment can become as high as in hypertrophic (extremely eutrophic) systems (Nixdorf et al., 1998). The low density of phytoplankton in Berkeley Pit Lake is not due to the low pH or high concentrations of metal ions, but due to the limited quantities of available nutrients (in particular, nitrogen and phosphorus). High levels of productivity can be achieved in Berkeley Pit

Lake water by increasing the availability of these nutrients, without raising the pH of the in situ acidified mine water or artificial medium (Mitman, 2002, Bartkowiak, 2002, and Tucci, 2005).

1.2. Biofuels and Biodiesel

1.2.1. Advantages of Biofuels and Biodiesel

In the 1970's through the 1990's (Knothe, 2005, eXtension, 2012, Covert et al., 2016), the need for greater energy independence and concern about the eventual depletion of accessible petroleum resources created interest in the development and utilization of alternatives to petroleum fuels, such as biofuels in the United States and in other countries. The interest in biofuels has since shifted towards sustainability, especially with regards to limiting climate change resulting from increasing concentrations of atmospheric carbon dioxide. Carbon dioxide released by burning fossil fuels, since the beginning of the industrial age, is now widely known to be one of the primary causes of global warming, resulting in the disruption of previously reliable climate patterns and an increase in the frequency and intensity of destructive weather events, fires and temperature extremes (NOAA, 2018, U.S. Global Change Research Program, 2014).

Unlike biofuels, petroleum-based fossil fuels release carbon into the atmosphere that had been captured and stored underground for millions of years, as fossilized remains of organisms that had accumulated over vast spans of geologic time. In addition to their impact on greenhouse gases in the atmosphere and the earth's climate, petroleum-based fuels also release a greater quantity and variety of toxic byproducts during their use, manufacture and extraction processes, directly impacting human health.

In spite of the human health costs of air pollutants and the alarming effects of climate change from fossil fuel combustion, technological advances have made previously inaccessible

fossil fuel sources available and inexpensive, and fossil fuel use continues to increase (Covert et al., 2016). Currently, interest in alternatives to fossil fuels has largely refocused towards developing cleaner, safer, carbon neutral fuels that would serve the same function as fossil fuels but better protect climate and human health.

Biodiesel, which is usually made from oils and fats from plants, is a cleaner-burning fuel than petroleum diesel. Except for nitrous oxides, biodiesel emits fewer particulates, sulfates and unburned hydrocarbons than petroleum diesel (Figure 4, USDE, 2017). Along with cleaner emissions and the potential for carbon neutrality, the advantages of biodiesel also include reduced engine wear, increased safety and compatibility with existing infrastructure. According to Knothe (2017), "advantages of biodiesel are low or no sulfur content, no aromatics content, high flash point, inherent lubricity, biodegradability, reduction of most regulated exhaust emissions, miscibility with petrodiesel in all blend ratios and compatibility with the existing fuel distribution infrastructure". Generally, due to its engine-protective qualities, biodiesel makes up a percentage of ultra-low sulfur diesel sold in the United States (Hanson and Agarwal, EIA, 2018).

Depending on the types of feedstocks used and the efficiency of the production process, biodiesel can be carbon neutral (having little to no net impact on greenhouse gases and climate). As a biofuel, the carbon emitted as CO_2 by burning biodiesel is from carbon that was recently removed from the atmosphere at the time the fuel crop was grown. The process of manufacturing biodiesel can be relatively energy efficient (with second and third generation fuels).

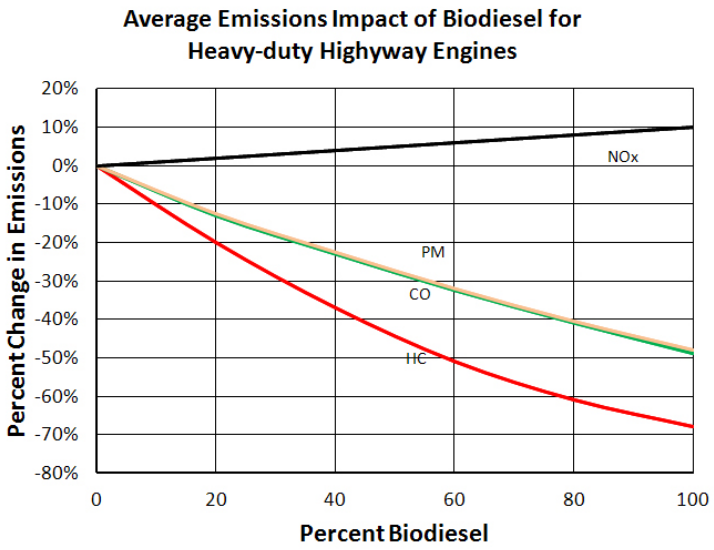

Figure 4: U.S. Department of Energy, Energy Efficiency and Renewable Energy (2017), Average Impact of Biodiesel for Heavy-duty Highway Engines. Biodiesel petroleum diesel blends are cleaner burning than petroleum diesel alone. NOx (nitrogen oxides), PM (particulate matter), CO (carbon monoxide), HC (hydrocarbons). (https://www.afdc.energy.gov/vehicles/diesels_emissions.html. Nov. 9, 2017.)

In addition to its environmental, climate and safety advantages, biodiesel has superior lubricating properties compared to petroleum diesel. Blending as little as 1% biodiesel with petroleum diesel significantly improves the fuel's engine lubricating properties (USDE Alternative Fuels Data Center, 2017, Sustainable Biodiesel Alliance, Biodiesel FAQ, 2016). As high-quality petroleum and other easily accessed fossil fuels become depleted, alternative fossil fuels may require the consumption of increasing quantities of energy and resources to obtain and process. Though the comparatively low cost of petroleum fuels now gives them a marketing advantage over biofuels, it is likely that the gap between the costs will narrow as biofuel production technologies improve.

1.2.2. History and Definition of Biodiesel

Biodiesel's history dates back to the 1890s when Rudolph Diesel used it to power the engines he designed, although the term "biodiesel" was not coined until much later (University of Idaho Biodiesel Short Course, 2016 and Knothe, 2017). The first patent for a fuel made of ethyl ester of palm oil was filed in Belgium in 1937, and this was used to fuel a city bus in 1938 (eXtension, 2016 and Knothe, 2017). Before petroleum become widely available and relatively inexpensive, it was common for farmers in remote locations to grow oil crops for fuel. Regular vegetable oils can be burned in diesel engines, but they do not perform well and their high viscosity can cause damage (eXtension, 2016).

Biodiesel fuel is made from biological lipids, especially triglycerides (also known as triacylglycerol, or TAG) from oil crops, surplus animal fats, or used cooking oils, and it can be burned in any engine that uses petroleum diesel. The type of feedstock influences the qualities of the biodiesel produced (Hanson and Agarwal, EIA, 2018). The US Dept. of Energy Alternative Fuels Data Center defines biodiesel as "a domestically produced, clean-burning, renewable substitute for petroleum diesel." and states that, "Using biodiesel as a vehicle fuel increases energy security, improves air quality and the environment, and provides safety benefits" (2017).

According to Biodiesel.org (2018), the ASTM International (formerly, American Society for Testing and Materials) biodiesel and biodiesel blends are classified according to the following technical definitions: "Biodiesel, n - a fuel comprised of mono-alkyl esters of long chain fatty acids derived from vegetable oils or animal fats, designated B100, and meeting the requirements of ASTM D 6751." and "Biodiesel Blend, n - a blend of biodiesel fuel meeting ASTM D 6751 with petroleum-based diesel fuel, designated BXX, where XX represents the volume percentage of biodiesel fuel in the blend." Biodiesel must meet all of the parameters as

defined within the ASTM specification D6751, “Standard Specification for Biodiesel Fuel Blend Stock (B100) for Middle Distillate Fuels.” Biodiesel has been registered with the U.S. EPA as a fuel and a fuel additive under Section 211(b) of the Clean Air Act (Archer Daniels Midland Company, adm-fact-sheet-biodiesel-technical-information.pdf, 2012).

In the United States, biodiesel is most widely sold as blends with petroleum diesel, most frequently as B20 (20% biodiesel) and B5 (5% biodiesel) (Biodiesel.org, 2018), though B100 is available from some suppliers.

1.2.3. Four Generations of Biofuels

Carbon released into the atmosphere when burning fossil fuels, whether from oil, coal or natural gas, was captured by photosynthetic organisms living millions of years ago and trapped underground until accessed by humans. The carbon that is released into the atmosphere during the use of biofuels is the same carbon that had recently been captured by photosynthesizing organisms. Therefore, biofuels are, or have the potential to be, carbon neutral, meaning that they do not add a net quantity of CO_2 to the atmosphere when they are burned.

Biofuels, including biodiesel, are often classified in terms of three to four generations, based on progress toward solving environmental, economic, social and health problems associated with conventional fossil fuels (Table II).

Table II: Biofuels, Generalized Comparison of Four Generations of Development.

	Example Feedstocks	Example Fuels	Advantages	Disadvantages
First Genreation	corn sugar cane soy bean oil canola oil cotton seed oil animal fats	bioethanol biodiesel biogas	existing crops existing infrastructure existing technology	increases in food prices clean water requirement fertile land requirement greenhouse gas emissions may be greater than carbon capture
Second Generation	used cooking oil Jatropha curcas cellulosic agricultural byproducts switchgrass poplar trees	bioethanol biodiesel biogas methane	non-food crops existing infrastructure utilization of surplus materials use marginal crop land	impact of land use change clean water requirement tecnology, horticultural improvements necessary high production cost
Third Generation	microalgae macroalgae	bioethanol biodiesel biogas biohydrogen jet fuel gasoline	rapid growth can use wastewater no effect on food prices minimal land requirement can use saltwater better carbon capture	culture contamination limited lipid production high nutrient requirements high production cost technological advances necessary to compete
Fourth Generation	genetically modified microalgae other microorganisms	bioethanol biodiesel biogas biohydrogen electrofuels	product harvest without biomass destruction enhanced lipid production enhanced carbon capture minimal land requirement rapid growth	production efficiency and speed need improvement high starting and production cost new, emerging technology

1.2.3.1. First Generation Biofuels

Fuels made from virgin (or edible) vegetable oils are considered to be first generation biofuels. These rely on crops traditionally regarded as food, for example, biodiesel made from soybean, canola or corn oil, or corn ethanol. First generation biofuels are produced using conventional technologies to produce fuels from food or oil crops, or from biomass. For example, the largest proportion of biodiesel currently produced in the United States is made from

soybean oil. This added up to 624 Million pounds of soybean oil out of the 1,194 million total pounds of feedstocks converted to biodiesel in one month. Soybean oil averaged approximately 65% (by weight) of the total of feedstocks used for biodiesel production from January 2016 to June 2018 (USEIA Monthly Biodiesel Production Report, 2018).

1.2.3.1. Second Generation Biofuels

Second generation biofuels, also known as advanced biofuels are, for the most part, those that do not come from food crops. They use waste materials, such as cornstalks and straw, leftover from food crops and other surplus types of biomass. Food crops can be used for second generation biofuels, but only after they have fulfilled their original purpose. For example, waste vegetable oil can be a source of second generation biofuel because it has been used for cooking and is no longer considered to be fit for human consumption.

1.2.3.2. Third Generation Biofuels

Third generation biofuels are generally those made from marine or freshwater algae, including seaweeds and microalgae (Ramaraj et al., 2015, Biofuel.org.uk, 2018). These can include biodiesel, bioethanol, biobutanol, aviation fuel (Bringezu et al., 2009) and biohydrogen (Melis et al., 2000). Algal biofuels are considered third generation biofuels because they offer several social and environmental improvements compared to first and second-generation biofuels (Lane, 2017). Algae can produce far more fuel per acre, sparing valuable fertile land and natural areas (Chisti, 2007). They can also use water that is not fit for drinking or agriculture, due to salinity or contamination, and algae can also perform secondary functions, such as carbon

capture and wastewater treatment, or produce secondary products such as agricultural and food products, pigments, and pharmaceuticals.

1.2.3.3. Fourth Generation Biofuels

Fourth-generation biofuels represent a newly emerging technology that employs genetically engineered microorganisms, including microalgae. For example, genetic manipulation can allow microalgae to double their lipid production without stopping growth (Ajjawi et al., 2017, Dutta, Daverey and Lin, 2014, Lü, Sheahan, and Fu, 2011 Courchesne et al., 2009). These fuel sources are currently in the early stages of research and development, but have the potential to solve many problems now associated with fossil fuels and with earlier generations of biofuels.

1.2.4. Manufacture of Biodiesel from Biological Fats and Oils (Lipids)

Fats and oils (types of lipids) are forms of energy storage in living organisms and they can store more energy than carbohydrates, because of their many carbon-hydrogen bonds (Evert and Eichhorn, 2013). Triglycerides (triacylglycerols) are the most prominent lipids in living organisms, and they are composed of three fatty acid units (Figure 5) linked to one glycerol unit. Fatty acids are biological monocarboxylic acids, and because of the metabolic pathway in which they are synthesized, nearly all of them have an even number of carbon atoms in an unbranched chain (Stoker, 2013). Saturated fatty acids are those that have hydrogen atoms at every position on the molecule that they can occupy. Unsaturated fatty acids have one or more carbon-carbon double bonds replacing pairs of hydrogen atoms.

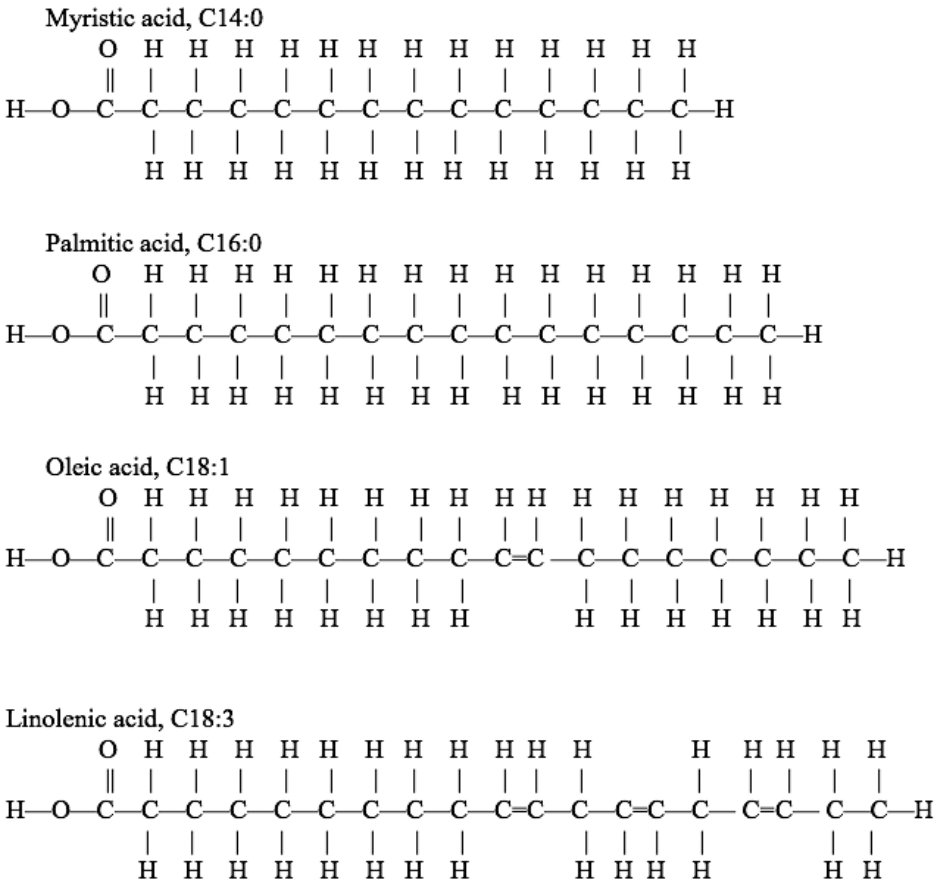

Figure 5: Four of the many types of fatty acids (FAs) found in vegetable oils. Fatty acids which have hydrogen atoms in every position that they can occupy are known as "saturated". Saturated fatty acid carbon chains form relatively straight lines. Those that have double bonds are considered to be "unsaturated". In reality, unsaturated fatty acid molecules are bent at the double bonds (not shown). The bent molecules of unsaturated fatty acids do not pack as densely as the straight ones of saturated FAs, and triglycerides containing more unsaturated fatty acids are more likely to remain liquid at lower temperatures.

The more unsaturated a fatty acid is, or the more unsaturated fatty acids in a triglyceride, the more likely it is to be liquid at room temperature. The bent fatty acid carbon chains of unsaturated fatty acids do not pack as densely as the straight ones in saturated fatty acids and this causes them to have a lower melting point (Stoker, 2013). For example, flax oil has a large proportion of linolenic acid and it is liquid at room temperature. Palm oil has a large proportion of palmitic acid and it is firm at room temperature. Olive oil has a large proportion of oleic acid and it can become cloudy in a cold room and nearly solid when refrigerated. Most natural oils

and fats in living organisms contain triglycerides, which are used primarily for energy storage. Organisms make a number of other types of lipids, including steroids; fatty acids attached to a protein; free fatty acids; glycolipids which have a sugar component; and phospholipids, which are hydrophilic on one end, hydrophobic on the other, and form the membranes enclosing cellular contents and organelles (Evert and Eichhorn, 2013).

Biodiesel is manufactured by transesterification (Figure 6), where triglycerides (more accurately known as triacylglycerols) are combined with an alcohol to become fatty acid esters and glycerol, in a chemical reaction that is most often facilitated by a catalyst such as sodium hydroxide (NaOH or lye). The fatty acids are separated from the glycerol, breaking up the triglycerides into smaller molecules (esters of fatty acids), to make a less viscous, more suitable liquid fuel for diesel engines. Glycerol (glycerin), a useful byproduct, is removed from the fuel mixture. Although other alcohols can be used, methanol is most common, producing a mixture of fatty acid methyl esters (FAMEs).

Most biodiesel production today uses a base for a catalyst, but transesterification reactions can also be catalyzed with an acid or a lipase enzyme, and they have numerous industrial and laboratory applications, besides producing biodiesel (Otera, 1993, Fukuda, Kondo and Noda, 2001). Additional steps may also be added to the process in order to convert other types of lipids to FAMEs, for example, an acid catalyst may be added in a second step to convert (to biodiesel) free fatty acids which may remain after the first transesterification step using a base.

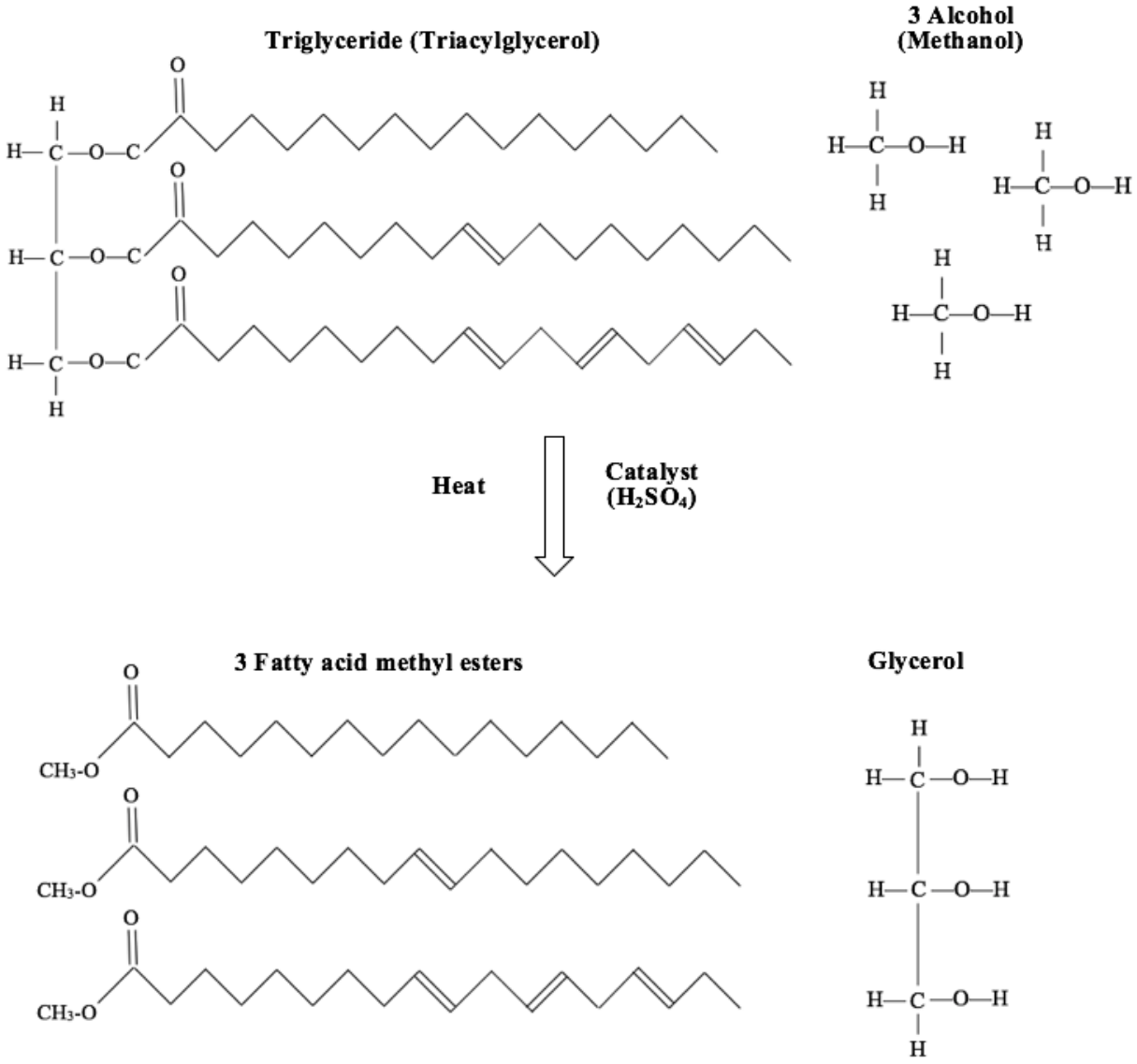

Figure 6: An example transesterification reaction with a triglyceride (also called triacylglycerol or TAG), methanol and sulfuric acid as a catalyst, like the method for this experiment (the C's and H's of the fatty acids have been left out for simplicity). The fatty acids pictured in the example triglyceride are palmitic acid (C16:0), oleic acid (C18:1) and linolenic acid (C18:3). These are connected by a glycerol "backbone". One triglyceride molecule and three of the alcohol yields three fatty acid methyl ester (FAME) molecules and one glycerol molecule. A catalyst is necessary to facilitate the reaction and the mixture may also be heated to speed up the reaction. The carbon chains of the fatty acids, and resulting FAMEs, may be various lengths and saturation or unsaturation, and may also be branched. FAMEs are more likely to remain liquid at low temperatures than the original triglycerides.

1.2.5. Quality of Biodiesel

The fatty acid profile of feedstocks strongly effects the quality and specific properties of the fuel made from them (Pinzi et al., 2009, Table 1, and Dunn, 2018). Three key properties of biodiesel that determine its quality are: cloud point, oxidative stability and cetane number. The cloud point describes the temperature below which the fuel will begin to solidify and form wax-like particles, which can obstruct fuel lines, filters and injectors. It is a particularly important factor to consider when operating machinery in cold climates. A high proportion of monounsaturated fatty acids (such as C16:1 and C18:1), in lipids used for biodiesel, improves its ability to remain liquid at low temperatures. Fatty acids that have only two or three unsaturations (such as C18:2 and C18:3) also positively influence cold temperature flow properties, but not as strongly as monounsaturated ones. High proportions of saturated fatty acids tend to make fuel more likely to thicken at cold temperatures.

Oxidative stability refers to the fuel's resistance to oxidation. Oxidation results in the build-up of impurities that adversely affect engine performance. A large proportion of polyunsaturated fatty acids dramatically decreases oxidative stability. Iodine Value (IV), a measure of total unsaturation, is related to oxidative stability. A high IV is related to lower oxidative stability. A low oxidative stability number (2.3 for ultra-low sulfur diesel) indicates better resistance to oxidation. Biodiesel is typically less resistant to oxidation than petroleum diesel. Oxidative stability can be improved by adjusting the diesel blend or by fuel additives.

Cetane number refers to the fuel's ignition properties and a higher cetane number indicates a cleaner-burning fuel and better engine performance. In general, biodiesel FAMEs with increased carbon chain length have a higher cetane number, although increasing unsaturation results in a lower cetane number. The minimum cetane number for ultra-low sulfur

diesel is usually 40, and biodiesel cetane numbers tend to be somewhat higher (Hanson and Agarwal, EIA, 2018).

Many algal species that have been studied for biodiesel have a wider range of fatty acids compared to vegetable oils, for example, higher proportions of short-chain saturated fatty acids, higher proportions of long-chain polyunsaturated fatty acids, and they may also contain more highly unsaturated fatty acids, with three or more double bonds (Hoekman et al., 2012).

1.3. Algae

1.3.1. Definition of Algae

"Algae" is a descriptive term for a diverse group of plant-like organisms that are not necessarily related to one another. Micro- and macroalgae include unicellular and multicellular organisms that mostly or entirely obtain their nutrition through photosynthesis, using light energy to fix atmospheric carbon, and therefore they serve as primary producers, the base of the food web, in aquatic environments. Microalgae and macroalgae are often referred to as phytoplankton and seaweeds. Algae include eukaryotic and prokaryotic organisms, but generally exclude terrestrial plants. Like land plants, algae require certain nutrients in order to grow, and the lack of any of these will limit their growth.

Conversely, excess nutrient concentrations, in particular nitrogen or phosphorus, can trigger algal blooms where growth increases dramatically until nutrients are depleted. In extreme bloom events, when very large quantities of algae or aquatic plants grow and die off, bacteria and fungi that decompose the biomass can deplete oxygen from the water, leading to anoxia and dead zones. Blooms of some species that produce toxins can result in the accumulation of these toxins in shellfish or fish.

1.3.2. *Chromulina freiburgensis* from Berkeley Pit Lake

One of the microalgae living in Berkeley Pit Lake has been identified as *Chromulina freiburgensis* Doflein, a chrysophyte or golden alga. *C. freiburgensis* was first observed and described by Franz Doflein, in 1921. He had found the species living in bogs in Germany's Schwarzwald near Freiburg (Doflein, 1921). This chrysophyte was first isolated from Berkeley Pit Lake in 1998, by Dr. Grant Mitman, as one of six microalgal species discovered by supplying water samples with nutrients to stimulate sparse algal populations to grow to detectible densities (Mitman, 1999). *C. freiburgensis* cells live independently or as part of a biofilm on submerged surfaces or the underside of the water's surface, but they do not form colonies. They can alternate between two basic forms, an active swimming form and a non-motile form.

The swimming form has an oblong, flexible shape, and it moves rapidly through the water (or aqueous medium) by means of one visible flagellum of about the same length as the cell body (a second, small flagellum may be present, but was not visible with light microscopy). The non-motile form is spherical in shape, and armored by in a smooth, glasslike, silica re-enforced layer beneath its outermost membrane (Huber-Pestalozzi, 1962). Both forms contain a single, large, more or less bowl-shaped, gold-colored chloroplast. The golden alga was identified as *C. freiburgensis* by Dr. Paul Kugrens at Colorado State University (Bocioaga, 2003, Henderson, 2005). Montana Tech graduate and undergraduate students subsequently studied this and other Berkeley Pit Lake microalgae, focusing on their potential utility for both biodiesel production and bioremediation (Dakel, 2001, Bartkowiak, 2002, Bocioaga, 2003, Tucci, 2005, Mondloch, 2012, Ostrom, 2012, Jonart, 2012, Kelly, 2013, Moslander, 2016).

This author hypothesized that *C. freiburgensis* was more readily able to adapt to an extremely acidic environment than other algae, due to its evolution and specialization in naturally acidic habitats. Peat bogs generally have a pH near 3.5 (Nixdorf, 2001) and are

oligotrophic (low in dissolved nutrients, containing a low-density phytoplankton population). Some eukaryotic phototrophs can be found in naturally-ocurring, extremely acidic environments, where eukaryote diversity is very low. Remarkably, several Chrysophytes, diatoms and Chlorophytes (green algae), can survive in extremely acidic environments associated with hydrothermal springs in Yellowstone National Park, ID, MT, WY and Lassen Volcanic National Park, CA. In fact, the genus, *Chromulina* has been found in a pH 1.8 pool at Lassen (Brown and Wolfe, 2006). Chrysophytes that were identified as belonging to the genus *Chromulina* have also been reported from U.S. water bodies, that had been polluted by acid mine drainage, from as long ago as 1938 (Lackey). It is possible that the golden alga had been introduced to Berkeley Pit Lake by a bird that had visited one of these natural sites, or possibly another acid mine drainage site where the alga had earlier become established.

C. freiburgensis appears to posess a competitive advantage over other microalgal species in these types of environments, repeatedly becoming the dominant alga in laboratory cultures grown in pH 2.5 to 2.7, nutrified Berkeley Pit Lake water (Dr. Grant Mitman, personal communication and Dakel, 2001).

1.3.3. Chrysophytes, Chromulinales and Stomatocysts

C. freiburgensis is currently classified in the kingdom Chromista, phylum Ochrophyta, and the class Chrysophyceae, which includes 670 known species. It is a member of the order Chromulinales, which currently includes approximately 608 species (Guiry and Guiry, 2018). Chrysophyceae are among a number of algae that are often called “golden algae” for their gold color (from “chrysos”, a Greek word for gold). A few chrysophytes, in particular, *Chromophyton rosanoffii* Woronin, previously classified as *Chromulina rosanoffii* (Woronin)

Blochmann, are known for creating a remarkable optical phenomenon that gives shaded forest ponds the appearance of having a layer of sparkling gold leaf, floating on the water's surface (Bauer, 1998, Guiry and Guiry, 2019).

Generally, chrysophytes are found in highest abundance in slightly acidic, oligotrophic (low-nutrient) freshwater environments (Sandgren, 1991). They are primarily photoautotrophs (providing their own nutrition through oxygenic photosynthesis (similarly to true plants), though some can become mixotrophs or rely on heterotrophy altogether, meaning that some species are also able to consume organic compounds or food particles, such as bacteria, depending on environmental conditions. Chrysophytes may be either unicellular (independent cells) or they can form colonies comprised of many cells.

Some species of chrysophytes (golden algae), diatoms and chlorophytes (green algae) can grow in naturally-occurring, extremely acidic environments (Brown and Wolfe, 2006), and these microalgae are among the pioneer species that first colonize acidic mining lakes. Many chrysophytes are also low-light and low phosphorus strategists (Nixdorf, Mischke and Leßmann, 1998). Previous experiments with *C. freiburgensis* had shown no increase in growth in response to increased medium phosphorus concentration (Dakel, 2001), supporting the suggestion that it also has a relatively low phosphorus requirement.

Chrysophytes, such as *C. freiburgensis*, and many other algae, are considered to be protists (microscopic eukaryotes). These groupings (protists and algae) are descriptive, but not based on taxonomic or genetic relatedness. Chrysophytes (a phylogenetic class and genetically related group) are characterized by their golden-brown accessory pigment, fucoxanthin in addition to chlorophyll a (the principal pigment for photosynthesis in eukaryotes), and chlorophyll c1 and c2, most often contained within one or two large chloroplasts. They store a

carbohydrate, chrysolaminarin, in vacuoles, and fats and oils in membrane-bound lipid bodies (lipid droplets or oil bodies).

Many chrysophytes are able to acquire nutrition through heterotrophy as well as through photosynthesis (absorbing organic carbon or consuming food particles such as bacteria), which has been reported to occur in the genus *Chromulina* (Graham, Graham and Wilcox, 2009). Individual chrysophyte cells can either assume a swimming form or a non-motile form that may be free or a member of a colony. Chrysophyte swimming cells generally have two flagella at the forward end, one large tinsel type, which pulls the cell forward, and a small, smooth one which is not used for swimming (the smaller one may be absent or not visible). They are phototactic, with a light-sensing organelle, either an "eyespot", or a photoreceptor, near the base of the smooth (small) flagellum (or where it would be, if the smooth flagellum is either not visible or absent) (Andersen, 2010). Non-motile cells can reproduce through mitosis. Many chrysophytes can also undergo sexual reproduction, but this has not been reported in *Chromulina* (Guiry and Guiry, 2019, Nicholls and Wujek, 2015, Doflein,1921 and Doflein, 1923).

A non-motile chrysophyte cell that is enclosed within a shell-like covering (cyst), and considered to be a resting stage, is known as a stomatocyst (statocyst or statospore). The stomatocyst of each species has a characteristic protective covering composed of silica, deposited by a specialized silica deposition vesicle, which is formed by the golgi apparatus, beneath the cell membrane. Each cyst has an exit pore or mouth (from, "stoma", a Greek word for mouth) which is often encircled by a collar, and is closed by a polysaccharide plug. Stomatocysts may arise from either sexual or asexual reproduction. Germination of the stomatocyst can occur with the release of two to four swimming daughter cells, which squeeze out through the narrow pore after its plug dissolves. Stomatocyst formation appears more likely

to be related to cell density, as opposed to other environmental factors, possibly in response to a chemical signal (Nicholls and Wujek, 2015, Graham, Graham and Wilcox, 2009). Chrysophyte species can be distinguished from one another by characteristic cyst features and ornamentation, such as collar type, pointed spikes or bumps (Holen, 2014). The silica covering makes these cells exceedingly durable, and hundreds of distinct types have been documented. Fossilized stomatocysts have been dated as far back as the early Cretaceous period (approximately 150 million years ago), and those deposited in sediment have been used to study long-term trends in aquatic ecology, such as the effects of acid rain and eutrophication (Graham, Graham, and Wilcox, 2009, Sandgren, 1991).

1.3.4. Biofuels from Algae

Like plants, microalgae fix atmospheric carbon as a means of harvesting solar energy. They convert sunlight to a chemical energy source that they can store for future energy requirements or use for the manufacture of the additional chemical compounds that they need for growth. The carbon that is released when algal biofuel is burned is the same carbon that they recently removed from the atmosphere, and that makes it possible to cultivate and market a carbon neutral fuel source, one that does not add a net quantity of greenhouse gases to the atmosphere.

The definition of photosynthesis is, “Conversion of light energy to chemical energy; the production of carbohydrates from carbon dioxide and water in the presence of chlorophyll by using light energy” (Figure 7, based on Evert and Eichhorn, 2013).

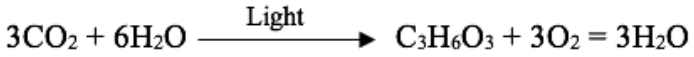

Figure 7: A simplified version of the balanced equation for photosynthesis in green plants and algae, where water serves as the electron donor. Pigments are necessary to harvest light energy in this manner, and chlorophyll a is the pigment directly involved in oxygen-generating photosynthesis. In many organisms, accessory pigments increase the useable range of light wavelengths and assist by directing light energy to chlorophyll a. These include chlorophyll b, chlorophyll c, phycobillins and carotenoids, including carotenes and xanthophylls. Chrysophytes, such as *C. freiburgensis*, use chlorophyll c in addition to chlorophyll a.

The chloroplast is the cellular organelle where photosynthesis occurs. It contains layers of thylakoid membranes, in which chlorophyll and accessory pigments are located, and it is positioned near the cell membrane where it is exposed to light. Carbohydrates and lipids are manufactured in the chloroplast, and then transported outside of it for storage. In terrestrial plants, leaf surface cells generally contain many small green chloroplasts. In *C. freiburgensis* and many other chrysophytes, each cell contains a single, large, gold-colored, bowl-shaped organelle.

1.3.5. Advantages of Algal Products as Biofuel Feedstocks

Microalgae are a promising source of lipids, especially triglycerides for biodiesel, because of their rapid growth rate and their relatively high lipid content, compared to terrestrial crops. One group of researchers cultured thirty different strains of microalgae under similar laboratory conditions, in nutrient replete media, and compared their lipid contents (Rodolfi et al., 2008). The lipid contents ranged from 8.5 to 39.8 percent (biomass). Another group of researchers tested twelve microalgal strains for both lipid productivity and lipid composition towards the qualities desired for biodiesel. They found that lipid content for their twelve strains ranged from 13.5 to 49.0 % of dry weight (Nascimento et al., 2013).

Microalgae have the potential to produce far more oil and consequently, fuel per acre than terrestrial crops (Chisti, 2007, Table III). Unlike terrestrial crops, they do not require fertile land, and because they are not relied on as a food crop, they would be unlikely to displace food crops or influence food prices. It is not necessary to consume valuable clean water, because they can be grown using agricultural, municipal or industrial wastewater, and serve as a step in the treatment process. Biodiesel from microalgae could become carbon neutral when an algal biofuel production facility could be built to supply all of the fuel for its own energy requirements, using, for example, biodiesel and methane from biomass, (Chisti, 2007).

Table III: Comparison of biodiesel crops, including microalgae and other biodiesel feedstocks, from data reported by Chisti (2007).

Biodiesel lipid (oil) Crops	Oil yield (L/ha)
Corn	172
Soybean	446
Canola	1190
Jatropa	1892
Coconut	2689
Oil Palm	5950
Microalgae (assuming 30% lipid by biomass)	58700

1.3.6. Challenges of Producing Algal Lipids for Biodiesel

Unique practical challenges must be overcome before algal fuels can replace fossil fuels or earlier generations of biofuels. The greatest obstacle is high production cost, which has prevented algal fuels from becoming cost-competitive in the market with conventional fuels and other forms of biodiesel. The high production cost is related to developing and adapting technology and methods for growing microalgae as a large-scale crop.

Harvesting substantial quantities of tiny cells from large volumes of liquid medium presents difficulties not encountered with other crops. Standard methods for harvesting and dewatering microalgal biomass generally involve centrifuges and filter membranes, which are equipment and energy intensive (Griffiths et al., 2012). Another disadvantage involves the high requirements many species have for nitrogen and phosphorus, which introduce their own negative environmental impacts related to polluted agricultural runoff and mining. In addition to using fossil fuels as an energy source to grow and harvest the algae, increasing quantities of fertilizers that would have to be mined, manufactured or imported would also increase greenhouse emissions to grow the algal crop, and could undo the expected carbon sequestration advantage (Biofuel.org, 2010). Effective solutions must be found for these problems to prevent them from cancelling out the potential economic and environmental benefits of growing microalgae for fuel.

1.3.7. Potential Solutions to Problems with Algal Biofuels

Some of the technological challenges that must be overcome to make algal fuels cost competitive include developing ways to reduce the cost and the amount of energy required for cultivation, harvest and processing to the point where a dry product is ready for lipid extraction for transesterification. Currently flocculation and centrifugation are common methods to separate algal cells from medium (Andersen, 2005). The comparatively greater cost of producing algal biofuels has been a significant challenge for establishing commercial-scale production. This is largely due to the lack of well-established, commercial-scale technology and infrastructure and the need to research and build cost-competitive production systems comparable to those that already exist for other fuels (Stephens et al., 2010).

According to Stephens et al., (2010), “If sustainable and profitable processes can be developed, the potential benefits of these technologies for the common good appear compelling and include the production on nonarable land of biodiesel, methane, butanol, ethanol, aviation fuel and hydrogen, using waste or saline water, as well as CO_2 from industrial or atmospheric sources.” The authors conducted a detailed industrial feasibility study, and concluded that the relatively high cost of microalgal fuel production would be begin to be resolved as the industry transitions from pilot study to commercial scale operations. Increasing petroleum oil prices and subsidies for cleaner fuels would benefit the algal fuel market, and marketing one or more high value products in addition to oil can protect against oil price fluctuations.

1.3.8. Lowering cost and energy expenditure

1.3.8.1. Co-culture as a Method to Reduce Costs Associated with Harvest and Nutrient Supply

Harvesting miniscule microalgal cells from large volumes of liquid medium is an important contributor to the high production cost, as they are too small for low-cost filters or strainers (Griffiths and Harrison, 2009). This can account for 20 to 30 percent of total costs of algal biomass production (Barros, et al., 2015, Zhou et al., 2013). Harvest can present unique mechanical challenges, such as designing filters to resist clogging, and it requires considerable energy input to run pumps and centrifuges.

Fungi and bacteria grown with microalgae can assist with biomass harvest by promoting flocculation (Barros, et al., 2015, Van Den Hende et al., 2011, Zhou et al., 2013). Many bacteria secrete sticky substances that promote flocculation, and many fungi grow long filamentous, hyphae.

Microalgal cells (phytoplankton), generally have a negative surface charge, which helps to keep them separated and in suspension in water. Fungal hyphae not only form a net-like matrix to capture algal cells, but they can also have a positive (+) surface charge, which attracts the negatively-charged (-) algal cells (Zhang and Hu, 2012, Zhou et al., 2013). Flocculation of algal cells makes them more readily harvested, by skimming or screening, and previous research has demonstrated that, with the addition of physical agitation (shaking), fungi-bound algal cells can be formed into pellets that are easily separated from the medium (Wrede et al., 2014, Zhou et al., 2013, Zhang and Hu, 2012, Zhou et al., 2012).

Many fungi are acid-tolerant, and able to adapt to and survive in extreme environments, including the acidic mine drainage of Berkeley Pit Lake (Phillip, 1999). For example, *Penicillium clavigerum* Demelius, a fungus found living with a green microalga from Berkeley Pit Lake, *Chlorella vulgaris* Beyerinck, is one of six Berkeley Pit Lake fungi that produce chemical compounds with potentially invaluable medical applications (Stierle and Stierle, 2005 and 2014, Stierle et al., 2014). This points out the possibility that the fungi chosen for co-culture with microalgae could themselves provide additional marketable side products, whether a large-scale algal culturing operation focuses on biodiesel, or on another primary purpose.

Another challenge has been relatively high nutrient requirements of many microalgae for rapid growth, in particular, nitrogen and phosphorus. Numerous species of prokaryotes fix atmospheric nitrogen, making it available to algae and plants. Some aerobic soil bacteria, for example, *Beijerinckia indica* (Starkey and De, 1939, Derx, 1950), can fix nitrogen at a pH as low as 2.5 to 3.0, and will grow well in a liquid medium (Becking, 2006, 1984 and 1961), therefore they may offer a means of reducing the cost associated with providing adequate nitrogen to promote rapid algal growth, even in an acid medium that excludes most contaminating

organisms. This bacterium also generates a sticky mucilage, that may be useful to promote flocculation. Co-culturing microalgae with bacteria and fungi can improve both biomass and lipid productivity (Barros, et al., 2015, Berthold, 2016, Kim et al., 2015). Sources of organic carbon can be added to the algal medium to support heterotrophic organisms, but such supplementation may only need to be minimal, or even unnecessary. Bacteria, fungi and nitrogen-fixing cyanobacteria all use the carbohydrates secreted by algae and plants to support their growth.

Some research has also demonstrated that increasing algal species diversity in laboratory culture, as in natural habitats, results in a corresponding increase not only in biomass productivity, but also in lipid yield (Stockenreiter et al., 2012). There is evidence that in highly diverse algal communities, like in other diverse biological communities, multiple species can utilize resources in a complementary way. Co-culture of microalgae along with fungi, bacteria or other algae shows promise for improving the cost-competitiveness and sustainability of the process.

1.3.8.2. Algal Side Products

Marketing side products or services is one way to improve cost-competitivness. The production of biodiesel from microalgae can occur simultaneously with the generation of several additional beneficial products and services, including economically valuable algal side products, phycoremediation and CO_2 capture and sequestration. High value algal side products can include food supplements, pharmaceutical ingredients, products used in cosmetics or feed ingredients for livestock and aquiculture, although edible products may not be compatible with the usage of contaminated wastewater. Some examples are polyunsaturated fatty acids such as

the ω-3 fatty acids, EPA and DHA, (eicosapentaenoic acid, C20:5, and docosahexaenoic acid, C22:6); pigments such as β-carotene, astaxanthin and phycobilins, as well as proteins, polysaccharides and a variety of pharmaceutical ingredients (Khozin-Goldberg et al., 2002, Yen et al., 2013, Pulz and Gross 2004).

Glycerol is an important side product of biodiesel production. The transesterification of triglycerides to yield FAMEs used in biodiesel releases one molecule of glycerol ($C_3H_8O_3$) for each three FAME molecules. Glycerol from biodiesel production usually contains remaining methanol, which can be retrieved, along with other impurities. It can be sold as crude glycerin or refined to improve its market value (Sims, 2011). Glycerol has an enormous variety of uses including, pharmaceuticals, foods, antifreeze, and in the production of pure hydrogen for fuel (PubChem, 2019, Bagnato et al., 2017, Wikipedia, 2018).

The surplus biomass remaining after lipid extraction contains nitrogen, phosphorus, micronutrients, protein, carbohydrates, and other organic carbon compounds. Microalgal biomass has water conserving and soil stabilizing physical properties as well as beneficial chemical properties as a soil amendment for agriculture, bioremediation, or habitat restoration (Pulz and Gross, 2004). If it does not accumulate toxic impurities from wastewater, it can also be used as a livestock feed supplement. After lipids have been extracted from microalgal biomass for biodiesel, it can yield additional valuable products, and it also becomes suitable feedstock for fermentation to produce bioethanol (Rawat et al., 2011, Harun, Danquaha and Forde, 2009). Nutrients, including nitrogen and phosphorus, can also be recovered from algal biomass, after lipid extraction, and reused to grow subsequent algal crops (Bagnoud-Velásquez et al., 2015).

1.3.8.3. Algal Services

1.3.8.3.1. Bioremediation, Phycoremediation and Wastewater Treatment

1.3.8.3.1.1. Agricultural Runoff

Microalgae can be used to remove nutrients, heavy metals and organic pollutants from municipal sewage, agricultural and industrial wastewater (Wong and Tam, 1998). Nitrogen and phosphorus are two of the most important plant nutrients required for agriculture and for algal culture. Although soil nitrogen can be increased using a variety of methods, such as rotation with nitrogen-fixing crops, phosphorus for fertilizers is traditionally obtained in sufficient quantities only by mining (USGS, 2017). A heavy reliance on commercial and synthetic fertilizers, in competition with agriculture, would make algal biofuels unsustainable, therefore research should emphasize nutrient recycling methods within algal biofuel production processes and alternative nutrients sources (Canter et al., 2015). Considerable quantities of both nutrients are lost from agriculture through runoff, resulting not only in an economic loss to farmers, but also in damaging eutrophication of freshwater bodies and ocean dead zones, harming fisheries, wildlife and human health. Microalgae can be used to retrieve and recycle both nitrogen and phosphorus from algal biofuel operations (Sandia National Laboratories, 2015) and can be utilized as a means of doing the same on a large scale with agricultural runoff and municipal wastewater (Wong and Tam, 1998), promising economic, environmental and health benefits.

1.3.8.3.1.2. CO_2 Removal from Flu Gas and Wastewater Treatment

Microalgae have been employed to remove CO_2 from flue gases in power plants and other applications that burn fossil fuels, biofuels or biomass. Microalgae have varied requirements and tolerances to CO_2. To be a suitable candidate for this purpose, an alga must be capable of growing well with concentrations of carbon dioxide greater that those normally found

in ambient air and the photic zones of most naturally-occurring water bodies. Because CO_2 is the source of carbon required for photosynthesis, a modest addition of CO_2 can enhance growth, but excess CO_2 will inhibit it (Varshney et al., 2016, Mortensen and Gislerød, 2015, Yue and Chen, 2005). Some strains of microalgae have been identified that can grow well at CO_2 concentrations as high as 20 to 30%. This is an unusual characteristic, and if they can also tolerate a wide range of temperatures and pH, they are especially well-qualified for flue gas carbon capture (Varshney et al., 2016, Yue and Chen, 2005, Hanagata et al., 1992). Many strains of microalgae are able to tolerate and grow well at CO_2 concentrations below 10%, but growth is usually limited or inhibited at higher CO_2 concentrations, even if the oxygen concentration is lowered, and if toxic flue gas contaminants are not present (Varshney et al., 2016, Mortensen and Gislerød, 2015). For example, out of 250 strains examined, only five grew well with 20% CO_2 (Hanagata et al., 1992).

Microalgae can be grown using media based on manure or effluent from dairy and swine farms (Kebede-Westhead et al., 2006, Martin et al., 1984, Wang et al., 2012, Zhu et al., 2013), and also from the nutrients generated by aquaculture, as a means of generating biomass. They can be used to reclaim nutrient byproducts that might otherwise cause environmental damage, for example, nitrogen and phosphorus, from one type of agricultural operation for use in another. Microalgae can be employed in the treatment of municipal wastewater and sewage, while cultivated as a biofuel crop, in much the same way as for agricultural wastewater (Rawat et al., 2011). CO_2 recapture from flue gas can be integrated with lipid production for biodiesel and nutrient removal from municipal, agriculture or aquiculture wastewater (Arbib et al., 2017, Kuo et al., 2016, Li et al., 2011, Van Den Hende et al., 2011, Woertz et al., 2009, Yadav and Sen, 2017, Zhu et al., 2013).

1.3.8.3.1.3. Industrial Wastewater and Acid Mine Drainage

Industrial and mining operations generate wastewaters with considerably higher concentrations of dissolved heavy metals than municipal and agricultural sources. Microalgae can be employed for the removal of heavy metals and sulfate and, to some extent, raise the pH of acidified water. Microalgae, such as *Chlorella sp.*, can be used to cost-effectively retrieve nutrients and remove and heavy metals from industrial wastewater (Chinnasamy et al., 2010, Wong and Tam, 1998).

Acid mine drainage is a world-wide problem, wherever mining is conducted in areas rich in iron pyrite (Bwapwa, Jaiyeola and Chetty, 2017). When rock containing pyrite is exposed to oxygen and water, it becomes an energy source for aerobic chemoautotrophic bacteria such as *Acidithiobacillus ferroxidans*, and their metabolic processes release sulfuric acid, as a byproduct, into the environment (Horikoshi and Grant, 1998, Madigan et al., 2015).

Bioremoval of heavy metals from acid mine drainage using microalgae may offer advantages over other methods, such as lime precipitation, particularly with regards to cost (Wilde and Benemann, 1993). A number of microalgae have adapted to acidic, dissolved metal-rich, freshwater habitats, and they have a high capacity for metal accumulation (Wong and Tam, 1998, He and Chen, 2014). Algal cells can accumulate a variety of metals by two different processes. The first is a rapid process of adsorption, where the metal ions are bound to polysaccharide and protein molecules of their cell walls, by both ionic and covalent bonds, generally taking several minutes. This is followed by a slow process of bioaccumulation by metabolic processes, throughout the life span of the cell, which is often irreversible (Wong and Tam, 1998). Because they occupy the base of the food chain, bioaccumulation of metals in microalgae has been known to negatively impact the health and survival of species that are higher on the food chain, for example, fish, birds and mammals, including humans

(Scheuhammer et al., 2007, King, 1964, Tao et al., 2012, Tchounwou et al., 2012, Jitar et al., 2015, Ayala-Parra et al., 2016). However, the same ability of microalgae to tolerate and accumulate heavy metals can be harnessed to retrieve and remove these from contaminated sites, and commercial applications have been developed to do this (Rose et al., 1998). In fact, metal adsorption on microalgal surfaces has been found to be higher than on abiotic adsorbing materials, such as activated carbon, silica gel and clay particles, though their efficiencies are highly variable, depending on both the chemical properties of the metals, and the types of algae (Wong and Tam, 1998, Wang and Wood, 1984).

Whole microalgal cells, and also the parts remaining after lipid extraction for biodiesel, have been successfully tested as a treatment for acid mine drainage. They were used as a means of recovering valuable metals, raising the pH of the medium and lowering its toxicity (Ayala-Parra, Sierra-Alvarez, and Field, 2016). A recent experiment demonstrated that, while high concentrations of nickel may impede growth, they also can induce microalgae to increase lipid production to approximately 6.8 times the normal average mass per cell in some species. The researchers found that two essentially unrelated species of microalgae (belonging to completely different taxonomic kingdoms) respond to increased Ni in their environment by increasing lipid production (Moussa et al., 2018).

According to Bwapwa, Jaiyeola and Chetty (2017), "Algae strains such as *Spirulina* sp., *Chlorella, Scenedesmus, Cladophora, Oscillatoria, Anabaena,* and *Phaeodactylum tricornutum* have shown the capacity to remove a considerable quantity of heavy metals from acid mine drainage." The authors also conclude that microalgae, "act as "hyper-accumulators" and "hyper-adsorbents" with a high selectivity for different elements", and they note that microalgae generally increase the alkalinity of the medium, which is necessary for precipitation of heavy

metals during acid mine drainage water treatment. However, characteristics of individual algal strains and pH strongly influence algal biosorption capabilities (Dönmez et al., 1999). An in-situ experiment to test whether nutrient supplementation of indigenous microalgae would result in the removal of significant amounts of dissolved metals was conducted in Berkeley Pit Lake in 2004 (Tucci, 2005). After six months, the algal populations, in particular *Euglena mutabilis* (a green alga) and *C. freiburgensis*, had increased from undetectable to 10^6 cells/mL, but dissolved metal concentrations remained stubbornly high. Tucci hypothesized that while a six-month period may not have been enough time to fully understand the effect of the native algae on dissolved metals, the low pH at the time (2.5 to 2.7), was probably the most important environmental factor preventing metal ions from binding to the algal surfaces (Tucci, 2005, Wang and Wood, 1984, Drever, 1997, Stumm and Morgan 1996, Leung et al., 2000). While the experiment in Berkeley Pit Lake was not able to demonstrate complete success with in-situ artificial eutrophication alone to quickly remove dissolved metals from a very large contaminated water body, it does not mean that a similar method would not succeed with smaller volumes and greater relative surface areas. The limnocorrals in which the nutrient supplementation occurred had a relatively small surface area (one meter surface diameter by three meters' depth) for gas exchange and lacked a means of circulation, which may have had a limiting effect on microalgal growth or species diversity. However, the growing algae increased oxygen levels by 58% and stimulated the growth of bacteria, which can capture and remove heavy metals from the environment by several biological and chemical processes (Tucci, 2005, Ullah et al., 2015, Leung et al., 2000).

Some of the least costly methods for treatment of acid mine drainage have involved passive systems including ponds, rock filters, and artificial wetlands. These often employ naturally occurring algae, aerobic and anaerobic microbes, and many other organisms, and they

have been used with varying levels of success (Gazea, Adam, and Kontopoulos, 1996). In fact, microalgae may be more effective for removing metal and sulfate from acid mine drainage when working symbiotically with acid-tolerant fungi and bacteria (Das et al., 2009). This is a potential additional use for surplus algal biomass from a biofuel operation, in particular, for acid-tolerant strains.

1.3.9. Large-Scale Algal Cultivation

Large scale microalgal culture systems share some similarities and technology with both aquaculture and with conventional farming, but have unique requirements in addition to those usually needed in terrestrial and aquatic farm systems. Microalgae require many of the same basic resources as terrestrial crops including light, water, carbon dioxide, oxygen, macronutrients and micronutrients. Macronutrients are the elements that are required in relatively large concentrations, and these include nitrogen, phosphorus, potassium, sulfur, magnesium, calcium, and in siliceous species, silicon. Micronutrients are elements that are also required for growth, but in trace amounts. These include iron, manganese, molybdenum, zinc, nickel, boron, chlorine and copper. All of these nutrients play critical roles in the functions of living cells, such as maintaining osmotic balance and the building of enzymes, pigments, nucleic acids, proteins, cell walls and organelles. All of these nutrients must be available to algal cells in sufficient concentrations, depending on the species' requirements, for growth to occur.

There are two basic growing systems commonly employed for cultivating microalgae in large quantities, open ponds or raceways, and closed systems, generally referred to as bioreactors, or more specifically, photobioreactors (Figure 8, Figure 9, and Table IV). These

systems can be modified and customized according to the requirements and purpose of the project.

1.3.9.1. Open Systems

Open ponds and/or raceways are relatively simple, durable, and less expensive to construct and maintain, outdoors or in greenhouses, and they can be built to nearly any size desired (Figure 8). In open ponds, even in greenhouses, the algae and their medium are more likely to be exposed to the air and outside environment, and therefore have more opportunities to become contaminated by unwanted organisms, which makes these systems less suited to maintain unialgal or axenic cultures. Productivity in ponds/raceways can be limited by the shading effects of cell density and depth, so these must be built shallow, for example 30 cm, and have a means of circulation, to optimize exposure of cells to light. Ponds/raceways should have rounded sides, to prevent buildup of cells in corners that could die and become anaerobic. Paddle wheels are one of the most common and effective methods for circulation. Algal cell density can also be controlled to allow optimal light exposure.

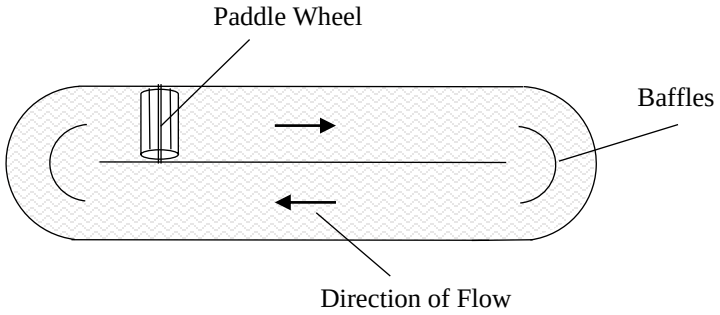

Figure 8: A simplified design for a raceway pond culture system for microalgae that can be built outdoors or in a greenhouse, to take advantage of natural sunlight (view from directly above). The aqueous medium containing cells can be piped out of the basin to harvest biomass. Scale and complexity can be customized to meet specific requirements. Ponds and raceways can also be covered, and supplemented with CO_2.

Air can be bubbled through these systems and CO_2 can also be supplemented by several different methods (Andersen, 2005). Arbib et al., 2017, describes a high rate algal pond continuous culture system for simultaneous municipal wastewater treatment and biodiesel production, with CO_2 supplementation, that functions best at a depth of 30 cm. CO_2 was added to improve the carbon to nitrogen ratio in the urban wastewater for algal growth. Yadav and Sen (2017) discuss the concept of a "microalgal green refinery", as a means of simultaneously capturing CO_2 from flue gases, reclaiming nutrients from wastewater, and producing algal lipids for biodiesel, biomass for bioethanol, and other valuable algal side products. They conclude that research should focus on open cultivation systems, for this concept to be successful and cost-effective.

1.3.9.2. Closed Systems

A bioreactor is a typical example of a closed system for cultivating microalgae (Figure 9). As defined by Merriam Webster (2018), it is "a device or apparatus in which living organisms… synthesize useful substances… or break down harmful ones…" Bioreactors can range from relatively simple to complex, but the algae and their liquid medium are contained and circulated within a sealed vessel or tubing, in which all their growth requirements are provided, including light, nutrients, and the necessary balance of CO_2 and oxygen. In bioreactors, or more specifically for when light is involved, photobioreactors (PBRs) the culture is isolated from the outside environment, with little chance of contamination. These apparatuses require relatively close monitoring and maintenance, and a reliable power source. Photosynthesis releases heat, and it is often necessary to have a means of cooling the medium. Productivity inside a photobioreactor can be limited by low carbon dioxide, which can be improved by supplementing

the air circulated through it with additional CO_2, for example, at a rate of 0.2 to five percent greater than ambient air (Andersen, 2005).

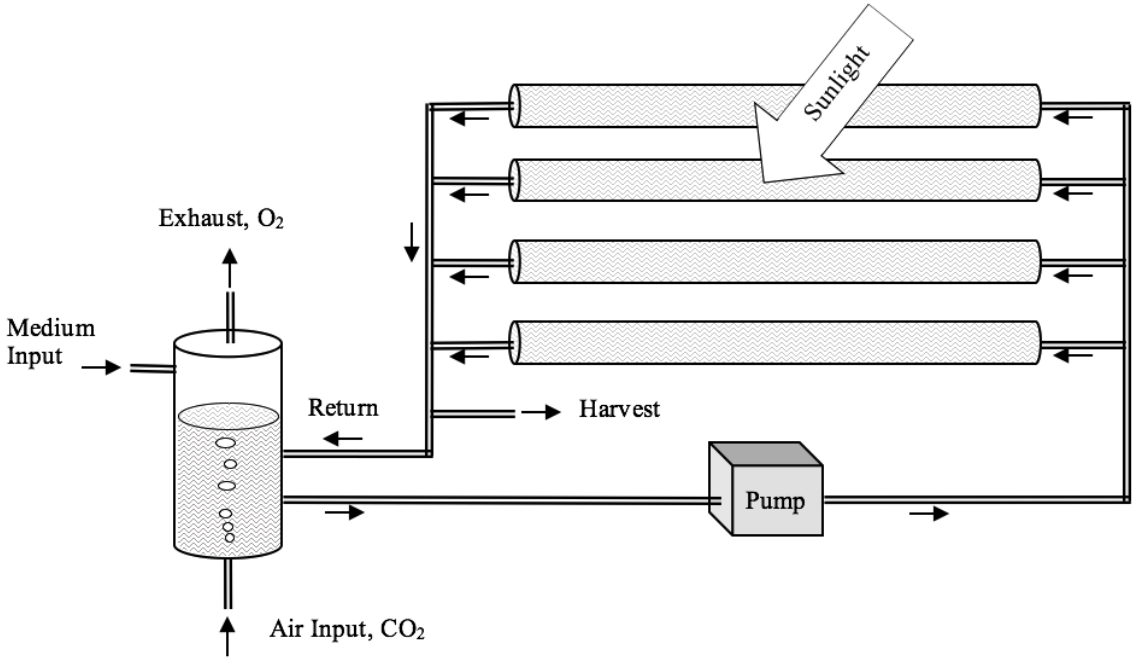

Figure 9: A simplified example of an outdoor or greenhouse photobioreactor that can be built to take advantage of natural sunlight. New medium is added to the reservoir and degassing column where the pH and the balance of gases in the medium can be adjusted, adding CO_2 and releasing excess oxygen generated during photosynthesis. Medium containing algal cells is circulated through a solar collector, a series of tubes arrayed to maximize each cell's exposure to sunlight or artificial lighting. Algal cells in depleted medium can be harvested as fresh medium is added. The temperature can be controlled by a heat exchange system, for example, by circulating cooled water through stainless steel coils submerged in the medium (Andersen, 2005, Chisti, 2007).

Large PBRs can be operated outdoors or in greenhouses, where they can take advantage of natural sunlight. Photobioreactors permit the cultivation of a single specialized species, for example, one genetically modified or selected for exceptionally high lipid yield, or to produce a particular high-value product. PBRs can provide the highest productivity, but to achieve this they generally require artificial lighting and a cooling system, in addition to systems for gas regulation and mixing, and their internal surfaces must be kept clean to prevent shading. Depending on their complexity and the materials from which they are built, PBRs can be more

expensive to build, operate, maintain and clean, more fragile, and have a shorter lifespan than open systems (Huang et al., 2017).

Table IV: A comparison of four promising photobioreactor designs (Huang, Jiang, Wang and Yang, 2017).

Photobioreactor Designs	Advantages	Disadvantages
Tubular	Simple; large illumination surface area	High temperature; photolimitation; high pH, CO2 and O2 gradients; high capital and operating costs
Plastic Bag	Low capital cost in the short term	Photolimitation; bad mixing; frailty to leakage; short lifespan
Column Airlift	Low power consumption; low shear stress; good mixing and mass transfer	High capital cost; high cleaning cost
Flat Panel Airlift	Low power consumption and shear stress; easy temperature control; good mixing and mass transfer; long lifespan; high ratio of illuminated surface area to volume; low operating cost	High capital cost

1.3.9.1. Batch vs. Continuous Cultures

Whether in an open or closed system, cultures can be maintained as either continuous or batch cultures, or as some combination of these methods. For a continuous culture, fresh medium is continually added while algal biomass is harvested along with depleted medium. The harvest and replacement are constantly occurring while the system is running. Batch cultures are started and allowed to grow for a period of time, until the desired cell density or growth stage is reached. At that point, the entire biomass in that batch is harvested at once.

In 2007, Chisti, in his review of relevant research, concluded that, “The only practicable methods of large-scale production of microalgae are raceway ponds and tubular photobioreactors”. According to Richardson, Johnson and Outlaw (2012), assuming the use of contemporary technology, neither photobioreactors nor open pond/raceway culture methods are economically feasible without substantial reductions in capital expenses and operation expenses,

because the cost of producing algal lipids is much higher than the cost of crude oil. However, they also concluded that these expense reductions were more achievable for open pond systems than for photobioreactors. Nonetheless, several new photobioreactor designs (Table IV) are currently being developed that show promise toward meeting the needs of large scale cultivation necessary for biofuel crops (Huang et al., 2017).

1.3.10. Algal Responses to Changes in Nutrient Concentrations

Most microalgae that have been studied begin amassing greater quantities of lipids, in particular triglycerides (triacylglycerols) only when they stop undergoing rapid growth. This is most often in response to the depletion of nitrogen, or another macronutrient, in their environment. This strategy has been successfully employed to coax increased lipid production in a number of different microalgal strains (Arias-Forero et al., 2013, Li, Fei, and Deng, 2012). Microalgae store energy as carbohydrates or lipids. Because lipids are more energy-dense than carbohydrates, they are better suited for long-term energy storage. It was hypothesized that *C. freiburgensis* cells, like those of other microalgae, respond to high nutrient concentrations by growing rapidly (algal blooms) and storing primarily carbohydrate (in this case, chrysolaminarin). When they begin to detect nutrient scarcity, they were expected to respond by amassing increasing quantities of lipids, an adaptation to tide them over for longer periods of nutrient scarcity, such as during a winter season. Rodolfi et al. (2009), found that (biomass) productivity and lipid content were generally inversely related, which they postulated was due to the high metabolic cost of lipid biosynthesis.

1.3.11. Light Requirements

Adequate light is necessary for photosynthesis, and it must also contain the correct wavelengths and intensity for the species. During photosynthesis, the carbon from CO_2 is first captured in carbohydrates which go on to provision the organism's growth and survival requirements. Photosynthetic organisms also respire, like heterotrophic organisms, using oxygen and releasing CO_2. The level of light intensity at which photosynthesis and respiration rates are balanced is known as the "compensation point". Higher light levels result in increasing rates of photosynthesis, up to a point where excess light results in "photoinhibition", a condition in which the respiration rate is higher than the rate of photosynthesis. If phytoplankton (microalgae) are unable to escape excess light, they will lose chlorophyll and their photosynthetic apparatus can become damaged (Graham and Wilcox, 2000).

Periods of darkness are generally assumed to be beneficial when culturing microalgae, in order for certain metabolic activities to occur, though it is difficult to know for certain how important they are. In the natural environment, photosynthetic organisms have adaptations to living with photoperiods and various light fluctuations, and photosynthetic organisms adjust pigment levels to optimize photosynthesis and to protect themselves from excess light. In an experiment comparing the growth of two diatoms in different light intensities and photoperiod lengths, it was observed that, "The growth rate in continuous light was never significantly higher than with 16 hours of light plus 8 hours of dark." (Paasche, 1968).

1.3.12. Balancing Carbon Dioxide and Oxygen

CO_2 concentrations, oxygen concentrations, and pH in natural bodies of water generally follow daily and seasonal fluctuations. Light, temperature and circulation influence

concentrations of dissolved gases in water. Photosynthesis during daylight hours increases oxygen and decreases CO_2 concentrations, while respiration by aquatic organisms at night increases CO_2 concentrations (Wurts and Durborow, 1992). Cold water bodies, with large surface areas relative to volume, or greater contact with air due to movement and circulation, generally contain higher concentrations of dissolved oxygen. Temperature increases, as may occur in shallow, still water during the summer, can result in low oxygen and high CO_2 extremes that become lethal to fish and other aquatic organisms. Bacterial decomposition of organic matter in eutrophic water bodies (those with high nutrient concentrations and high biomass productivity) can also cause lethal, anoxic conditions. Since microalgae have evolved to live in nearly every aquatic habitat and growing condition on earth, some species can be expected to have adaptations for surviving relatively high CO_2 concentrations, while others would not.

1.3.13. Stability of pH

It is necessary to provide a stable pH for microalgae, and if the balance of gases dissolved in the medium is unstable, it can make the environment too acidic (because of excess CO_2) or, most often, too basic (due to CO_2 depletion) (Fogg, 1975, Wurts and Durborow, 1992). In bright light, with high densities of algal cells, photosynthesis can increase medium or water pH to as high as 10 to 11 (Talling, 1976), which can trigger untimely flocculation and culture crash (Sunda, Price and Morel, 2005, Ogunsakin, 2017). Disruption in the pH of the medium can change important ion concentrations, impede growth or kill algal cells, or promote the growth of undesirable organisms. Most microalgae in cultivation grow at a pH between 7 and 9 (Lavens et al., 1996), neutral to slightly basic for a natural water body. Aeration and CO_2 supplementation, especially in closed systems, is one means of helping to stabilize the balance of these gases and

medium pH. A medium, such as MAM, that behaves as a buffer, or that has had buffering ingredients added, also helps to prevent undesired changes in pH.

1.3.14. Micronutrients and Concentrations of Metal Ions

In addition to macronutrients (such as carbon, nitrogen, phosphorus and silicon), microalgae require the correct concentrations of major ions including Na^{+}, K^{+}, Mg^{2+}, Ca^{2+}, Cl^{-} and SO_4^{2-}, and also micronutrients in the form of trace metal ions (of Fe, Mn, Zn, Co, Cu, Mo, and Se). The concentrations of ions in the medium is strongly influenced by pH, and they can bind to one another, precipitate out of solution, or reach toxic concentrations. Soil extract is one solution to this problem, and it has often been used to provide the necessary micronutrients and trace elements in adequate, non-toxic concentrations, in solution and available for the alga. In soil, these micronutrients are contained in humic compounds with humic acids. However, the concentrations of these elements in the medium from soil extracts are variable and difficult to predict. Adding EDTA (ethylenediaminetetraacetic acid) provides a way to keep metal ions in solution, either chelated with the EDTA, or free and available to microalgae, in stable, predictable concentrations. The ions are gradually released from the chelated complexes that they form with EDTA, in proportion to the decreasing concentrations of free ones in the solution, as these are consumed by the algae. The combination functions as a “metal ion buffer”, keeping the concentrations of the required micronutrient ions in the medium stable (Sunda, Price and Morel, 2005).

1.3.15. Microalgal Growth Patterns

Although the process of mitosis in eukaryotic cells is completely different from binary fission in prokaryotes, the resulting growth pattern (as change in cell density over time) of many unicellular organisms is similar. Microalgae growing in batch culture, including *C. freiburgensis* (a eukaryotic organism) exhibit this predictable pattern. A typical growth cycle (Figure 10) includes four distinct phases known as lag, exponential, stationary, and death (crash or lysis). There is also a transitional period, when growth slows, between the exponential and stationary growth phases (Fogg, 1975, Palenik and Wood, 1998, Wood, Everroad and Wingard, 2005). The lag phase refers to the period of time after inoculation during which cells acclimate and adjust their metabolic processes to new conditions, before beginning exponential growth. This phase can be shortened by selecting starter cells from a culture that is already in exponential growth (or has not fully transitioned to the stationary phase). Exponential growth occurs as long as cells can easily acquire all the nutrients necessary for rapid growth from their environment. Growth rates begin to slow down when one or more nutrients becomes depleted and more difficult for cells to obtain. The stationary growth phase is a period of time during which cells multiply and die at about the same rate, and the overall density of living cells remains constant. The final phase of the growth cycle in batch culture is known as the death or "crash" phase, which occurs when mortality exceeds growth. The population crash generally results from a combination of nutrient depletion and the buildup of metabolic byproducts that become toxic to cells and impede their growth, but it may also involve the activities of pathogenic or predatory organisms, if they enter the culture environment.

The transition between exponential and stationary growth is seldom mentioned as a separate growth phase in published literature, but it has been described as "phase of declining

relative growth rate" (Fogg, 1975, Price et al., 2013), and also as two transitional phases, "T1 and T2" (Palenik and Wood, 1998).

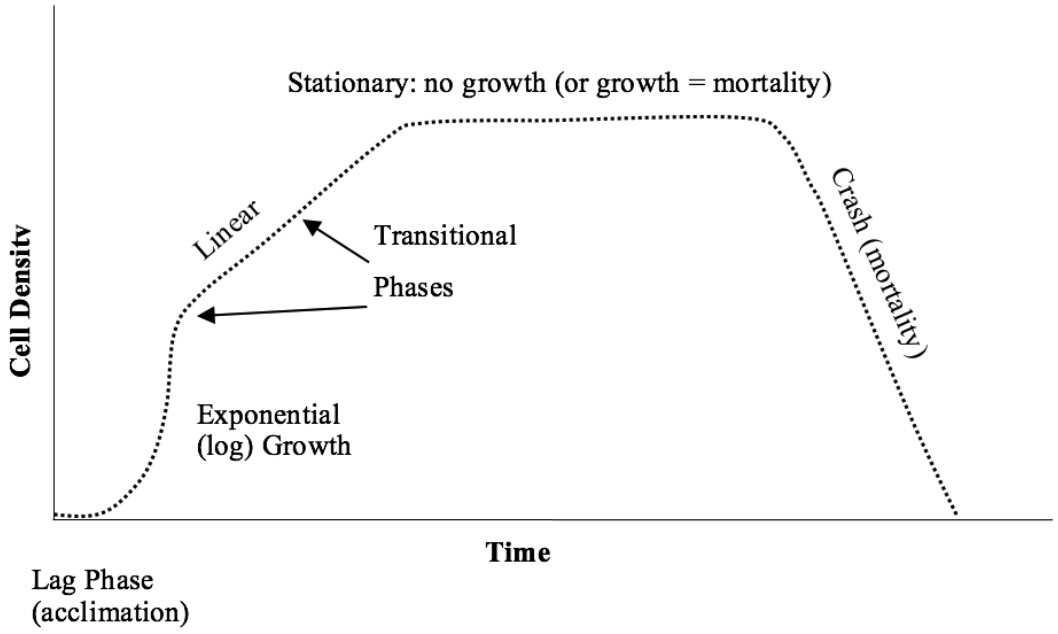

Figure 10: A typical growth pattern for unicellular organisms in batch culture, with five distinct growth phases, Lag, Exponential, Transitional, Stationary, and Death or "Crash". Cell density is a measure or estimate of the cell count per unit of liquid medium volume. Cells can be counted by various methods, using either visual microscopic observation, spectrophotometry or flow cytometry. Time can be any unit of time, but it is generally measured in hours or days.

1.4. Potential Advantages of *C. freiburgensis* from Berkeley Pit Lake

1.4.1. Potential High Lipid Content

Microalgae that have been investigated or successfully cultured for the high lipid yield that is desirable in a biodiesel crop, vary widely in terms of lipid content. Many are within the range of 20 to 50 percent lipid by dry weight (biomass). Lipid production is strongly influenced by environmental conditions, especially nutrient availability (Mata, Martins and Caetano, 2010). Based on visual observations and previous research by students at Montana Tech, *C. freiburgensis* appeared to be able to accumulate lipids within the range of other relatively high-

lipid microalgae. A Montana Tech undergraduate thesis research project combined BODIPY 505/515 (4, 4-Difluoro-3a, 4a-diaza-s indacane), a fluorescent stain for lipid in live cells, and ImageJ (2012) software, to determine the lipid content of *C. freiburgensi*s (Jonart, 2012). This method detected 25.2% average lipid content (by volume) with a high detected value of 34.48%, after approximately 57 days of growth in standard Modified Acid Medium (control treatment). Jonart's treatments with higher concentrations of nitrogen and phosphorus (combined) resulted in a 3.3% decrease in average lipid content. The higher nutrient medium resulted in an average detected lipid content of 21.2% and a maximum of 30.51% (by volume) after approximately 53 days. Her results were consistent with the expected response to higher nutrient concentrations, increased growth and cell densities, but lower lipid content.

C. freiburgensis in laboratory culture also produces a few extra-large cells that appear to contain an unusually large proportion of lipid (Figure 11). Cells undergoing active growth appear to contain little lipid, but once growth slows in response to lower concentrations of nutrients in the medium, cells begin to accumulate lipid stores (Figure 12).

Accumulating lipid when nutrient concentrations are low and they are not undergoing rapid growth is consistent with the behavior of other microalgae (Fidalgo et al. 1998). According to Vechtel, Eichenberger and Ruppell (1992), under nutrient-limited conditions, algae synthesize large amounts of triacylglycerols (triglycerides), which are stored in lipid droplets (oil bodies). Griffiths and Harrison (2009), state that "Nutrient deficiency, typically nitrogen or silicon deficiency, is well known to enhance the lipid content of algae". Because *C. freiburgensis* is adapted to oligotrophic conditions, it is hypothesized to have an effective means of stockpiling energy, such as amassing large lipid stores, to last through long periods of nutrient-scarce conditions. Since the nature of the *C. freiburgensis* extra-large cells is not yet

known, a hypothesis is that these cells are a specialized type of resting cyst, provisioned with an exceptionally large proportion of stored lipid.

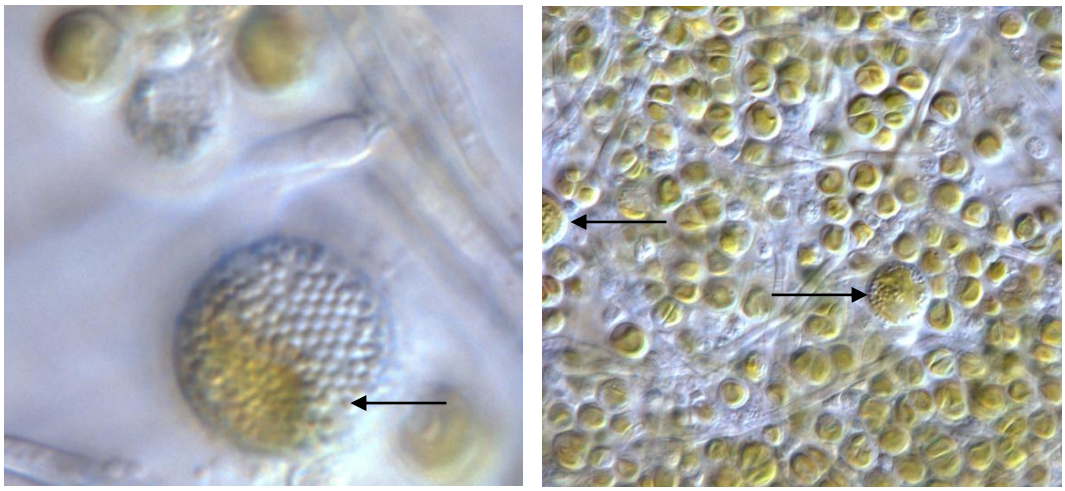

Figure 11: An extra-large cell (Left) of lab cultured *C. freiburgensis,* late in the growth cycle (approximately 12 µm in diameter), after nutrients have become depleted from the medium and cells have settled into flocs with fungal hyphae. The small (approx. 1 µm) colorless spheres are stored lipid droplets. The smaller cells are normal-sized (5 to 7 µm) non-motile cells within silica cysts. Under lower magnification (approximately 1000 X), of an algal/fungal floc (Right), two extra-large cells are visible (one whole cell at lower Right center and a partial one at far-Left center).

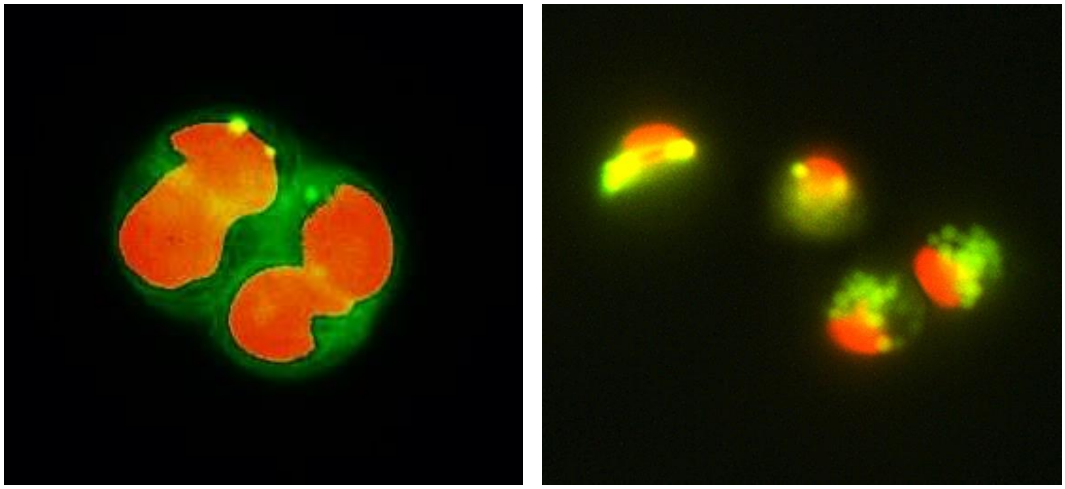

Figure 12: *C. freiburgensis* non-motile cells that have been treated with Nile Red stain and viewed with epifluorescence lighting and filters. The large, red objects are chloroplasts with chlorophyll autofluorescence. The small (1 µm) yellow-green spheres are lipid droplets. Left, a cluster of actively growing cells (each approximately 5 µm in diameter). Right, normally-sized cells (5 to 7 µm) that have stopped active growth and have begun to accumulate larger quantities of lipid, but also contain a visible quantity of chlorophyll in their chloroplasts.

C. freiburgensis from Berkeley Pit Lake appears to be the first extremely acid-tolerant chrysophyte examined as a potential biofuel feedstock. To thrive such an acidic environment, with high concentrations of toxic dissolved metals, where most organisms could not survive, requires unique survival strategies and biological chemical adaptations (Brake and Hasiotis, 2010). For example, diatoms found growing in water bodies impacted by acidic drainage from a mine in Portugal showed increased antioxidant enzyme activity, compared to those growing in a nearby water body without acid mine drainage (Luís et al., 2019). Some of these unique adaptations may prove to be useful in a biofuel candidate.

At this time, *C. freiburgensis* appears to be either the first, or one of very few, chrysophytes that have been examined for their potential as a biofuel crop, based on a search of published literature. A few microalgae which were previously counted among the Chrysophyceae, but after closer microscopic observation and genetic research, are now classified with other organisms, have been evaluated as potential biofuel sources. For example, *Isochrysis zhanjiangensis* and *I. galbana* have been examined as biofuel candidates and were once thought to be chrysophytes (Feng et al., 2011, Griffiths and Harrison, 2009, Fidalgo et al., 1998), however, they are no longer considered to be members of this class (Guiry and Guiry, 2018). *Poterioochromonas malhamensis* (Pringsheim) was also studied as a representative "chrysophyte" in a diverse algal community (Stockenreiter et al., 2012), but it is now classified in the Synurophyceae (Guiry and Guiry, 2019). Several diatoms, which have golden-brown pigments and are often rich in lipids, have been examined as potential biofuel sources. Diatoms currently belong to the Phylum Bacillariophyta, Class Bacillariophyceae, and the genus *Isochrysis* is in the Phylum Haptophyta and Class Coccolithophyceae. Two other genera that were listed as Chrysophyceae, *Boekelovia* sp., (Shamzi Mohamed, Wei, and Ariff, 2011) and

Poterioochromonas malhamensis Pringsheim, which was studied as a representative "chrysophyte" in a diverse algal community (Stockenreiter et al., 2012), are now considered to be members of the class, Synurophyceae (Guiry and Guiry, 2019). Green algae (Chlorophyceae) represent the largest number of microalgal species identified as potential sources of lipids for biofuels. It is more likely that they were selected because they are ubiquitous and relatively easy to isolate and grow, rather than their being more prolific lipid producers (Hu et al., 2008).

1.4.2. Potential for Reduced Costs Associated with Contamination

Outdoor or greenhouse ponds and raceways, with their relative technological simplicity, are generally considered to be more economical to construct and operate, but they are especially vulnerable to contamination by faster-growing, but undesired algal competitors, predators and pathogens. Outdoor ponds and greenhouses may also require, to an extent depending on the climate and locality, heating and artificial lighting. *C. freiburgensis* from Berkeley Pit Lake grows vigorously in pH 2.5 medium (to densities exceeding 30,000,000 cells/mL). The acidity of the medium provides a competitive advantage for *C. freiburgensis*, and a hostile environment for most other microalgae, heterotrophic protists and other organisms likely to cause culture contamination. The alga is most productive at a relatively low temperature, 10 ˚C (Dakel, 2001), and was observed to survive and grow in a wide range of indoor lighting conditions, indicating that it is likely to tolerate shade well. These adaptations make *C. freiburgensis* an excellent candidate for large, open systems. Losses due to contamination or problems with lighting would likely be infrequent, but a reliable cooling system would probably be necessary.

1.4.3. Potential for Use and Treatment of Acid Mine Drainage Water

Because *C. freiburgensis* is adapted to living in an acid mine drainage environment containing sulfuric acid and high concentrations of dissolved heavy metals, it would be worth investigating whether acidic mine or industrial wastewater could be used in a growth medium as a first step in wastewater treatment. Algae, like land plants, secrete carbohydrates into their environment, and these are an important source of organic carbon that supports the growth of fungi and bacteria. Many microorganisms that can use secreted algal carbohydrates to support growth can also remove dissolved heavy metals from solution and detoxify them (Pepper, Gerba and Gentry 2014). A biodiesel production operation that was able to utilize acidic wastewater could both conserve clean water and also provide a bioremediation service.

1.4.4. Potential for CO_2 Capture

If the Berkeley Pit Lake strain of *C. freiburgensis* is able to grow well with higher than average CO_2 concentrations, then it could be useful to retrieve carbon from flue gases emitted by power plants or industrial operations. Because it can grow vigorously in pH 2.5 medium, changes in pH due to fluctuations in CO_2 concentration may be tolerated well. It is often necessary to provide additional CO_2 to maintain high densities of microalgae in a bioreactor, and supplemental CO_2 can also support higher cell densities in covered ponds (Andersen, 2005).

1.5. Experiment to Investigate Biomass Productivity, Lipid Content and FAME Composition, in Response to Changes in Nutrient and CO_2 Concentrations

The purpose of the experiment was to investigate responses of *C. freiburgensis* to changes in the growing medium, including lowered nitrogen concentrations, lowered phosphorus concentrations, supplemental CO_2, and intermittent feeding of nitrogen, in comparison to a standard, nutrient-replete Modified Acid Medium. Specifically, the experiment sought to determine which changes would be most likely to result in responses by the alga that would improve its production of the lipids, especially triglycerides, that would yield a high proportion of the FAMEs most desirable for biodiesel, while maintaining adequate biomass production.

Important responses to changes to growing conditions would include changes in biomass production (dry weight), lipid production, and in changes in fatty acid methyl ester (FAME) composition, after transesterification of lipids. Changes in FAME composition that would increase the proportion of monounsaturated FAMEs, relative to saturated and polyunsaturated FAMEs would result in an improved mixture for biodiesel.

It was anticipated that *C. freiburgensis* could also increase numbers of extra-large cells or swimming cells, relative to normal, 5 to 7 µm, non-motile cells, in response to one or more of the experimental treatments. A notable change in the proportion of either of these cell types in one of the experimental treatments would point to ways that nutrient concentrations in the medium could be adjusted to induce greater proportions of extra-large, lipid-filled cells, or prevent mass conversion to swimming cells.

1.5.1. Medium Nitrogen Concentration

Experiments previously conducted by a Montana Tech student, demonstrated a decrease in lipid production in response to an increase in medium nitrogen concentration (Jonart, 2012). Conversely, previous experiments (Figure 13, Mosslander and Mohler Mitman, 2016), showed that lipid content in *C. freiburgensis* cells increased, with time, as biomass increased. It was postulated that the lipid increase was in response to depletion of nutrients in the medium, that had been consumed by the growing population of cells. In general, it has been established that microalgae begin to increase their lipid content, and slow their growth, in response to lowered concentrations of macronutrients, especially nitrogen and silicon (Zienkiewicz et al., 2016, Griffiths, van Hille and Harrison, 2012, Boyle et al., 2012, Breuer et al., 2012, Chen et al., 2011, Roessler, 1988). Therefore, it was predicted that lowering the concentration of nitrogen in the medium would result in lower biomass production, but that the lipid content in those cells would increase more rapidly than in cells that were started in medium with high concentrations of nitrogen.

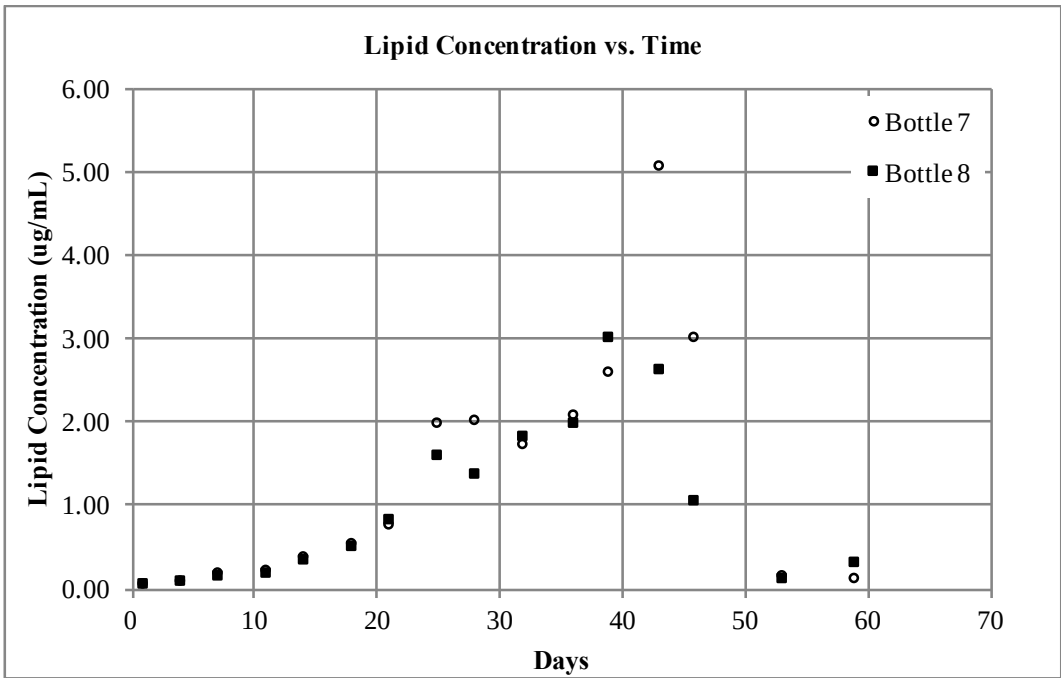

Figure 13: Increase in lipid content, with growing time, of *C. freiburgensis* cells grown in standard MAM at pH 2.5 (Moslander and Mohler Mitman, 2016) unpublished data.

1.5.2. Medium Phosphorus Concentration

Based on earlier observations of cultures started in medium with lower concentrations of phosphorus, it was anticipated that, most likely, the growth of *C. freiburgensis* would not be limited a great deal by reducing the phosphorus concentration in the medium to 10% of that in standard MAM. Also, Challagulla, Fabbro, and Nayar (2015) found that total lipid content in a green alga, *Rhopalosolen saccatus* Filarsky, did not change with reduced concentrations of phosphorus, but the relative concentrations of several fatty acids, including C16:1, increased.

1.5.3. Supplemental CO_2 vs. Ambient Air Only

In addition to comparing the alga's responses to adjustments in the concentrations of nitrogen and phosphorus in the medium, it was also of interest to determine how it would respond to a CO_2 concentration higher than that from ambient air. If the response was positive,

for example, improved growth or lipid production, or neutral (no negative impact on growth) then *C. freiburgensis* could also have potential as an alga that could be employed to retrieve and utilize CO_2 from flue gases or other industrial sources.

1.5.4. Timing of Harvest Relative to Growth Stage

Harvest timing was also an important factor to investigate, because *C. freiburgensis* cells were not expected to begin increasing quantities of storage lipids until after the end of the exponential growth phase. The alga was not expected to substantially increase its lipid content until net growth stopped or slowed considerably. The length of time that exponential growth would continue was anticipated to differ, depending on the treatment. In particular, it was expected that it would stop earlier in the treatments with lowered concentrations of nitrogen. It was expected that the transition from exponential to stationary growth, or a period of linear growth, would occur when one of the macronutrients in the medium would begin to become depleted, and it was not known when the alga would detect and respond to depletion of medium nutrients.

1.6. Suitability of *C. freiburgensis* as a Source of Lipids for Biodiesel

1.6.1. *Lipid Content*

To discover whether *C. freiburgensis* could be cultivated successfully for biodiesel production, it is necessary to determine whether it can produce adequate quantities of lipids for the purpose. Since most cultivated microalgae will increase lipid production when they enter the stationary growth phase, in response to the concentrations of one or more nutrients becoming

depleted, it is necessary to ascertain the proportions of nutrients that will result in adequate growth (biomass production) with high lipid content.

1.6.2. Fatty Acid Composition of Algal Lipids for FAME Composition of Biodiesel Product

According to Pinzi et al., (2009), biodiesel should be made from inedible oils, for the reasons previously discussed, but it must also contain a mixture of fatty acids that result in a high-quality fuel that provides reliable engine performance, and can be stored and used over a range of environmental temperatures. The authors recommend as an ideal composition, "a high presence of monounsaturated fatty acids (as oleic and palmitoleic acids), reduced presence of polyunsaturated acids, and controlled saturated acids". The authors point out that a high-quality biodiesel composition should ideally contain a large proportion of C18:1 and (or) C16:1 FAMEs. It should have lower proportions of polyunsaturated FAMEs for oxidative stability, and also lower proportions of saturated FAMEs, for cold weather performance.

It is expected that reducing the concentration of nutrients, specifically nitrogen and phosphorus, in the medium would result in a more rapid onset of lipid production; however, the composition of the lipids, for the purpose of manufacturing a high-quality fuel product, which would require few modifications, is also quite important. High proportions of long chains of saturated fatty acids in a fuel would be expected to lead to poor performance in cold weather, as the fuel would more readily begin to solidify. A high proportion of polyunsaturated fatty acids (PUFAs) would reduce oxidative stability, and could possibly require more additives to prevent oxidation in the fuel, however, these could also be marketed as a valuable side product. For example, algal PUFAs are needed in aquaculture feed, as they are essential dietary components for the growth of fish larvae, shrimp and mollusks (Fidalgo et al., 1998). Fidalgo et al., also

found that neutral lipid proportions in *Isochrysis galbana* increased in the late stationary growth phase along with a decrease in phospholipids. The proportion of PUFAs were found to be highest during the early part of the stationary phase. Based on the results of Fidalgo et al. and others, along with preliminary observations of *C. freiburgensis*, a high quantity and quality of fatty acids was expected to be found in the low nitrogen treatments, during the stationary phase of growth, possibly during the late part of the stationary phase.

2. Methods

2.1. Preparation of Materials and Culture Methods

2.1.1. Preparation of Glassware, Materials and Equipment

All containers and stoppers used for algal culture were soaked for a minimum of 24 hours in a mild sulfuric acid solution (1 to 2% by volume) to loosen mineral and other residues, scrubbed with warm tap water, and rinsed five times with deionized or distilled water. All tubing, stoppers and connectors that were new were treated the same, except for the sulfuric acid soak. The components of the culture system, except for plastic tubing connectors, were also autoclaved for 30 minutes at 15 psi (100 kPa) and 121°C, prior to use. Some plastic tubing connectors could not be autoclaved. In order to minimize potential sources of contamination from these parts, they were cleaned as described and then immersed, for 5-10 minutes, in hot (95 to 105 ˚C), boiled, deionized water immediately prior to use.

Glassware that was not used for algal culture was washed with detergent and it was not soaked in mild H_2SO_4 solution. Containers used for lipid detection by Nile Red fluorescence spectrometry and for transesterification in preparation for GC/MS analysis were washed between uses with warm water and dish detergent, thoroughly rinsed with warm water, and rinsed for a minimum of five times with deionized or distilled water. After washing and rinsing, they were allowed to air dry at room temperature. Between uses, the quartz glass cuvette used for fluorescence spectrometry was cleaned with acetone, rinsed with warm tap water and deionized water, and patted dry with a delicate, lint-free tissue (Kimwipes, Kimberly-Clark).

2.1.2. Observation Methods

The majority of observations and all cell counts were conducted under light microscopy using a Nikon Eclipse E800, which was equipped with differential interference contrast, mercury lamp epifluorescence and filters including an 61002 DAPI/FITC/Texas Red Triple Filter, an excitation filter and an emission filter. Changes in cell density, type and behavior were noted, including interactions among *C. freiburgensis* cells and, later in the growth cycle, with fungal hyphae.

Cells were stained with Nile Red for epifluorescence observation by adding 40µL of Nile Red stock solution to one mL of culture medium containing live cells. This was mixed for one minute using a Vortex mixer, and spun for a few seconds in a microcentrifuge tube to concentrate the cells. A drop of medium containing the stained cells was placed on a standard glass slide and observed with oil immersion, using the Nikon Eclipse E800 with epifluorescence lighting and filters. A Q-Imaging Micropublisher 3.3 RTV digital camera and Image-Pro Plus 7.0.0.591 (Media Cybernetics, 2009) software were used for microphotography.

In addition to light microscopy, Dr. Bill Granath and Dr. Jim Driver at University of Montana Emtrix Electron Microscopy Facility, contributed scanning electron micrographs which allowed for the observation of some of the external features of the non-motile, cyst-type cells (Figures 43 – 44, In “Results”).

2.1.3. Culture System and Laboratory Growing Conditions

All batch cultures were maintained in one-liter or eight-liter glass aspirator bottles under controlled temperature and lighting within a Percival Scientific culture chamber (Model IR-89). The chamber was equipped with daylight balanced cool white fluorescent lighting, providing a

light intensity of approximately 100µmol per m^2 per second. The light source was set for a cycle of 16 hours of light alternating with 8 hours of darkness per day. The temperature was maintained at a steady 10 °C for 24 hours per day. Backup cultures were stored, in the same culture chamber, in 60 mL plastic centrifuge tubes with loosely threaded caps to allow gas exchange.

2.1.4. Modified Acid Medium (MAM)

Modified Acid Medium (Canadian Phycological Culture Centre, CPCC, 2015, Olaveson and Stokes, 1989), was selected because *C. freiburgensis* had been growing well in the medium, and the low pH deterred the growth of competing organisms. The pH was adjusted with sulfuric acid, for all of the batch cultures. This was done by adding concentrated sulfuric acid (H_2SO_4) to deionized water to make a 10% solution (by volume). Small amounts of 10% sulfuric acid (in drops or one milliliter portions depending on the volume of medium) were added to each container of medium while it was stirred using a magnetic stirrer. A Cole Parmer pHWand handheld pH meter with an Oakton (WD-35804-08) electrode was calibrated immediately before each use, with pH 7.00 and pH 4.01 reference buffers (Cole Parmer). The pH electrode was placed in the medium and the pH was monitored while H_2SO_4 was slowly added, until it became stable at 2.5 (± approximately 0.05).

A standard MAM composition (CPCC, 2015), containing high concentrations of nitrogen and phosphorus (enough to maintain growth beyond 40 days), was chosen to represent the "control" condition. Standard MAM does not contain a source of silicon, though it is also a limiting nutrient for Chrysophytes. No source of silicon was added to any of the six experimental treatments. Silicates are ubiquitous in the environment in dust, on container

surfaces and as impurities in other medium ingredients, and therefore not easily excluded from culture medium (Werner, 1977), and *C. freiburgensis* had previously been cultured successfully (with densities exceeding 30,000,000 cells/mL) without this addition.

2.1.5. Re-isolation of *C. freiburgensis* from a Dormant Berkeley Pit Lake Algal Culture

Modified Acid Medium (MAM, Table VIII) was prepared and adjusted to three low pH versions, pH 2.8, 2.5, and 2.4. Two 15 mL plastic centrifuge tubes were filled with each medium and loosely capped. A one-liter aspirator bottle that had been used by students five months earlier (on 4/23/2015) to culture Berkeley Pit Lake algae, and had not yet been cleaned, was retrieved from a storage room. The bottle contained some remaining liquid medium and a thin, dark-colored biofilm on the glass interior near the top of the bottle. A few small scrapings (0.5 to 2 mm^2) of this biofilm was transferred to each tube. These were placed in the culture chamber and observed. After 20 days, vigorous growth was observed in all six tubes. The cells growing in the tubes were observed microscopically, and they were identified as *C. freiburgensis*. It appeared to be the only algal species growing in all six tubes (Figure 14). The visible characteristics of the cells growing in each tube were observed and recorded.

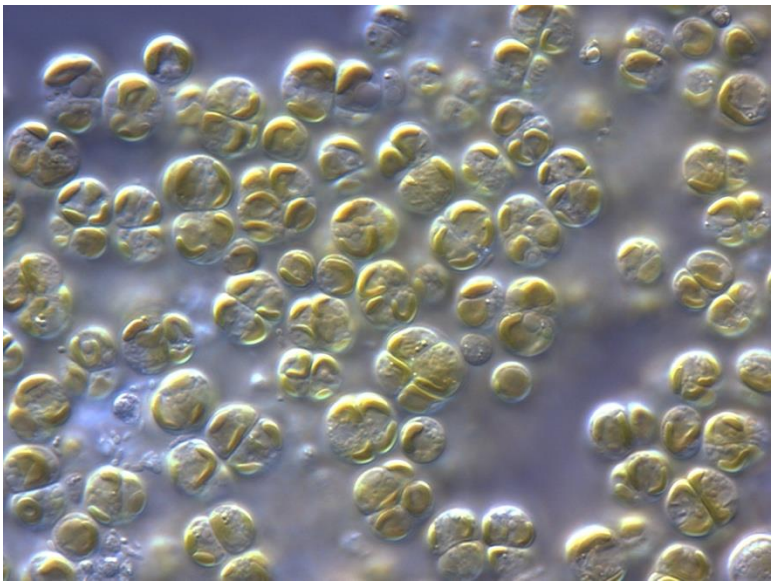

Figure 14: *C. freiburgensis* from Berkeley Pit Lake growing as a biofilm on glass, in MAM at pH 2.5. Each normally-sized cell measures 5 to 7 µm, and contains a single, large, gold-colored, more or less bowl-shaped chloroplast. Many clusters of cells are visibly growing, by the process of mitotic division, with two to four (or more) cells that have not yet completely separated from one another.

2.1.6. Trial Run Cultures for Stock and Selection of Growing Conditions

Two one-liter aspirator bottles were prepared with MAM, Bottle No. 1 with pH 2.5 and Bottle No. 2 with pH 2.4 medium. Because growth in the pH 2.5 medium appeared to be somewhat more vigorous than in the pH 2.4 medium, cells from the former were chosen to inoculate a set of one-liter cultures (Figure 15). Suspended cells in these cultures were counted at intervals of two to 16 days, and samples from these cultures were used to test and make adjustments to a Nile Red fluorescence method for lipid detection and quantification (Kelly, 2013, Alonzo and Mayzaud, 1999) that had been developed with another algal species earlier. After the first set of cultures, subsequent pairs of one-liter cultures were maintained in standard MAM, at pH 2.5, to provide samples and starter culture cells as needed.

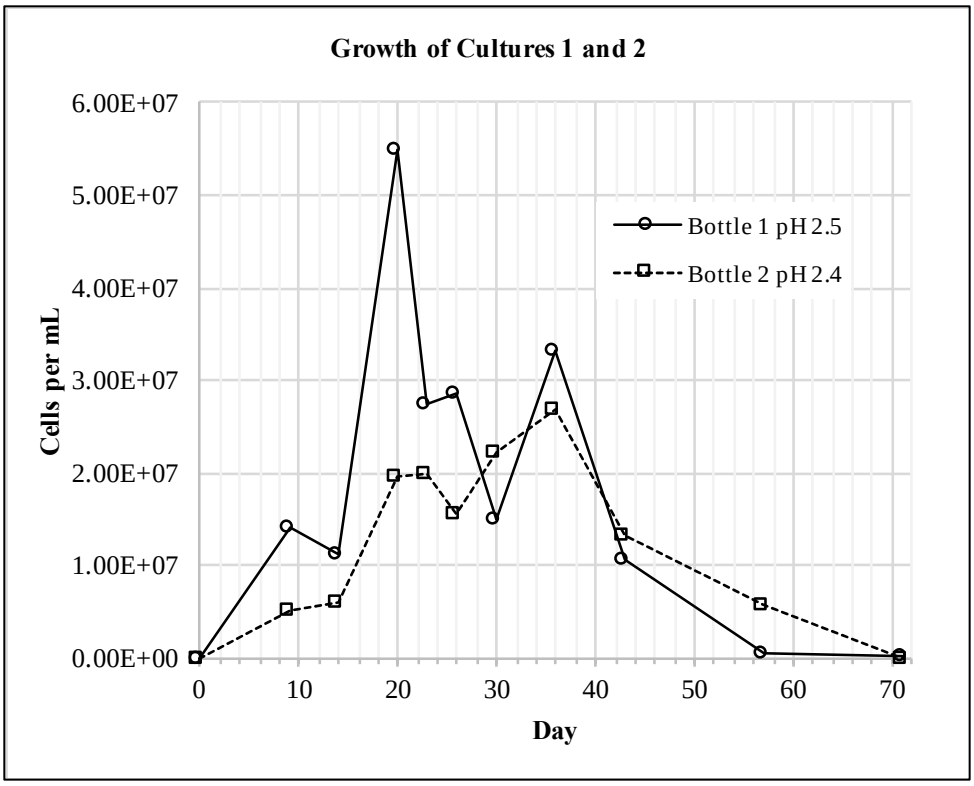

Figure 15: Initial one-liter cultures. Cell counts for the first two cultures should be considered to be estimates, due to a relatively high margin of error (possibly ± 35%). Suspended cell counts were made using an older, damaged counting chamber that was found not to hold a consistent volume, and later replaced with an accurate one. In addition, the volume of air circulating through the medium fluctuated, which may have contributing to sampling error.

2.1.7. Preliminary Test to Observe Responses to Lower Nutrient Concentrations

Prior to starting eight-liter cultures, the alga's response to nutrient adjustments was first tested by starting two one-liter culture bottles with lower concentrations of nitrogen and phosphorus: one with 10% of the nitrogen source in standard MAM and one with 10% of the phosphorus source. Regular cell counts were made to monitor growth over a period of 46 days. A comparison was made to the average counts over the same period of cultures in two one-liter bottles growing in standard MAM (Figure 16). It was determined that growth with 10% of the standard nitrogen and phosphorus sources would be adequate to produce enough biomass for the intended transesterification and GC-MS analysis.

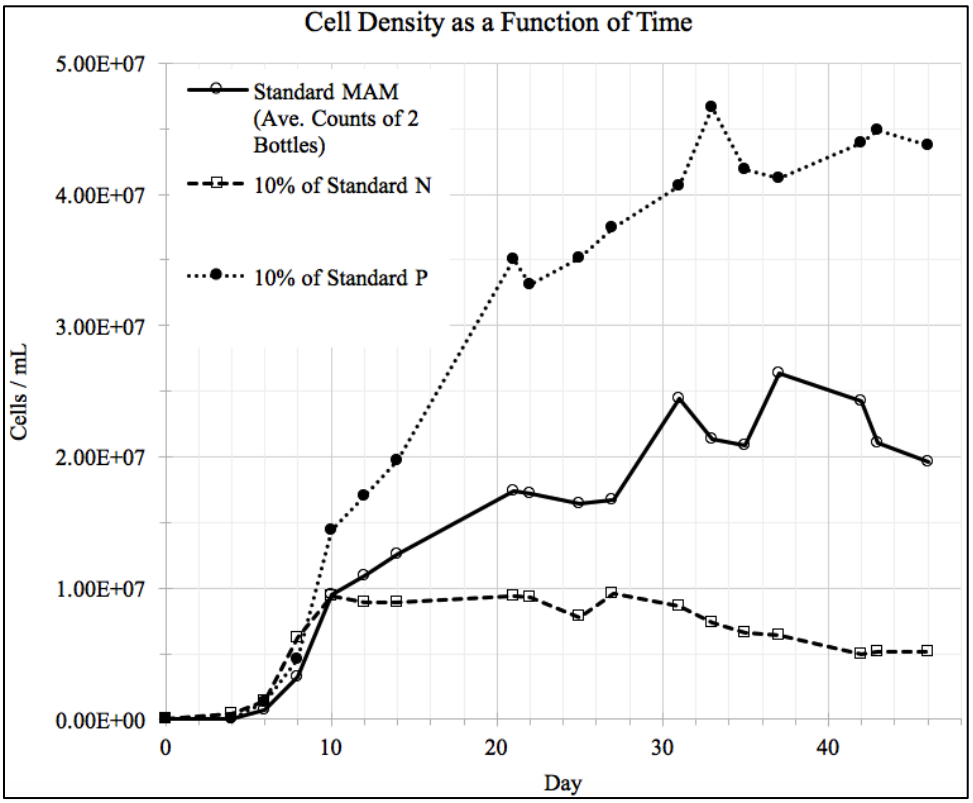

Figure 16: A preliminary test to observe growth with decreased nitrogen and decreased phosphorus compared to growth with standard MAM (all three at pH 2.5). After ten days, all three cultures transitioned out of exponential growth. Cells growing in low-nitrogen MAM (10% of standard concentration), immediately entered the static phase (cell density remained steady at approximately 9.45 x10^6 cells/mL). Cell numbers in low-phosphorus MAM (10% of standard concentration), continued to increase to high densities (4.66 x 10^7 cells/mL). Cells growing in standard, high-nutrient medium showed an intermediate pattern. Both of the high-nitrogen cultures prolonged linear growth in the transitional phase and delayed entering the static phase for 15 to 20 days. Counting error is estimated to be approximately ± 5%.

2.1.8. Monitoring Growth

2.1.8.1. Cell Counting Method

Growth was monitored by recording changes in suspended cell density during regular cell counts. A Hausser Bright-Line Hemacytometer with a Neubauer ruling was chosen (to replace the less accurate counting chamber) to count live non-motile cells. Each Hausser Bright-Line Hemacytometer contains two ruled surface plateaus, 0.1 mm below the cover slip, which hold a fixed volume of liquid (10 µL, each). The center 1 mm square is divided into 25 0.20 mm

squares (each further divided into 16 0.05 mm squares) (Figure 17, Neubauer ruling, and Figure 18, cells on its grid). If the number of cells per central 1 mm square was approximately 100 (or fewer), the entire central square was counted. If the count per 1 mm square clearly exceeded 100 cells, a systematically selected subsample of five of the 25 central squares was counted (four corners and the center). For each cell count, an average of the counts from the two etched grids on the hemacytometer was designated to represent the final count. The volume of liquid over one square mm grid is 0.1 mm^3. The count for one 1 mm^2 was multiplied by 10,000 to determine the number of cells per mL (or by 50,000 for a subsample of $1/5^{th}$ of the volume).

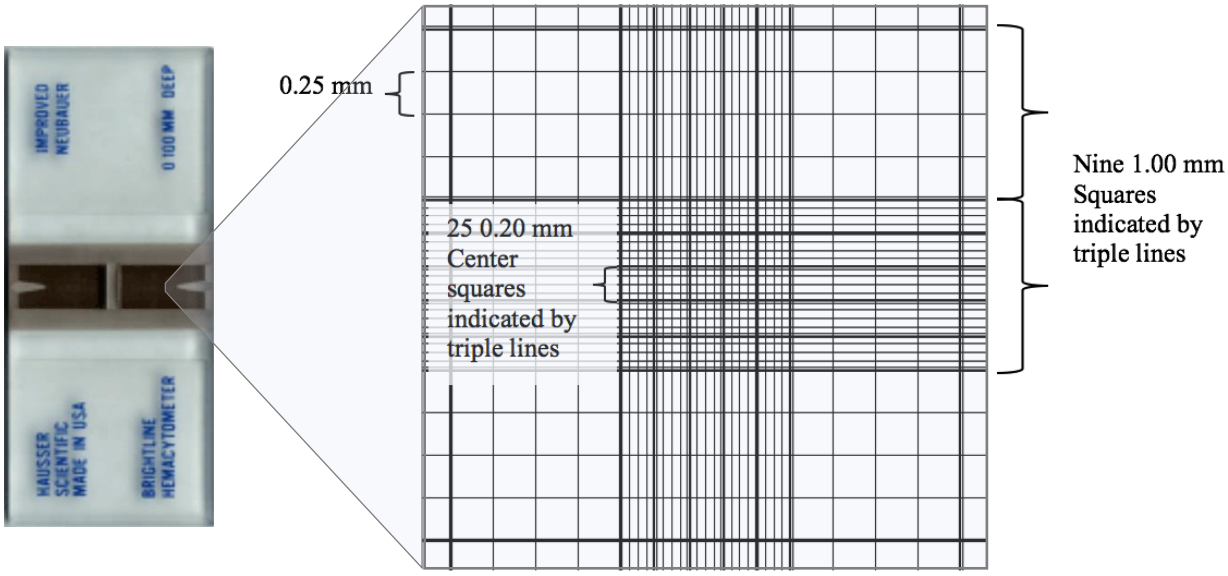

Figure 17: Features of the Neubauer Ruling of a Hausser Hemacytometer, a specialized etched glass microscope slide (counting chamber) that is designed to count blood cells. The smallest squares in the center grid measure 0.05 mm^2.

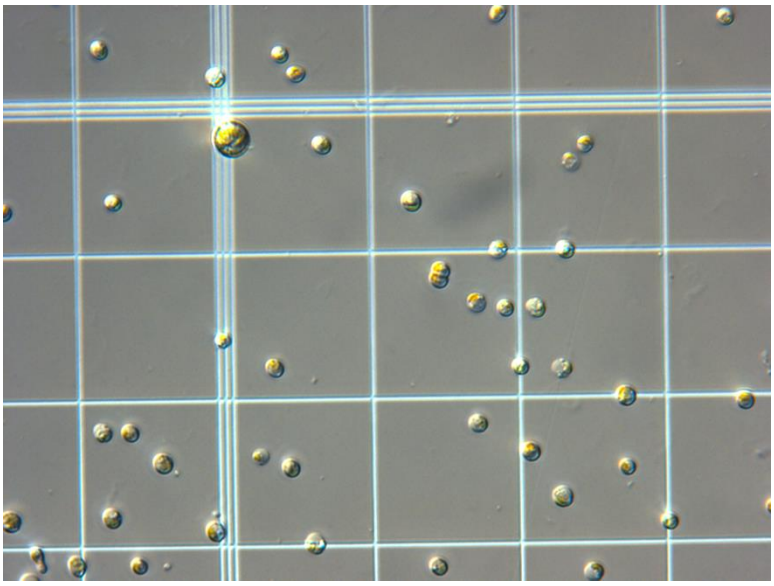

Figure 18: *C. freiburgensis* non-motile cells in the Hausser counting chamber with Neubauer ruling. The etched triple line denotes the boundary of one 0.20 mm^2 square. The single lines indicate the boundary of 0.05 mm squares. One extra-large cell (12 µm) can be seen in the upper left corner, the others are normal size (5 to 7 µm).

With the counting chamber method, errors in cell counts can sometimes be above 30 percent (Celeromics, 2015), unless steps are taken to minimize them. Methods that were described by Stein (1979), Madigan et al. (2015) and recommended by Bastidas (2015) and Rouge (2002), for obtaining the most accurate counts with a ruled hemacytometer, were followed to reduce counting and sampling error. The actual error in cell counts was estimated to be close to 5%. To estimate counting error, the average and standard deviation were determined from three repeated counts of the same sample (averaging 336 cells/1 mm^2 grid). The standard deviation was ± 0.8% of the mean final count (± 132,288 cells out of 16,800,000 cells). To estimate sampling error, two sets of three samples from the same two cultures were counted (averaging 132 and 838 cells/grid). The standard deviations of these sample sets were ± 2.5% and 5.8% of the mean final counts. Sampling and counting error due to cell aggregation was not

estimated, but was expected to increase as densities approached 20,000,000 cells/mL (after day 20 in standard MAM), with increased density, aggregation size and flocculation of cells.

Swimming cells and dead cells were not counted. Cells that had shattered or missing a visible chloroplast were assumed to be dead. Whole cells with an intact chloroplast were assumed to be live. Swimming cells were not counted due to their rapid movement between squares, and because they became trapped at the edges of the counting plateau, where they were not clearly visible, therefore it was determined that a different method would be necessary to accurately count them. However, the approximate percentage of swimming cells, relative to non-motile calls, was noted. Cells in the process of division were counted as two (or more), if each contained a chloroplast and the wall forming between them had become clearly visible.

2.1.8.2. Methods of Determining Growth Rates and Phase of Growth Cycle

To determine an expected growth rate under standard conditions, initial growth rates were determined by observing algal growth in one pair of one-liter culture bottles under previously determined standard conditions (standard MAM adjusted with sulfuric acid to pH 2.5, at 10 °C, illuminated by daylight balanced cool white fluorescent lighting for 16 hours of light, and an 8-hour dark period per day). Cell counts were made daily, for one 60-day period (from January 21st to March 21st, 2016), (Figure 19). A pattern was observed that included an extended period of linear growth, after exponential growth had slowed, during the transition to the stationary growth phase (Figure 20). The same conditions on a larger (8 liter) scale were later selected to represent the nutrient-replete “control” (treatment No. 1) to compare the effects of six different experimental treatments.

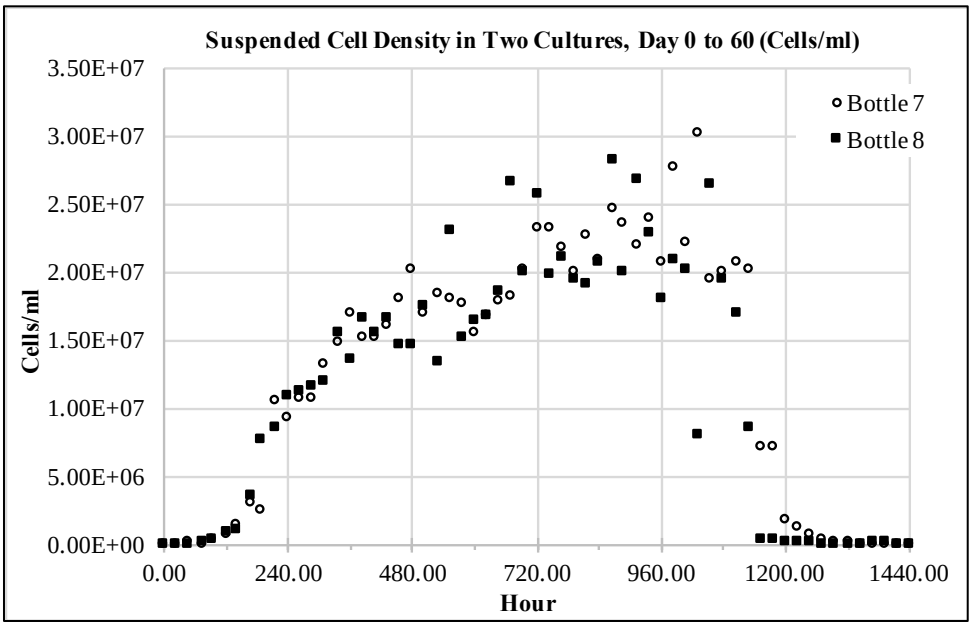

Figure 19: Cell density was monitored daily for 60 days in two one-liter cultures in pH 2.5, standard MAM.

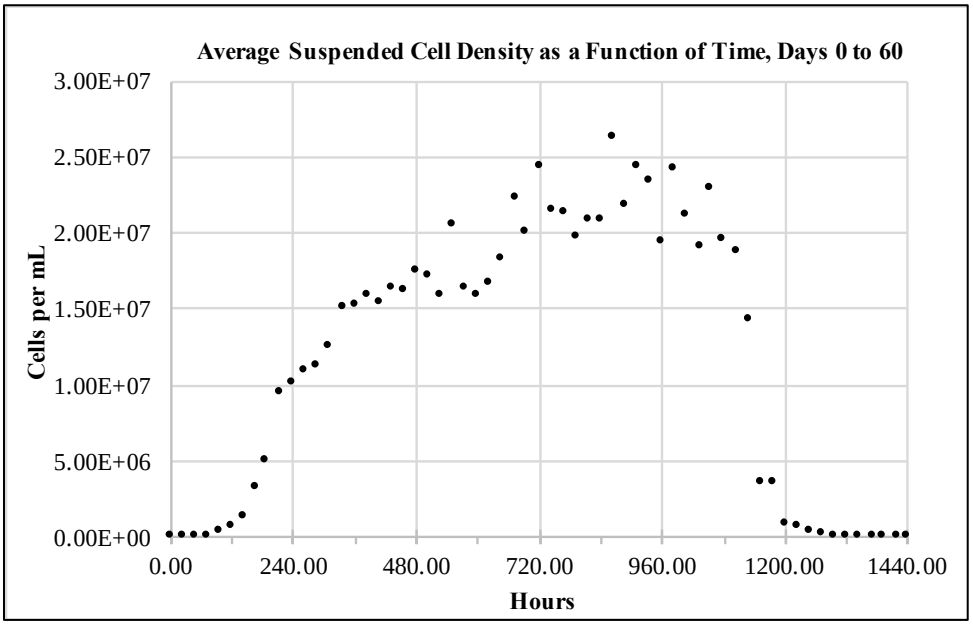

Figure 20: The average of daily cell counts from two one-liter *C. freiburgensis* cultures grown in regular, standard MAM at pH 2.5, illustrates a typical growth pattern for a batch culture, except for the transitional growth phase. The period of linear growth at the transition from exponential (log) growth and stationary growth, is relatively long, lasting approximately 25 days (600 hours).

Growth rates during the exponential growth period were calculated by the method of Wood, Everroad, and Wingard (2005), to determine the growth rate constant (r), doublings per day (k) and doubling time (T_2) (Table V).

The exponential growth period was determined by plotting the log of suspended cell density versus time (Microsoft Excel, version 15.33, 2017), so that the exponential increase appears as a straight line (Figure 21 and 22). The same method was used for subsequent exponential growth rate calculations.

Table V: Definitions of terms for calculating growth rates.

Exponential Growth Definitions:

r = proportional rate of change (during exponential growth)
"specific growth rate"
r = growth constant = K_e

Exponential Growth Relationship:

$dn/dt = rN$ **(1)**

$dN/dt = K_eN$ **(2)**

$N_t = N_0e^{rt}$ **(3)**

$r = \ln (N_t /N_0)/\mathbf{\Delta}t$ **(4)**

$r = (\ln N_t - \ln N_0)/\mathbf{\Delta}t$ **(5)**

N_0 = Population size at start of interval
N_t = Population size at end of interval

$\mathbf{\Delta}t = t_t - t_0$ **(6)**

t_0 = time at start of interval
t_t = time at end of interval

k = doublings per day

$k = r/\ln 2$ **(7)**

$k = r/0.6931$ **(8)**

$k = \text{Log}(2) (Nt/N0))\mathbf{\Delta}t$ **(9)**

T_2 = population doubling time

$T_2 = \ln 2/r$ **(10)**

$T_2 = 0.6931/r$ **(11)**

r = proportional rate of change
Equivalent to the growth equation: $r = \mu - m$, when $m = 0$
μ = specific population growth rate
m = mortality

Linear Growth Definitions:

Linear Change = $(N_t - N_0)/\mathbf{\Delta}t$ **(12)**

Linear Change = $(\mathbf{\Delta}N)/\mathbf{\Delta}t$ **(13)**

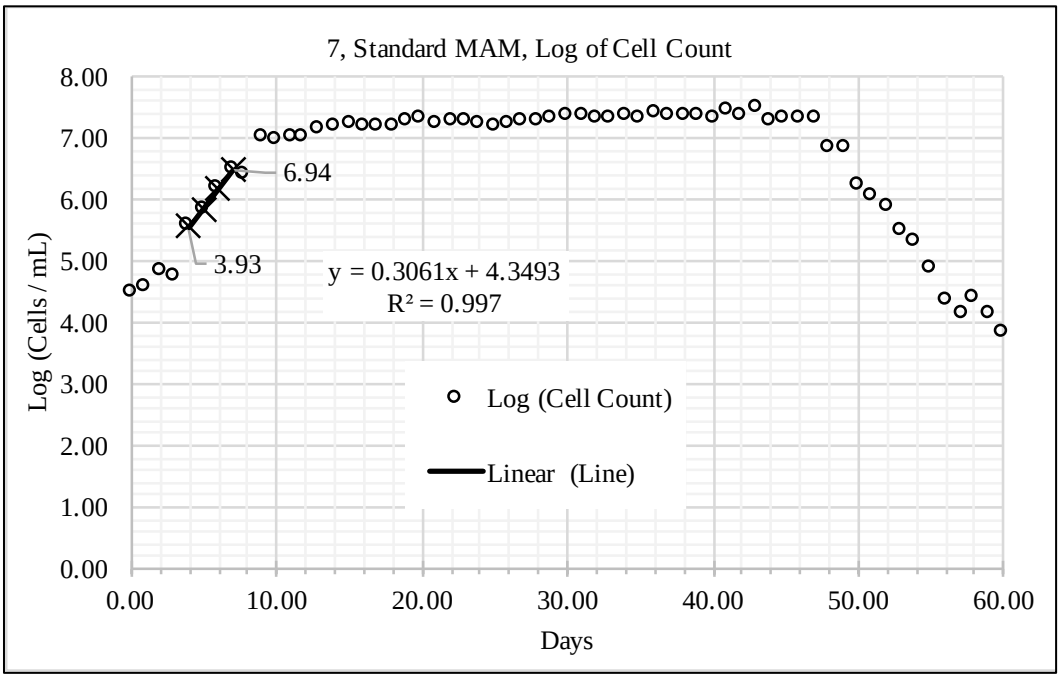

Figure 21: Determination of growth rates during exponential growth by plotting the log of the cell density versus time. Exponential growth appears as a straight line relationship.

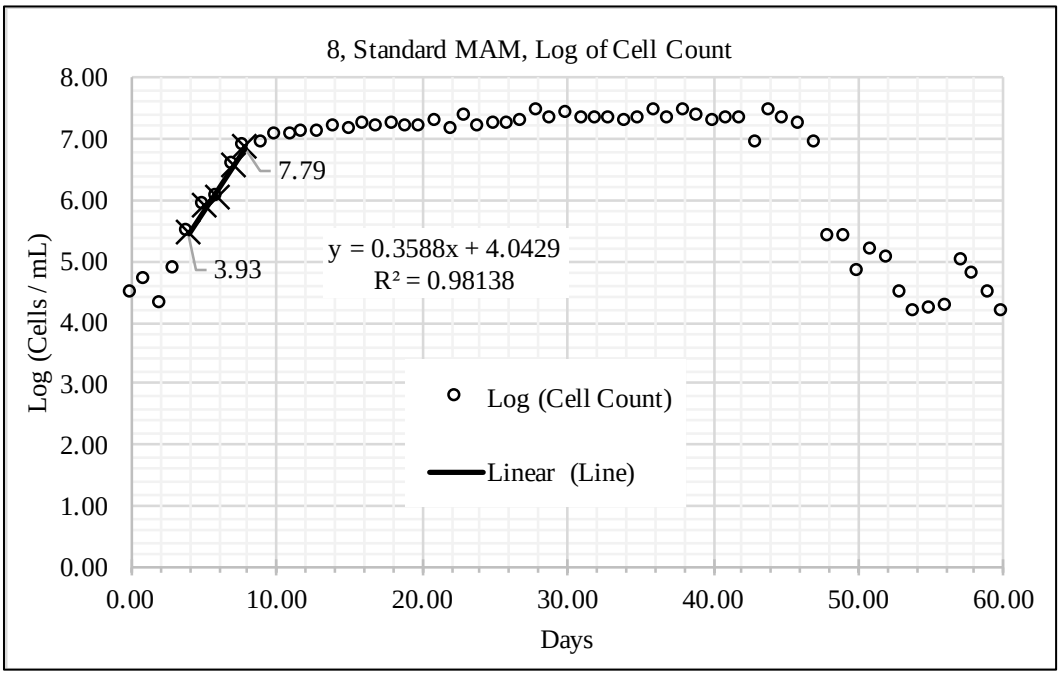

Figure 22: Determination of growth rates during exponential growth by plotting the log of the cell density versus time.

Linear growth was calculated from the change in cell density between two points within the linear (transitional) growth period. The period of linear growth was identified by plotting the suspended cell density versus time, and choosing the series of points that best fit a linear trend line. The stationary growth phase was identified by the appearance of a horizontal line (zero slope) relationship between suspended cell density and time in the same plot. The crash (death) phase of the growth cycle could not be determined with a high level of accuracy, due to the continuation of growth after cells had flocculated or adhered to the sides of the culture container, however it was hypothesized to begin within a few days of the point at which suspended cell counts began to exhibit a decreasing trend.

Multiple pairs of dividing cells and small clusters of dividing cells were considered to be evidence of ongoing growth (Figure 23). Evidence of the cessation of growth was observed microscopically when pairs of dividing cells became scarce and was an indicator, in addition to a static cell count, of the culture entering stationary growth phase. Flocculation and settling also result in stationary or decreasing counts of suspended cells and can be a source of counting error. Evidence of cell death was apparent when shattered cells, fragments and numerous empty silica cysts could be observed in samples (Figure 24). Empty cysts could also result from conversion from non-motile to swimming cells, but their appearance in high numbers, along with cell fragments and without visible swimming cells, is consistent with the cells having died.

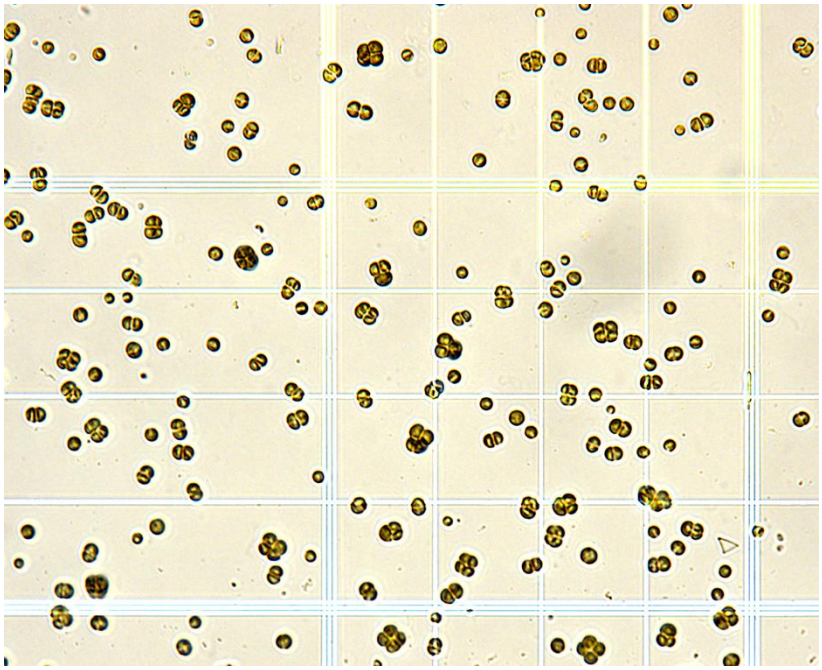

Figure 23: *C. freiburgensis* non-motile cells on a Hausser hemacytometer counting grid, that have reached a high density (approaching 30,000,000 cells/mL). Numerous pairs of dividing cells and small clusters (3 to 6 cells) indicate that the alga is actively growing. The square outlined by a triple etched line measures 0.20 mm^2 and is further divided into 16 0.05 mm^2 squares.

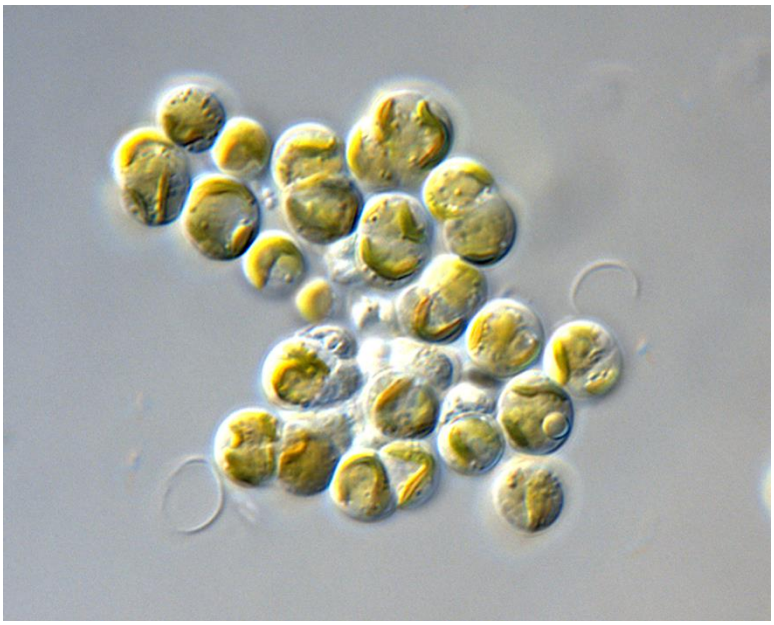

Figure 24: Empty silica cysts (at lower left and middle right of cell cluster above) may result from cell death or from conversion of non-motile cells to the swimming form, which exits the cyst through its pore (stoma). They can be one indicator of increasing cell mortality, if there is other evidence as well, such as cells that appear to be breaking down or have no chloroplast, and there are no swimming cells present. Most of the live, whole cells (pictured above) appear to be in a healthy state.

2.1.9. Batch Culture Method, Simple Bioreactor

Experimental and stock batch cultures were maintained in glass aspirator bottles of two volume sizes, one-liter and eight-liter, in a simple photobioreactor assembly (Figures 25 and 26). The one-liter volume was chosen for preliminary tests and observations, and to maintain stock cultures. The eight-liter volume was chosen for the experimental treatment cultures, in order to collect a greater number of relatively large samples without reducing the culture volume to the point that would be likely to affect circulation and growth. Ambient air was pumped through a hydrophobic 0.2 µm (Gelman) inline air filter into autoclaved deionized water inside a glass aspirator bottle, through a glass pipette, upstream of each culture container, in order to increase humidity and prevent loss of medium volume by evaporation. The humidified air was directed to each culture container through a port located at its base, circulating the medium in the culture container, evenly exposing algal cells to light, and keeping them in suspension. Exhaust air was released through another 0.2 µm inline air filter mounted in the stopper of each culture bottle. Culture medium was not replenished, except in treatment No. 6. A supplemental carbon dioxide delivery method was assembled for treatment No. 5 (Figure 27).

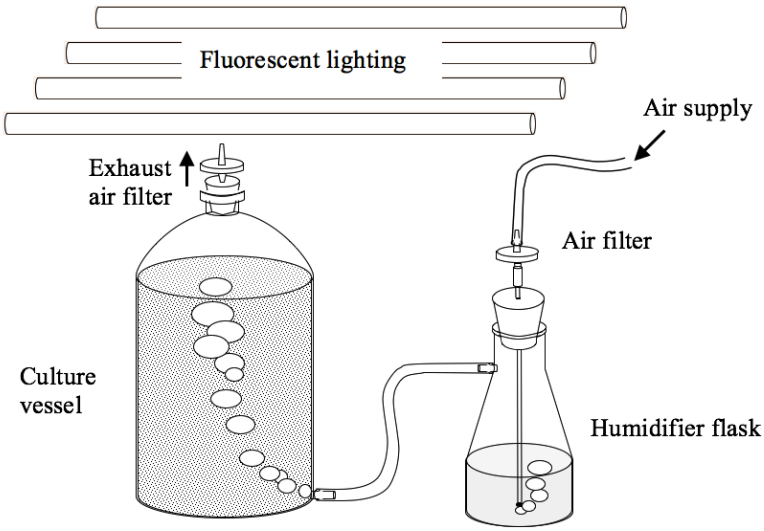

Figure 25: Simplified indoor photobioreactor assembly, using an eight-liter aspirator bottle, attached to an air supply, routed through autoclaved deionized water as a humidity source, for experimental cultures.

Figure 26: Simplified photobioreactor assembly for six experimental treatments in 8-liter bottles (Right center) and one stock culture (lower Right in 1-liter bottle). Each bottle receives air from a humidifier flask (behind bottles), which is connected to a common air supply. CO_2 (lower Left), passes through a regulator into a box (depicted in Figure 28) containing an air pump. From the box, CO_2 flows through two small flowmeters, anti-siphon devices and an inline air filter, into the humidifier flask for treatment No. 5, where it mixes with air (which is likewise monitored and regulated at a third flow meter) before entering the culture bottle.

2.1.10. Source of Starter Cells for Inoculation

Each experimental culture vessel was inoculated with 16 mL of growing cells, in standard, pH 2.5 MAM, from the same fourteen-day-old culture, which had reached a suspended cell density of 1.35 x 10^7 cells/mL. The starter culture had recently transitioned from exponential to linear growth.

2.1.11. Six Experimental Treatments

Six experimental treatments were chosen to compare total lipid content and fatty acid methyl ester quantities and composition. All six treatments were grown under the same temperature and lighting conditions, in pH 2.5 medium, based on Modified Acid Medium (CPCC, 2015). The nutrient levels were adjusted in five of the six treatments, providing less nitrogen, less phosphorus, or lower concentrations of both nutrients than in the standard medium (Table VI). One treatment (No. 5) combined lower nutrients with supplemental carbon dioxide (CO_2). The purpose of the six chosen treatments was to determine which strategy would provide the maximum lipid yield, and which would result in the most optimal composition of fatty acid methyl esters (FAMEs). The purpose of examining samples collected at various times during the growth cycle was to determine optimal harvest timing for maximum yield of biomass, lipid content, and FAME composition.

The six experimental treatments varied only by concentrations of nitrogen and phosphorus in the medium (Table VII and Table VIII), except that one treatment No. 5 was also supplied with a modest volume of carbon dioxide in addition to the concentration in ambient air. Each treatment was a single batch without replication, but all six were run concurrently. All six experimental batch cultures were started in eight-liter glass aspirator bottles, which were topped

with filters to allow ventilation but prevent contamination, and all were supplied with approximately 3.0 - 3.5 liters per minute (LPM) of humidified ambient air, which was bubbled through the medium from the base of the bottle. This volume of air provided adequate circulation in each bottle to keep algal cells in suspension and prevent them from adhering to surfaces, settling, and forming clumps that would cause shading. The air supplied to each culture vessel was humidified by first passing it through autoclaved deionized water in a two-liter glass aspirator flask placed upstream of the culture vessel. The water in this flask was replenished as it evaporated, and this step prevented any observable loss of volume, due to evaporation of water from the medium, in the culture vessel during the growth period. The first treatment was regarded as a "control" and the culture vessel was filled with eight liters of standard, pH 2.5 MAM. The second contained MAM with a lowered concentration of nitrogen, the third contained MAM with decreased phosphorus, the fourth and fifth treatments contained MAM with the concentrations of both nitrogen and phosphorus decreased. The fifth treatment received a small volume of supplemental carbon dioxide. The sixth treatment contained decreased concentrations of nitrogen and phosphorus, but small portions of nitrogen were added at regular intervals. All six treatments received (as much as possible) 16 hours per day of the same intensity of light (approximately 100 µmol per m^2 per second) and was kept at a constant 10 ˚C (± 1 ˚C).

Table VI: Plan for experimental treatments, in six eight-liter batch cultures. Changes are indicated by shaded squares. The nutrient source concentrations represent the concentrations at the start of the growth period (day 0). *Treatment 6 (intermittent N feeding) requires 2.7 to 4 mL of $(NH_4)_2SO_4$ stock solution to be added at four-day intervals until the total mg of $(NH_4)_2SO_4$ added reaches approximately 50% of that in standard MAM (250 mg).

Treatments	Nitrogen Source $(NH_4)_2SO_4$	Phosphorus Source KH_2PO_4	CO_2 relative to ambient air
1. Control	100% (500 mg/L)	100% (300 mg/L)	100% (no change)
2. Low N	10% (50 mg/L)	100% (300 mg/L)	100% (no change)
3. Low P	100% (500 mg/L)	10% (30 mg/L)	100% (no change)
4. Low N & Low P	10% (50 mg/L)	10% (30 mg/L)	100% (no change)
5. Low N & Low P	10% (50 mg/L)	10% (30 mg/L)	≤ 105% (increase)
6. Intermittent N Feeding*	5% (25 mg/L)	10% (30 mg/L)	100% (no change)

Table VII: Medium concentrations of three macronutrients at the start (day 0), for six experimental treatments.

Treat-ment No.	Medium	Nitrogen (N) (g/L)	Nitrogen (N) (mg/L)	Phosphorus (P) (g/L)	Phosphorus (P) (mg/L)	Potassium (K) (g/L)	Potassium (K) (mg/L)
1	**Standard MAM (100% of N & P)**	0.1076	107.64	0.0683	68.28	0.0862	86.19
1	**Low N (10%)**	0.0108	10.76	0.0683	68.28	0.0862	86.19
3	**Low P (10%)**	0.1076	107.64	0.0068	6.83	0.0862	86.16
4 & 5	**Low N and P (10%)**	0.0108	10.76	0.0068	6.83	0.0862	86.16
6	**Ex-Low N (5%) & Low P (10%)**	0.0054	5.38	0.0068	6.83	0.0862	86.16

Table VIII: Adjustments to Modified Acid Medium (CPCC, 2015, Olaveson and Stokes, 1989) for six experimental treatments. Changes to standard nutrient concentrations are indicated by shaded squares. Potassium sulfate is not included in the original formulation and Provasoli's ASP 6 B Vitamin Solution was substituted for F/2 Vitamin mix as a source of B vitamins.

Treatments:			**1**	**2**	**3**	**4 & 5**	**6**
Modified Acid Medium CPCC 2015 with Provasoli's substituted for F/2 Vitamin Soln.			**Standard MAM**	**Low N (10%)**	**Low P (10%)**	**Low N and P (10%)**	**Ex-Low N (5%) & Low P (10%)**
Stocks	**Salts**	**Stock (g/L)**	**mL Stock/L**	**mL Stock/L**	**mL Stock/L**	**mL Stock/L**	**mL Stock/L**
1	$(NH_4)_2SO_4$	50	10	1	10	1	0.5
2	$CaCl_2 \cdot 2H_2O$	1	10	10	10	10	10
3	$MgSo_4 \cdot 7H_2O$	50	10	10	10	10	10
4	KH_2PO_4	30	10	10	1	1	1
5	NaCl	3	10	10	10	10	10
6	$Na_2EDTA \cdot 2H_2O$	20	0.5	0.5	0.5	0.5	0.5
7	***Trace Metal Mix**	(See Below)	1	1	1	1	1
8	$FeSO_4 \cdot 7H_2O$ + H_2SO_4	4.98 g/L + 1mL	1	1	1	1	1
9	Provasoli's ASP 6 B Vitamin Solution (1000X concentrate, Sigma Aldrich)		1	1	1	1	1
10 New	K_2SO_4	15	0	0	11.52	11.52	11.52
mL Stocks			53.5	44.5	56.02	47.02	46.52
mL Deionized Water			946.5	955.5	943.98	952.98	953.48
Adjust pH with 5% or 10% H_2SO_4 (added by drops)			<1	<1	<1	<1	<1
Total Volume (mL)			1000	1000	1000	1000	1000

***Trace Metal Mix**	**Trace Metals**	**Stock Solution g/L**
1	H_3BO_3	2.86
2	$MnCl_2 \cdot 4H_2O$	1.81
3	$ZnSO_4 \cdot 7H_2O$	0.222
4	$NaMoO_4 \cdot 2H_2O$	0.39
5	$CuSO_4 \cdot 5H_2O$	0.079
6	$Co(NO_3)2 \cdot 6H_2O$	0.0494

2.1.11.1. Treatment 1, Standard MAM, Nutrient-Replete Control

Treatment number one was designated as the "control" treatment. The culture vessel contained standard MAM, with pH adjusted to 2.5 by the addition of small amounts of sulfuric acid. Provasoli's ASP 6 B Vitamin Solution (Provasoli, McLaughlin, and Droop, 1957), from concentrate (Sigma) was substituted for F/2 Vitamin mix as a source of B vitamins. The vitamin solution was the only ingredient with a source of organic carbon, therefore it was not added to the medium until after inoculation with algal cells, to prevent the early stimulation of fungal and bacterial growth.

2.1.11.2. Treatment 2, Low Nitrogen Medium

Treatment number two contained MAM with 10% of the nitrogen source contained in standard MAM, $(NH_4)_2SO_4$, but was otherwise, to the extent possible, identical to treatment number one.

2.1.11.3. Treatment 3, Low Phosphorus Medium

Treatment number three contained MAM with 10% of the phosphorus contained in standard MAM. Because the source of phosphorus in original MAM is K_2HPO_4 (dipotassium phosphate, K_2SO_4 (potassium sulfate) was added to replace the missing potassium. All other ingredients were the same as in treatment one. The relatively small increase in sulfur was not expected to noticeably influence growth, because the Berkeley Pit Lake strain of *C. freiburgensis* had not been previously observed to be sensitive to high concentrations of sulfur in its environment. (Grant Mitman, personal communication, 2017).

2.1.11.4. Treatment 4, Low Nitrogen and Low Phosphorus Medium

Treatment number four contained MAM with 10% of the standard concentration of both nitrogen and phosphorus, with K_2SO_4 added to replace potassium. All other nutrient concentrations were the same as for treatment number one.

2.1.11.5. Treatment 5, Low Nitrogen and Low Phosphorus Medium with Supplemental CO_2

Treatment No. 5 received CO_2-enriched air, but contained the same medium as treatment number four (reduced nitrogen and phosphorus). Additional carbon dioxide was mixed into the humidified ambient air, and the air mixture was circulated through the medium, maintaining the portion of CO_2 at a rate between one and five percent of the total air volume. An apparatus was assembled to deliver the CO_2 during the day (light period) and stop its flow at night (dark period). Algae have varied tolerances to CO_2. Although an adequate CO_2 supply is necessary for photosynthesis, excess CO_2 can inhibit growth (Silva and Pirt, 1984). Although some highly CO_2 tolerant microalgae can grow with levels up to 100%, others would be impaired or killed at much lower concentrations. Optimal growth in several species occurs with 2% to 10% additional CO_2 supplementation (Salih, 2011, Chiu et al., 2009). It was not possible to regulate the gas flow precisely with the equipment available. It was determined that setting a target of an increase in CO_2 at five percent or lower of ambient air volume would be unlikely to negatively impact growth or become lethal to the alga (personal communication, Martha Apple and Grant Mitman, 2017), but it could augment its growth.

2.1.11.5.1. Supplemental Carbon Dioxide Delivery Method

CO_2 was added to the ambient air entering the humidifier flask, where it mixed with air entering the culture vessel, at a rate between two and five percent of the volume of air circulating through the vessel. During dark periods, the flow of CO_2 was stopped automatically by a timer that controlled an aquarium air pump (Figure 27). The CO_2 flow was monitored two to five times per day, and regular adjustments were necessary to keep it within the desired range. Changes in water level in the humidifier flask, water siphoning into tubing with pressure changes from clogged filters and air leaks contributed to CO_2 flow fluctuations from zero to fifteen percent of ambient air, and these were corrected by adjusting or replacing flowmeters, valves and filters. The CO_2 supply lasted until day 26, and at that point supplementation was discontinued.

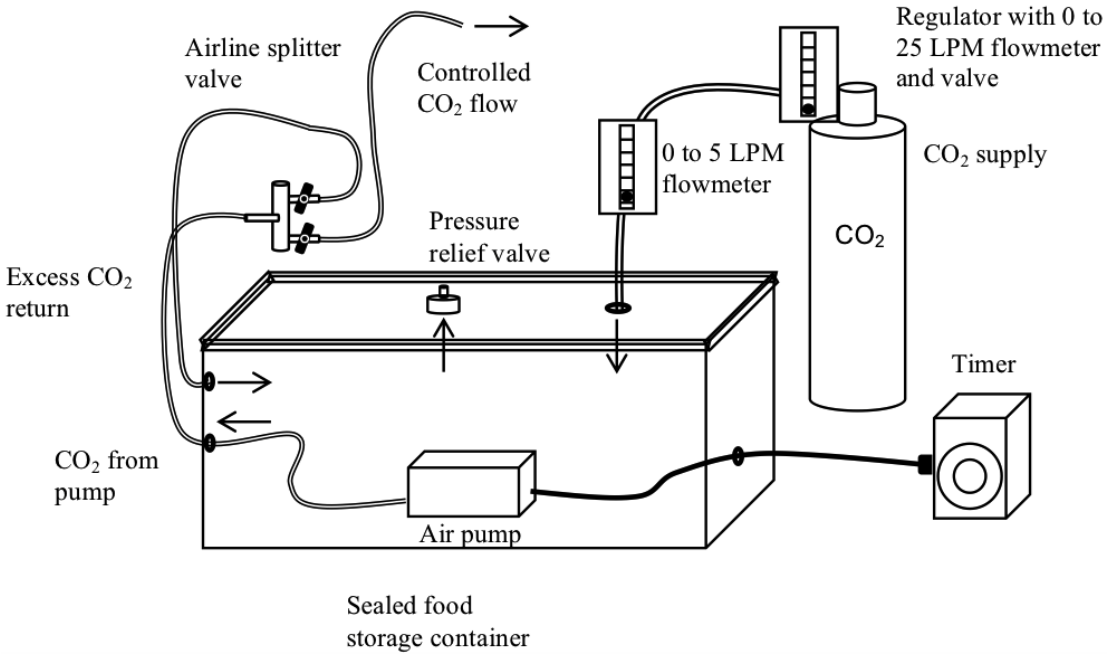

Figure 27: Supplemental CO_2 Delivery Method. A sealed box, aquarium pump and a timer was used to deliver a small volume of CO_2 to treatment No. 5, and for automatically stopping the flow at night (eight-hour dark period). A tank of carbon dioxide was connected to a sealed plastic food storage box, and a low flow (less than 1 LPM) was established to keep the box filled with CO_2. A timer switched on and off an aquarium air pump, that delivered CO_2 from the box to a flowmeter (not pictured), which regulated the flow of CO_2 added to a humidifier flask with ambient air (also regulated by another flow meter). By making frequent adjustments, it was possible to maintain the additional CO_2 flow volume between 2% and 5% of the ambient air circulating through the culture during the daytime (16-hour light period), except for a few fluctuations outside of the desired range (from 0 to 15%).

2.1.11.6. Treatment 6, Intermittent Nitrogen Feeding

An intermittent nitrogen feeding method has been successfully employed to induce other microalgae, for example, *Nannochloris sp*., to significantly increase lipid reserves, and the triglyceride proportion of cellular lipid, while maintaining an acceptable cell density (Takagi et al., 2000). Treatment number six contained MAM with lowered nitrogen and phosphorus. The phosphorus concentration was reduced to 10% of the concentration found in standard MAM. At the time of inoculation (Day 0), nitrogen was lowered to 5% of the concentration found in standard MAM. Intermittent feeding of nitrogen was accomplished by adding 2.7 to 4.0 mL of ammonium sulfate stock solution (Table VIII) at intervals of four days, until day 24, during the period when exponential and linear growth was expected to occur. Volumes of stock solution were added that were approximately 0.05% of the current total volume of medium in the bottle. The total volume of nitrogen solution added was 47.43% of that contained in standard MAM. Nitrogen feeding was discontinued after day 24. The object of treatment No. 6 was to maintain relatively high biomass (as in treatments number 1 and 3) with increased lipid and triglyceride content that would be comparable to the expected response to nitrogen depletion (as in treatments number 2, 4 and 5).

2.1.12. Sampling and Cell Counting for Experimental Treatments

Samples were harvested from each culture on the same day, immediately before cell counts were made. Algal cells were harvested while suspended and mixed homogenously in their medium, before any settling could occur. The date of inoculation was labeled as “day 0”. Samples for lipid (fluorescence) analysis and FAME (GC/MS) analysis were harvested on days 6, 8, 9, 12, 15, 19, 23, 27, 34 and 52. Ten sets samples (of 346 to 450 mL from each of the six

treatments) were removed and frozen at -20 to -25 ˚C for later GC/MS analysis. Ten sets of samples (4 mL) were removed for Nile Red fluorescence analysis, and these were either analyzed within a few hours of harvest, or frozen until they could be thawed and analyzed at a later date. Twelve additional sample sets (60 mL of medium with algal cells) were removed, six sets for nitrogen analysis and six for phosphorus analysis. Cell counts were made of each of the six experimental treatment cultures, every three days, starting on day 0. After 15 days, counts were conducted every four days. After day 23, counts were made after longer time intervals.

2.1.13. Monitoring Nitrogen and Phosphorus Concentrations

To obtain a more precise interpretation of the quantity of nitrogen and phosphorus in the medium associated with exponential growth, linear growth, and static phase (little to no growth), which is associated with increased lipid production, six sets of six 50 mL samples of culture medium were vacuum filtered using 0.2 µm, 90mm, Millipore filters to remove algal cells and other particles, and mailed to University of Georgia's Laboratory for Environmental Analysis (LEA). At LEA, the six sets of six samples were each divided for analysis of total nitrogen and phosphorus concentrations. Phosphorus concentration was determined by an ICPMS (Inductively Coupled Plasma Mass Spectrometry) method. Although details regarding the methods for determining total nitrogen (nitrates, nitrites and ammonia) were not available, the LEA website states that nitrogen species are mostly determined by spectrophotometric or ion chromatography methods. Nitrogen and phosphorus samples for days 0, 7, 15, 21, 28 and day 57 were analyzed.

2.1.14. Monitoring pH

The pH of the culture medium was tested four times during the growth period (on days 0, 12, 15 and 23) and once after the majority of cells had become attached to algal-fungal flocs or surfaces and the rate of cell mortality appeared to clearly exceed the growth rate, at 105 days after inoculation.

2.2. Nile Red Fluorescence Method to Monitor Lipid Content

A lipophilic fluorescent stain, Nile Red (or 9-(diethylamino)benzo[a]phenoxazin-5-one, PubChem, 2019) was chosen to indicate total lipid content in whole, freshly sampled live algal cells suspended in their liquid medium (Figure 28 and Figure 29). Nile Red (NR) selectively stains cellular lipids and has been found to be useful to evaluate lipid content of live cells (Cooksey et al., 1987, De La Jara et al., 2003, Kelly, 2013, Alemán-Nava et al., 2016). It does not fluoresce in a polar solvent, such as water, but does when dissolved in a non-polar solvent such as a lipid. According to Alemán-Nava et al. (2016), Nile Red fluorescence has been used in the analysis of 40 strains of microalgae since 1995, and serves as a rapid method for monitoring TAG content in microalgae. Determining the TAG content of the algal lipids detected by the Nile Red method was outside the scope of this experiment, however it was postulated that TAG makes up a large proportion of the stored lipids, as it commonly does in other photosynthetic eukaryotes. The authors also advise, “Since NR's fluorescence is mainly controlled by its diffusion though the cell wall, the protocol must be customized and calibrated for individual strains”. Montana Tech students had tested a Nile Red fluorescence method on a green microalgal species from Berkeley Pit Lake, *Stichococcus bacillaris* Nageli, and found it to be

successful (Kelly, 2013, Henderson, 2005). Prior to beginning the experiment described here, a method was developed that appeared to work well for *C. freiburgensis* (Moslander, 2016).

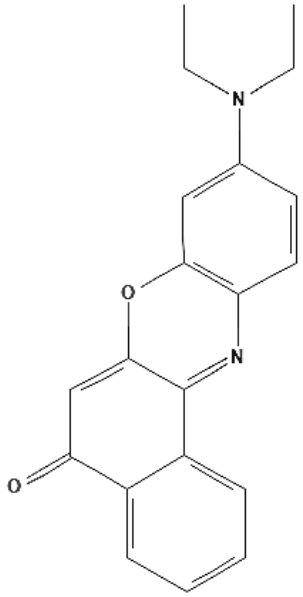

Figure 28: Nile Red fluorescent stain (9-(diethylamino)benzo[a]phenoxazin-5-one) (Nile Red 2 D Structure Image from PubChem Open Chemistry Database, 2019).

A stock solution of 0.025 mg/mL of Nile Red stain (Sigma Life Sciences) in dimethyl sulfoxide (DMSO) was prepared. Ten sets of six 20 mL samples of fresh, live *C. freiburgensis* cells in liquid MAM were harvested and either analyzed within the next few hours, or placed in 50 mL capped centrifuge tubes and frozen at -20 to -25 °C, for later analysis. Samples were frozen when it was not possible to run the fluorescence analysis immediately after harvest, in order to prevent cellular metabolism from altering lipid content from that at the time of their harvest. Samples that had been frozen were thawed immediately before fluorescence lipid analysis, by resting the tubes in slightly warm tap water (approximately 20 °C) for a few minutes. Thawed samples were thoroughly mixed to re-suspend cells, by placing the tubes on a Vortex mixer for one minute, at the high setting, before removing the portion to be analyzed.

Freezing was not expected to significantly affect lipid content or fluorescence, except to preserve samples in the condition that they were in when harvested, and *C. freiburgensis* cells were expected to survive freezing (Grant Mitman, 2016, personal communication).

2.2.1. Equipment

A Florolog (Horriba Jobin Yvon Inc.) fluorescence spectrometer with FluorEssence 3.5 software was used to detect and quantify fluorescence. The spectrometer was set at 530 nm for excitation and 580 nm for emission. The wavelengths were chosen for the optimal fluorescence measurements of Nile Red stain in non-polar solvent, and the results from previous experiments with *C. freiburgensis* and *S. bacillaris* (Moslander, 2016, Kelly, 2013). The calibration curve for the fluorescence measurements was established using triolein (also known as glyceryl trioleate, $C_{57}H_{104}O_6$), as a representative lipid for the standards (Figure 29).

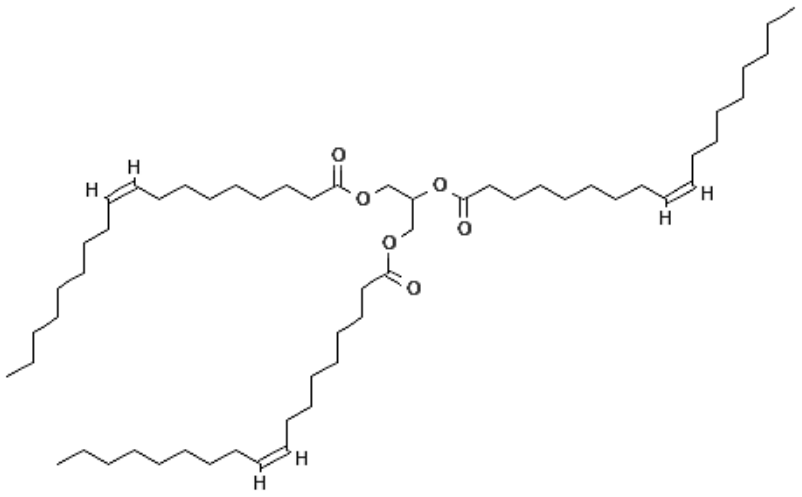

Figure 29: Triolein, a triglyceride (triacylglycerol or TAG) which is composed of three oleic acid (C18:1) units and one glycerol unit. Triolein occurs in high abundance in olive oil (2D Structure image from PubChem Open Chemistry Database 2018).

2.2.2. Standard Preparation and Calibration

A series of six triolein standard solutions between 0.05 mg/mL and 0.55 mg/mL were prepared (Table IX). To establish a calibration curve, 40 µL of each triolein standard was mixed into 4 mL of filtered standard MAM for one minute with a Vortex mixer on a high setting. 40 Microliters of Nile Red stock solution was added and mixed into the diluted standard in the same way. For a blank, 40 µL of isopropanol/chloroform (Fisher Scientific) solvent was substituted for triolein standard. Immediately after mixing in the Nile Red, the sample was placed into a 4 mL quartz glass cuvette and it was placed directly into the fluorescence spectrometer. The cuvette was rinsed with acetone and deionized water between samples, to remove any Nile Red stained lipid that remained on the inner surfaces. A 0.60 mg/mL standard was also tested, but replaced by the 0.55 mg/mL standard, as it fell outside the linear portion of the resulting calibration.

Table IX: Preparation of Triolein Standards for Fluorescence Calibration.

		Isopropanol (mL)	Chloroform (mL)
Solvent, 100 mL		95	5
	Stock (1mg/mL)	**Isopropanol/ Chloroform Solvent (mL)**	**Triolein (mg)**
Triolein Stock, 50 mL		50	50
Standards		**Triolein Stock (mL)**	**Isopropanol/ Chloroform Solvent (mL)**
			Fill to
1	0.05 mg/mL	0.5	10
2	0.1 mg/mL	1	10
3	0.25 mg/mL	2.5	10
4	0.375 mg/mL	3.75	10
5	0.5 mg/mL	5	10
6	0.55 mg/mL	5.5	10

2.2.3. Sample Preparation and Data Collection

Samples of medium containing live or freshly thawed algal cells were treated in a similar manner as the triolein standards. Each sample was mixed for one minute, 4 mL was placed into a 20 (to 30 ml) glass flask, to which 40 µL of Nile Red stock was added. It was mixed for one minute again, and immediately placed into the cuvette, and then into the fluorescence spectrometer. If the signal was beyond the high end of the calibration curve, the sample was diluted with filtered MAM, and the process was repeated with the dilute sample. A new calibration curve, from four or five standards, was determined during, or within a few days before or after, the fluorescence analysis for each set of algal samples. At least two of the standards, one at the low end of the linear portion of the calibration curve and one at the high end, were analyzed along with each set of algal standards.

2.2.4. Data Analysis

Calibration curves, based on the prepared standards, were plotted in Microsoft Excel (version 15.33, 2017), with fluorescence signal values on the y axis, and the x axis values representing the concentrations of lipids. The relationship between the fluorescence signal and concentration of lipid in the sample can be described as a straight line in the central, linear portion of the calibration curve. The upper and lower regions of the calibration curve have changing slopes. However, the calibration was not linear at the lower concentrations of lipids found in some of the samples. Final concentrations were calculated based on a polynomial relationship instead of the linear one (Figures 30 – 31). All lipid concentration calculations were corrected to account for dilution.

A linear relationship (Figure 30) can be described by the following equation, in slope-intercept form:

$$y = mx + b \quad (14)$$

where x and y are the coordinates of a point on a line, m is the slope of the line, and b is the x coordinate of the point where the line intercepts the y axis.

$$x = (y-b)/m \quad (15)$$

is the same linear equation as equation No. 1, but written in a different order.

A polynomial relationship, like the one used to calculate lipid concentrations, can be described by the following equation:

$$y = ax^2 + bx + c \quad (16)$$

where y represents the fluorescence signal value, x represents the concentration of lipid in the sample, and a, b and c are values that are known (a is not 0). There are two solutions for x, and the one that makes sense (for example, the one that is > 0), represents the concentration of lipid in the sample.

The two solutions for x can be found by placing the four known values into the quadratic formula:

$$x = (-b \pm \sqrt{(b^2 - 4*a*c)})/(2*a) \quad (17)$$

where a, b and c are three known values, y represents the fluorescence signal value, and x, the unknown variable, has two solutions, one of which represents the lipid concentration. The values for a, b, and c were found in the best-fitting polynomial trendline equations calculated by Excel software, for the known concentrations of the standards (y) and their corresponding fluorescence signal values (x).

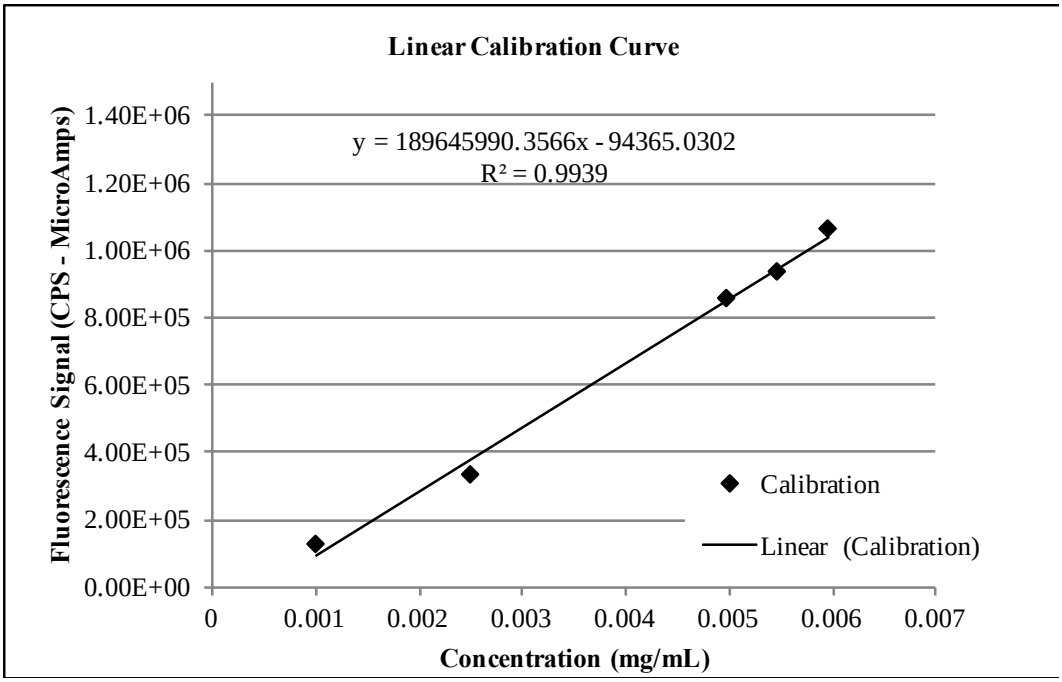

Figure 30: Example Linear Calibration Curve. Line equation: y = 120213444.7588x + 8629.9842 or x = (y+8629.9842)/120213444.7588. The unknown lipid concentration of the algal samples is represented by "x" in this equation.

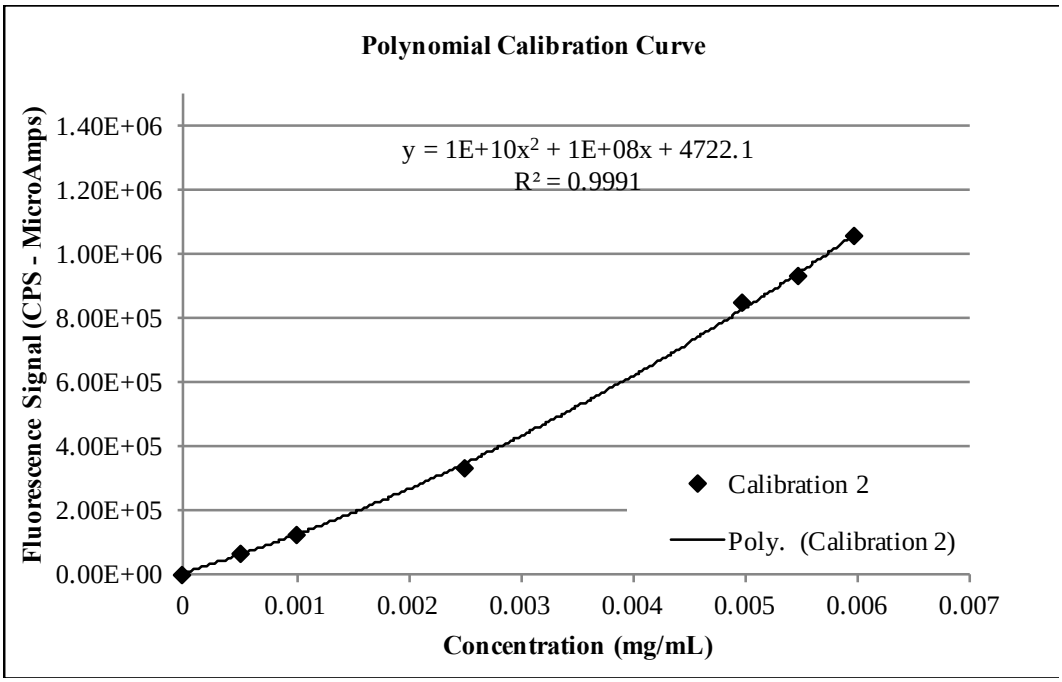

Figure 31: Example Polynomial Calibration Curve. Line equation: y = 1E+10x2 + 1E+08x + 4722.1 or y = 11662541583.3965x2 + 107765870.4909x + 4722.1108 and x = (-b±√(b^2 - 4*a*c))/(2*a). One of the two solutions for "x" represents the lipid concentration of the algal sample. The polynomial relationship included lower and higher fluorescence signal values than the linear model and it provided a better match to the actual observed relationship between the range of lipid concentrations that were found and their Nile Red fluorescence signal values.

2.3. Dry Weight Biomass Determination and Freeze-drying Method

Samples of 250 to 396 mL of fresh, live algal cells suspended in liquid medium, were removed from the cultures and placed in new 16 oz. (473 mL) plastic drinking cups inside zipper plastic bags and frozen at -20 °C to -25 °C in a chest freezer. The frozen samples were transferred to 6000 mL glass flasks and freeze-dried, using a Labconco FreeZone Benchtop freeze dryer, at -45 °C and 0.18 to 0.24 Torr. Samples were checked several times per day until no visible ice or cold spots remained. Drying time varied from 71 to 118 hours depending on sample volume and whether one or two samples were dried at a time. Samples were considered to be completely dry when they had become a dark or light green powdery substance with a small amount of white mineral residue. Freeze-dried *C. freiburgensis* was difficult to transfer

due to its static charge, causing it to scatter and cling to plastic and glass containers, therefore aluminum foil was used to weigh and transfer the dry material. The weight (g) of each sample was recorded, and compared to the volume of liquid culture that had been dried to determine the biomass yield (g/L). Dried samples were stored in 50 mL sealed plastic centrifuge tubes in a freezer (away from light, at approximately -24 °C). Entire dried algal samples were processed to convert lipids to FAMEs. After the dry sample was transferred to a container for transesterification, the empty sample tube was weighed again to correct analyzed sample mass for any dry algal residue remaining inside the plastic tube.

2.4. GC/MS Method for Determining FAME Composition

A gas chromatograph/mass spectrometry (GC/MS) method had been developed at Montana Tech to characterize fatty acid methyl esters in general (Harkey, Cameron and Chang, 2009). The method was refined to identify and determine the proportions of FAMEs in lipids extracted from *C. freiburgensis*, specifically (Cameron and Stewart, 2010). A similar method was employed to examine the proportions and quantities of FAMEs in samples harvested at various time intervals during growth of the six experimental treatments. The primary goal of examining the FAME composition of *C. freiburgensis* samples cultured in media with varying nutrient compositions, for varying lengths of time, is to determine which combination of conditions results in the highest relative proportion of C18:1 and C16:1, and the lowest relative proportion of saturated fatty acids and polyunsaturated fatty acids in the transesterified product.

2.4.1. Sample Preparation

2.4.1.1. Lipid Extraction and Transesterification

Approximately 0.5 g of dried algal sample was placed in a 50 mL round-bottomed tempered glass flask, and any clumps were gently crushed using a round-tipped glass rod, to a uniform fine powder. Sulfuric acid (J.T. Baker) was diluted to 2.5% in methanol (Fisher Scientific, ACS certified). 2.5 To 3.0 mL of H_2SO_4/methanol solution was added to the dry sample and the flask was placed in a heated, clean sand bath, atop a hotplate, where it was kept at 60 °C (with temperature fluctuations of ± approximately 5 °C). The mixture was constantly stirred, with a magnetic stirrer, at a medium speed, for two hours.

2.4.1.2. 2.4.2.2 Filtering to Remove Algal Solids

Each transesterified sample was transferred to a Whatman three-part vacuum filtering apparatus using Whatman, No. 540 hardened, ashless, 2.1 cm circular filter papers (Cat. no. 1540 321) to remove all solid materials from each sample. A small amount of deionized water (approx. 1 to 2 mL) was used to rinse remaining solids from the flask, magnetic stir bar and sides of filter container onto the papers. Depending on the amount of solid material in the sample, from one to eight filter papers were required per sample.

2.4.1.3. FAME Extraction

Each filtered sample was transferred to a 60 mL glass separatory funnel, and 3 mL of hexane (Fisher Scientific, ACS Certified, 4.2% various methylpentanes) was added. The funnel was capped with a glass stopper and the contents were mixed manually by gently shaking for 15 minutes. Afterwards, the mixture was allowed to stand for five minutes. The hydrophilic bottom

layer was reserved in a 50 mL glass beaker, and the hydrophobic upper layer was reserved in a separate beaker. The hydrophilic layer was returned to the separatory funnel, and washed in the same manner again with 3 mL of hexane, repeating the process for a total of three times. With each wash, approximately three mL of hydrophobic solution containing hexane and algal FAMEs was reserved, for a total volume of approximately 9 mL. After three hexane washes, the hydrophilic bottom layer was discarded. The reserved hydrophobic mixture was washed, by gentle manual shaking in the funnel, for 15 minutes using 10 mL of deionized water. It was allowed to stand for five minutes, and the hydrophilic layer was discarded. If the mixture did not separate neatly into two layers, but contained a foamy emulsion between the hydrophobic and hydrophilic layers, trapping some water, a small amount (1 to 1.5 g) of A.C.S. reagent grade anhydrous sodium sulfate was added to the funnel. This caused the emulsion to dissipate. To remove any remaining water, the hydrophobic layer was filtered through a small amount (approximately 1 g) of anhydrous Na_2SO_4 on a fragment of clean cotton fiber inside one or two glass Pasteur pipettes, and transferred to a sealed 25 mL glass EPA vial. If no emulsion formed, only the second method was used.

2.4.1.4. Concentration by Evaporation

Approximately 9 ml of hexane containing algal FAME mixture was concentrated to a volume of 0.5 mL, by placing the EPA vial on warm (35 to 45 °C) sand, loosely covered with aluminum foil. The hexane was allowed to evaporate until less than 0.5 mL of liquid remained in the vial. The sample was then transferred to a 1.5 mL glass Agilent vial and a small amount of hexane (a few tenths of one mL) was added to the EPA vial to retrieve and transfer any

remaining sample and bring the final volume up to 0.5 mL, according to the marking on the side of each vial.

2.4.2. Naphthalene Internal Standard

Naphthalene was chosen for an internal standard, to calculate the proportion of each FAME from chromatographic peak area values. A stock solution was prepared using 517.4 mg naphthalene (Sigma) dissolved in sufficient hexane for a final volume of 10 mL. This stock solution was diluted again with hexane to a concentration of 1.035 mg/ml (200 µL in 10 mL) for the internal naphthalene standard. This standard solution was added at a proportion of 10 µL per 0.5 mL directly to the 0.5 mL concentrated, algal FAME sample before EI and CI GC-MS analysis, for a final concentration of 0.0270 mg/mL in the sample.

2.4.3. GC/MS Equipment, Data Collection and Analysis

The combination of Gas Chromatography (GC) and Mass Spectrometry (MS) can provide both quantitative and qualitative information about a sample. A Thermo Scientific Trace GC Ultra (model No. K24300000000080) with an ITQ 900 Ion Trap and Xcaliber 2.0 software was configured for the algal FAME samples (Appendix).

2.4.3.1. GC/MS Electron Ionization Method

Thirty-one algal FAME samples were analyzed by an electron ionization (EI) method which yielded data on amount of each FAME, based on the signal intensity represented as peak area. Substances that enter the GC column at the same time, exit the column at different times, depending primarily on their molecular mass, polarity and shape. The molecules enter the mass

spectrometer where they are ionized and fragmented, such that the molecular ions and fragment ions are separated by their mass to charge ratio (m/z). These ions are subsequently detected and the ion signals are recorded as a function of time. The sum of these signals is recorded as peaks in the gas chromatogram (Figure 32). The signal intensity is related to the amount of the substance in the sample, and it is indicated by the height and area of each peak. The retention time (RT) is the time at the apex of each peak, indicating the maximum signal intensity, since the sample entered the column. Comparison of the retention times of known compounds to unknown compounds in a sample can be used to identify the unknown ones. A software library comparison was done between the mass spectra obtained from compounds in the FAME samples to the mass spectra of standard FAME compounds. An example of a library search of these spectra at a selected time is given below (Figure 33). This identification method is used in conjunction with a comparison of the mass spectra of known compounds to the mass spectra of the separated compounds from the samples.

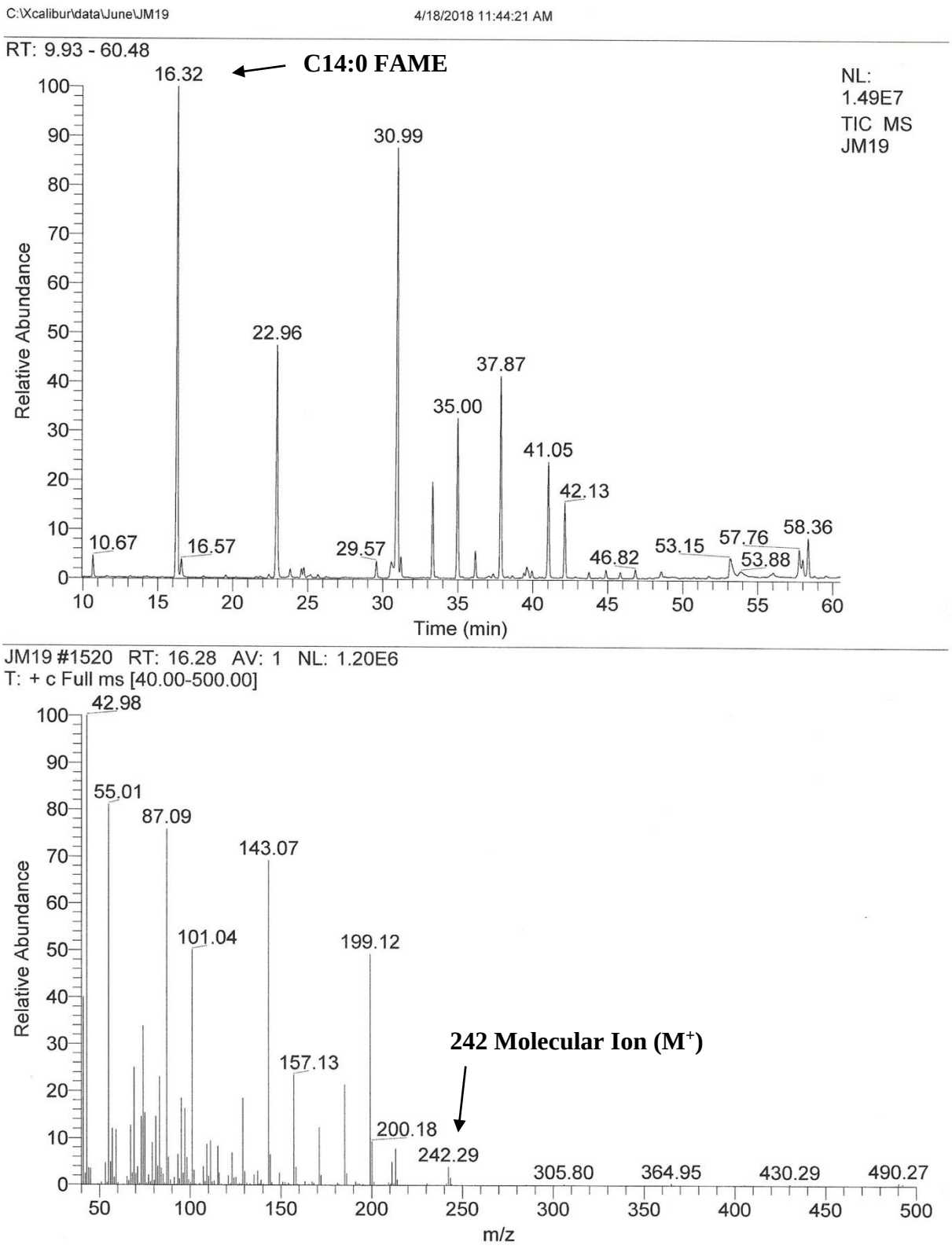

Figure 32: The mass spectrum (lower section) of the peak at 16.32 (16.28) minutes, selected in the EI chromatogram from treatment No. 2, day 27 (upper section). A GC/MS instrument software library search found a likely match for a C14:0 FAME with a peak at that retention time (Figure 33).

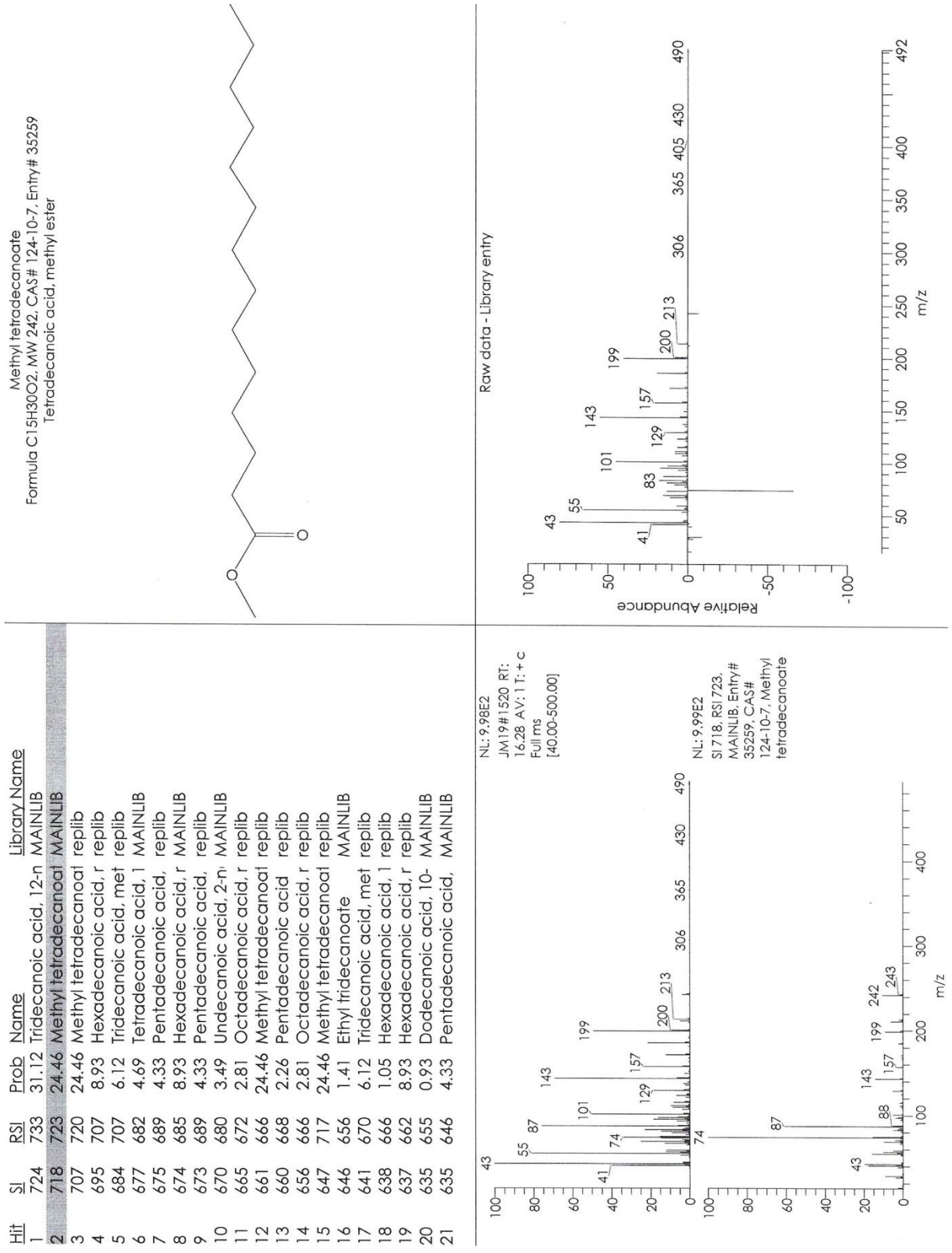

Hit	SI	RSI	Prob	Name	Library Name
1	724	733	31.12	Tridecanoic acid, 12-n	MAINLIB
2	718	723	24.46	Methyl tetradecanoat	MAINLIB
3	707	720	24.46	Methyl tetradecanoat	replib
4	695	707	8.93	Hexadecanoic acid, r	replib
5	684	707	6.12	Tridecanoic acid, met	replib
6	677	682	4.69	Tetradecanoic acid, 1	MAINLIB
7	675	689	4.33	Pentadecanoic acid,	replib
8	674	685	8.93	Hexadecanoic acid, r	MAINLIB
9	673	689	4.33	Pentadecanoic acid,	replib
10	670	680	3.49	Undecanoic acid, 2-n	MAINLIB
11	665	672	2.81	Octadecanoic acid, r	replib
12	661	666	24.46	Methyl tetradecanoat	replib
13	660	668	2.26	Pentadecanoic acid	replib
14	656	666	2.81	Octadecanoic acid, r	replib
15	647	717	24.46	Methyl tetradecanoat	replib
16	646	656	1.41	Ethyl tridecanoate	MAINLIB
17	641	670	6.12	Tridecanoic acid, met	replib
18	638	666	1.05	Hexadecanoic acid, 1	replib
19	637	662	8.93	Hexadecanoic acid, r	replib
20	635	655	0.93	Dodecanoic acid, 10-	MAINLIB
21	635	646	4.33	Pentadecanoic acid,	MAINLIB

Figure 33: A library search found an identified compound, tetradecanoic acid methyl ester, a C14:0 FAME from a saturated fatty acid, as a likely match for the peak at 16.32 (16.28) min.

2.4.3.2. GC/MS Chemical Ionization Method

Nine algal FAME samples, that had been analyzed by the electron ionization method, were also analyzed by a chemical ionization (CI) method. Acetonitrile was used as the reagent gas, and the ions generated from the gas reacted with and ionized the FAMEs in the sample. Saturated FAMEs yielded one main type of ion (M+1) which could be identified by its mass to charge ratio (m/z) (Figure 34). A separate ionization reaction occurred with each unsaturated FAME at the position of a double bond, resulting in three (most numerous) types of ions (M+1 protonated FAMEs; M+40, adduct FAMEs and M+54 imine adduct FAMEs), which could also be identified by their m/z (Figures 35 – 39).

The retention times of peaks (at the apex) in the chromatogram were selected and the m/z ratios associated with each retention time were examined to determine whether they were characteristic of a known FAME. If so, the mean retention times of these compounds were assigned the identity of the particular FAME. Table X lists the identified FAMEs, their corresponding retention times and the molecular weights of ions generated in their reaction with acetonitrile. Peaks in the chromatograms from non-FAME substances, such as pigments and phthalates from plastics, were not identified, but did occur in the samples.

The retention time error from variation in the time that it takes to inject a sample (a few hundredths of a minute) was accounted for by subtracting the mean retention time of the internal standard, naphthalene (10.64 minutes) from the retention times of each peak. The mean retention time of each FAME identified by the CI method, minus 10.64 minutes, was the retention time used to identify the peak from that FAME in the remaining samples that were run with EI only (Figure 40).

Five sets of six samples were processed and analyzed by the GC/MS methods described above. These included sample sets from the six treatments that were harvested on days 6, 9, 19, 27, and 52 of the growth period. An additional sample from treatment No. 5, day 15, was later added to these.

Table X: Retention times of identified FAMEs and the molecular weights of ions that were expected to be observed in the mass spectrum after chemical ionization (CI) of the FAMEs with acetonitrile gas.

GC/MS Identified Peaks		Molecular Weights (AMU) of FAMEs and Ions Expected to be Observed in m/z Spectrum					
RT at Peak Apex (Minutes)	FAME Detected (Carbon Chain Length and No. of Unsaturations)	FAME Lenght and Saturation		Saturated (and Unsaturated) FAMEs Weight (Mass)		Unsaturated FAMEs Weight (Mass)	
10.64	Napthalene (Internal Standard)	C (No.)	C=C (No.)	FAME	"+CH3O2" M+1	Imine M + 54	ACN. (CH3CN) M + 40
16.24	C14:0	14	0	242	243		
19.49	C15:0	15	0	256	257		
22.91	C16:0	16	0	270	271		
24.24	C16:1	16	1	268	269	322	308
24.54	C16:1	16	1	268	269	322	308
24.69	C16:1	16	1	268	269	322	308
25.00	C16:1	16	1	268	269	322	308
25.16	C17:0	17	0	284	285		
26.17	C20:0	20	0	326	327		
27.43	C16:2	16	2	266	267	320	306
28.86	C16:2	16	2	266	267	320	306
29.53	C18:0	18	0	298	299		
30.45	C17:2 and/or C18:1 (RT overlap)	17	2	280	281	334	320
30.88	C18:1	18	1	296	297	350	336
31.17	C18:1	18	1	296	297	350	336
33.31	C18:2	18	2	294	295	348	334
34.99	C18:3	18	3	292	293	346	332
36.14	C18:3	18	3	292	293	346	332
37.11	C18:4	18	4	290	291	344	330
37.86	C18:4	18	4	290	291	344	330
39.54	C18:4	18	4	290	291	344	330
39.91	C18:5	18	5	288	289	342	328
41.01	C20:3	20	3	320	321	374	360
41.79	C22:0	22	0	354	355		
42.10	C20:4	20	4	318	319	372	358
43.05	C22:1	22	1	352	353	406	392
43.71	C20:4	20	4	318	319	372	358
44.85	C20:5	20	5	316	317	370	356
45.39	C21:4	21	4	332	333	386	372
48.06	C22:4	22	4	346	347	400	386
50.69	C22:5	22	5	344	345	398	384
51.69	C22:6	22	6	342	343	396	382
55.98		25	1	394	395	448	434
	C25:1, C26:8, aromatic FAME or unknown compound (not FAME)						
57.69	C25, C26:7, C20:8 or other aromatic FAME						
58.31	Unknown or pthalic acid (software library)						

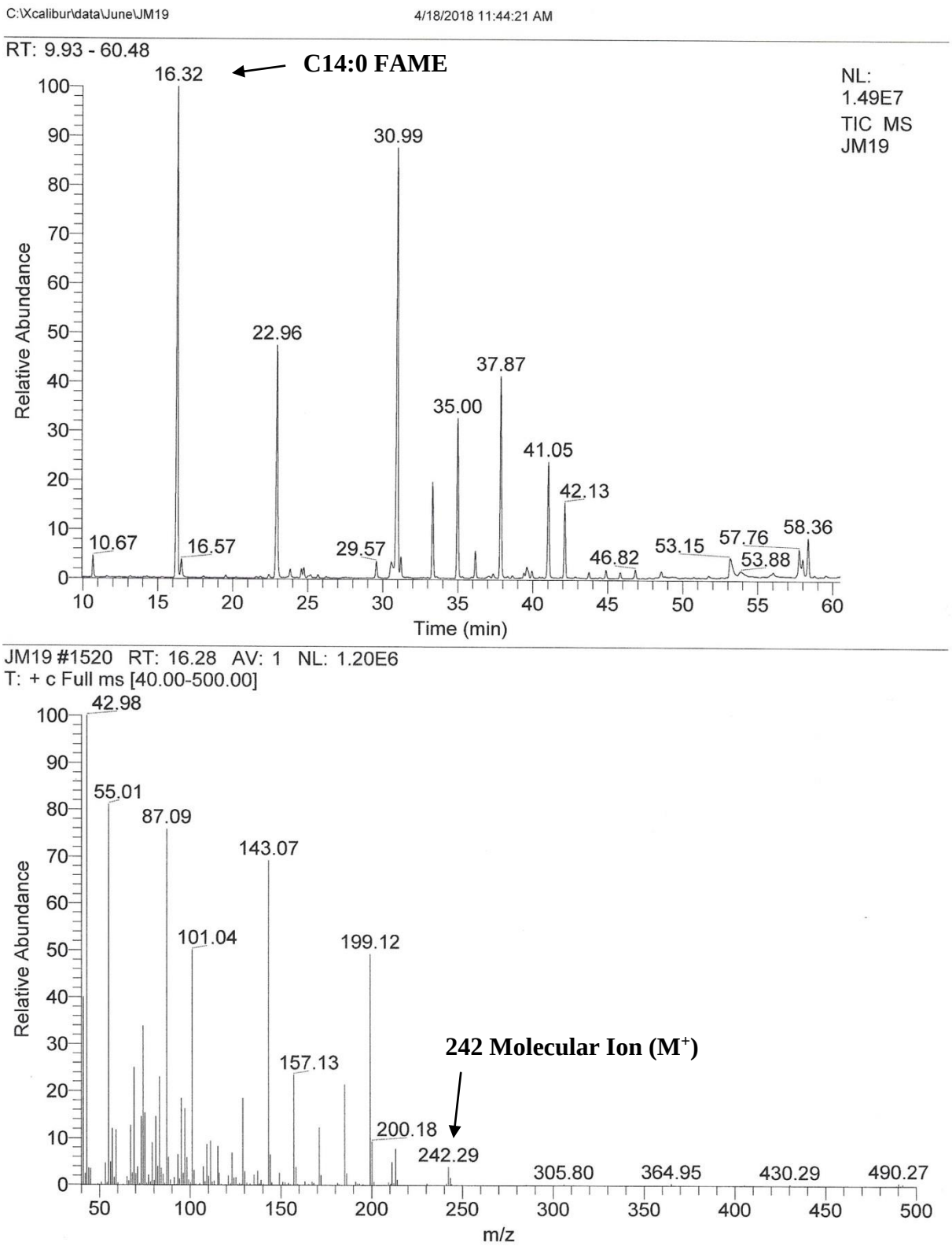

Figure 34: The EI chromatogram (upper chart) from treatment No. 2, day 27 with the mass spectrum of a saturated FAME, C14:0, selected (lower chart). The average retention times remain the same (except for slight variation in the time it takes to inject a sample) for each FAME, in each EI and CI run.

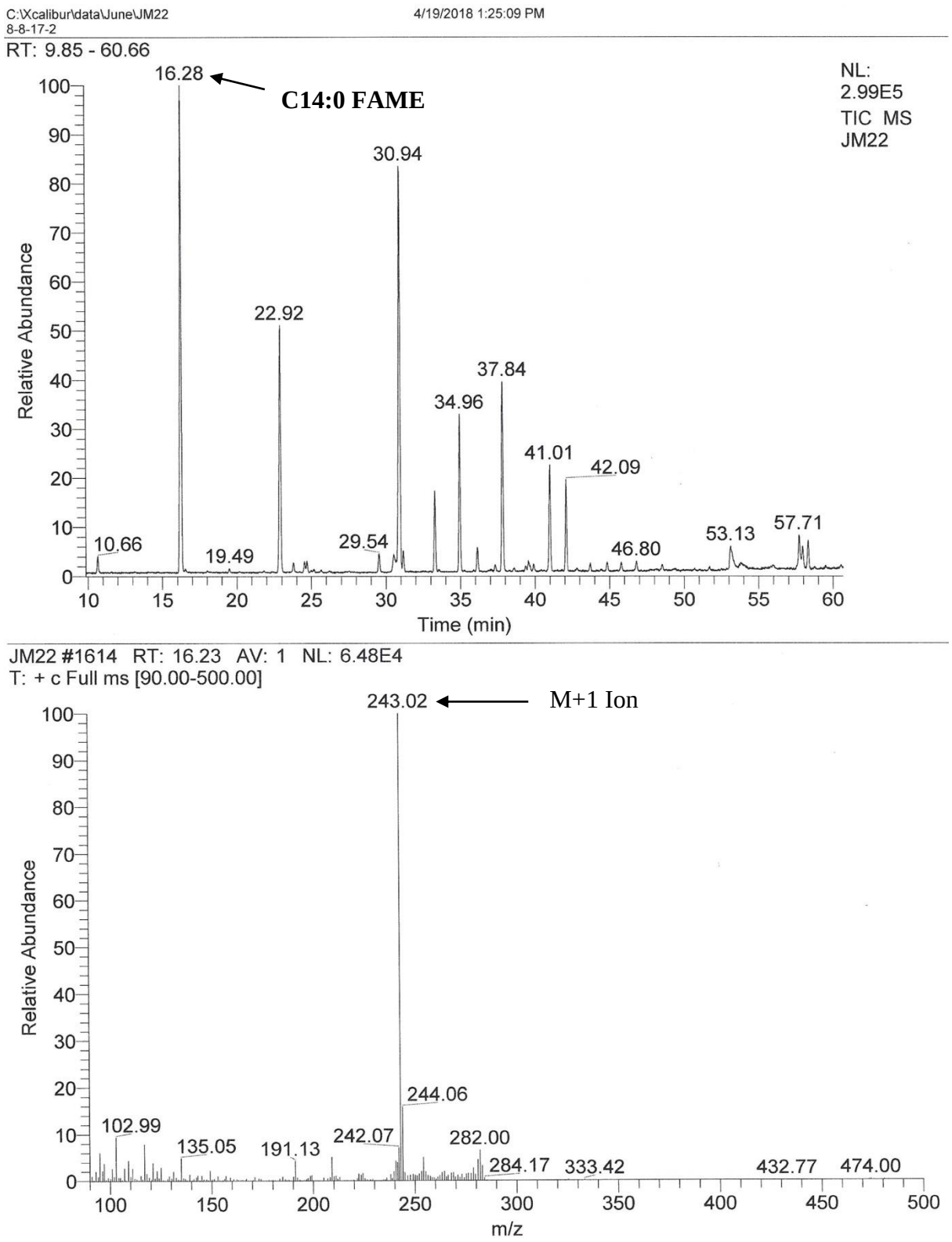

Figure 35: The CI Chromatogram for treatment No. 2, sample day 27 (upper chart), with the mass spectrum from a saturated FAME, C14:0, selected (lower chart). The molecular weight of the "M+1" ion from C14:0 is 243 AMU, and the mass spectrum shows that a high concentration of ions of that weight were detected at that retention time, confirming the identity of the FAME.

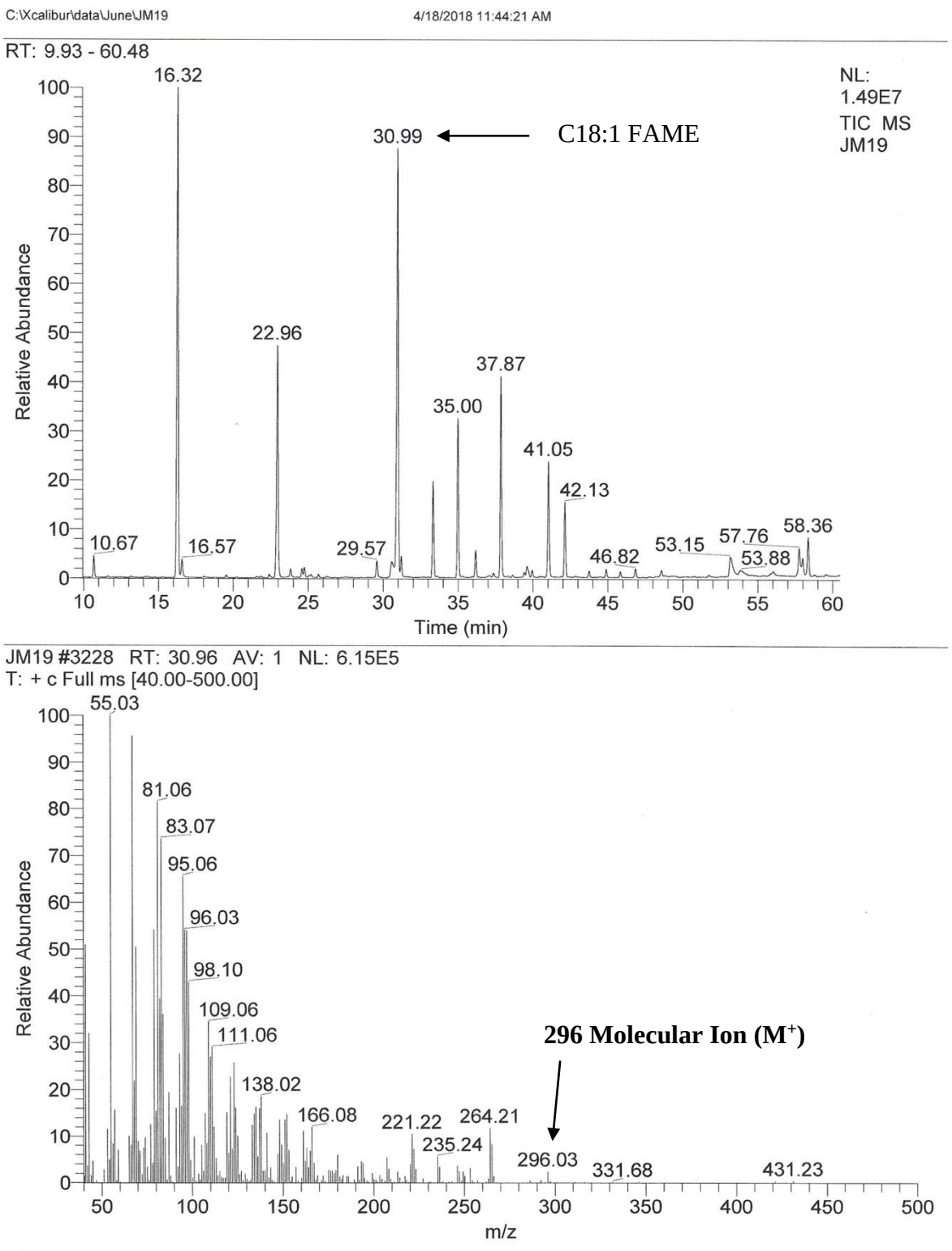

Figure 36: The EI chromatogram (upper chart) from treatment No. 2, day 27 with the mass spectrum of an unsaturated FAME, C18:1, at 30.96 to 30.99 minutes, selected (lower chart).

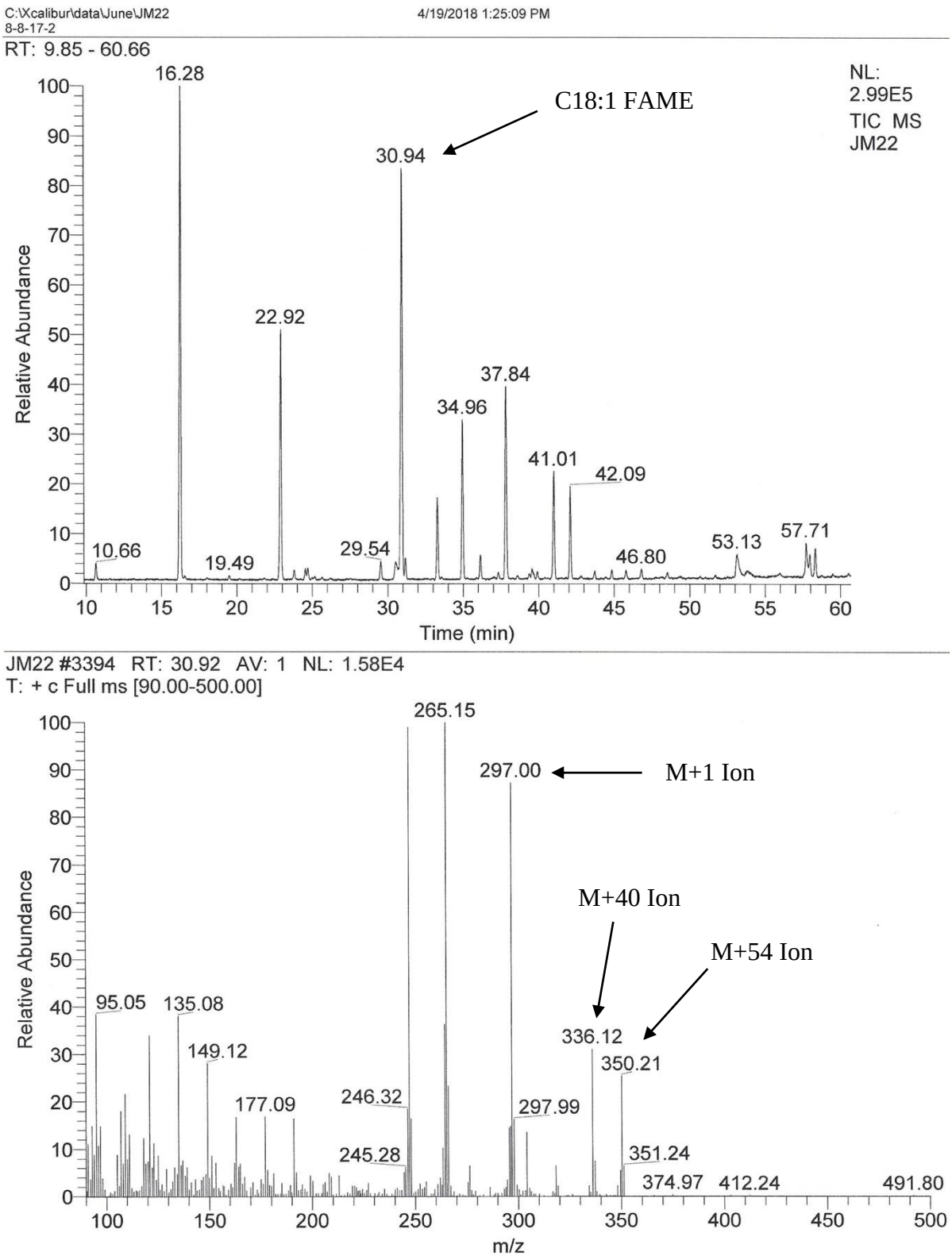

Figure 37: The CI Chromatogram for treatment No. 2, sample day 27 (upper chart), with the mass spectrum from an unsaturated FAME, C18:1, selected (lower chart). The molecular weights of the M+1, M+54 and M+40 ions from C18:1 are 297, 350 and 336 AMU. High concentrations of ions of these weights were detected at that retention time, confirming the identity as a C18:1 FAME.

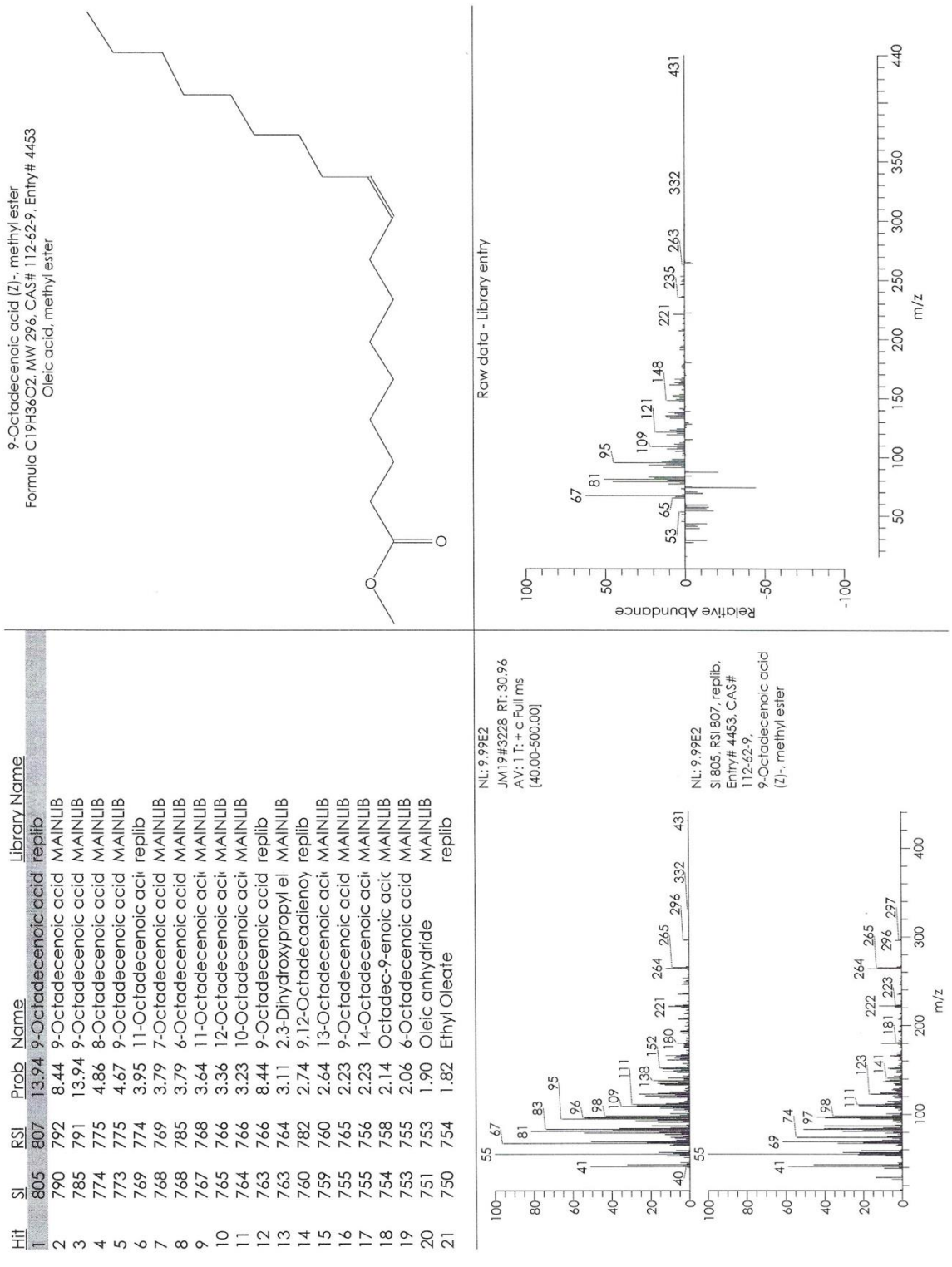

Hit	SI	RSI	Prob	Name	Library Name
1	805	807	13.94	9-Octadecenoic acid	replib
2	790	792	8.44	9-Octadecenoic acid	MAINLIB
3	785	791	13.94	9-Octadecenoic acid	MAINLIB
4	774	775	4.86	8-Octadecenoic acid	MAINLIB
5	773	775	4.67	9-Octadecenoic acid	MAINLIB
6	769	774	3.95	11-Octadecenoic aci	replib
7	768	769	3.79	7-Octadecenoic acid	MAINLIB
8	768	785	3.79	6-Octadecenoic acid	MAINLIB
9	767	768	3.64	11-Octadecenoic aci	MAINLIB
10	765	766	3.36	12-Octadecenoic aci	MAINLIB
11	764	766	3.23	10-Octadecenoic aci	MAINLIB
12	763	766	8.44	9-Octadecenoic acid	replib
13	763	764	3.11	2,3-Dihydroxypropyl el	MAINLIB
14	760	782	2.74	9,12-Octadecadienoy	replib
15	759	760	2.64	13-Octadecenoic aci	MAINLIB
16	755	765	2.23	9-Octadecenoic acid	MAINLIB
17	755	756	2.23	14-Octadecenoic aci	MAINLIB
18	754	758	2.14	Octadec-9-enoic acic	MAINLIB
19	753	755	2.06	6-Octadecenoic acid	MAINLIB
20	751	753	1.90	Oleic anhydride	MAINLIB
21	750	754	1.82	Ethyl Oleate	replib

Figure 38: A Library search of the EI chromatogram peak retention time of 30.96 (to 30.99) minutes found a C18:1 FAME from oleic acid, which agrees with identification based on the molecular weights of three most common ions expected to be generated by CI of that FAME and detected in the sample (Figure 37).

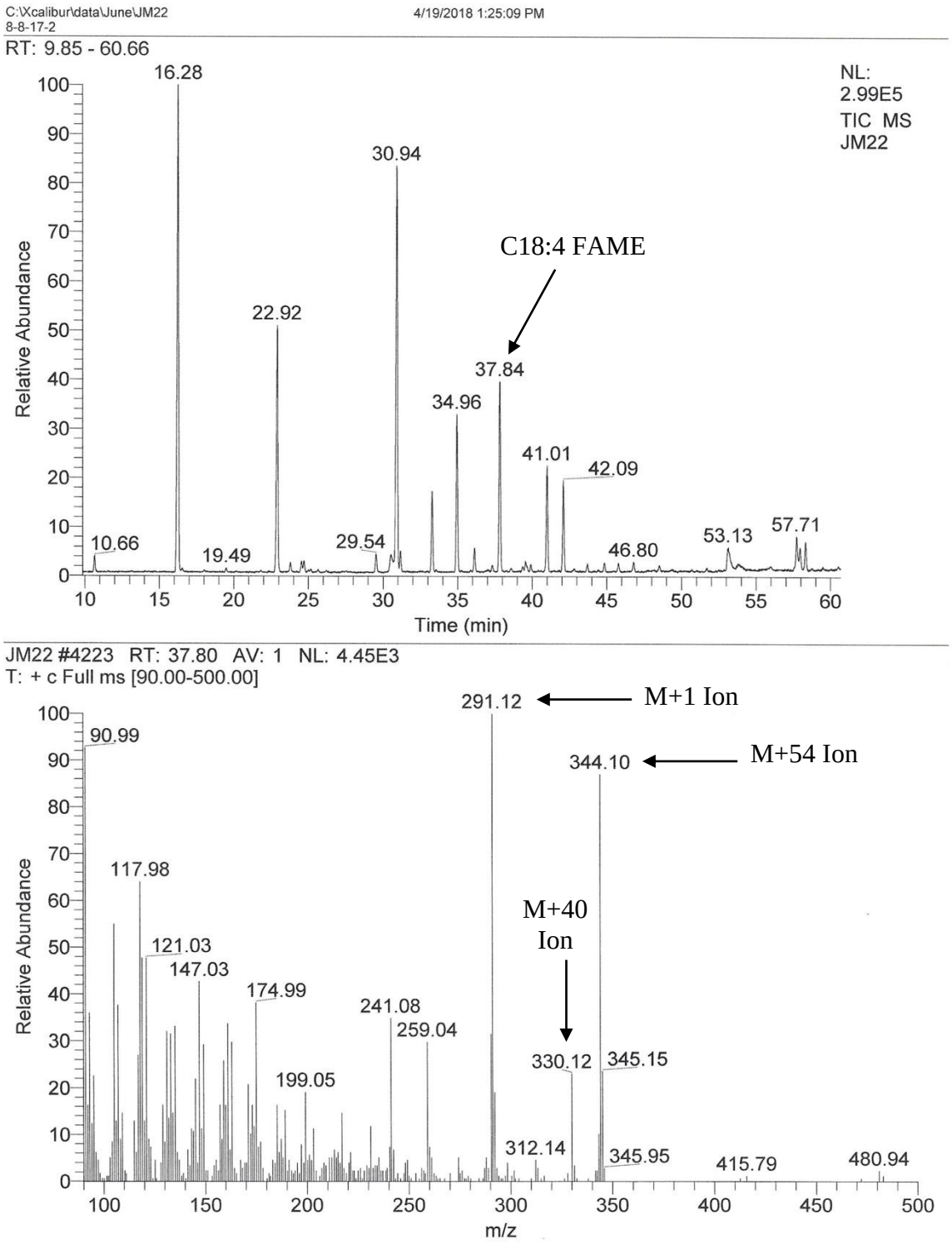

Figure 39: The CI chromatogram for treatment No. 2, Day 27, with the peak at 37.80 to 37.84 selected. The mass spectrum indicates high concentrations of ions with molecular weights 291, 344 and 330 AMU. These weights correspond to the M+1, M+54 and M+40 ions from a C18:4 FAME.

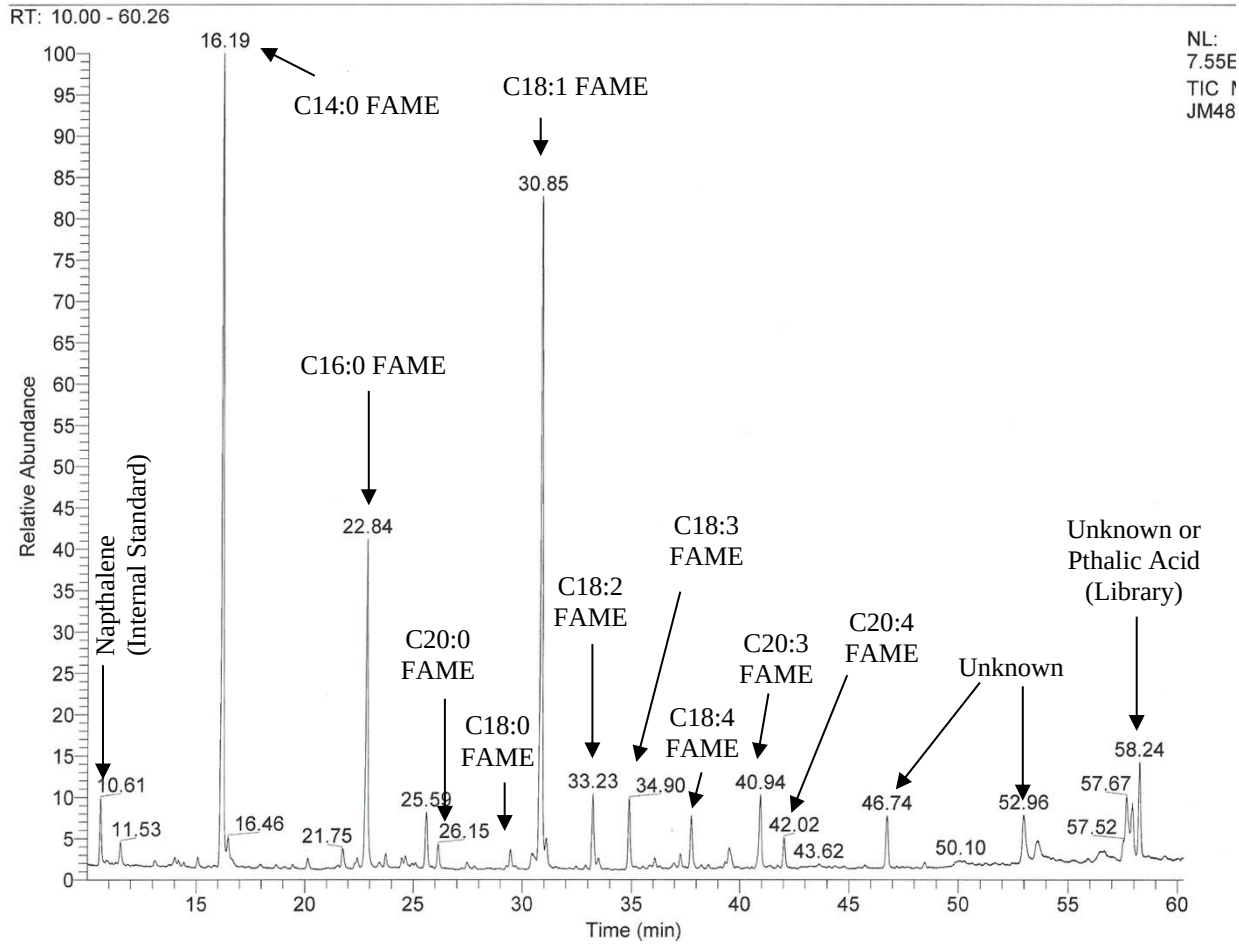

Figure 40: The EI chromatogram from treatment No. 5, sample day 27, with the peaks matched to the retention times of FAMEs that were identified by the CI method. The peaks represent the signal intensities at the retention times of the detected compounds.

2.4.4. Relating EI Chromatography Peak Areas (Signal Intensities) to Quantities of FAMEs in Each Sample

The areas of each peak (representing signal intensity) observed in the EI chromatogram of a sample are related to the amount of each compound in the sample, but also on the individual physical and chemical characteristics of the compound. The amount of a FAME in the sample can be calculated if a response factor from a standard of the same (or very similar) type of FAME is known, and if a known quantity of internal standard has also been added to the sample.

2.4.4.1. Response Factors from FAME Standards

Response factors (describing the correlation between peak area and concentration) had been previously calculated from sets of five dilutions (each) of seventeen representative known FAME standards (Mondloch, 2012, Ostrom, 2012). The mean response factor (excluding outlying values) from fourteen sets of dilutions was chosen to calculate concentrations of each FAME, relative to the peak area values from the EI signal (Table XI). For identified FAMEs that did not correspond to one of the previously determined response factors, response factor values were estimated, based on the most similar FAMEs for which response factors had been determined. When both the peak area value and an appropriate response factor value for an identified FAME were known, the concentration of that FAME in the sample could be determined (Table XII).

Table XI: Relationship between peak area values and FAME concentrations. The following equations are two ways of expressing the same relationship.

Equations:

$$RF = (A_{FA}/ C_{FA})/(A_{IS}/C_{IS}) \quad \textbf{(18)}$$

$$C_{FA}= ((C_{IS} * A_{FA})/A_{IS})/RF \quad \textbf{(19)}$$

Definitions of Terms:

RF = Response Factor

A_{FA} = Peak Area of Fatty Acid Methyl Ester

C_{FA} = Concentration of FAME in the Sample

A_{IS} = Peak Area of Internal Standard

C_{IS} = Concentration of Internal Standard

Table XII: Mean response factors and estimated response factor values based on FAME standards with similar properties. The GC/MS CI method indicated a peak at 19.82 minutes with molecular weights representing C17:2 in some samples, C18:1 in others, or a combination of the two. The GC-MS software library identified several peaks, including one at 47.67 minutes, as representing phthalic acid, which is likely to be a contaminant from plastic containers.

Mean RT-Naphthalene RT (Minutes)	FAME Detected	Mean Response Factors	Mean Response Factor of RF Estimate based on Closest Match
0.00	(Naphthalene)		
5.60	C14:0	1.53	
8.86	C15:0	1.22	
12.27	C16:0	1.47	
13.61	C16:1	1.16	
13.91	C16:1	1.16	
14.05	C16:1	1.16	
14.36	C16:1	1.16	
14.53	C17:0	1.14	
15.53	C20:0	1.38	
16.79	C16:2	1.16	Estimate
18.23	C16:2	1.16	Estimate
18.90	C18:0	1.56	
19.82	C17:2 and/or C18:1	1.24	Estimate
20.25	C18:1	1.24	
20.53	C18:1	2.68	
22.68	C18:2	2.93	Estimate
24.35	C18:3	1.44	Estimate
25.51	C18:3	1.44	Estimate
26.48	C18:4	1.44	Estimate
27.22	C18:4	1.44	Estimate
28.90	C18:4	1.44	Estimate
29.28	C18:5	1.44	Estimate
30.37	C20:3	1.38	Estimate
31.16	C22:0	0.72	Estimate
31.47	C20:4	1.38	Estimate
32.42	C22:1	0.72	Estimate
33.08	C20:4	1.38	Estimate
34.21	C20:5	0.66	
34.75	C21:4	0.72	Estimate
37.43	C22:4	0.72	Estimate
40.06	C22:5	0.72	Estimate
41.06	C22:6	0.72	Estimate
45.34	C25:1, C26:8, aromatic FAME or unknown (not FAME)		
47.05	C25:0, C26:7, C20:8 or other aromatic FAME		
47.67	unknown/phthalic acid		

2.5. Additional FAME Analysis by Algal Genomics and Synthetic Biology Laboratory, National Research Council Canada

A sample set that was harvested on day 34 was sent for analysis to Dr. Stephen J.B. O'Leary and Dr. Fabrice Berrue at Algal Genomics and Synthetic Biology Laboratory, National Research Council, Canada. The sample was divided and prepared by two methods, whole biomass FAME conversion and chloroform/methanol lipid extraction (a similar method is described by Bligh and Dyer, 1958), and both sets were analyzed by GC-FID (Flame Ionization Detection) and nuclear magnetic resonance spectroscopy (NMR) by Dr. Fabrice Berrue.

3. Results and Discussion

3.1. Initial Observations of Culture Re-Isolated from a Dormant Culture

C. freiburgensis non-motile cells, growing on a surface appear as a thin, black coffee-colored biofilm. After placing scrapings of this biofilm from a bottle that had contained a culture the previous year (April 23, 2015), into centrifuge tubes containing MAM with pH ranging from 2.4 to 2.8, and allowing them to become acclimated in the lighted culture chamber for 20 days, vigorous growth was observed in all six tubes. The cells growing in all six tubes were identified as *C. freiburgensis*, and no other algal species appeared to be growing in any of the six. In the tubes containing pH 2.5 and 2.4 medium, three types of *C. freiburgensis* cells were observed, normal-sized (5-7 µm), smooth, round, non-motile cells; oblong, flagellated (4 – 5 µm) swimming cells; and extra-large (12-16 µm), round, non-motile cells, which were hypothesized to be specialized resting, nutrient-storing cells similar to auxospores (in diatoms). The extra-large cells contained numerous uniformly-sized, translucent, colorless spheres, which were hypothesized to be lipid droplets, as illustrated in early species descriptions (Doflein, 1921) and in descriptions of other chrysophytes (Andersen, 2010). In tubes containing pH 2.8 medium, normal-sized, round, non-motile cells were present. Fungal hyphae were also observed to be present in five of the six tubes. All six centrifuge tubes contained plentiful algal growth, but the cells growing in the tubes containing pH 2.5 medium appeared to be slightly more robust than in the others, and these were chosen to start subsequent cultures.

3.2. Cell Types and Behavior

Throughout the experiment, the dominant form taken by *C. freiburgensis* cells was the normal-sized (5 – 7 µm), spherical non-motile (cyst) form, in all six treatments. This was

observed to be the actively growing cell type. Until nutrient levels began to become depleted, normal-sized non-motile cells each contained a single, gold-colored chloroplast and were covered by a translucent, glass-like cyst (shell-like covering). No cyst surface ornamentation, scales or collar was visible by light microscopy. Also, though no pore or plug was observed by light microscopy, SEM images had revealed the presence of a pore, without a collar, in cells from a previous batch culture in a previous experiment by a Montana Tech student (Figure 41, Bocioaga, 2003). When actively growing, cells were most often observed as pairs or clusters of three or four cells in the process of dividing.

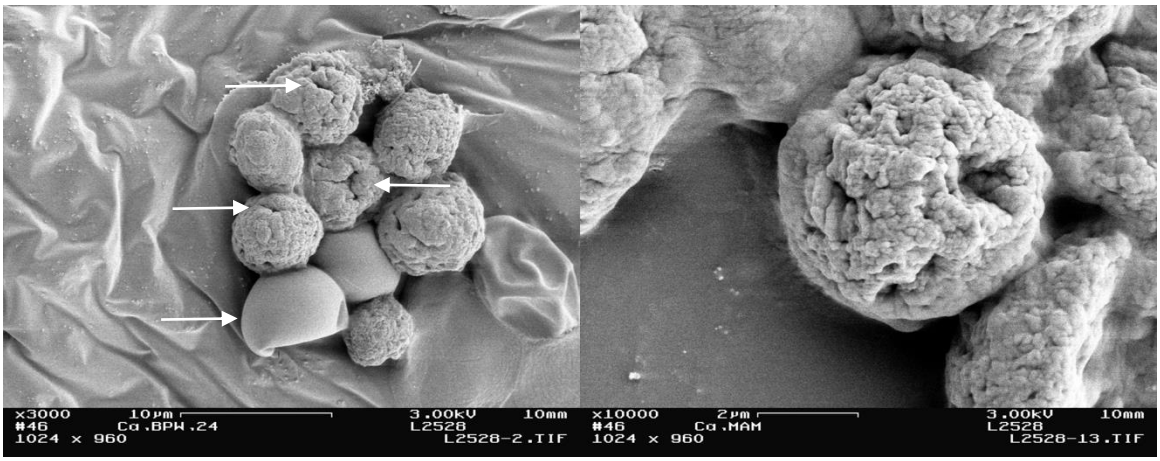

Figure 41: SEM images of Berkeley Pit Lake *C. freiburgensis* non-motile cells by Daniela Bocioaga (2003). Pores are visible on three cells in a cluster with two empty cysts (Left). The empty cysts do not appear to have external ornamentation (scales or spines), and no collars are visible on the pair above. A pore is clearly visible (Right center), but a prominent collar is not visible. It is possible that small collars may be hidden beneath the two empty cysts or by the external membrane and mucilage, which were not removed in preparation for SEM examination.

An event where the majority of cells converted to the swimming form was not observed in any of the six treatments, but a few swimming cells were observed on the eighth day in Treatment No. 2 (low nitrogen), No. 5 (low nitrogen, low phosphorus and CO_2) and No. 6 (intermittent nitrogen feeding). Small numbers of swimming cells were observed to occur in all treatments with the exception of No. 4 (low nitrogen and phosphorus without supplemental

CO_2). They were observed to be active only during brief intervals (one to three days) in two low nitrogen treatments (No. 2 and No. 5) and in the intermittent nitrogen feeding treatment (No. 6). Swimming cells were present throughout the growth period starting by day 15 in Treatment No. 1 (nutrient replete "control"), and starting on day 9 in Treatment No. 3 (low phosphorus). A complete conversion from non-motile to swimming cells (≥ 90% of cells at a time) was not observed in any of the six treatments, though such an event had been observed in a pair of one-liter batches growing with the same treatment conditions (except for volume) as No. 1 (high nutrient "control").

Extra-large cells were observed to occur in all six treatments, however, they were not observed until day 52 in No. 1 (high-nutrient "control"). Extra-large cells were observed earliest, on day 8, in the two low nitrogen, low phosphorus treatments (No. 4 and 5). Four days later they began to appear in the low phosphorus treatment (No. 3) and the intermittent nitrogen feeding treatment (No. 6).

3.3. Observation of External Features of Cell Wall and Siliceous Cyst

Dr. Bill Granath and Dr. Jim Driver, at University of Montana, Missoula accepted samples and prepared Scanning Electron Microscope (SEM) images of samples from a one-liter culture in standard MAM that was nearing the end of its growth cycle (late stationary phase). It had been anticipated that external cyst ornamentation, if any, and especially a pore collar, would be observed. A few of the images did appear to show a cyst with no external ornamentation (Figures 42 and 43), which is consistent with descriptions of *C. freiburgensis* (Doflein, 1921). Indentations in some cells may indicate the position of a pore without a collar or with a very small collar, but these may also be artifacts of the SEM preparation process. None of the SEM

images clearly revealed a pore collar or pore plug. Ideally, preparation of chrysophyte cysts for SEM observation should include chemical removal of the outer membrane and mucilage covering, to reveal identifying features of the siliceous cyst.

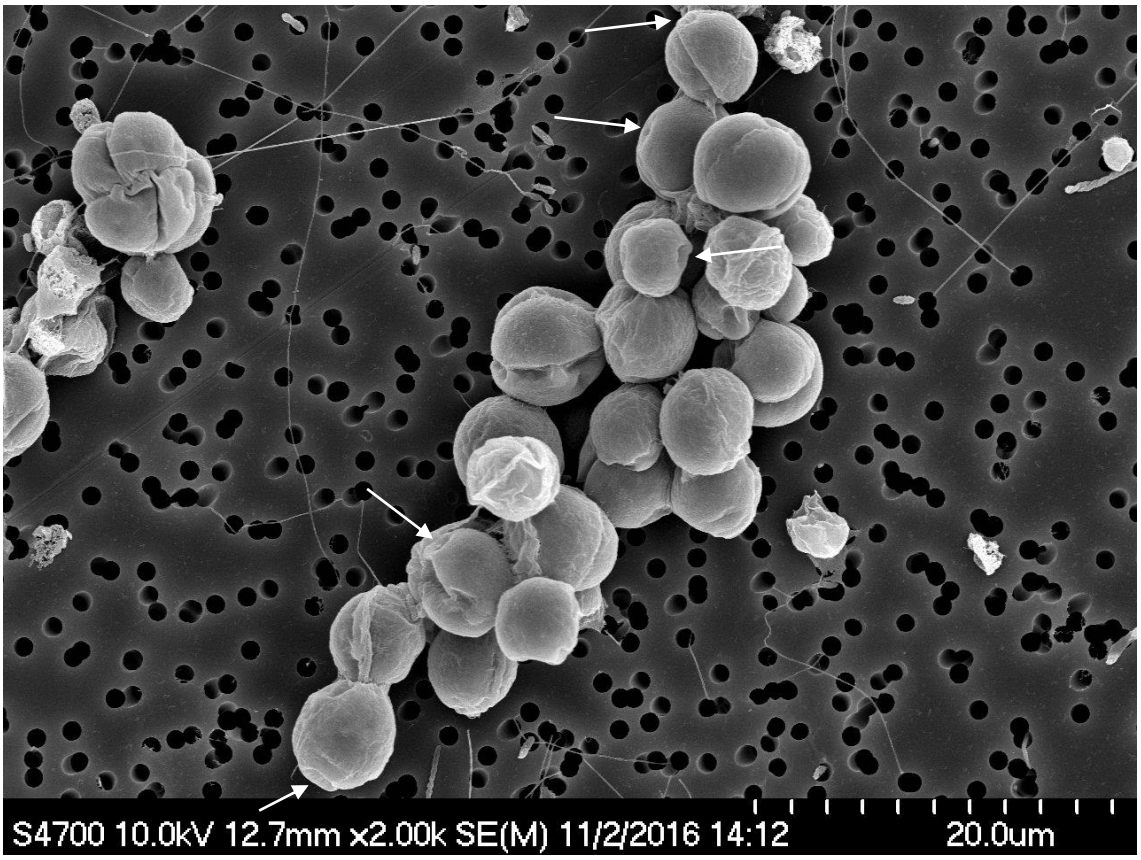

Figure 42: SEM image (Dr. Jim Driver, 2016) of *C. freiburgensis* non-motile cells. The cells' outer surfaces appear smooth, lacking external spines or scales. A few cells have indentations which may indicate the location of a pore without a collar, or with a very small collar (arrows). The presence of longitudinal creases indicate that some cells are in the process of mitotic division, and growing, though the sample was collected late in the stationary phase. Fungal hyphae and bacteria are also visible in the image.

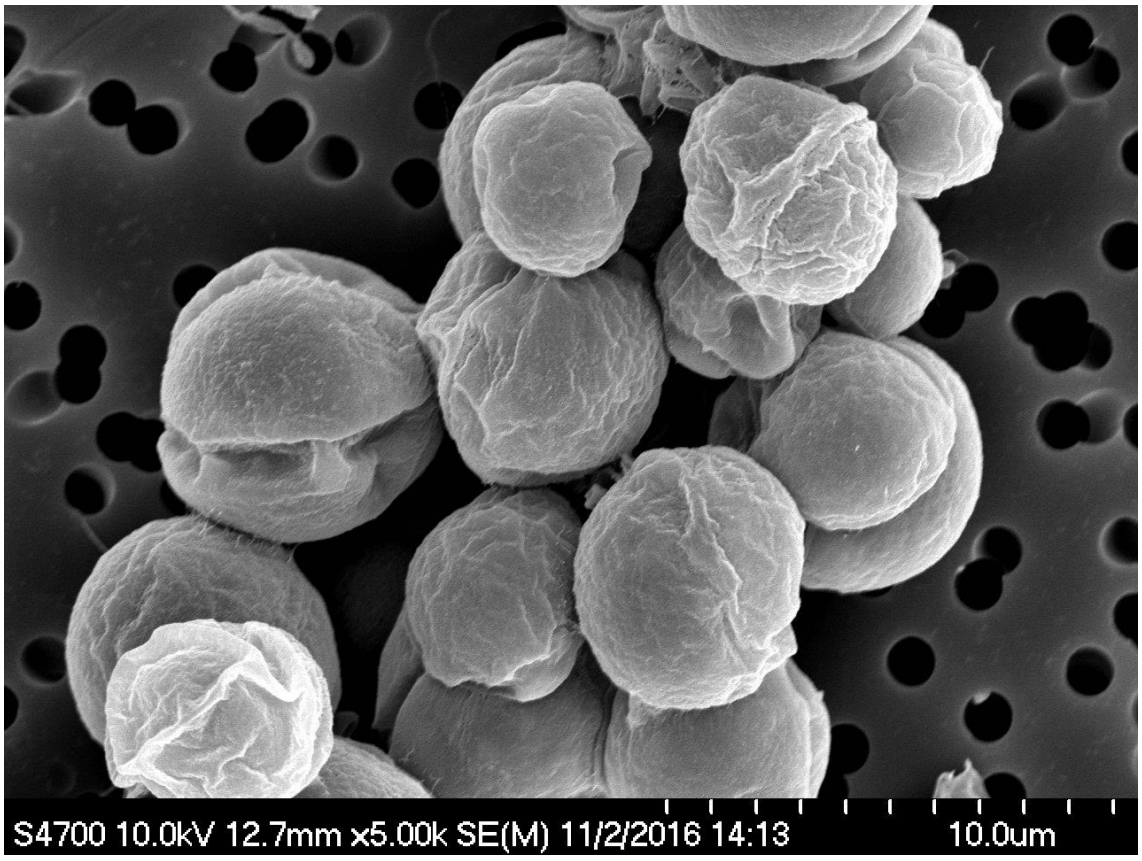

Figure 43: SEM image of *C. freiburgensis* non-motile cells (Dr. Jim Driver, 2016). An indentation in the surface of one cell that may indicate the position of a pore (arrow). Ideally, the outer covering of membrane and mucilage should be removed for a clear view of the siliceous cyst.

3.4. Growth and Cell Density

After ten days, the difference in growth response to each of the treatments, in particular, between the low nitrogen and the high nitrogen treatments, became visible and obvious, and the difference became more apparent with time. At a glance, the color distinguished three of the low nitrogen treatments No. 2, No. 4, and No. 5 from the others. Because of the increasing difference in cell densities, the two high nitrogen treatments (No. 1 and No. 3) quickly became darker in color until, at peak density, they resembled opaque black coffee, while the three low nitrogen treatments became a translucent green-gold color. Microscopic examination revealed that the lighter color observed in the low nitrogen treatments was not only caused by lower cell

densities, but the pigmentation of the chloroplasts in the low nitrogen cells also appeared to be fading. After approximately 34 days, the suspended cell densities of the three higher nitrogen cultures (No. 1, No. 3, and No. 6) had all begun to decrease, while the three low nitrogen cultures (No. 2, No. 4, and No. 5) remained static.

3.5. Slight Decrease in Medium pH of Three Treatments

It was expected that photosynthesis by the alga could result in a slight increase in pH in all six experimental treatments, or that there would be no measurable change in pH, because MAM functions as a buffer. The pH of the medium was monitored four times (on day 12, 15, 23 and after 105 days), in all six experimental treatments, after cultures were started (Appendix C).

No increase in pH above 2.5 was observed in any of the six treatments. A small decrease in pH was observed in treatments No. 1 (nutrient replete MAM), No. 3 (low phosphorus) and No. 6 (intermittent nitrogen feeding). The change in pH occurred prior to day 23, and pH remained stable from day 23 to day 105 (after culture crash in all six treatments and 53 days after the final algal sample was collected). After 105 days, the greatest change was observed in treatment No. 3 (low phosphorus), with a decrease of 0.26, from pH 2.5 to pH 2.24. The observed decrease was unexpected, and the reason for it is not known. The error in pH measurements was estimated to be approximately ± 0.05 of a unit. If the pH measurement error is greater than estimated, the observed decrease may not be significant.

3.6. Growth Changes in Responses to Experimental Nutrient Concentrations

C. freiburgensis followed a predictable pattern, similar to that of many different microorganisms, when grown in batch culture (Figure 44). The six treatments differed in growth rates and in the amount of time spent in each growth phase (Table XIII and XIIV). As expected, starting with cells from a younger culture, that was in the transitional phase, starting linear growth, shortened the lag phase of growth. For the shortest possible lag phase, it is best to start with cells that are in the exponential growth phase. The lag phase lasted approximately three days, and *C. freiburgensis* cells in all six treatments had entered the exponential growth phase by the end of the third day after inoculation.

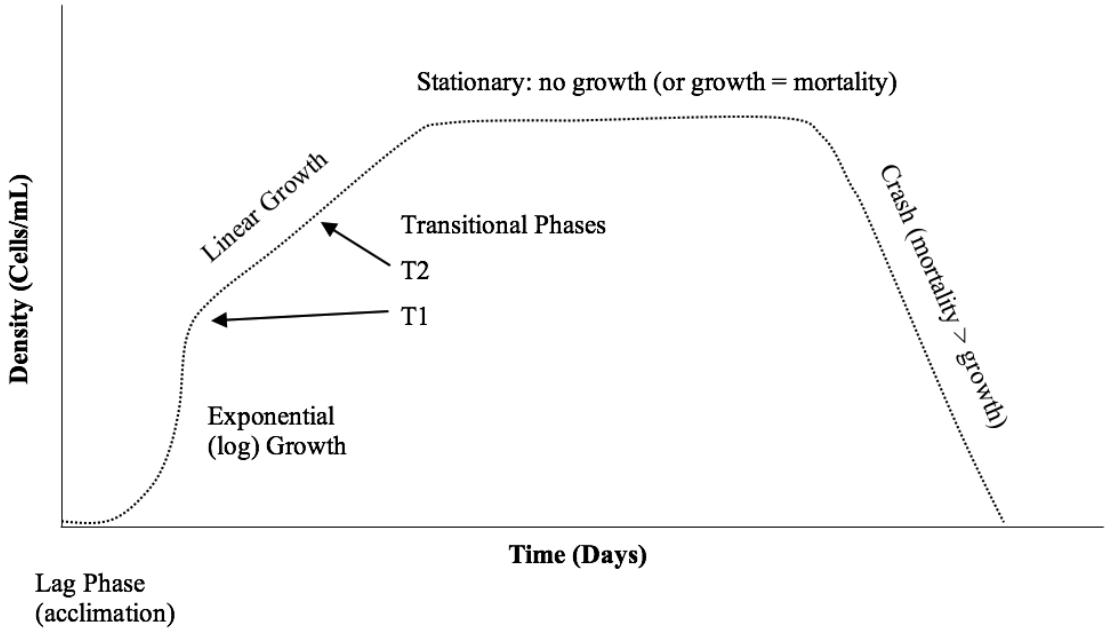

Figure 44: A generalized growth curve for a microalgal species in batch culture. The transition between exponential and stationary growth may include a period of linear growth, and is shown as two transitional phases (described as T1 and T2 by Palenik and Wood, 1998).

Table XIII: Differences in the lengths of growth phases between six experimental treatments (unshaded portion, treatments No. 1 – No. 6). *Precise timing of "crash" phase was not possible because cells formed flocs, fell out of suspension or adhered to vessel walls, and could no longer be counted, while slow growth continued. Because only suspended cells could be counted, it was not possible to determine when mortality exceeded generation of new live cells. Information from earlier cultures (No. 7 – No. 10) is included.

Culture Volume (L)	Culture or Treatment No.	Days Until Peak Cell Density	Approx. Lag Time (Days)	Approx. No. of Days of Exponential Growth	Approx. No. of Days of Transitional or Linear Growth	Approx. No. of Days from Inoculation to beginning of Crash*
1.00	No. 7, Standard MAM	36.04	3	3 to 7	38	≥44
1.00	No. 8, Standard MAM	43.03	3	4 to 6	36	≥45
1.00	No. 9, Standard MAM	53.94	12	14	56	≥76
1.00	No. 10, Standard MAM	53.94	12	7 to 11	54	≥76
8.00	No. 1, Standard MAM	34.02	3	5	≥25	≥52
8.00	No. 2, Low N	12.04	3	5	3	≥52
8.00	No. 3, Low P	34.02	3	5	≥25	≥52
8.00	No. 4, Low N & Low P	19.03	3	5	6	≥52
8.00	No. 5, Low N & Low P + CO_2	23.86	3	6	3	≥52
8.00	No. 6, Intermittent N Feeding	27.02	3	5	≥15	≥52

Table XIV: Comparison of 10 cultures (No. 7 – No. 10 were grown before No. 1 – No. 6). Length of lag phase (Table XII, above) is most often positively correlated to the age of the starter culture.

Culture or Treatment No.	Culture Volume (L)	Age of Starter Culture (Days)	Growth Stage of Starter Cells	Inoculation Date (Day 0)	Length of Lag Phase (Days Until Start of Exponential Phase)	Maximum (Peak) Cell Density (cells/ml)
No. 7, Standard MAM	1.0	50	Stationary	1/21/16	3	3.01E+07
No. 8, Standard MAM	1.0	50	Stationary	1/21/16	3	2.81E+07
No. 9, Standard MAM	1.0	58	Late Stationary	3/19/16	12	2.85E+07
No. 10, Standard MAM	1.0	58	Late Stationary	3/19/16	12	3.82E+07
No. 1, Standard MAM	8.0	14	Transitional	7/12/17	3	3.33E+07
No. 2, Low N	8.0	14	Transitional	7/12/17	3	9.70E+06
No. 3, Low P	8.0	14	Transitional	7/12/17	3	2.78E+07
No. 4, Low N & Low P	8.0	14	Transitional	7/12/17	3	9.83E+06
No. 5, Low N & Low P + CO_2	8.0	14	Transitional	7/12/17	3	1.11E+07
No. 6, Intermittent N Feeding	8.0	14	Transitional	7/12/17	3	2.43E+07

The length of the period of exponential growth can be identified by plotting the log of the cell counts versus time (Figure 45). Choosing counts and times of two points within the exponential growth phase allows the calculation of a growth constant, that reveals the doubling time (T_2) and the number of times cells double per day (k) (Table V and XVI). Cells in all six treatments maintained exponential growth for between five and six days. The most obvious difference in growth occurred in response to the concentration of nitrogen in each treatment.

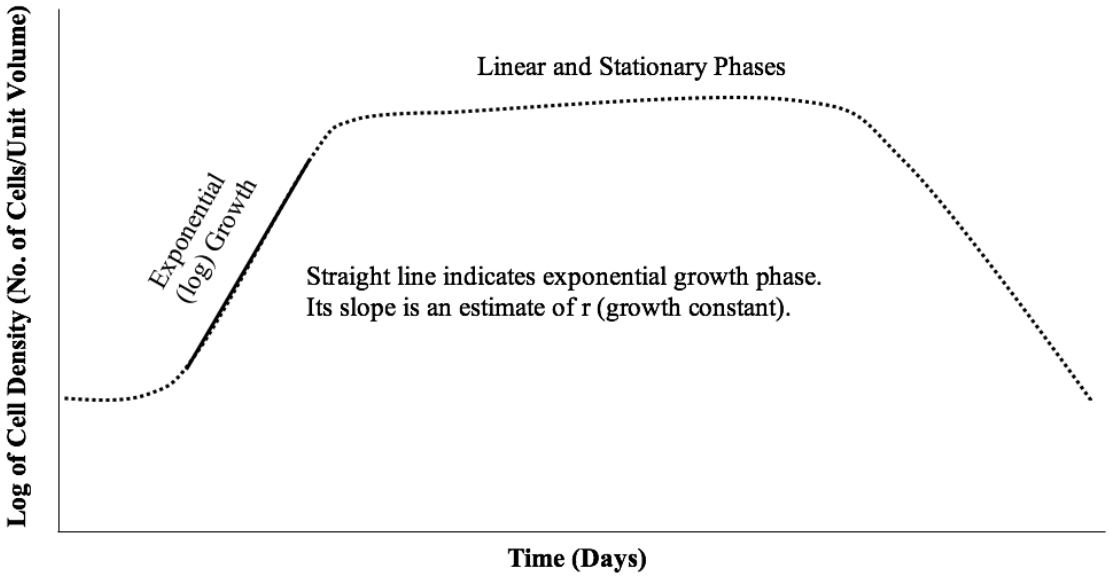

Figure 45: Cells are undergoing exponential growth during the period of time where there is a linear relationship between the log of the cell density (No. of cells/unit volume) vs. time.

3.6.1. Rapid Transition to Stationary Phase in Low Nitrogen Treatments

All three treatments with low nitrogen (No. 2, No. 4, and No. 5) began to transition out of the exponential growth phase on day 8 or 9, and had entered the stationary phase by day 15 (Figure 46). They exhibited relatively short transitional phases, compared to the three high nitrogen treatments. All three low nitrogen treatments reached maximum cell densities, of approximately 10,000,000 cells/mL, between day 12 and 15.

3.6.2. Extended Phase of Linear Growth in High Nitrogen Treatments

All three treatments with higher nitrogen concentrations (No. 1, No. 3 and No. 6) began to transition out of exponential growth near the same time as the three low nitrogen treatments, but these entered an extended period of linear growth, before entering a stationary phase that occurred approximately 10 to 20 days later and was difficult to characterize (Figure 46 and Table XV). All high nitrogen treatments reached cell densities greater than 24,000,000 cells/mL by day 27, and Treatment 1 (high-nutrient "control") reached 33,000,000 cells/mL on day 34.

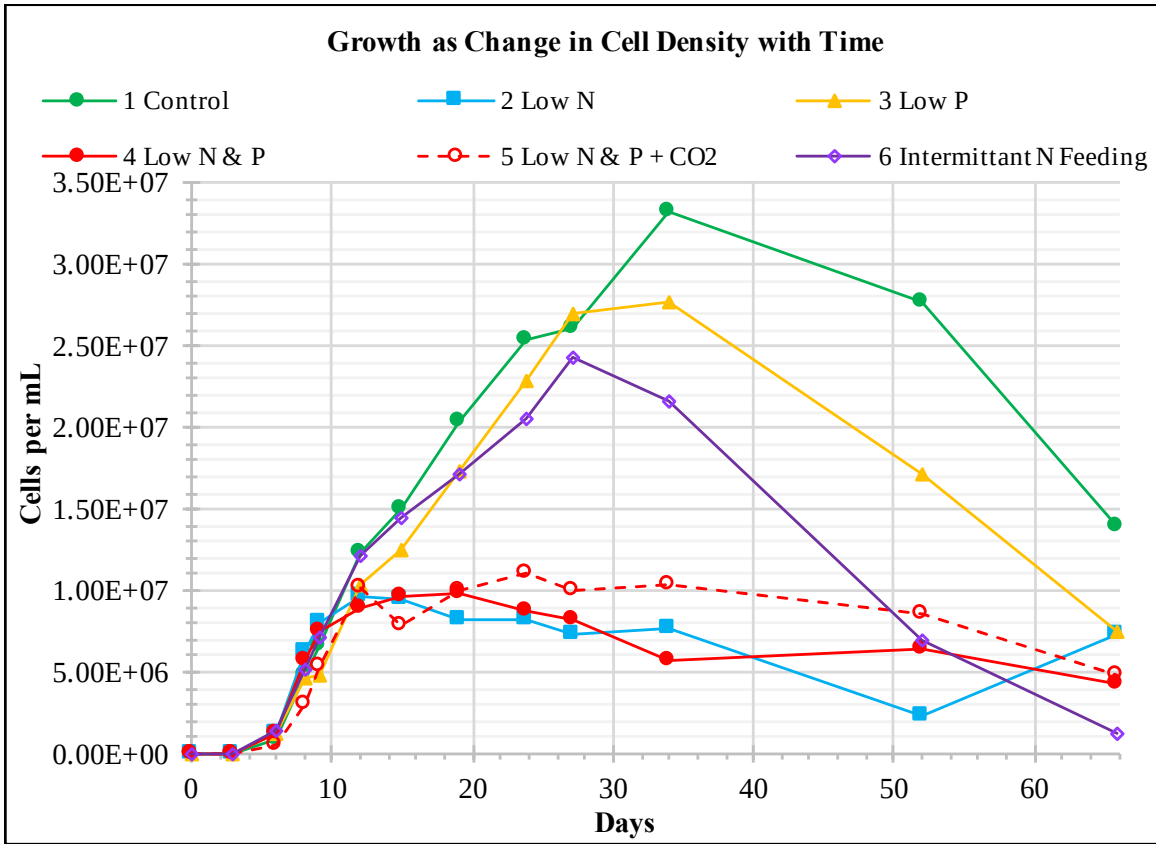

Figure 46: Comparison of *C. freiburgensis* growth, as change in cell densities (cells/mL) over time, in six experimental treatments. Decreasing cell densities in treatments number one, three and six, after day 27 to 34, do not indicate actual decline in numbers of living cells. Large clumps of cells, attached cells and flocculation of algal cells with fungal hyphae prevented accurate counts after high suspended cell densities were reached.

Table XV: Cell counts in six experimental treatments (illustrated in Figure 46). Peak cell densities for each treatment culture are shown in bold font.

Day	Day (Fraction)	1. Control	2. Low N	3. Low P	4. Low N & P	5. Low N & P + CO2	6. Intermittent N Feeding
0	0.00	2.69E+04	2.69E+04	2.69E+04	2.69E+04	2.69E+04	2.69E+04
3	2.92	3.39E+04	7.78E+04	7.89E+04	6.94E+04	5.83E+04	7.94E+04
6	5.94	8.20E+05	1.18E+06	1.24E+06	1.28E+06	6.20E+05	1.50E+06
8	8.03	4.80E+06	6.30E+06	4.63E+06	5.65E+06	3.10E+06	5.13E+06
9	9.05	6.70E+06	8.00E+06	4.90E+06	7.60E+06	5.33E+06	7.15E+06
12	12.04	1.23E+07	**9.70E+06**	1.05E+07	8.90E+06	1.02E+07	1.21E+07
15	14.94	1.50E+07	9.55E+06	1.26E+07	9.73E+06	7.83E+06	1.45E+07
19	19.03	2.04E+07	8.15E+06	1.73E+07	**9.83E+06**	1.01E+07	1.72E+07
24	23.86	2.54E+07	8.23E+06	2.30E+07	8.75E+06	**1.11E+07**	2.06E+07
27	27.02	2.61E+07	7.38E+06	2.70E+07	8.28E+06	9.95E+06	**2.43E+07**
34	34.02	**3.33E+07**	7.65E+06	**2.78E+07**	5.65E+06	1.04E+07	2.17E+07
52	51.98	2.77E+07	2.36E+06	1.73E+07	6.45E+06	8.60E+06	6.98E+06
66	65.90	1.40E+07	7.30E+06	7.58E+06	4.31E+06	4.81E+06	1.30E+06

3.6.1. Changes in Growth Rates as a Response to Nitrogen Depletion

Growth rates during the exponential phase did not appear to slow down earlier when the initial medium nitrogen concentration was lowered to 10% of that in the standard MAM formulation, therefore the length of the exponential growth phase was nearly the same in all six treatments. However, growth rates were affected by differences in nitrogen concentrations after the exponential growth phase had ended (Figure 47). In the three treatments with the lowest medium nitrogen concentrations (No. 2, No. 4 and No. 5), growth slowed abruptly during the transition out of the exponential growth phase. In the two treatments with the highest nitrogen concentrations (No. 1 and No. 3), growth slowed gradually after the end of the exponential phase, which resulted in an extended period of continued, linear net growth. In treatment No. 6 (intermittent nitrogen feeding), growth also slowed gradually after the end of the exponential phase, in a pattern more similar to the high nitrogen treatments than that of the low nitrogen

treatments. Slower initial growth in treatment No. 5 may be attributable to a temporary spike in CO_2 concentration. Cells in treatment No. 5 quickly recovered, and biomass and lipid yields did not appear to be negatively impacted.

Table XVI: *C. freiburgensis* growth rates during exponential growth phase in six experimental treatments (treatments No. 1 through No. 6) and four one-liter cultures (shaded squares).

Culture or Treatment No.	Culture Volume (L)	Time Interval, $\Delta t = t_t - t_0$ (Days)	N_t / N_0	$\ln (N_t / N_0)$	Growth Constant, r (*Day^{-1}) = $\ln (N_t / N_0)/\Delta t$	Increase in Cell Density from 2 Points (cells/ml) *Day^{-1}	Doublings per Day: k = r/ln2	Doubling Time (Days): T_2 = ln2/r	Doubling Time (Hours)
No. 7, Standard MAM	1.00	3.01	8.15	2.099	0.70	8.86E+05	1.01	0.99	23.86
No. 8, Standard MAM	1.00	3.86	25.69	3.246	0.84	1.90E+06	1.21	0.82	19.77
No. 9, Standard MAM	1.00	13.85	8608.28	9.060	0.65	1.04E+06	0.94	1.06	25.44
No. 10, Standard MAM	1.00	7.08	117.24	4.764	0.67	1.04E+06	0.97	1.03	24.72
No. 1, Standard MAM	8.00	2.09	141.64	4.953	2.37	2.28E+06	3.42	0.29	7.01
No. 2, Low N	8.00	2.09	81.00	4.394	2.11	2.98E+06	3.04	0.33	7.90
No. 3, Low P	8.00	2.09	58.63	4.071	1.95	2.18E+06	2.81	0.36	8.53
No. 4, Low N & Low P	8.00	2.09	81.36	4.399	2.11	2.67E+06	3.04	0.33	7.89
No. 5, Low N & Low P + CO_2	8.00	3.10	91.29	4.514	1.45	1.70E+06	2.10	0.48	11.44
No. 6, Intermittent N Feeding	8.00	2.09	64.51	4.167	2.00	2.42E+06	2.88	0.35	8.33

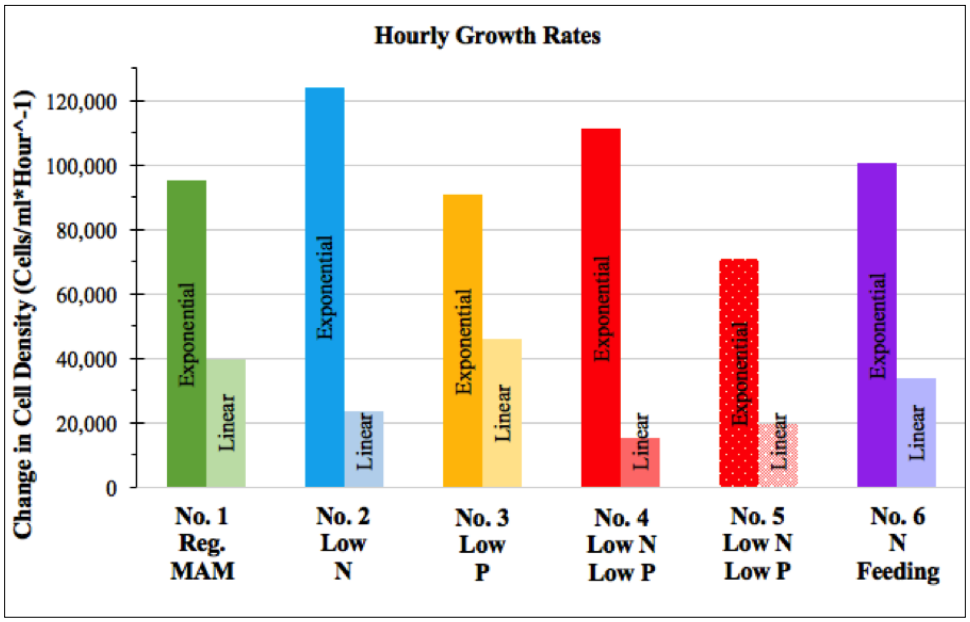

Figure 47: Comparison of hourly growth rates (increase in No. of cells per mL per hour) during the exponential growth phase and during linear growth (transitional phase) in cells per mL.

3.6.2. Physiological Changes Associated with Lipid Accumulation

After 15 to 24 days, cells in the low nitrogen batches began to lose their normal gold color, and their chloroplasts began to shrink, eventually becoming nearly invisible. The number of lipid droplets in the cytoplasm increased most rapidly in the low-nitrogen treatment cells, and they began to merge into larger drops (Figure 48). Between day 15 and 24, a few broken cells became evident in all but the nutrient-replete "control" treatment (No. 1); and, as time progressed, counting became more difficult for the low nitrogen treatments due to lipid-filled cells collapsing during microscopic observation. Their outer cysts and cell membranes had apparently become so fragile, that the change in their environment from placing them in the counting chamber, caused them to disintegrate.

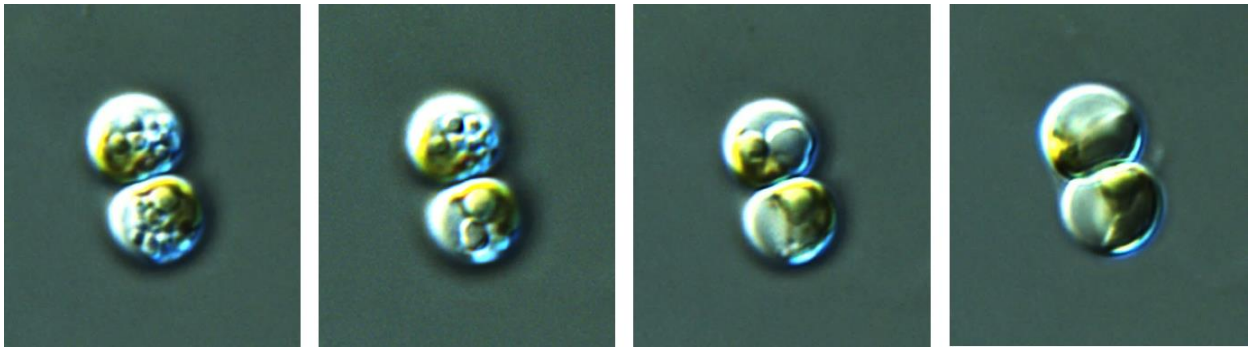

Figure 48: A sequence of photos of the same two cells in treatment No. 4 (low nitrogen and low phosphorus), taken at intervals of approximately 30-seconds to one minute apart, on day 25. From Left to Right, as the live cells begin to lose structural integrity, uniformly-sized lipid droplets within the cytoplasm begin to merge with one another until they become one large drop. By day 25, lipid-filled cells have become so fragile, that within a few minutes of transferring a sample from the culture vessel to a counting slide on the microscope stage, the cells begin to break down.

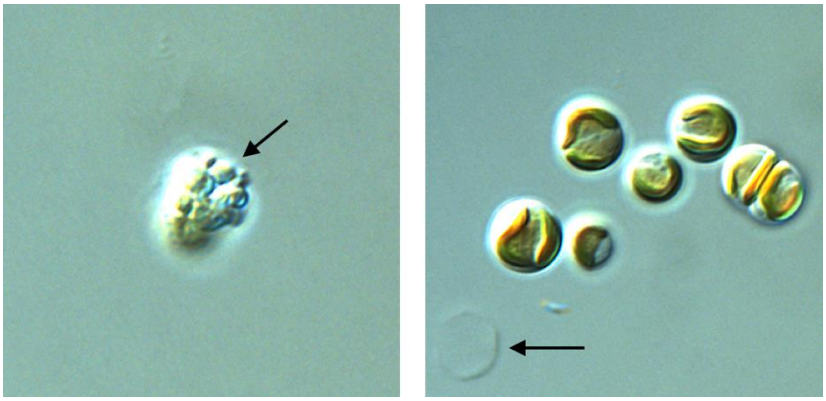

Figure 49: Left: A fragile, lipid-filled cell from treatment No. 6 (intermittent nitrogen feeding), on day 25, has shattered, leaving a cluster of lipid drops, free in the medium. Right: For comparison, cells from treatment No. 3 (low phosphorus only), on the same day, contain relatively few lipid droplets, and they appear to have maintained robust external and internal structures, including prominent, normally-colored chloroplasts (cell diameter is 5 to 7 µm). The presence of empty cysts (arrow) may either indicate cell mortality, or remain after some cells have transitioned to the swimming form).

Soon after the lipid droplets merge, the cells shatter, leaving visible lipid drops free in the medium (Figure 49). The fragility of the algal cells in this experiment may be partially due to insufficient silicon concentration in the medium, leading to a weaker cyst covering. However, cells in treatments number one and three (nutrient-replete and low phosphorus only), retained their structural integrity and the exceptional cell fragility was only observed to occur in the four

lower nitrogen treatments. Therefore, it is unlikely that insufficient silicon was a major contributor to cell fragility.

Because microalgal cells have been found to respond to nitrogen scarcity by prioritizing triglyceride production over growth (Griffiths, van Hille, and Harrison, 2012, Breuer et al., 2012), it is more likely that the cells became progressively more fragile as they diverted their resources and metabolic processes toward TAG accumulation, at the expense of those necessary to maintain structural strength. For example, lipids could be reallocated from cellular and organelle membranes, composed of phospholipids (Boyle et al., 2012, Fidalgo et al., 1998), and converted into TAG storage lipids. (Goncalves et al. (2013) reported that lipid bodies began to accumulate as early as three hours after nitrogen was removed from the medium, and organelles began to collapse after only 48 hours in one strain of the green alga, *Chlorella vulgaris* Beijerinck. Yoon et al. (2012) observed that chloroplasts were degraded as TAG (stored in lipid droplets) accumulated in *Chlamydomonas reinhardtii* Dangeard. The membrane containing the intracellular lipid droplets (or lipid bodies) may have become weakened if phospholipids from these were recycled for TAG production. It is conceivable that TAG accumulation in response to nitrogen depletion may also take precedence over the building and maintenance of elements of the cytoskeleton or the siliceous cyst.

3.6.3. Aggregation, Settling and Algal-Fungal Flocculation

It was hypothesized that cells in the three high nitrogen treatments entered the stationary growth phase within a few days of reaching peak cell densities, but cell counts did not illustrate stationary growth in these three treatments, because the counting method excluded cells that were no longer in suspension. At high densities, cells began to form clusters that increased in

size, and began to settle. Nourished by increasing concentrations of organic carbon provided by the alga (most likely secreted carbohydrates), fungal hyphae (of a yet-to-be-identified species) began to grow, speeding up formation of algal-fungal flocs (Figure 50). Algal-fungal flocs fell out of suspension and many attached to the inner surfaces of the culture vessels.

The counting method worked well for free cells and small clusters (≤ 30 cells) in suspension. However, it could not account for continued growth of cells in flocs that had fallen out of suspension or attached to surfaces, which resulted in decreasing cell counts, reflecting decreasing suspended cell densities. When flocs began to form, and they were observed microscopically, they contained large numbers of living algal cells, and little evidence of dead cells.

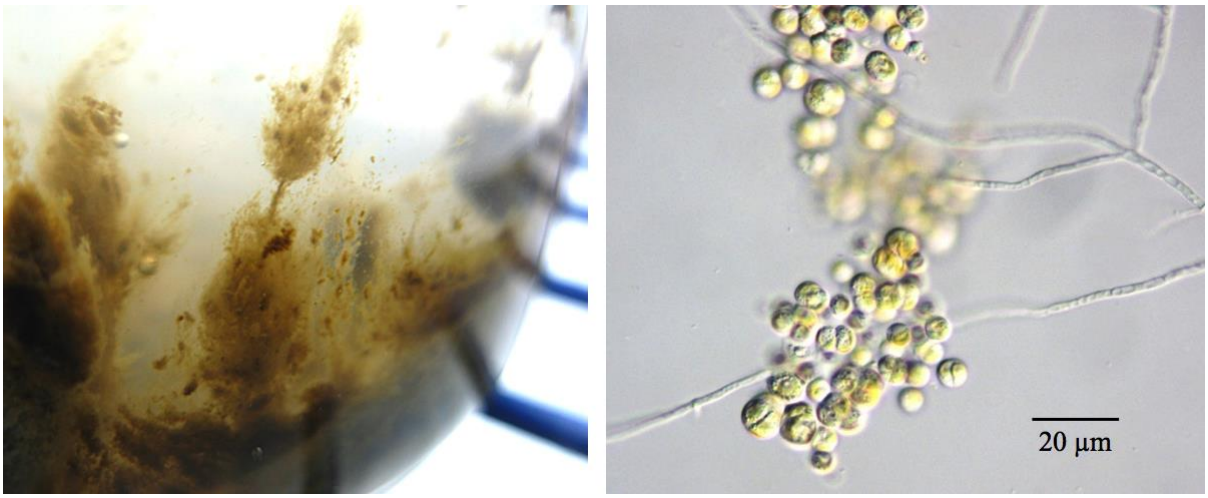

Figure 50: Algal-fungal flocs at the bottom of a one-liter culture vessel, macroscopic view (Left) and under magnification (Right). *C. freiburgensis* non-motile cells begin to cluster around fungal hyphae after these begin to grow in the medium. Fungal hyphae appear to collect algal cells, which may be related to some fungi having a positive (+) surface charge (Zhang and Hu, 2012). Microalgal cells generally have a negative (-) surface charge.

Because of flocculation that occurred in the three high nitrogen treatments, it was not possible to determine when cell mortality began to exceed growth, which would have indicated

the end of the stationary phase. It is hypothesized that the "crash" phase of *C. freiburgensis* in the six treatments most likely began at some point after 52 days in all six treatments, based on the appearance of increasing numbers of dead cells. In previous one-liter cultures grown in standard MAM, the "crash" most often appeared to occur at times ranging between 44 and 76 days after inoculation. Interestingly, fungal hyphae that grew in the low nutrient treatment cultures, after algal cells had amassed a large number of lipid droplets, appeared to contain lipid droplets themselves (Figure 51).

Figure 51: Fungal hyphae (of an unidentified species) surrounding *C. frieburgensis* cells that have amassed a large quantity of lipid droplets toward the end of their growth cycle. Several algal cells are visible that have lost the pigmentation of the chloroplast and become fragile. Fungal hyphae appear to contain numerous lipid droplets, presumably released from ruptured algal cells.

3.6.4. Swimming Behavior

Swimming behavior appeared to correlate to high nitrogen concentration (Table XVII), which was opposite of the conditions that were expected to trigger swimming behavior. Because swimming allows cells to disperse to new habitats, it was expected that cells would begin swimming in response to stressful environmental conditions, for example, nitrogen depletion, darkness or high or low temperatures. The greatest proportions of swimming cells were observed for the longest periods of time in treatments No. 1 and No. 3, the two highest nitrogen treatments. Swimming cells were observed on two sampling days in treatment No. 6 (intermittent nitrogen feeding). Swimming cells were only observed once, or not at all, in the three treatments with the lowest nitrogen concentrations (No. 2, No. 4 and No. 5).

Prior to the six experimental cultures, an event was observed where nearly all cells (approximately 90% to >95%) converted to the swimming form for a period of approximately four days, from day 7 to day 10 (Figure 52). On day 11, nearly all cells had resumed a non-motile form, leaving fewer than 1% swimming. This occurred simultaneously in two one-liter cultures (Bottles No. 7 and No. 8), while daily cell counts and observations were made. It was hypothesized at the time that a change in temperature may have triggered the swimming mass conversion event, but this potential cause was not confirmed. The transition from non-motile to swimming was observed as flexible, motile cells were observed to squeeze out through the pore of the spherical cyst of the non-motile form. Swimming cells appeared in two sizes, normally-sized (approximately 5 µm long, not including the flagellum) and smaller (approximately 3 µm long, not including the flagellum). Swimming cells assumed both the expected oblong shape and a spherical form that appeared to be transitional, as swimming cells began to form cysts. A similar event was not observed in any of the six experimental eight-liter cultures. In all five

treatments where swimming cells were observed during counting and sampling events, their relative proportion remained low (≤ 10%) compared to non-motile cell numbers.

Sexual reproduction has not been reported in the genus *Chromulina*, and its documentation was beyond the scope of these experiments. However, swimming can be a means of bringing cells in contact with one another for that purpose. Pairs of swimming cells were observed to remain in close contact for extended periods of time during the observed mass swimming event and also in treatment No. 1 (nutrient-replete "control") on day 34. It was not possible at the time to determine whether the prolonged contact was purposeful or if the motile cells had become entangled by chance.

For *C. freiburgensis* from Berkeley Pit Lake, swimming may not only be a means of escape from potentially stressful environmental conditions, but it may also be a response to high nutrient concentrations, and it may be a means of dispersal into new areas when cell densities are high. Swimming may also be associated with sexual reproduction, though it was not definitively observed in this experiment, and is not known to occur in *Chromulina*.

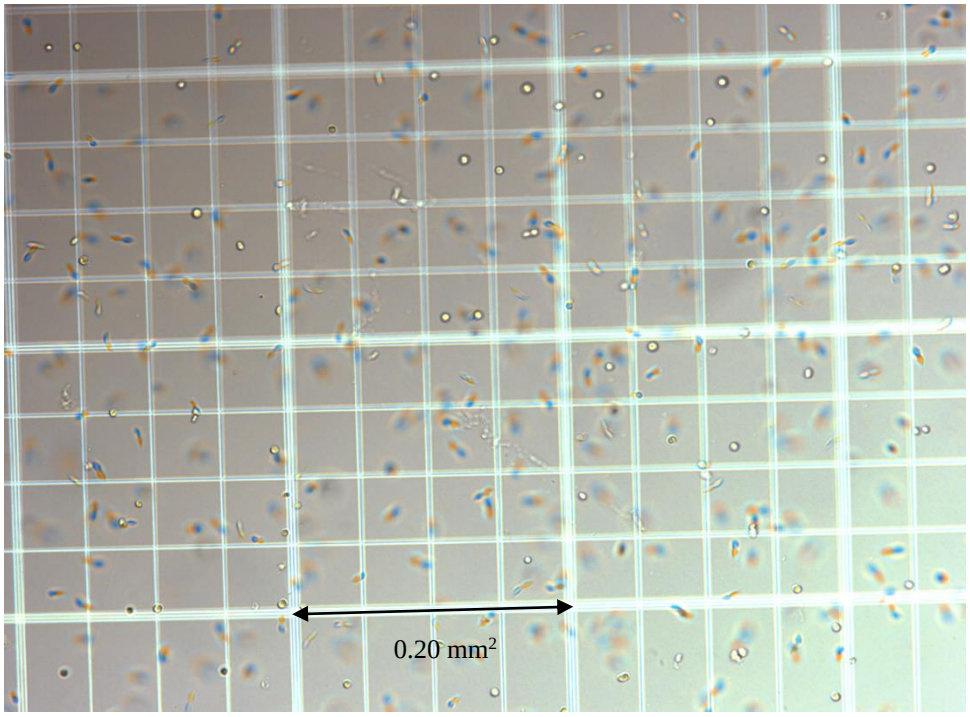

Figure 52: *C. freiburgensis* swimming cells in one-liter bottles No. 7 and No. 8, with standard MAM at pH 2.5. Nearly all non-motile cells converted to the swimming form for a period lasting approximately four days. Each triple etched line square measures 0.20 mm^2 and each single etched line small square measure 0.05 mm^2.

Table XVII: Comparison of changes in cell appearance and behavior in six treatment cultures. As low nitrogen cells accumulated large lipid stores, chloroplast color faded until they became nearly invisible, while cells became fragile. Cells in higher nitrogen treatments maintained active growth and structural integrity for a longer period, and began to amass lipid stores later.

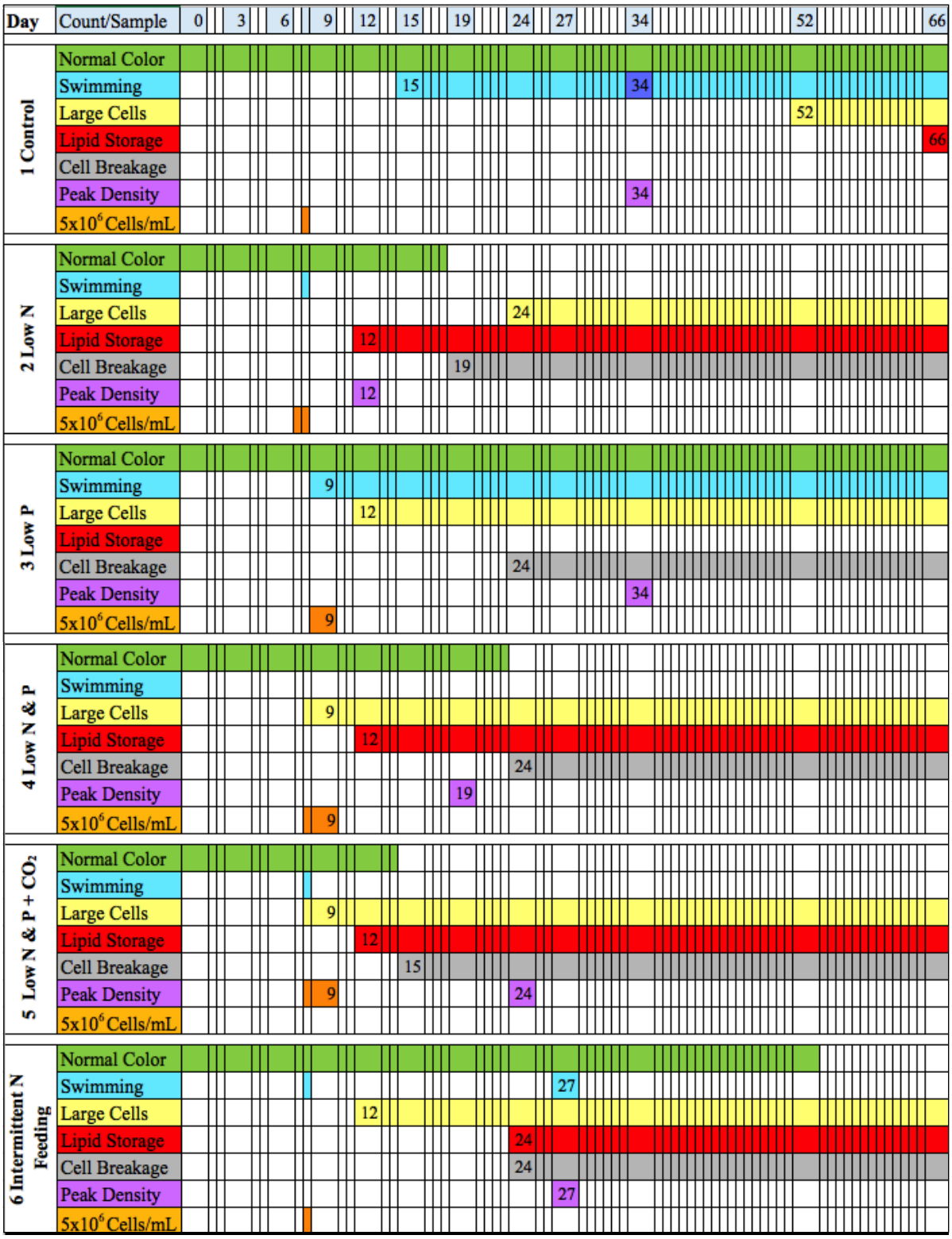

3.6.5. Extra-Large Cells

Extra-large cells (Figure 53) were observed earlier in all five treatments in which one or more nutrient concentrations were lowered. This supports the hypothesis that they may be a form of energy-storing, resting cell that occurs as a response to decreasing nutrients in the environment (Table XVII). Extra-large cells appeared earliest (on day 8) in the two treatments where both nitrogen and phosphorus concentrations were lowered (treatments No. 4 and No. 5). Interestingly, they were observed earlier (on days 9 – 12) in the four treatments with lowered phosphorus concentrations, No. 3 (low phosphorus only), and No. 4, No. 5, and No. 6 (low nitrogen and low phosphorus), than they were in treatment No. 2 (low nitrogen only). Extra-large cells were not observed until day 52 in treatment No. 1 (nutrient-replete "control"). Some extra-large cells appear to contain as many as six chloroplasts, while others only appear to contain a single chloroplast, as in a normally-sized cell. Numerous chloroplasts may result from incomplete cell division, where the contents of what would have normally been multiple cells end up sharing a single cell wall. Extra-large cells may also be a result of sexual reproduction or they could be the cells that form and release (4) gametes, which would have essentially the same appearance as asexual swimming cells.

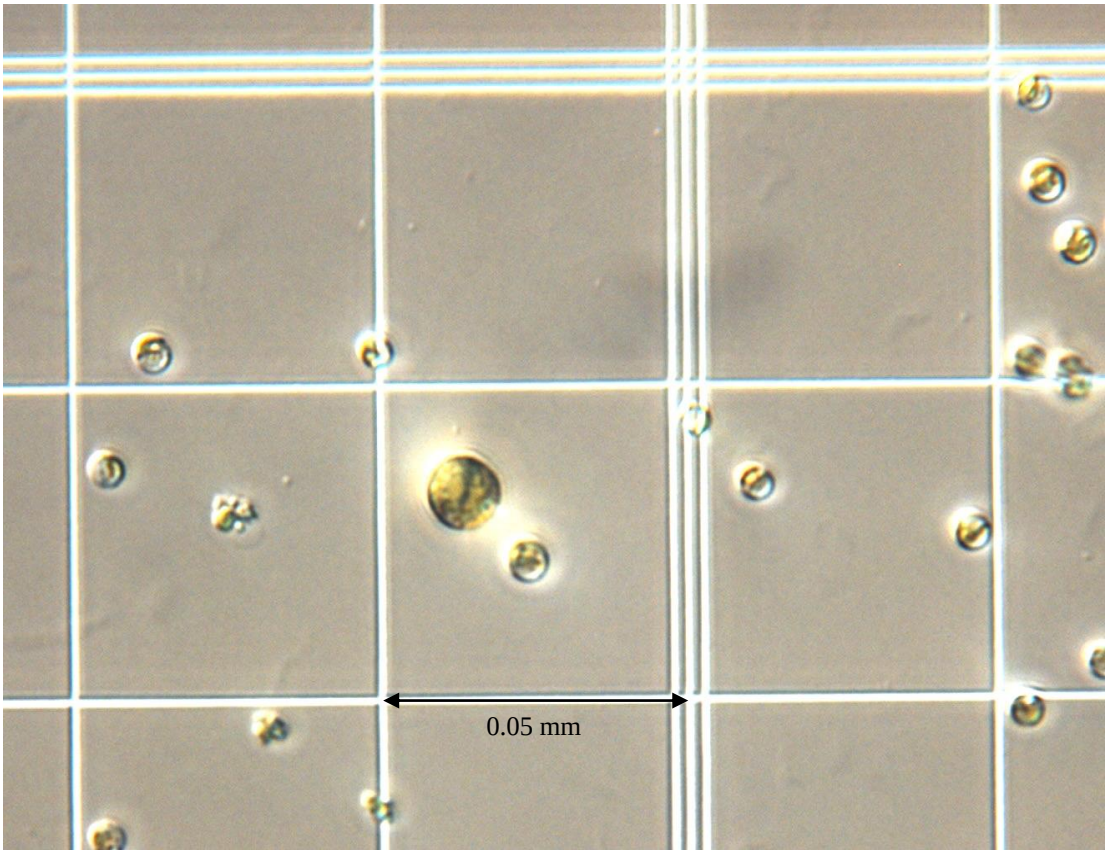

Figure 53: One *C. freiburgensis* extra-large cell (center Left) with normally-sized cells in treatment No. 4 (low nitrogen and low phosphorus). Large masses of lipid droplets have accumulated in many of the cells, and a few have shattered, spilling out lipid droplets (center Left).

3.7. Nitrogen and Phosphorus Concentrations

3.7.1. Nitrogen

The nitrogen concentrations that coincided with transition out of exponential growth in *C. freiburgensis* were between 90 and 110 ppm (parts per million) in the two treatments that started out with the highest nitrogen concentrations (No. 1 and No. 3, with 100% of the nitrogen in standard MAM). University of Georgia, Laboratory for Environmental Analysis (LEA) results are listed in Figure 54 and Table XVIII. However, the four treatments that started out with approximately 10% of the nitrogen in standard MAM, transitioned from exponential growth, directly to stationary growth (where net increase in cell density stops) at about the same

time as treatments No. 1 and No. 3 transitioned to linear growth. The additional nitrogen appears to have supported the extended periods of linear growth that occurred in treatments No. 1 and No. 3. Treatment No. 6 (intermittent nitrogen feeding) also resulted in an extended period of linear growth, similar to the resulting growth in treatments No. 1 and No. 3, but with consistently lower nitrogen concentrations, between 1.98 and 9.07 ppm, that were about the same as the concentrations detected in treatments No. 2, No. 4 and No. 5 (the three other low-nitrogen treatments). An explanation for linear growth in treatment No. 6 with low concentrations of nitrogen detected in the medium, is that the alga quickly consumed the small portions of nitrogen that were added during six four-day feeding intervals until day 24, and this nitrogen (47.43% of that in standard MAM) was adequate to support linear growth until approximately day 27.

Table XVIII: LEA Results for dissolved nitrogen (N) as total nitrates and nitrites, and phosphorus (P) in parts per million (ppm). One ppm is approximately equivalent to 1mg/L.

	1. Reg. MAM		2. Low N		3. Low P		4. Low N & P		5. Low N & P + CO2		6. N Feeding	
Day	N (ppm)	P (ppm)	N (ppm)	P (ppm)	N (ppm)	P (ppm)	N (ppm)	P (ppm)	N (ppm)	P (ppm)	N (ppm)	P (ppm)
0	113.90	4.70	12.63	242.23	113.10	4.99	11.69	2.36	11.69	2.36	6.50	2.36
7	110.90	5.18	10.26	4.29	107.30	0.59	9.94	0.52	9.16	0.53	9.07	0.54
15	87.00	5.57	2.99	5.28	76.90	0.32	2.88	0.42	2.78	0.34	2.99	0.27
21	66.28	4.52	3.67	4.20	58.99	0.19	2.85	0.31	2.84	0.32	2.82	0.20
28	47.88	246.19	2.97	254.76	43.59	4.33	2.96	18.83	2.37	29.38	2.23	4.99
57	16.19	231.03	2.63	239.60	17.48	0.20	3.13	35.97	1.86	22.13	1.98	9.61

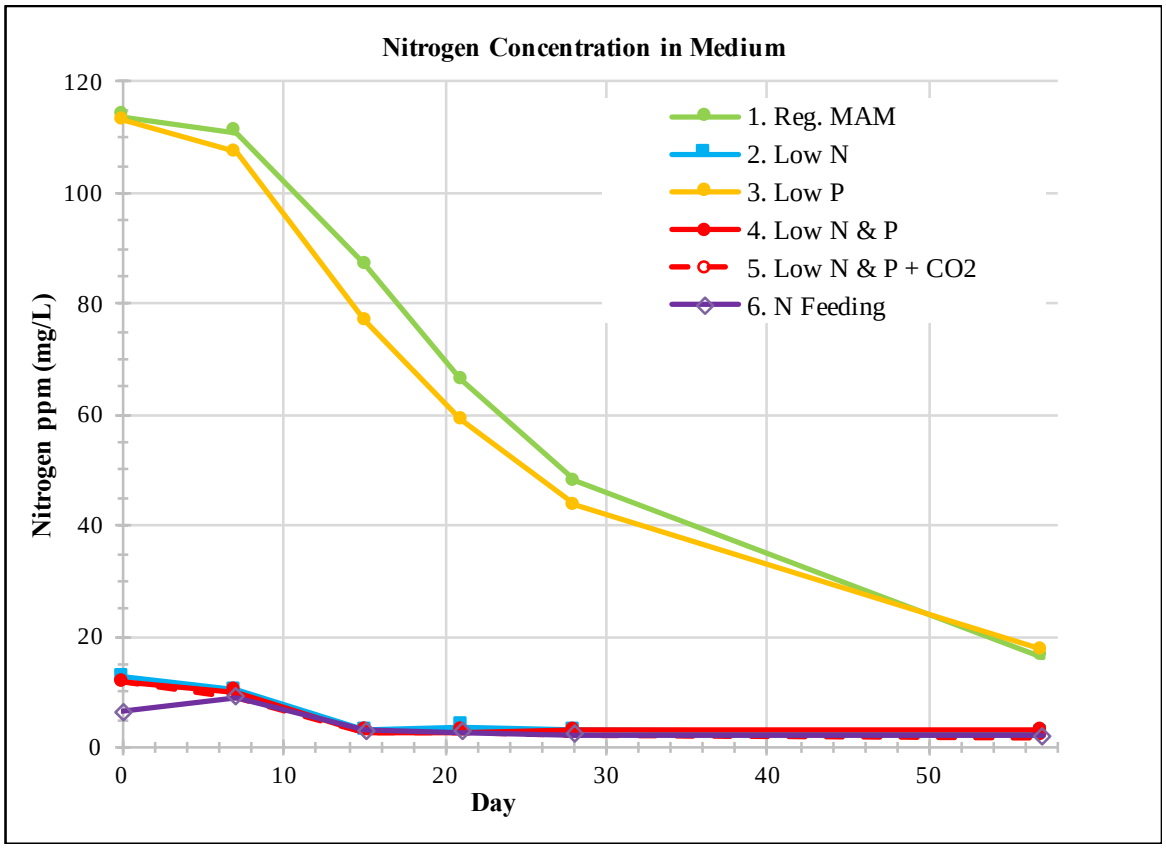

Figure 54: Comparison of Nitrogen Concentrations in Six Experimental Treatments. The results are from an analysis by University of Georgia LEA (Appendix). The margin of error is estimated to be approximately 5%.

3.7.2. Phosphorus

The phosphorus requirements of *C. freiburgensis* for growth are thought to be relatively low, because it is found in oligotrophic habitats, and is likely to have some adaptations to low-nutrient environments. In fact, phosphorus concentrations in Berkeley Pit Lake were too low to be detected at the time *C. freiburgensis* was found to be living there (Mitman, 1999). A decrease in detectable medium phosphorus concentration was expected to occur in some of the six treatments, but it was not clearly evident from the analysis results provided by LEA (Table XVIII and Figure 55). The explanation for this may be a combination of factors. Due to the alga's relatively low phosphorus requirements, it was not expected to consume a large proportion

of available phosphorus from the medium. A confounding factor may also involve dissolved phosphorus becoming bound to iron and other substances in the medium (Bartkowiak, 2002), which makes it more difficult to determine what proportion is actually available for use by the alga. Binding to metals may also account for the apparent error in the results of the analysis, especially with regards to samples collected on day 6 through day 21.

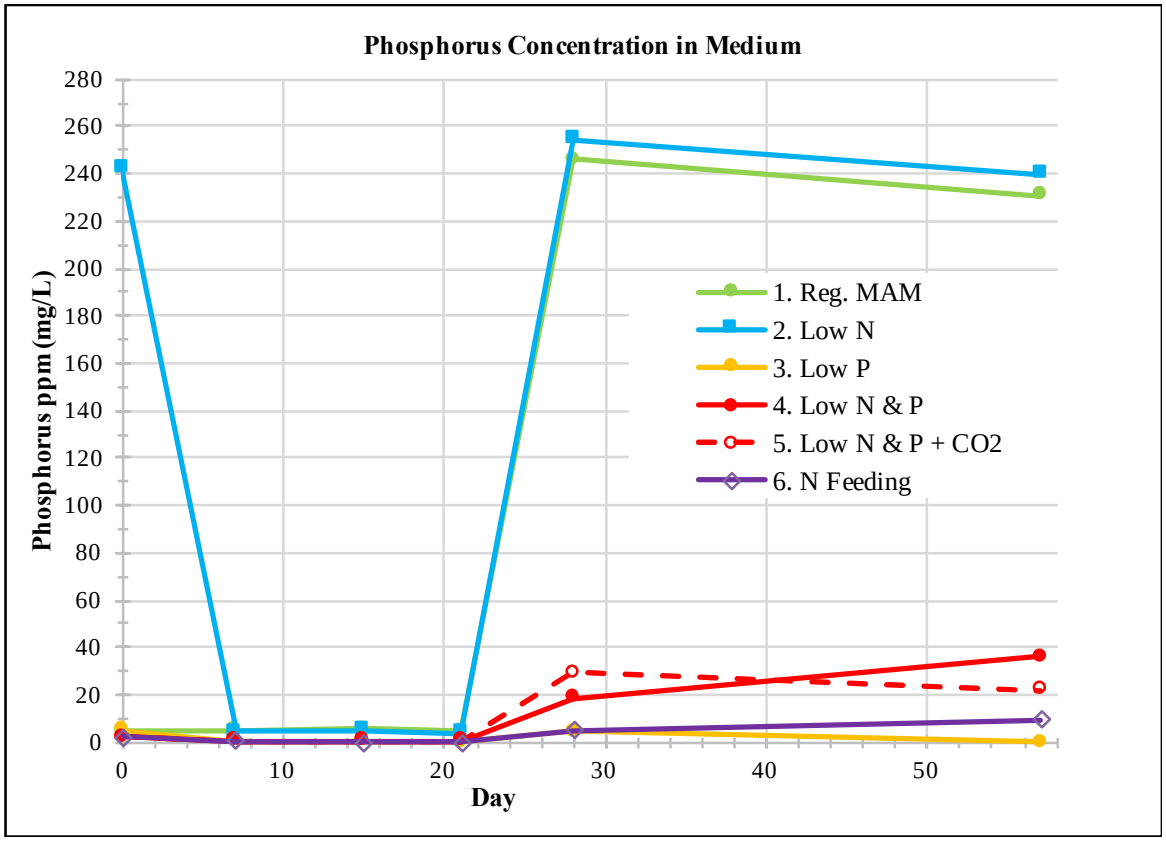

Figure 55: Comparison of Phosphorus Concentrations in Six Experimental Treatments from results of an analysis by University of Georgia LEA (Appendix). The margin of error was estimated to be approximately 5%. The results from samples collected between day 6 and day 21, and for treatment No. 1 on day 0, are most likely to represent errors, possibly due to an unknown mishap, which may have caused damage to the samples, or a failure of the method of the analysis (which may have been attributable to the phosphorus binding to iron or other substances in the medium). Results from day 28 to day 57 are likely the most accurate, as they reflect the reduction (by 90%) of the phosphorus source in the medium of treatments No. 3 through No. 6).

3.8. Biomass (Dry Weight) Productivity Responses to Treatments

The highest biomass yields, in dry algal product per volume liquid, were found in the two treatments with the highest concentrations of nitrogen. Treatment No. 1 (standard MAM, high nutrient) yielded 2.244 mg/mL at day 52, and treatment No. 3 (low phosphorus), yielded 2.083 mg/mL at 34 days (Figures 56, 58 and 62). These two treatments yielded the highest peak biomass, but the lowest total lipid content, based on the Nile Red fluorescence method (Figure 65).

The treatments that resulted in the highest lipid content (No. 4, low nitrogen and low phosphorus and No. 5, low nitrogen and low phosphorus with added CO_2) had lower overall biomass yields (Figure 62), as expected, because increased lipid production was expected to occur after growth had slowed, during the stationary growth phase (Figures 57, 59, 60 and 65). High biomass and high lipid content were not expected to occur, simultaneously in the same treatment. Growth and energy storage are opposing survival strategies for photoautotrophic microalgae. They generally alternate between the two, depending on environmental conditions. When nutrients are plentiful in the environment, microalgae typically allocate their resources toward growth. When one or more limiting nutrients reaches some minimum concentration, microalgae typically stop active growth and begin to amass lipids as an efficient means of storing energy. Stored lipids can provide energy for all functions, during periods when conditions are not favorable for growth. Treatments No. 4 and No. 5 resulted in a peak biomass yields of 1.46 and 1.48 mg of dry product per milliliter of liquid medium.

Treatment number six (intermittent nitrogen feeding) was expected to yield higher biomass by dry weight than the three lower nitrogen treatments (No. 2, No. 4 and No. 5), with a higher lipid content than the two highest nitrogen treatments (No. 1 and No. 3). Treatment No. 6 resulted in somewhat higher peak biomass (1.54 mg/mL) with somewhat higher lipid content

(Figure 61). It is possible that the biomass and lipid yields could be further improved by adjustments to the time intervals of the feeding schedule, quantity of nitrogen per feeding, and nitrogen source.

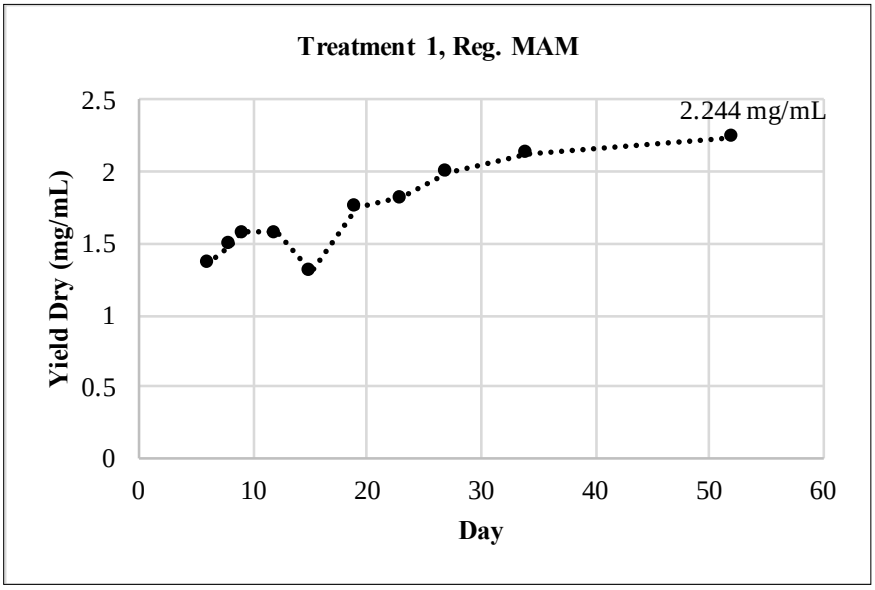

Figure 56: Biomass production in treatment 1, nutrient-replete (control) medium. The highest-biomass sample, day 52, contained 2.244 mg dry alga per mL medium.

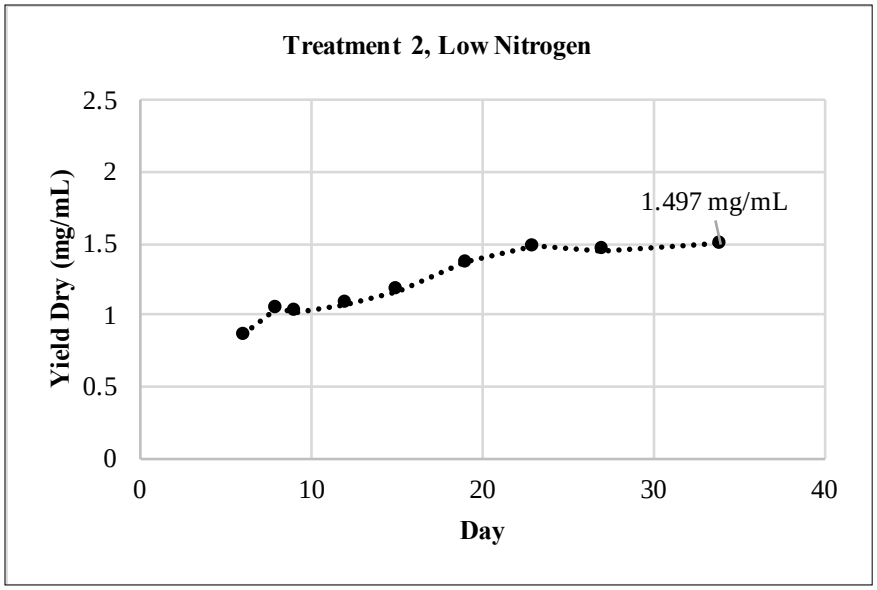

Figure 57: Biomass production in treatment 2, limited nitrogen medium. The highest-biomass sample, day 52, contained 1.497 mg dry alga per mL medium.

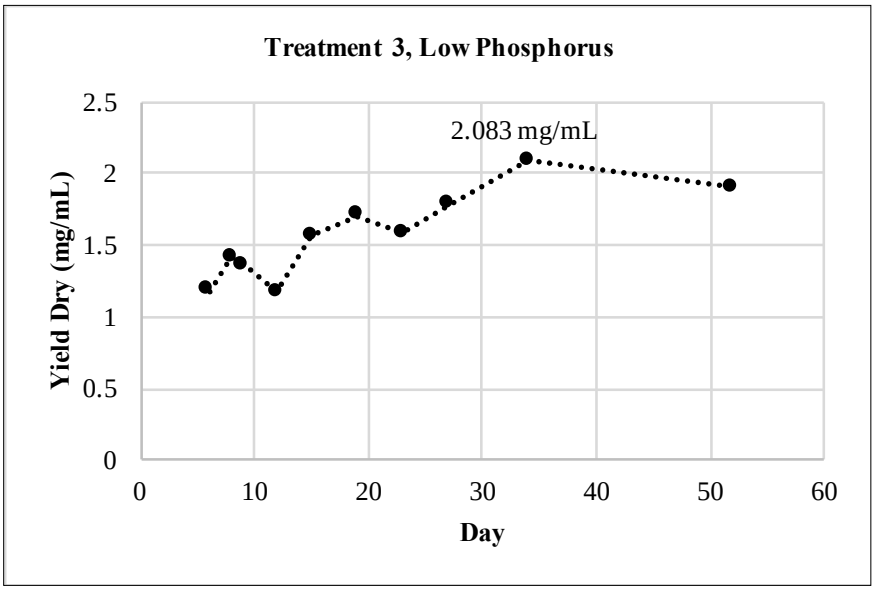

Figure 58: Biomass production in treatment 3, limited phosphorus medium. The highest-biomass sample, day 34, contained 2.083 mg dry alga per mL medium.

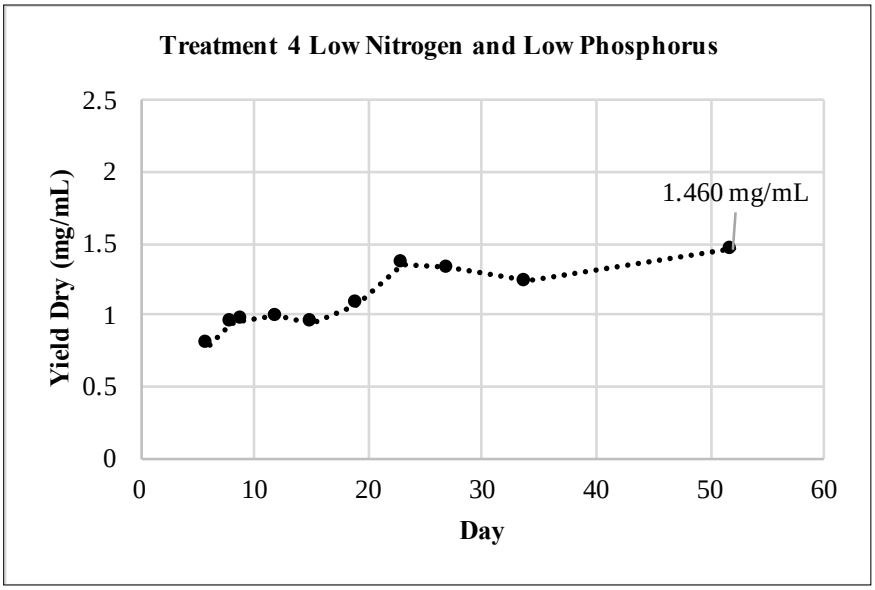

Figure 59: Biomass production in treatment 4, with limited nitrogen and phosphorus. The highest-biomass sample, day 52, contained 1.460 mg dry alga per mL medium.

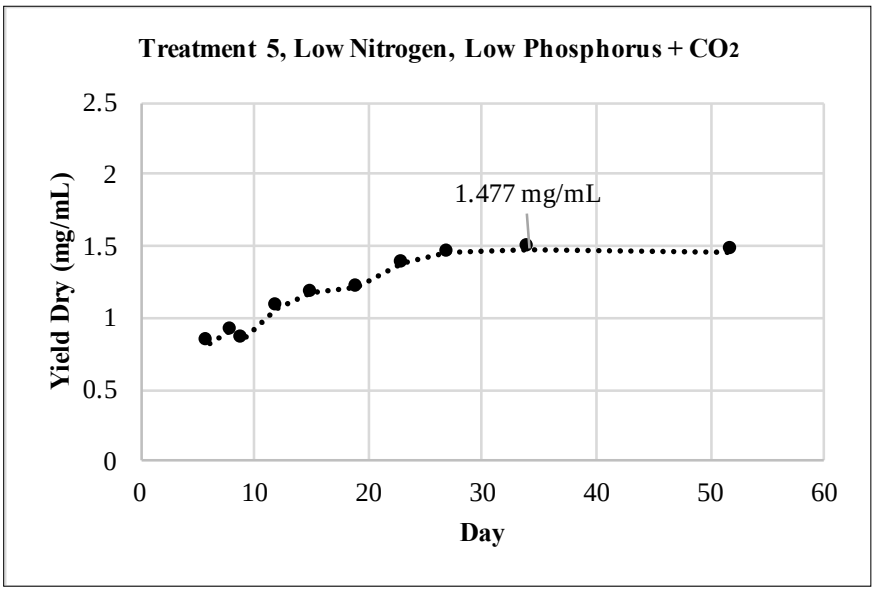

Figure 60: Biomass production in treatment 5, with limited nitrogen and phosphorus and supplemental CO_2 until day 26. The highest-biomass sample was day 34, with 1.477 mg dry alga per mL medium.

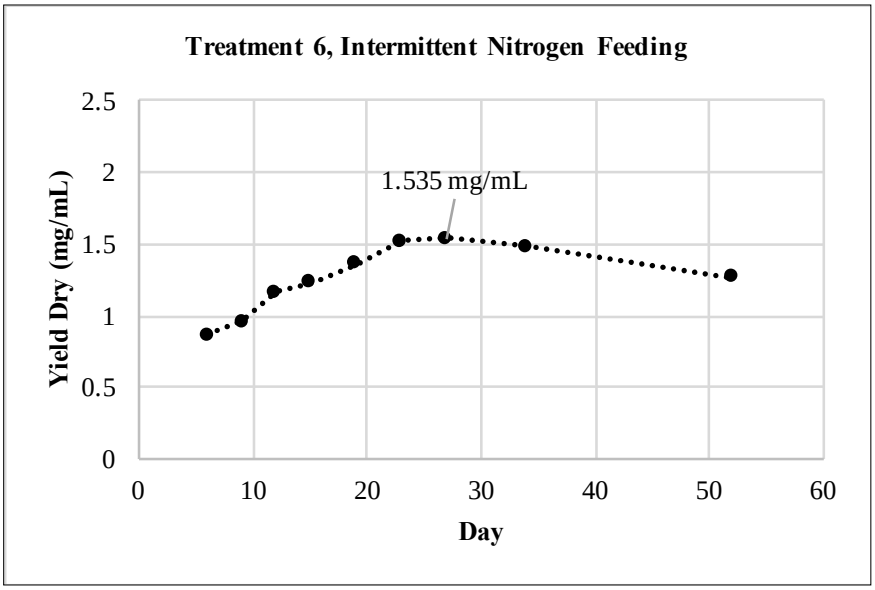

Figure 61: Biomass production in treatment 6, with intermittent nitrogen feeding until day 24. The highest biomass sampled was on day 27, at 1.535 mg dry alga per mL medium.

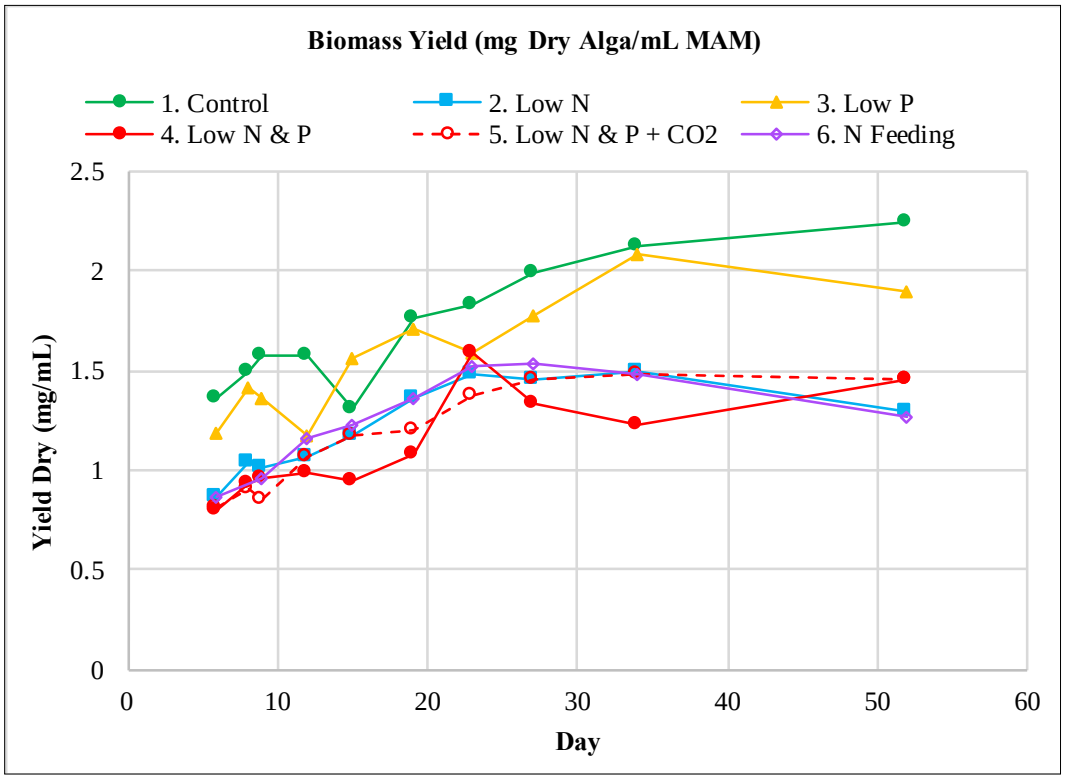

Figure 62: Comparison of biomass (mg dry weight per mL liquid culture) results of six experimental treatments.

3.9. Relationship Between Nutrient Concentrations, Biomass and Lipid Content

The three treatments (No. 1, No. 3 and No. 6) that yielded the highest maximum detected biomass in mg per mL MAM corresponded with the three treatments that yielded the three lowest detected maximum lipid contents, as percent of dry weight (Figures 63 and 64). Lower nitrogen concentrations corresponded with lower biomass production and higher lipid content. Higher nitrogen concentrations corresponded with higher biomass production of cells with a lower lipid content (Figure 63). Lower phosphorus concentrations, in combination with lower nitrogen, corresponded with the highest detected lipid contents. As biomass increased in the three low nitrogen treatments, lipid content also increased, though a linear relationship between biomass and lipid content was not especially strong (Figure 64). In the three treatments with the most nitrogen, there did not appear to be a strong relationship between biomass and lipid content.

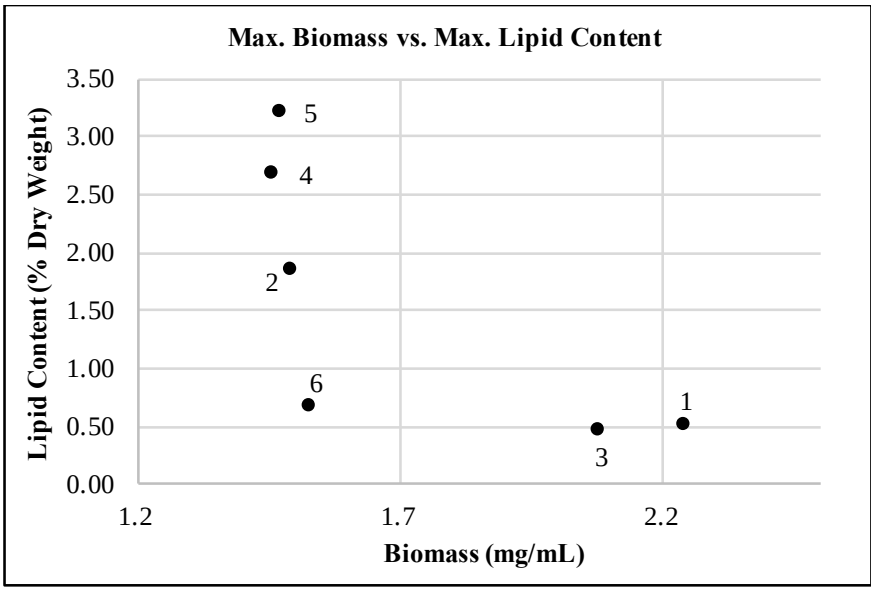

Figure 63: A comparison of the maximum detected biomass and maximum detected lipid content in six experimental treatments, No. 1 (nutrient-replete control), No. 2 (low nitrogen), No. 3 (low phosphorus), No. 4 (low nitrogen and low phosphorus), No. 5 (low nitrogen and low phosphorus with supplemental CO_2), and No. 6 (intermittent nitrogen feeding). The two highest nitrogen treatments correspond to the two lowest (maximum) lipid contents.

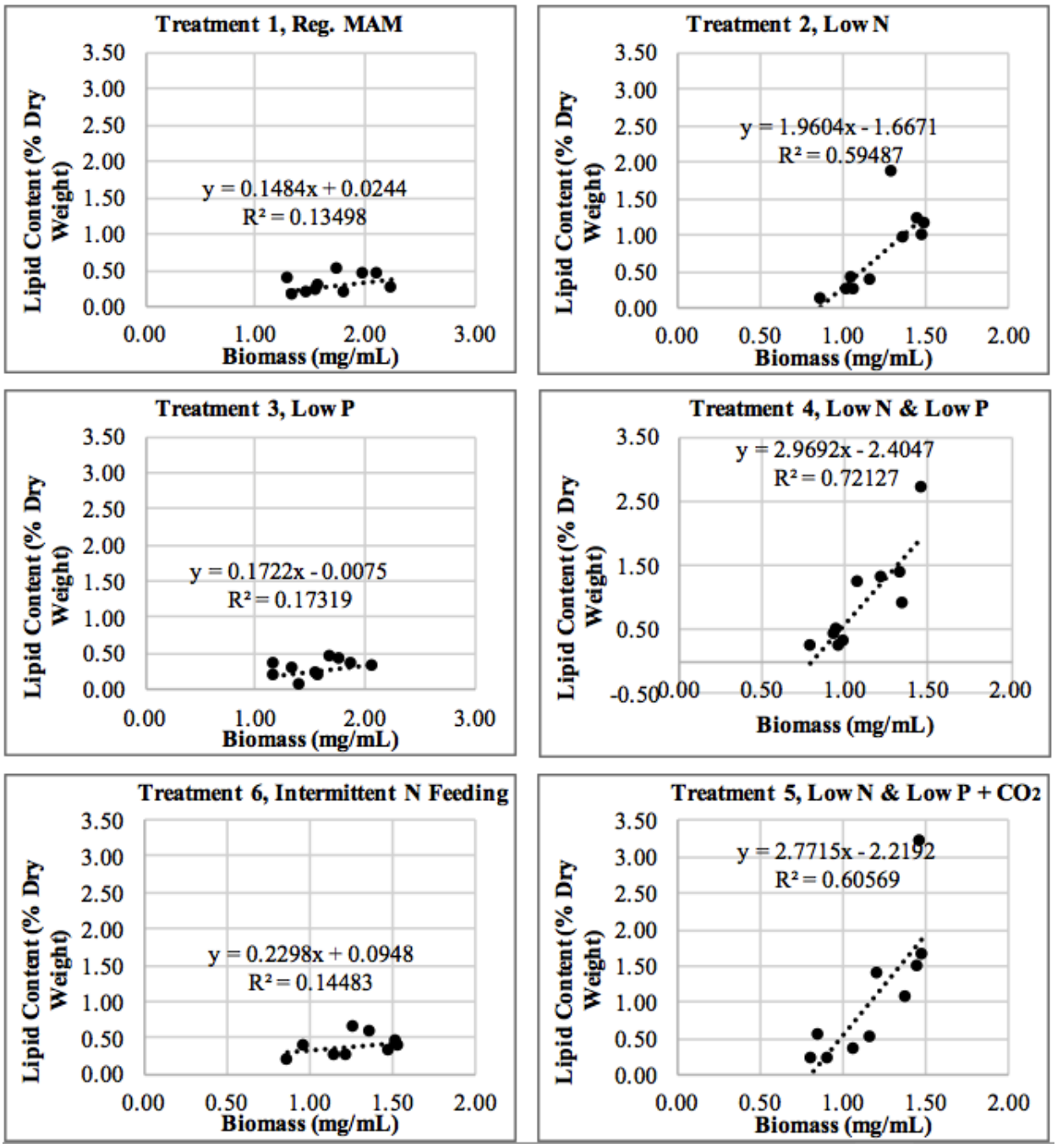

Figure 64: Lipid content increased along with increasing biomass in the three lowest nitrogen treatments (at Right). Lipid content did not appear to increase along with biomass in the three higher nitrogen treatments (at Left).

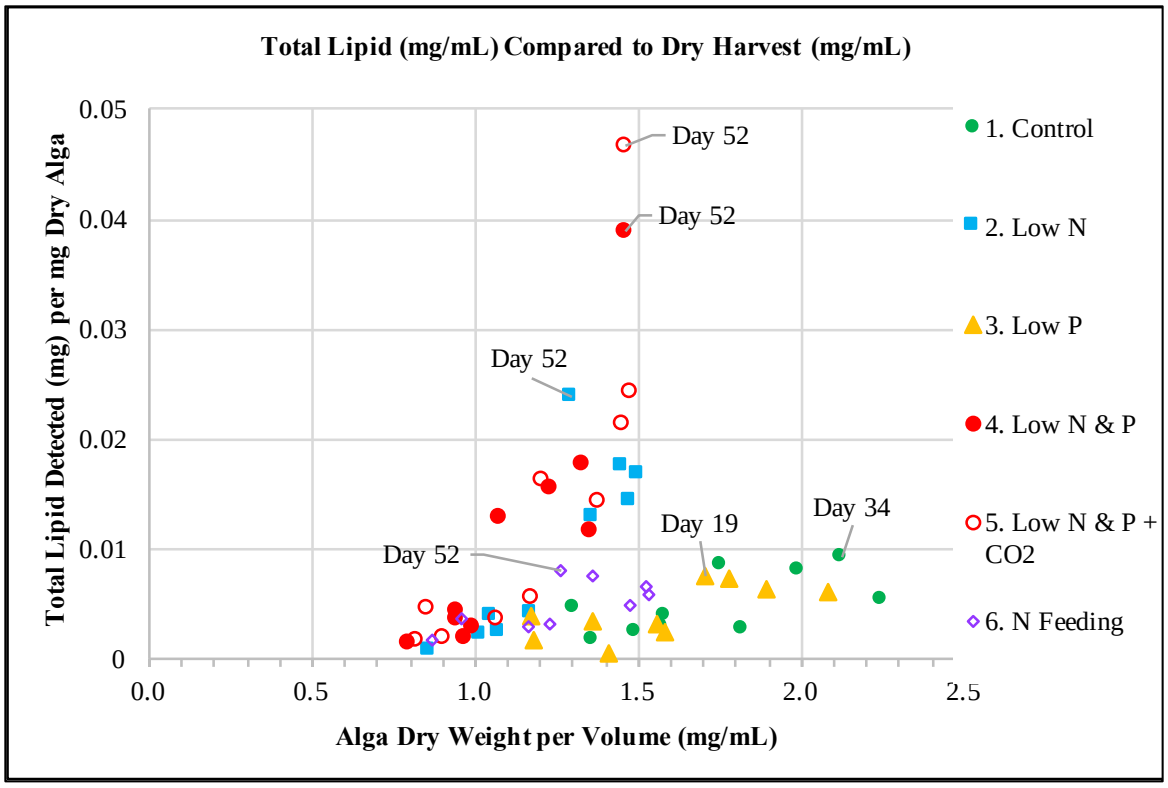

Figure 65: The harvest day in each treatment on which the highest lipid content (mg lipid/mg biomass) was detected, and its corresponding biomass harvest (mg dry weight/mL medium).

3.10. Total Lipid Content, Nile Red Fluorescence and CNRC Results

Microscopic examination showed rapid accumulation of large numbers of intercellular lipid droplets in all three of the low (10%) nitrogen treatments (No. 2, Figure 66, No. 4 and No. 5), compared to the two high-nitrogen treatments (No. 1 and No. 3) and the intermittent nitrogen feeding treatment (No. 6). The highest overall lipid concentrations, from Nile Red fluorescence spectroscopy results, were detected in the three low nitrogen treatments, and the total lipid content (by percent of dry weight) increased over time in all three of these treatments (Figure 67).

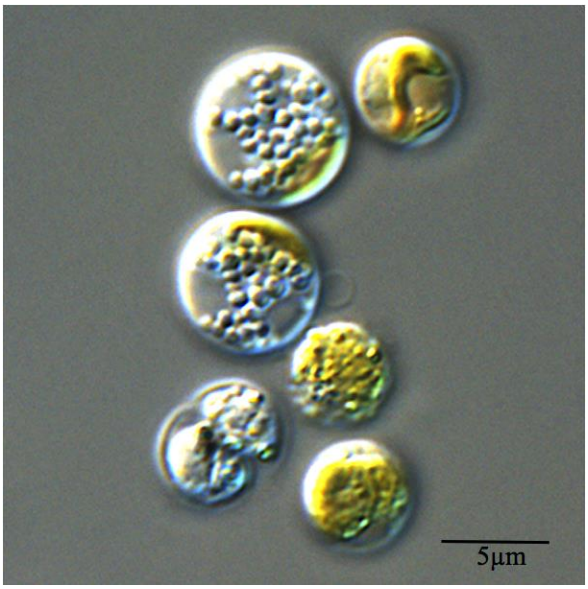

Figure 66: Accumulation of lipid droplets (lipid bodies) in *C. freiburgensis* cells in treatment No. 2 (low nitrogen). Lipid droplets are the uniformly-sized colorless spheres. As cells accumulate storage lipids, they stop active growth and reallocate resources from cellular structures, including the chloroplast (large gold-colored object). Cell walls and membranes also become fragile, and extremely lipid filled, normally sized cells are prone to rupturing. The cell at upper Right contains an intact chloroplast and few lipid droplets. The cell at lower Left no longer contains a visible chloroplast, and the lipid droplets have merged to become large globules.

Treatment No. 5, (low nitrogen and low phosphorus, with supplemental CO_2) showed the highest maximum lipid content, based on the results from this method (3.2% at 52 days). Trends of increasing lipid content over time in the Nile Red fluorescence data were consistent with microscopic observations of increasing numbers of lipid droplets accumulating in the cells. This change was observed in the three lowest nitrogen treatments.

In summary, the highest overall lipid concentrations, from Nile Red fluorescence spectroscopy results, were detected in the low nitrogen treatments, and the total lipid content (by percent of dry weight) increased over time in all three of these treatments (Figure 67.) Treatment No. 5, (low nitrogen and low phosphorus, with supplemental CO_2) showed the highest maximum lipid content, based on the results from this method (3.20% at 52 days). Trends of increasing

lipid content over time in the Nile Red fluorescence data were consistent with microscopic observations of conspicuously increasing numbers of lipid droplets in the cells of the three low nitrogen treatments.

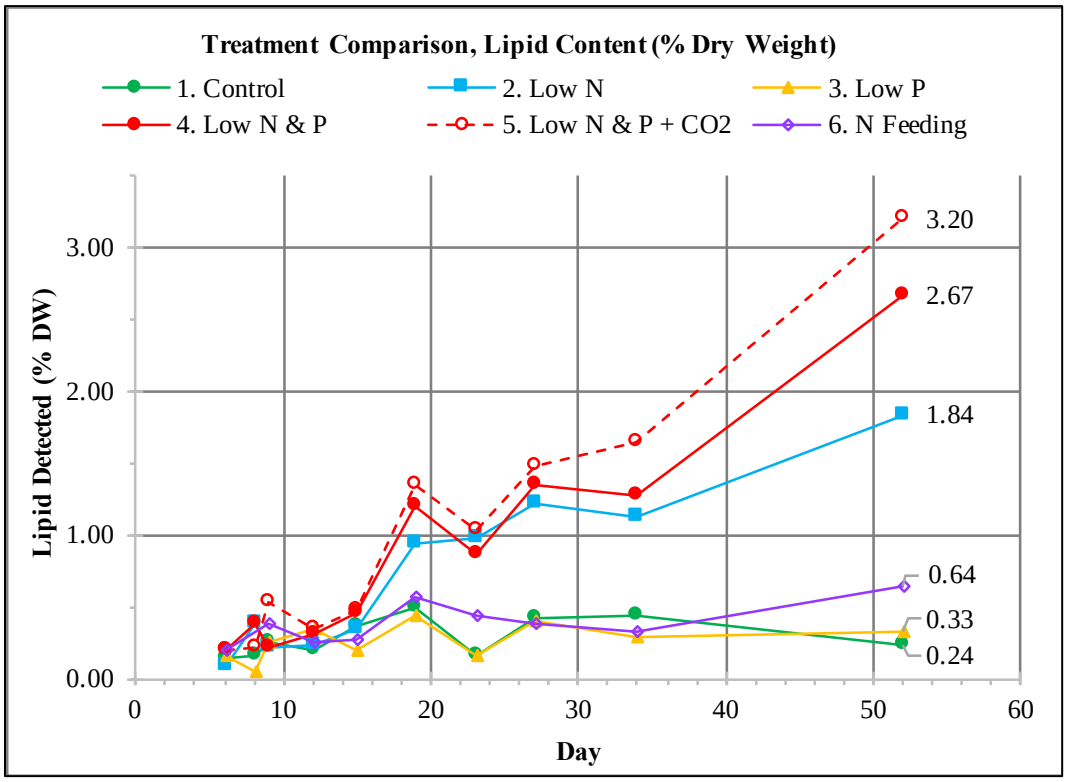

Figure 67: Comparison of lipid content in six experimental treatments, detected by Nile Red fluorescence method. Treatment No. 5 (low nitrogen, low phosphorus and supplemental CO_2) resulted in the highest detected lipid content, followed by treatment No. 4 (low nitrogen and low phosphorus) and treatment No. 2 (low nitrogen only). Treatment No. 6 (intermittent nitrogen feeding) resulted in a somewhat higher lipid content than treatments No. 1 (nutrient-replete control) and No. 3 (low phosphorus only).

The Canadian National Research Council (CNRC) laboratory (Appendix) recovered the highest total lipid content, from chloroform/methanol extraction, on sample day 34, in treatment No. 2 (Low nitrogen only), at 7.83 % (Table XIX). The CNRC method was expected to provide the most accurate results for total lipid yield, though some lipid was expected to be lost along with biomass that was removed by this method, and the actual lipid content is likely to be slightly higher (Dr. Stephen O'Leary and Dr. Fabrice Berrue, personal communication, 2018).

The CNRC laboratory chloroform/methanol extraction method yielded four to 23 times higher lipid contents (by % dry weight) in all six samples, on sample day 34, than the Nile Red fluorescence method.

Table XIX: CNRC laboratory lipid content results from chloroform/methanol extraction (contributed by Dr. Fabrice Berrue), from dry alga, for six experimental treatments harvested on sample day 34, compared to Nile Red fluorescence lipid content results for day 34, and highest detected lipid content from Nile Red fluorescence method.

Treatments	Percent Total Lipid (by Dry Weight)			
	CNRC Day 34	Nile Red Day 34	Nile Red Highest	
1. Standard MAM, High Nutrient	6.23	0.43	0.48	Day 19
2. Low Nitrogen	7.83	1.12	1.84	Day 52
3. Low Phosphorus	5.84	0.29	0.44	Day 19
4. Low Nitrogen and Low Phosphorus	5.75	1.26	2.67	Day 52
5. Low Nitrogen and Low Phosphorus + CO_2	7.04	1.64	3.20	Day 52
6. Intermittent Nitrogen Feeding	7.70	0.33	0.64	Day 52

The low lipid percentages found by the Nile Red fluorescence method also seem to be inconsistent with the large volumes of intercellular lipid droplets observed microscopically in the cells of the three low nitrogen treatments (Figure 68).

It is likely that the Nile Red fluorescence method provided underestimates of the actual total lipid content, and several factors may have contributed to the discrepancy. The Nile Red method has proven to be useful as a means of for monitoring lipid content directly from live algal cells in culture while they are growing. However, its effectiveness varies considerably depending on the algal species, and traits that could interfere with the stain reaching internal lipid bodies (Chen et al., 2009). For example, thick cell walls and a large amount of chlorophyll, common characteristics of green algae, made detecting lipids by the Nile Red fluorescence more difficult and likely to result in underestimates of lipid content (Cooper et al., 2010). With its large chloroplast and glassy cyst, *C. freiburgensis* may present a similar challenge as some of the green algae.

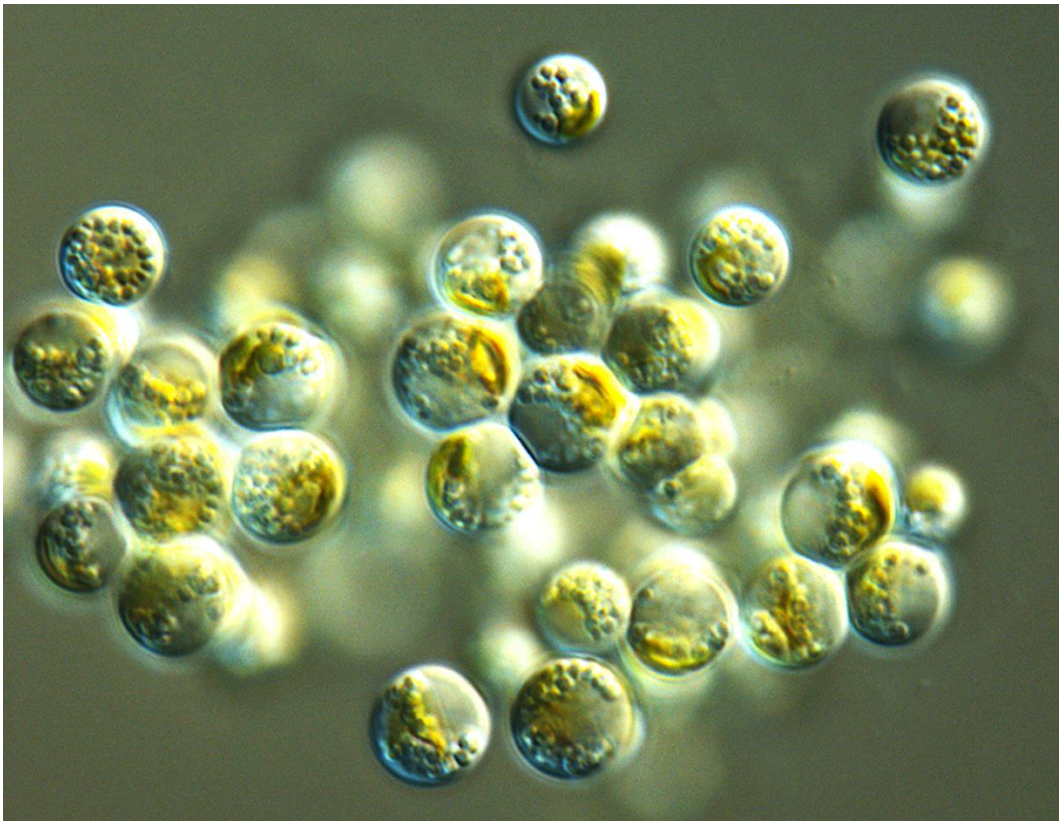

Figure 68: Lipid-filled cells in treatment No. 2 (low nitrogen only), on day 25 (after 25 days of growth). Nile Red fluorescence indicated approximately 1.2% lipid (by dry weight) in these cells at the time of the photograph above (see Figure 67). The highest lipid content found by CNRC was in treatment No. 2 cells at 7.83% (by dry weight, solvent extraction method, day 34).

Chen et al. found that combining Nile Red stain with DMSO facilitates its permeating external cell structures to bind with the internal cellular lipid bodies, but also that the temperature of the sample influences its permeability to the stain and the intensity of the fluorescence signal. *C. freiburgensis* in the non-motile form, has a rigid, silica-based outer cell covering which may, to some extent, delay or lower its permeability to Nile Red stain, even with DMSO. Mixing for one minute (at 20 to 25˚ C), may not have provided sufficient time for the stain to completely permeate all of the cellular lipid bodies. Triolein represents the algal triglycerides well as a standard, however, when mixed into filtered MAM, it is unlike algal lipid droplets, in that its droplets are free from any membranes, cell walls, or other coverings. Some microalgal surfaces

may not only interfere with complete permeation of the stain into the lipid droplets, but they may also reflect or absorb some light radiation, preventing it from reaching the stained droplets, or fluorescence emission from reaching the detector.

Based on the trends observed in the Nile Red fluorescence results and the lipid content results determined by CNRC, *C. freibergensis* from Berkeley Pit Lake can probably actually accumulate 14 to 15 % lipid by dry weight, in approximately 52 days, when grown in similar conditions to those of the three low nitrogen treatments (Table XX). Supplemental CO_2 and intermittent nitrogen feeding may also speed up or increase lipid accumulation. An NMR analysis conducted at CNRC, for the six treatments sampled on day 34, found that the highest total fatty acid content (mM/mg) and the highest triacylglycerols (TAG) were also associated with low nitrogen MAM (treatment No. 2).

Table XX: Estimates of lipid content based on CNRC results and the lipid accumulation trend observed in the results of the Nile Red fluorescence method.

Day 34 Lipid Content Results (% d.w.)			**Nile Red Fluorescence Method, Day 52**	**Change in % Lipid from Day 34 to Day 52 (Nile Red)**	**Percent Increase (Nile Red Method)**	**Estimated % Lipid on Day 52 (Based on CNRC % and Nile Red Trend)**	
CNRC Chloroform/Methanol Extraction Percent Total Lipid from Biomass (Before FAME Analysis)		**Nile Red Fluorescence Method, Day 34**					
Sample No.	% Lipid	% Lipid	% Lipid			% Lipid Est.	
1. Reg. MAM	6.23	0.43	0.24	-0.19	-44%	3.46	
2. Low N	7.83	1.12	1.84	0.72	64%	12.86	
3. Low P	5.84	0.29	0.33	0.04	14%	6.65	
4. Low N & Low P	5.75	1.26	2.67	1.40	111%	12.14	
5. Low N & P + CO_2	7.04	1.64	3.20	1.56	95%	13.71	
6. N Feeding	7.70	0.33	0.64	0.31	93%	14.90	*
Average for Low N	6.87	1.34	2.57	1.23	91%	**12.90**	
Average for High N	6.59	0.35	0.41	0.05	15%	8.34	

* Most extreme difference between CNRC and Nile Red result. Percent increase in lipid may not provide an accurate prediction.

3.11. Triglyceride (Triacylglycerol) Portion of Total Algal Lipids

CNRC found that triglycerides (triacylglycerols or TAGs) represented a fraction of total detected lipids on day 34, in all six treatments (Figure 69). However, a comparison of triglycerides to total lipid content was not made. An accurate comparison to total lipid content would require additional data and a larger set of samples. The three low nitrogen treatments (No. 2, No. 4 and No. 5) showed the highest proportion of TAGs compared to other types of lipids. Glycolipids and free fatty acids appeared to be comparatively dominant in the two treatments that were started with the highest nitrogen concentrations, No. 1 (nutrient-replete) and No. 3 (low phosphorus). Treatment No. 6 (intermittent nitrogen feeding) appeared to have begun accumulating a greater proportion of TAG than in No. 1 and 3, but less than in treatments No. 2, No. 4 and No. 5.

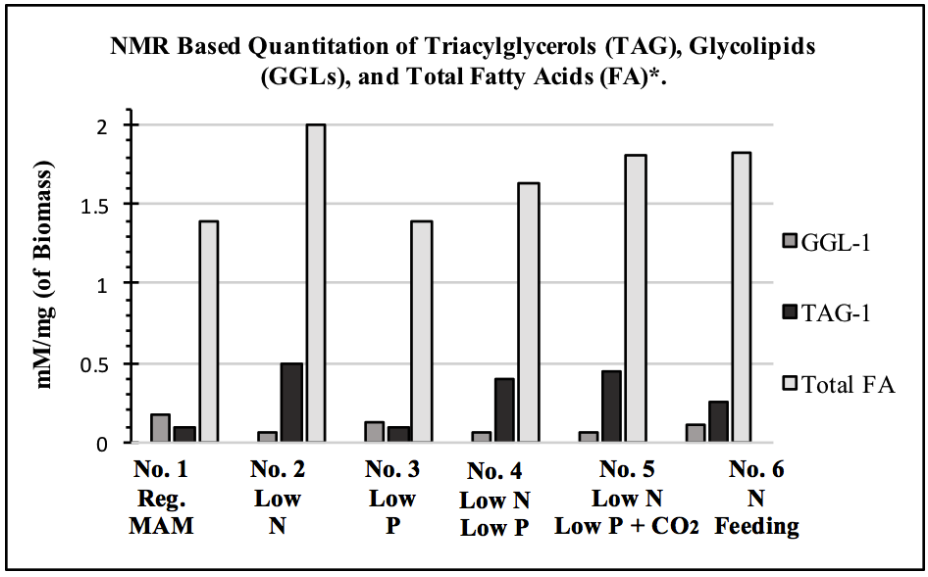

Figure 69: NMR based quantitation of Triacylglycerols (TAG), Glycolipids (GGLs), and Total Fatty Acids (FA) by National Research Council, Canada (CNRC) for day 34 sample set. *Total FA was estimated by integrating all the methyl signals (0.80-1.0 ppm) and can be attributed to TAG, GGLs, or free fatty acids (FA). Samples from Treatments No. 2, 4, and 5 exhibit the highest amount of TAGs while free FAs appear to be the major lipids in No. 1 and No. 3.

3.12. GC/MS Results for FAME Composition

3.12.1. FAMEs detected in Transesterified Algal Lipids

Approximately 32 different FAME compounds were detected by the GC/MS EI and CI methods (Table XXI). The different FAMEs could be distinguished by their unique retention times, which reflected their varying carbon chain lengths and degrees of saturation or unsaturation. FAMEs that have the same chemical formula may have more than one retention time because of differing placement of the same number of unsaturations along the length of their carbon chains or differences in its branching. The retention times of two FAME compounds or a FAME and another type of molecule may be nearly identical and overlap, making it difficult to distinguish them from one another. For example, two FAMEs, C17:2 and C18:1 appeared to have nearly identical retention times, and it was not possible to determine quantitatively, what mixture of the two FAMEs was represented by the peak at 30.45 minutes. However, even numbers of carbon atoms, such as in C18 fatty acids, are most likely to be found in biological lipids.

Table XXI: List of 32 identified FAMEs detected by GC/MS methods, in order of retention time at peak apex, and a few unidentified peaks.

GC/MS Identified Peaks	Retention Time (Minutes)	FAME Detected (Carbon Chain Length and No. of Unsaturations)
1	10.64	(Naphthalene internal standard)
2	16.24	C14:0
3	19.49	C15:0
4	22.91	C16:0
5	24.24	C16:1
6	24.54	C16:1
7	24.69	C16:1
8	25.00	C16:1
9	25.16	C17:0
10	26.17	C20:0
11	27.43	C16:2
12	28.86	C16:2
13	29.53	C18:0
14	30.45	C17:2 and/or C18:1 (RT overlap)
15	30.88	C18:1
16	31.17	C18:1
17	33.31	C18:2
18	34.99	C18:3
19	36.14	C18:3
20	37.11	C18:4
21	37.86	C18:4
22	39.54	C18:4
23	39.91	C18:5
24	41.01	C20:3
25	41.79	C22:0
26	42.10	C20:4
27	43.05	C22:1
28	43.71	C20:4
29	44.85	C20:5
30	45.39	C21:4
31	48.06	C22:4
32	50.69	C22:5
33	51.69	C22:6
34	55.98	C25:1, C26:8, aromatic FAME or unknown
35	57.69	C25, C26:7, C20:8 or other aromatic FAME
36	58.31	unknown or phthalic acid (software library)

3.12.1. Changes in FAME Concentrations with Time

The GC/MS combination of EI and CI methods revealed fatty acid carbon chain lengths, and extent of unsaturation, from C14:0 to C22:6. The GC/MS methods ran for 80 minutes, and FAMEs with retention times between 10.64 to 51.69 minutes were identifiable. Identifiable FAMEs were not distinguishable from background noise before the retention time for the internal standard, naphthalene, at 10.64 minutes. The first identifiable FAME, C14:0, had a retention time of 16.24 minutes. The FAME with the longest retention time, that was consistently identifiable, was C22:6 at 51.69 minutes. Compounds with retention times longer than 51.69 minutes were not reliably identifiable because they were present in low abundances and their MS spectra did not clearly match any of the library reference spectra. Retention times after 51.69 minutes often appeared to overlap (they were too similar to distinguish) for multiple compounds. These low-abundance compounds may include longer carbon chain FAMEs, aromatic FAMEs, substances similar to phthalic acid ester, and other unidentified compounds that may include pigments. Additionally, molecules eluting later than 51.69 minutes were not identifiable because they often co-eluted, with more than one substance having similar mass to charge ratios. The GC/MS method was able to reliably identify fatty acid methyl esters with carbon chain lengths between C:14 and C:22. FAMEs with carbon chains shorter than C:14 were not detected, and those with carbon chains longer than C:22 were not identified, however both may have been present in the algal samples in very small amounts.

Total detected FAME (by dry weight, mg/g) and the proportions of individual FAMEs both changed, in all six treatments, over time. The total detected FAME content reached its highest point at different times during the growth period in the six treatments. Because of the limited number of samples analyzed and the multi-day time intervals between samples, it is not possible to precisely determine the day of the growth cycle that each treatment reached its

maximum FAME content. However, a trend became apparent from the GC/MS result. Decreasing nutrient levels at the start of the batch culture appears to speed up FAME accumulation, as it does for lipid accumulation, with a decreasing nitrogen having a more pronounced effect than that of decreasing phosphorus (Figure 70). In the nutrient-replete treatment, No. 1 (standard MAM) the total FAME increased at the slowest rate and was highest on day 52, when the last sample was taken, toward the end of the growth cycle. In the other five treatments, where starting nutrient concentrations were decreased, peak detected FAME contents occurred earlier. They occurred on day 9 in No. 2, when nitrogen only was decreased, on day 15 and 19 in No. 4 and No. 5, when nitrogen and phosphorus were decreased, and the peak FAME content occurred on day 27 in No. 3, where only phosphorus was decreased. In all three low nitrogen treatments, the total detected lipid content continued to increase throughout the growth cycle (Figure 70), while it leveled off for treatments No. 1 and No. 2 (high nitrogen). Total detected FAME did not necessarily continue to increase in proportion to increasing total detected lipid content. In fact, while lipid production continues after day 27 in the three low-nitrogen treatments, FAME accumulation appears to stop earlier in all but the nutrient-replete “control” treatment (No. 1).

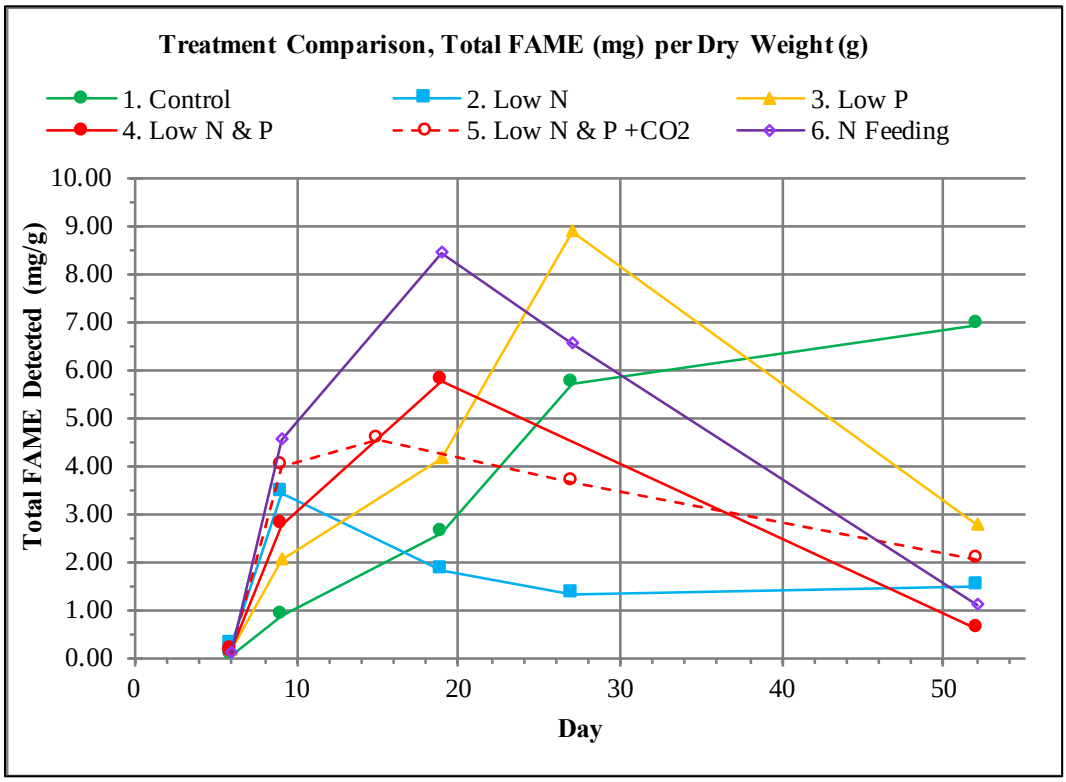

Figure 70: Accumulation of total FAMEs (mg/g) detected by GC/MS method. The actual peak value for treatment No. 2 (low nitrogen) may have occurred close to day 15, but the sample from day 15 for treatment No. 2 was not analyzed. All total detected FAME results from the GC/MS sample preparation method are far lower than total FAME results from methods at CNRC laboratory for day 34, and should be considered to be probable underestimates of the actual total FAME that could have been recovered and detected by different methods.

3.12.2. Interpreting GC/MS Results, with Comparison to FAME Composition Results from CNRC GC and NMR Methods.

The CNRC GC analysis of biomass from day 34 detected five to 15 times the amount of total FAME (mg/g) that was detected by the Montana Tech GC/MS method that was used for all other sample days (Table XXII). Because the results for total detected FAME differed so greatly between the GC/MS method and the CNRC GC method, it was not possible to precisely determine how close sample day 34 was to the time of maximum FAME accumulation.

Table XXII: Proportions (percent of total detected FAMEs) of C18:1 compared to saturated C14 and C16 and polyunsaturated C18:3 and C18:4. The highest proportion of C18:1 occurred earliest in the two treatments that combined reduced concentrations of both nitrogen and phosphorus (No. 4 and No. 5). Treatment No. 5, which combined low nitrogen, low phosphorus and supplemental CO_2, achieved the highest proportion of C18:1 (31.2%) at the earliest time (27 days). The standard deviation for percent of C18:1 is 0.8%. CNRC results are indicated by shaded squares.

Treatment	Day	% C14:0 and C16:0	% C18:1	% C18:3 and C18:4	Total Detected FAME by dry Wt. (mg/g)	
1. Reg. MAM	6	39.8%	2.8%	26.0%	0.035	
	9	36.4%	2.5%	38.1%	0.846	
	19	22.2%	1.5%	56.0%	2.610	
	27	20.2%	1.7%	55.1%	5.692	
	34	22.6%	2.6%	45.6%	35.455	**CNRC**
	52	23.7%	**3.5%**	42.9%	**6.926**	
2. Low N	6	56.7%	2.9%	7.1%	0.276	
	9	32.6%	5.1%	37.7%	**3.397**	
	19	30.6%	16.2%	34.3%	1.789	
	27	35.4%	26.8%	19.9%	1.314	
	34	19.5%	**45.1%**	15.0%	51.018	**CNRC**
	52	34.9%	31.0%	15.8%	1.449	
3. Low P	6	56.3%	4.1%	17.2%	0.117	
	9	30.2%	2.1%	43.2%	2.058	
	19	24.2%	1.9%	52.4%	4.143	
	27	21.3%	2.2%	49.4%	**8.850**	
	34	28.3%	2.7%	42.8%	40.947	**CNRC**
	52	19.9%	**4.7%**	48.0%	2.749	
4. Low N & Low P	6	47.2%	3.3%	22.8%	0.146	
	9	44.4%	6.0%	28.1%	2.745	
	19	28.8%	26.6%	26.7%	**5.776**	
	27	42.4%	27.2%	15.4%	0.488	
	34	23.8%	**50.1%**	9.9%	39.046	**CNRC**
	52	49.5%	20.5%	15.5%	0.580	
5. Low N & Low P + CO2	6	72.5%	3.4%	7.9%	0.099	
	9	36.0%	3.1%	35.3%	3.999	
	15	45.3%	25.7%	15.4%	**4.554**	**Mean of 3**
	19	34.0%	26.9%	21.6%	1.236	**Mean of 3**
	27	41.7%	31.2%	14.4%	3.633	
	34	20.9%	**48.1%**	14.0%	51.148	**CNRC**
	52	32.2%	29.3%	18.4%	2.031	
6. Intermittent N Feeding	6	72.3%	2.9%	7.3%	0.112	
	9	29.4%	2.4%	38.8%	4.537	
	19	25.4%	9.3%	41.9%	**8.450**	
	27	24.0%	11.6%	37.5%	6.558	
	34	21.5%	17.8%	24.9%	47.285	**CNRC**
	52	27.4%	**26.5%**	22.0%	1.065	

It is most likely that the CNRC results for day 34 do not represent a maximum accumulation of FAMEs, unless FAME content actually reached its maximum close to day 34. Based on GC/MS results, and supposing that while these are probable underestimates, they are consistent underestimates, the maximum FAME content of the transesterification product of the algal lipids most likely occurred earlier in the growth cycle, (between day 9 and day 19) for treatments No. 2, No. 4, No. 5 and No. 6 (lower nitrogen treatments). Based on the GC/MS results, the actual peak FAME content for treatment No. 1 (regular, high nutrient MAM) probably occurred after day 34. The actual maximum FAME content probably occurred close to or shortly before day 34 in treatment No. 3 (low phosphorus, high nitrogen MAM).

Although the CNRC method detected much higher overall FAME, their results for relative proportions of individual FAMEs were similar and generally consistent with the results from the GC/MS method, and they appeared to fit within the pattern of increases and decreases in FAME classes, with time, revealed by the GC/MS method.

3.12.3. Highest Total Detected FAME Content and Highest Proportion of C18:1

The sample preparation, GC and NMR methods which were followed by the CNRC laboratory to detect and identify FAMEs in the sample set from day 34 detected a far higher total FAME content than the GC/MS method that was used for the other sample sets. The CNRC laboratory methods are currently used for similar testing, and proven to be dependable. The sample preparation and GC/MS methods being tested and developed for this experiment are in an experimental stage and have not been standardized. Therefore, where the two sets of methods appear to show conflicting results, the CNRC result should be considered to be most reliable.

The treatments resulting in the highest yields of detected FAMEs (mg/g) differed from those that resulted in the highest proportion of C18:1, within total quantity of all FAMEs detected (Figures 71 – 73 and Table XXII).

3.12.3.1. Accumulation of Total Detected FAME Yield Over Time

The total FAME content from all five sets of samples analyzed by the GC/MS method (day 6, 9, 19, 27 and 52) were combined to de-emphasize fluctuations with time, and to roughly simulate what the cumulative FAME yields from multiple harvests over a 50 to 60 day growth period might look like.

It appeared that cumulative total FAME production, over the time of the growth period, was highest in the three treatments with the *higher* quantities of nitrogen made to the alga (No. 1, 3 and 6), which was not expected (Figure 71). The treatments resulting in the highest total lipid content and the highest maximum detected FAME content were the ones that were expected to also have the highest FAME content from the combined GC/MS results.

The high cumulative FAME results could not be attributed to algae increasing total lipid accumulations in the higher nitrogen treatments late in the growth cycle. The Nile Red fluorescence results show that they did not do this (Figure 67). It is possible that the composition of lipids in the higher nitrogen treatments contained a higher proportion of the types of lipids that were later converted to the FAMEs that were detected. The cells in the higher nitrogen treatments may have maintained higher proportions of these (unknown) types of lipids throughout the growth cycle, than the cells in the low nitrogen treatments.

In summary, the three treatments with the highest initial or cumulative (in treatment No. 6) quantities of nitrogen the medium were the three that produced the highest cumulative FAME

content, as detected by the GC/MS method. While the combined results from these three treatments showed higher FAME totals, they had relatively low proportions of C18:1 in the FAME mixture. The total FAME content from five samples detected by the GC/MS method was also much lower than the quantity of FAMEs detected by the CNRC method in a single sample.

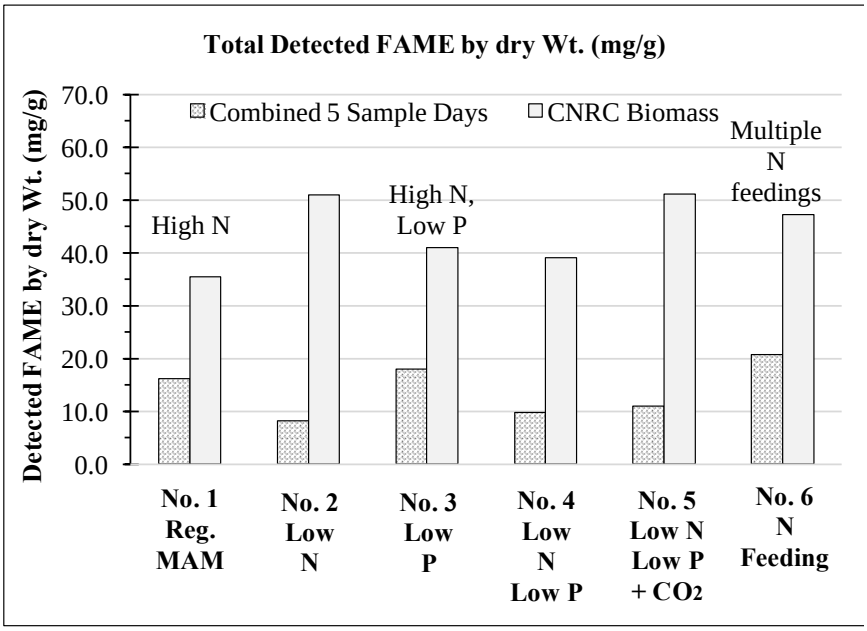

Figure 71: Total detected FAME by dry weight (mg/g) from the sum of results of five sample days by the GC/MS method and one sample day (day 34) by the CNRC GC method. The CNRC GC method detected a far higher FAME content than the GC/MS method. The three treatments with the highest initial and cumulative nitrogen in the medium produced the highest cumulative detected FAME content.

3.12.3.2. Highest Detected Total FAME on One Sample Day

The highest total FAME content that was detected by the GC/MS method was 8.850 mg FAME per gram of dry alga from treatment No. 3 (low phosphorus with high nitrogen) on day 27 (Figure 72). One set of samples, those from Day 34, were analyzed by the CNRC laboratory method. The highest total FAME content that was detected by the CNRC method on day 34 was 51.148 mg FAME per gram of dry alga in treatment No. 5 (low nitrogen, low phosphorus and CO_2. These results do not appear to provide enough data, on their own, to point to any clear

relationship between the experimental treatments and the total FAME content from the algal lipids.

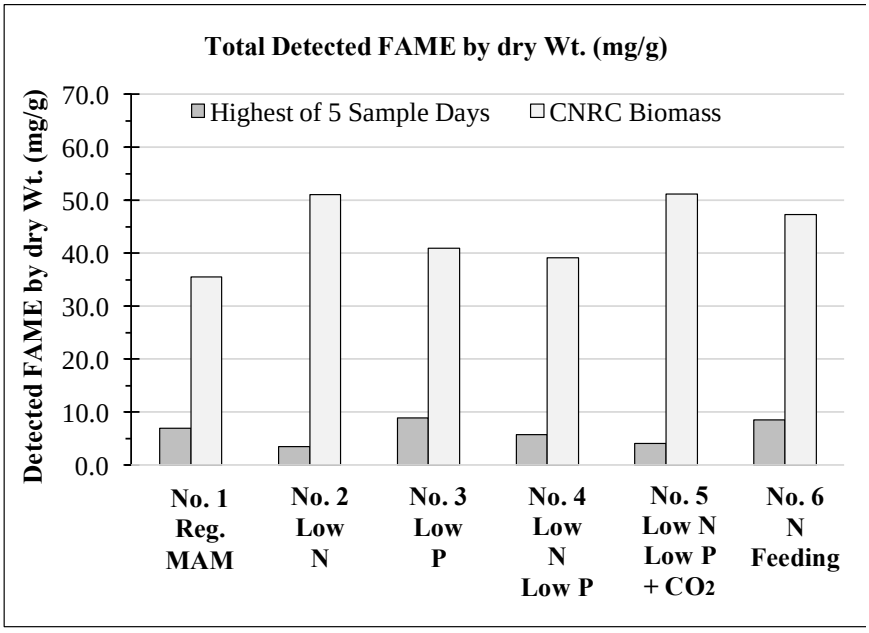

Figure 72: Total detected FAME by dry weight (mg/g) from the highest measure of five sample days by the GC/MS method and one sample day (day 34) by the CNRC GC method. The CNRC GC method detected a far higher total FAME content than the GC/MS method.

3.12.3.3. Treatments Resulting in the Highest Proportions of C18:1

Treatment No. 2 (low nitrogen) and treatment No. 5 (Low nitrogen, low phosphorus and supplemental CO_2) showed relatively high proportions of both total FAME and C18:1, on day 34 (Table XXII, and Figure 73). Peak accumulation of C18:1, relative to other FAMEs, appeared to occur later than peak accumulation of FAMEs in all treatments, except in nutrient-replete "control" treatment (No.1). For all three low-nitrogen treatments (No. 2, No. 4 and No. 5), the highest relative proportion of C18:1 appeared to occur close to day 34. For treatment No. 1 (high nutrient "control") and No. 6 (intermittent nitrogen feeding), the highest relative proportion of C18:1 occurred close to day 52. However, the relative proportion of C18:1 in treatment No. 1 and treatment No. 3 (low phosphorus) which both started with the highest nitrogen

concentrations, remained very low (3.5% and 4.7%) throughout the growth cycle. The highest relative proportions of C18:1 were accumulated in treatments No. 2, No. 4 and No. 5, which all started with the lowest nitrogen concentrations. Treatments No. 4 (low nitrogen and low phosphorus), and No. 5 (low nitrogen, low phosphorus and supplemental CO_2) accumulated the highest relative proportions of C18:1 at 50.1% and 48.1% of total FAME. Treatment No. 6 (intermittent nitrogen feeding) accumulated an intermediate amount (26.5%), later in the growth cycle (day 52).

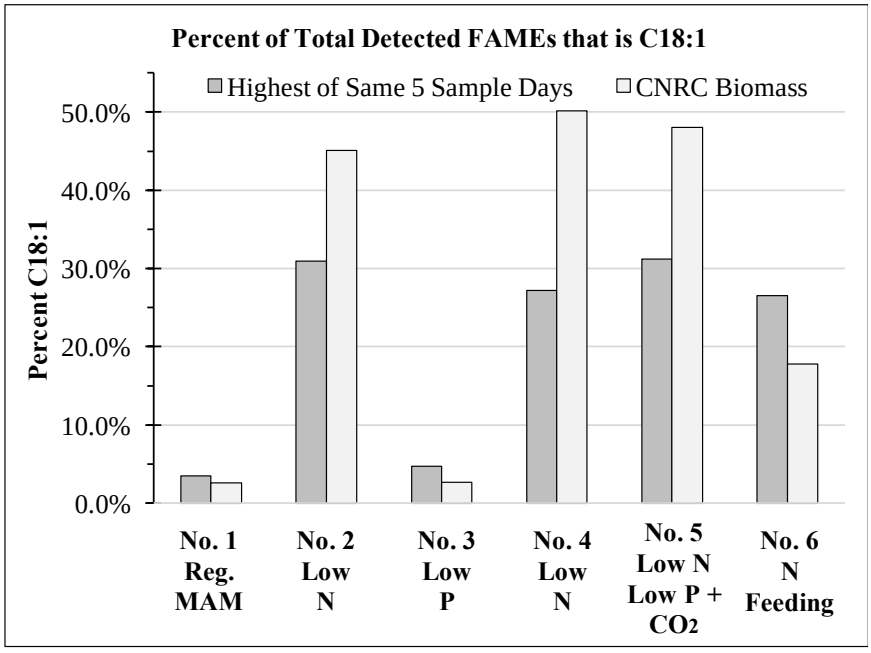

Figure 73: Highest percent of total FAME that is C18:1 out of the same five sample days of each treatment, detected by the GC/MS method and one sample day (day 34) by the CNRC GC method.

3.12.4. Disparity in Detected Total FAME Between GC/MS Methods and CNRC Methods

The CNRC laboratory employed two sample preparation methods for detecting and characterizing FAME content in the day 34 sample set. One method involved solvent extraction of total lipids before analyzing FAME content that would be found in the transesterified product. The second method involved analysis of the FAME content after conversion of lipids from whole dry biomass, without first extracting them. The day 34 samples were prepared by both methods and the resulting 12 samples were analyzed by GC-FID (Flame Ionization Detection) and nuclear magnetic resonance spectroscopy (NMR). The second CNRC (whole biomass) sample preparation method was expected to be less likely to result in the loss of algal lipid and FAMEs during sample preparation, and therefore most accurate. Both CNRC methods consistently resulted in far higher total combined FAME concentrations per unit mass of the dry alga than the sample preparation and GC/MS methods that were developed and used at Montana Tech (Table XXIII), for all of the other sample sets.

Table XXIII: Comparison of the range of results for total FAME recovery per unit mass dry alga from GC/MS methods with the results for total FAME recovery per unit mass dry alga from CNRC methods (day 34 samples only).

Total FAME Results, GC/MS Methods (Range from Day 6 – Day 52) and CNRC Methods (Day 34)						
Treatments	**1. Reg. MAM**	**2. Low N**	**3. Low P**	**4. Low N & Low P**	**5. Low N & Low P + CO_2**	**6. N Feeding**
Highest Total FAME (mg/g) from GC/MS methods	6.926	3.397	8.850	5.776	4.554	8.450
Lowest Total FAME (mg/g) from GC/MS methods	0.035	0.276	0.117	0.146	0.099	0.112
Day 34 Total FAME (mg/g) from biomass	35.455	51.018	40.947	39.046	51.148	47.285
Day 34 Total FAME (mg/g) from lipid extract	16.014	29.831	13.814	20.408	26.048	22.041

The CNRC methods were more successful at recovering and detecting FAME product from dry algal biomass, and their results for day 34, from the whole biomass sample preparation method should be considered to be the most accurate.

This disparity appears to indicate that the sample preparation and GC/MS methods that were developed for this experiment and used for all sample sets, except for day 34, did not convert and recover as much of the algal lipids, or detect FAMEs after transesterification, as the CNRC methods. Based on the disparity between the results of the different sets of methods and analyses, it appears likely that a significant portion of the total algal lipids were not fully converted to FAMEs, or FAMEs that could have been recovered were lost during the transesterification and extraction process used for the GC/MS methods.

There are a number of possible reasons why the transesterification process may not have effectively converted all (nearly all) algal lipids into FAMEs, as intended. Some algal lipid may have been trapped inside solid parts of cells, and not available for the reaction with the methanol. There may have been an inadequate quantity of methanol/H_2SO_4 mixture to complete the transesterification reaction with all of the algal lipids. Two hours may not have allowed adequate time for all of the lipids to react, at 60 ˚C. Also, the temperature fluctuations that occurred during the reaction may have resulted in less-than-optimal conditions for all algal lipids being converted to FAMEs.

Other problems with the sample preparation method may have resulted in low recovery of converted FAMEs. It is possible that a significant portion of FAMEs may have been lost with the algal solids removed during the filtering process. Algal FAMEs may also have been lost during the hexane and water washes used for recovering the hydrophobic portion from the mixture after transesterification and filtering. Some of the hydrophobic portion of the sample

that contained the FAMEs may have been lost as it adhered to the insides of the funnel and containers. Possibly more problematic, was the formation of an emulsion layer between the hydrophobic and hydrophilic parts of the sample/solvent mixture on several occasions, that made the complete separation and recovery of the hydrophobic portion of the sample more difficult.

The relatively small sample size (approximately 0.5 g) may have exaggerated the loss of algal FAMEs somewhat. If significant algal FAME product was actually lost during the sample preparation process in one or more of the ways described, it is possible that the same methods may have worked better with a larger sample size, because the relative portion of algal FAMEs lost may have been smaller.

Though the transesterification, extraction and GC/MS methods most likely resulted in underestimates for total FAME content of the transesterified sample, these underestimates are expected to be consistent for all of the samples (except for day 34) because the samples were, to the extent possible, treated the same way at every step. The general trends in FAME content over time during the growth period are still likely to follow the observed trends, though the actual amounts detected are underestimates.

3.12.5. Consistent Results for Percentages of individual FAME Types Between GC/MS Methods and CNRC Methods

There appeared to be far less disparity with regards to types of FAMEs, and their percentages relative to total FAME content, detected between the CNRC methods and the GC/MS methods. The GC/MS results for FAME composition as a percent of each individual FAME relative to total FAME content, were fairly similar and consistent with CNRC results from day 34. The CNRC day 34 results, for the most part, fit into the pattern of increasing and

decreasing proportions of FAME types that was revealed in the analyses of the other sample sets by the GC/MS methods (Figures 74 – 76, and 77 – 82).

3.12.6. Changes in Fatty Acid Composition and Proportions FAMEs with Time

The GC/MS results support the hypothesis that harvest timing would make a difference in the FAME compositions. After transesterification of lipids from *C. freiburgensis* biomass (freeze-dried whole cells), the result of the changing composition of fatty acids in the algal lipids became evident.

3.12.7. Common Patterns of Change in FAME Compositions with Time

The proportions of each type of FAME detected in the transesterified product of each dried algal sample differed, depending on harvest timing, uniquely in each of the six experimental treatments. However, based on the results of GC/MS FAME composition analysis, three common patterns were shared in all six treatments. First, the proportion of two, shorter chain, saturated FAMEs (C14:0 and C16:0) began relatively high, followed by a general decreasing trend in all six treatments, though it rebounded, notably in treatment No. 4 (Figure 74).

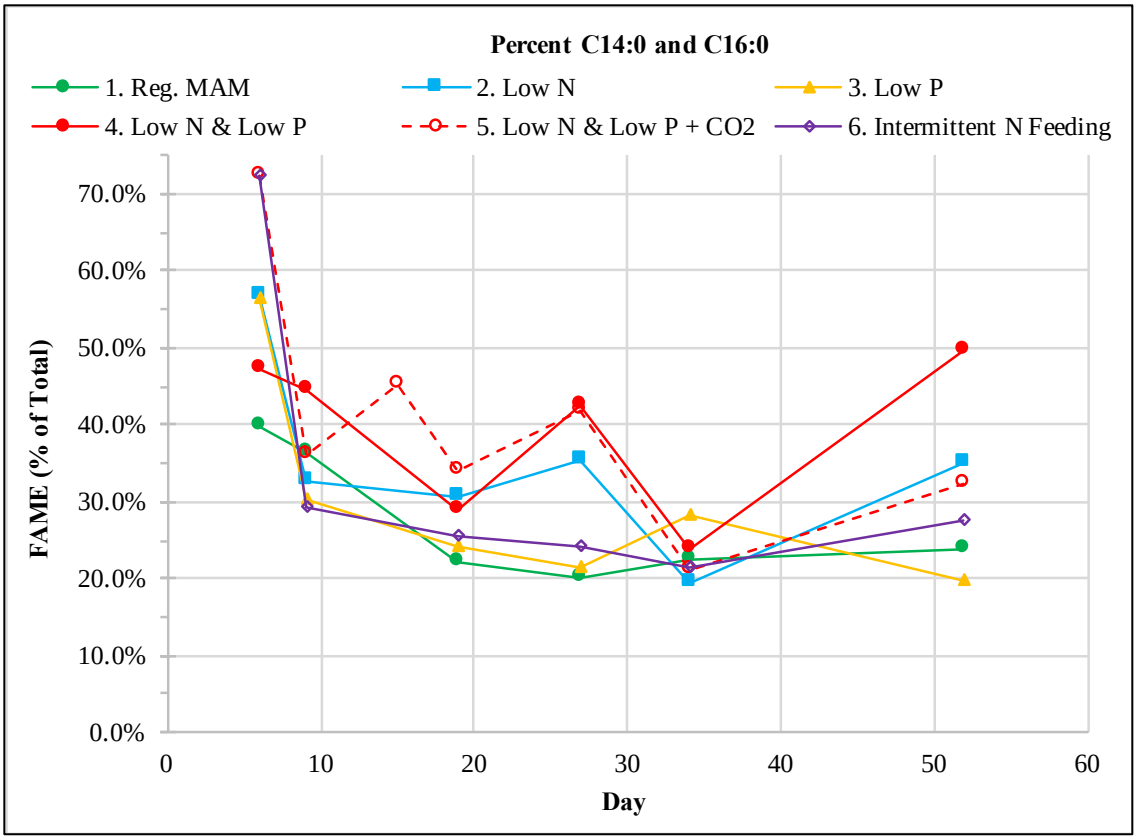

Figure 74: The proportions of the two predominant saturated FAMEs, C14:0 and C16:0, followed a generally decreasing trend followed by an increase. The three treatments with the lowest nitrogen concentrations at the start, appeared to have also resulted in a possible cyclical fluctuation in the proportions of saturated FAMEs, though the trend from treatment 6 (intermittent nitrogen feeding) appeared to be similar to that of the two high-nitrogen treatments.

Second, the proportion of two polyunsaturated FAMEs (C18:3 and C18:4) started low, increased, and then began to decrease in all six treatments (Figure 75). In the three low nitrogen treatments and treatment No. 6, C18:1 increased as the two polyunsaturated FAMEs decreased. The proportions of the two shorter chain, saturated FAMEs and the two longer chain, polyunsaturated FAMEs appeared to be somewhat inversely related to one another (Figures 77 – 82). The third pattern was a general increase in C18:1 (a FAME from oleic acid) in all six treatments, but with much different rates and proportions, depending on medium nutrient concentrations (Figure 76). The proportion of C18:1, relative to other FAMEs, increased rapidly

in the treatments that had lower nitrogen concentrations, reaching proportions of around 50%, before beginning to decrease. In the high-nitrogen treatments, the increase was much slower, and the proportions remained below 5%.

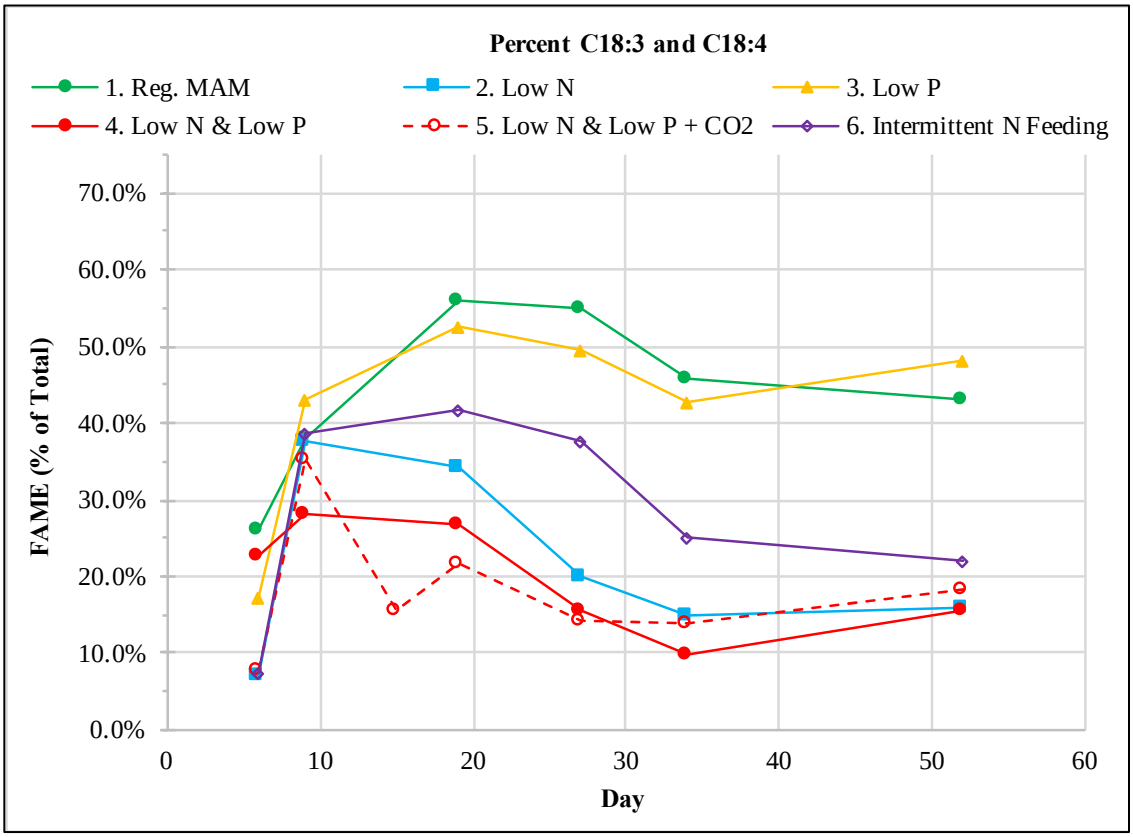

Figure 75: The predominant polyunsaturated FAMEs found in the transesterified lipids of *C. freiburgensis*, C18:3 and C18:4, showed a general increasing trend followed by a decrease. Polyunsaturated FAME proportions appeared to peak earlier than day 19 in all six treatments.

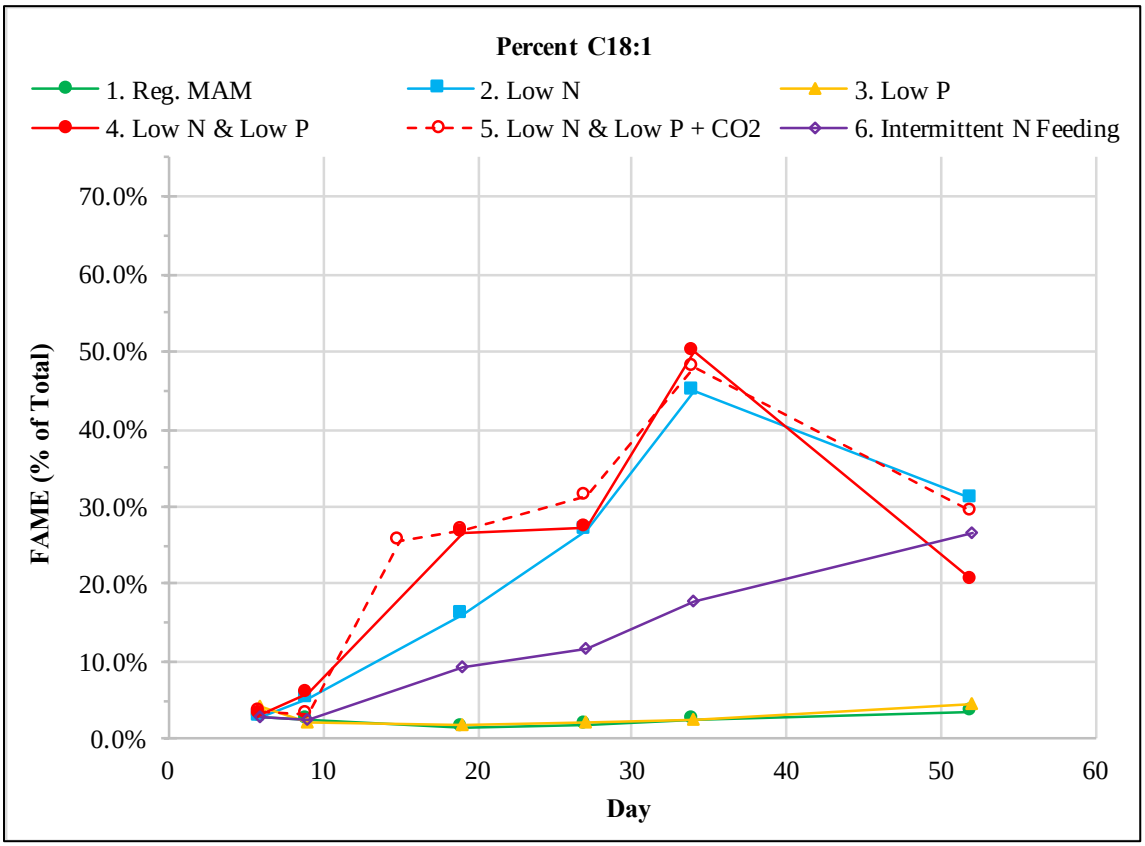

Figure 76: The proportion of the predominant monounsaturated FAME found in the transesterified lipids of *C. freiburgensis*, C18:1, increased over the growth period most notably in all four of the treatments where nitrogen concentrations were lowered. The most rapid increases were observed in treatments No. 2, No. 4 and No. 5, which started with 10% of the nitrogen source found in regular MAM (No. 1) and had no additional nitrogen added. These three treatments also resulted in a peak proportion of C18:1 near day 34. Treatment No. 6, which started with 5% of the nitrogen in regular MAM, but was fed additional portions at four day intervals, showed a steady, slower increase in proportion of C18:1.

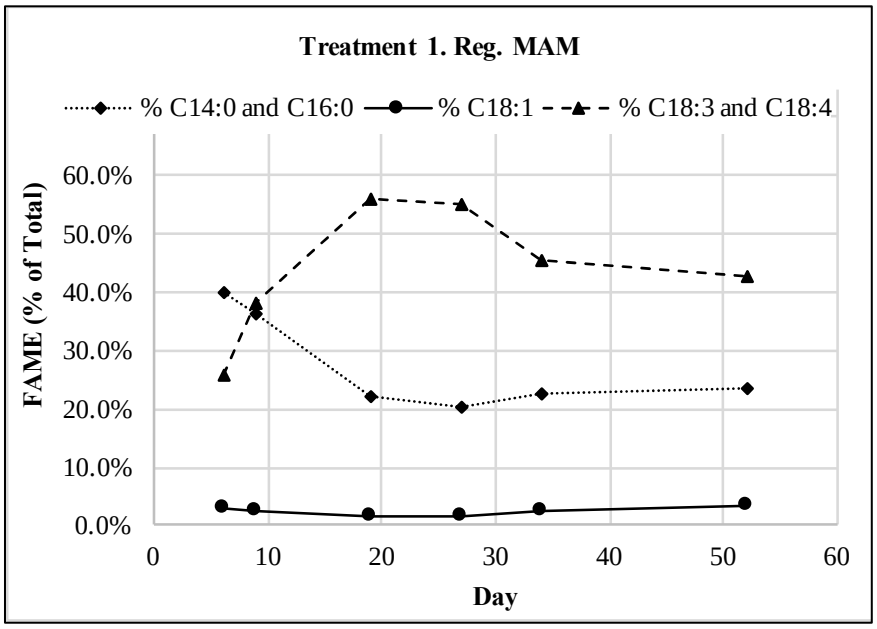

Figure 77: Treatment 1, C. freiburgensis in standard MAM (high-nutrient "control") trends in proportions of saturated C14 and C16, monounsaturated C18:1, and polyunsaturated C18:3 and C18:4 with growing time.

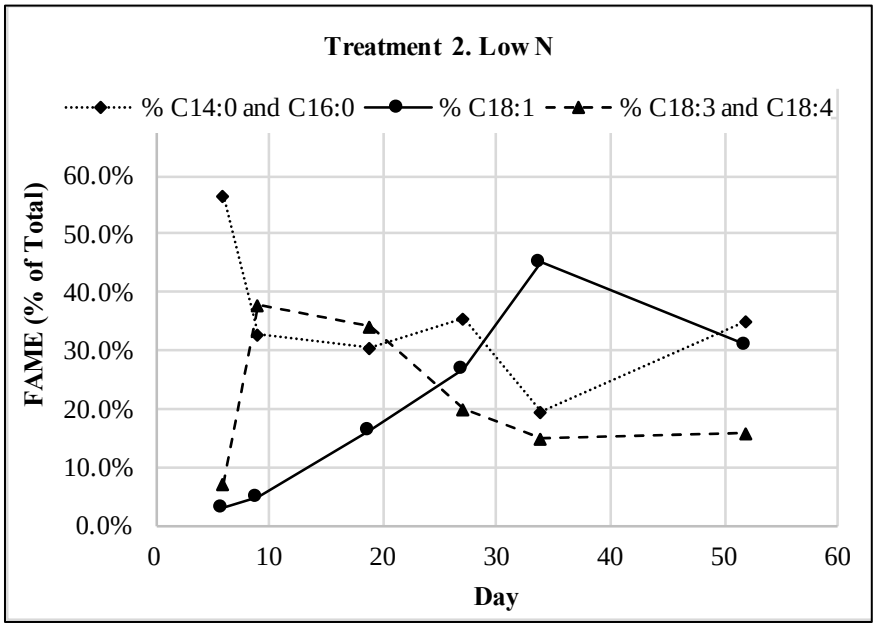

Figure 78: Treatment 2, *C. freiburgensis* in low nitrogen MAM and trends in proportions of saturated C14 and C16, monounsaturated C18:1, and polyunsaturated C18:3 and C18:4 with growing time.

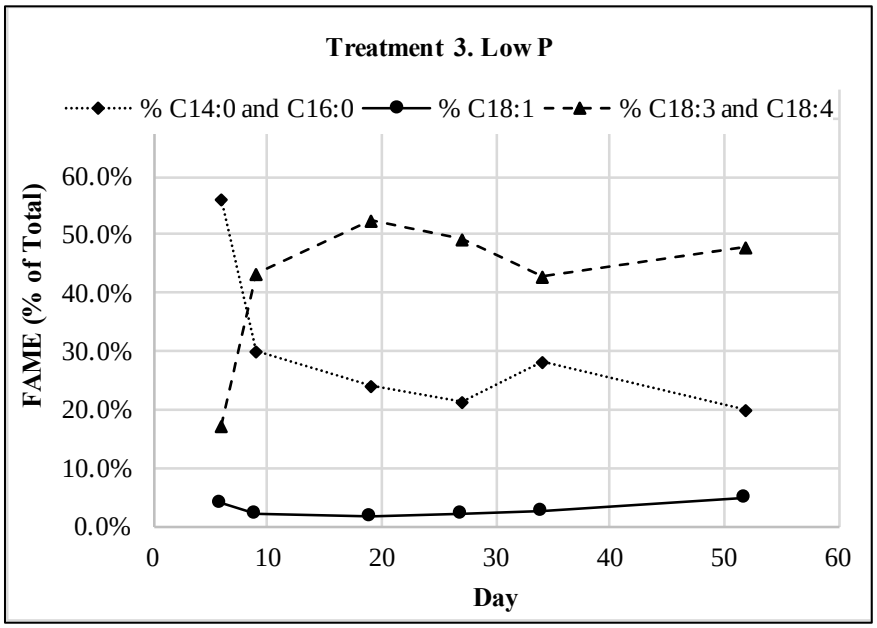

Figure 79: Treatment 3, *C. freiburgensis* in low phosphorus MAM and trends in proportions of saturated C14 and C16, monounsaturated C18:1, and polyunsaturated C18:3 and C18:4 with growing time.

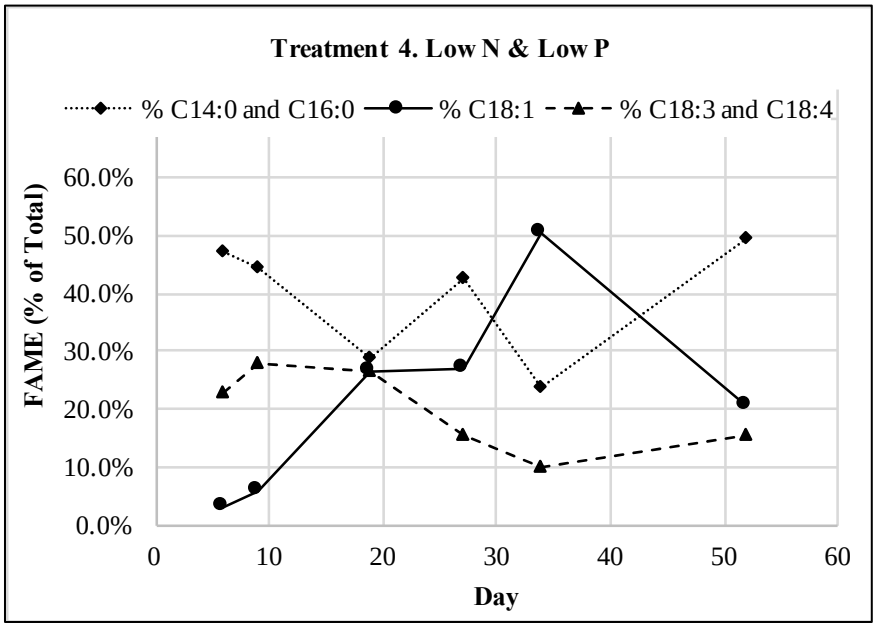

Figure 80: Treatment 4, *C. freiburgensis* in low nitrogen and phosphorus MAM, and trends in proportions of saturated C14 and C16, monounsaturated C18:1, and polyunsaturated C18:3 and C18:4 with growing time.

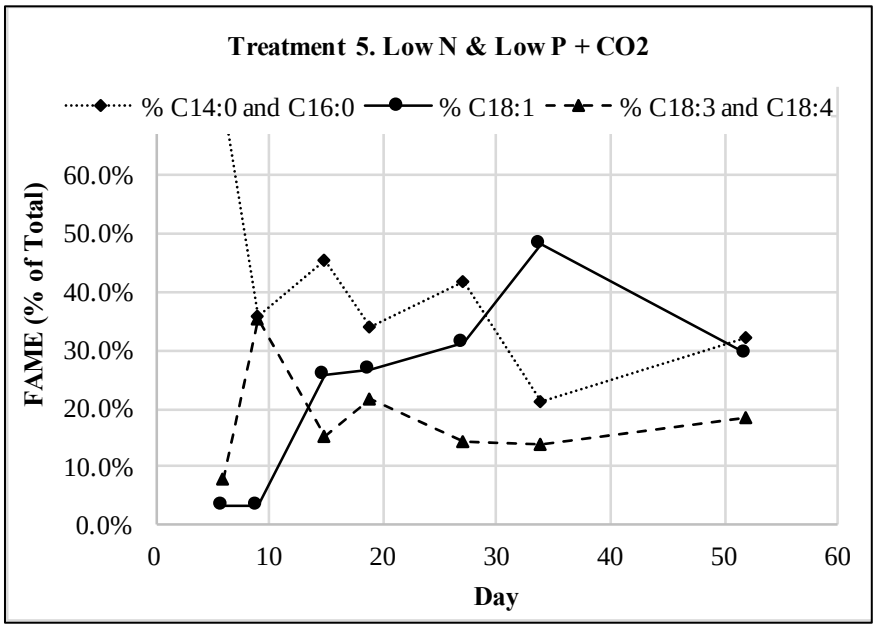

Figure 81: Treatment 5, *C. freiburgensis* in low nitrogen and phosphorus MAM, with supplemented CO_2, and trends in proportions of saturated C14 and C16, monounsaturated C18:1, and polyunsaturated C18:3 and C18:4 with growing time. The results for sample day 19 are suspected to represent an error. However, the preparation of the day 19 GC/MS sample was investigated, and no problem was found that would have been likely to have damaged it. Sample day 15 was added, and its results are expected to be more accurate than those from day 19.

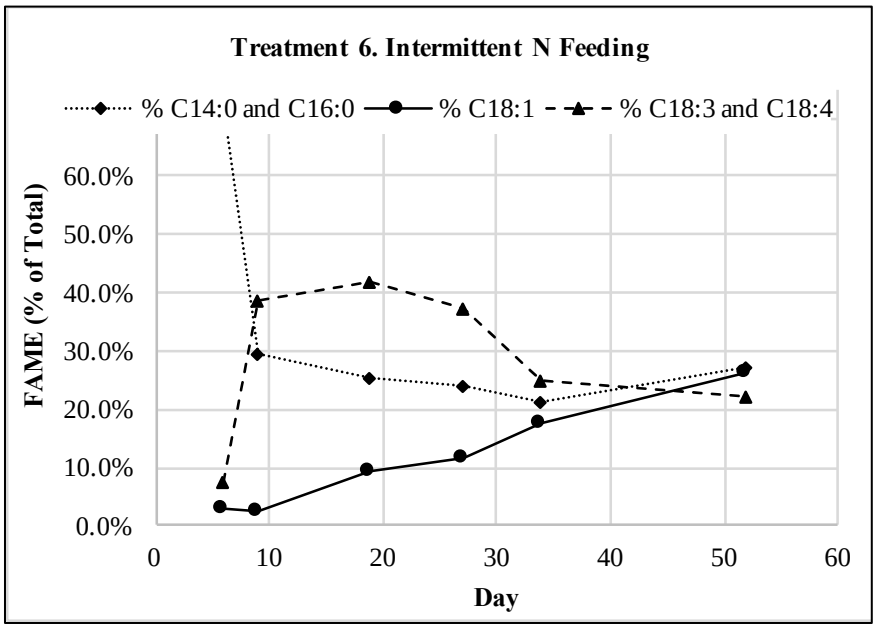

Figure 82: Treatment 6, *C. freiburgensis* in low nitrogen MAM with intermittent nitrogen feeding, and trends in proportions of saturated C14 and C16, monounsaturated C18:1, and polyunsaturated C18:3 and C18:4 with growing time.

3.12.8. Contrasting Patterns of Change in FAME Compositions with Time

3.12.8.1. Treatment 1, Nutrient Replete, Standard MAM

In treatment No. 1 (standard MAM/nutrient-replete "control") the proportion of C18:1 remained low (1.5% to 3.5%) in comparison to FAMEs from polyunsaturated fatty acids, especially C18:4, throughout the growth period (Table XXII and Figures 83 – 90). Treatment No. 1 showed the most noticeable decrease in the proportions of C14:0 and C16:0, and an increase in C18:3 and C18:4, which reached a maximum of 56.0% of total FAMEs on day 19. The total FAME content in treatment No. 1 continued to increase throughout the growth period until day 52 (the final sampling event), but remained relatively low (Figure 90).

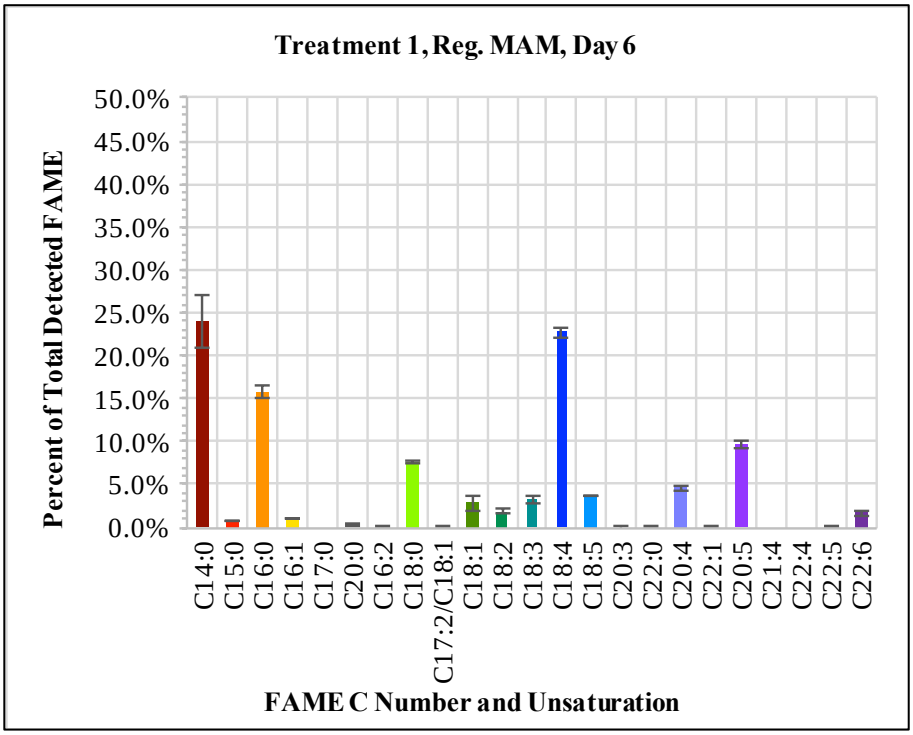

Figure 83: Treatment No. 1 (standard MAM/nutrient-replete "control") FAME composition from sample day 6, GC/MS method.

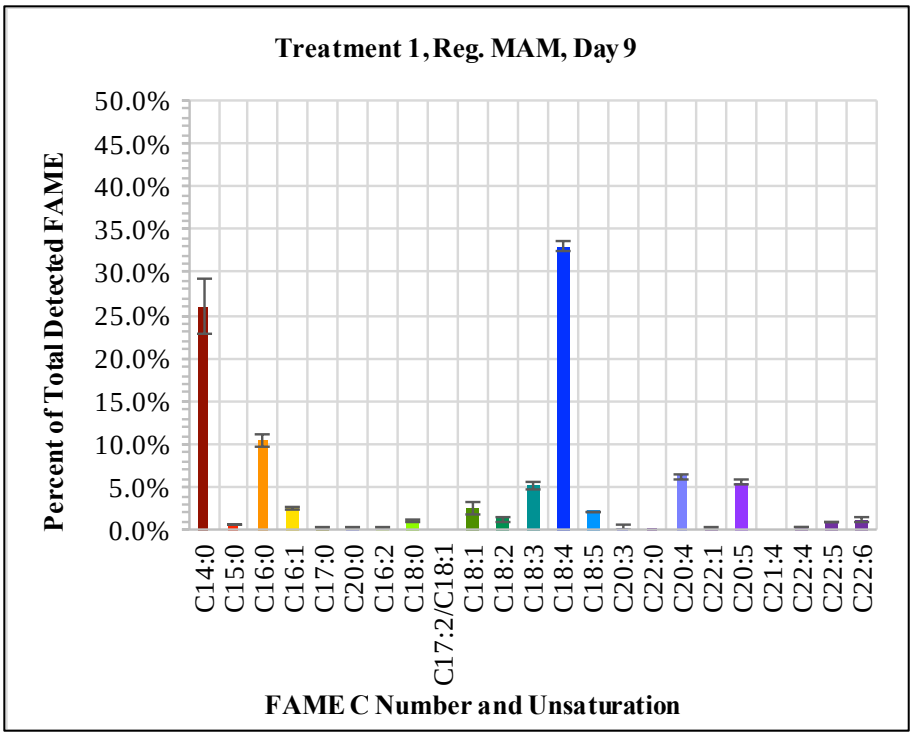

Figure 84: Treatment No. 1 (standard MAM/nutrient-replete "control") FAME composition from sample day 9, GC/MS method.

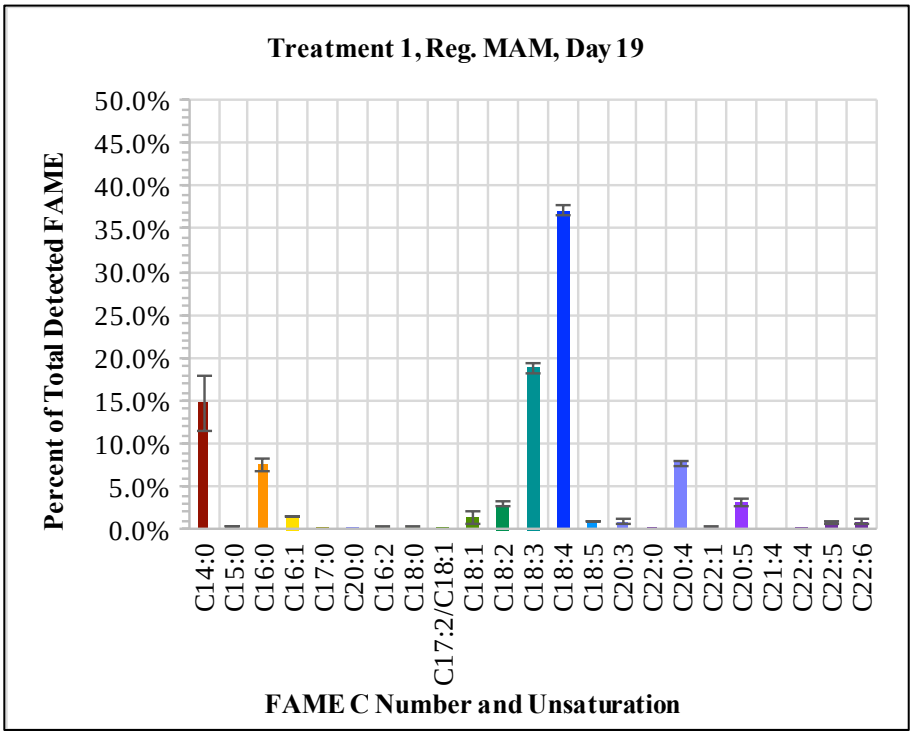

Figure 85: Treatment No. 1 (standard MAM/nutrient-replete "control") FAME composition from sample day 19, GC/MS method.

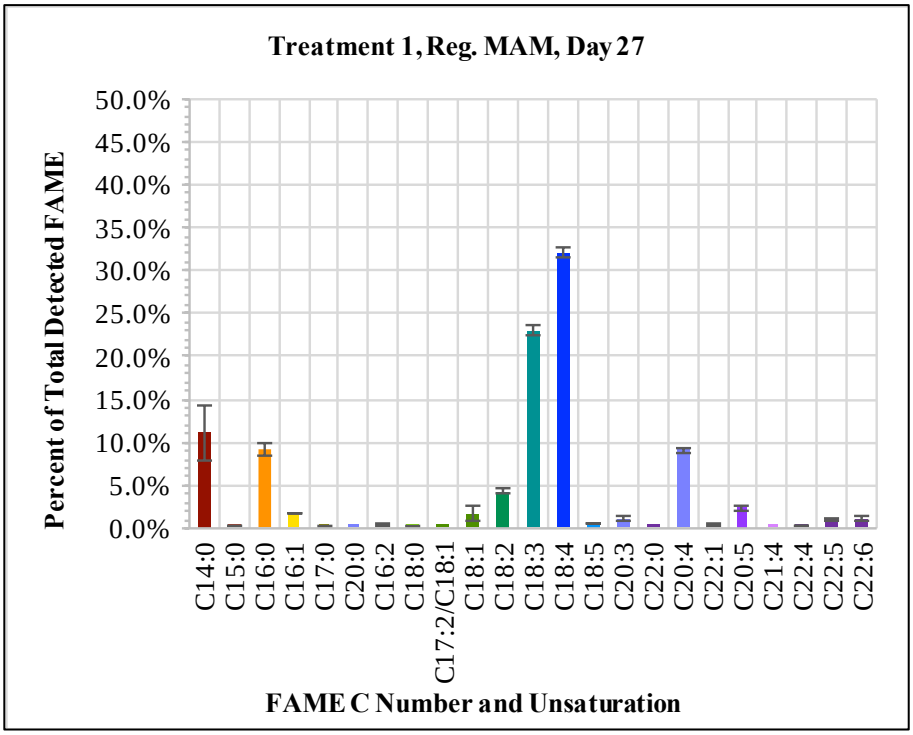

Figure 86: Treatment No. 1 (standard MAM/nutrient-replete "control") FAME composition from sample day 27, GC/MS method.

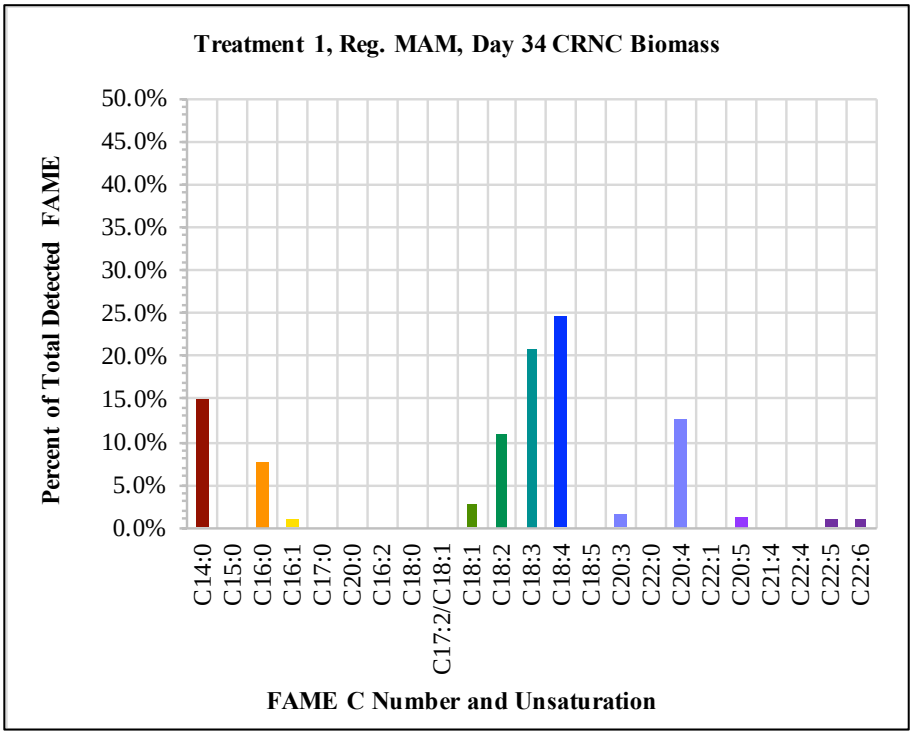

Figure 87: Treatment No. 1 (standard MAM/nutrient-replete "control") FAME composition from sample day 34 from CNRC biomass extraction method.

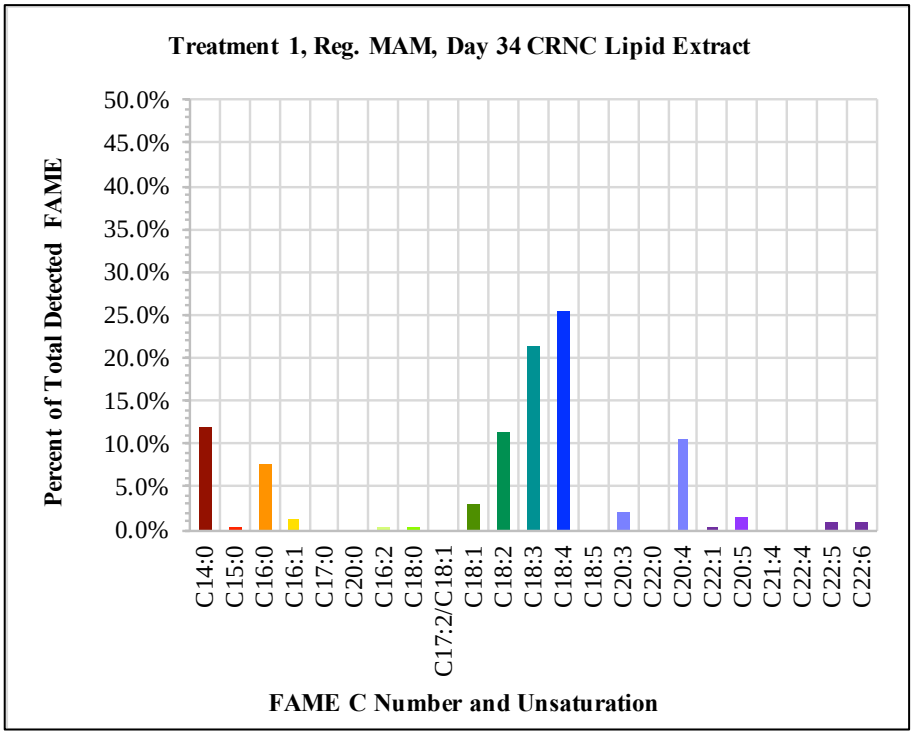

Figure 88: Treatment No. 1 (standard MAM/nutrient-replete "control") FAME composition from sample day 34 from CNRC lipid extraction method.

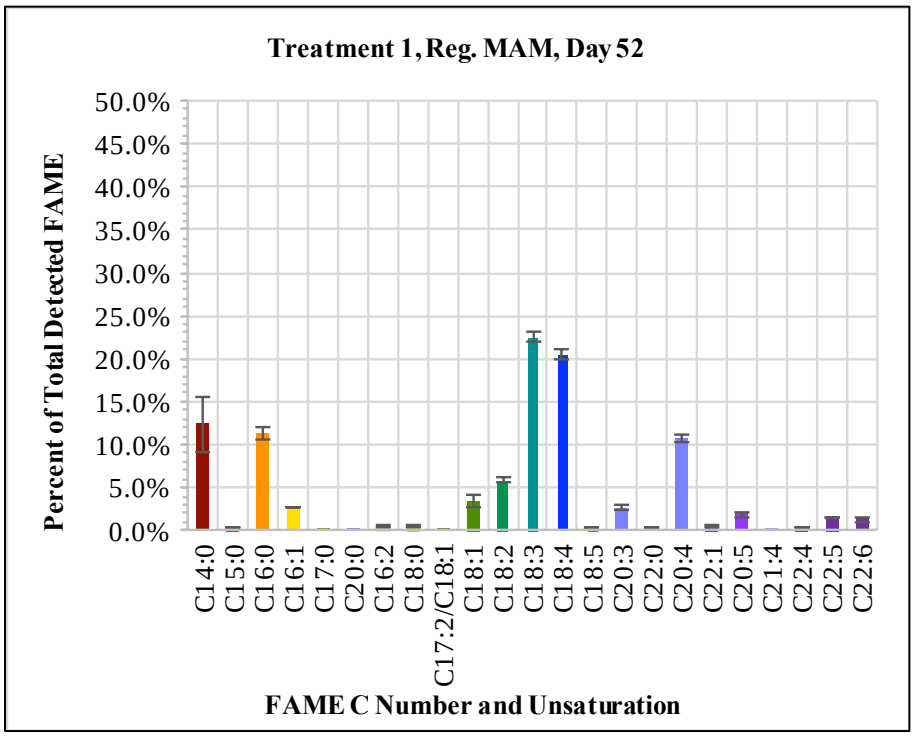

Figure 89: Treatment No. 1 (standard MAM/nutrient-replete "control") FAME composition from sample day 52, GC/MS method.

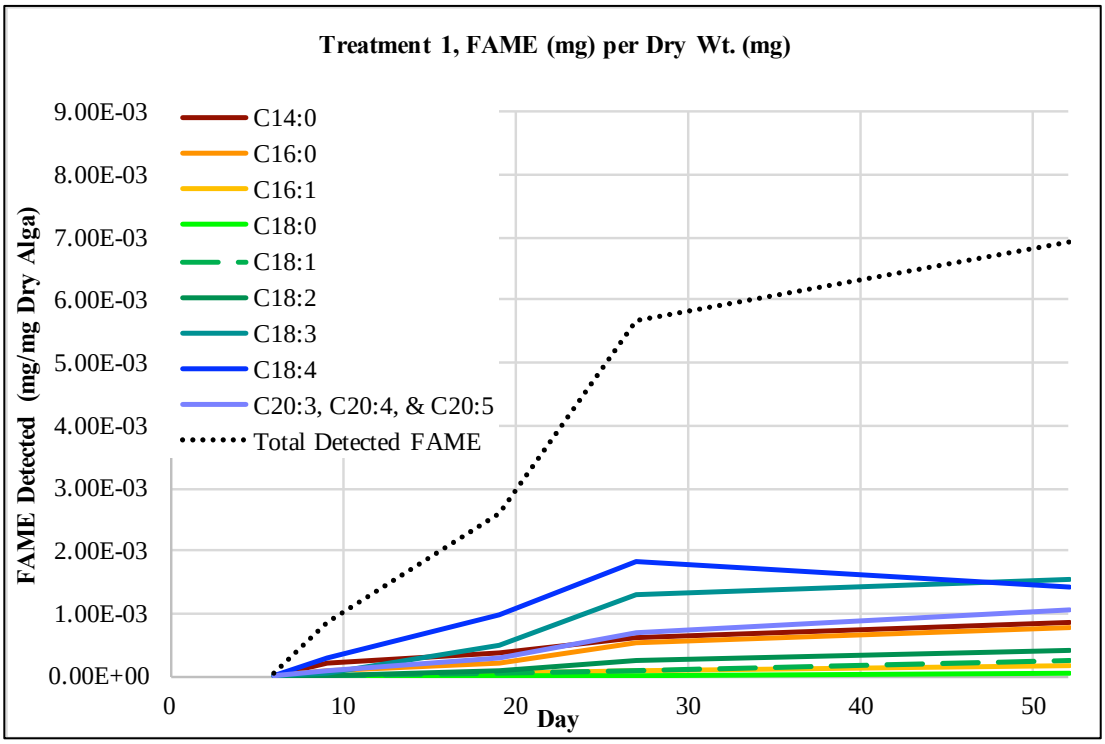

Figure 90: Treatment No.1, Standard MAM (high-nutrient medium, "control"), FAME proportion of dry weight and change with time of sample harvest. The above results are from GC/MS analysis only.

3.12.8.2. Treatment 2, Low Nitrogen MAM

In treatment No. 2 (low nitrogen MAM), the highest proportion of the monounsaturated FAME, C18:1 (45.1%) was detected on sample day 34, by the CNRC lipid extraction method. The highest total FAME content, detected by the CNRC biomass extraction method, was 51.018 mg/g on day 34 (Table XXII). However, it is likely that the total FAME content actually reached its peak earlier in the growth cycle, between day 9 and 19, when the highest total FAME content was detected by the GC/MS method (Figures 91 – 97).

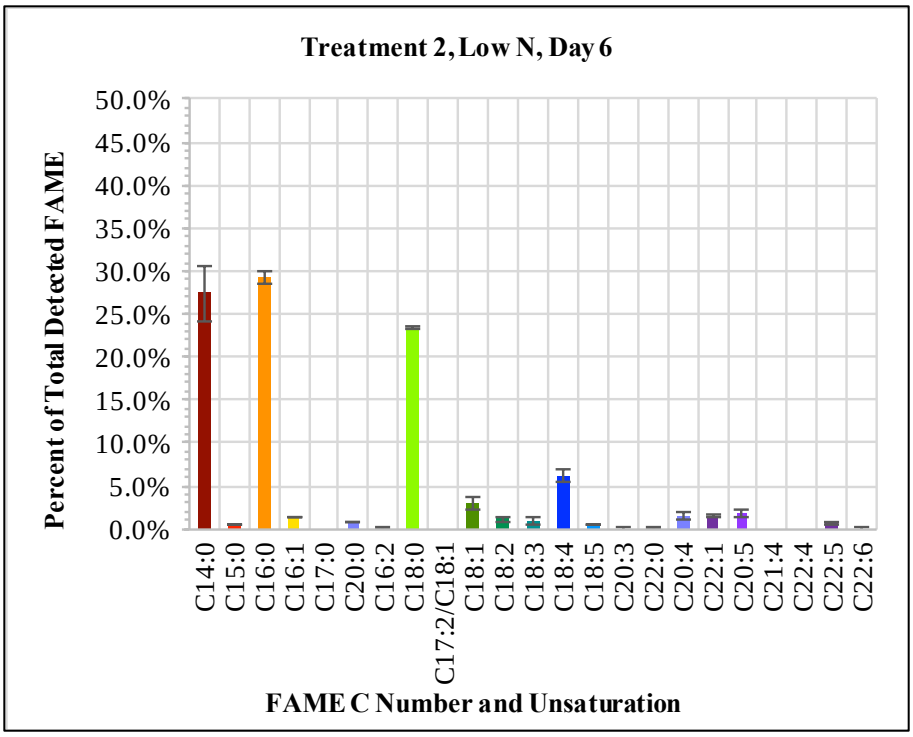

Figure 91: Treatment No. 2 (low nitrogen MAM) FAME composition from sample day 6, GC/MS method.

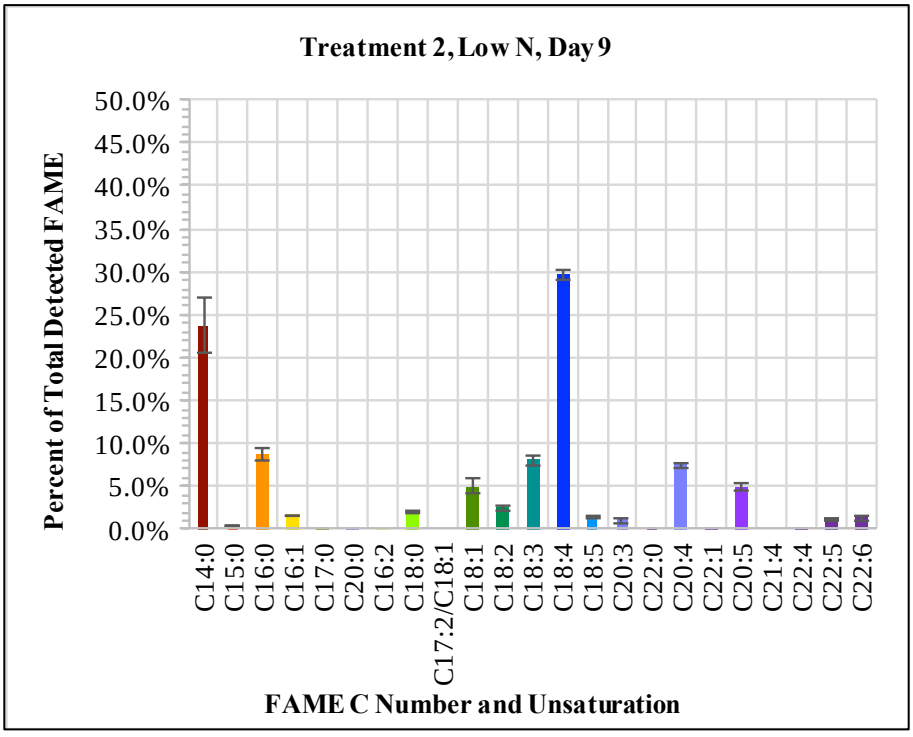

Figure 92: Treatment No. 2 (low nitrogen MAM) FAME composition from sample day 9, GC/MS method.

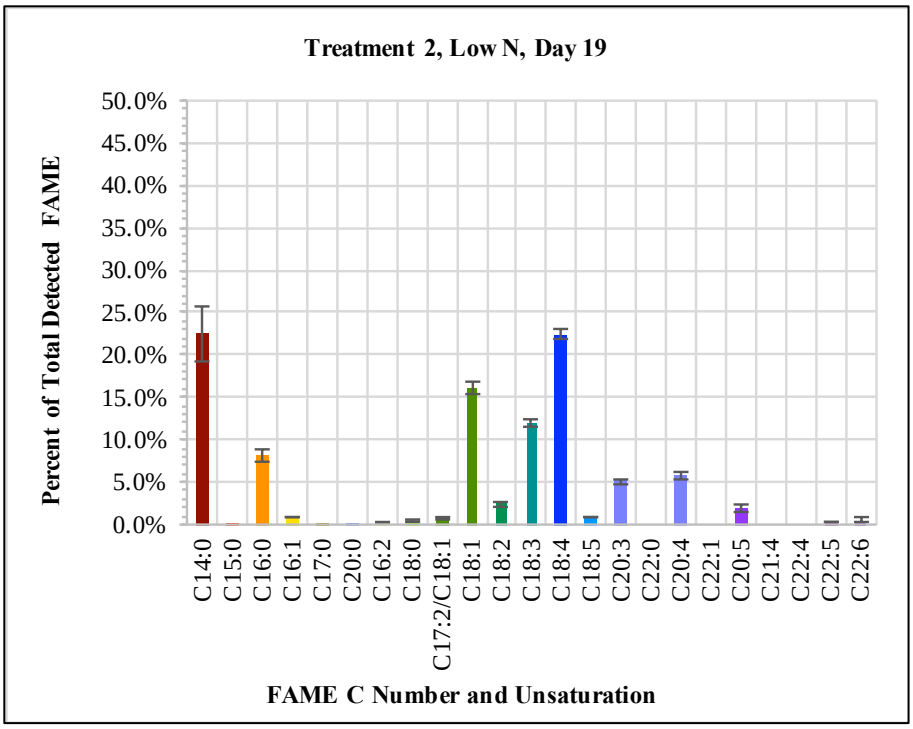

Figure 93: Treatment No. 2 (low nitrogen MAM) FAME composition from sample day 19, GC/MS method.

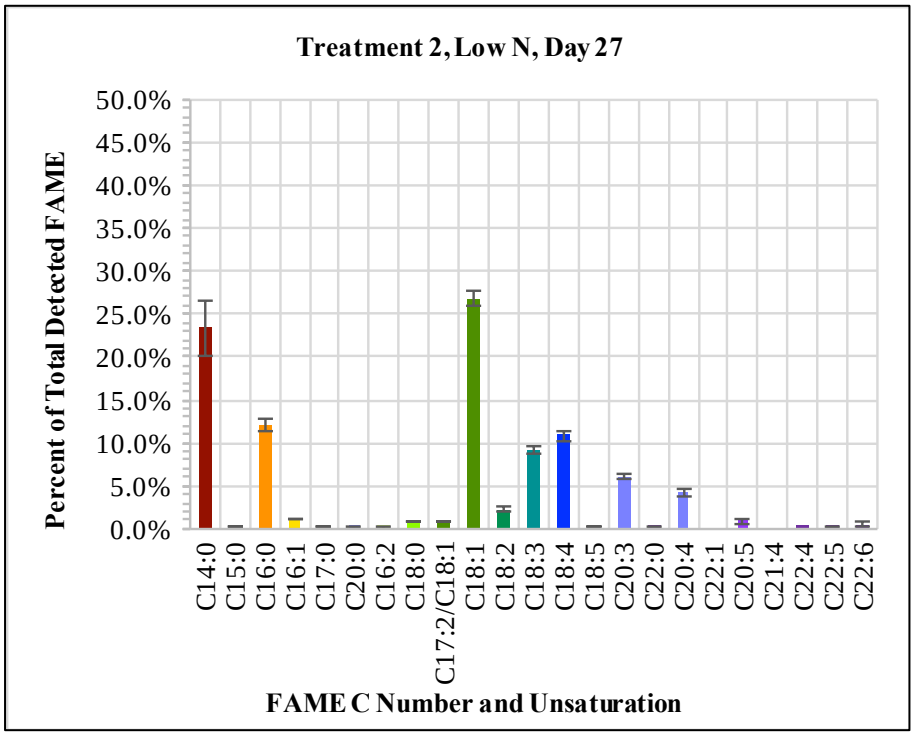

Figure 94: Treatment No. 2 (low nitrogen MAM) FAME composition from sample day 27, GC/MS method.

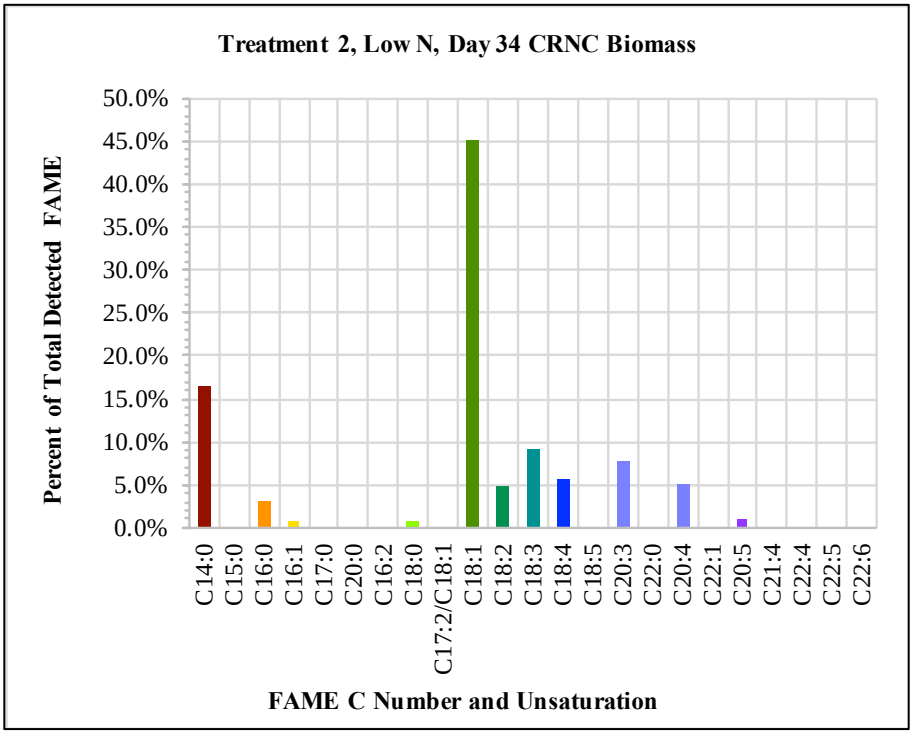

Figure 95: Treatment No. 2 (low nitrogen MAM) FAME composition from sample day 34 from CNRC biomass extraction method.

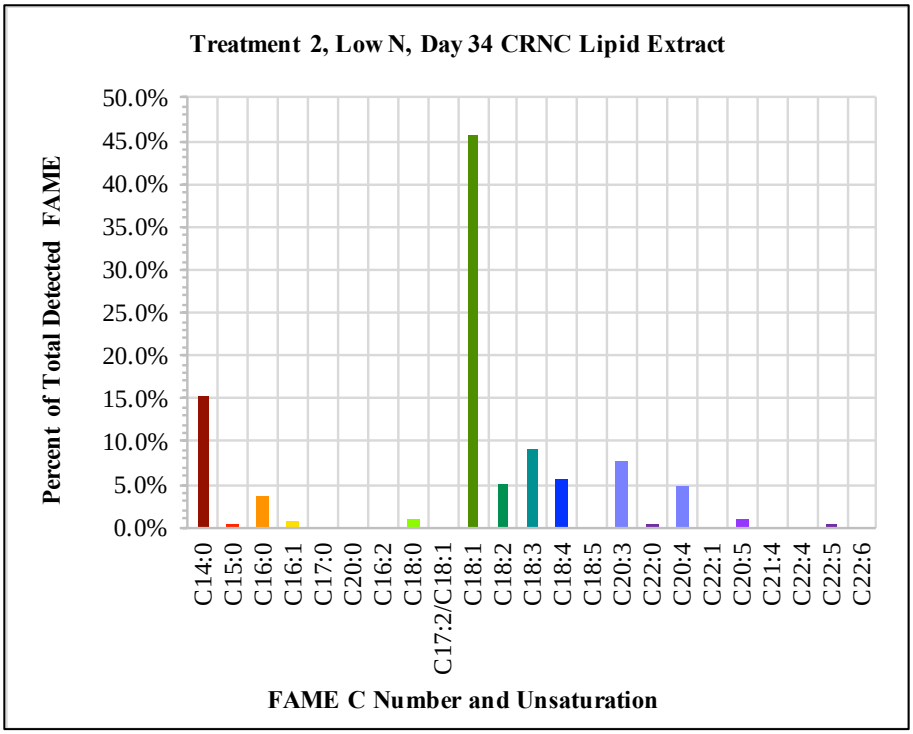

Figure 96: Treatment No. 2 (low nitrogen MAM) FAME composition from sample day 34 from CNRC solvent lipid extraction method.

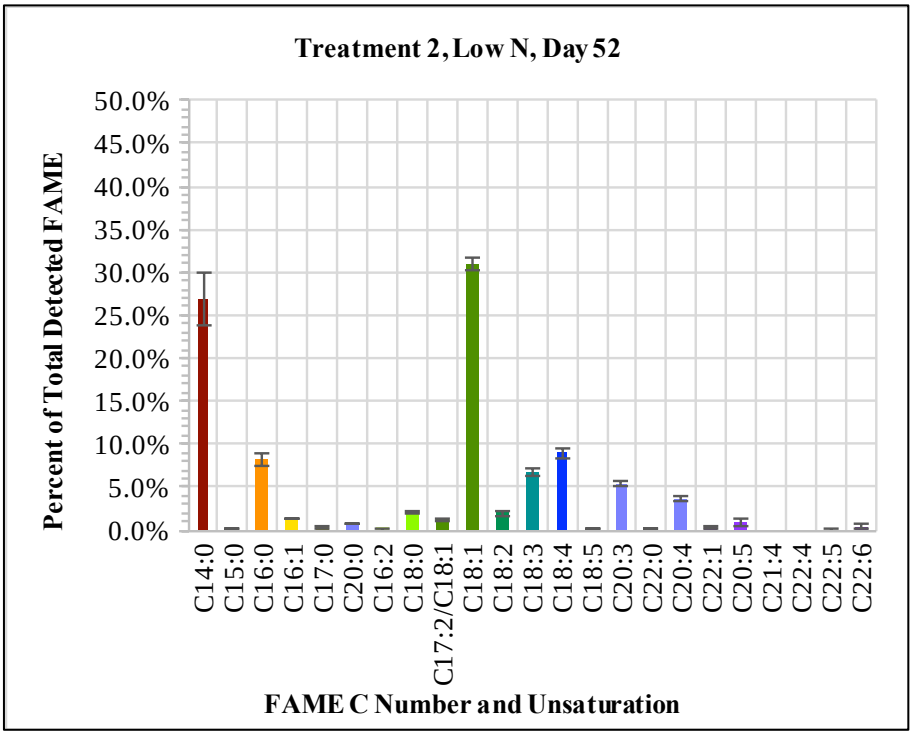

Figure 97: Treatment No. 2 (low nitrogen MAM) FAME composition from sample day 52, GC/MS method.

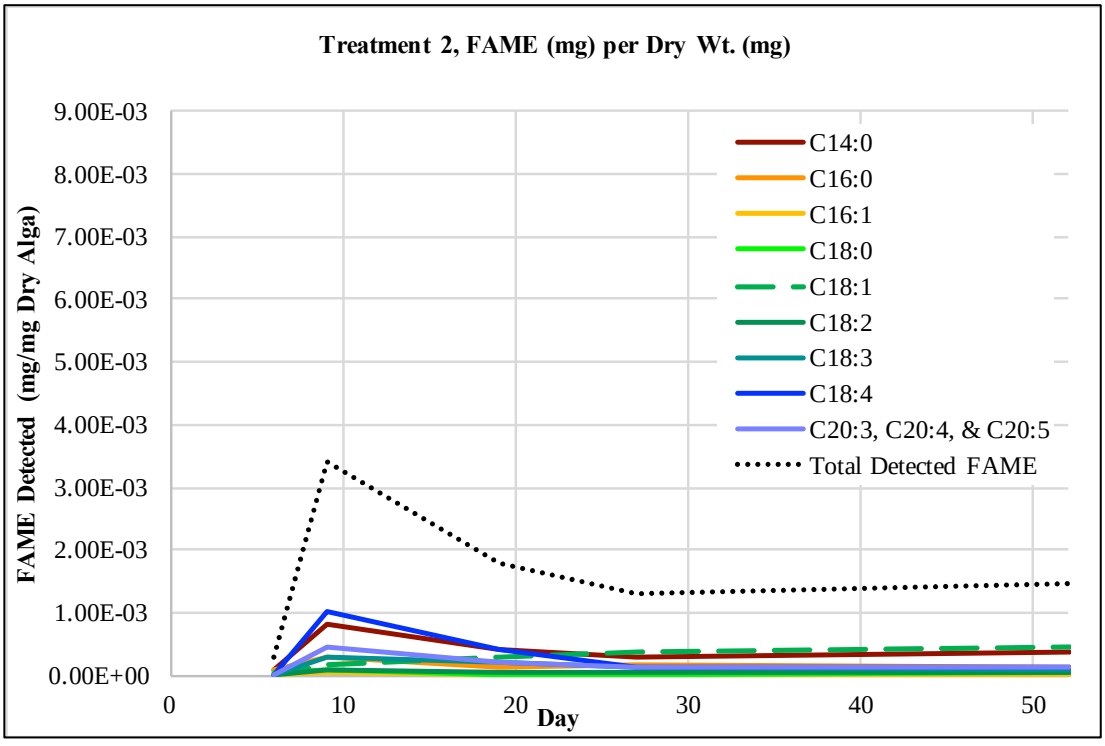

Figure 98: Treatment No.2, (low nitrogen MAM), FAME proportion of dry weight and change with time of sample harvest. The above results are from GC/MS analysis only.

3.12.8.3. Treatment 3, Low Phosphorus MAM

In treatment No. 3 (low phosphorus MAM), the highest proportion of the monounsaturated FAME, C18:1 (4.7%) was detected on sample day 52, the last sample to be collected. The highest total FAME content, detected by the CNRC biomass extraction method, was 40.947 mg/g on day 34 (Table XXII). However, it is likely that the total FAME content was actually highest closer to day 27, based on GC/MS results (Figures 98 – 105). Challagulla, Fabbro, and Nayar (2015) found that C16:1 increased in *Rhopalosolen saccatus* (a green alga) with lowered medium phosphorus, but no notable increase in the proportion of C16:1 FAME was observed in *C. freiburgensis* in response to treatment No. 3.

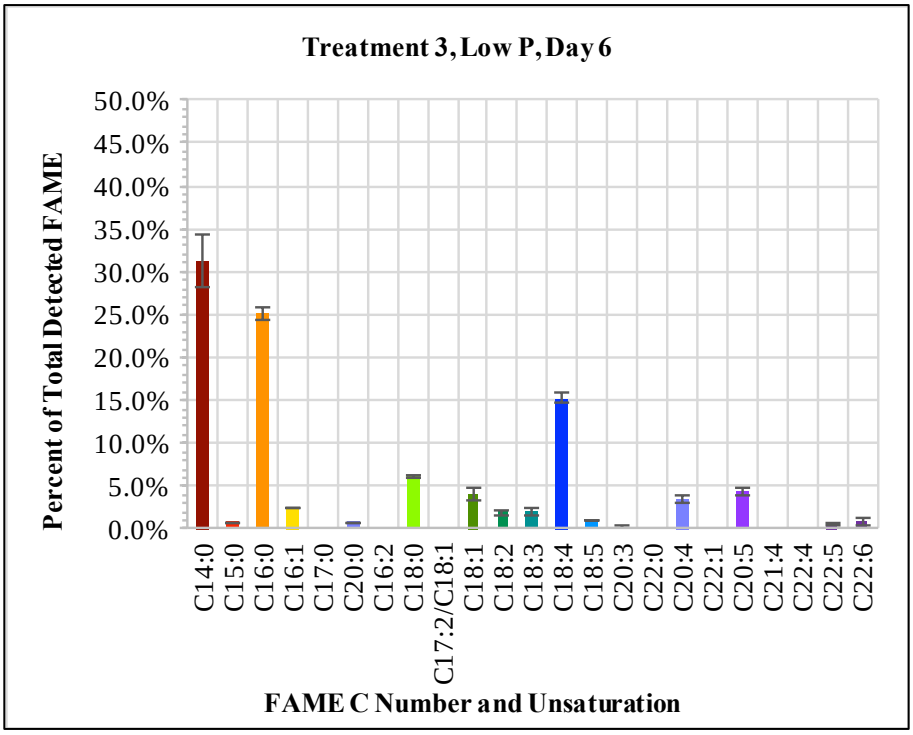

Figure 99: Treatment No. 3 (low phosphorus MAM) FAME composition from sample day 6, GC/MS method.

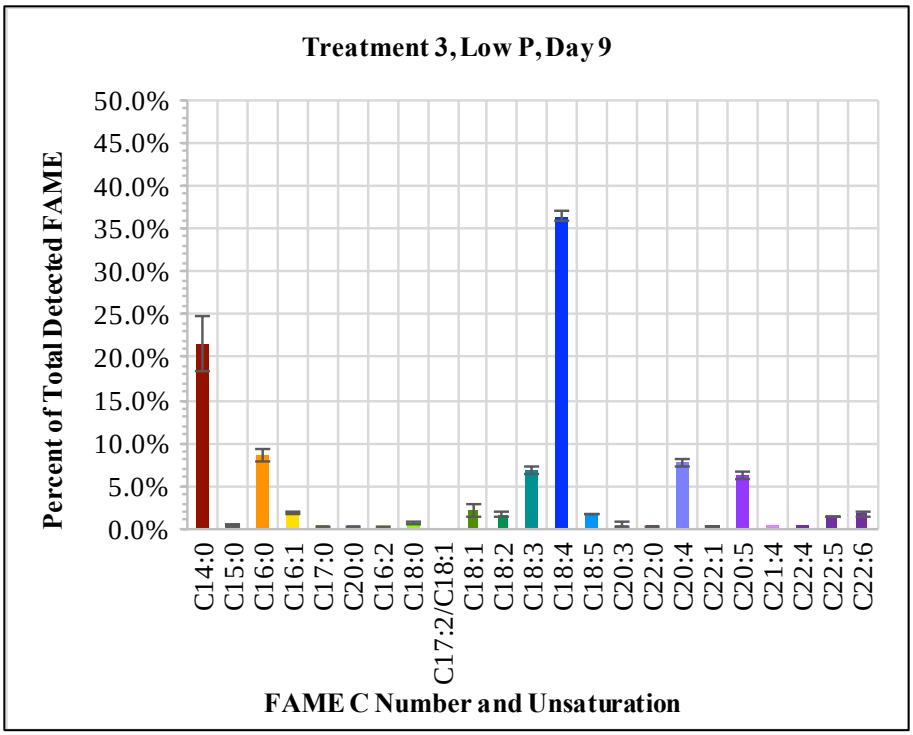

Figure 100: Treatment No. 3 (low phosphorus MAM) FAME composition from sample day 9 from GC/MS method.

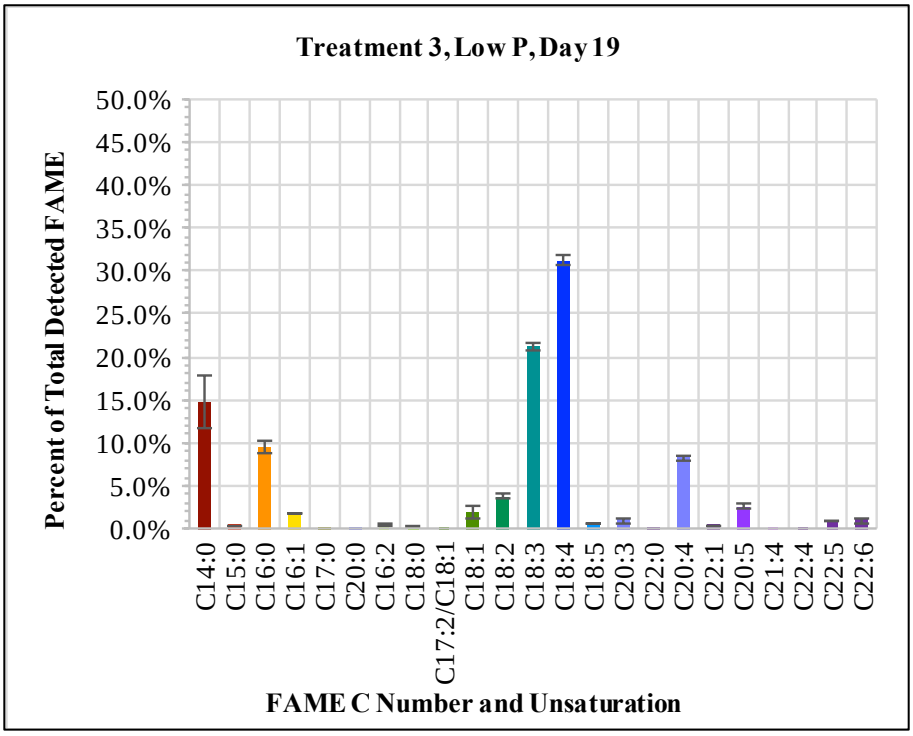

Figure 101: Treatment No. 3 (low phosphorus MAM) FAME composition from day 19, GC/MS method.

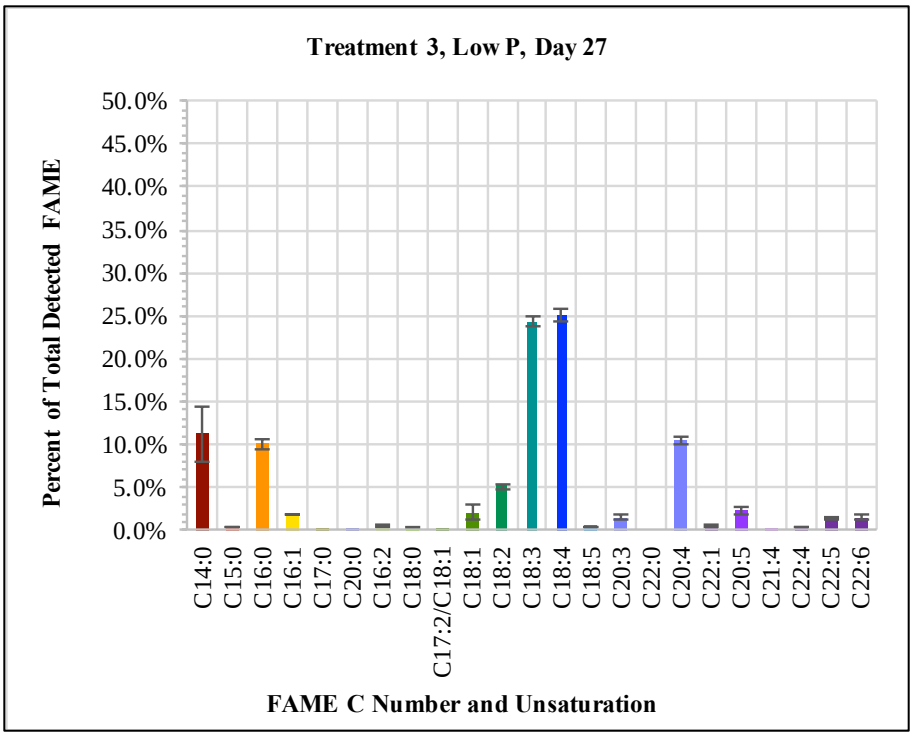

Figure 102: Treatment No. 3 (low phosphorus MAM) FAME composition from day 27, GC/MS method.

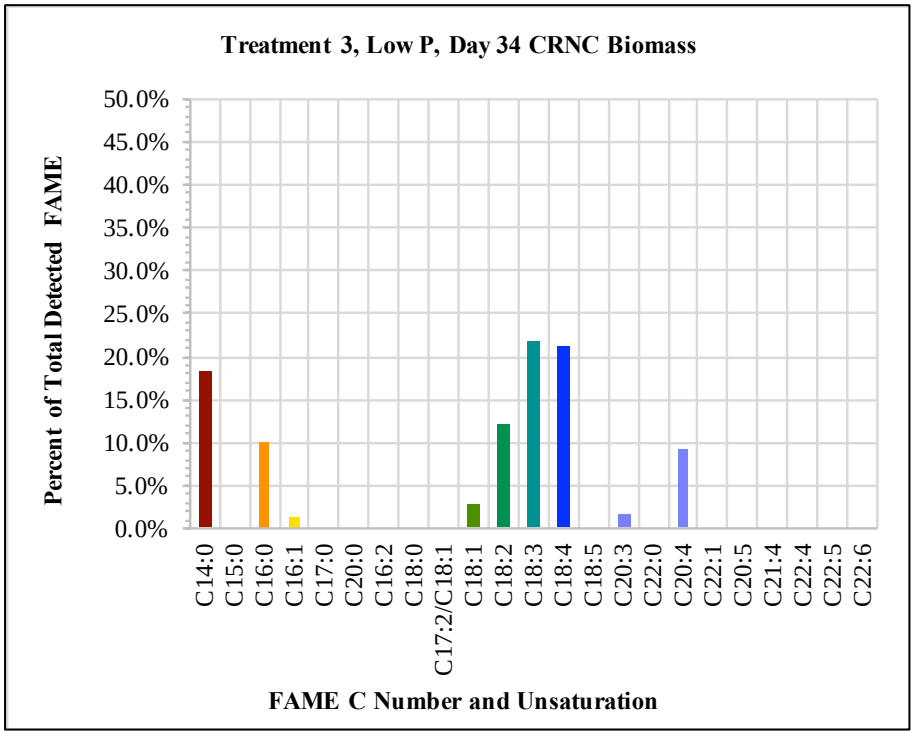

Figure 103: Treatment No. 3 (low phosphorus MAM) FAME composition from day 34, CNRC biomass method.

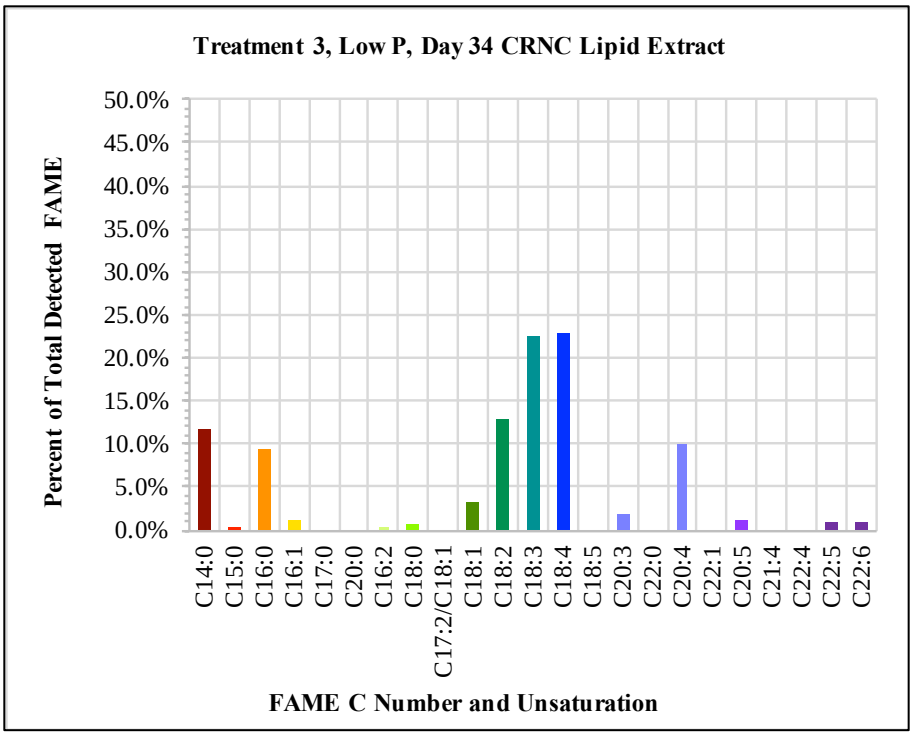

Figure 104: Treatment No. 3 (low phosphorus MAM) FAME composition from sample day 34 from CNRC lipid extraction method.

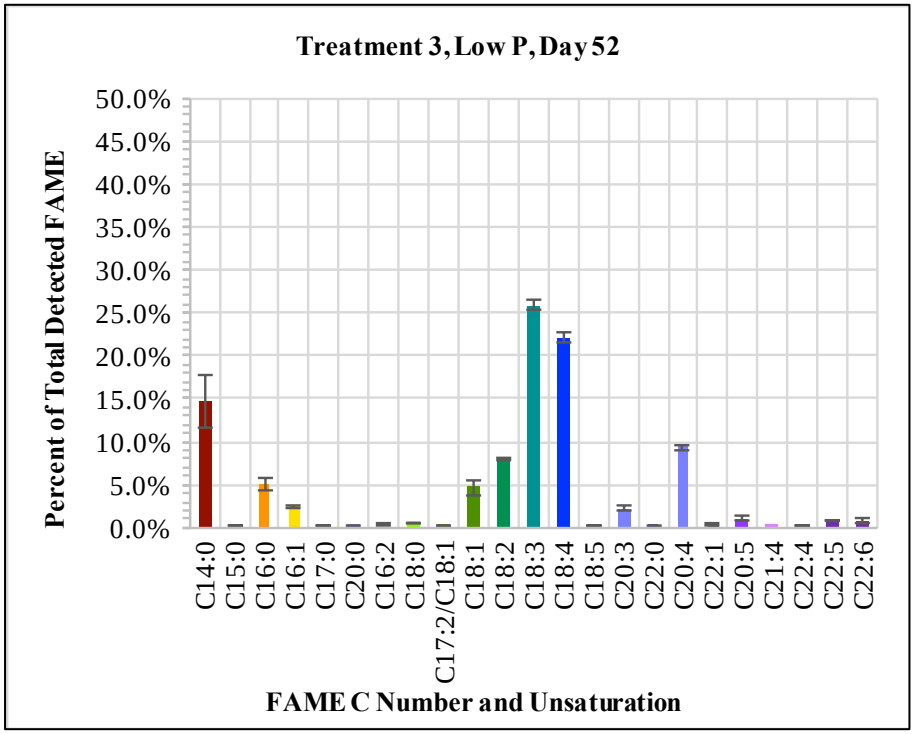

Figure 105: Treatment No. 3 (low phosphorus MAM) FAME composition from sample day 52, GC/MS method.

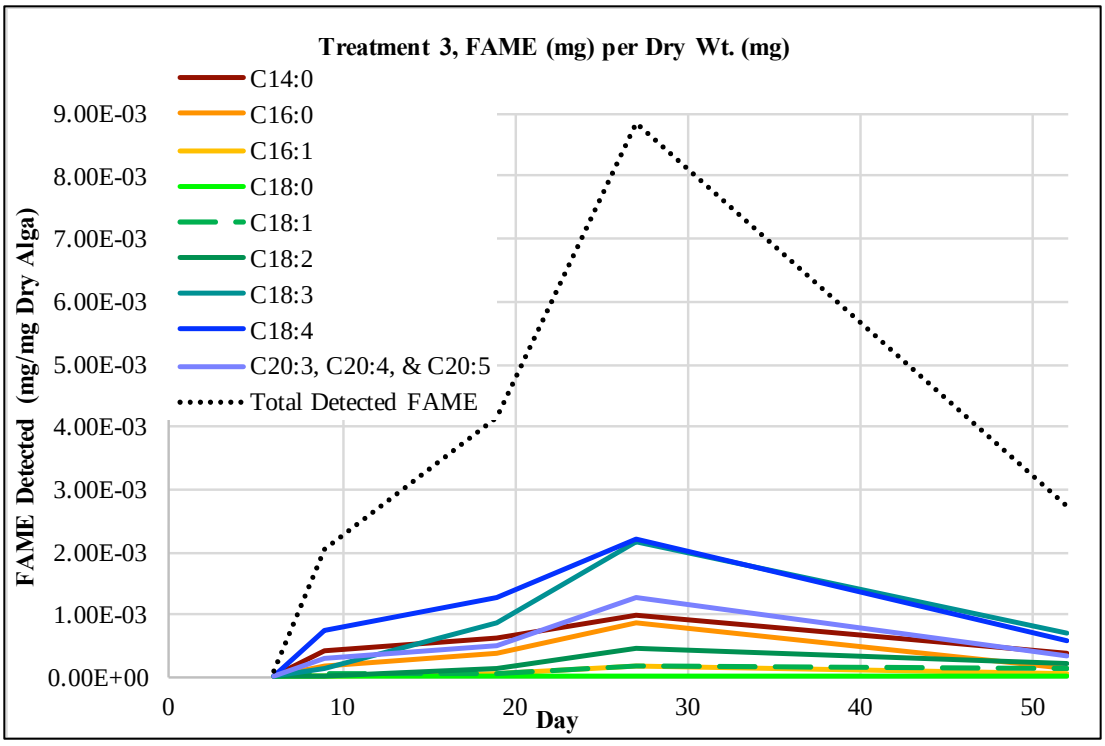

Figure 106: Treatment No. 3 (low phosphorus MAM), FAME proportion of dry weight and change with time of sample harvest. The above results are from GC/MS analysis only.

3.12.8.4. Treatment 4, Low Nitrogen and Low Phosphorus MAM

In treatment No. 4 (low nitrogen and low phosphorus MAM), the highest proportion of the monounsaturated FAME, C18:1 (50.1%) was detected on sample day 34 by the CNRC biomass extraction method. The highest total FAME content, detected by the CNRC biomass extraction method, was 39.046 mg/g on day 34 (Table XXII). However, it is more likely that the total FAME content was actually at its highest point between day 9 and day 19, based on GC/MS results (Figures 106 – 113).

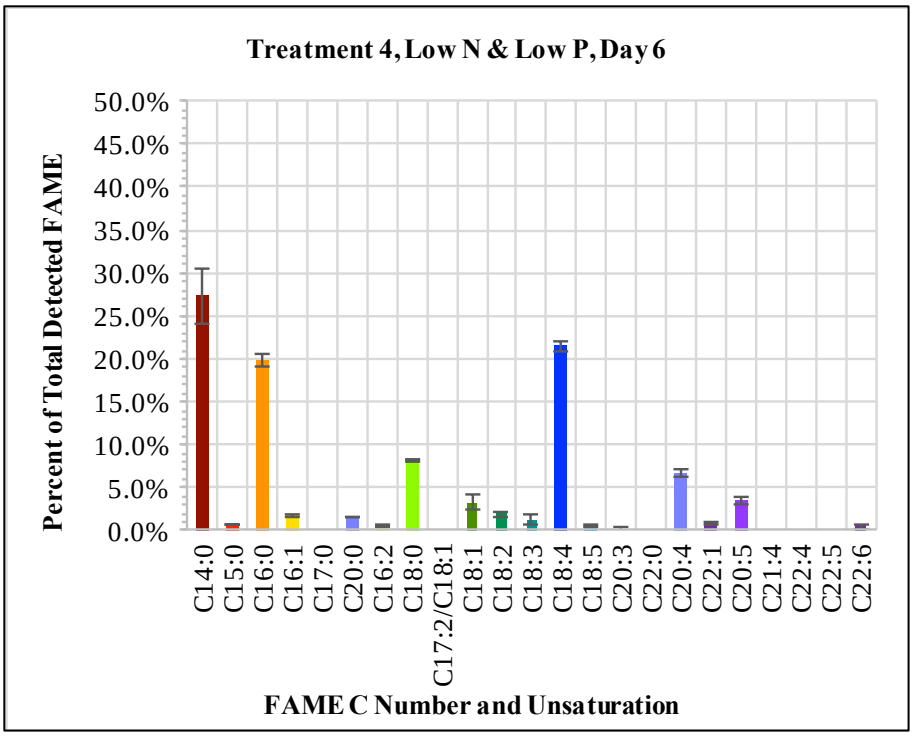

Figure 107: Treatment No. 4 (low nitrogen and low phosphorus MAM) FAME composition from sample day 6, GC/MS method.

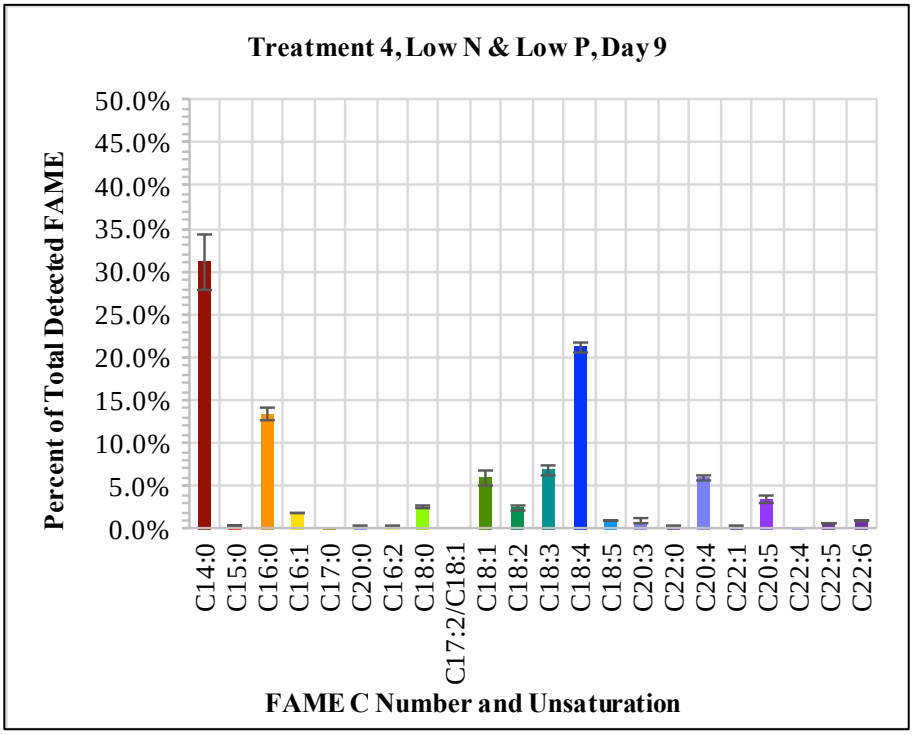

Figure 108: Treatment No. 4 (low nitrogen and low phosphorus MAM) FAME composition from sample day 9, GC/MS method.

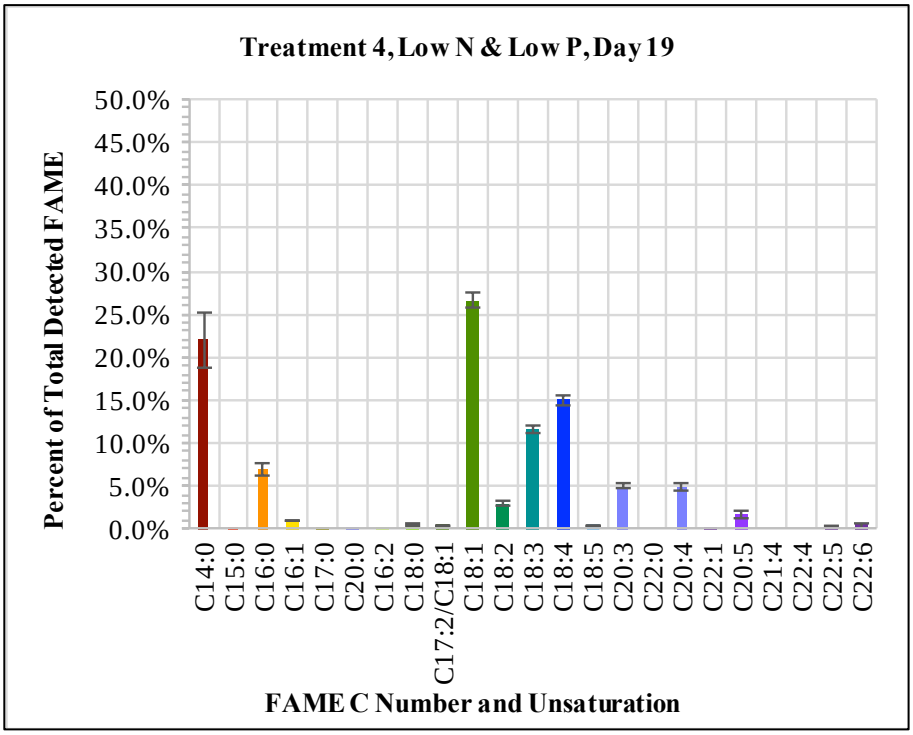

Figure 109: Treatment No. 4 (low nitrogen and low phosphorus MAM) FAME composition from sample day 19, GC/MS method.

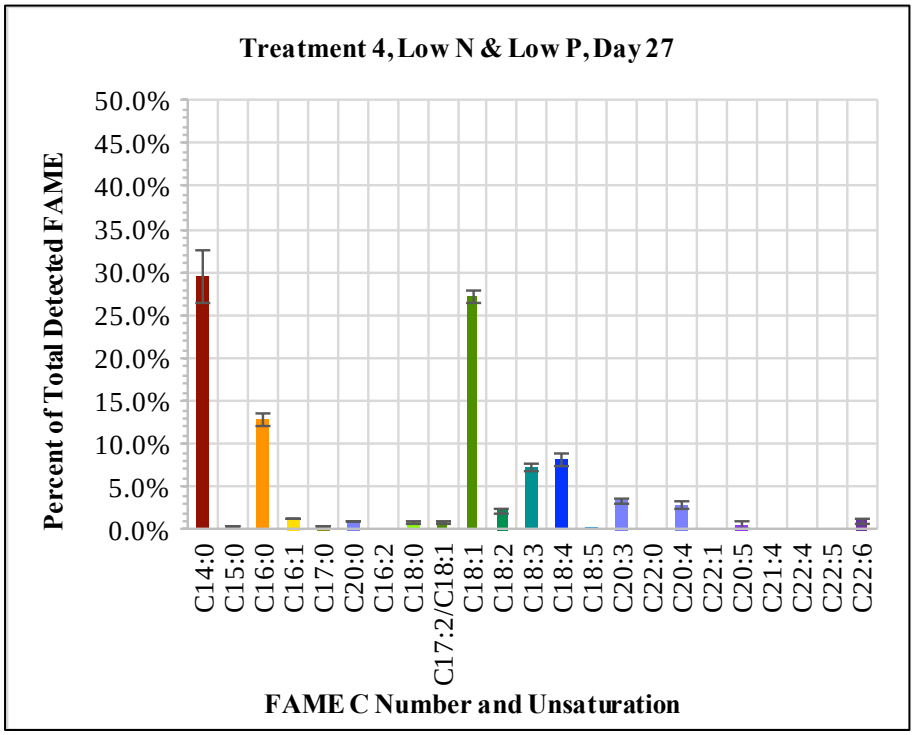

Figure 110: Treatment No. 4 (low nitrogen and low phosphorus MAM) FAME composition, day 27, GC/MS method.

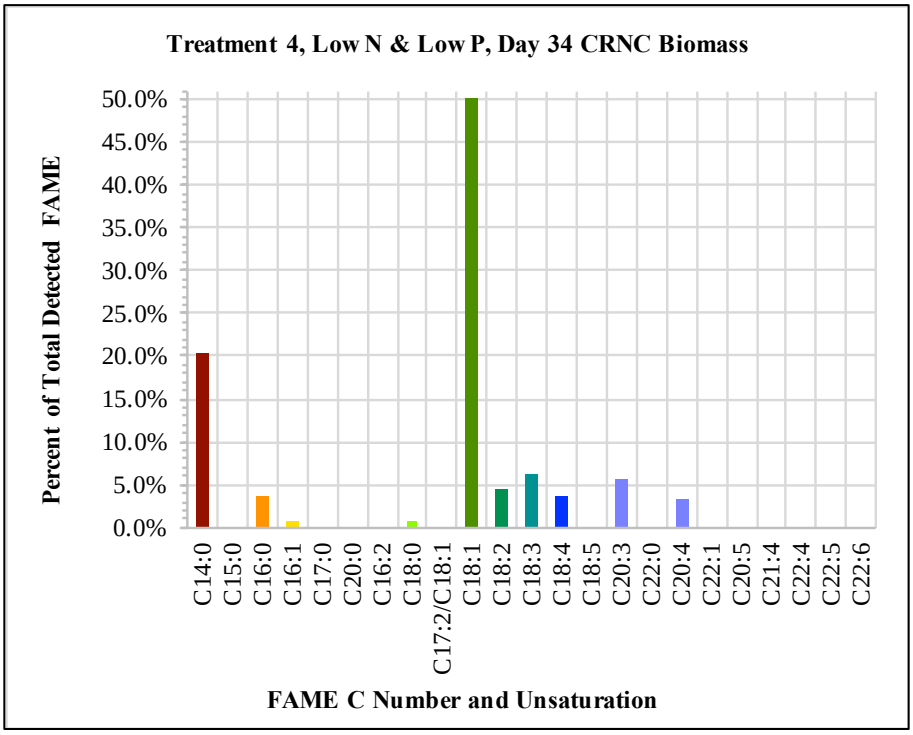

Figure 111: Treatment No. 4 (low nitrogen and low phosphorus MAM) FAME composition from sample day 34 from CNRC biomass method.

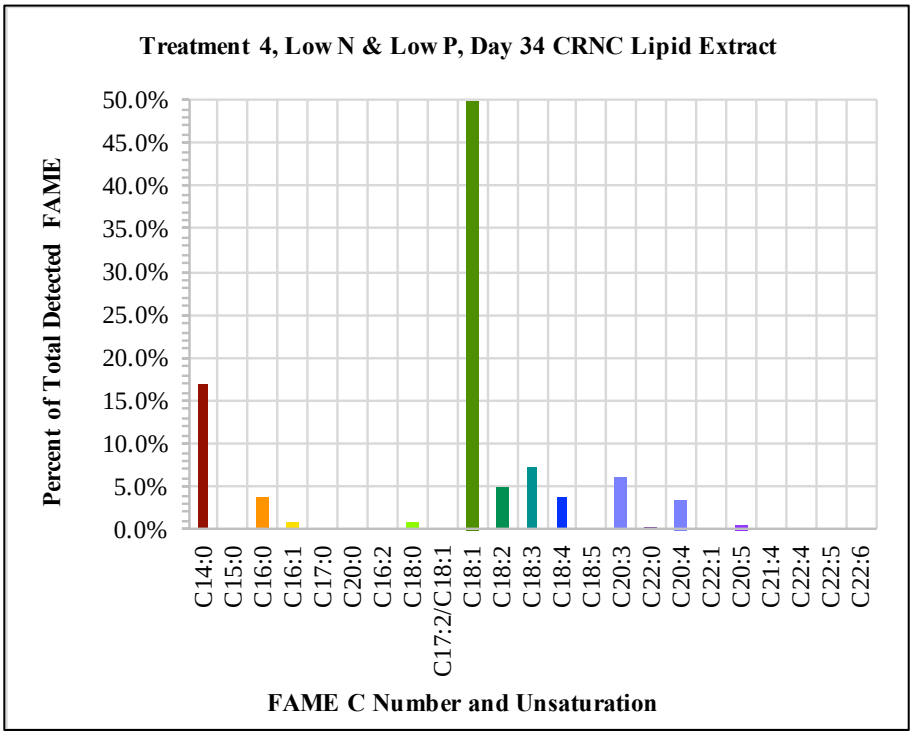

Figure 112: Treatment No. 4 (low nitrogen and low phosphorus MAM) FAME composition from sample day 34 from CNRC lipid extract method.

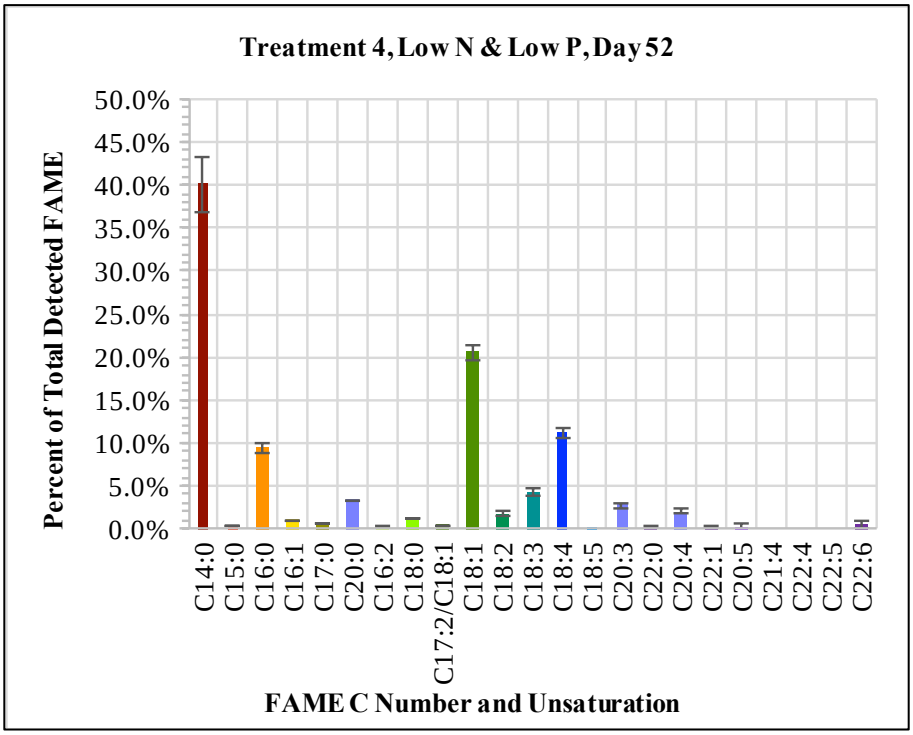

Figure 113: Treatment No. 4 (low nitrogen and low phosphorus MAM) FAME composition, day 52, GC/MS method.

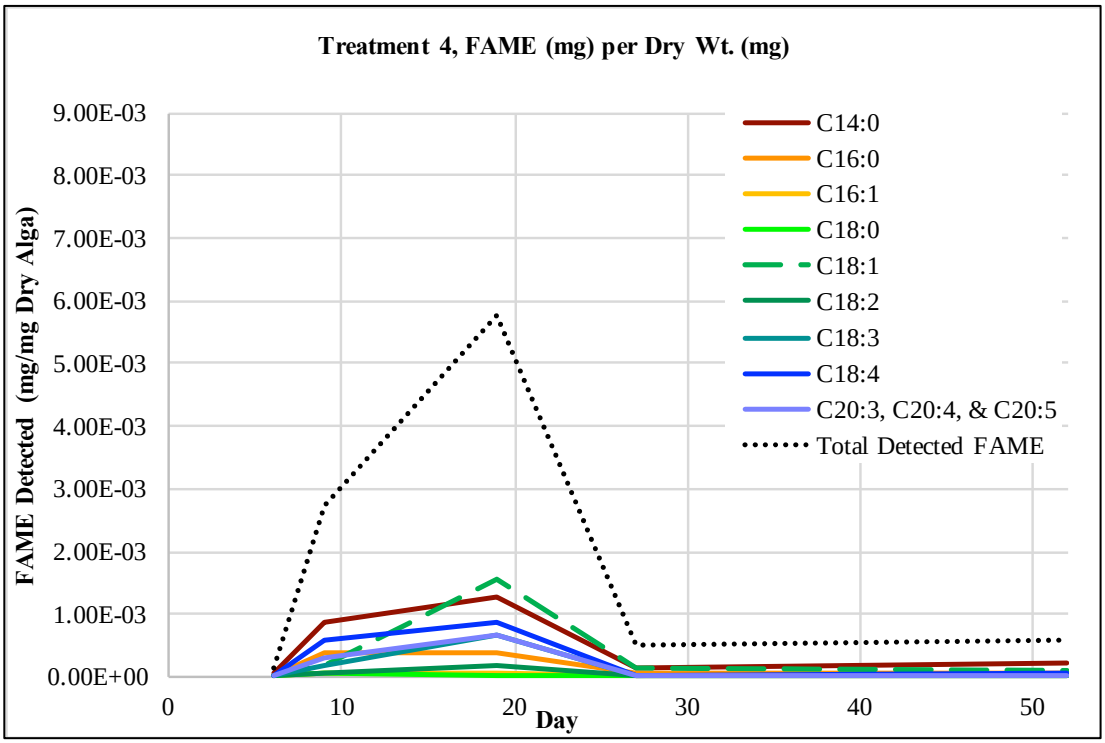

Figure 114: Treatment No. 4 (low nitrogen and low phosphorus MAM), FAME proportion of dry weight and change with time of sample harvest. The above results are from GC/MS analysis only.

3.12.8.6. Treatment 5, Low Nitrogen, Low Phosphorus MAM with Supplemental CO_2

In treatment No. 5 (low nitrogen, low phosphorus MAM with supplemental CO_2), the highest proportion of the monounsaturated FAME, C18:1 (48.1%) was detected on sample day 34, by the CNRC biomass extraction method. The highest total FAME content, also detected by the CNRC biomass extraction method on day 34, was 51.148 mg/g (Table XXII). However, it is likely that the total FAME content was actually highest close to day 15, based on GC/MS results (Figures 114 – 122). Treatment No. 5 resulted in the second-highest proportion of C18:1 combined with the highest total FAME content of all six experimental treatments.

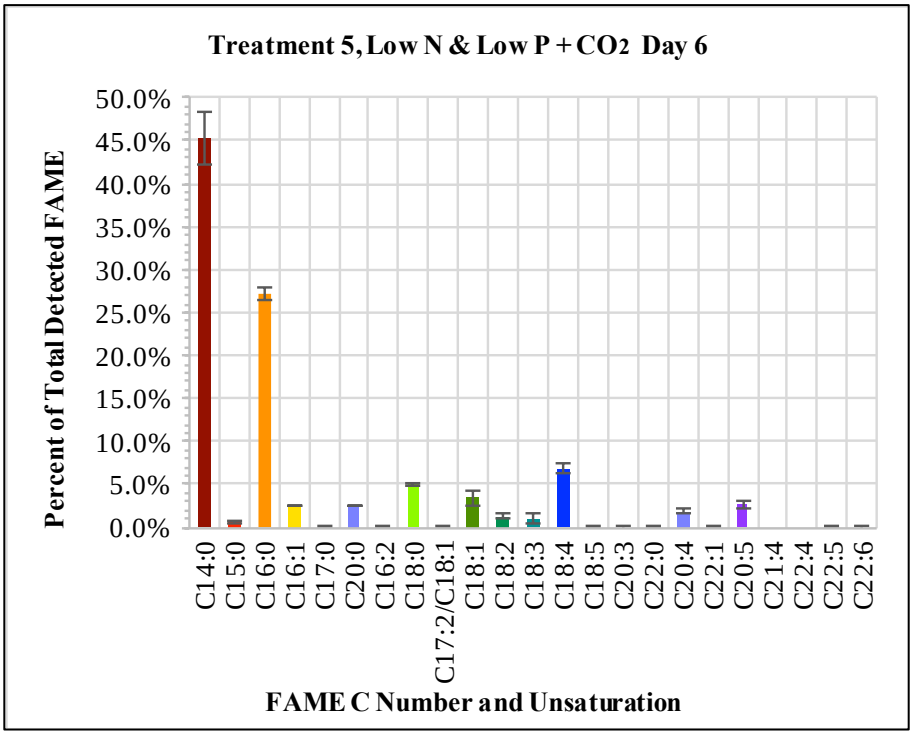

Figure 115: Treatment No. 5 (low nitrogen, low phosphorus and supplemental CO_2) FAME composition, from sample day 6, GC/MS method.

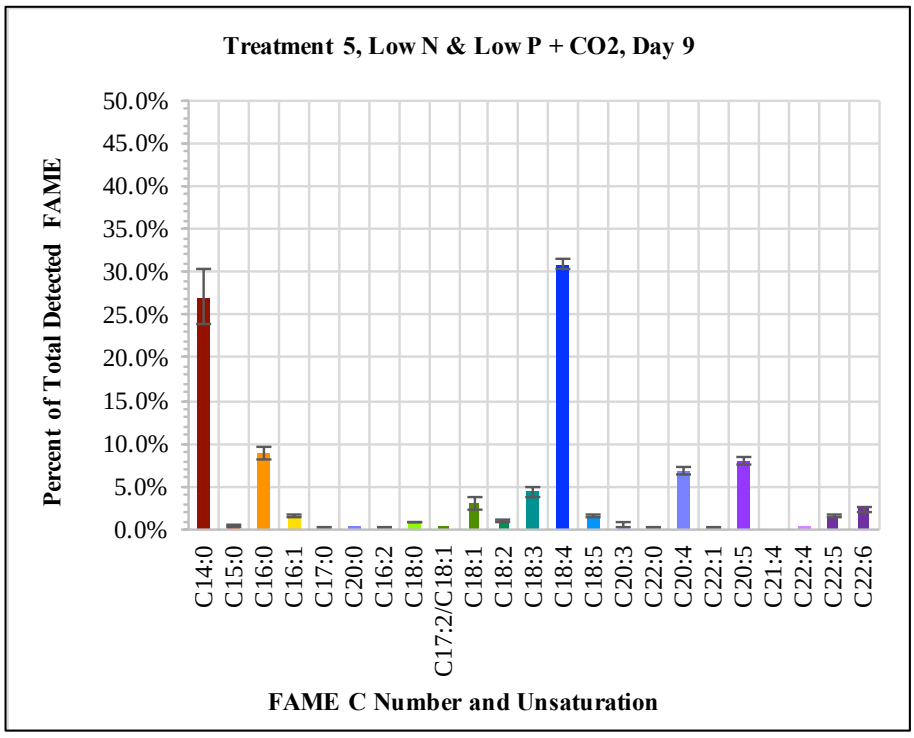

Figure 116: Treatment No. 5 (low nitrogen, low phosphorus and supplemental CO_2) FAME composition from sample day 9, GC/MS method.

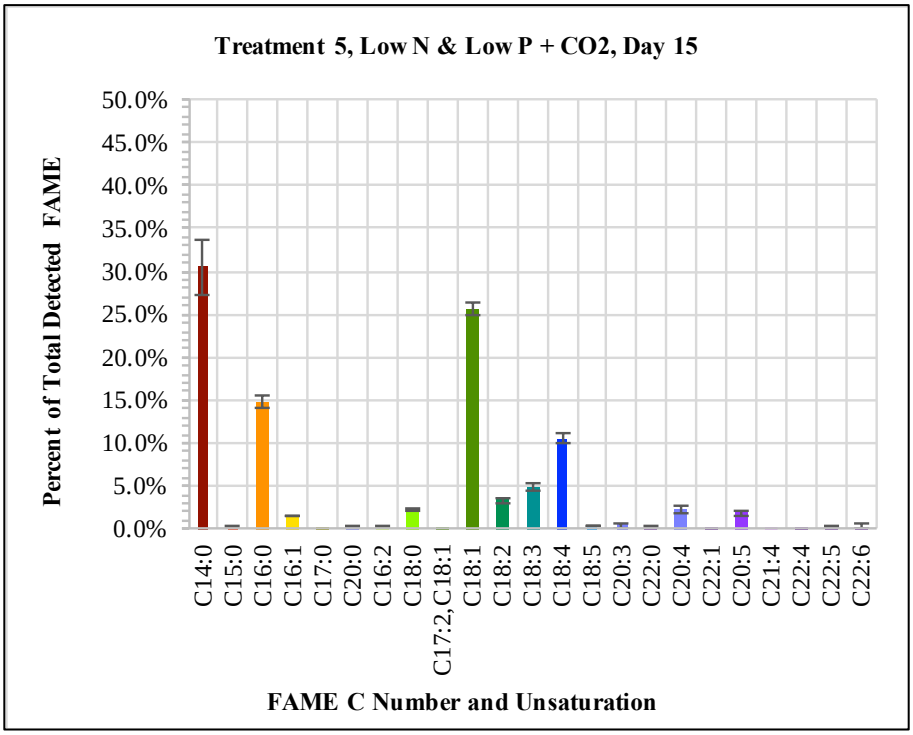

Figure 117: Treatment No. 5 (low nitrogen, low phosphorus and supplemental CO_2) FAME composition from sample day 15, GC/MS method.

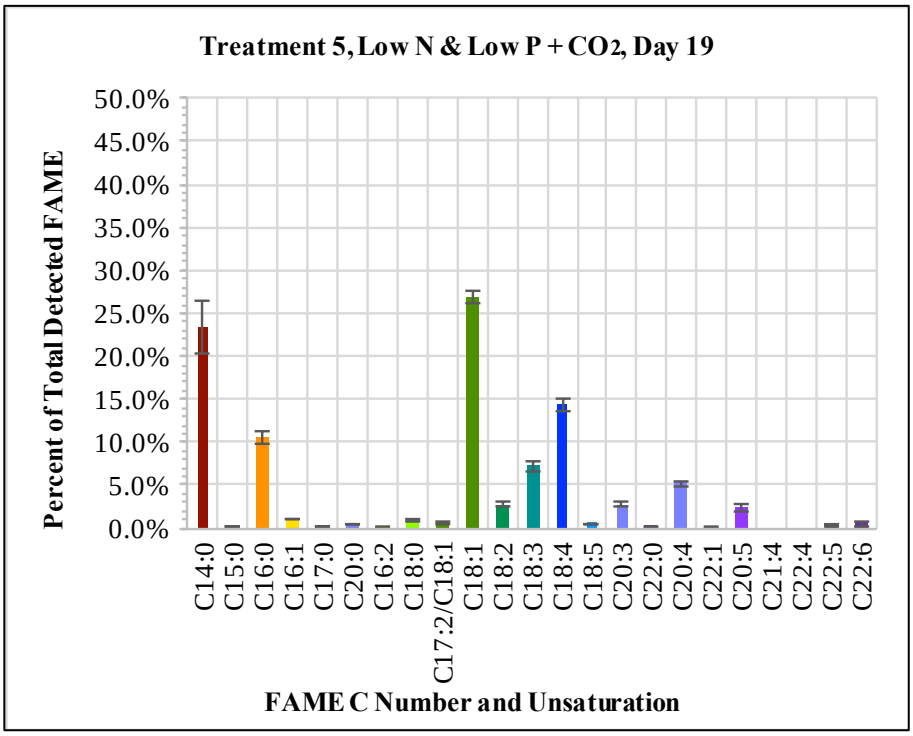

Figure 118: Treatment No. 5 (low nitrogen, low phosphorus and supplemental CO_2) FAME composition from sample day 19, GC/MS method.

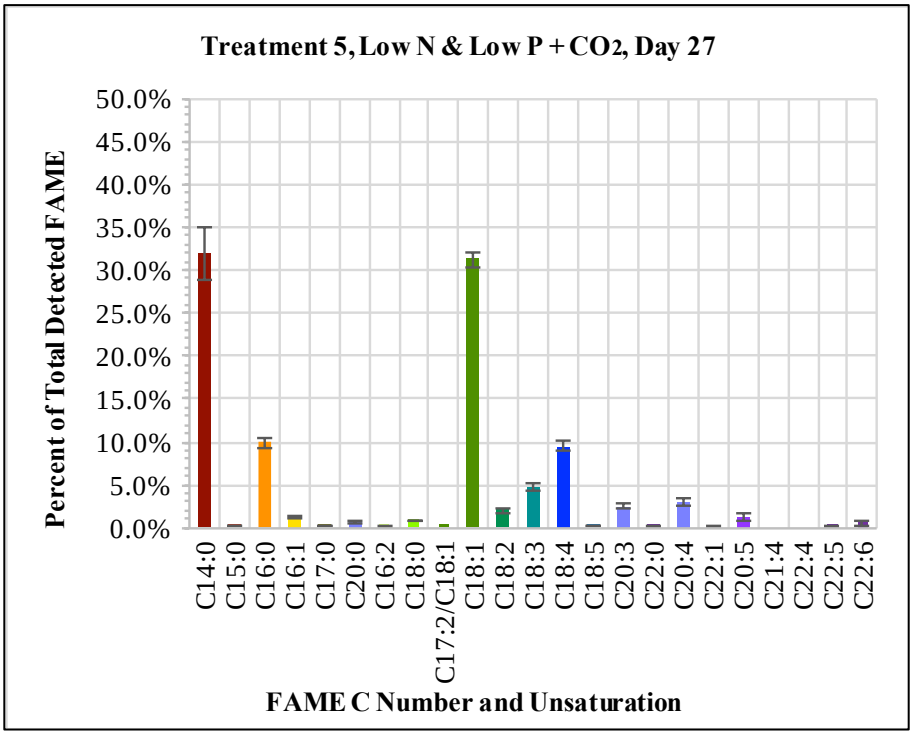

Figure 119: Treatment No. 5 (low nitrogen, low phosphorus and supplemental CO_2) FAME composition from sample day 27, GC/MS method.

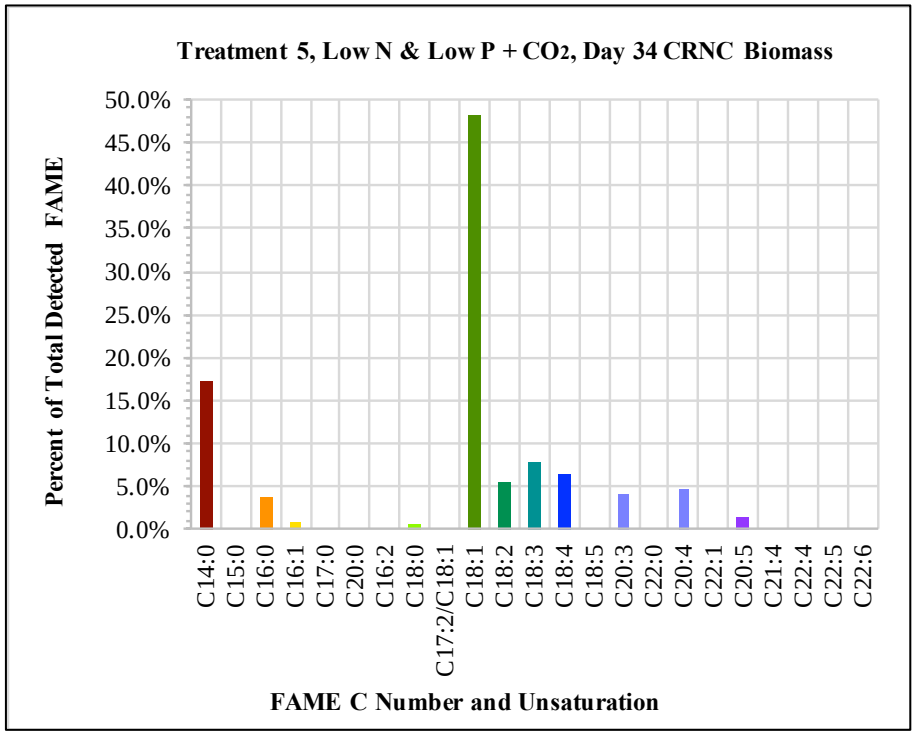

Figure 120: Treatment No. 5 (low nitrogen, low phosphorus and supplemental CO_2) FAME composition from sample day 34 from CNRC biomass method.

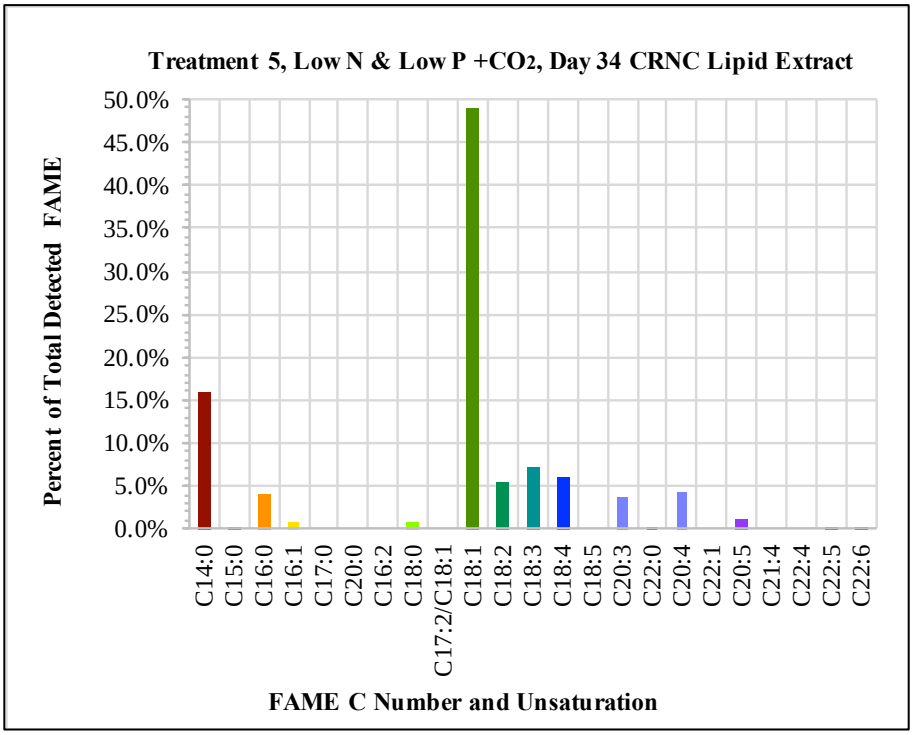

Figure 121: Treatment No. 5 (low nitrogen, low phosphorus and supplemental CO_2) FAME composition from sample day 34 from CNRC lipid extract method.

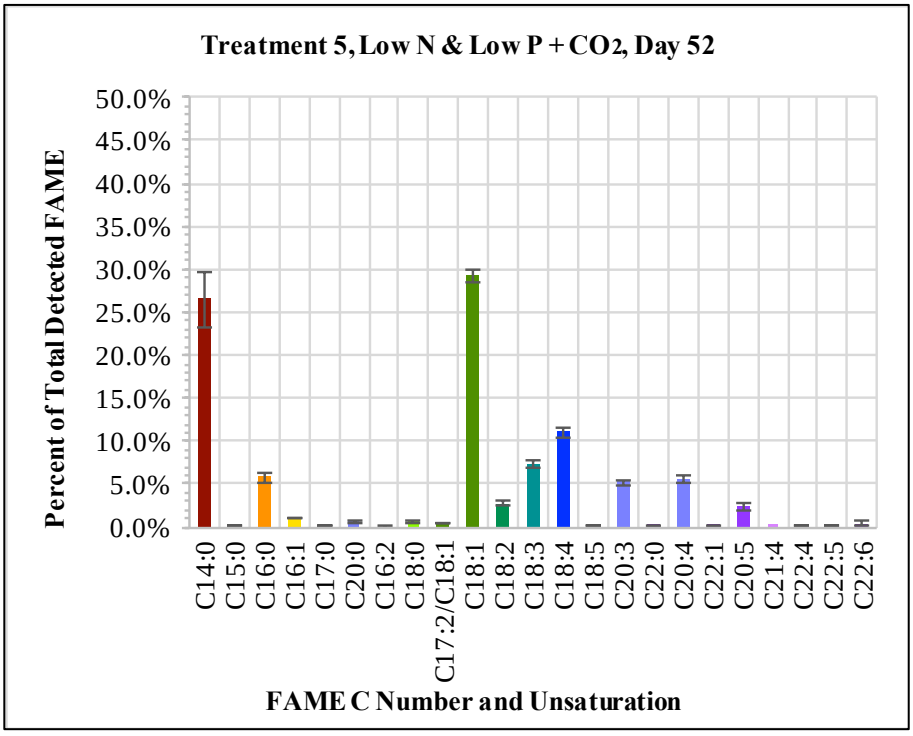

Figure 122: Treatment No. 5 (low nitrogen, low phosphorus and supplemental CO_2) FAME composition from sample day 52, GC/MS method.

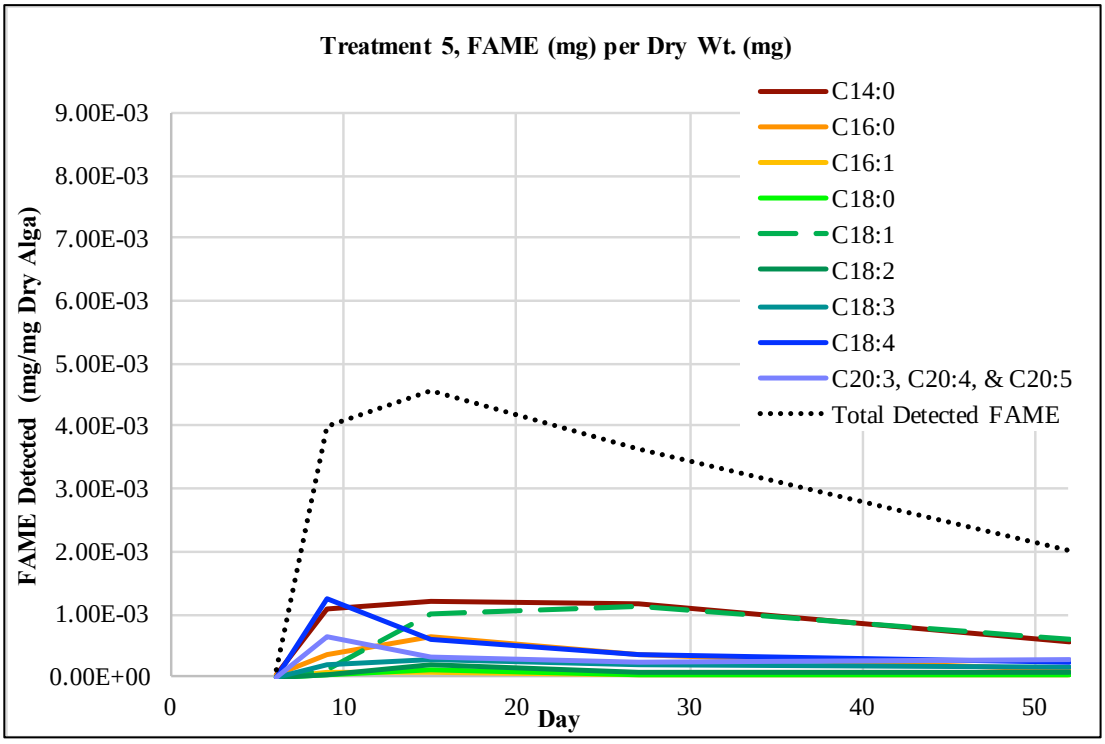

Figure 123: Treatment No. 5 (low nitrogen, low phosphorus, and supplemental CO_2), FAME proportion of dry weight and change with time of sample harvest. The above results are from GC/MS analysis only.

3.12.8.7. Treatment 6

In treatment No. 6 (low nitrogen and phosphorus MAM, with intermittent nitrogen feeding), the highest proportion of the monounsaturated FAME, C18:1 (26.5%) was detected on sample day 52, the last sample to be collected. The highest total FAME content, detected by the CNRC biomass extraction method, was 47.285 mg/g on day 34 (Table XXII). However, it is likely that the total FAME content was actually highest closer to day 19, based on GC/MS results (Figure 123 – 130).

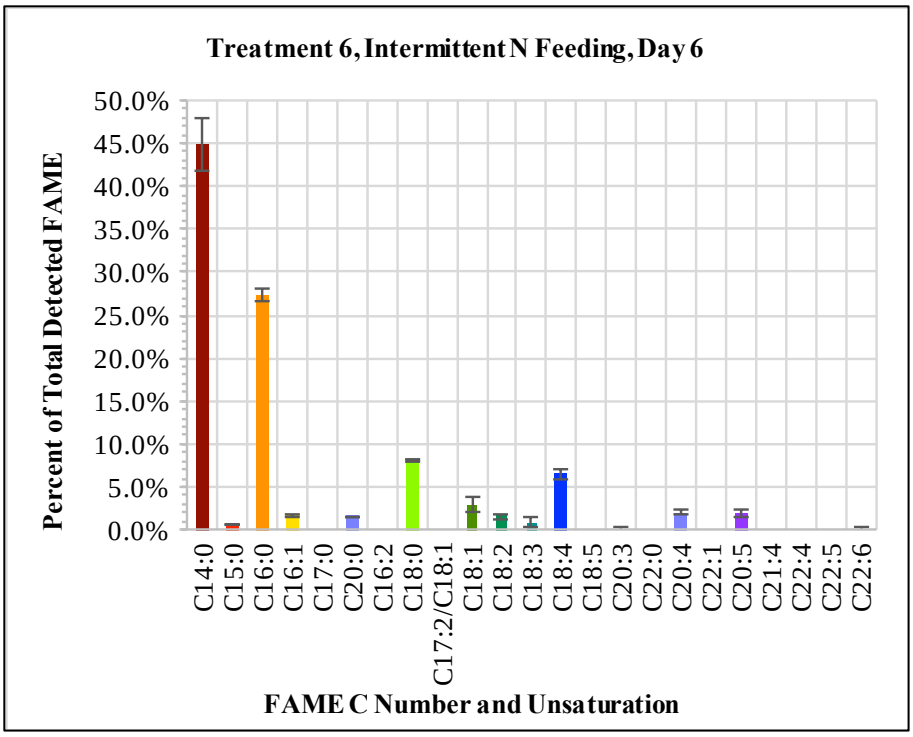

Figure 124: Treatment No. 6 (intermittent nitrogen feeding) FAME composition from sample day 6, GC/MS method.

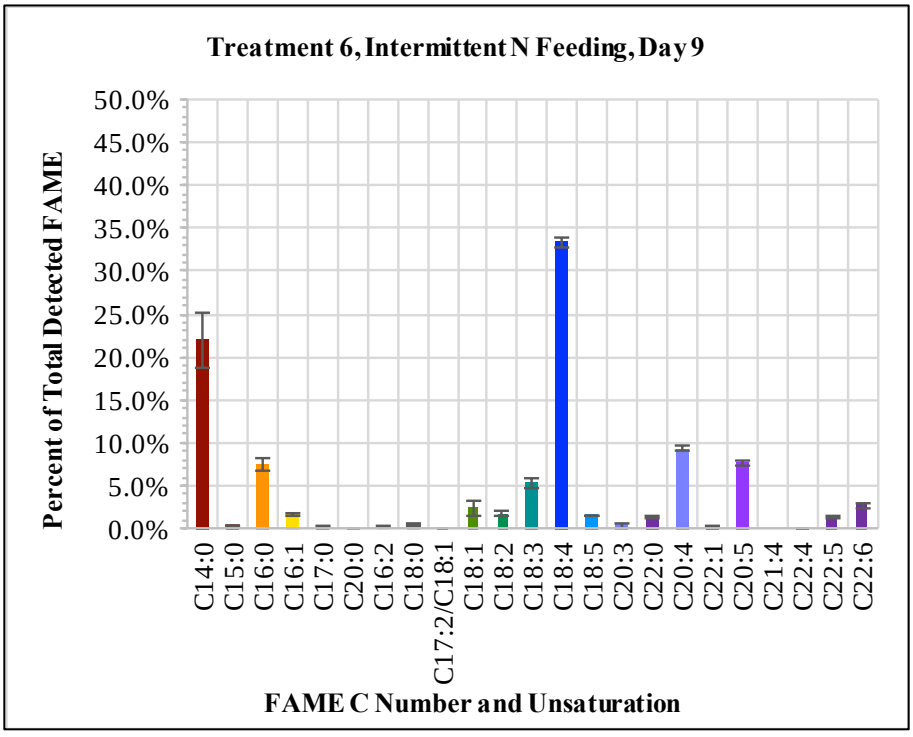

Figure 125: Treatment No. 6 (intermittent nitrogen feeding) FAME composition from sample day 9, GC/MS method.

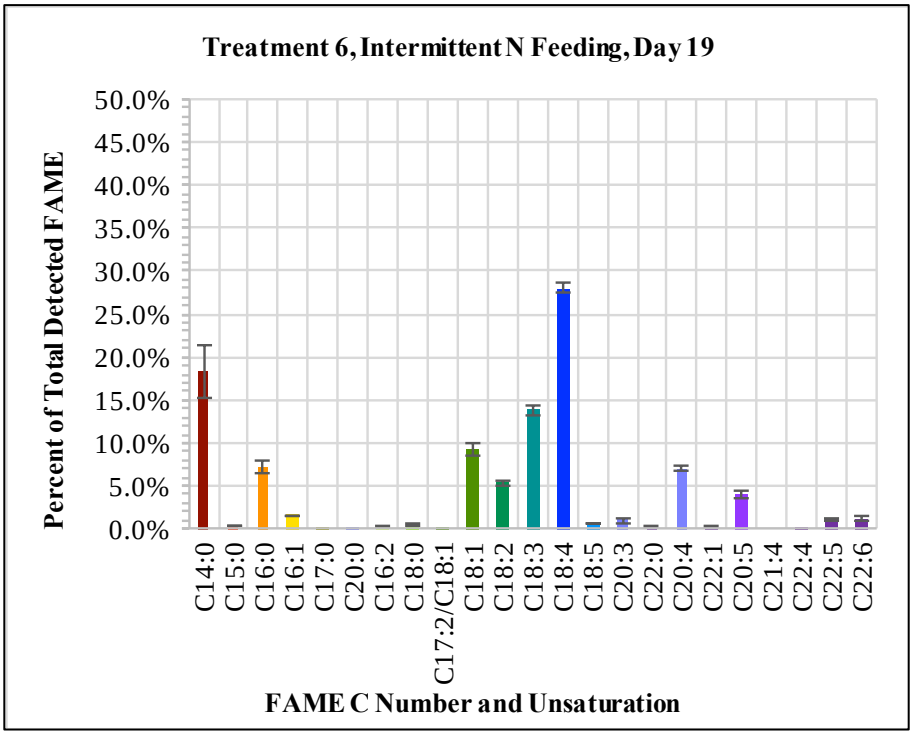

Figure 126: Treatment No. 6 (intermittent nitrogen feeding) FAME composition from sample day 19, GC/MS method.

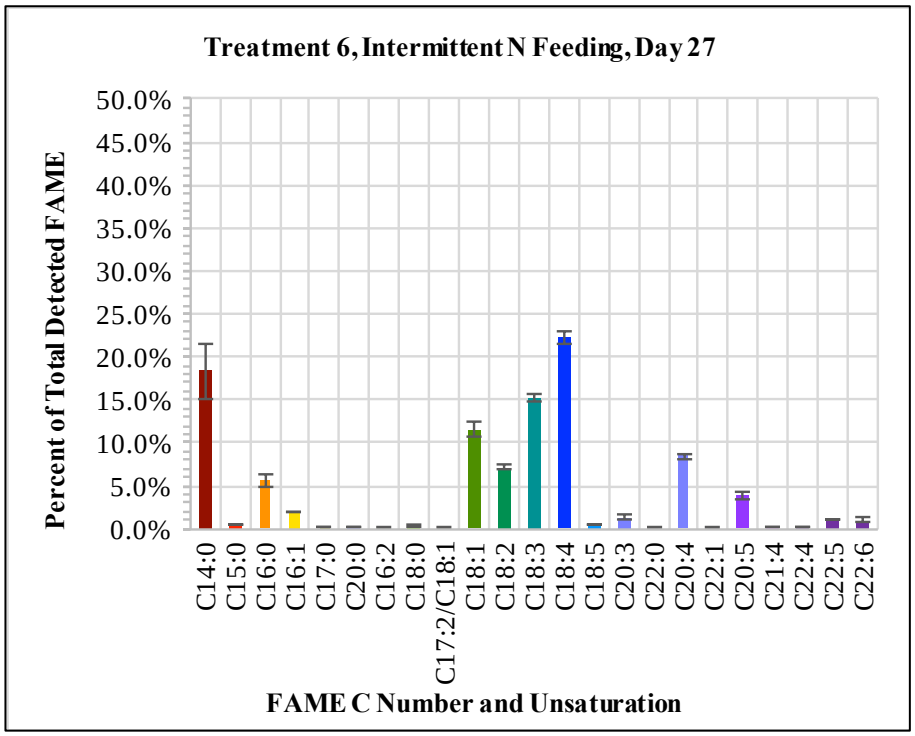

Figure 127: Treatment No. 6 (intermittent nitrogen feeding) FAME composition, day 27, GC/MS method.

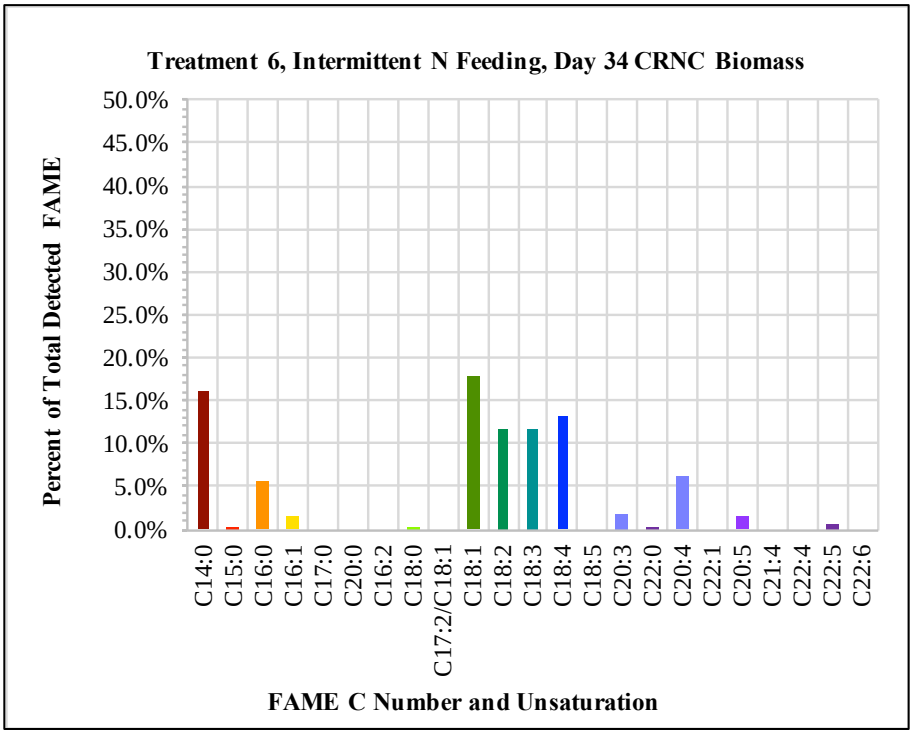

Figure 128: Treatment No. 6 (intermittent nitrogen feeding) FAME composition from sample day 34 from CNRC biomass method.

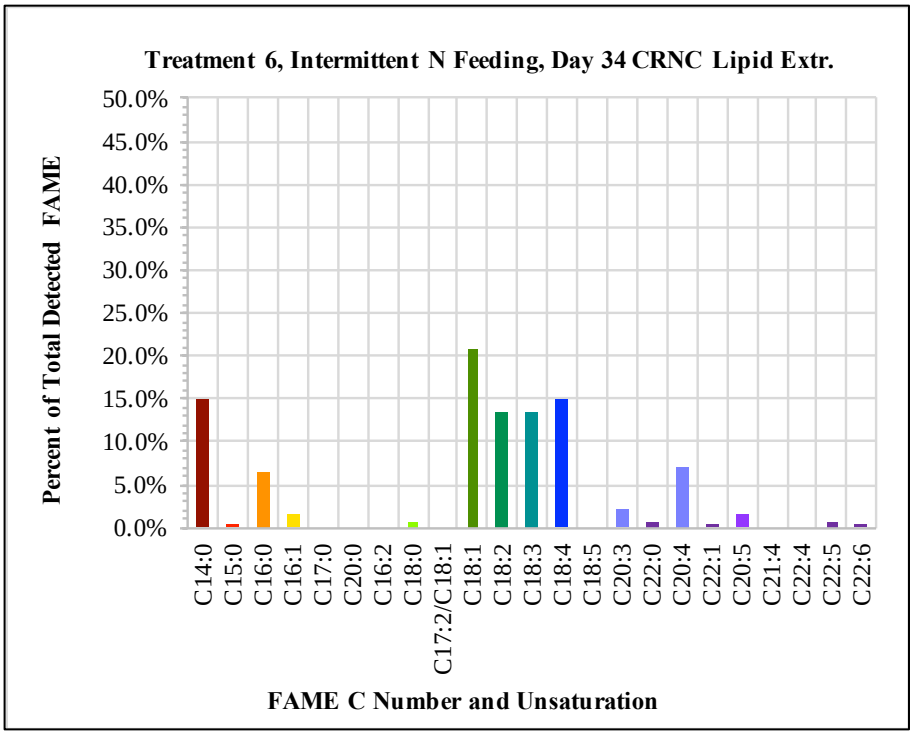

Figure 129: Treatment No. 6 (intermittent nitrogen feeding) FAME composition from sample day 34 from CNRC lipid extract method.

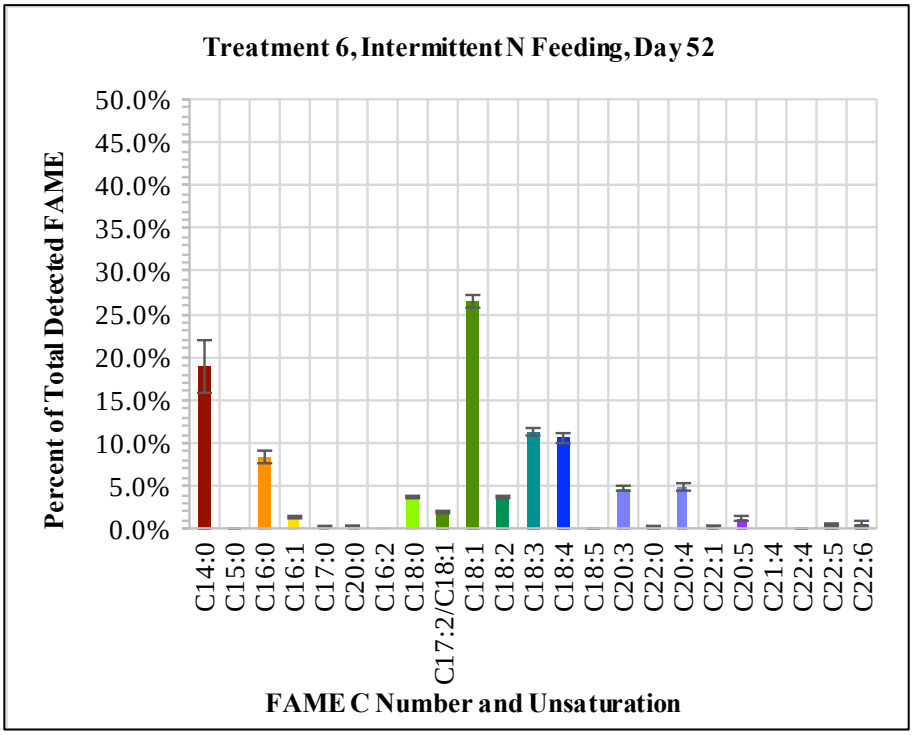

Figure 130: Treatment No. 6 (intermittent nitrogen feeding) FAME composition from sample day 52, GC/MS method.

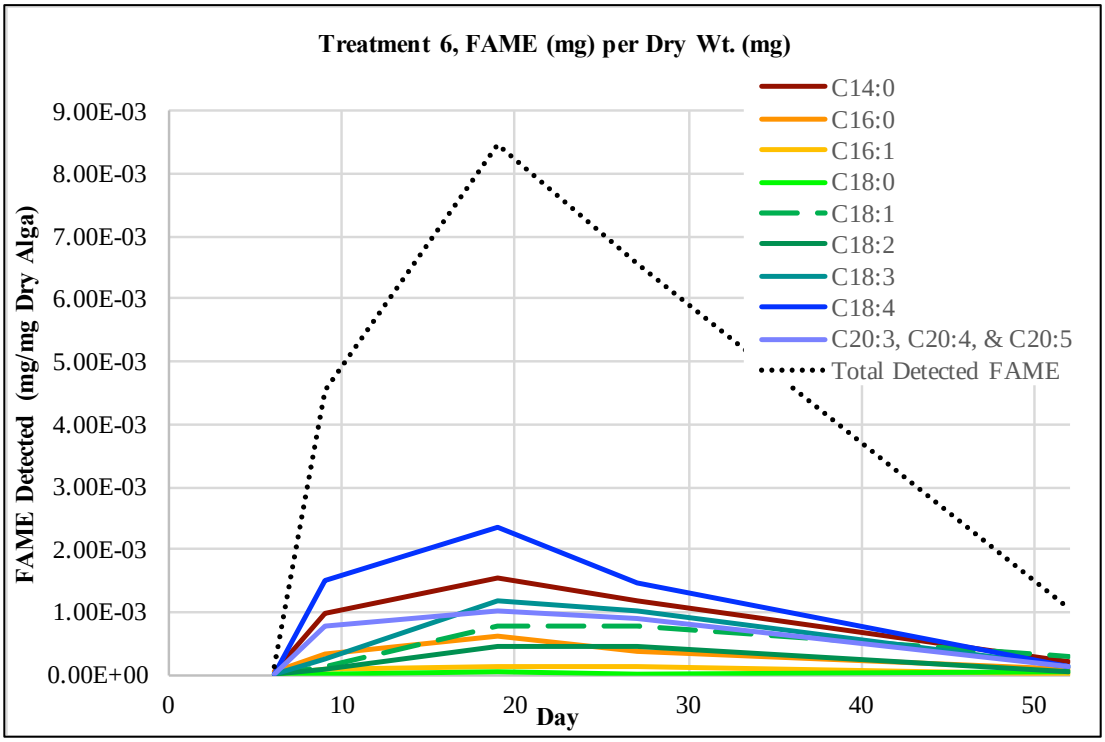

Figure 131: Treatment No.6 (intermittent nitrogen feeding), FAME proportion of dry weight and change with time of sample harvest. The above results are from GC/MS analysis only.

4. Summary

4.1. The Effects of Nutrients on Growth, Biomass Production, and Lipid Content

4.1.1. Starting Nitrogen Concentration

Lowering the medium nitrogen concentration had a clearly significant impact on lipid accumulation and biomass production. When the algal cells stopped exponential growth, and the nitrogen concentration in the medium was between 5 and 10 mg/L (ppm), they quickly entered the stationary growth phase after a brief (3 to 6 day) transitional period. The exponential growth phase lasted five to six days in all six treatments and not appear to be influenced by nitrogen concentration, but the length of time that linear growth was maintained afterwards clearly depended on nitrogen concentration. Lowering the nitrogen concentration of the medium resulted in not only the most rapid lipid accumulation, but also the highest total cellular lipid contents. However, because lipid accumulation occurred when active growth stopped, it was at the expense of biomass production.

The difference in biomass between the low nitrogen and higher nitrogen treatments was due to the growth rate during, and length of time in the linear growth period. Ideally, a high lipid content with high biomass would be desirable, but the metabolic survival strategies of microalgae generally prioritize one of these activities in opposition to the other. Research is underway to introduce genetic modifications into microalgae that would enhance traits related to improved biofuel production and the production of other valuable products (Shuba and Kifle, 2018). This may soon result in new microalgal strains that could yield much higher lipid and triglyceride contents along with high biomass. This research sought to examine ways to achieve a relatively high lipid content with adequate biomass. One treatment that was not included in the experiment, would be to provide enough nitrogen to achieve fairly high biomass, and lower the

nitrogen concentration after the desired cell density is reached. It was not possible to lower nutrient concentrations in the medium after growth had begun, with the batch culture method used for the experiment.

4.1.2. Intermittent Nitrogen Feeding (Treatment No. 6)

Intermittent nitrogen feeding has been demonstrated to result in adequate biomass with improved lipid content in other microalgae (Takagi et al., 2000). This method was tested in treatment No. 6. Treatment No. 6 was started with a low nitrogen concentration, but small portions of additional nitrogen were added every four days until day 24. Treatment No. 6 resulted in somewhat higher lipid accumulation, throughout the growth cycle (after day 12) than in the two treatments with high nitrogen concentrations, No. 1 (high nitrogen and phosphorus "control") and No. 3 (high nitrogen/low phosphorus). However, treatment No. 6 resulted in a lower lipid content than the three lowest nitrogen treatments (Figure 67). Intermittent nitrogen feeding also resulted in higher suspended cell densities, and slightly larger harvests of dry biomass (mg/mL) than in the three low nitrogen treatments.

An analysis of the sample from treatment No. 6, day 34 by CNRC showed higher total fatty acids and higher TAG than in the two high nitrogen treatments. The combined results from five samples from treatment No. 6 that were analyzed by the GC/MS method showed the highest cumulative FAME yield, and the GC/MS results also detected the second highest total FAME in a single sample from treatment No. 6 (Figures 71 and 72).

Treatment No. 6 also resulted in a higher percent of the total FAME content that was identified as C18:1 FAME, from the most favorable sample day (Figure 73), compared to the

two high nitrogen treatments. On day 34, the CNRC analysis also detected a high proportion of C18:1, comparable to the day 34 results of the three low nitrogen treatments.

In summary, the total lipid, total FAME and proportion of C18:1 resulting from treatment No. 6 were found to be intermediate between the high nitrogen treatments and the low nitrogen treatments.

4.1.3. Phosphorus

Based on previous observations of *C. freiburgensis* from Berkeley Pit Lake, lowering the phosphorus concentration of the medium was not expected to have as impressive an effect on growth and lipid production as lowering the nitrogen concentration. Lowering only the phosphorus concentration (treatment No. 3) appeared to have little impact on lipid accumulation and biomass production. However, the combination of low nitrogen and low phosphorus (treatments No. 4 and No. 5) resulted in higher lipid content than lowering nitrogen only (treatment No. 2), throughout the growth period (Figure 67).

4.2. Lipid Content and FAME Yields for the Final Product

The two highest FAME contents from day 34 transesterified samples, which were analyzed by CNRC, were found in treatments No. 2 (low nitrogen only) and No. 5 (low nitrogen, low phosphorus and supplemental CO_2). The highest FAME contents detected in transesterified samples, by the GC/MS method, were found in samples No. 3 (low phosphorus only) and No. 6 (intermittent nitrogen feeding and low phosphorus). Unfortunately, these few data (Table XXIV) do not point to a clear pattern of lower nutrient levels relating to higher FAME content in the final product.

Table XXIV: Comparison of highest FAME content detected in the final product from one sample, after transesterification, by GC/MS and CNRC methods.

Treatment	Sample Day	Total Detected FAME by dry Wt. (mg/g)	Methods
	34	35.455	CNRC
1. Reg. MAM	52	6.926	GC/MS
	9	3.397	GC/MS
2. Low N	34	51.018	CNRC
	27	8.850	GC/MS
3. Low P	34	40.947	CNRC
	19	5.776	GC/MS
4. Low N & Low P	34	39.046	CNRC
	15	4.554	GC/MS (Mean of 3 runs)
5. Low N & Low P + CO_2	34	51.148	CNRC
	19	8.450	GC/MS
6. Intermittent N Feeding	34	47.285	CNRC

The Nile Red Fluorescence lipid content results, combined with microscopic observation, demonstrate that, in *C. freiburgensis* from Berkeley Pit Lake, high lipid content results from the accumulation of storage lipids (lipid droplets or oil bodies). Triglycerides are generally considered to make up the predominant storage lipids in the fats and oils of algae, plants and animals (Evert and Eichhorn, 2013) and they are the desired lipids for transesterification into FAMEs for biodiesel. Nevertheless, the actual triglyceride content of microalgal storage lipid droplets is still in the early stages of being documented (Goold et al., 2014), and it is likely to vary between individual algal strains. For example, Wang et al. (2009) found that triglycerides made up 90% of the total lipid content of purified lipid bodies from a starchless mutant strain of the green microalga, *Chlamydomonas reinhardtii* (Dangeard), that has a very high lipid content. Nguyen et al. (2011) found 19 proteins in the lipid bodies (lipid droplets) of *C. reinhardtii* grown with low nitrogen, that are involved in triacylglycerol (triglyceride) synthesis. These results support the popular premise that the primary functions of these organelles are the building and storage of triglycerides.

Based on these observations, a high triglyceride content was expected to be found with a high lipid content. However, because the transesterification reaction is not selective for triglycerides only, it is reasonable to expect that a higher lipid content would result in a proportionately higher FAME content in the transesterified sample, whether or not the algal lipids contained an especially high proportion of triglycerides.

NMR analysis by CNRC on day 34 samples found the highest triacylglycerol content in treatments No. 2, No. 4 and No. 5, the three lowest nitrogen treatments, and the lowest triacylglycerol contents in the two high nitrogen treatments, No. 1 and No. 3 (Figure 69). Treatment No. 6 (intermittent nitrogen feeding with low phosphorus), had an intermediate quantity of triacylglycerol on that day. Total fatty acids were found to be highest in treatments No. 2, No. 4, No. 5 and No. 6, the four of six treatments that had lowered nitrogen concentrations.

The discrepancy between the results for FAME content and lipid content in the samples may be explained by the low number of samples analyzed, the small biomass of the samples, and the sample processing methods. For the GC/MS FAME analysis method, there were several ways that lipids and FAMEs could have been lost from the sample during preparation. In this case, total lipid content may be more indicative of the actual FAME content, per unit biomass, that could be expected with a larger quantity of biomass or an improved method for transesterification and extraction.

When the results for FAME content after transesterification of samples, lipid content from Nile Red fluorescence, and CNRC NMR results for triacylglycerol and fatty acid content are all considered, lowering nitrogen clearly had the strongest influence toward increasing FAME content per unit of biomass, after transesterification of the algal lipids.

Based on lipid content results, lowering phosphorus only did not appear to have a noticeable effect on lipid production, but lowering both phosphorus and nitrogen appeared to be more effective at increasing lipid content than lowering nitrogen only, and lowering both nutrients could reasonably be expected to have a positive influence on FAME content as well.

4.3. FAME Composition

The monounsaturated FAME with carbon chain length and unsaturation of C18:1, as in oleic acid, is a preferred ingredient for high-quality biodiesel. The two treatments that combined low nitrogen and low phosphorus resulted in the highest detected proportions (as percent of total FAME content) of C18:1 (Table XXV). Lowering nitrogen only (treatment No. 2) also resulted in a high proportion of C18:1. Intermittent nitrogen feeding with low phosphorus (treatment No. 6) resulted in a proportion of C18:1 that was intermediate between the three lowest nitrogen treatments and the two treatments with high nitrogen concentrations. The two treatments with the highest nitrogen concentrations, No. 1 (nutrient-replete, standard MAM) and No. 3 (low phosphorus only) resulted in the lowest proportions of C18:1.

Table XXV: Six experimental treatments, ranked from highest to lowest, by proportion of total FAME content (in transesterified samples) that is C18:1.

% of FAMEs that are C18:1	Combined GC/MS Results from Six Samples from Each Treatment	CNRC Results for Sample Day 34	% C18:1 of Total FAMEs on Day 34
Highest	5. Low N & Low P + CO_2	4. Low N & Low P	50.10%
↑	4. Low N & Low P	5. Low N & Low P + CO_2	48.10%
↕	2. Low N	2. Low N	45.10%
↕	6. Intermittent N Feeding	6. Intermittent N Feeding	17.80%
↓	3. Low P	3. Low P	2.70%
Lowest	1. Reg. MAM	1. Reg. MAM	2.60%

4.4. Harvest Timing

Lipid content and FAME content and composition, in the transesterified product both changed over the growth period, in each of the experimental treatments. Optimal harvest timing for biodiesel production would be at a point in the growth cycle when the alga had produced adequate biomass with high lipid content and a high proportion of C18:1 (oleic acid) in its stored lipids. The proportion of C18:1, in the FAME mixture of the transesterified product, increased most significantly during stationary growth in all low nitrogen treatments, and lowering phosphorus as well resulted in the highest proportions of C18:1, relative to saturated and polyunsaturated FAMEs. Although lipid content (by dry weight) increases throughout stationary and declining growth, based on GC/MS data, total FAME content in the transesterified product may not continue increasing with total lipid content, and may begin decreasing between day 15 and day 30. The proportion of C18:1 also does not appear to continue to increase, relative to saturated and polyunsaturated FAMEs, for the entire stationary growth period, and it reaches its peak well before day 52. Based on GC/MS results for samples taken from the low nitrogen treatments on day 27, 34 and 52, it appears most likely that the peak proportion of C18:1 occurs

near or a few days after day 34 of the growth period, and it can be expected to reach approximately 50% of the composition of the FAMEs in the transesterified sample under comparable growing conditions.

Lipid content and the proportion of C18:1 may continue to increase after suspended cell density begins to decrease. Depending on the harvest method, a decrease in suspended cell density is likely to represent a decrease in harvestable biomass. Therefore, optimal harvest timing is most likely to be before a decrease in cell density is observed. Considering biomass production, lipid content and FAME composition, for treatments No. 2 (low nitrogen), No. 4 (low nitrogen and low phosphorus) and No. 5 (low N, low P and CO_2), the optimal point in the growth period for harvest is most likely to be between day 34 and day 40.

Because nitrogen limited conditions occurred later in treatment No. 6 (intermittent nitrogen feeding with low phosphorus), the peak proportion of C18:1 also occurred later. On the day of the final sampling event (day 52), in treatment No. 6, C18:1 was at 26.5%, but it is possible that it had not yet reached its highest proportion relative to saturated and polyunsaturated FAMEs. For treatment No. 6, the desired goal would have been satisfied by a greater biomass harvest than in the low nitrogen treatments, in combination with a comparatively high lipid content and a high proportion of C18:1. Treatment No. 6 did not result in significantly higher harvested biomass, by dry weight, than in treatments No. 2, No. 4 and No. 5, after day 34. However, the FAME composition and lipid content results for treatment No. 6 were more favorable than in the two high nitrogen treatments, No. 1 (high-nutrient, regular MAM) and No. 3 (low phosphorus). A period of linear growth was observed between day 12 and day 27, where total FAME yield per dry weight also appeared to increase, but an expected corresponding increase in biomass harvest and total lipid content was not observed during that period. With

further adjustments to the nitrogen feeding schedule and a later harvest timing, it may be possible to achieve a more satisfactory combination of higher biomass with a favorable lipid content and FAME composition, but the conditions of treatment No. 6 did not achieve that by day 52.

4.5. Fatty Acid and FAME Composition

The composition of fatty acids in *C. freiburgensis* lipids are the source of, and contribute directly to the proportions of FAMEs found in the transesterified product. The predominant saturated fatty acids found in the FAME composition of *C. freiburgensis* from Berkeley Pit Lake are C14:0 and C16:0 (Table XXVI and Table XXVII). The predominant monounsaturated fatty acid is C18:1, and the predominant polyunsaturated fatty acids are C18:2, C18:3, C18:4 and C20:4. C20:5 is also present (Table XII provides a complete list of detected FAME carbon chain lengths and unsaturation). The alga was able to increase the proportion of C18:1, a FAME that is a preferred component of high-quality biodiesel, to 50.1% of total FAME mixture in treatment No. 4 (low nitrogen and low phosphorus) and nearly 50% in treatment No. 5 (low nitrogen, low phosphorus and supplemental CO_2). All treatments resulted in relatively high proportions of saturated C14:0 and C16:0 early in the growth cycle. High-nitrogen treatments resulted in increasing proportions of polyunsaturated C18:3 and C18:4, while low-nitrogen treatments resulted in increasing proportions of C18:1 (Figures 74 – 76; 77 – 82; 83 – 130).

Breuer, et al., (2013), who selected *Scenedesmus obliquus* (Turpin) Kützing, a green microalga, for its high lipid productivity, observed a pattern of increasing C18:1, with a corresponding decrease in C18:3, in their low-nitrogen treatments, which was similar to the trends observed in this experiment. By making adjustments to medium nitrogen concentration, temperature and pH (between 7.0 and 9.0), they were able to increase the triglyceride content

from approximately 2% to 30% – 40% (of dry weight) with lowered nitrogen, at pH 7 and 27.5 °C. Their highest C18:1 content reached 32% – 53%, as a portion of total fatty acids. Interestingly, they also found that increasing the light intensity above 200 μmol m^{-2} sec^{-1} resulted in a modest increase in the proportion of C18:3 in the algal fatty acid composition. *C. freiburgensis* was grown at a lower light intensity (approximately 100 μmol m^{-2} sec^{-1}) in all six treatments, and its effect on FAME composition was not investigated.

Although it's total lipid productivity may be lower, *C. freiburgensis* from Berkeley Pit lake appears to perform about as well as *S. obliquus*, with regards to fatty acid composition, but at pH 2.5 and 10 °C.

Halim, et al. (2011) compared several lipid extraction methods for a saltwater green microalga, *Chlorococcum* sp. that was grown in a medium containing approximately 24.7 mg/L nitrogen. They found it to produce a maximum total lipid yield of 7.1% (of dry biomass). Importantly, they also found that the fatty acid composition of the lipids extracted from the alga differed depending on the extraction method that was used. For example, hexane extraction from dry biomass resulted in a fatty acid composition with approximately 53.1% C18:1, 35.6% C16:0 and 4.7% C18:2 (by dry weight) (Table XXVIII). Supercritical CO_2 extraction at 60 °C resulted in a notable increase in the proportion of C18:1, with a fatty acid composition containing approximately 63.6% C18:1, 18.8% C16:0 and 4.7% C18:2 (by dry weight). Halim et al. concluded that *Chlorococcum* sp. had a fatty acid profile favorable for biodiesel, though it's lipid content was relatively low.

C. freiburgensis from Berkeley Pit lake is likely to be capable of exceeding the lipid production of *Chlorococcum* sp., with a fatty acid composition that is probably higher in polyunsaturated fatty acids, and somewhat lower in C18:1, but also suitable for biodiesel.

Table XXVI: Predominant fatty acids in microalgae, based on Hu et al., 2008. *C. freiburgensis* from Berkeley Pit Lake is listed at far right for comparison with eight most prominent fatty acid types, based on GC/MS FAME analysis results. *Chrysophyceae: Hu et al. mentions the class in general, but no species currently classified as Chrysophyceae, could be found that had been evaluated as potential sources of lipids for biofuels.

Fatty acid (length and unsaturation)		Bacillariophyceae (Diatoms) "D"	Chlorophyceae (Green Algae) "Ch"	Chrysophyceae (Golden Algae) "G"	Cryptophyceae "Cr."	Cyanobacteria (Blue-green Algae) "BG"	Dinophyceae (Dinoflagellates) "Di"	Euglenophyceae "E"	Eustigmatophyceae "Eu"	Coccolithophyceae (Prymnesiophycidae) "Co"	Rhodophyceae (Red Algae) "R"	Xanthophyceae (Yellow Green Algae) "X"	***C. freiburgensis* (8 most predominant) "CF"**	**Soybean Oil* "S"**
Saturated Fatty Acids	**C10:0**					BG								
	C14:0				Cr	BG						X	CF	
	C16:0	D	Ch	G	Cr	BG	Di	E	Eu	Co	R	X	CF	S
	C18:0												CF	
Monounsaturated Fatty Acids	**C16:1**	D		G		BG				Co		X		
	C18:1		Ch	G		BG		E	Eu	Co			CF	S
	C20:1				Cr									
Polyunsaturated Fatty Acids	**C16:3**		Ch									X		
	C18:2		Ch			BG		E		Co	R		CF	S
	C18:3		Ch		Cr	BG		E		Co			CF	S
	C18:4				Cr								CF	
	C18:5						Di							
	C20:3								Eu					
	C20:4		Ch						Eu				CF	
	C20:5	D	Ch	G	Cr				Eu		R	X		
	C22:5			G								X		
	C22:6	D		G						Co				

Table XXVII: Lowest and highest percentages (range of proportions) of predominant fatty acids found in *C. freiburgensis* FAME composition.

Predominant Fatty Acids in FAME Composition	Lowest % of FAMEs	Day	Treatment		Highest % of FAMEs	Day	Treatment
C14:0	11.1%	27	1. Reg. MAM		45.3%	6	5. Low N, Low P + CO_2
C16:0	3.1%	34	2. Low N		29.3%	6	2. Low N
C18:0	0.0%	34	1. Reg. MAM		23.5%	6	2. Low N
C18:1	1.5%	19	1. Reg. MAM		50.1%	34	4. Low N & Low P
C18:2	1.2%	6	2. Low N		13.4%	34	6. N Feeding
C18:3	0.8%	6	6. N Feeding		25.9%	52	3. Low P
C18:4	3.5%	34	4. Low N & Low P		37.2%	19	1. Reg. MAM
C20:4	2.1%	52	4. Low N & Low P		12.7%	34	1. Reg. MAM

The most common feedstock for biodiesel, in the United States, is soybean oil. Between 2016 and 2018, soybean oil accounted for between 63.5% and 67.2% (by weight) of the total sum of feedstocks (fats and oils) used to produce biodiesel in the U.S. (USEIA Monthly Biodiesel Production Report, Jun. 2018). Soybean biodiesel is considered to be a first generation biofuel, because it is made from a product that would otherwise be considered edible. Increasing its production is very likely to raise prices and affect the availability of foods and cooking oil made from soy beans, and for this reason, it is not considered to be an ideal biofuel feedstock.

This research provides convincing evidence that the fatty acid content of the lipids in *C. freiburgensis*, in all three low nitrogen treatments, contain a higher percentage of monounsaturated fatty acids than soybean oil, based on both the CNRC GC-FID analysis and GC-MS analysis of FAME mixtures in the transesterified lipids from dry biomass, as compared to the fatty acid composition of soybean oil (Jokić et al., 2013). The analysis of the FAME composition of *C. freiburgensis* from treatment No. 4 (low nitrogen and low phosphorus), yielded the highest proportion of C18:1 (50.1%) when harvested on day 34 (Figure 131 and

Table XXVIII). The FAME composition of all day 34 samples was determined by CNRC. An example from treatment No. 5 (low nitrogen, low phosphorus and supplemental CO_2), FAME composition from GC-MS analysis, also compares favorably to soybean oil, although the sample was from earlier in the growth period, before the peak proportion of C18:1 occurred. Only seven sets of samples were tested for FAME composition in the transesterified product, over a 52-day period, which limited the data available to interpret the effect of harvest timing on FAME composition. If the actual peak concentration of C18:1 did not occur on day 34, it is possible that a proportion of C18:1 FAME higher than 50.1% could have been (or could be) found in algal biomass harvested at a point in the growth period before or after day 34.

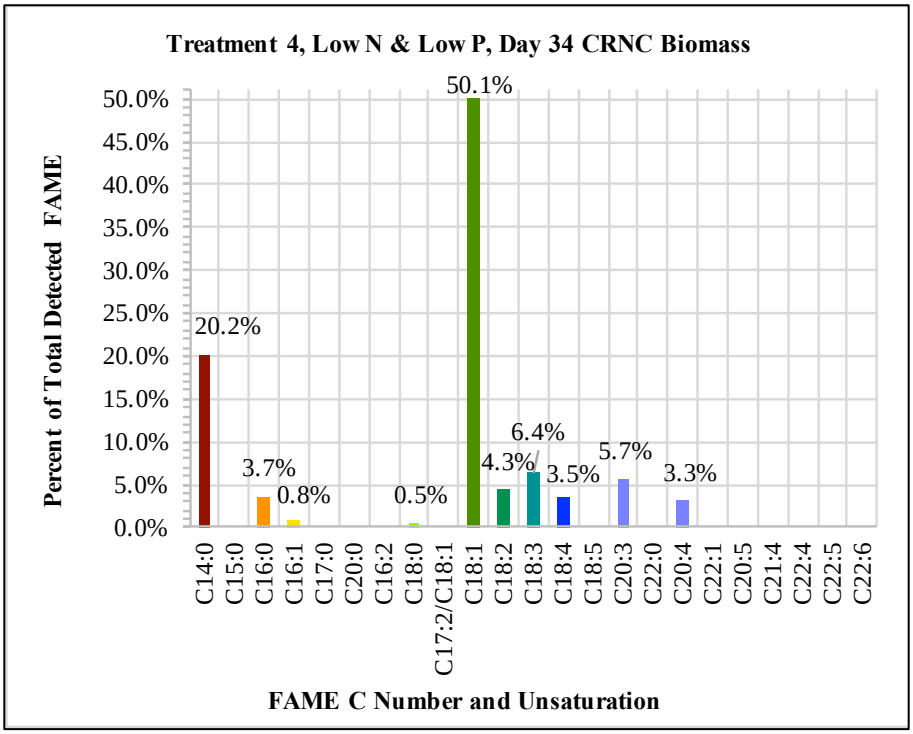

Figure 132: *C. freiburgensis* FAME composition results from treatment No. 4, harvested on day 34 (based on CNRC GC-FID analysis if FAMEs from lipids in dry algal biomass). Treatment No. 4 from day 34 contained the highest detected proportion of C18:1, relative to the proportion of other FAMEs.

Microalgae are an extremely diverse group of organisms, each strain has its own range of nutrient, temperature, pH, salinity, and lighting and lighting requirements, and their lipid composition may be as dissimilar from one another as each are from terrestrial plants. Methods for extracting lipids and determining lipid yield, triglyceride content, and fatty acid composition also vary among researchers, and the answers to questions about lipid content and fatty acid composition are presented in different forms and contexts, depending on the researchers' objective and chosen methods. Because of the diversity in the field of algal biofuels research, it is difficult to make direct comparisons between potential microalgal feedstocks, and between microalgal lipids and vegetable oils, from the range of different organisms and research sources. *C. freiburgensis* FAME compositions from two of the treatments with favorable results were summarized and compared to the fatty acid compositions of two green microalgae and soybean oil in Table XXVIII. The summarized data in Table XXVIII is meant to represent "ballpark" estimates, but not a direct ("apples to apples") comparison, which could only be done if the lipids from each of the feedstocks were extracted and analyzed by the same methods.

Table XXVIII: *C. freiburgensis* FAME composition results from treatment No. 5 (day 27), based on GC/MS results and No. 4 on day 34 (based on CNRC GC-FID analysis if FAMEs from lipids in dry algal biomass), In comparison to fatty acid composition of *Scenedesmus obliquus* (based on data from Fig. 6, Breuer et al., 2013), *Chlorococcum* sp. (estimated from data in Fig. 4, Halim et al., 2011), and soybean oil (based on data from Jokić et al., 2013, extraction by supercritical CO_2.

	***C.f.* Treatment 5 Day 27 from GC-MS FAME Composition**		***C.f.* Treatment 4, Day 34 from CNRC GC-FID FAME Composition**		***Scenedesmus obliquus* Fatty Acid Composition of TAG (Breuer, et al., 2013)**		***Chlorococcum* sp. Fatty Acid Comp. of Total Lipid (Hexane Extraction from Dry Alga, Halim et al., 2011)**		**Soybean Oil Fatty Acid Composition of Total Lipid (Supercritical CO_2 Extraction, Jokic, et al. 2013)**	
Percent Saturated Fatty Acids	C14:0	31.88%	C14:0	20.2%			C14:0	1.88%	C14:0	0.06%
	C15:0	0.17%								
	C16:0	9.86%	C16:0	3.7%	C16:0	18.13%	C16:0	35.63%	C16:0	10.66%
	C17:0	0.18%								
	C18:0	0.81%	C18:0	0.5%	C18:0	3.75%	C18:0	2.81%	C18:0	5.15%
	C20:0	0.61%							C20:0	0.60%
	C22:0	0.13%							C22:0	0.35%
									C24:0	0.15%
	Sum:	**43.65%**		**24.4%**		**21.88%**		**40.32%**		**16.97%**
Percent Mono-unsaturated Fatty Acids	C16:1	1.27%	C16:1	0.8%	C16:1	2.81%	C16:1	3.13%		
	C18:1	31.24%	C18:1	50.1%	C18:1	44.06%	C18:1	53.13%	C18:1	22.79%
									C22:1	0.37%
	Sum:	**32.50%**		**50.9%**		**46.87%**		**56.26%**		**23.16%**
Percent Polyunsaturated Fatty Acids					C16:2	4.69%				
					C16:3	2.19%				
	C18:2	1.98%	C18:2	4.3%	C18:2	7.50%	C18:2	4.69%	C18:2	53.98%
	C18:3	4.81%	C18:3	6.4%	C18:3	12.50%			C18:3	5.91%
	C18:4	9.55%	C18:4	3.5%						
	C18:5	0.16%								
	C20:3	2.47%	C20:3	5.7%						
	C20:4	2.95%	C20:4	3.3%						
	C20:5	1.21%								
									C22:1	0.37%
	C22:5	0.10%								
	C22:6	0.57%								
	Sum:	**23.80%**		**23.2%**		**26.88%**		**4.69%**		**60.26%**

4.6. CO_2 Supplementation

4.6.1. Biomass Productivity with Supplemental CO_2

The results from treatment No. 5 (low nitrogen, low phosphorus MAM with supplemental CO_2), were comparable to those from treatment No. 4 (low nitrogen, low phosphorus MAM without supplemental CO_2). The total lipid productivity was somewhat higher than, and the biomass productivity and FAME composition were very similar to those of treatment No. 4. In all but a few samples, throughout the growth period, biomass yield appeared to slightly exceed that of treatment No. 4.

4.6.2. Lipid Productivity and FAME Composition with Supplemental CO_2

The highest lipid content, detected by Nile Red fluorescence, occurred in treatment No. 5, and lipid content in treatment No. 5 remained higher than all five other treatments for nearly the entire period, between day 12 and day 52. Adding a small volume of CO_2 to the air circulating through low nitrogen and low phosphorus MAM (treatment No. 5), resulted in the second highest detected proportion of C18:1 monounsaturated FAME (as percent of total FAME mixture) along with the highest total FAME content after transesterification of the algal lipids. Increasing CO_2 above the 0% to 5% that was added to ambient air in treatment No. 5 may further improve results for biomass production and the production of desirable lipids, and continued investigation could discern an ideal proportion of supplemental CO_2 for optimal growth, lipid content, FAME composition or carbon retrieval from flue gases. The results of treatment No. 5 indicate that *C. freiburgensis* from Berkeley Pit Lake is able to tolerate slightly elevated CO_2 concentrations well, and it is likely to be a suitable candidate for carbon capture from sources such as flue gases.

5. Conclusions

5.1. Changes in Biomass Production in Response to Nutrient Concentrations and CO_2 Supplementation

C. freiburgensis from Berkeley Pit Lake can attain suspended cell densities of 33 million cells per milliliter (3.33×10^7 cells/mL) after 34 days of growth in standard, nutrient-replete MAM at pH 2.5. When the nitrogen concentration of the medium was reduced to 10% of standard MAM, cell densities peaked at approximately ten million cells per milliliter (1.00×10^7 cells/mL) around day 12. Intermittent nitrogen feeding until day 24 (treatment No. 6) resulted in peak cell densities of around 24 million cells per milliliter ($2.43\ 10^7$ cells/mL) on day 27. However, dry weight yields were not noticeably higher in treatment No. 6 than those of the three low nitrogen treatments. A decrease in suspended cell densities also did not clearly correspond to a decrease in dry biomass harvest in any of the six treatments, indicating that the mass of individual cells can vary depending on growing conditions and growth phase. Cell density alone did not reliably predict dry harvest weight.

Phosphorus concentrations appeared to have a lesser influence on biomass versus lipid production, which may be related to *C. freiburgensis*'s low phosphorus requirements relative to other microalgae. Lowering phosphorus concentrations alone had little impact on biomass production, lipid production, and FAME composition. However, lowering the phosphorus concentration along with lowered nitrogen appeared to have a noticeable positive influence on lipid production and the FAME composition of the transesterified product.

The addition of supplemental CO_2 did not appear to noticeably affect biomass yield as dry weight, however, an unexpected spike in the concentration of CO_2 in the medium is suspected to be have been the cause of the abrupt, temporary decrease in cell density observed on day 15 in treatment No. 5.

5.2. Changes in Lipid Production in Response to Nutrient Concentrations and CO_2 Supplementation

As in the majority of microalgae studied, lipid accumulation in *C. freiburgensis* happened at the expense of biomass production, after medium nitrogen decreased to a certain minimum concentration. This research demonstrated how *C. freiburgensis* responded to lowered nutrient concentrations by prioritizing lipid production over growth and structural integrity.

Total lipid content (as percent of dry weight) increased in all six experimental treatments with time. The highest total lipid yields, detected by the Nile Red fluorescence method, were observed in the three treatments with the lowest medium nitrogen concentrations. Lowering medium phosphorus alone did not result in a higher lipid yield. However, lowering both nitrogen and phosphorus concentrations resulted in higher measurements for total lipid content than lowering nitrogen alone. CO_2 supplementation also appeared to increase total lipid content.

Although the Nile Red method did not detect high yields for total lipid content, relative to other microalgae studied, *C. freiburgensis* produced lipids that yielded, in the transesterified product, a FAME composition which is favorable for biodiesel.

5.3. Changes in FAME Composition in Response to Nutrient Concentrations and CO_2 Supplementation

All four treatments that included lowered medium nitrogen concentrations resulted in increasing percentages of C18:1 FAME in the transesterified samples (up to approximately 50% of the FAME composition). As C18:1 increased, percentages of C18:3 and C18:4 decreased. Lowering phosphorus alone resulted in an increase in C18:2, but not in C18:1. In the two treatments with the highest nitrogen concentrations, the percentage of C18:1 remained low and the percentages of C18:3 and C18:4 remained relatively high throughout the growth period. The

percentage of short-chain, saturated C14:0 and C16:0 FAMEs initially decreased in the transesterified products of all six experimental treatments, however, these later began to increase in the low nitrogen treatments. The most favorable FAME compositions for biodiesel (those with the highest percentage of C18:1 and lowest percentage of polyunsaturated FAMEs) resulted from the combination of lowered nitrogen and lowered phosphorus. This favorable FAME composition was similar, with and without CO_2 supplementation.

5.4. Change in FAME Composition with Harvest Timing

The proportions of each FAME, as a percent of total FAME content, changed with time in all six experimental treatments. For biodiesel, the relative amounts of saturated FAMES, monounsaturated FAMEs and polyunsaturated FAMEs strongly influence the performance of the fuel. High proportions of FAMEs from saturated fatty acids can cause the fuel to be more likely to coagulate in cold temperatures, while high proportions of polyunsaturated FAMEs can lower oxidative stability even more than environmental factors.

In the three lowest nitrogen treatments, the highest percentages of C18:1 (approximately 50%) were detected in samples that were collected on day 34, which were analyzed by CNRC. An increase in the percentage of C18:1 had been observed in samples from these treatments prior to day 34. This increase and the high proportion of C18:1 were not observed in samples from the two high nitrogen treatments, where C18:1 remained below 5% throughout the growth period. In the treatment with intermittent nitrogen feeding (No. 6), the proportion of C18:1 increased more slowly than in the three lowest nitrogen treatments, reaching 25.4% on day 52, when the last sample set was collected.

A high proportion of C18:1 FAME provides both the favorable cold weather performance and the oxidative stability that are required for the production of a high quality of biodiesel. This research demonstrated that the proportion of monounsaturated C18:1 FAME, in relation to both saturated (C14:0 and C16:0) FAMEs and polyunsaturated (C18:3 and C18:4) FAMEs, in the final product can be optimized by controlling nutrient concentrations and harvest timing.

5.5. Differences Between the Total Lipid and Total FAME Content Reported by CNRC and Those Detected by the Nile Red and GC/MS Methods

5.5.1. Total Lipid Content Detection by Nile Red Fluorescence Method Compared to CNRC Solvent Extraction Method

The Nile Red fluorescence method detected lipids inside live cells suspended in medium. It has the advantage of rapid measurements to monitor actively growing cultures, and it need not kill the cells being examined. Because of these advantages, Nile Red fluorescence can be used to select high-lipid cells to start new cultures.

The Nile Red method detected maximum total lipid contents ranging from 0.24% to 3.20% of dry weight on day 52. Day 52 represented the last sample set collected at the end of the growth period, and the highest lipid content measured in all six treatments. These lipid content measurements were much lower than expected, based on microscopic observations of the cells. The CNRC lipid detection method, which detected lipids extracted from dry samples using chloroform and methanol, resulted in a total lipid content range from 5.75% to 7.83% on day 34. The methods used by CNRC are considered to be standardized and a reliable way of determining lipid content. The accuracy of the Nile Red fluorescence method is known to vary, depending on individual characteristics of the microalgal species being studied. The reason for the low

measurements in this experiment is not known, but may be related to characteristics of *C. freiburgensis* cells that could affect either the behavior of Nile Red stain or of light.

5.5.2. Nile Red Detection of Lipid Increase and Differences in Total Lipid Content

While the Nile Red method almost certainly resulted in underestimated lipid productivity for *C. freiburgensis*, it nevertheless provided useful data. The Nile Red fluorescence method succeeded as a means of detecting the relative differences in the responses of the alga to the six experimental treatments, in terms of lipid productivity. The method also provided a way to document a trend of increasing lipid content over time in all six treatments.

5.5.3. Total FAME Content Detection by GC/MS Method Compared to CNRC Methods

The total FAME content detected by the GC/MS method ranged from 0.035 mg/g to 8.850 mg/g of dry alga in all of the samples analyzed. The CNRC laboratory methods detected a range of 35.455 mg/g to 51.148 mg/g in the transesterified lipids from dry algal biomass. CNRC detected a range of 13.814 mg/g to 29.831mg/g in the transesterified lipids that had first been extracted from dry algal biomass using methanol and chloroform. The CNRC lab analyzed one set of samples from the six experimental treatments collected on day 34.

The CNRC methods should be considered to be standardized and reliable. The CNRC FAME content results for the day 34 sample set should be considered to most closely represent the actual FAME content in the two types of samples that they tested. The GC/MS sample preparation and analysis methods described in this research are still in an early stage of development. It is most likely that the total FAME contents detected by the GC/MS methods are

underestimates. The specific reasons for the underestimates are not known, but are suspected to be related to the loss of a portion of the FAMEs during the sample preparation process.

5.5.4. FAME Composition Detection by GC/MS Method Compared to CNRC Methods

The FAME composition detected by the CNRC laboratory methods was very similar to the FAME composition of the transesterified algal lipids detected by the CG/MS method. The percentages of the FAMEs that were detected by CNRC in the day 34 sample set fit well into the trends in FAME percentages that had been observed in the FAME compositions detected by the GC/MS methods in the sample sets collected before and after day 34. The agreement between the different methods of the two laboratories indicate that the FAME compositions that were detected are likely to well represent the actual FAME compositions of transesterified *C. freiburgensis* lipids.

6. Suggestions for Future Work

6.1. Replication of Experimental Treatments

Future experiments based on this research should include replicate experimental treatments. Conclusions about the results of this experiment were limited by the absence of replicates of the six treatments, because it was not possible to determine the statistical significance of the differences in the observed results.

6.2. Suggestions for Future Experiments Investigating Nutrient Concentrations

The key difference in the growth cycles between low and high nitrogen treatments was the extended period of linear growth (≥ 25 days) after exponential growth had ended in the high-nitrogen cultures. Linear growth lasted for approximately 15 days in the intermittent nitrogen feeding treatment (No. 6). A transitional growth phase occurred in all six experimental treatments between day 9 and 12, however, the two lowest nitrogen treatment cultures quickly transitioned to stationary growth. This accounted for the notable differences in maximum cell density and dry biomass yields between samples from the low nitrogen and the high nitrogen treatments.

It may be possible to obtain a higher biomass yield before the stationary growth phase and lipid production begins, while maintaining high lipid production, by further adjustments to nutrient concentrations. Alternatively, intermittent nitrogen feeding, with additional adjustments to nitrogen concentrations and timing, may further improve lipid production. Takagi et al. (2000), demonstrated significantly improved lipid production with intermittent nitrate feeding. They found that when nitrate (as KNO_3) was fed to *Nannochloris sp.* (a green alga) ten times during the exponential (log) growth phase, added to their initial low nitrogen medium, the dry

weight (g/L) was comparable to that of their low nitrate treatment. However, they found that the lipid content and the percentage of triglycerides both increased, from 31.0% to 50.9% and 26.0 to 47.6%, respectively, compared to cells cultured in medium containing the same low nitrogen concentration at the start, without additional feeding. A continuous culture system, where nutrients are added and biomass is harvested in an ongoing manner, may provide more opportunities to make adjustments, and potentially improve lipid content results.

6.3. Supplemental CO_2 and the Potential for Carbon Capture from Flu Gas Emissions

It was also demonstrated that neither *C. freiburgensis* growth nor its lipid production was negatively impacted by slightly elevated CO_2. The FAME composition of the transesterified lipids resulting from the treatment with elevated CO_2 was also favorable for a biodiesel feedstock. Therefore, it is conceivable that *C. freiburgensis* from Berkeley Pit Lake would be a suitable candidate for a biofuel crop that could utilize acidic industrial wastewater-based medium and simultaneously capture some of the carbon from industrial sources such as flue gases. The experimental treatment added a modest additional volume of CO_2 (approximately 0 - 5%) to ambient air. The optimal volume of supplemental CO_2 to maintain or improve biomass or lipid productivity, was not determined, and the alga may be tolerant of, or benefit from, a larger volume than was supplied in treatment No. 5. The alga's physiological adaptations to acidic conditions may also afford some protection from sudden decreases in pH that may result from spikes in CO_2.

6.4. Potential for Bioremediation, Acid Mine Drainage Use and Treatment

C. freiburgensis from Berkeley Pit Lake is an alga that can grow rapidly and out-compete other microalgae as free-living cells in a liquid medium at pH 2.5, reaching densities of 35,000,000 cells/mL, and it is tolerant of high concentrations of dissolved metals. Therefore, it can be grown to high densities in acid mine drainage water, if the appropriate nutrients are supplied. It is an excellent candidate for use in biological treatment of acidic wastewater, including mitigation of acid mine drainage and recovery of dissolved metals, especially if co-cultured with bacteria and fungi.

6.5. Potential for Fungus-assisted Flocculation and Co-culture to Improve Productivity

The potential for fungus-assisted flocculation and co-culture with other organisms to further improve lipid production by *C. freiburgensis* deserve investigation. One, or both methods combined, could be employed to improve the efficiency of lipid production for biodiesel, while simultaneously accomplishing bioremediation functions, such as wastewater treatment or carbon (CO_2) capture. The energy required to harvest microalgal biomass, by conventional methods, can contribute as much as 50% to the production cost of algal biofuel, and fungal-assisted harvesting technology (bio-flocculation) can offer a solution to that problem (Wrede et al., 2014, Zhang and Hu, 2012, Zhou et al., 2012 and 2013). *C. freiburgensis* coexists, in the laboratory, with at least one acid-tolerant fungus, and probably with many in the field. During the experiment, it was observed that fungal hyphae began to grow as the density of algal cells increased, presumably stimulated by organic carbon compounds released into the medium by the algal cells (Figure 50). These hyphae not only gathered algal cells, but also appeared to sequester lipid droplets themselves, which may have been lost as fragile, lipid-filled algal cells

began to rupture (Figure 51). Zhang and Hu, Zhou et al. and Wrede et al. demonstrated that co-culturing a fungus with microalgal cells, when combined with physical agitation, can gather the algal cells into round pellets which are far more easily, and less-expensively harvested from liquid medium than free microalgal cells.

Co-culturing with other acid-tolerant microalgae could also be a way to further improve lipid yield from the algal crop, due to resource use complementarity (Stockenreiter et al., 2012).

Perhaps one of the most important considerations for developing a sustainable operation is to find a source of nitrogen that is environmentally protective, for example, agricultural or municipal wastewater. However, co-culture with an organism that is able to fix atmospheric nitrogen in a low-pH environment could also offer a solution, and it would be an excellent topic to include in future research involving co-culture with *C. freiburgensis*. *B. indica*, a free-living, nitrogen fixing soil bacterium, may be a perfect candidate to examine for this purpose, as it has been found to fix nitrogen in pH conditions as low as 2.5 to 3.0, and it secretes a sticky mucilage that may be useful as an algal cell flocculating agent (Becking, 2006, 1984 and 1961). Fungi and *B. indica* thrive on the organic carbon compounds secreted by photosynthetic organisms such as plants and microalgae, and it may not be necessary to supplement an additional nutrition source for these once an algal culture becomes established.

6.6. Remaining Unanswered Questions

There remain several unanswered questions that are relevant to lipid production or the potential production of additional valuable algal side products. Few clues to the nature or significance in the life cycle of extra-large (12 to 14 µm), non-motile, cyst-type cells were found that point to any definite answers about them. Clearly, extra-large cells can be packed with

exceptionally large lipid stores, and increasing the proportion of them in the population would result in increased lipid yields. It would be fortunate to discover an environmental condition or chemical cue that would promote their formation. Extra-large cells have been observed to contain multiple chloroplasts (possibly as many as six) which would be consistent with either abnormal incomplete mitotic division, or the formation swimming daughter cells with flagella that would soon germinate. Two or four chloroplasts would be the expected number for two to four swimming daughter cells from most Chrysophyte stomatocysts (Graham, Graham and Wilcox, 2009). If daughter cells germinate from the extra-large cells, then they could be considered to be true stomatocysts. Likewise, the experiment did not reveal an event or condition that would reliably trigger a mass-germination of swimming cells from either non-motile cells, or true stomatocysts, if they are not.

It is not certain whether the normally-sized (5 to 7 μm) non-motile form of *C. freiburgensis* growing under laboratory conditions is a true stomatocyst. The presence of extra-large cells lends to the confusion, and the normally sized non-motile cells reliably contain only a single chloroplast, indicating that two to four daughter cells have not formed within the cyst. Instead, the normally-sized non-motile cells reproduce by simple mitosis, separating into pairs, occasionally remaining attached to one-another, after formation of new walls, in groups of three, four, six, etc. However, a single swimming cell was observed to exit from a normally-sized cyst during an event when many swimming cells were present. Also, the one event where two separate cultures simultaneously converted nearly every cell to the swimming form was not preceded by formation of a large number of extra-large cells.

Prior to and during this research, it was observed that the strain of *C. freiburgensis* from Berkeley Pit Lake, grown under laboratory conditions, did not appear or behave or appear

exactly as described by Franz Doflein in 1921. Dr. Robert A. Andersen (Friday Harbor Marine Laboratories, University of Washington), who specializes in chrysophyte algae, after viewing micrographs of the Berkeley Pit Lake golden alga, confirmed this suspicion (personal communication, Nov. 19, 2016). For example, Dr. Andersen pointed out that a stomatocyst should be a normally sized non-motile cell and it should have an obvious plug. He also mentioned that the pattern of mitotic division of this alga resembles that of *Chrysosphaera sp*. in that a cell will often divide once and then quickly again, resulting in a cluster of four cells. On the other hand, normally-sized cells of this species only contain a single chloroplast, but those in the genus *Chrysosphaera* generally contain more (between one and eight chloroplasts each).

There are currently 60 taxonomically accepted species of *Chromulina* and eight that have been noted as possible additional distinct species (Guiry and Guiry, 2019). *C. freiburgensis* from Berkeley Pit Lake was positively identified by Paul Kugrens (Colorado State University), also a chrysophyte specialist, in 1998 (Bocioaga, 2003, Mitman, 1999). Therefore, if the alga is not *C. freiburgensis*, it is likely to be a closely related species. Ideally, genomic analysis, by one of the methods that have since become available, could confirm that the species name the alga has been known by until today is correct, or indicate whether another name would be more accurately assigned to it.

6.7. A Unique Alga that Deserves Further Study

C. freiburgensis from Berkeley Pit Lake is a unique organism in several ways, and it deserves further study, not only as a potential source of lipids for biofuels, but also for its potential utility in bioremediation and carbon capture. It is either the first, or one of very few, of its class that have been evaluated as a potential lipid source for biofuels. Although the lipids

produced by a few species of freshwater chrysophytes, such as *Dinobryon divergens* Imhof, have been studied (Cranwell et al., 1988), published articles that examine any species in the class Chrysophyceae, as a potential producer of lipids for biofuels are scarce. For example, Hu et al., 2008 mentions the class Chrysophyceae in general, but lists no genera or species. A search of published literature, including the references cited by Hu et al. did not uncover any examples of species currently classified as Chrysophyceae, that have been evaluated as potential sources of lipids for biofuels. *C. freiburgensis* from Berkeley Pit Lake is also an acidophilic extremophile, which is a unique ecological niche among algae studied for biofuels.

This experiment serves as a starting point from which to fine tune the timing of harvest, concentrations of nutrients, and concentration of supplemental CO_2, in order to optimize lipid production and the proportions of fatty acids required, for the manufacture of a high-quality biodiesel product, from a unique species with capabilities and potential applications that distinguish it from other microalgae that have been previously studied.

7. References Cited

Alemán-Nava, G. S.; Cuellar-Bermudez, S. P.; Cuaresma, M.; Bosma, R.; Muylaert, K.; Ritmann, B. E.; Parra, R. How to use Nile Red, a Selective Fluorescent Stain for Microalgal Neutral Lipids. *J. Microbiol. Methods* **2016**, *128,* 74-79.

Alonzo, F.; Mayzaud, P. Spectrofluorometric Quantification of Neutral and Polar Lipids in Zooplankton Using Nile Red. *Mar. Chem.* **1999**, *67(3-4)*, 289-301.

American Trucking Associations, Inc. - Alternative Fuels in Trucking. **1997**, *6(1)*. www.afdc.energy.gov/pdfs/truk6-1.pdf. Accessed on 11/30/2018.

Andersen, Robert A. Algal Culturing Techniques, Elsevier Academic Press: Burlington, MA, **2005**.

Andersen, Robert A. Ch. 11, Chrysophyta, in Algae Source to Treatment, Manual of Water Supply Practices M57. American Water Works Association, 1st Ed.: Denver, CO, **2010**; pp 249-270.

Arbib, Z.; de Godos, I; Ruiz, J.; Perales, J. A. Optimization of Pilot High Rate Algal Ponds for Simultaneous Nutrient Removal Lipids Production. *Sci. Total Environ*. **2017**, *589*, 66-72.

Archer Daniels Midland Company, adm-fact-sheet-biodiesel-technical-information. https://www.biodiesel.org/docs/ffs-basics/adm-fact-sheet-biodiesel-technical-information.pdf?sfvrsn=4

Arias-Forero, D.; Hayashida, G.; Aranda, M.; Araya, S.; Portilla, T.; García, A.; Díaz-Palma, P. Protocol for Maximizing the Triglycerides-Enriched Lipids Production from *Dunaliella salina* SA32007 Biomass, Isolated from the Salar de Atacama (Northern Chile). *Adv. Biosci. Biotechnol*. **2013**, *4(8),* 830.

Ajjawi, I.; Verruto, J.; Aqui, M.; Soriaga,L.B.; Coppersmith, J.; Kwok, K.; Peach, L. Lipid Production in *Nannochloropsis gaditana* is Doubled by Decreasing Expression of a Single Transcriptional Regulator. *Nat. Biotechnol*. **2017**, *35(7)*, 647.

Arunakumara, K. K. I. U.; Zhang, X. Heavy Metal Bioaccumulation and Toxicity with Special Reference to Microalgae. *J. Ocean Univ. China* **2008**, *27(1)1*, 60-64.

Ayala-Parra; P.; Sierra-Alvarez R.; Field J. A. Algae as an Electron Donor Promoting Sulfate Reduction for the Bioremediation of Acid Rock Drainage. *J. Hazard. Mater*. **2016**, *317*, 335-343.

Bagnoud-Velásquez, M. U.; Schmid-Staiger, G. P., Vogel, F.; Ludwig, C. First Developments Towards Closing the Nutrient Cycle in a Biofuel Production Process. *Algal Res.* **2015**, *8*, 76-82.

Bagnato, G.; Iulianelli, A.; Sanna, A.; Basile, A. Glycerol Production and Transformation: A Critical Review with Particular Emphasis on Glycerol Reforming Reaction for Producing Hydrogen in Conventional and Membrane Reactors. *Membranes* **2017** *7(2),* 17. doi:10.3390/membranes7020017

Barros, A. I.; Gonçalves, A. L.; Simões, M.; Pires, J. C. M.. Harvesting Techniques Applied to Microalgae: a Review. *Renewable Sustainable Energy Rev.* **2015**, *41*, 1489-1500.

Bartkowiak, Algal Stimulation of the Berkeley Pit Lake System, Thesis, Montana Tech, **2002**.

Bastidas, O. Technical Note, Low Concentration Cell Counting. Celeromics, www. Celeromics.com **2015** (Website discontinued, see Appendix).

Bastidas, Oscar, Technical Note, Cell Counting with Neubauer Chamber, Basic Hemocytometer Usage, Celeromics, www. Celeromics.com **2015** (Website discontinued, see Appendix).

Bauer, P.; Teufel, D, - Beitrag im Jahrbuch **1998** des Stadtteilvereins Handschuhsheim. Gold auf dem Heiligenberg? http://www.upi-institut.de/_handschuhsheim/goldauf.htm (accessed on 4/5/2019).

Becking, J. H. The genus *Beijerinckia*. The Prokaryotes: Volume 5: Proteobacteria: Alpha and Beta Subclasses. **2006**, 151-162.

Becking, J. H. Studies on the Nitrogen-Fixing Bacteria of the Genus Beijerinckia: II. Mineral Nutrition and Resistance to High levels of Certain Elements in Relation to Soil Type. *Plant Soil* **1961**, 297-322.

Becking, **1984** Genus Beijerinckia, in Bergey's Manual of Systematic Bacteriology, Vol. 1: Section 4. Krieg, Noel R. and John Holt, editors, Williams and Wilkins, Publ. Baltimore.

Berthold, E. D. MS Thesis, Enhancing Algal Biomass and Lipid Production Through Bacterial and Fungal Co-culture, Florida International University, **2016**.

Biodiesel Basics, Biodiesel.org, National Biodiesel Board, http://biodiesel.org, **2018**.

Biofuel.org, http://biofuel.org.uk/third-generation-biofuels.html, 1**2/6/2018.**

Bligh, E. G.; Dyer, W. J. A Rapid Method of Total Lipid Extraction and Purification. Can. J. *Biochem. Physiol*. **1959,** *37(8)*, 911-917.

Bocioaga, D. Thesis, MS Geochemistry, Montana Tech of The University of Montana, **2003**.

Bocioaga, D.; Mitman, G. G. *Chlamydomonas acidophila* from the Berkeley pit lake – A Strain Adapted to an Extreme Environment. *J. Phycol.* **2004**, *39(1)*, 4.

Boyle, N.R.; Page, M.D.; Liu, B.; Blaby, I.K.; Casero, D.; Kropa, J.; Cokus, S.J.; Hong-Hermesdorf, A.; Shaw, J.; Karpowicz, S.J.; Gallaher, S.D,; Johnson, S.; Benning, C.; Pellegrini, M.; Grossman, A.; Merchant, S.S.; Three Acyltransferases and Nitrogen-responsive Regulator are Implicated in Nitrogen Starvation-induced Triacylglycerol Accumulation in *Chlamydomonas*. *J. Biol. Chem.* **2012**, *287(19),* 15811-15825.

Brake, S. S.; Hasiotis, S. T.; Eukaryote-dominated Biofilms and Their Significance in Acidic Environments. *Geomicrobiology* **2010**, *27(6-7),* 534-558.

Breuer, G.; Lamers, P. P.; Martens, D. E.; Draaisma, R. B.; Wijffels, R. H. Effect of Light Intensity, pH, and Temperature on Triacylglycerol (TAG) Accumulation Induced by Nitrogen Starvation in *Scenedesmus obliquus*. *Bioresour.* Te*chnol.* **2013**, *143*, 1-9.

Breuer, G.; Lamers, P. P.; Martens, D. E.; Draaisma, R. B.; Wijffels, R. H. The Impact of Nitrogen Starvation on the Dynamics of Triacylglycerol Accumulation in Nine Microalgae Strains. *Bioresour. Technol.* **2012**, *124*, 217-226.

Bringezu, S.; Schütz, H.; O´Brien, M.; Kauppi, L.; Howarth, R. W.; McNeely, J. Towards Sustainable Production and Use of Resources: Assessing Biofuels. United Nations Environment Programme. Biofuels Working Group, and United Nations Environment Programme. International Panel for Sustainable Resource Management. Towards sustainable production and use of resources: assessing biofuels. UNEP/Earthprint, **2009**.

Brown, P. B.; Wolfe, G. V. Protist Genetic Diversity In The Acidic Hydrothermal Environments Of Lassen Volcanic National Park, USA. J. Eukaryotic *Microbiol.* **2006**, *53(6)*, 420-431.

Burgess, 11.4 Economics of Biodiesel Production, Including Economics of Al. https://www.e-education.psu.edu **2018**.

Bwapwa, J. K.; Jaiyeola, A. T.; Chetty, R. Bioremediation of Acid Mine Drainage Using Algae Strains: A Review. *S. Afr. J. Chem. Eng*. **2017**, *24*, 62-70.

Cameron, D.; Stewart, A. Low-pressure positive chemical ionization GC/MS for the analysis of lipids from *Chromulina freibugensis* Defl., a Potential Biofuel Source, 58th ASMS Conference on Mass Spectrometry, Salt Lake City, UT, **May 23-27, 2010**.

Canadian Phycological Culture Centre (CPCC), Modified acid medium (MAM) https://uwaterloo.ca/canadian-phycological-culture-centre/cultures/culture-media/modified-acid-medium **(Accessed July, 2015**).

Canter, C. E.; Blowers, P.; Handler, R.M.; Shonnard, D. R. Implications of Widespread Algal Biofuels Production on Macronutrient Fertilizer Supplies: Nutrient Demand and Evaluation of Potential Alternate Nutrient Sources. *Appl. Energy* **2015**, *143*, 71-80.

Celeromics, Technical Note - Error in Cell Counting www. Celeromics.com **2015** (Website discontinued, see Appendix).

Challagulla, V.; Fabbro, L.; and Nayar, S.; Biomass, Lipid Productivity and Fatty Acid Composition of Fresh Water Microalga *Rhopalosolen Saccatus* Cultivated Under Phosphorous Limited Conditions. *Algal Res.* **2015**, *8*, 69-75.

Chen, W.; Zhang, C.; Song, L.; Sommerfeld, M.; Hu, Q. A High Throughput Nile Red Method for Quantitative Measurement of Neutral Lipids in Microalgae. *J. Microbiol. Methods* **2009**, *77(1),* 41-47.

Chen, C-Y.; Yeh, K-L.; Aisyah, R.; Lee, D-J.; Chang, J-S.; Cultivation, Photobioreactor Design and Harvesting Of Microalgae for Biodiesel Production: A Critical Review. *Bioresour. Technol.* **2011**, *102(1),* 71-81.

Chen, J.; Li, J.; Dong, W.; Zhang, X.; Tyagi, R. D.; Drogui, P.; Surampalli, R.Y. The Potential of Microalgae in Biodiesel Production. Renewable *Sustainable Energy Rev.* **2018**, *90*, 336-346.

Chen, M.; Tang, H.; Ma, H.; Holland, T. C.; Ng, K. Y. S.; Salley, S. O. Effect of Nutrients on Growth and Lipid Accumulation in The Green Algae D*unaliella tertiolecta*. *Bioresour. Technol.* **2011**, 10*2(2),* 1649-1655.

Chinnasamy S.; Bhatnagar A.; Hunt, R. W.; Das, K.C. Microalgae Cultivation In A Wastewater Dominated by Carpet Mill Effluents For Biofuel Applications. *Bioresour. Technol*. **2010**, *101(9),* 3097-105.

Chisti, Y. Biodiesel from *Microalgae. Biotechnol. Adv.* **2007**, *25(3),* 294-306.

Chiu, S-Y.; Kao,C-Y.; Tsai, M-T.; Ong, S-C.; Chen, C-H.; Lin, C-S. Lipid Accumulation and CO_2 Utilization of *Nannochloropsis oculata* in Response to CO^2 Aeration. *Bioresour. Technol.* **2009**, 10*0(2),* 833-838.

Chiu, S-Y.; Kao,C-Y.; Chen, T-Y.; Chang, Y-B.; Kuo, C-M.; Lin, C-S. Cultivation of Microalgal *Chlorella* for Biomass and Lipid Production Using Wastewater as Nutrient Resource. *Bioresour. Technol.* **2015**, *184*, 179-189.

Citizens Technical Environmental Committee (CTEC) 27 W. Park Street, Butte, MT 59701 http://www.buttectec.org (Accessed on **April 15, 2019**).

Cooksey, K. E., ed. Molecular Approaches to the Study of the Ocean. First Ed. Chapman and Hall: NY, **1998**.

Cooksey, K. E.; Guckert, J. B.; Williams, S. A.; Callis, P. R. Fluorometric Determination of the Neutral Lipid Content of Microalgal Cells Using Nile Red. *J. Microbiol. Methods* **1987**, *6(6)*, 333-345.

Cooksey - Collection and Screening of Microalgae for Lipid Production. **1987**. https://www.nrel.gov/docs/legosti/old/15388.pdf.

Cooper, M. S.; Hardin, W. R.; Petersen, T.W.; Cattolico, R. A. Visualizing Green Oil in Live Algal Cells. *J. Biosci. Bioeng.* **2010**, 1*09(2),* 198-201.

Cranwell, P. A.; Creighton, M. E.; Jaworski G. H. M. Lipids of Four Species of Freshwater Chrysophytes. *Phytochemistry* **1988**, 2*7(4),* 1053-1059.

Courchesne, N. M. D.; Parisien, A.; Wang, B.; Lan, C. Q. Enhancement of Lipid Production Using Biochemical, Genetic and Transcription Factor Engineering Approaches. *J. Biotechnol.* **2009**, *141(1-2),* 31-41.

Covert, T.; Greenstone, M.; Knittel, C. R. Will We Ever Stop Using Fossil Fuels? J. of *Economic Perspectives* **2016**, *30(1),* 117-38.

Dakel, S. M.; Mitman, G. G. Bioremediative Potential of *Chromulina freiburgensis* in Culture from The Berkeley Pit. **2003**, MS thesis, Montana Tech of The University of Montana.

Das, B. K.; Roy, A.; Koschorreck, M.; Mandal, S. M.; Wendt-Potthoff, K.; Bhattacharya, J. Occurrence and Role of Algae And Fungi in Acid Mine Drainage Environment with Special Reference to Metals and Sulfate Immobilization. *Water Res.* **2009**, *43(4),* 883-894.

de la Jara, A.; Mendoza, H.; Martel, A.; Molina, C.; Nordström, L.; de la Rosa, V.; Diaz-Diaz, R. Flow Cytometric Determination of Lipid Content in a Marine Dinoflagellate, *Crypthecodinium cohnii. J. Appl. Phycol*. **2003**, *15*, 433-438.

Derx, H. G. *Beijerinckia*, a new genus of nitrogen-fixing bacteria in tropical soils. *Repr. Meded. Konink. Ned. Akad. Wetens.* **1950**, *53(2).*

Doflein, F. Mitteilungen über Chrysomonadinen aus dem Schwarzwald. *Zoologischer Anzeiger* **1921**, *53(7/8)*, 153-173.

Doflein, F. Untersuchungen über Chrysomonadinen III. Arten von C*hromulina* und *Ochromonas* aus dem badischen Schwarzwald und ihre Cystenbildung. *Archiv für Protistenk* **1923**, *46*, 267-327.

Doflein, F. Die Gattung *Chloramoeba* Bohlin Und Ihre Stellung Im Reich Der Organismen. *Acta Zoologica* **1921**, *2(3),* 431-443.

Dönmez, G. Ç.; Aksu, Z.; Öztürk, A.; Kutsal, T. A Comparative Study on Heavy Metal Biosorption Characteristics of Some Algae. Process. *Biochemistry*, **1999**, *34(9),* 885-892.

Drever, J. I. The Geochemistry of Natural Waters: Surface and Groundwater Environments. Third Ed. Prentice Hall: New York, **1997**, Vol. 436.

Du, Z-Y.; Benning, C. Triacylglycerol Accumulation In Photosynthetic Cells In Plants and Algae in Lipids in Plant and Algae Development. *Subcellular Biochemistry* **2016**, *86*, 179-205.

Duaime, T. E.; McGrath, S. F.; Icopini, G. A.; Thale, P.R. Montana Bureau of Mines and Geology. Butte Mine Flooding Operable Unit Water-Level Monitoring and Water-Sampling 2016 Consent Decree Update Butte Montana 1982-2016 prepared for Montana Department of Environmental Quality, Remediation Division and U.S. Environmental Protection Agency, Region VIII. **2017**.

Dunlap, S. Metals, Acid In Berkeley Pit Water Killed Geese, Report Confirms. Montana Standard, **April 18, 2017**.

Dunlap, Susan. Migrating Snow Geese Land in Berkeley Pit Water - And Survive. Montana Standard, **November 30, 2016**.

Dunlap, Susan. Bird Deterrent Demonstration Sends 200 Mph Blast of Air Through Berkeley Pit. Montana Standard, **May 31, 2017**.

Dunn, R. O. Correlating the Cloud Point of Biodiesel to the Concentration and Melting Properties of the Component Fatty Acid Methyl Esters. *Energy Fuels* **2018**, *32(1),* 455-464.

Dutta, K.; Daverey, A.; Lin, J-G. - Evolution Retrospective for Alternative Fuels- First to Fourth Generation. *Renewable Energy* **2014**, *69*, 114-122.

Evert, R. F.; Eichhorn, S. E. Raven, Biology of Plants, 8th Ed, W.H. Freeman and Co.: New York, **2013**.

eXtension, Algae for Biofuel Production, Farm Energy, **January 31, 2014** https://articles.extension.org/pages/26600/algae-for-biofuel-production (accessed Mar 29, 2017).

Environmental Protection Agency (EPA), What is Superfund? https://www.epa.gov/superfund/what-superfund (accessed **3/21/2019**).

Feng, D.; Chen, Z.; Xue, S.; Zhang, W. Increased Lipid Production of the Marine Oleaginous Microalgae *Isochrysis zhangjiangensis* (Chrysophyta) by Nitrogen Supplement. *Bioresour. Technol.* **2011**, *102(12),* 6710-6716.

Feng, Y.; Li, C.; Zhang, D. Lipid Production of *Chlorella vulgaris* Cultured in Artificial Wastewater Medium. *Bioresour. Technol.* **2011**, *102(1),* 101-5.

Fidalgo, J. P.; Cid, A.; Torres, E.; Sukenik, A.; Herrero C. Effects of Nitrogen Source and Growth Phase on Proximate Biochemical Composition, Lipid Classes and Fatty Acid Profile of the Marine Microalga *Isochrysis galbana*. *Aquaculture* **1998** *166(1-2),* 105-116.

Fogg, G. E. Algal Cultures and Phytoplankton Ecology, 2nu Ed., University of Wisconsin Press, London, **1975**.

Fukuda, H.; Kondo, A.; Noda, H. Biodiesel Fuel Production by Transesterification of Oil. *J. Biosci. Bioeng.* **2001**, *92(5),* 405-416.

Funakoshi, H.; Yamada, A. Transition Phenomena in Bacterial Growth Between Logarithmic and Stationary Phases. *J. Math Biol.* **1980**, *9(4),* 369-87.

Gammons, C. H.; Duaime, T. E. Long Term Changes in the Limnology and Geochemistry of the Berkeley Pit Lake, Butte, Montana. *Mine Water Environ.* **2006**, *25(2)*, 76-85.

Gammons, Christopher H., John J. Metesh, and Terence E. Duaime. An overview of the mining history and geology of Butte, Montana. *Mine Water Environ.* **2006**, 2*5(2),* 70-75.

Gazea, B.; Adam, K.; Kontopoulos, A. A Review of Passive Systems for the Treatment of Acid Mine Drainage. *Miner. Eng.* **1996**, *9(1),* 23-42.

Goold, H.; Beisson, F.; Peltier, G.; Li-Beisson, Y. Microalgal Lipid Droplets: Composition, Diversity, Biogenesis and Functions. *Plant Cell Rep.* **2015**, *34(4),* 545-555.

Graham, L. E.; Graham, J. M; Wilcox, L. W. Algae, 2nd ed.; Benjamin Cummings: San Francisco, **2009**.

Graham, L. E.; Wilcox, L. W. Algae; Prentice Hall, Inc. New Jersey, **2000**.

Griffiths, M. J.; van Hille, R. J.; Harrison, S. T. L. Lipid Productivity, Settling Potential and Fatty Acid Profile of 11 Microalgal Species Grown Under Nitrogen Replete and Limited Conditions. *J. Appl. Phycol*. **2012**, *24(5),* 989-1001.

Griffiths, M. J.; Harrison, S.T.L. Lipid Productivity As A Key Characteristic For Choosing Algal Species for Biodiesel Production. *J. Appl. Phycol.* **2009**, *21(5),* 493-507.

Grima, E. M.; Belarbi, E-H.; Fernández, F. G. A.; Medina, R. A; Chisti, Y. Recovery of Microalgal Biomass and Metabolites: Process Options and Economics. *Biotechnol. Adv.* **2003**, *20 (7),* 491-515.

Guiry, M.D in Guiry, M.D.; Guiry, G.M. *Chromulina freiburgensis* Doflein AlgaeBase. **2019**. World-wide electronic publication, National University of Ireland, Galway. http://www.algaebase.org; searched on 13 April 2019.

Guiry, M.D in Guiry, M.D.; Guiry, G.M. **2019**. Chromulina AlgaeBase. World-wide electronic publication, National University of Ireland, Galway. http://www.algaebase.org; searched on 11 March 2019.

Guiry, M.D in Guiry, M.D.; Guiry, G.M. **2019**. *Isochrysis zhanjiangensis* H.-J.Hu & H.-R.Liu AlgaeBase. World-wide electronic publication, National University of Ireland, Galway. http://www.algaebase.org; searched on 13 April 2019.

Guiry, M.D in Guiry, M.D.; Guiry, G.M. **2019**. AlgaeBase. *Chromulina rosanoffii* (Woronin) Blochmann, 1895. World-wide electronic publication, National University of Ireland, Galway. http://www.algaebase.org; searched on 13, Mar. 2019.

Guiry, M.D in Guiry, M.D.; Guiry, G.M. **2019**. AlgaeBase. *Chromophyton* Woronin, 1880. World-wide electronic publication, National University of Ireland, Galway. http://www.algaebase.org; searched on 05 February 2019.

Guiry, M.D in Guiry, M.D.; Guiry, G.M. **2019**. *Boekelovia* M.F.E.Nicolai & L.G.M.Baas-Beck, 1935 *AlgaeBase*. World-wide electronic publication, National University of Ireland, Galway. http://www.algaebase.org; searched on 27 February 2019

Goncalves, E, C.; Johnson, J. V.; Rathinasabapathi, B. Conversion Of Membrane Lipid Acyl Groups To Triacylglycerol And Formation Of Lipid Bodies Upon Nitrogen Starvation In Biofuel Green Algae *Chlorella* UTEX29. *Planta* **2013**, *238(5),* 895-906.

Halim, R.; Gladman, B.; Danquah, M. K.; Webley, P. A. Oil Extraction from Microalgae for Biodiesel Production. *Bioresour. Technol*. **2011**, *102(1),* 178-185.

Hanagata, N.; Takeuchi, T.; Fukuju, Y.; Barnes, D. J.; Karube, I. Tolerance of Microalgae to High CO2 and High Temperature. *Phytochemistry* **1992**, *31(10),* 3345-3348.

Harun, R.; Danquah, M. K.; Forde, G. M. Microalgal Biomass as A Fermentation Feedstock for Bioethanol Production. *J. Chem. Technol. Biotechnol.* **2010**, *85(2),* 199-203.

Harkey, G. A.; Cameron, D.; Chang, J. The use of low-pressure positive chemical ionization GC/MS for the characterization of fatty acid methyl esters (FAME), 57th ASMS Conference on Mass Spectrometry, Philadelphia, PA, **May 31-June 4, 2009.**

He, J.; Chen, P. J. A Comprehensive Review on Biosorption of Heavy Metals by Algal Biomass: Materials, Performances, Chemistry, and Modeling Simulation Tools. *Bioresour. Technol.* **2016**, *160*, 67-78.

Henderson, M. E. Stabilization of Mine Waste Rock Using Moss, MS Thesis, **2005**, Montana Tech

Hoekman, S. K.;, Broch, A.; Robbins, C.; Ceniceros, E.; Natarajan, M.; Review of Biodiesel Composition, Properties, and Specifications. *Renewable Sustainable Energy Rev.* **2012**, *16(1),* 143-169.

Holen, D. A. Chrysophyte Stomatocyst Production in Laboratory Culture and Descriptions of Seven Cyst Morphotypes. *Phycologia* **2014**, *53 (5),* 426-432.

Horikoshi, K.; Grant, W. D. editors, Extremophiles: Microbial Life in Extreme Environments. Wiley-Liss Inc.: New York 1**998**.

Hu, Q.; Sommerfeld, M.; Jarvis, E.; Ghirardi, M.; Posewitz, M.; Seibert, M.; Darzins, A. Microalgal Triacylglycerols as Feedstocks for Biofuel Production: Perspectives and Advances. *The Plant Journal* **2008**, *54(4),* 621-639.

Huber-Pestalozzi, G. *Das* Phytoplankton des Süsswassers Systematik und Biologie: Chrysophyceen; Farblose Flagellaten; Heterokonten. (In book series, Thienemann, August, *Die Binnengewässer*, Band XVI, Teil 2, 1. Hälfte, Schweizerbart (publisher), Stuttgart, **1962**.

Huang, Q.; Jiang, F.; Wang, L.; Yang, C. Design of Photobioreactors for Mass Cultivation of Photosynthetic Organisms. *Engineering* **2017** *3(3),* 318-329.

Hu, Q., Zhang, C., Sommerfeld, M. Biodiesel From Algae: Lessons Learned Over The Past 60 Years And Future Perspectives. Annual meeting of the Phycological Society of America, July 7–12, **2006**, Juneau, Alaska, pp. 40–41.

Hu, Q., Sommerfeld, M., Jarvis, E., Ghirardi, M., Posewitz, M., Seibert, M., Darzins, A. Microalgal Triacylglycerols As Feedstocks For Biofuel Production: Perspectives And Advances. *Plant Journal* **2008**, *54*, 621–639.

Hughes, S. R.; Gibbons, W.R.; Moser, B. R.; Rich, J. O. Sustainable Multipurpose Biorefineries for Third-Generation Biofuels and Value-Added Co-Products. **2013** https://www.semanticscholar.org/paper/Sustainable-Multipurpose-Biorefineries-for-Biofuels-Hughes-Gibbons/2753766d2c1435babb954127bb2886f1020659e7

Imahara, H.; Minami, E.; Saka, S. Thermodynamic Study on Cloud Point Of Biodiesel With Its Fatty Acid Composition. *Fuel* **2006**, *85(12–13),* 1666-1670.

ImageJ, https://imagej.nih.gov/ij/index.html (Accessed on 2/5/2019) See Schneider, et al. **2012**.

Jitar, O.; Teodosiu, C.; Oros; A. Plavan, G.; Nicoara, M. Bioaccumulation of Heavy Metals in Marine Organisms from the Romanian Sector of the Black Sea. *New Biotechnol.* **2015**, *32(3),* 369-378.

Jokić, S.;, Sudar, R.; Svilović, S.; Vidović, S.; Bilić, M.; Velić, D.; Jurković, V. Fatty Acid Composition of Oil Obtained from Soybeans by Extraction with Supercritical Carbon Dioxide. *Czech J. Food Sci.* **2013**, *31(2),* 116-125.

Jonart, L. **2012**. Undergraduate Research Paper, (unpublished) Exploring the Lipid Content of *Chromulina freiburgensis* Dofl. and Poster: Exploring the Lipid Content of an Acidiphilic Alga *Chromulina freiburgensis* Dofl. Isolated from the Berkeley Pit.

Kebede-Westhead, E.; Pizarro, C.; Mulbry, W. W. Treatment of Swine Manure Effluent Using Freshwater Algae: Production, Nutrient Recovery, and Elemental Composition of Algal Biomass at Four Effluent Loading Rates. *J. Appl. Phycol.* **2006**, *18(1),* 41-46.

Kelly, J. A Comparison of Gravimetric and Fluorescence Techniques for Determining the Lipid Content of Microalgae. Department of Chemistry and Geochemistry, Honors Thesis, Montana Tech of the University of Montana, **2013**.

Khozin-Goldberg, I.; Didi-Cohen, S.; Shayakhmetova, I.; Cohen, Z. Biosynthesis of Eicosapentaenoic Acid (EPA) In the Freshwater Eustigmatophyte *Monodus subterraneus* (Eustigmatophyceae). *J. of Phycol.* **2002**, *38(4)*, 745-756.

Kim, H-J,; Choi, Y-K.; Jeon, H. J.; Bhatia, s. K.; Kim, Y-H.; Kim, Y-G.; Choi, K-Y. Growth Promotion of *Chlorella Vulgaris* by Modification of Nitrogen Source Composition with Symbiotic Bacteria, *Microbacterium* Sp. HJ1. *Biomass Bioenergy* **2015**, *74*, 213-219.

King, S. F. Uptake and Transfer of Cesium-137 by *Chlamydomonas, Daphnia*, and Bluegill Fingerlings. *Ecology* **1964**, *45(4)*, 852-859.

Knothe, G. Improving Biodiesel Fuel Properties by Modifying Fatty Ester Composition. Energy *Environ. Sci.* **2009**, *2(7)*, 759-766.

Knothe, G.; Razon, L. F. Biodiesel Fuels. *Prog. Energy Combust. Sci.* **2017**, *58*, 36-59.

Kugrens, P. Colorado State University, Fort Collins, CO, personal communication with Grant Mitman, **1998**.

Kuo, C. M.; Jian, J. F.; Lin, T. H.; Chang, Y. B.; Wan, X. H.; Lai, J. T.; Chang, J. S.; Lin, C. S Simultaneous Microalgal Biomass Production and CO2 Fixation by Cultivating *Chlorella* sp. GD with Aquaculture Wastewater and Boiler Flue Gas. *Bioresour. Technol.* **2016**, *221*, 241-250.

Lackey, J. B. The Flora and Fauna of Surface Waters Polluted by Acid Mine Drainage. *Public Health Rep.* **1938**, *53(34)*, 1499-507.

Lane, J. What are–and who's making – 2G, 3G and 4G biofuels? Biofuels Digest, **May 18, 2010**, https://web.archive.org/web/20100521143237/http://www.biofuelsdigest.com/bdigest/2010/05/18/3g-4g-a-taxonomy-for-far-out-%E2%80%94-but-not-far-away-%E2%80%94-biofuels/

Lane, Jim- Ethanol and biodiesel/ dropping below the production cost of fossil fuels? **2017**/ Biofuels Digest. https://www.biofuelsdigest.com/bdigest/2017/05/18/ethanol-and-biodiesel-dropping-below-the-production-cost-of-fossil-fuels/

Lavens, Patrick and Patrick Sorgeloos, Editors, 2.3. Algal Production. Manual on the Production and Use of Live Food for Aquaculture **1996** Laboratory of Aquaculture and *Artemia* Reference Center, University of Ghent, Ghent, Belgium, Rome 1996, Food and Agriculture Organization of the United Nations http://www.fao.org/docrep/003/W3732E/w3732e06.htm 10/14/2018 (Same as: 2.3. Algal Production. FAO Corporate Document Repository. Fisheries and Aquaculture Department, Wed. 23 Sept. 2012., http://www.fao.org/docrep/003/W3732E/w3732e06.htm)

Lawton, R. J.; de Nys, R.; Paul, N. A. Selecting Reliable and Robust Freshwater Macroalgae for Biomass Applications. *PLoS One* **2013**; *8(5)*, e64168.

Lee, Y-K.; Tay, H-S. High CO_2 Partial Pressure Depresses Productivity and Bioenergetic Growth Yield of *Chlorella pyrenoidosa* Culture. *J. Appl. Phycol.* **1991**, *3(2)*, 95-101.

Leung, W. C.; Wong, M-F.; Chua, H.; Lo, W.; Yu, P. H. F.; Leung, C. K. Removal and Recovery of Heavy Metals by Bacteria Isolated from Activated Sludge Treating Industrial Effluents and Municipal Wastewater. *Water Sci. Technol.* **2000**, *41(12)*, 233-240.

Li, Y.; Fei, X.; Deng, X. Novel Molecular Insights into Nitrogen Starvation-Induced Triacylglycerols Accumulation Revealed by Differential Gene Expression Analysis in Green Algae *Micractinium pusillum*. *Biomass Bioenergy* **2012**, *42*, 199-211.

Lohman, E. J.; Gardner, R. D.; Pedersen, T.; Peyton, B.M.; Cooksey, K. E.; Gerlach, R. Optimized Inorganic Carbon Regime for Enhanced Growth and Lipid Accumulation in *Chlorella vulgaris Biotechnol. Biofuels* **2015**, *8*, 82.

Lü, J.; Sheahan, C.; Fu, P. Metabolic Engineering of Algae for Fourth Generation Biofuels Production. *Energy Environ. Sci.* **2011**, *4(7)*, 2451-2466.

Mackay, S.; Gomes, E.; Holliger, C.; Bauer, R.; Schwitzguébel, J-P. Harvesting Of *Chlorella sorokiniana* by Co-Culture with the Filamentous Fungus *Isaria fumosorosea*: A Potential Sustainable Feedstock for Hydrothermal Gasification. *Bioresour. Technol.* **2015**, *185*, 353-361.

Madigan, M. T.; Martinko, J. M.; Bender, K. S.; Buckley, D. H.; Stahl, D. A. Biology of Microorganisms, Brock Biology of Microorganisms (14th Edition);Pearson Education Inc.: New York, **2015**.

Martin, C., J. De la Noüe; Picard, G. Intensive Cultivation of Freshwater Microalgae on Aerated Pig Manure. *Biomass* **1985**, *7(4)*, 245-259.

Mata, T. M.; Martins, A. A.; Caetano, N. S. Microalgae for Biodiesel Production and Other Applications: A Review. Renewable Sustainable *Energy Rev.* **2010**, *14(1)*, 217-232.

Malins, C. (**2017**). Thought for food - A review of the interaction between biofuel consumption and food markets. https://www.transportenvironment.org/sites/te/files/publications/Cerulogy_Thought-for-food_September2017.pdf

Mansour, M. P.; Volkman, J.K.; Blackburn, S. The Effect of Growth Phase on The Lipid Class, Fatty Acid and Sterol Composition in the Marine Dinoflagellate, *Gymnodinium* sp. in Batch Culture. *Phytochemistry* **2003**, *63(2)*, 145-53.

Meng, X.; Yang, J,; Xu, X.; Zhang, L.; Nie, Q.; Xian, M. Biodiesel Production from Oleaginous Microorganisms. *Renewable Energy* **2009**, *34(1)*, 1-5.

Merriam Webster Dictionary, accessed online, **11/13/2018**, https://www.merriam-webster.com/dictionary/bioreactor

Mesner and Geiger - **2005** Understanding Your Watershed- What is pH?, Utah State University, Extension, Water Quality Fact Sheets, https://extension.usu.edu/waterquality/wq-publications/index (accessed on 3/14/2019)

Michigan State University - Advancing Algae's Viability as a Biofuel | Lab Manager http://www.labmanager.com/news/**2014/02**/advancing-algae-s-viability-as-a-biofuel#.WwcUZS-ZP-Y

Mitman, G. G. A Biological Survey of the Berkeley Pit Lake System, Final Report **(1999)**, Mine Waste Technology Program, Activity IV, Project 10, for Montana Tech of The University of Montana, Butte Montana, and U.S. Environmental Protection Agency National Risk Management Research Laboratory Cincinnati, Ohio, IAG ID No. DW89938513-01-0

Mitman, G. G. - Abstract - Algal Bioremediation of The Berkeley Pit Lake System. *J. of Phycology* **2000**, *36(3)*, 49.

Mitman, G. G. Bacterial Effects and Algae Bioremediation by *Chlorella ellipsoidea* Gerneck of the Berkeley Pit Lake System. *J. of Phycology* **2001,** *37(3)*, 36.

Mitman, G. G. - Mine Waste Technology Program, Activity IV, Project 30 Final Report 261–Algal Bioremediation of the Berkeley Pit Lake System/ An In Situ Test Using Limnocorrals. EPA/ DOE **2007**. Government Documents.

Mitman, G. G. - Pit Lake System Characterization and Remediation phase III Activity IV Project 16. EPA/ DOE **2007**. Government Documents.

Mondloch, A. Analysis of Lipids From *Chromulina Freiburgensis* for Their Potential Use as Biofuels, Thesis, Interdisciplinary Master of Science, Montana Tech of The University of Montana, **2012**.

MBMG GWIC, **2018**. Montana Bureau of Mines and Geology, Ground Water Information Center, MBMG Data Center Montana Tech of The University of Montana. http://mbmggwic.mtech.edu/ 11/19/2018.

MBMG, **2019** (Montana Bureau of Mines and Geology) Berkeley Pit/Butte Mine-Flooding http://www.mbmg.mtech.edu/env/env-berkeley.html (Accessed on 2/22/2019).

MBMG-GWIC. **2000** Montana Bureau of Mines and Geology Ground Water Information Center Analysis, ID 2000Q0525.

Mortensen, L. M.; Gislerød, H. R. The Growth of Chla*mydomonas reinhardtii* as Influenced by High CO_2 And Low O_2 in Flue Gas from a Silicomanganese Smelter. *J. Appl. Phycol.* **2015**, *27(2)*, 633-638.

Moslander, H. Maximization and Quantification of Fatty Acid Methyl Esters for Biofuels from *Chromulina freiburgensis*, Senior Research Paper, Montana Tech, Chemistry Department (unpublished), **2016**.

Munday, P. Butte Mining, 1864-2005: A Brief Cultural and Environmental History. **2005**. https://buttearchives.pastperfectonline.com/library/699C94C7-E6EC-471F-8884-825585776521.

Moussa, I. D-B.; Athmouni, K.; Chtourou, H.; Ayadi, H.; Sayadi, S.; Dhouib, A. Phycoremediation Potential, Physiological, and Biochemical Response of *Amphora subtropica* and *Dunaliella* sp. to Nickel Pollution. *J. Appl. Phycol.* **2018**, *30(2)*, 931-941.

Mutanda T.; Ramesh D.; Karthikeyan S.; Kumari S.; Anandraj A.; Bux F. Bioprospecting for Hyper-Lipid Producing Microalgal Strains for Sustainable Biofuel Production. *Bioresour. Technol.* **2011**, *102(1)*, 57-70.

Murakami, H.; Levin, E.; Delworth, T. L.; Gudgel, R.; Hsu P-C. Dominant Effect of Relative Tropical Atlantic Warming on Major Hurricane Occurrence Dominant Effect of Relative Tropical Atlantic Warming on Major Hurricane Occurrence. *Science* **2018**, *16(362), Issue 6416*, 794-799.

Nascimento, I.A.; Marques, S.S.; Cabanelas, I.T.; Pereira, S.A., Druzian, J.I.; Souza, C.D.; Vich, D.V.; Carvalho, G.C.,; Nascimento, M.A. Screening Microalgae Strains for Biodiesel Production: Lipid Productivity and Estimation of Fuel Quality Based on Fatty Acids Profiles as Selective Criteria. *BioEnergy Res.* **2012***, 6*, 1-13.

National Biodiesel Education Program, University of Idaho. https://biodieseleducation.org/index.html **(12/7/2018)**

National Climate Assessment. U.S. Global Change Research Program, **2014**, 1800 G Street, NW, Suite 9100, Washington, D.C. 20006 USA https://nca2014.globalchange.gov/highlights/report-findings/extreme-weather, 9/22/2018

Nicholls, Kenneth H. and Daniel E. Wujek, 2**015**, Ch. 12, Chrysophyceae and Phaeothamniophyceae, in Freshwater Algae of North America Ecology and Classification, Second Edition, Edited by John D. Wehr, Robert G. Sheath, and Patrick Kociolek, c. 2015, Academic Press, Elsevier, Inc. San Diego, CA, Waltham, MA, London, UK and Oxford, UK.

Nixdorf, B.; Mischke, U.; Leßmann, D. Chrysophytes and Chlamydomonads: Pioneer Colonists in Extremely Acidic Mining Lakes (Ph< 3) In Lusatia (Germany). *Hydrobiologia* **1998**, *369*, 315-327.

Nguyen, H. M.; Baudet, M.; Cuiné, S.; Adriano, J-M.; Barthe, D.; Billon, E.; Bruley, C. Proteomic Profiling of Oil Bodies Isolated From the Unicellular Green Microalga *Chlamydomonas reinhardtii*: with Focus on Proteins Involved in Lipid Metabolism. *Proteomics* **2011**, *11(21)*, 4266-4273.

NOAA, National Centers for Environmental Information, National Oceanic and Atmospheric Administration, Global Climate Change Indicators, How do we know humans are the primary cause of the warming?, **9/22/2018** https://www.ncdc.noaa.gov/monitoring-references/faq/indicators.php

Ogunsakin, O. R. **2017**, Thesis, Evaluation of The Fertilization Properties of Algal Biomass and Assessment of KOH-Induced Flocculation of PW95 Algal Cells.

Olaveson, M. M.; Stokes, P. M. Responses of The Acidophilic Alga *Euglena mutabilis* (Euglenophyceae) to Carbon Enrichment at pH 3. J. *Phycol.* **1989**, *25*, 529-539. (Original Reference for MAM).

O'Leary, Stephen, and Berrue, Fabrice, September to November, **2018**, personal communication, National Research Council, Canada, Algal Genomics and Synthetic Biology.

Oram, Brian. The pH of Water, Water Research Center, Education Guide for Private Well Users and City Water Customers, BF Environmental Consultants, Inc., https://www.water-research.net/index.php/ph **(accessed 11/21/2018)**

Ostrom, Jessica, The Characterization of *Chromulina freiburgensis* As a Potential Source for Biomass Fuel: The Effect of Nitrogen And Phosphorus Limitation, Thesis, Interdisciplinary Masters of Science, Montana Tech of The University of Montana, **2012**.

Palenik, B.; Wood, M. A. Molecular Markers of Phytoplankton Physiological Status and Their Application at the Level of Individual Cells. In Molecular Approaches to The Study of The Ocean, First Ed. **1998**, Chapman and Hall, NY, pp 187-205.

Paasche, E. Marine Plankton Algae Grown With Light-Dark Cycles. II. *Ditylum brightwellii* and *Nitzschia turgidula. Physiol. Plant.* **1968,** *21(1)*, 66-77.

Patidar, S. K.; Kim, S-H.; Ho, J.; Jungsoo, K.; Bum, P.; Park, S.; Han, M-S. *Pelagibaca bermudensis* Promotes Biofuel Competence of *Tetraselmis striata* in A Broad Range of Abiotic Stressors: Dynamics of Quorum-Sensing Precursors and Strategic Improvement in Lipid Productivity. *Biotechnol. Biofuels* **2018**, *11*, 102.

Pepper, I. L.; Gerba, C. P.; Gentry, T. J. eds. Environmental Microbiology. Third Ed. Elsevier Inc.: New York, **2014**.

Phillip, Mark **(1999)** MS Thesis, An Investigation of Sulfate Reducing Bacteria Activity in the Berkeley Pit Lake System, Montana Tech of The University of Montana, Butte Montana.

Pienkos, P. T.; Darzins, A. The Promise and Challenges of Microalgal-Derived Biofuels. Biofuels, *Bioprod. Bioref.* **2009**, *3*, 431–440.

Pinzi, S.; Garcia, I. L.; Lopez-Gimenez, F. J.; Luque de Castro, M. D.; Dorado, G.; Dorado, M. P. The Ideal Vegetable Oil-Based Biodiesel Composition: A Review of Social, Economical and Technical Implications. *Energy Fuels* **2009**, *23(5)*, 2325-2341.

Pit Watch, Berkeley Pit News and Info. (website) Berkeley Pit Public Education Committee, Butte-Silver Bow Planning Department, Butte, MThttp://www.pitwatch.org/berkeley-pit-history/ (accessed on **3/21/2019**).

Provasoli, L.; McLaughlin, J. J. A.;Droop, M. R. The Development of Artificial Media for Marine Algae. *Archiv für Mikrobiologie* 1**957**, *25(4)*, 392-428.

PubChem Open Chemistry Database, Nile Red, National Center for Biotechnology Information. PubChem Compound Database; CID=65182, https://pubchem.ncbi.nlm.nih.gov/compound/65182 (accessed **Mar.10, 2019**).

PubChem Open Chemistry Database https://pubchem.ncbi.nlm.nih.gov Thiessen, Kim S, PA, Bolton EE, Chen J, Fu G, Gindulyte A, Han L, He J, He S, Shoemaker BA, Wang J, Yu B, Zhang J, Bryant SH. PubChem Substance and Compound databases. *Nucleic Acids Res.* **2016 Jan 4**; 44(D1):D1202-13. Epub 2015 Sep 22 [PubMed PMID: 26400175] doi: 10.1093/nar/gkv951.

PubChem, Glycerol, National Center for Biotechnology Information. PubChem Compound Database; CID=753, https://pubchem.ncbi.nlm.nih.gov/compound/753 (Accessed **Mar. 14, 2019**).

PubChem Open Chemistry Database, Glyceryl trioleate https://pubchem.ncbi.nlm.nih.gov/compound/Triolein#section=Top (Accessed **3/14/2019**).

Pulz, O.; Gross, W. Valuable Products from Biotechnology of Microalgae. Appl. *Microbiol. Biotechnol.* **2004**, *65(6),* 635-648.

Ramaraj, R.; Unpaprom, Y.; Whangchai, N.; Dussadee, N. Culture of Macroalgae *Spirogyra ellipsospora* for Long-Term Experiments, Stock Maintenance and Biogas Production. *Emergent Life Sciences Research* **2015**, *1(1)*, 38-45.

Rawat, I.; Kumar, R, R.; Mutanda, T.; Bux, F. Dual Role of Microalgae: Phycoremediation of Domestic Wastewater and Biomass Production for Sustainable Biofuels Production. *Appl. Energy* **2011** *88(10)*, 3411-3424.

Richardson, J. W.; Johnson, M. D.; Outlaw, J. L.;. Economic Comparison of Open Pond Raceways to Photo Bio-Reactors for Profitable Production of Algae for Transportation Fuels in the Southwest. *Algal Res.* **2012**, *1(1)*, 93-100.

Roberts D.A.; de Nys, R.; Paul, N, A. The Effect of CO_2 On Algal Growth In Industrial Waste Water for Bioenergy and Bioremediation Applications. *PLoS One*. **2013**, *8(11)*:e81631.
.

Rodolfi L.; Chini Z. G; Bassi, N; Padovan, G; Biondi, N; Bonini, G; Tredic, M.R. Microalgae for oil: strain selection, induction of lipid synthesis and outdoor mass cultivation in a low-cost photobioreactor. *Biotechnol Bioeng.* **2009**, *1*, 100–112.

Roessler, P. G. Effects of Silicon Deficiency on Lipid Composition and Metabolism in the Diatom *Cyclotella cryptica*. *J. Phycol.* 1**988**, *24(3)*, 394-400.

Rose, P. D.; Boshoff, G. A.; Van Hille, r. P.; Wallace, L. C. M.; Dunn, K. M.; Duncan, J. R. An Integrated Algal Sulphate Reducing High Rate Ponding Process for the Treatment of Acid Mine Drainage Wastewaters. *Biodegradation* **1998**, *9(3-4)*, 247-257.

Rouge, M. **(2002)** Counting Cells with a Hemacytometer, Collection and Evaluation of Semen, Pathophysiology of the Reproductive System, Hypertexts for Biomedical Sciences, Colorado State University. http://www.vivo.colostate.edu/hbooks/pathphys/reprod/semeneval/hemacytometer.html

Salih, F. M. Microalgae Tolerance to High Concentrations of Carbon Dioxide: A Review. *J. Environ. Prot.* **2011**, *2(5)*, 648.

Salisbury, F. B.; Ross, C.W. Plant Physiology. 4th. Ed.. Wadsworth Belmont, CA, **1992**: 23-52.

Samek, O.; Pilát, A. J. Z.; Zemánek, P.; Nedbal, L.; Tříska, J.; Kotas, P.; Trtílek, M.. Raman Microspectroscopy of Individual Algal Cells: Sensing Unsaturation of Storage Lipids *In Vivo*. *Sensors* **2010**, *10(9)*, 8635-8651.

Samenow, J. Study: Warming ocean waters intensified devastating **2017** Atlantic Hurricane Season Washington Post 09/27/2018.

Sandgren, C. D. Chrysophyte Reproduction and Resting Cysts: A Paleolimnologist's Primer. *J. of Paleolimnology* **1991**, *5(1)*, 1-9.

Sandia National Laboratories **August 21, 2015**, Algae Nutrient Recycling is a Triple Win.http://www.labmanager.com/news/2015/08/algae-nutrient-recycling-is-a-triple-win#.WwXmrS-ZOu4 (Accessed 05/23/2018).

Sharma, K. K.; Schuhmann, H.; Schenk, P. M.. High Lipid Induction in Microalgae for Biodiesel Production. *Energies* **2012**, *5(5)*, 1532-1553.

Sheehan J. D.; T, Benemann, J. R.; Roessler, P. **1998**. A Look Back at the U.S. Department of Energy's Aquatic Species Program: Biodiesel from Algae. Closeout Report. National Renewable Energy Lab, Department of Energy, Golden, CO, USA. Report NREL/TP-580-24190.

Shamzi M.; Mohd, L. Z. W.; Arbakariya, B. A. Heterotrophic Cultivation of Microalgae for Production of Biodiesel. *Recent Pat. Biotechnol.* **2011**, *5(2)*, 95-107.

Sims, B. (**25 October 2011**). Clearing The Way For Byproduct Quality: Why Quality for Glycerin is Just as Important for Biodiesel. Biodiesel Magazine.

Scheuhammer, A. M.; Meyer, M. W.; Sandheinrich, M. B.; Murray, M. W. Effects of Environmental Methylmercury on the Health of Wild Birds, Mammals, and Fish. *AMBIO: a Journal of the Human Environment* **2007**, *36(1)*, 12-19.

Schneider, C. A.; Rasband, W. S.; Eliceiri, K. W. NIH Image to ImageJ: 25 Years of Image Analysis. *Nat. Methods* **2012**, *9*, 671-675.

Shuba, E. S.; Kifle, D. Microalgae to Biofuels:'Promising'alternative and Renewable Energy, Review. *Renewable Sustainable Energy Rev.* **2018**, *81*,743-755.

Silva, H. J.; Pirt, J. Carbon Dioxide Inhibition of Photosynthetic Growth of *Chlorella*. *Microbiology* **1984**, *130(11)*, 2833-2838.

Starkey, R. L.; De, P. K. A New Species of Azotobacter. *Soil Sci.* **1939**, *47(4)*, 344-346.

Stein, Janet R. (Editor) Handbook of Phycological Methods Culture Methods & Growth Measurements, Cambridge University Press: London, **1979**.

Stephens, E.; Ross, I. L.; Mussgnug, J. H.; Wagner, L. D.; Borowitzka, M. A.; Posten, C.; Kruse, O.; Hankamer, B. Future Prospects of Microalgal Biofuel Production Systems. Trends *Plant Sci.* **2010**, *15(10)*, 554-564.

Stierle, A. A.; Stierle, D. B.; Mitman, G. G.; Snyder, S.; Antczak, C.; Djaballah, H. Phomopsolides And Related Compounds From The Alga-Associated Fungus, *Penicillium clavigerum*. *Nat. Prod. Commun*. **2014**, *9(1)*, 87-90.

Stierle, A. A.; Stierle, D. B. Bioprospecting in The Berkeley Pit: Bio Active Metabolites from Acid Mine Waste Extremophiles. In Studies in natural products chemistry, vol. 32, pp. 1123-1175. Elsevier: New York, **2005**.

Stierle, A. A.; Stierle, D. B. Bioactive Secondary Metabolites from Acid Mine Waste Extremophiles. *Nat. Prod. Commun.* **2014**, *9(7)*, 1934578X1400900738.

Stockenreiter, M.; Graber, A-K. Haupt, F.; Stibor, H. The Effect of Species Diversity on Lipid Production by Micro-Algal Communities. *J. Appl. Phycol.* **2012**, *24(1)*, 45-54.

Stoker, H. Stephen, Organic and Biological Chemistry, 6th Ed. Brooks/Cole Cengage Learning: New York, **2013**.

Stumm, W.; Morgan, J. J. Aquatic Chemistry: Chemical Equilibria and Rates in Natural Waters. Vol. 1022, Wiley, New York, **1996**.

Sunda, W. G.; Price, N. M. and Morel, F.M. Trace Metal Ion Buffers And Their Use In Culture Studies. In Andersen, Robert A. Algal Culturing Techniques, Elsevier Academic Press: Burlington, MA, 2005, pp 35-63, **2005**.

Sustainable Biodiesel Alliance, Biodiesel FAQ, http://test.sustainablebiodieselalliance.com/SBA/?page_id=169 (accessed **Oct 9, 2016**).

Takagi, M.; Watanabe, K.; Yamaberi, K.; Yoshida, T. Limited Feeding of Potassium Nitrate for Intracellular Lipid and Triglyceride Accumulation of *Nannochloris* sp. UTEX LB1999. *Appl. Microbiol. Biotechnol.* **2000**, *54(1)*, 112-117.

Tao, Y.; Yuan, Z.; Xiaona, H.; Wei, M. Distribution and Bioaccumulation of Heavy Metals in Aquatic Organisms of Different Trophic Levels and Potential Health Risk Assessment from Taihu Lake, China. *Ecotoxicol. Environ. Saf*. **2012**, **81**, 55-64.

Talling, J. F. The depletion of carbon dioxide from lake water by phytoplankton. *J. Ecol.* **1976**, 79-121.

Tchounwou, P. B.; Yedjou, C, G.; Patlolla, A. K.; Sutton D. J. Heavy Metal Toxicity and the Environment. In Molecular, clinical and environmental toxicology,. Springer: Basel, pp. 133-164, **2012**.

Thienemann, A. Die Binnengewässer, Band XVI, Teil 2, 1. Halfte, Das Phytoplankton des Süsswassers. Stuttgart, (p. 33-35). (Contains chapter by Huber-Pestalozzi, Gottfried. Das Phytoplankton des Süsswassers Systematik und Biologie: Chrysophyceen; Farblose Flagellaten; Heterokonten), **1976**.

Thiessen, K. S; Bolton, P. A.; Chen, J.; Fu, G.; Gindulyte, A.; Han, L.; He, J.; He, S.; Shoemaker, B. A.; Wang, J.; Yu, B.; Zhang, J.; Bryant, S. H. PubChem Substance and Compound databases. Nucleic Acids Res. **2016 Jan 4**; 44(D1):D1202-13. Epub 2015 Sep 22 [PubMed PMID: 26400175] doi: 10.1093/nar/gkv951.
PubChem Open Chemistry Database, https://pubchem.ncbi.nlm.nih.gov

Tucci, N. J. Mine Waste Technology Program Activity IV, Project 30 Final Report–Algal Bioremediation of the Berkeley Pit Lake System: An In Situ Test Using Limnocorrals. EPA/DOE Government Documents, **2005**.

Ullah, A.; Heng, S.; , M.; Munis, H.; Fahad, S.; Yang. X. Phytoremediation of Heavy Metals Assisted by Plant Growth Promoting (PGP) Bacteria: A Review. *Environ. Exp. Bot.* **2015**, *117*, 28-40.

University of Idaho, Biodiesel Short Course, http://web.cals.uidaho.edu/biodiesel/biodiesel-shortcourse-history/ (accessed **Oct 2016**).

University of Michigan, Center for Sustainable Systems, Biofuels Factsheet (**2018**). http://css.umich.edu/factsheets/biofuels-factsheet (accessed 3/14/2019)

US Department of Energy, Energy.gov - Researchers Strive to Reduce Cost and Time of Algal Biofuel Production **2017**. https://www.energy.gov/eere/bioenergy/articles/researchers-strive-reduce-cost-and-time-algal-biofuel-production.

US Department of Energy, USDE alternative Fuels Data Center, https://www.afdc.energy.gov/vehicles/diesels_emissions.html (Accessed **November 9, 2017**).

U.S. Department of Energy, USDE alternative Fuels Data Center Glossary. (https://afdc.energy.gov/glossary.html)**11/30/2018**

U.S. Department of Energy, USDE biodiesel handling use guide DOE/GO-102016-4875 **November 2016**
(afdc.energy.gov/uploads/publication/biodiesel_handling_use_guide.pdf)

US Department of Energy, Office of Energy Efficiency and Renewable Energy, http://www.energy.gov/eere/bioenergy/algal-biofuels (accessed **Nov 11, 2016).**

U. S. Energy Information Administration (USEIA) Monthly Biodiesel Production Report - Energy Information Administration. https://www.eia.gov/biofuels/biodiesel/production/ (accessed **9/24/18**)

U. S. Energy Information Administration (USEIA), Monthly Biodiesel Production Report With data for **June 2018**, https://www.eia.gov/biofuels/biodiesel/production/archive/2018/2018_06/biodiesel.php (accessed 9/24/18).

U. S. Environmental Protection Agency (USEPA) A Comprehensive Analysis of Biodiesel Impacts on Exhaust Emissions.pdf.
A Comprehensive Analysis of Biodiesel Impacts on Exhaust Emissions - Draft Technical Report (EPA-420-P-02-001, **October 2002**)2012-09-12
https://archive.epa.gov/ncea/biofuels/web/pdf/p02001.pdf 11/19/2018

USEPA National Recommended Water Quality Criteria EPA -**2004**.
https://www.epa.gov/quality/national-recommended-water-quality-criteria-2004, 11/19/2018

U.S. Geological Survey (USGS), Phosphate Rock, Mineral Commodity Summaries, January **2017**.

USGS, **2018** U.S. Geological Survey, Water Science School, https://water.usgs.gov/edu/ph.html, accessed on 11/21/2018

USGS, The National Map, U.S. Department of the Interior, U.S. Geological Survey, https://viewer.nationalmap.gov (Yankee Doodle Creek, Butte Montana, https://viewer.nationalmap.gov/advanced-viewer/viewer/index.html?marker=-112.5022437,46.0446491&level=13) Accessed on **1/16/2019**

Van Den Hende, S., Vervaeren, H., Desmet, S., & Boon, N. Bioflocculation of microalgae and bacteria combined with flue gas to improve sewage treatment. *New Biotechnology.* **2011**, *29(1)*, 23-31.

Varshney, P.; Sohoni, S.; Wangikar, P. P.; Beardall, J. Effect of High CO_2 Concentrations on the Growth and Macromolecular Composition of a Heat-And High-Light-Tolerant Microalga. *J. Appl. Phycol.* **2016**, *28(5)*, 2631-2640.

Vechtel, B.; Eichenberger, W.; Ruppel, G. Lipid Codies in *Eremosphaera viridis* De Bary (Chlorophyceae). *Plant Cell Physiol.* **1992**, *33(1)*, 41-48.

Wang, Z. T.; Ullrich, N.; Joo, S.; Waffenschmidt, S.; Goodenough, U. Algal Lipid Bodies: Stress Induction, Purification, and Biochemical Characterization in Wild-Type and Starchless *Chlamydomonas reinhardtii*. *Eukaryotic Cell* **2009**, *8(12)*, 1856-1868.

Wang, T.; Tian, X.; Liu, T.; Wang, Z.; Guan, W.; Guo, M.; Chu, J.; Zhuang, Y. Enhancement of Lipid Productivity with a Novel Two-Stage Heterotrophic Fed-Batch Culture of *Chlorella protothecoides* and a Trial of CO_2 Recycling by Coupling with Autotrophic Process. *Biomass Bioenergy* **2016**, *95*, 235-243.

Wang, H.; Xiong, H.; Hui, Z.; Zeng, X. Mixotrophic Cultivation of *Chlorella pyrenoidosa* with Diluted Primary Piggery Wastewater to Produce Lipids. *Bioresour. Technol.* **2012**, *104*, 215-220.

Wang, H. K.;, Wood, J. M. Bioaccumulation of Nickel by Algae. *Environ. Sci. Technol.* **1984**, *18(2)*, 106-109.

Wehr, John, D. Robert G. Sheath, and Patrick Kociolek, editors, Freshwater Algae of North America Ecology and Classification, Second Edition, c. **2015**, Academic Press, Elsevier, Inc. San Diego, CA, Waltham, MA, London, UK and Oxford, UK.

Wehr, John D., Robert G. Sheath, and J. Patrick Kociolek, eds. **(2015)**. Freshwater algae of North America: ecology and classification. Academic Press, Elsevier, London, (p. 546-553).

Werner, Dietrich (editor and chapter author) **1977**, The Biology of Diatoms, Botanical Monographs Vol. 13, University of California Press, Ch. 4, Silicate Metabolism

Wurts, William A., and Robert M. Durborow. Interactions of pH, carbon dioxide, alkalinity and hardness in fish ponds. **(1992)**: 1-3. https://agrilifecdn.tamu.edu/fisheries/files/2013/09/SRAC-Publication-No.-464-Interactions-of-pH-Carbon-Dioxide-Alkalinity-and-Hardness-in-Fish-Ponds.pdf

Wilde, E. W.; Benemann, J. R.. Bioremoval of Heavy Metals by the Use of Microalgae. *Biotechnology Advances* **1993**, *4*, 781-812.

Wikipedia - https://en.wikipedia.org/wiki/Glycerol#Applications accessed **05/25/2018**.

Wong, Y-S.; Tam, N. F. Y. Editors, Wastewater Treatment with Algae. Springer-Verlag: Berlin, **1998**.

Woertz, I.; Feffer, A.; Lundquist, T.; Nelson, Y. Algae Grown on Dairy and Municipal Wastewater for Simultaneous Nutrient Removal and Lipid Production for Biofuel Feedstock. *Journal of Environmental Engineering (J. Environ. Sci.)* **2009**, *135(11).*

Wood, M. A.; Everroad, R. C.; Wingard, L. M. Measuring Growth Rates in Microalgal Cultures, Ch. 18, Algal Culturing Techniques, Elsevier Academic Press, **2005**.

Wrede, **2014** Co-Cultivation of Fungal and Microalgal Cells as an Efficient System for Harvesting Microalgal Cells, Lipid Production and Wastewater Treatment. https://journals.plos.org/plosone/article?id=10.1371/journal.pone.0113497

Yadav, G.; Sen, R. Microalgal Green Refinery Concept for Biosequestration Of Carbon-Dioxide Vis-À-Vis Wastewater Remediation aBioenergy Production: Recent Technological Advances In Climate Research. *J. of CO_2 Utilization* **2017**, *17*, 188-206.

Yen, H-W.; Hu, I-C.; Chen, C-Y.; Ho, S-H.; Lee, D.-J.; Chang, J-S. Microalgae-Based Biorefinery–from Biofuels to Natural Products. *Bioresour. Technol*. **2013**, *135*, 166-174.

Yoon, K.; Han, D.; Li, Y.; Sommerfeld, M.; Hu, Q. Phospholipid: Diacylglycerol Acyltransferase is a Multifunctional Enzyme Involved in Membrane Lipid Turnover and Degradation While Synthesizing Triacylglycerol in the Unicellular Green Microalga *Chlamydomonas reinhardtii. The Plant Cell* **2012**, 112.

Yue, L.; Chen, W. Isolation and Determination of Cultural Characteristics of a New Highly CO_2 Tolerant Fresh Water Microalgae. Energy Convers. *Manage.* **2005**, *46(11-12)*, 1868-1 876.

Zienkiewicz, K.; Du, Z-Y.; Vollheyde, W. M. K. Benning, C. Stress-Induced Neutral Lipid Biosynthesis in Microalgae—Molecular, Cellular and Physiological Insights. *Biochimica et Biophysica Acta (BBA)-Molecular and Cell Biology of Lipids* **2016**, *1861(9),* 1269-1281.

Zhang, J.; Hu, B. A Novel Method to Harvest Microalgae Via Co-Culture Of Filamentous Fungi to Form Cell Pellets. *Bioresour. Technol.* **2012**, *114*, 529-535.

Zhou, W.; Min, M.; Hu, B.; Ma, X.; Liu, Y.; Wang, Q.; Shi, J.; Chen, P.; Ruan, R. Filamentous Fungi Assisted Bio-Flocculation- A Novel Alternative Technique For Harvesting Heterotrophic And Autotrophic Microalgal Cells. *Sep. Purif. Technol.* **2013**,*107*, 158-165.

Zhou, W.; Cheng, Y.; Li, Y.; Wan, Y.; Liu,Y.; Lin, X; Rua, R. Novel Fungal Pelletization-Assisted Technology for Algae Harvesting and Wastewater Treatment. *Appl. Biochem. Biotechnol*. **2012**, *167(2)*, 214-28.,

Zhu, L.; Zhongming W.; Takala, J.; Hiltunen, E.; Qin, L.; Xu, Z,; Qin, X.; Yuan, Z. Scale-Up Potential of Cultivating *Chlorella zofingiensis* In Piggery Wastewater for Biodiesel Production. *Bioresour. Technol.* **2013**, *137*, 318-325.

Zhu, L.; Wang, Z.; Shu, Q.; Takala, J.; Hiltunen, E.; Feng, P.; Yuan, Z. Nutrient Removal and Biodiesel Production by Integration of Freshwater Algae Cultivation with Piggery Wastewater Treatment. *Water Res.* **2013**, *47(13)*, 4294-4302.

8. Appendix A: Technical Note - Error in Cell Counting, Celeromics, 2015

A publication that provided brief, concise explanations of common sources of counting error that are associated with hemacytometer/counting chamber visual cell counting methods is no longer available online. The company that had provided online life sciences tools, including the following publication, no longer maintains a website under the name, “Celeromics”. Procedures that were recommended in the Celeromics (2015) publication to reduce counting error were followed to improve the accuracy of cell counts, and they may be of interest to readers who use similar counting methods. A copy of this publication is included on the following pages.

Most common errors in cell counting.

Most significative errors.

ERROR IN OBTAINING THE SAMPLE

"The sample is not the population"

Usually, a small quantity is extracted from the original sample in order to carry out the counting. This sample will have a different concentration than the original one. Once this is done, the content is pipetted into the counting chamber

How to reduce this error?

In order to reduce this error it is convenient to shake the sample with a shaker, and extract the necessary quantity to carry out the cell counting as soon as possible.
Likewise, a pipette can be used to shake the sample, pipetting repeatedly into the recipient where the sample is taken from.

ERROR IN LOADING THE NEUBAUER CHAMBER

It is common to load the Neubauer chamber with a quantity slightly greater or smaller than 10 microliters. When the quantity is greater than 10 microliters, the coverglass will slightly rise in order to allocate the overload. When the quantity is smaller than 10 microliters, the chamber will not hold enough quantity, leading to an error.

Our estimation is that this error moves around 3-5%

How to reduce this error?

1) Being careful when introducing the simple in the chamber not to overload it.
2) Some technicians slightly heat up the coverglass with their breath, before putting it on the counting chamber. Later, they observe that some multicolor rings have been created around the surface of the coverglass, indicating that it has been attached properly.
3) Keeping the micro-pipettes perfectly calibrated.

STATISTICAL ERROR

This error is encountered when trying to approximate a population (original sample) to a sample from that population that is too small.

Most of lab-technicians use 4 or 5 grids of the counting chamber, regardless the concentration.

This error moves around 20-30%

How to reduce this error?

1) In order to reduce this error, the size of the sample should be taken into account when calculating the concentration and the number of samples used.

For a culture of 100ml with a Neubauer Chamber:

Concentration	Number of Samples (1)	Maximum Error Range (confidence. 95%)	Maximum Error Range (confidence. 90%)
1.0 x 10^6 cel/ml	1	43,10%	36,19%
1.0 x 10^6 cel/ml	2	30,49%	25,59%
1.0 x 10^6 cel/ml	3	24,89%	20,59%
1.0 x 10^6 cel/ml	4	21,56%	18,09%

NOTE: The estimation of the error has been carried out presuming a confidence interval for variance of 22% for the samples

(1) A sample is considered when 5 grids of the Neubauer chamber have been counted.

1) As a general rule, some laboratories count 80 or 100 cells, regardless the concentration. This sometimes implies loading some counting chambers to calculate a concentration, if this is very small.

ERROR IN THE ALLOCATION OF THE CELLS AROUND THE NEUBAUER CHAMBER.

Occasionally, the sample does not distribute equally around the counting chamber, due to its inclination or manipulation

How to reduce this error?

1) Shake the sample before introducing it into the counting chamber.

2) Make sure that the counting chamber lies completely flat when introducing the sample

HUMAN ERRORS

There are various types of errors that are made by the person who carries out the cell counting, directly or indirectly.

- Bad visualization of the sample: if the person who carries out the cell counting does not visualize the sample properly, some of the cells may be left out. Moreover, other elements might be taken for cells, when they are not.

  How to reduce this error?: using an optimal microscope in good state. Carrying out the manipulation of the microscope properly and using the appropriate optic for the size of the cells.

- To lose count: if the person who carries out the cell counting loses count, he/she should start again.

  How to reduce this error?: using an automated counter. It is also important that the person who carries out the cell counting is always the same.

- Error when applying the formula: if the *counting* formula is applied in the wrong way, wrong results will be obtained. This is one of the main sources of confusion and error when carrying out the cell counting.

  How to reduce this error? Using an automated counter and the same counting chamber. Check the size of the chamber and make sure that the formula applied makes sense.

- Error in counting the borders: it occurs when the person who carries out the cell counting can't tell whether a cell is in or out of the counting. It is estimated that this error is smaller than 1%.

  How to reduce this error? Using an automated cell counter. Using a clear criteria when selecting the borders

ERROR IN DILUTION

Any error made when using the liquids to carry out the dilution will translate into an error made in the diluted sample.

How to reduce this error?: to calibrate periodically the pipettes and other measurement instruments.

ERROR IN CULTURING DEAD AND APOPTOTIC CELLS

When culturing cells, it is necessary to know the percentage of dead and alive cells (viability). If we only count the total amount, we will be making an error proportional to the viability of the sample. Only alive cells will grow.

How to reduce this error? to calculate manually or automatically the viability.

ERROR WHEN COUNTING DUE TO AGGREGATES

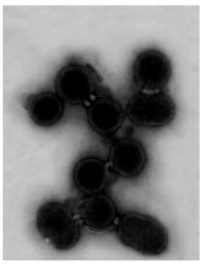

Under certain circumstances, some types of cells tend to aggregate, making it harder or even impossible to count.

Flow Cytometers are especially problematic when dealing with aggregates, since a group of various cells will be counted as one single cell.

This error moves around 20-30%.

How to reduce this error? to make sure that the simple in good conditions. Carry out the counting immediately after loading the counting chamber.

REFERENCES

[1] A SIMPLIFIED METHOD OF PHYTOPLANKTON COUNTING, Eva Willen. Br. Phycol. J. 11:235-278, September 1976.

9. Appendix B: Table of Dry Weight Biomass Yields

Sample Date	Day	Treatment No.		GC-MS	Fluorescence?	Volume Freeze Dried (mL)	Dry Weight (g)	Dry wt. per L (g/L)	Drying Time (Hrs)	Notes/ Conditions
7/18/17	6	1	EI	CI	OK	350.0	0.476	1.360	92.00	
7/18/17	6	2	EI	CI	Re-Done	344.8	0.297	0.861	64.00	
7/18/17	6	3	EI	CI	OK	349.2	0.413	1.183	92.00	
7/18/17	6	4	EI	CI	OK	349.0	0.278	0.797	98.75	
7/18/17	6	5	EI	CI	OK	348.2	0.285	0.818	69.75	
7/18/17	6	6	EI	CI	OK	348.2	0.302	0.302	73.83	
7/20/17	8	1			OK	345.8	0.516	1.492	74.25	
7/20/17	8	2			OK	345.8	0.362	1.047	74.25	
7/20/17	8	3			OK	345.8	0.489	0.940	70.33	
7/20/17	8	4			OK	345.8	0.325	1.414	70.33	
7/20/17	8	5			OK	345.8	0.313	0.940	67.50	
7/20/17	8	6			Lost/spilled	0.0	0.000	0.000	0.00	Lost/spilled
7/21/17	9	1	EI		OK	395.8	0.626	1.582	75.33	
7/21/17	9	2	EI		Re-Done	390.8	0.398	1.018	68.25	
7/21/17	9	3	EI		OK	395.8	0.538	1.359	71.00	
7/21/17	9	4	EI		Re-Done	390.8	0.377	0.965	93.50	
7/21/17	9	5	EI		OK	395.8	0.337	0.851	71.00	
7/21/17	9	6	EI		OK	395.8	0.381	0.963	75.00	
7/24/17	12	1			OK	391.1	0.617	1.578	75.00	
7/24/17	12	2			Re-Done	391.1	0.419	1.071	68.75	Power Outage
7/24/17	12	3			OK	391.1	0.459	1.174	118.00	Power Outage
7/24/17	12	4			Re-Done	391.1	0.387	0.990	68.75	Power Outage
7/24/17	12	5			Re-Done	391.1	0.416	1.064	72.08	
7/24/17	12	6			Re-Done	391.1	0.454	1.161	93.50	
7/27/17	15	1			OK	345.3	0.450	1.303	118.00	Power Outage
7/27/17	15	2			OK	345.3	0.405	1.173	76.00	
7/27/17	15	3			Re-Done	345.3	0.539	1.561	74.42	
7/27/17	15	4			OK	345.3	0.327	0.947	96.00	
7/27/17	15	5	EI		OK	345.3	0.405	1.173	95.25	
7/27/17	15	6			Re-Done	345.3	0.425	1.231	93.17	
7/31/17	19	1	EI		OK	396.0	0.696	1.758	96.50	
7/31/17	19	2	EI		OK	396.0	0.540	1.364	96.50	
7/31/17	19	3	EI		OK	396.0	0.675	1.705	75.60	
7/31/17	19	4	EI		OK	396.0	0.427	1.078	94.68	
7/31/17	19	5	EI		OK	396.0	0.478	1.207	72.75	
7/31/17	19	6	EI		OK	396.0	0.540	1.364	92.92	
8/4/17	23	1			OK	391.8	0.715	1.825	95.25	
8/4/17	23	2			OK	391.8	0.579	1.478	67.67	
8/4/17	23	3			OK	391.8	0.621	1.585	75.25	
8/4/17	23	4			OK	391.8	0.530	1.353	67.67	
8/4/17	23	5			OK	391.8	0.540	1.378	73.17	
8/4/17	23	6			OK	391.8	0.597	1.524	73.17	

Sample Date	Day	Treatment No.	GC-MS		Fluorescence?	Volume Freeze Dried (mL)	Dry Weight (g)	Dry wt. per L (g/L)	Drying Time (Hrs)	Notes/ Conditions
8/8/17	27	1	EI	CI	OK	396.0	0.790	1.995	91.75	
8/8/17	27	2	EI	CI	OK	396.0	0.575	1.452	91.75	
8/8/17	27	3	EI	CI	OK	396.0	0.705	1.780	77.58	
8/8/17	27	4	EI		OK	396.0	0.527	1.331	96.33	
8/8/17	27	5	EI		OK	396.0	0.576	1.455	91.42	Dryer malfunction
8/8/17	27	6	EI		OK	396.0	0.608	1.535	76.25	Dryer malfunction
8/15/17	34	1			OK	396.0	0.842	2.126	78.67	CNRC analyzed
8/15/17	34	2			OK	396.0	0.593	1.497	78.67	CNRC analyzed
8/15/17	34	3			OK	396.0	0.825	2.083	94.84	CNRC analyzed
8/15/17	34	4			OK	396.0	0.487	1.230	98.59	CNRC analyzed
8/15/17	34	5			OK	396.0	0.585	1.477	66.25	CNRC analyzed
8/15/17	34	6			OK	396.0	0.586	1.480	94.50	CNRC analyzed
9/2/17	52	1	EI		OK	450.0	1.010	2.244	73.83	
9/2/17	52	2	EI		OK	450.0	0.582	1.293	69.50	
9/2/17	52	3	EI		OK	450.0	0.854	1.898	51.00	
9/2/17	52	4	EI		OK	450.0	0.657	1.460	69.50	
9/2/17	52	5	EI		OK	450.0	0.657	1.460	94.50	
9/2/17	52	6	EI		OK	450.0	0.570	1.267	74.75	

10. Appendix C: Monitoring pH in Experimental Treatments

The pH decreased slightly in three experimental treatments. The cause of the decrease is not known. Because the change in pH is not far outside of the estimated error in pH measurements (± 0.05), it is possible that it is not significant.

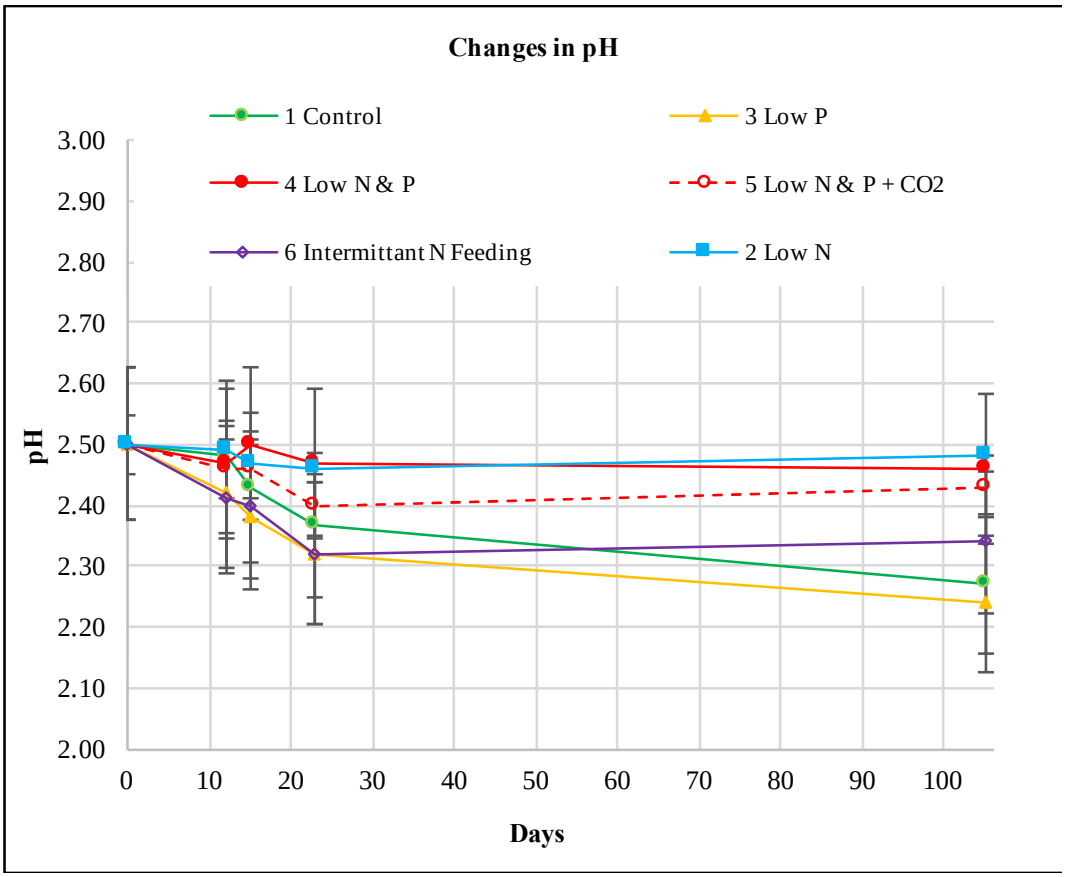

		pH Measurements					
Date	Sample Days	1. Control	2. Low N	3. Low P	4. Low N & P	5. Low N & P + CO_2	6. N Feeding
7/12/17	0	2.50	2.50	2.50	2.50	2.50	2.50
7/24/17	12	2.48	2.49	2.42	2.47	2.46	2.41
7/27/17	15	2.43	2.47	2.38	2.50	2.46	2.40
8/4/17	23	2.37	2.46	2.32	2.47	2.40	2.32
10/25/17	105	2.27	2.48	2.24	2.46	2.43	2.34

11. Appendix D: Nile Red Fluorescence Lipid Calculations

11.1. Example Excel Charts: Fluorescence Results for Triolein Standards and Algal Samples

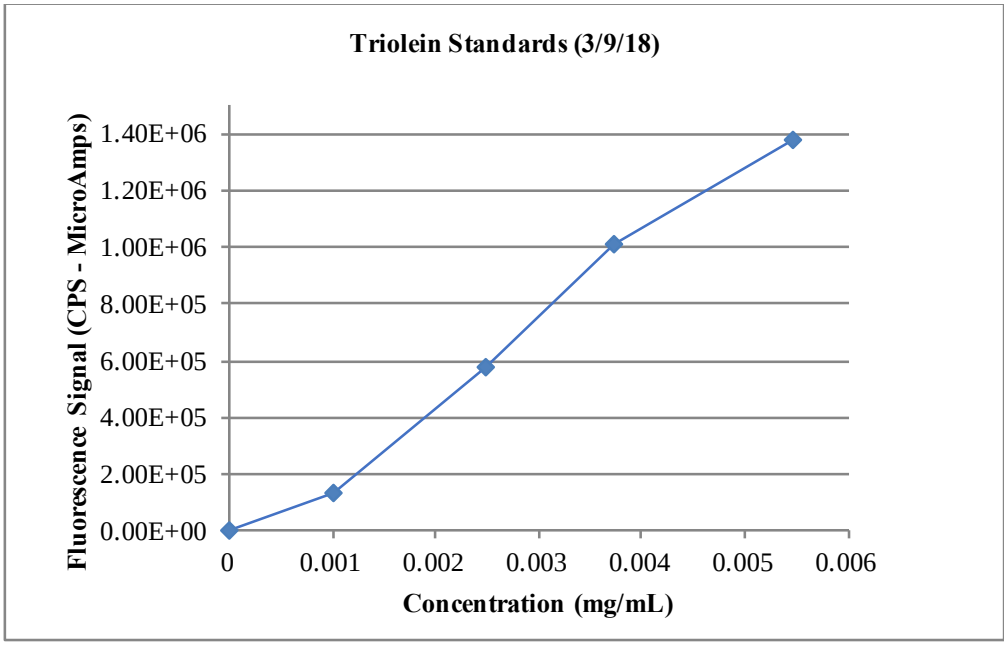

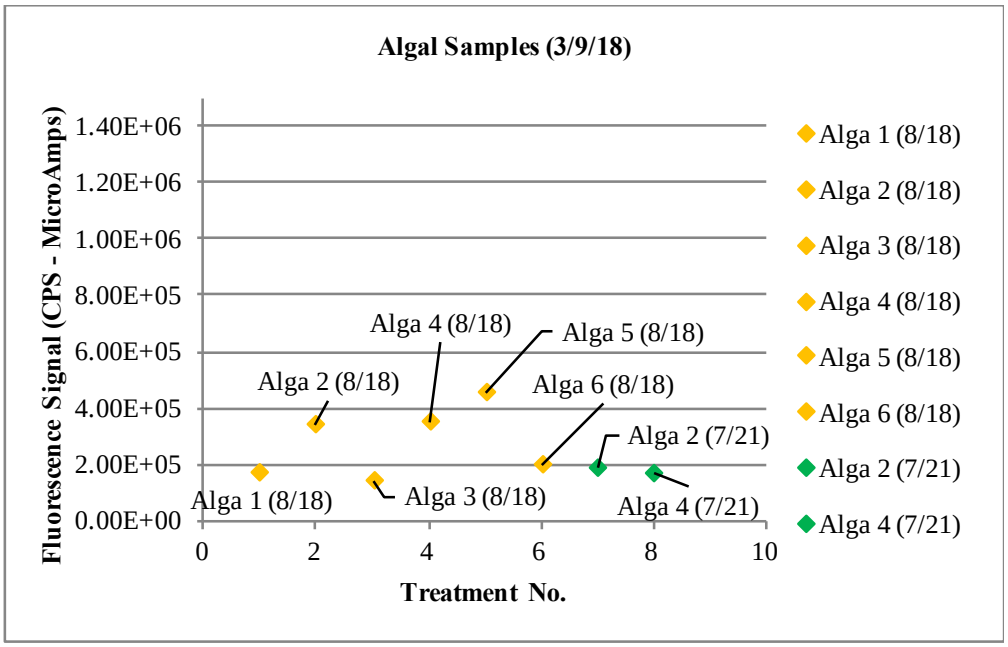

Example Excel Charts: Fluorescence results for triolein standards and algal samples from July 21 and August 18, 2017, that were re-run on March 3rd, 2018.

11.2. Example: Nile Red Fluorescence Data from March 3rd, 2018

Sample Date		Samples	Std. Conc. (mg/mL)	Fin. Conc. (mg/mL)	CPS - MicroAmps	Signal - Blank
3/9/18	Sample 2	Blank	0.000	0.000000	31302.19	0.00E+00
3/9/18	Sample 3	Trio 0.10	0.100	0.000999	167708.86	1.36E+05
3/9/18	Sample 4	Trio 0.25	0.250	0.002494	610582.19	5.79E+05
3/9/18	Sample 5	Trio 0.375	0.375	0.003736	1039540.00	1.01E+06
3/9/18	Sample 6	Trio 0.55	0.550	0.005470	1407230.00	1.38E+06
8/8/17	Sample 7	Alga 1 (8/18)	8/8/17		196448.85	1.65E+05
8/8/17	Sample 8	Alga 2 (8/18)	8/8/17		372742.19	3.41E+05
8/8/17	Sample 9	Alga 3 (8/18)	8/8/17		173068.85	1.42E+05
8/8/17	Sample 10	Alga 4 (8/18)	8/8/17		378845.52	3.48E+05
8/8/17	Sample 11	Alga 5 (8/18)	8/8/17		481018.86	4.50E+05
8/8/17	Sample 16	Alga 6 (8/18)	8/8/17		226015.52	1.95E+05
7/21/17	Sample 13	Alga 2 (7/21)	7/21/17		221105.52	1.90E+05
7/21/17	Sample 14	Alga 4 (7/21)	7/21/17		194655.52	1.63E+05

Line Equation 5 (3/9/18)	Min.	Max.
	1.36E+05	1.38E+06

11.3. Nile Red Fluorescence Calibration Curves

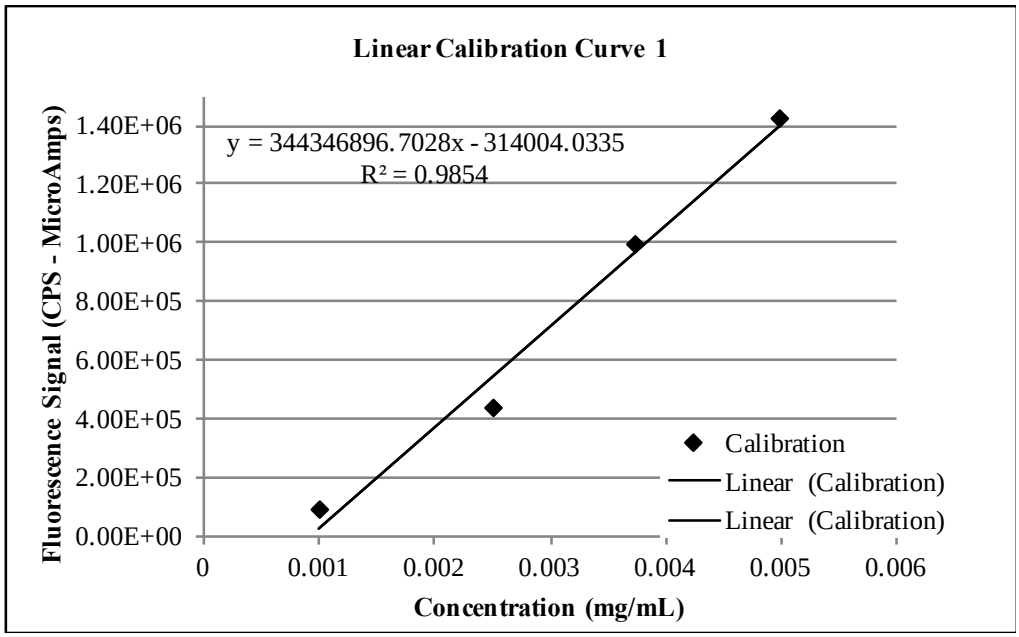

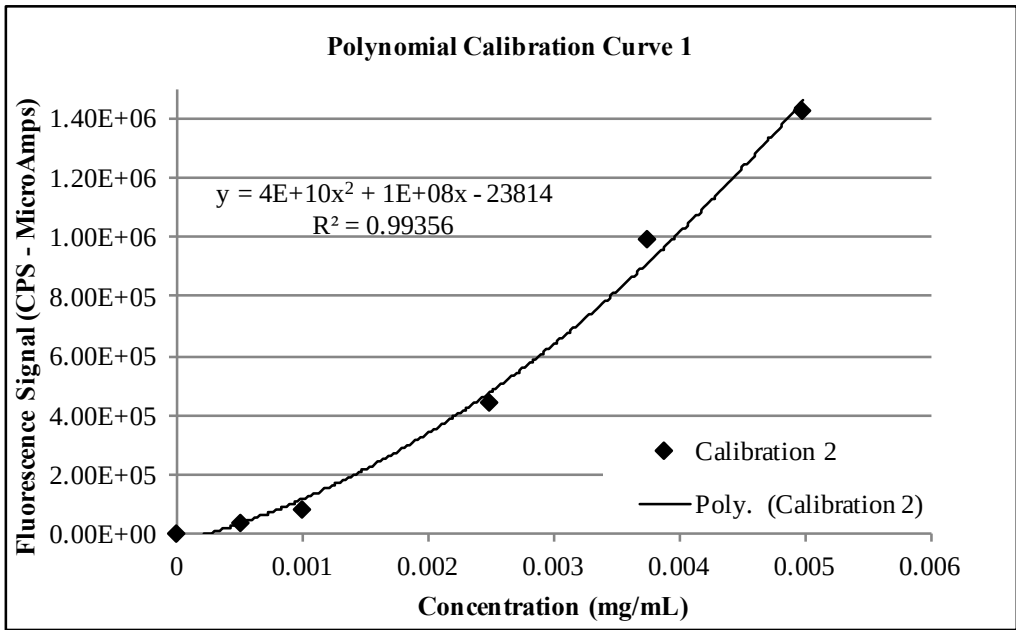

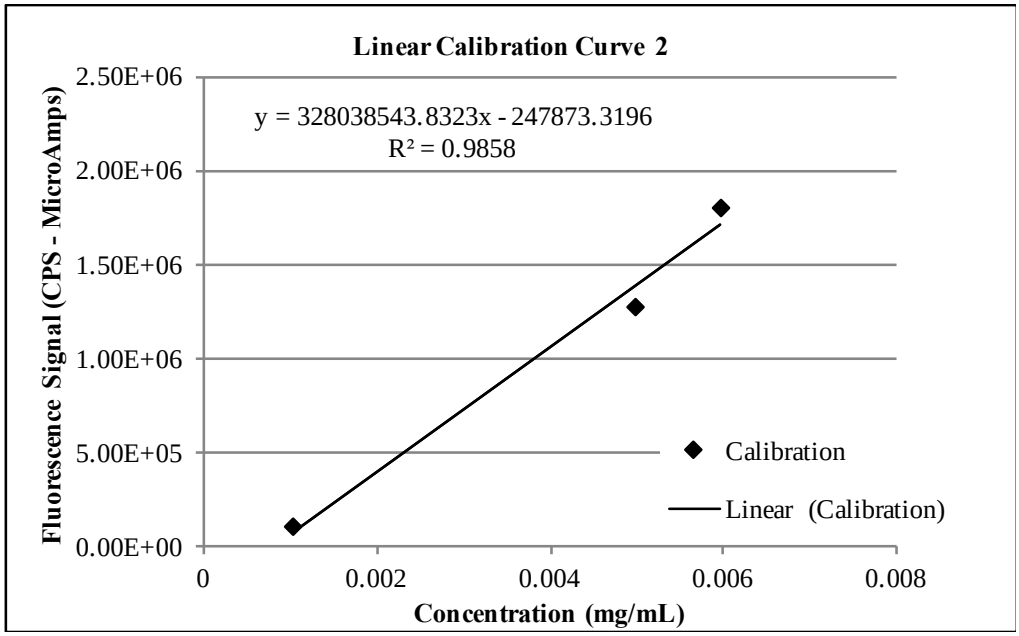
Linear Calibration Curve 2
y = 328038543.8323x - 247873.3196
R² = 0.9858
Fluorescence Signal (CPS - MicroAmps)
2.50E+06
2.00E+06
1.50E+06
1.00E+06
5.00E+05
0.00E+00
0
0.002
0.004
0.006
0.008
Concentration (mg/mL)
Calibration
Linear (Calibration)

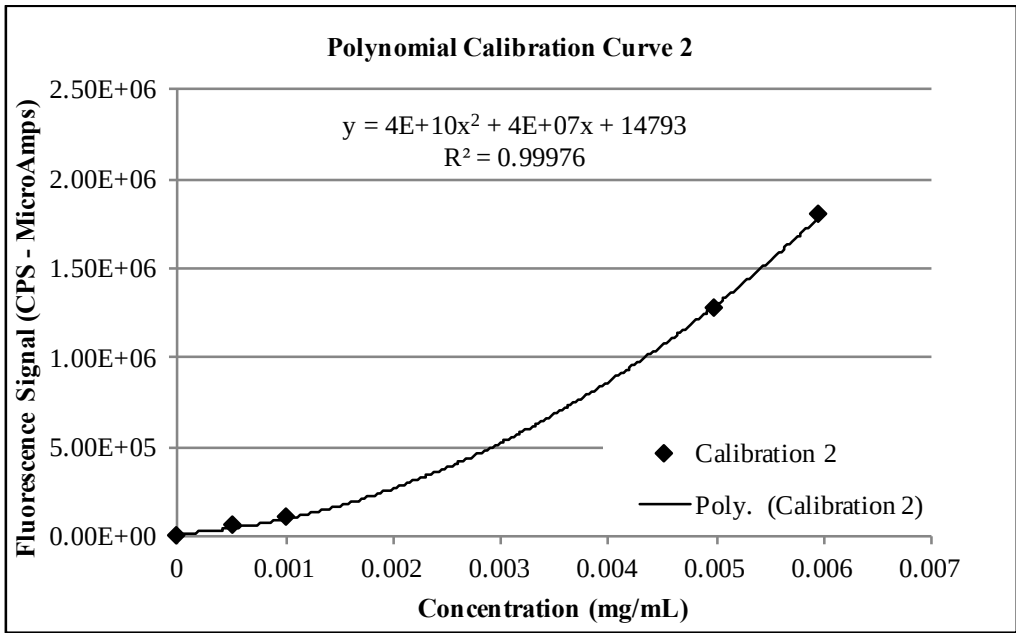
Polynomial Calibration Curve 2
y = 4E+10x² + 4E+07x + 14793
R² = 0.99976
Fluorescence Signal (CPS - MicroAmps)
2.50E+06
2.00E+06
1.50E+06
1.00E+06
5.00E+05
0.00E+00
0
0.001
0.002
0.003
0.004
0.005
0.006
0.007
Concentration (mg/mL)
Calibration 2
Poly. (Calibration 2)

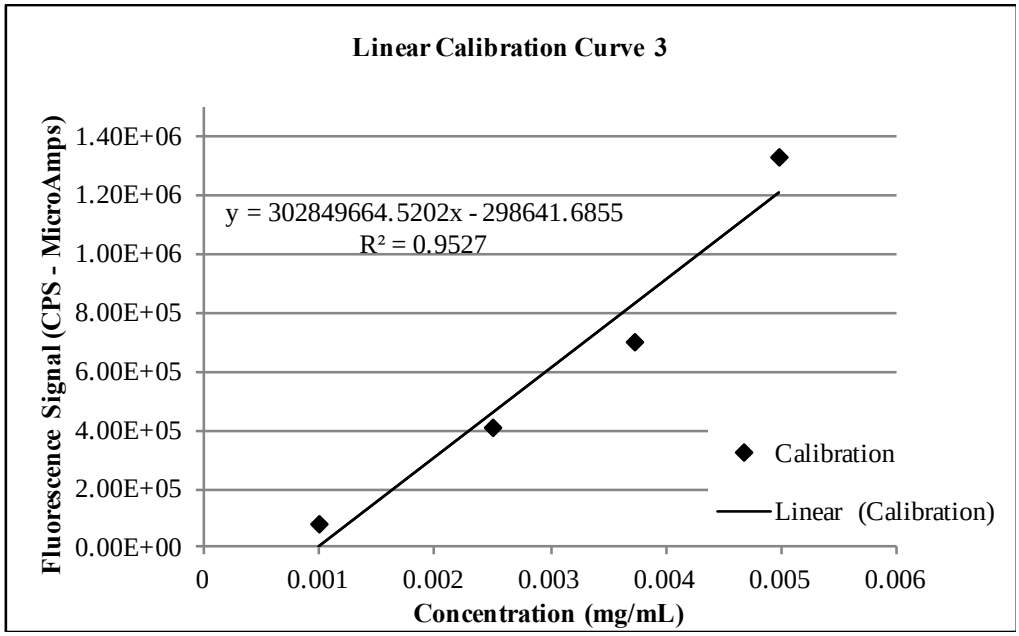
Linear Calibration Curve 3
Fluorescence Signal (CPS - MicroAmps)
1.40E+06
1.20E+06
1.00E+06
8.00E+05
6.00E+05
4.00E+05
2.00E+05
0.00E+00
y = 302849664.5202x - 298641.6855
R² = 0.9527
Calibration
Linear (Calibration)
0
0.001
0.002
0.003
0.004
0.005
0.006
Concentration (mg/mL)

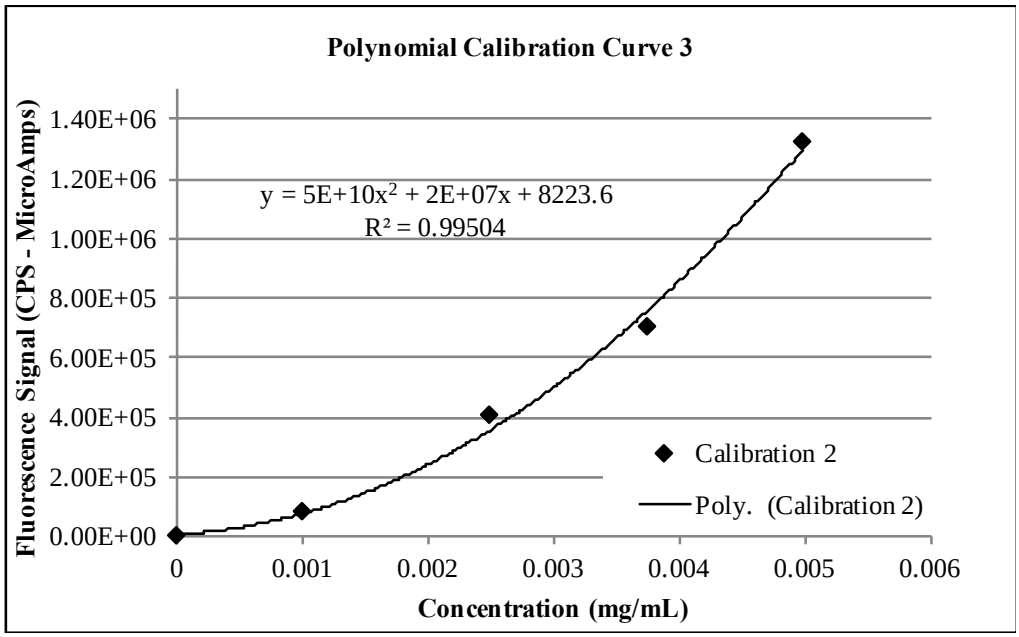
Polynomial Calibration Curve 3
Fluorescence Signal (CPS - MicroAmps)
1.40E+06
1.20E+06
1.00E+06
8.00E+05
6.00E+05
4.00E+05
2.00E+05
0.00E+00
y = 5E+10x² + 2E+07x + 8223.6
R² = 0.99504
Calibration 2
Poly. (Calibration 2)
0
0.001
0.002
0.003
0.004
0.005
0.006
Concentration (mg/mL)

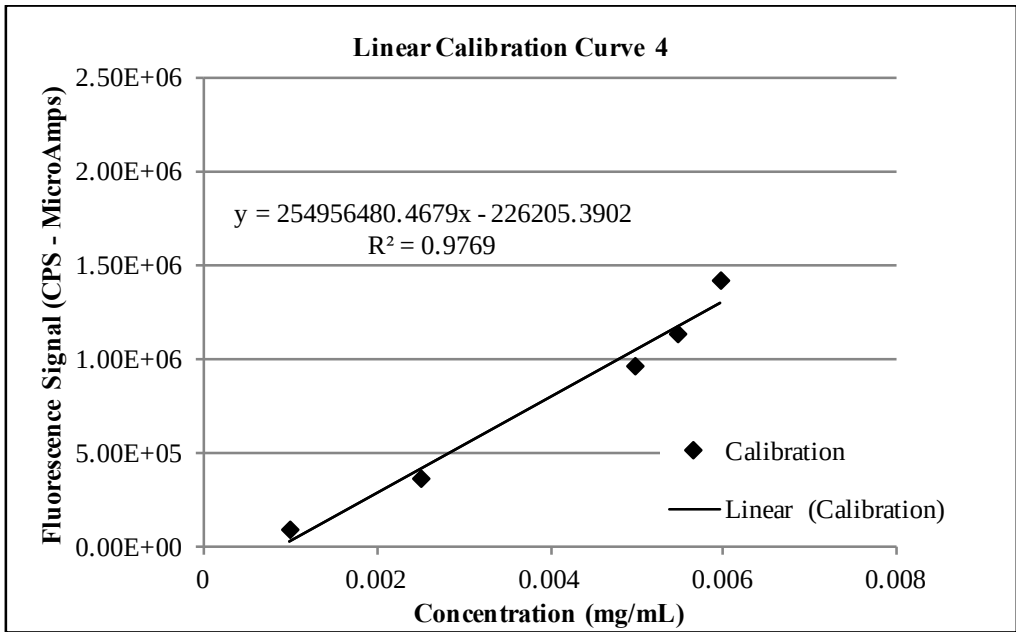
Linear Calibration Curve 4
Fluorescence Signal (CPS - MicroAmps)
2.50E+06
2.00E+06
1.50E+06
1.00E+06
5.00E+05
0.00E+00
y = 254956480.4679x - 226205.3902
R² = 0.9769
Calibration
Linear (Calibration)
0
0.002
0.004
0.006
0.008
Concentration (mg/mL)

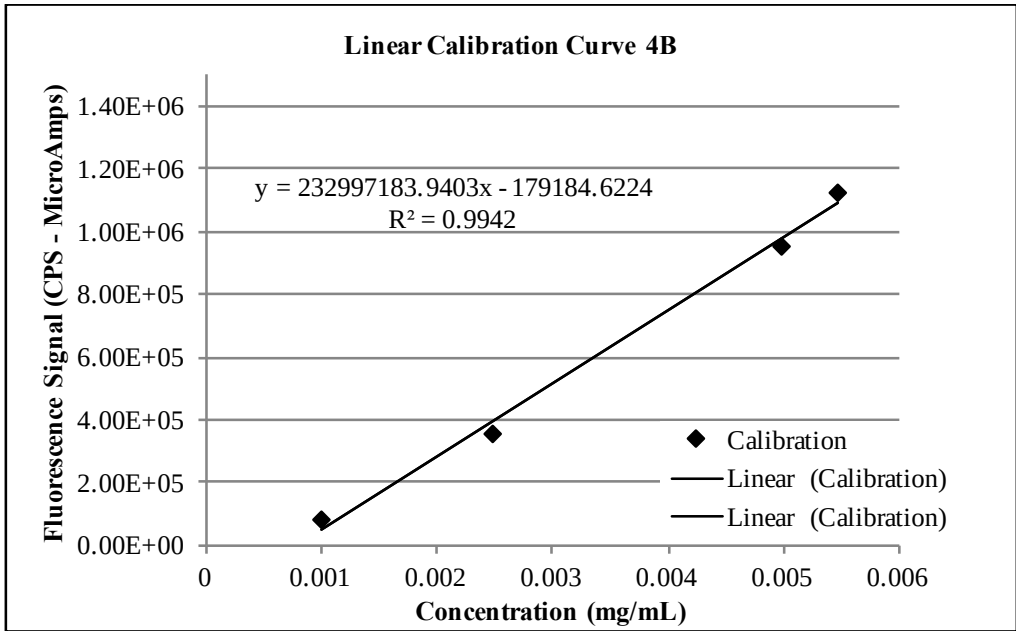
Linear Calibration Curve 4B
Fluorescence Signal (CPS - MicroAmps)
1.40E+06
1.20E+06
1.00E+06
8.00E+05
6.00E+05
4.00E+05
2.00E+05
0.00E+00
y = 232997183.9403x - 179184.6224
R² = 0.9942
Calibration
Linear (Calibration)
Linear (Calibration)
0
0.001
0.002
0.003
0.004
0.005
0.006
Concentration (mg/mL)

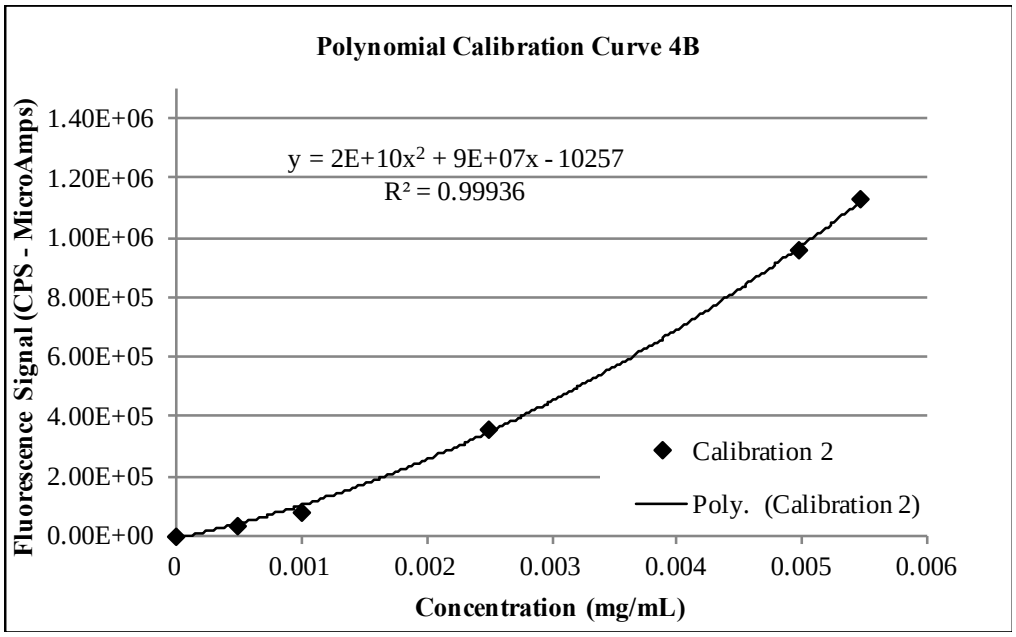
Polynomial Calibration Curve 4B
Fluorescence Signal (CPS - MicroAmps)
1.40E+06
1.20E+06
1.00E+06
8.00E+05
6.00E+05
4.00E+05
2.00E+05
0.00E+00
y = 2E+10x² + 9E+07x - 10257
R² = 0.99936
Calibration 2
Poly. (Calibration 2)
0
0.001
0.002
0.003
0.004
0.005
0.006
Concentration (mg/mL)

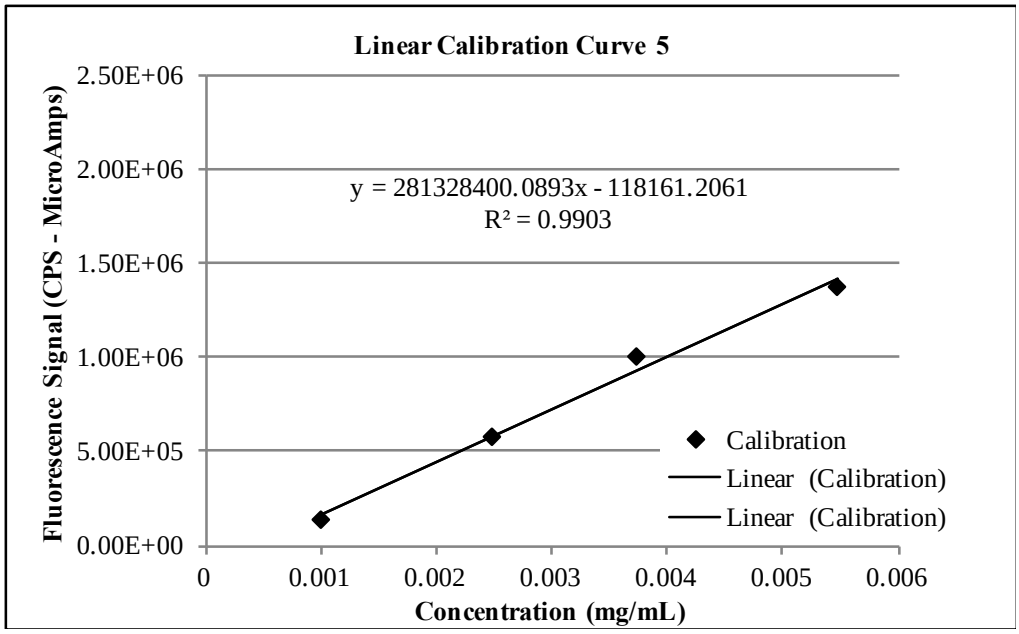
Linear Calibration Curve 5
Fluorescence Signal (CPS - MicroAmps)
2.50E+06
2.00E+06
1.50E+06
1.00E+06
5.00E+05
0.00E+00
y = 281328400.0893x - 118161.2061
R² = 0.9903
Calibration
Linear (Calibration)
Linear (Calibration)
0
0.001
0.002
0.003
0.004
0.005
0.006
Concentration (mg/mL)

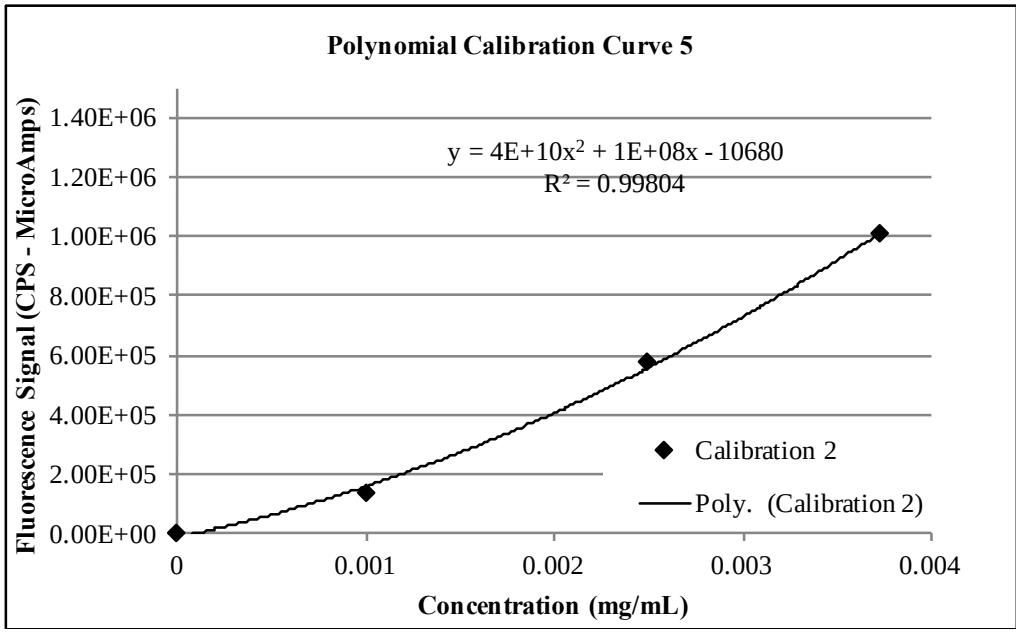
Polynomial Calibration Curve 5
Fluorescence Signal (CPS - MicroAmps)
1.40E+06
1.20E+06
1.00E+06
8.00E+05
6.00E+05
4.00E+05
2.00E+05
0.00E+00
y = 4E+10x² + 1E+08x - 10680
R² = 0.99804
Calibration 2
Poly. (Calibration 2)
0
0.001
0.002
0.003
0.004
Concentration (mg/mL)

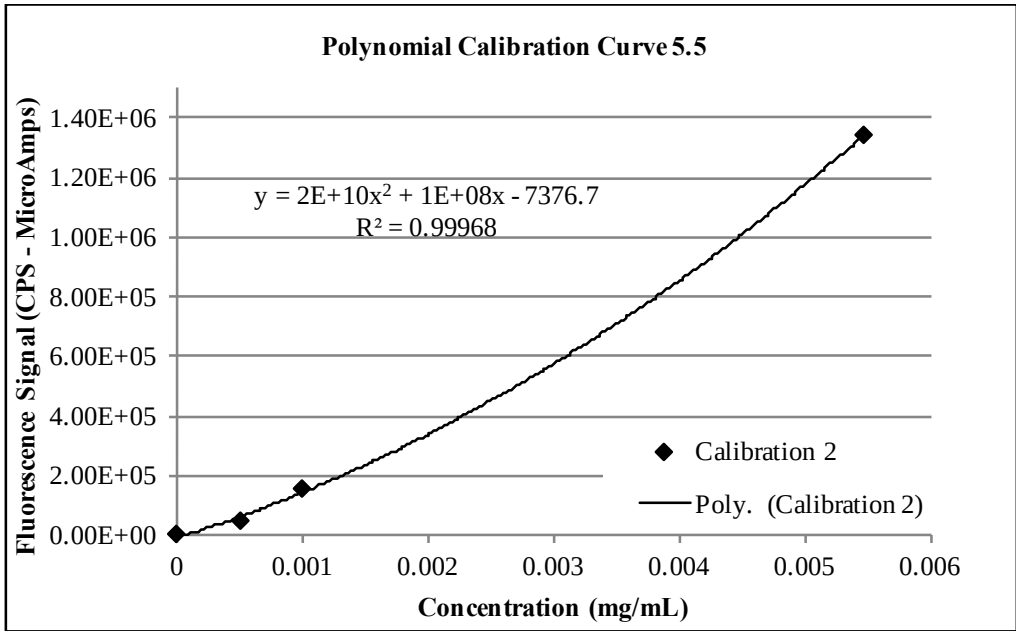
Polynomial Calibration Curve 5.5
Fluorescence Signal (CPS - MicroAmps)
1.40E+06
1.20E+06
1.00E+06
8.00E+05
6.00E+05
4.00E+05
2.00E+05
0.00E+00
y = 2E+10x² + 1E+08x - 7376.7
R² = 0.99968
Calibration 2
Poly. (Calibration 2)
0
0.001
0.002
0.003
0.004
0.005
0.006
Concentration (mg/mL)

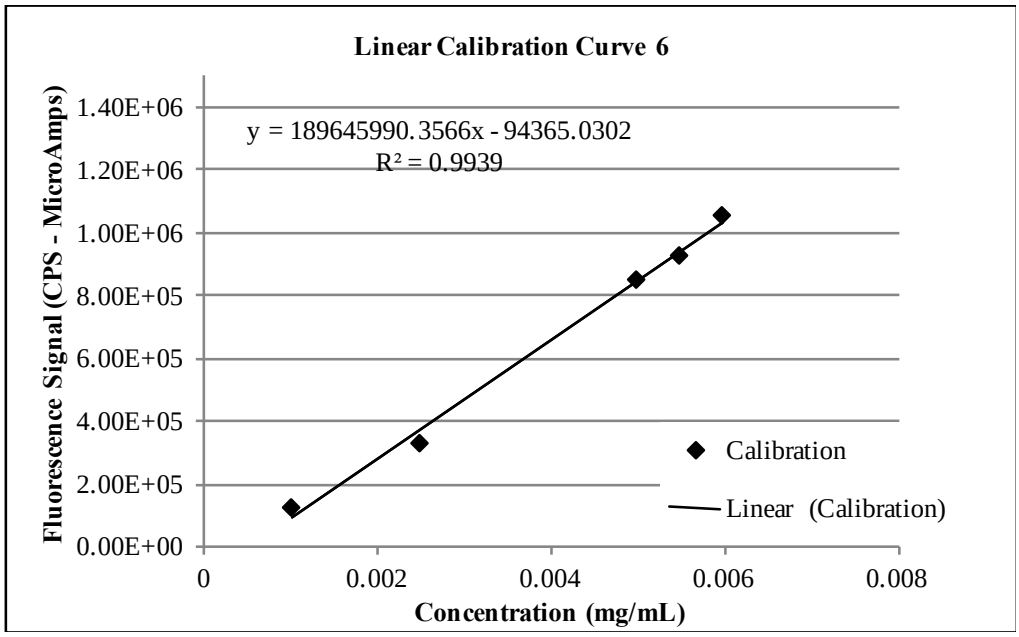
Linear Calibration Curve 6
y = 189645990.3566x - 94365.0302
R² = 0.9939
Fluorescence Signal (CPS - MicroAmps)
1.40E+06
1.20E+06
1.00E+06
8.00E+05
6.00E+05
4.00E+05
2.00E+05
0.00E+00
0
0.002
0.004
0.006
0.008
Concentration (mg/mL)
Calibration
Linear (Calibration)

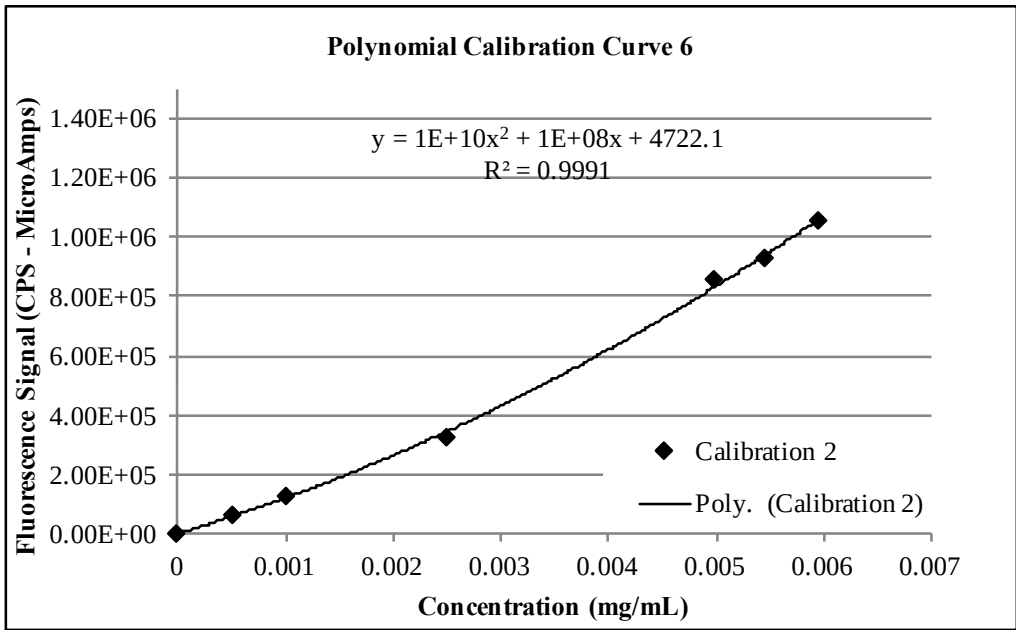
Polynomial Calibration Curve 6
y = 1E+10x² + 1E+08x + 4722.1
R² = 0.9991
Fluorescence Signal (CPS - MicroAmps)
1.40E+06
1.20E+06
1.00E+06
8.00E+05
6.00E+05
4.00E+05
2.00E+05
0.00E+00
0
0.001
0.002
0.003
0.004
0.005
0.006
0.007
Concentration (mg/mL)
Calibration 2
Poly. (Calibration 2)

11.4. Line Equations from Linear Calibration Curves

Calibration for initial calculations

Line Equation 1 (7/18/17)	Min.	Max.
y = 344346896.7028x - 314004.0335	8.84E+04	1.42E+06
x=(y+314004.0335)/344346896.7028		

Line Equation 2 (7/27/17)	Min.	Max.
y = 328038543.8323x - 247873.3196	1.02E+05	1.80E+06
x=(y+247873.3196)/328038543.8323		

Line Equation 3 (8/4/17)	Min.	Max.
y = 302849664.5202x - 298641.6855	7.99E+04	1.32E+06
x=(y+298641.6855)/302849664.5202		

Line Equation 4 (3/1/18)	Min.	Max.
y = 254956480.4679x - 226205.3902	8.32E+04	1.41E+06
x=(y+226205.3902)/254956480.4679		

Line Equation 4 B (3/1/18)	Min.	Max.
y = 232997183.9403x - 179184.6224	8.32E+04	1.13E+06
x=(y+179184.6224)/232997183.9403		

Line Equation 5 (3/9/18)	Min.	Max.
y = 281328400.0893x - 118161.2061	1.36E+05	1.38E+06
x=(y+118161.2061)/281328400.0893		

Line Equation 6 (3/16/18)	Min.	Max.
y = 189645990.3566x - 94365.0302	1.29E+05	1.06E+06
x=(y+94365.0302)/189645990.3566		

Line Equation 6 B (3/16/18)	Min.	Max.
y = 120213444.7588x + 8629.9842	6.87E+04	1.29E+05
x=(y+8629.9842)/120213444.7588		

11.1. Line Equations from Polynomial Calibration Curves

Calibration for final calculations

Polynomial Calibration Line Equations $y = ax^2 + bx + c$

a	b	c 1

Line Equation 1 (7/18/17) Polynomial

$y = 38379100821.8940x^2 + 106990709.2282x - 23813.6855$

Line Equation 2 (7/27/17) Polynomial

$y = 43168914934.0981x^2 + 40274627.7827x + 14793.1878$

Not used in final calculations

Line Equation 3 (8/4/17) Polynomial

$y = 47740876223.5334x^2 + 21934989.2527x + 8223.6296$

Line Equation 4 B (3/1/18) Polynomial

$y = 21619821628.2397x^2 + 88964886.5422x - 10256.6881$

Line Equation 5 (3/9/18) Polynomial

$y = 37722178381.2629x^2 + 133895384.7334x - 10680.1551$

Line Equation 5.5 (3/15/18) Polynomial

$y = 21153207080.7422x^2 + 131396328.0950x - 7376.7021$

Not used in final calculations

Line Equation 6 (3/16/18) Polynomial

y = 11662541583.3965x2 + 107765870.4909x + 4722.1108

Formulas:

x = (-b±√(b^2 - 4*a*c))/(2*a)

c 2 = c 1 - y

c 2 = AA2-U2

D = (b)^2*4*a*c

D = (Z2)^2 - (4*(Y2*AB2))

x 1 = (-(Z2) + (SQRT(AC2)))/(2*Y2)

x 2 = (-(Z2) - (SQRT(AC2)))/(2*Y2)

11.1. Nile Red Fluorescence Data and Calculations Summary Table

A	B	C	D	E	F	G	H	I	J	K
Sample set	Sample No.	Sample Date	Day	Fluorescence Date	Treatment No.	Volume Freeze-Dried (mL)	Volume Freeze-Dried (L)	Dry Weight (g)	Yield Dry Alga (mg/mL)	Yield Dry Alga (g/L)
1	1	7/18/17	6	7/18/17	1	350.0	0.3500	0.476	1.360	1.360
Re-run	2	7/18/17	6	3/15/18	2	344.8	0.3448	0.297	0.861	0.861
	3	7/18/17	6	7/18/17	3	349.2	0.3492	0.413	1.183	1.183
	4	7/18/17	6	7/18/17	4	349.0	0.3490	0.278	0.797	0.797
	5	7/18/17	6	7/18/17	5	348.2	0.3482	0.285	0.818	0.818
	6	7/18/17	6	7/18/17	6	348.2	0.3482	0.302	0.867	0.867
2	7	7/20/17	8	7/20/17	1	345.8	0.3458	0.516	1.492	1.492
	8	7/20/17	8	7/20/17	2	345.8	0.3458	0.362	1.047	1.047
	9	7/20/17	8	7/20/17	3	345.8	0.3458	0.489	1.414	1.414
	10	7/20/17	8	7/20/17	4	345.8	0.3458	0.325	0.940	0.940
	11	7/20/17	8	7/20/17	5	345.8	0.3458	0.313	0.905	0.905
Error/Lost	12	7/20/17	8	7/20/17	6	0.0	0.0000		#DIV/0!	#DIV/0!
3	13	7/21/17	9	7/21/17	1	395.8	0.3958	0.626	1.582	1.582
Re-run	14	7/21/17	9	3/9/18	2	390.8	0.3908	0.398	1.018	1.018
	15	7/21/17	9	7/21/17	3	395.8	0.3958	0.538	1.359	1.359
Re-run	16	7/21/17	9	3/9/18	4	390.8	0.3908	0.377	0.965	0.965
	17	7/21/17	9	7/21/17	5	395.8	0.3958	0.337	0.851	0.851
	18	7/21/17	9	7/21/17	6	395.8	0.3958	0.381	0.963	0.963
Re-run 4	19	7/24/17	12	3/15/18	1	391.1	0.3911	0.617	1.578	1.578
Re-run	20	7/24/17	12	3/15/18	2	391.1	0.3911	0.419	1.071	1.071
Re-run	21	7/24/17	12	3/15/18	3	391.1	0.3911	0.459	1.174	1.174
Re-run	22	7/24/17	12	3/15/18	4	391.1	0.3911	0.387	0.990	0.990
Re-run	23	7/24/17	12	3/15/18	5	391.1	0.3911	0.416	1.064	1.064
Re-run	24	7/24/17	12	3/15/18	6	391.1	0.3911	0.454	1.161	1.161
Re-run 5	25	7/27/17	15	3/15/18	1	345.3	0.3453	0.450	1.303	1.303
Re-run	26	7/27/17	15	3/15/18	2	345.3	0.3453	0.405	1.173	1.173
Re-run	27	7/27/17	15	3/15/18	3	345.3	0.3453	0.539	1.561	1.561
Re-run	28	7/27/17	15	3/15/18	4	345.3	0.3453	0.327	0.947	0.947
Re-run	29	7/27/17	15	3/15/18	5	345.3	0.3453	0.405	1.173	1.173
Re-run	30	7/27/17	15	3/15/18	6	345.3	0.3453	0.425	1.231	1.231
6	31	7/31/17	19	3/1/18	1	396.0	0.3960	0.696	1.758	1.758
	32	7/31/17	19	3/1/18	2	396.0	0.3960	0.540	1.364	1.364
	33	7/31/17	19	3/1/18	3	396.0	0.3960	0.675	1.705	1.705
	34	7/31/17	19	3/1/18	4	396.0	0.3960	0.427	1.078	1.078
	35	7/31/17	19	3/1/18	5	396.0	0.3960	0.478	1.207	1.207
	36	7/31/17	19	3/1/18	6	396.0	0.3960	0.540	1.364	1.364

A	B	C	D	E	F	G	H	I	J	K
Sample set	Sample No.	Sample Date	Day	Fluorescence Date	Treatment No.	Volume Freeze-Dried (mL)	Volume Freeze-Dried (L)	Dry Weight (g)	Yield Dry Alga (mg/mL)	Yield Dry Alga (g/L)
Re-run 7	37	8/4/17	23	2/22/18	1	391.8	0.3918	0.715	1.825	1.825
Re-run	38	8/4/17	23	2/22/18	2	391.8	0.3918	0.579	1.478	1.478
Re-run	39	8/4/17	23	2/22/18	3	391.8	0.3918	0.621	1.585	1.585
Re-run	40	8/4/17	23	2/22/18	4	391.8	0.3918	0.530	1.353	1.353
Re-run	41	8/4/17	23	2/22/18	5	391.8	0.3918	0.540	1.378	1.378
Re-run	42	8/4/17	23	2/22/18	6	391.8	0.3918	0.597	1.524	1.524
8	43	8/8/17	27	3/9/18	1	396.0	0.3960	0.790	1.995	1.995
	44	8/8/17	27	3/9/18	2	396.0	0.3960	0.575	1.452	1.452
	45	8/8/17	27	3/9/18	3	396.0	0.3960	0.705	1.780	1.780
	46	8/8/17	27	3/9/18	4	396.0	0.3960	0.527	1.331	1.331
	47	8/8/17	27	3/9/18	5	396.0	0.3960	0.576	1.455	1.455
	48	8/8/17	27	3/9/18	6	396.0	0.3960	0.608	1.535	1.535
9	49	8/15/17	34	3/12/18	1	396.0	0.3960	0.842	2.126	2.126
	50	8/15/17	34	3/12/18	2	396.0	0.3960	0.593	1.497	1.497
	51	8/15/17	34	3/12/18	3	396.0	0.3960	0.825	2.083	2.083
	52	8/15/17	34	3/12/18	4	396.0	0.3960	0.487	1.230	1.230
	53	8/15/17	34	3/12/18	5	396.0	0.3960	0.585	1.477	1.477
	54	8/15/17	34	3/12/18	6	396.0	0.3960	0.586	1.480	1.480
10	55	9/2/17	52	3/14/18	1	450.0	0.4500	1.010	2.244	2.244
	56	9/2/17	52	3/14/18	2	450.0	0.4500	0.582	1.293	1.293
	57	9/2/17	52	3/14/18	3	450.0	0.4500	0.854	1.898	1.898
	58	9/2/17	52	3/14/18	4	450.0	0.4500	0.657	1.460	1.460
	59	9/2/17	52	3/14/18	5	450.0	0.4500	0.657	1.460	1.460
	60	9/2/17	52	3/14/18	6	450.0	0.4500	0.570	1.267	1.267

A	B	L	M	N	O	P	Q	R	S
Sample set	Sample No.	**Y: Signal - Blank**	Dilution (mL Culture/mL Filtered MAM)	Line Equation No.	**X: Vol. Lipid (mg/mL) Linear**	**X: Vol. Lipid (mg/mL) Polynomial**	**Vol. Lipid (mg/ml) Corrected for Dilution**	**Lipid (mg)/Dry Wt. (mg)**	**Lipid (%) Dry Wt.**
1	1	3.14E+05	1.000	1	0.0018229	0.0018829	0.0018829	0.0013845	0.14
Re-run	2	9.60E+04	1.000	6	0.0008701	0.0007808	0.0007808	0.0009064	0.09
	3	3.09E+05	1.000	1	0.0018106	0.0018660	0.0018660	0.0015778	0.16
	4	2.41E+05	1.000	1	0.0016120	0.0015802	0.0015802	0.0019837	0.20
	5	2.59E+05	1.000	1	0.0016645	0.0016583	0.0016583	0.0020261	0.20
	6	2.87E+05	1.000	1	0.0017453	0.0017748	0.0017748	0.0020463	0.20
2	7	4.53E+05	1.000	1	0.0022269	0.0023959	0.0023959	0.0016056	0.16
	8	1.01E+06	1.000	1	0.0038305	0.0039680	0.0039680	0.0037905	0.38
	9	5.41E+04	1.000	1	0.0010690	0.0005995	0.0005995	0.0004239	0.04
	10	8.59E+05	1.000	1	0.0034052	0.0035995	0.0035995	0.0038299	0.38
	11	3.26E+05	1.000	1	0.0018577	0.0019302	0.0019302	0.0021324	0.21
Error/Lost	12	-9.66E+04	1.000				0.0000000	#DIV/0!	#DIV/0!
3	13	9.66E+05	1.000	1	0.0037172	0.0038724	0.0038724	0.0024484	0.24
Re-run	14	1.90E+05	0.500	5	0.0010947	0.0011346	0.0022692	0.0022282	0.22
	15	8.01E+05	1.000	1	0.0032381	0.0034471	0.0034471	0.0025360	0.25
Re-run	16	1.63E+05	0.500	5	0.0010007	0.0010115	0.0020230	0.0020971	0.21
	17	1.26E+06	1.000	1	0.0045798	0.0045621	0.0045621	0.0053581	0.54
	18	9.15E+05	1.000	1	0.0035681	0.0037438	0.0037438	0.0038892	0.39
Re-run 4	19	1.48E+05	0.400	6	0.0012783	0.0011795	0.0029487	0.0018691	0.19
Re-run	20	1.60E+05	0.500	6	0.0013388	0.0012637	0.0025275	0.0023592	0.24
Re-run	21	4.30E+05	0.750	6	0.0027642	0.0029823	0.0039764	0.0033882	0.34
Re-run	22	1.92E+05	0.500	6	0.0015089	0.0014942	0.0029884	0.0030200	0.30
Re-run	23	2.41E+05	0.500	6	0.0017701	0.0018322	0.0036645	0.0034451	0.34
Re-run	24	3.09E+05	0.750	6	0.0021249	0.0022648	0.0030198	0.0026014	0.26
Re-run 5	25	3.17E+05	0.500	6	0.0021684	0.0023160	0.0046320	0.0035543	0.36
Re-run	26	2.75E+05	0.500	6	0.0019484	0.0020531	0.0041062	0.0035010	0.35
Re-run	27	3.28E+05	0.750	6	0.0022272	0.0023846	0.0031794	0.0020368	0.20
Re-run	28	2.97E+05	0.500	6	0.0020619	0.0021901	0.0043801	0.0046252	0.46
Re-run	29	4.01E+05	0.500	6	0.0026121	0.0028180	0.0056359	0.0048051	0.48
Re-run	30	3.38E+05	0.750	6	0.0022815	0.0024474	0.0032631	0.0026512	0.27
6	31	2.04E+05	0.200	4B	0.0016446	0.0017034	0.0085169	0.0048458	0.48
	32	2.42E+05	0.150	4B	0.0018083	0.0019310	0.0128732	0.0094404	0.94
	33	1.74E+05	0.200	4B	0.0015138	0.0015110	0.0075552	0.0044324	0.44
	34	2.42E+05	0.150	4B	0.0018081	0.0019307	0.0128715	0.0119371	1.19
	35	3.38E+05	0.150	4B	0.0022179	0.0024506	0.0163371	0.0135345	1.35
	36	1.21E+05	0.150	4B	0.0012899	0.0011552	0.0077015	0.0056478	0.56

A	B	L	M	N	O	P	Q	R	S
Sample set	Sample No.	**Y: Signal - Blank**	Dilution (mL Culture/mL Filtered MAM)	Line Equation No.	**X: Vol. Lipid (mg/mL) Linear**	**X: Vol. Lipid (mg/mL) Polynomial**	**Vol. Lipid (mg/ml) Corrected for Dilution**	**Lipid (mg)/Dry Wt. (mg)**	**Lipid (%) Dry Wt.**
Re-run 7	37	3.96E+05	1.000	4B	0.0024698	0.0027422	0.0027422	0.0015026	0.15
Re-run	38	1.61E+05	0.100	4B	0.0014596	0.0014281	0.0142812	0.0096639	0.97
Re-run	39	3.61E+05	1.000	4B	0.0023187	0.0025694	0.0025694	0.0016211	0.16
Re-run	40	1.23E+05	0.100	4B	0.0012958	0.0011651	0.0116507	0.0086127	0.86
Re-run	41	1.61E+05	0.100	4B	0.0014612	0.0014306	0.0143062	0.0103799	1.04
Re-run	42	5.81E+04	0.100	4B	0.0010186	0.0006623	0.0066229	0.0043465	0.43
8	43	1.65E+05	0.125	5	0.0010070	0.0010200	0.0081603	0.0040905	0.41
	44	3.41E+05	0.100	5	0.0016337	0.0017586	0.0175856	0.0121111	1.21
	45	1.42E+05	0.125	5	0.0009239	0.0009069	0.0072549	0.0040751	0.41
	46	3.48E+05	0.100	5	0.0016554	0.0017814	0.0178138	0.0133857	1.34
	47	4.50E+05	0.100	5	0.0020186	0.0021438	0.0214375	0.0147383	1.47
	48	1.95E+05	0.200	5	0.0011121	0.0011569	0.0057845	0.0037676	0.38
9	49	1.45E+05	0.100	5	0.0009361	0.0009237	0.0092366	0.0043441	0.43
	50	2.17E+05	0.075	5	0.0011909	0.0012555	0.0167394	0.0111784	1.12
	51	2.09E+05	0.200	5	0.0011635	0.0012216	0.0061079	0.0029318	0.29
	52	1.97E+05	0.075	5	0.0011191	0.0011658	0.0155436	0.0126392	1.26
	53	3.58E+05	0.075	5	0.0016909	0.0018184	0.0242452	0.0164121	1.64
	54	1.58E+05	0.200	5	0.0009802	0.0009840	0.0049202	0.0033249	0.33
10	55	1.35E+05	0.200	6	0.0012108	0.0010840	0.0054202	0.0024149	0.24
	56	2.34E+05	0.075	6	0.0017298	0.0017813	0.0237503	0.0183636	1.84
	57	1.60E+05	0.200	6	0.0013406	0.0012662	0.0063310	0.0033360	0.33
	58	4.19E+05	0.075	6	0.0027057	0.0029196	0.0389279	0.0266630	2.67
	59	5.25E+05	0.075	6	0.0032652	0.0035005	0.0466738	0.0319684	3.20
	60	2.11E+05	0.200	6	0.0016119	0.0016297	0.0081486	0.0064331	0.64

B	U	V	W	X 2	Z	AA	AB	AC	AD
Sample No.	Line Equation No.	y	x 1	x 2	a	b	c 1	c 2	D
1	1	313699.9964	0.0018829	-4.671E-03	3.84E+10	1.07E+08	-2.38E+04	-3.38E+05	6.33E+16
2	6	95969.9998	0.0007808	-1.002E-02	1.17E+10	1.08E+08	4.72E+03	-9.12E+04	1.59E+16
3	1	309476.6620	0.0018660	-4.654E-03	3.84E+10	1.07E+08	-2.38E+04	-3.33E+05	6.26E+16
4	1	241079.9962	0.0015802	-4.368E-03	3.84E+10	1.07E+08	-2.38E+04	-2.65E+05	5.21E+16
5	1	259159.9959	0.0016583	-4.446E-03	3.84E+10	1.07E+08	-2.38E+04	-2.83E+05	5.49E+16
6	1	286969.9971	0.0017748	-4.563E-03	3.84E+10	1.07E+08	-2.38E+04	-3.11E+05	5.92E+16
7	1	452823.3366	0.0023959	-5.184E-03	3.84E+10	1.07E+08	-2.38E+04	-4.77E+05	8.46E+16
8	1	1005017.8767	0.0039680	-6.756E-03	3.84E+10	1.07E+08	-2.38E+04	-1.03E+06	1.69E+17
9	1	54113.3324	0.0005995	-3.387E-03	3.84E+10	1.07E+08	-2.38E+04	-7.79E+04	2.34E+16
10	1	858566.6654	0.0035995	-6.387E-03	3.84E+10	1.07E+08	-2.38E+04	-8.82E+05	1.47E+17
11	1	325679.9989	0.0019302	-4.718E-03	3.84E+10	1.07E+08	-2.38E+04	-3.49E+05	6.51E+16
12				#DIV/0!					
13	1	965991.2029	0.0038724	-6.660E-03	3.84E+10	1.07E+08	-2.38E+04	-9.90E+05	1.63E+17
14	5	189803.3276	0.0011346	-4.684E-03	3.77E+10	1.34E+08	-1.07E+04	-2.00E+05	4.82E+16
15	1	801023.3248	0.0034471	-6.235E-03	3.84E+10	1.07E+08	-2.38E+04	-8.25E+05	1.38E+17
16	5	163353.3254	0.0010115	-4.561E-03	3.77E+10	1.34E+08	-1.07E+04	-1.74E+05	4.42E+16
17	1	1263051.2029	0.0045621	-7.350E-03	3.84E+10	1.07E+08	-2.38E+04	-1.29E+06	2.09E+17
18	1	914661.2029	0.0037438	-6.532E-03	3.84E+10	1.07E+08	-2.38E+04	-9.38E+05	1.56E+17
19	6	148056.6675	0.0011795	-1.042E-02	1.17E+10	1.08E+08	4.72E+03	-1.43E+05	1.83E+16
20	6	159536.6672	0.0012637	-1.050E-02	1.17E+10	1.08E+08	4.72E+03	-1.55E+05	1.88E+16
21	6	429846.6680	0.0029823	-1.222E-02	1.17E+10	1.08E+08	4.72E+03	-4.25E+05	3.14E+16
22	6	191783.3324	0.0014942	-1.073E-02	1.17E+10	1.08E+08	4.72E+03	-1.87E+05	2.03E+16
23	6	241326.6649	0.0018322	-1.107E-02	1.17E+10	1.08E+08	4.72E+03	-2.37E+05	2.27E+16
24	6	308613.3288	0.0022648	-1.151E-02	1.17E+10	1.08E+08	4.72E+03	-3.04E+05	2.58E+16
25	6	316863.3339	0.0023160	-1.156E-02	1.17E+10	1.08E+08	4.72E+03	-3.12E+05	2.62E+16
26	6	275140.0000	0.0020531	-1.129E-02	1.17E+10	1.08E+08	4.72E+03	-2.70E+05	2.42E+16
27	6	328013.3318	0.0023846	-1.162E-02	1.17E+10	1.08E+08	4.72E+03	-3.23E+05	2.67E+16
28	6	296673.3324	0.0021901	-1.143E-02	1.17E+10	1.08E+08	4.72E+03	-2.92E+05	2.52E+16
29	6	401013.3334	0.0028180	-1.206E-02	1.17E+10	1.08E+08	4.72E+03	-3.96E+05	3.01E+16
30	6	338316.6687	0.0024474	-1.169E-02	1.17E+10	1.08E+08	4.72E+03	-3.34E+05	2.72E+16
31	4B	204013.3342	0.0017034	-5.818E-03	2.16E+10	8.90E+07	-1.03E+04	-2.14E+05	2.64E+16
32	4B	242146.6700	0.0019310	-6.046E-03	2.16E+10	8.90E+07	-1.03E+04	-2.52E+05	2.97E+16
33	4B	173536.6697	0.0015110	-5.626E-03	2.16E+10	8.90E+07	-1.03E+04	-1.84E+05	2.38E+16
34	4B	242103.3385	0.0019307	-6.046E-03	2.16E+10	8.90E+07	-1.03E+04	-2.52E+05	2.97E+16
35	4B	337590.0019	0.0024506	-6.566E-03	2.16E+10	8.90E+07	-1.03E+04	-3.48E+05	3.80E+16
36	4B	121370.0034	0.0011552	-5.270E-03	2.16E+10	8.90E+07	-1.03E+04	-1.32E+05	1.93E+16

B	U	V	W	X 2	Z	AA	AB	AC	AD
Sample No.	Line Equation No.	y	x 1	x 2	a	b	c 1	c 2	D
43	5	165146.6631	0.0010200	-4.570E-03	3.77E+10	1.34E+08	-1.07E+04	-1.76E+05	4.45E+16
44	5	341439.9977	0.0017586	-5.308E-03	3.77E+10	1.34E+08	-1.07E+04	-3.52E+05	7.11E+16
45	5	141766.6631	0.0009069	-4.456E-03	3.77E+10	1.34E+08	-1.07E+04	-1.52E+05	4.09E+16
46	5	347543.3306	0.0017814	-5.331E-03	3.77E+10	1.34E+08	-1.07E+04	-3.58E+05	7.20E+16
47	5	449716.6640	0.0021438	-5.693E-03	3.77E+10	1.34E+08	-1.07E+04	-4.60E+05	8.74E+16
48	5	194713.3295	0.0011569	-4.706E-03	3.77E+10	1.34E+08	-1.07E+04	-2.05E+05	4.89E+16
49	5	145176.6660	0.0009237	-4.473E-03	3.77E+10	1.34E+08	-1.07E+04	-1.56E+05	4.14E+16
50	5	216876.6673	0.0012555	-4.805E-03	3.77E+10	1.34E+08	-1.07E+04	-2.28E+05	5.23E+16
51	5	209176.6671	0.0012216	-4.771E-03	3.77E+10	1.34E+08	-1.07E+04	-2.20E+05	5.11E+16
52	5	196676.6677	0.0011658	-4.715E-03	3.77E+10	1.34E+08	-1.07E+04	-2.07E+05	4.92E+16
53	5	357523.3311	0.0018184	-5.368E-03	3.77E+10	1.34E+08	-1.07E+04	-3.68E+05	7.35E+16
54	5	157606.6656	0.0009840	-4.534E-03	3.77E+10	1.34E+08	-1.07E+04	-1.68E+05	4.33E+16
55	6	135250.0056	0.0010840	-1.032E-02	1.17E+10	1.08E+08	4.72E+03	-1.31E+05	1.77E+16
56	6	233686.6731	0.0017813	-1.102E-02	1.17E+10	1.08E+08	4.72E+03	-2.29E+05	2.23E+16
57	6	159873.3392	0.0012662	-1.051E-02	1.17E+10	1.08E+08	4.72E+03	-1.55E+05	1.89E+16
58	6	418766.6650	0.0029196	-1.216E-02	1.17E+10	1.08E+08	4.72E+03	-4.14E+05	3.09E+16
59	6	524870.0039	0.0035005	-1.274E-02	1.17E+10	1.08E+08	4.72E+03	-5.20E+05	3.59E+16
60	6	211326.6721	0.0016297	-1.087E-02	1.17E+10	1.08E+08	4.72E+03	-2.07E+05	2.13E+16
43	5	165146.6631	0.0010200	-4.570E-03	3.77E+10	1.34E+08	-1.07E+04	-1.76E+05	4.45E+16
44	5	341439.9977	0.0017586	-5.308E-03	3.77E+10	1.34E+08	-1.07E+04	-3.52E+05	7.11E+16
45	5	141766.6631	0.0009069	-4.456E-03	3.77E+10	1.34E+08	-1.07E+04	-1.52E+05	4.09E+16
46	5	347543.3306	0.0017814	-5.331E-03	3.77E+10	1.34E+08	-1.07E+04	-3.58E+05	7.20E+16
47	5	449716.6640	0.0021438	-5.693E-03	3.77E+10	1.34E+08	-1.07E+04	-4.60E+05	8.74E+16
48	5	194713.3295	0.0011569	-4.706E-03	3.77E+10	1.34E+08	-1.07E+04	-2.05E+05	4.89E+16

12. Appendix E: GC/MS Instrument Method Settings

12.1. Electron Ionization (EI) Settings

```
MS Method

Acquisition Time:   GC Run Time
Cal Gas:            Off
Reagent Gas:        Off
Acquire Profile:    No
Acq Threshold:      0
Source Temp:        280 C

Segment 1
Start Time:         3.00 minutes
Mult Offset:        +0 V
Detector:           On
Reagent Gas Flow:   Off
Damping Gas Flow:   0.3 mL/min
Emission Current:   Use Tune File

   Scan Event 1
   Micro Scans:        3
   Max Ion Time:       25 ms
   Mass Defect:        0.00 mmu/100 amu
   Polarity:           POS
   Tune File:          autotune
   Scan Mode:          Full Scan
   First Mass:         40.0
   Last Mass:          500.0
```

TRACE GC Ultra Method

Oven Method

Initial Temperature (C):	100
Initial Time (min):	1.00
Number of Ramps:	2
Rate #1 (deg/min):	2.0
Final Temperature #1 (C):	250
Hold Time #1 (min):	1.00
Rate #2 (deg/min):	15.0
Final Temperature #2 (C):	280
Hold Time #2 (min):	1.00
Post Run Temperature:	Off
Enable Cryogenics:	Off
Maximum Temperature (C):	350
Prep Run Timeout (min):	5.00
Equilibration Time (min):	0.50

Right PTV Method

Base Temperature:	On
Base Temperature (C):	280
Mode:	PTV Split
Split Flow:	On
Split Flow Flow (ml/min):	10
Splitless Time (min):	0.00
Solvent Valve Temperature:	Off
Solvent Valve Temperature (C):	100
Surge Pressure (psi):	0.50
Surge Duration (min):	0.00
Constant Purge:	On
Stop Purge At: (min):	0.00
Evaporation Phase:	Off
Cleaning Phase:	Off
Ramped Pressure:	Off
Sub-ambient:	Off
Backflush:	Off
Inject Time (min):	0.1
Transfer Rate (deg/sec):	14.5
Transfer Temperature (C):	280
Transfer Time (min):	1.0

Right Carrier Method

Mode:	Constant Flow
Initial Value:	On
Initial Value (ml/min):	1.00
Initial Time:	1.00
Gas Saver:	Off
Gas Saver Flow (ml/min):	20
Gas Saver Time:	2.00
Vacuum Compensation:	On

```
TRACE GC Ultra Method

No Left Inlet
-------------------------------------------------------------
No Right Detector
-------------------------------------------------------------
No Left Detector
-------------------------------------------------------------
No Aux Detector
-------------------------------------------------------------
Aux Zones
   Aux 1 MS Transfer Line:                On
   Aux 1 MS Transfer Line (C):            270
   Aux 2 :                                Off
   Aux 2  (C):                            30
-------------------------------------------------------------
Run Table
   External Event #1 Prep-Run Default:    Off
   External Event #2 Prep-Run Default:    Off
   External Event #3 Prep-Run Default:    Off
   External Event #4 Prep-Run Default:    Off
   External Event #5 Prep-Run Default:    Off
   External Event #6 Prep-Run Default:    Off
   External Event #7 Prep-Run Default:    Off
   External Event #8 Prep-Run Default:    Off
-------------------------------------------------------------
```

12.1. Chemical Ionization (CI) Settings

MS Method

Acquisition Time:	GC Run Time
Cal Gas:	Off
Reagent Gas:	On
Reagent Gas Type:	Methane
Acquire Profile:	No
Acq Threshold:	0
Source Temp:	280 C

Segment 1

Start Time:	3.00 minutes
Mult Offset:	+0 V
Detector:	On
Reagent Gas Flow:	0.0 mL/min
Damping Gas Flow:	0.3 mL/min
Emission Current:	Use Tune File

Scan Event 1

Micro Scans:	3
Max Ion Time:	25 ms
Mass Defect:	0.00 mmu/100 amu
Polarity:	POS
Tune File:	autotune
Scan Mode:	Full Scan
First Mass:	90.0
Last Mass:	500.0

TRACE GC Ultra Method

Oven Method

Initial Temperature (C):	100
Initial Time (min):	1.00
Number of Ramps:	2
Rate #1 (deg/min):	2.0
Final Temperature #1 (C):	250
Hold Time #1 (min):	1.00
Rate #2 (deg/min):	15.0
Final Temperature #2 (C):	270
Hold Time #2 (min):	1.00
Post Run Temperature:	Off
Enable Cryogenics:	Off
Maximum Temperature (C):	350
Prep Run Timeout (min):	5.00
Equilibration Time (min):	0.50

Right PTV Method

Base Temperature:	On
Base Temperature (C):	280
Mode:	PTV Splitless
Split Flow:	On
Split Flow Flow (ml/min):	10
Splitless Time (min):	0.00
Solvent Valve Temperature:	Off
Solvent Valve Temperature (C):	100
Surge Pressure (psi):	0.50
Surge Duration (min):	0.00
Constant Purge:	On
Stop Purge At: (min):	0.00
Evaporation Phase:	Off
Cleaning Phase:	Off
Ramped Pressure:	Off
Sub-ambient:	Off
Backflush:	Off
Inject Time (min):	0.1
Transfer Rate (deg/sec):	14.5
Transfer Temperature (C):	280
Transfer Time (min):	1.0

Right Carrier Method

Mode:	Constant Flow
Initial Value:	On
Initial Value (ml/min):	1.00
Initial Time:	1.00
Gas Saver:	Off
Gas Saver Flow (ml/min):	20
Gas Saver Time:	2.00
Vacuum Compensation:	On

```
TRACE GC Ultra Method

No Left Inlet
-------------------------------------------------------------
No Right Detector
-------------------------------------------------------------
No Left Detector
-------------------------------------------------------------
No Aux Detector
-------------------------------------------------------------
Aux Zones
   Aux 1 MS Transfer Line:                On
   Aux 1 MS Transfer Line (C):            270
   Aux 2 :                                Off
   Aux 2  (C):                            30
-------------------------------------------------------------
Run Table
   External Event #1 Prep-Run Default:    Off
   External Event #2 Prep-Run Default:    Off
   External Event #3 Prep-Run Default:    Off
   External Event #4 Prep-Run Default:    Off
   External Event #5 Prep-Run Default:    Off
   External Event #6 Prep-Run Default:    Off
   External Event #7 Prep-Run Default:    Off
   External Event #8 Prep-Run Default:    Off
-------------------------------------------------------------
```

12.2. Appendix F: GC/MS File Name List

Treatment No.	Sample Day	Sample Date	GC-MS File Name	EI or CI	Note
1	6	7/18/17	JM01	EI	OK
~~1~~	~~6~~	~~7/18/17~~	~~JM02~~	EI	Problem with run
1	6	7/18/17	JM12	CI	
1	9	7/21/17	JM26-180427	EI	
~~1~~	~~19~~	~~7/31/17~~	~~JM33~~	EI	Problem with run
1	19	7/31/17	JM33-180610	EI	OK
1	27	8/8/17	JM18	EI	
1	27	8/8/17	JM23	CI	
~~1~~	~~52~~	~~9/2/17~~	~~JM34~~	EI	Problem with run
1	52	9/2/17	JM35	EI	OK
2	6	7/18/17	JM03	EI	
2	6	7/18/17	JM13	CI	
2	9	7/21/17	JM28	EI	
2	19	7/31/17	JM42	EI	
2	27	8/8/17	JM19	EI	
2	27	8/8/17	JM22	CI	
2	52	9/2/17	JM36	EI	
3	6	7/18/17	JM04	EI	
3	6	7/18/17	JM14	CI	
3	9	7/21/17	JM29	EI	
3	19	7/31/17	JM43	EI	
3	27	8/8/17	JM20	EI	
3	27	8/8/17	JM21	CI	
3	52	9/2/17	JM37	EI	
~~4~~	~~6~~	~~7/18/17~~	~~JM05~~	EI	Problem with run
~~4~~	~~6~~	~~7/18/17~~	~~JM07~~	EI	Problem with run
~~4~~	~~6~~	~~7/18/17~~	~~JM10~~	EI	Problem with run
4	6	7/18/17	JM11	EI	OK
4	6	7/18/17	JM15	CI	
4	9	7/21/17	JM30	EI	
4	19	7/31/17	JM45	EI	
4	27A	8/8/17	JM24	EI	
4	27B	8/8/17	JM48	EI	
4	27C	8/8/17	JM48_181021162032	EI	
~~4~~	~~52~~	~~9/2/17~~	~~JM38~~	EI	Problem with run
4	52	9/2/17	JM39	EI	OK
5	6	7/18/17	JM08	EI	
5	6	7/18/17	JM16	CI	
5	9	7/21/17	JM31	EI	
5	15A	7/27/17	JM51	EI	
5	15B	7/27/17	JM52	EI	
5	15C	7/27/17	JM53	EI	

Treatment No.	Sample Day	Sample Date	GC-MS File Name	EI or CI	Note
5	19A	7/31/17	JM44	EI	
5	19B	7/31/17	JM46_181019125	EI	
5	19C	7/31/17	JM47_1810191427	EI	
5	19D	7/31/17	JM50	EI	
5	27	8/8/17	JM25	EI	
5	52	9/2/17	JM40	EI	
6	6	7/18/17	JM09	EI	
6	6	7/18/17	JM17	CI	
6	9	7/21/17	JM32	EI	
6	19	7/31/17	JM46	EI	
6	27	8/8/17	JM26	EI	
6	52	9/2/17	JM41	EI	

12.3. Appendix G: GC/MS Electron Ionization Chromatograms

12.3.1. Treatment 1, Standard MAM (Nutrient Replete)

12.3.1.1. Treatment 1, Standard MAM, Day 6

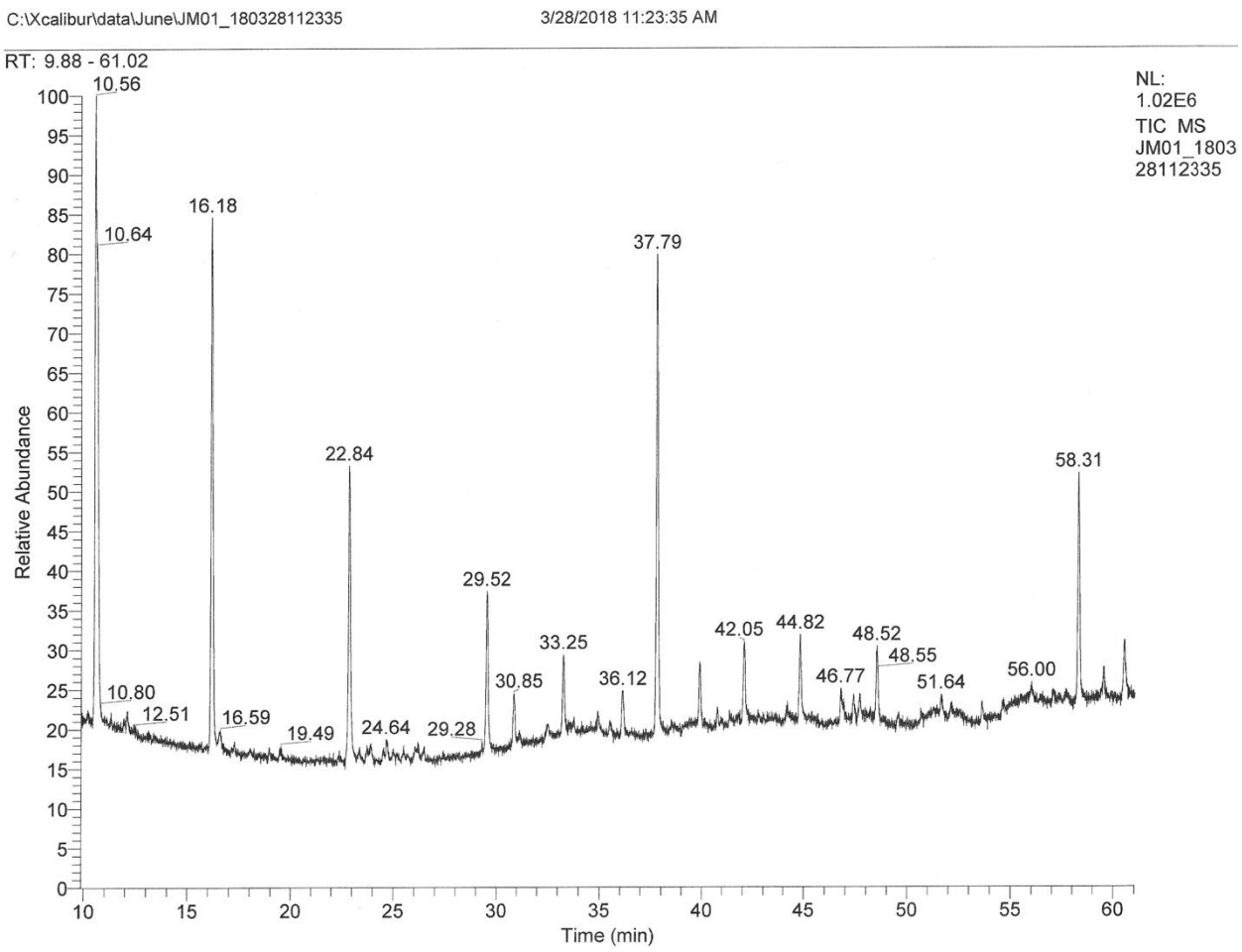

12.3.1.2. Treatment 1, Standard MAM, Day 9

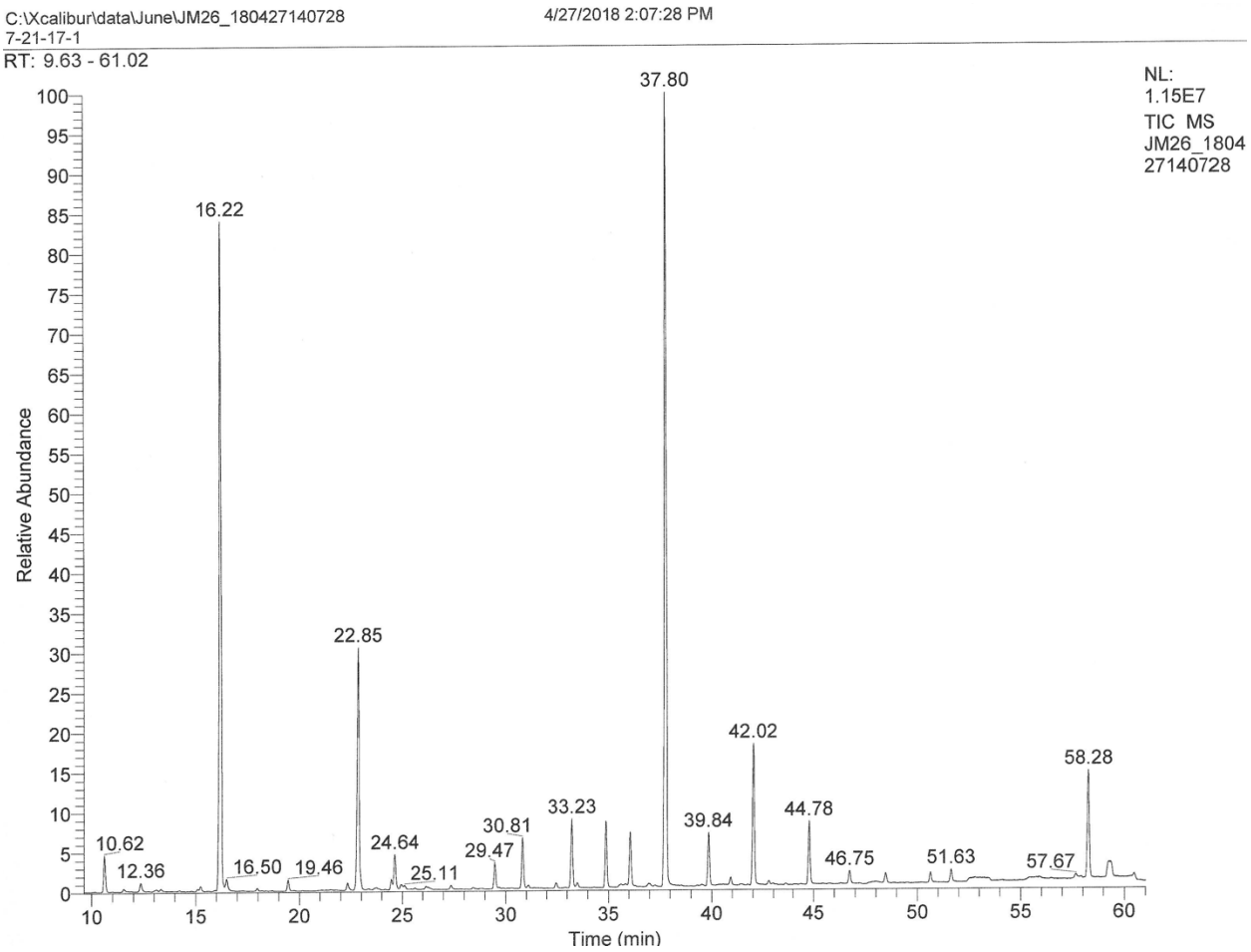

12.3.1.2.1. Treatment 1, Standard MAM, Day 19

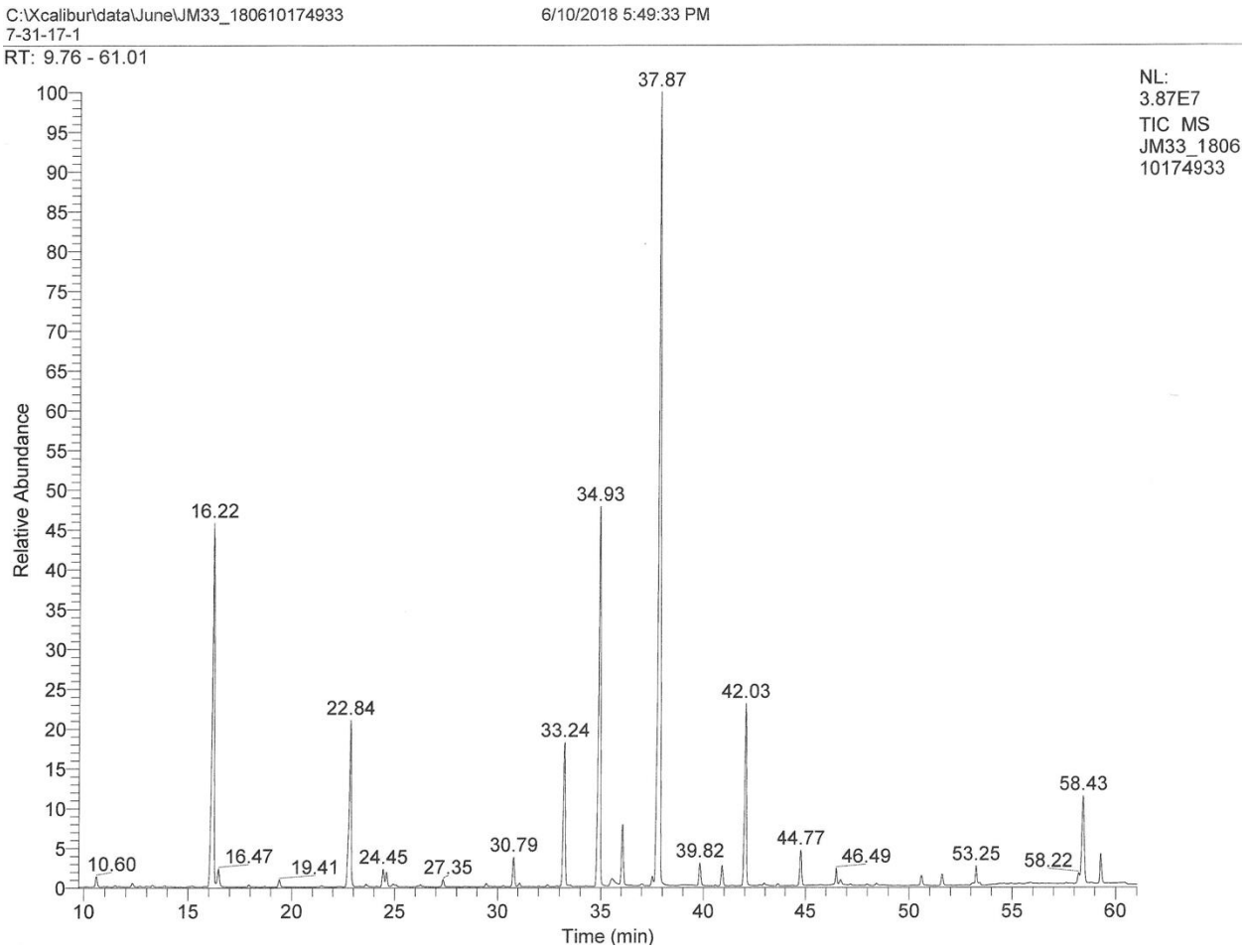

12.3.1.2.2. Treatment 1, Standard MAM, Day 27

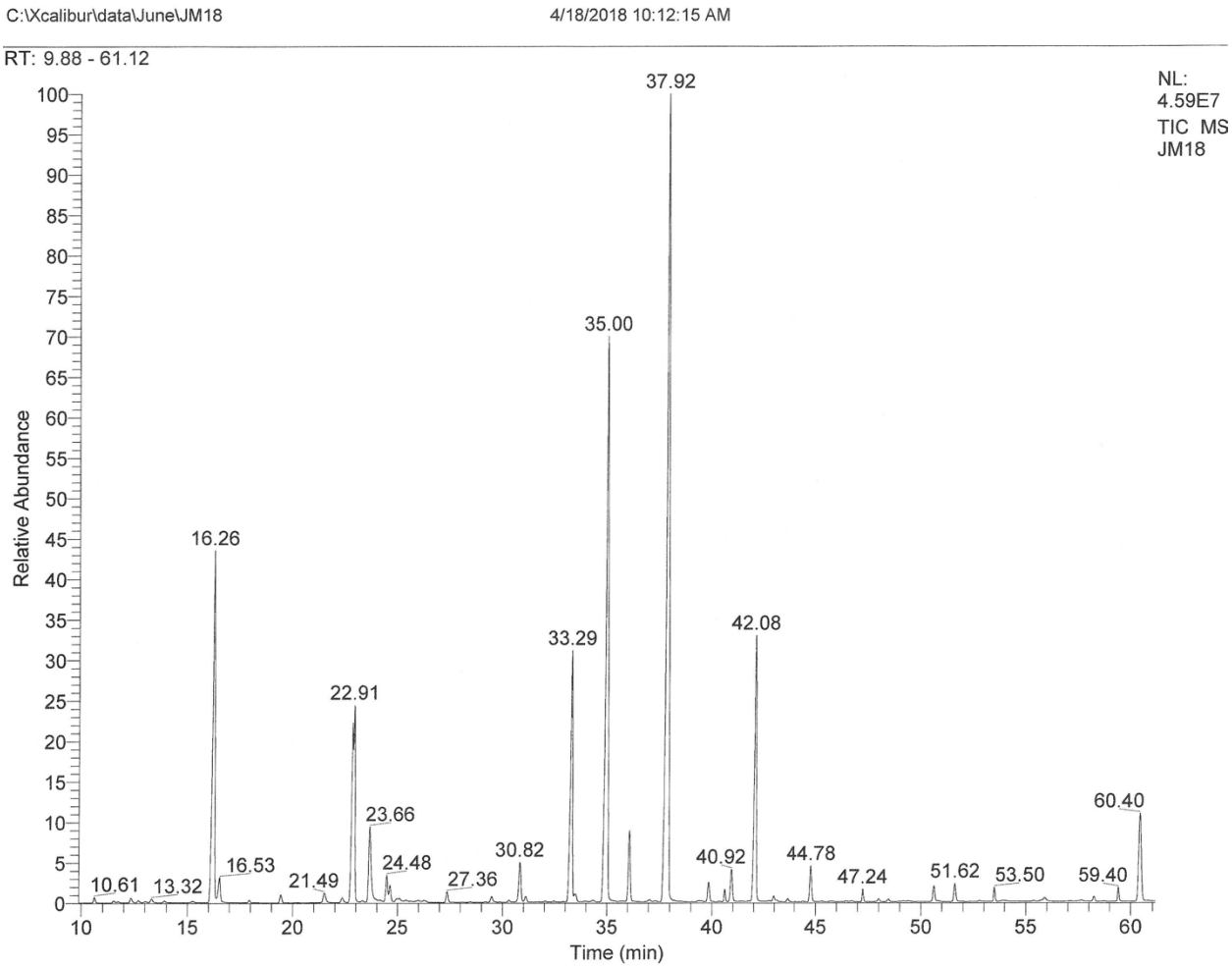

12.3.1.3. Treatment 1, Standard MAM, Day 52

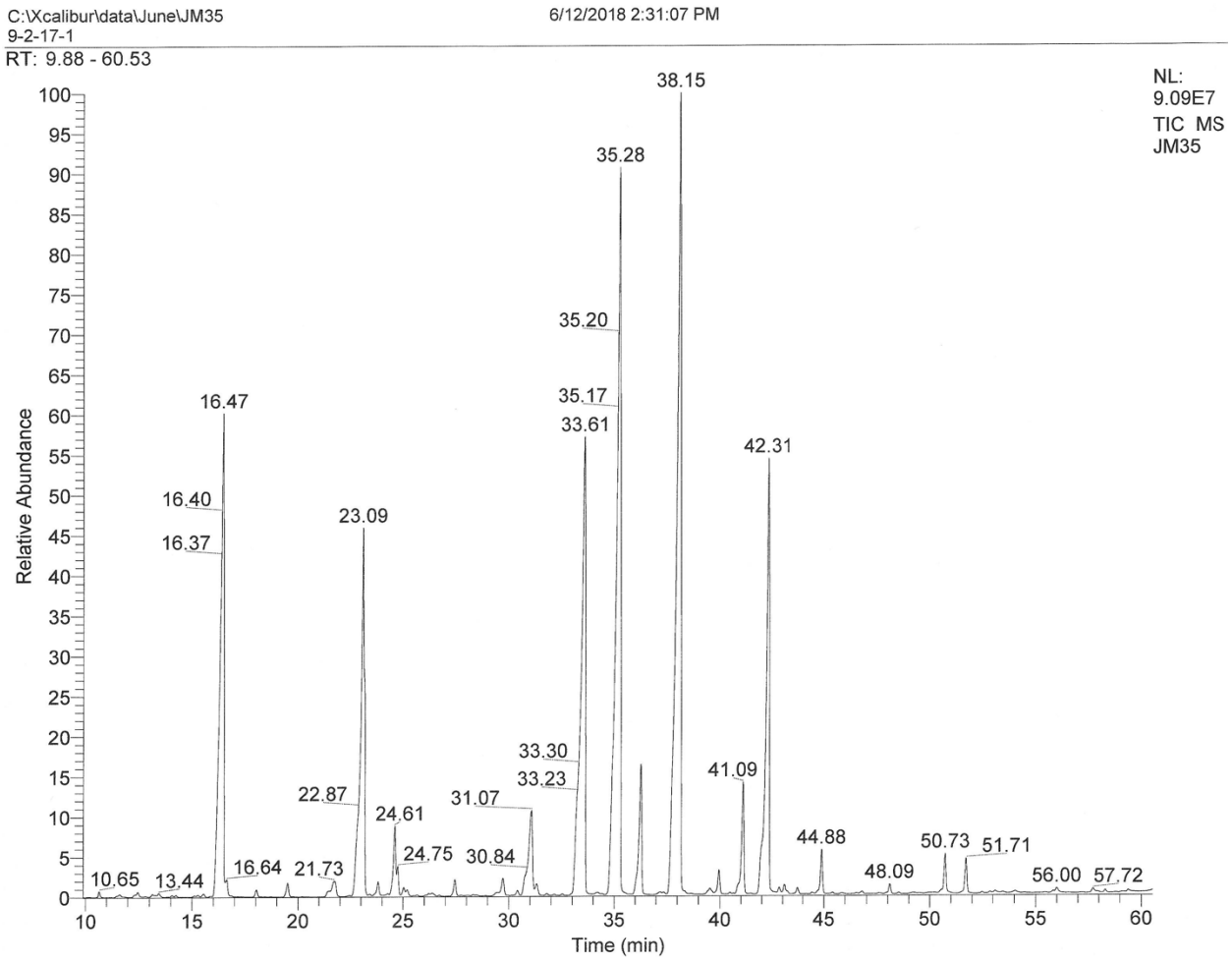

12.3.2. Treatment 2, Low Nitrogen

12.3.2.1. Treatment 2, Low Nitrogen, Day 6

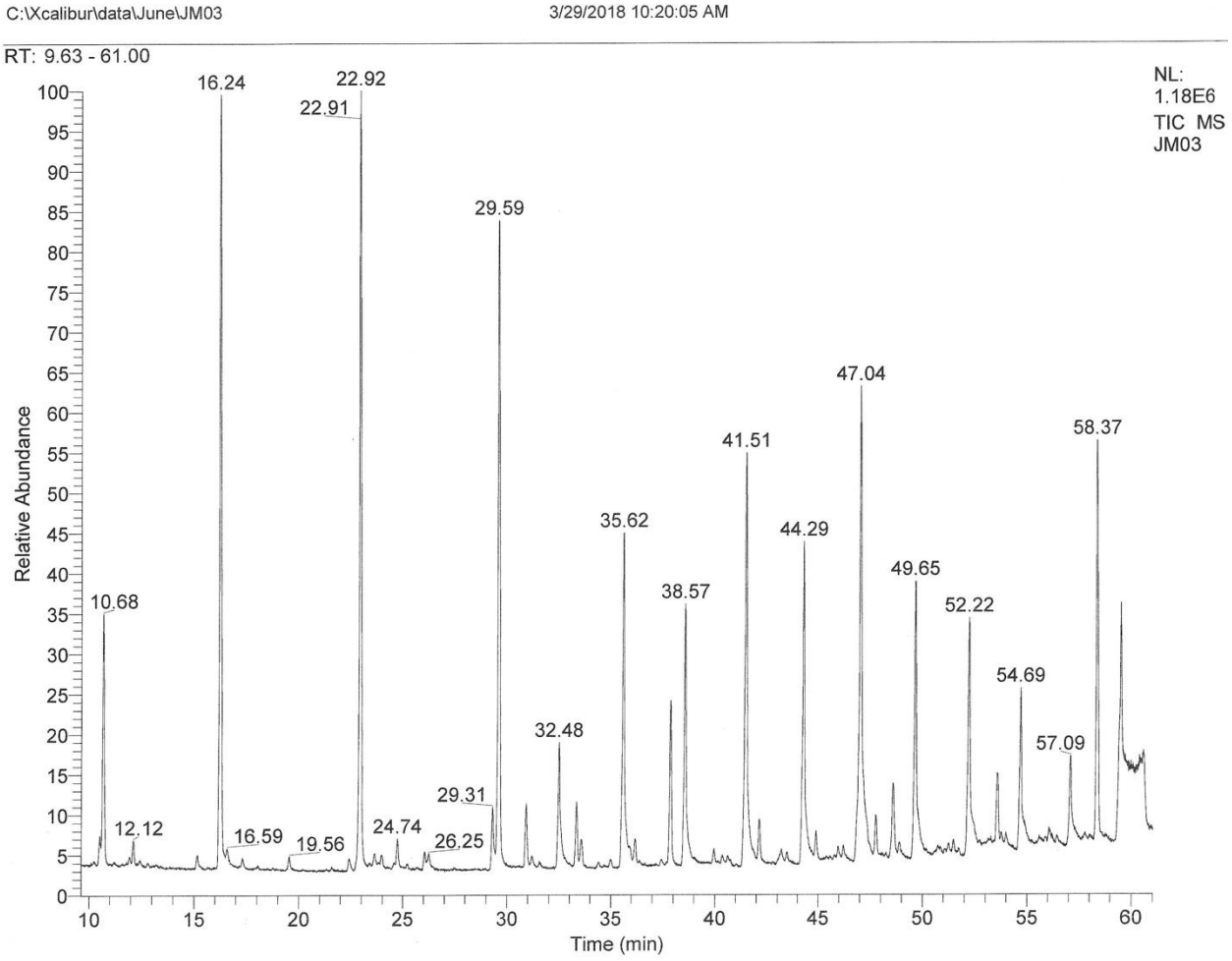

12.3.2.2. Treatment 2, Low Nitrogen, Day 9

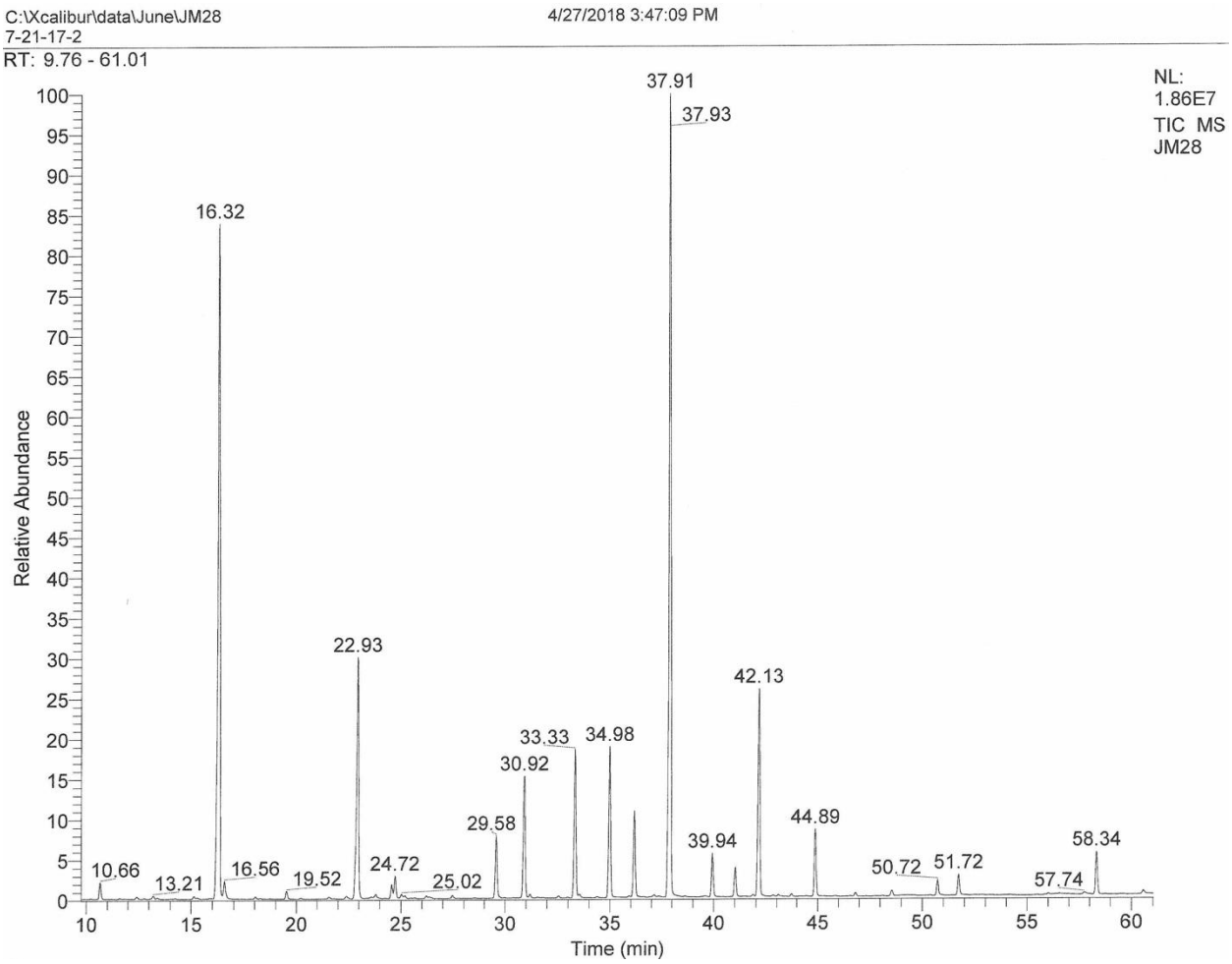

12.3.2.3. Treatment 2, Low Nitrogen, Day 19

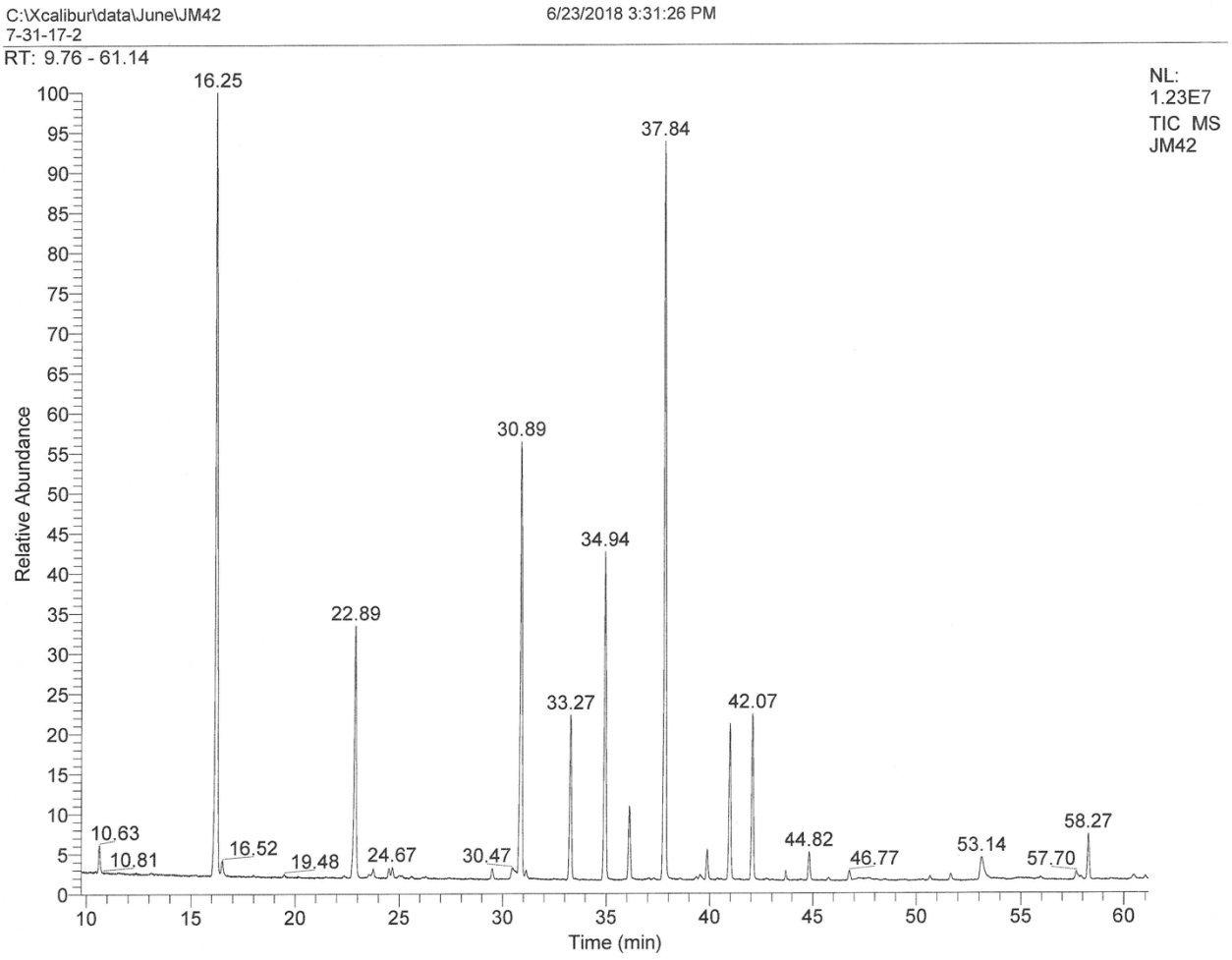

12.3.2.4. Treatment 2, Low Nitrogen, Day 27

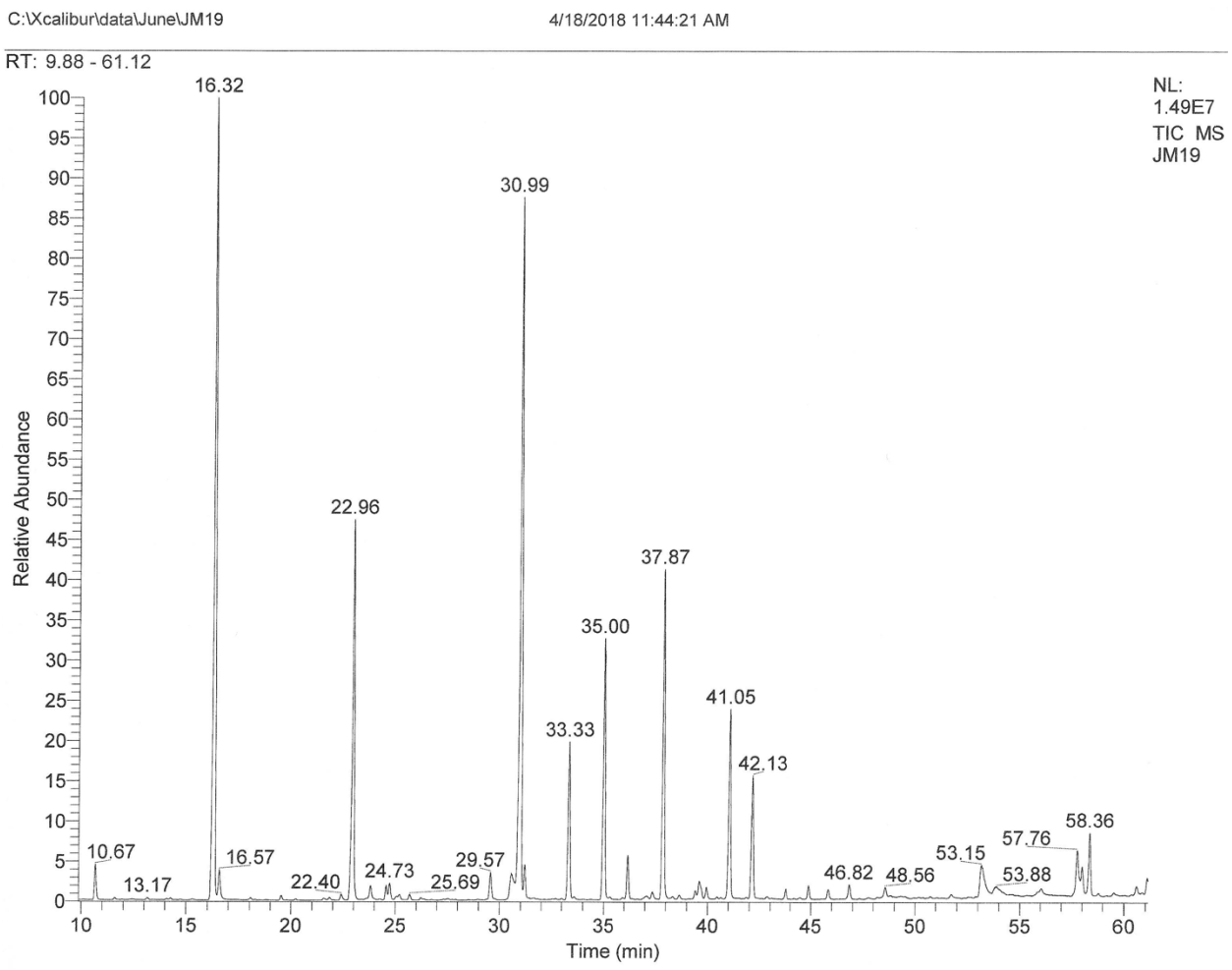

12.3.2.5. Treatment 2, Low Nitrogen, Day 52

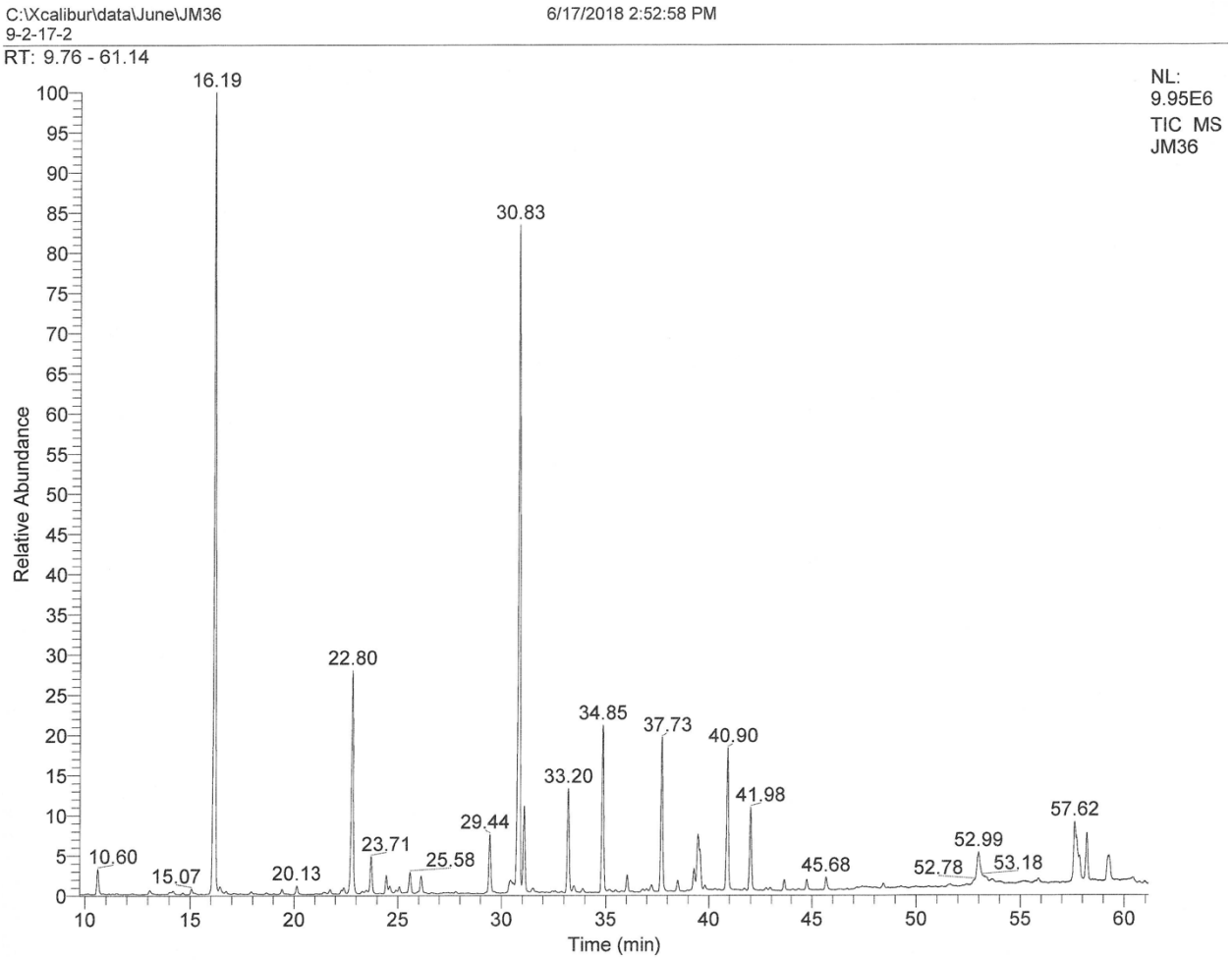

12.3.3. Treatment 3, Low Phosphorus

12.3.3.1. Treatment 3, Low Phosphorus, Day 6

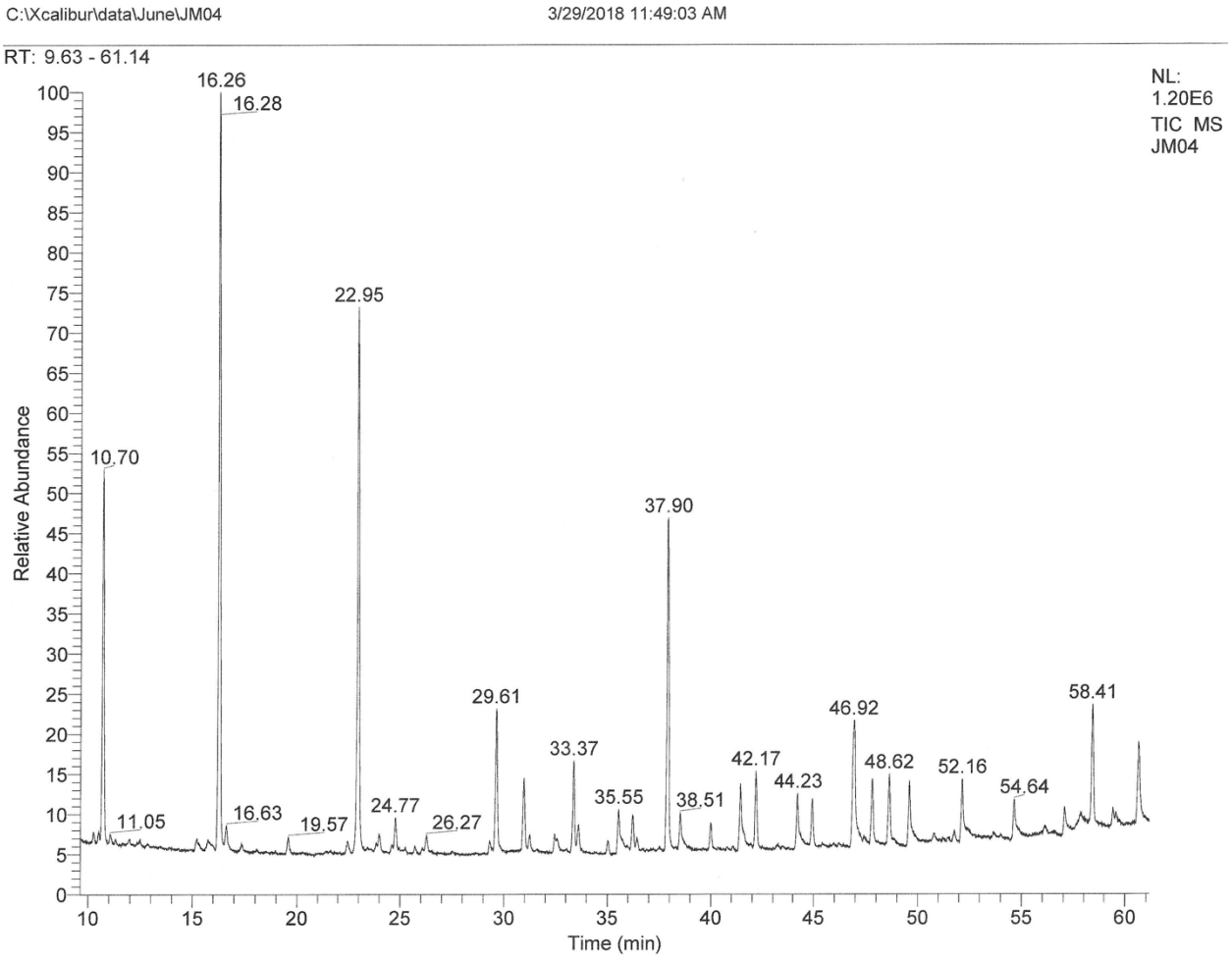

12.3.3.2. Treatment 3, Low Phosphorus, Day 9

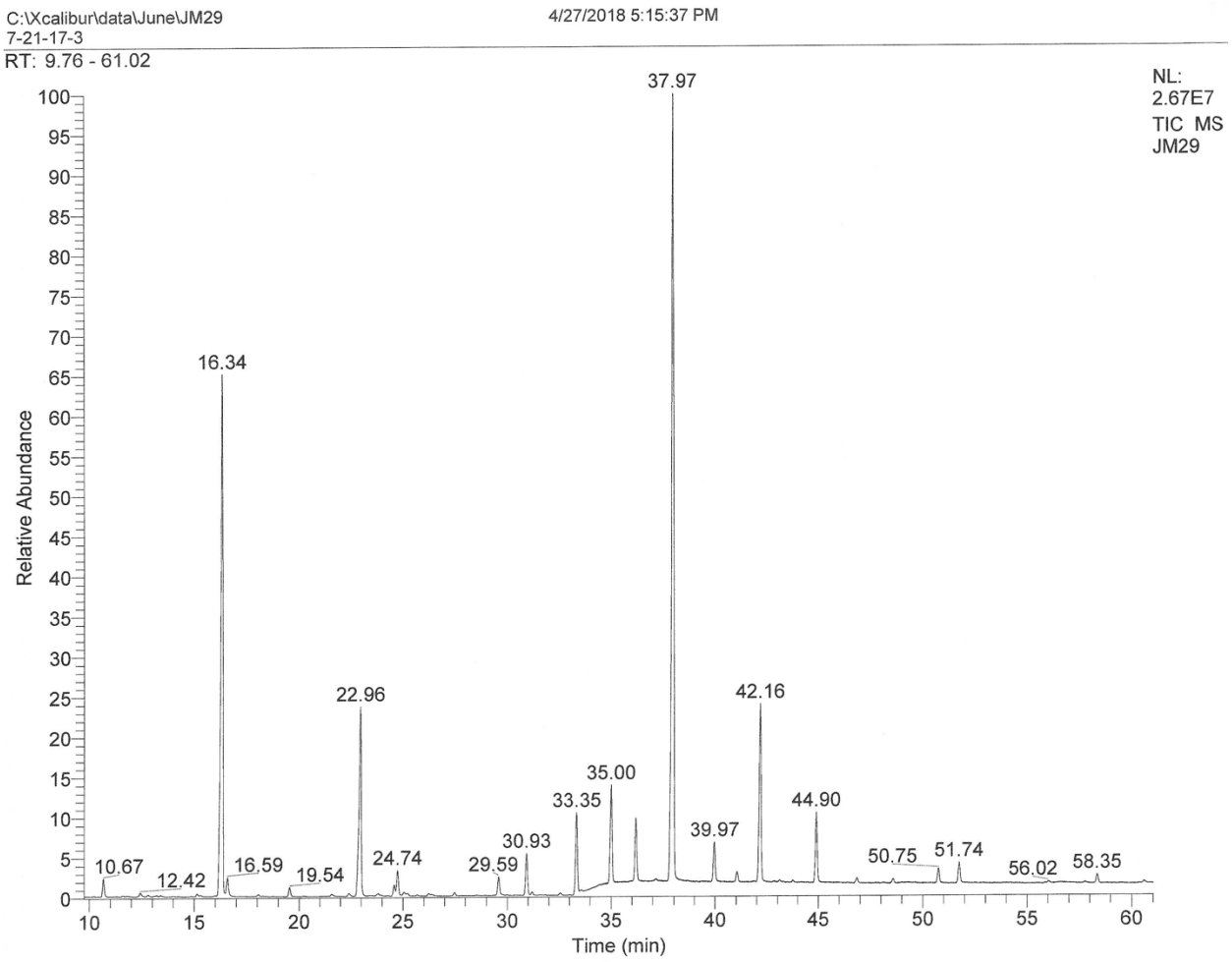

12.3.3.3. Treatment 3, Low Phosphorus, Day 19

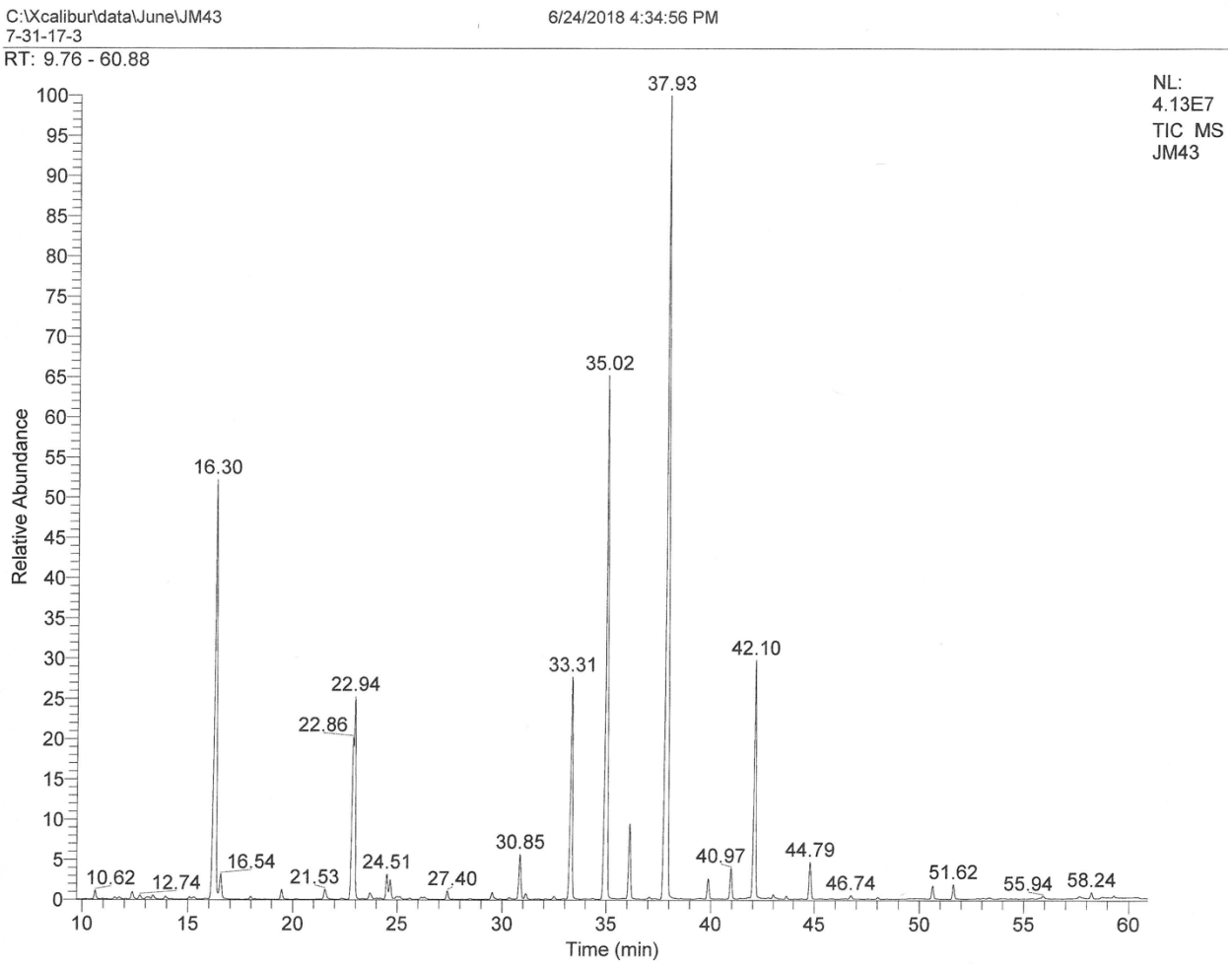

12.3.3.4. Treatment 3, Low Phosphorus, Day 27

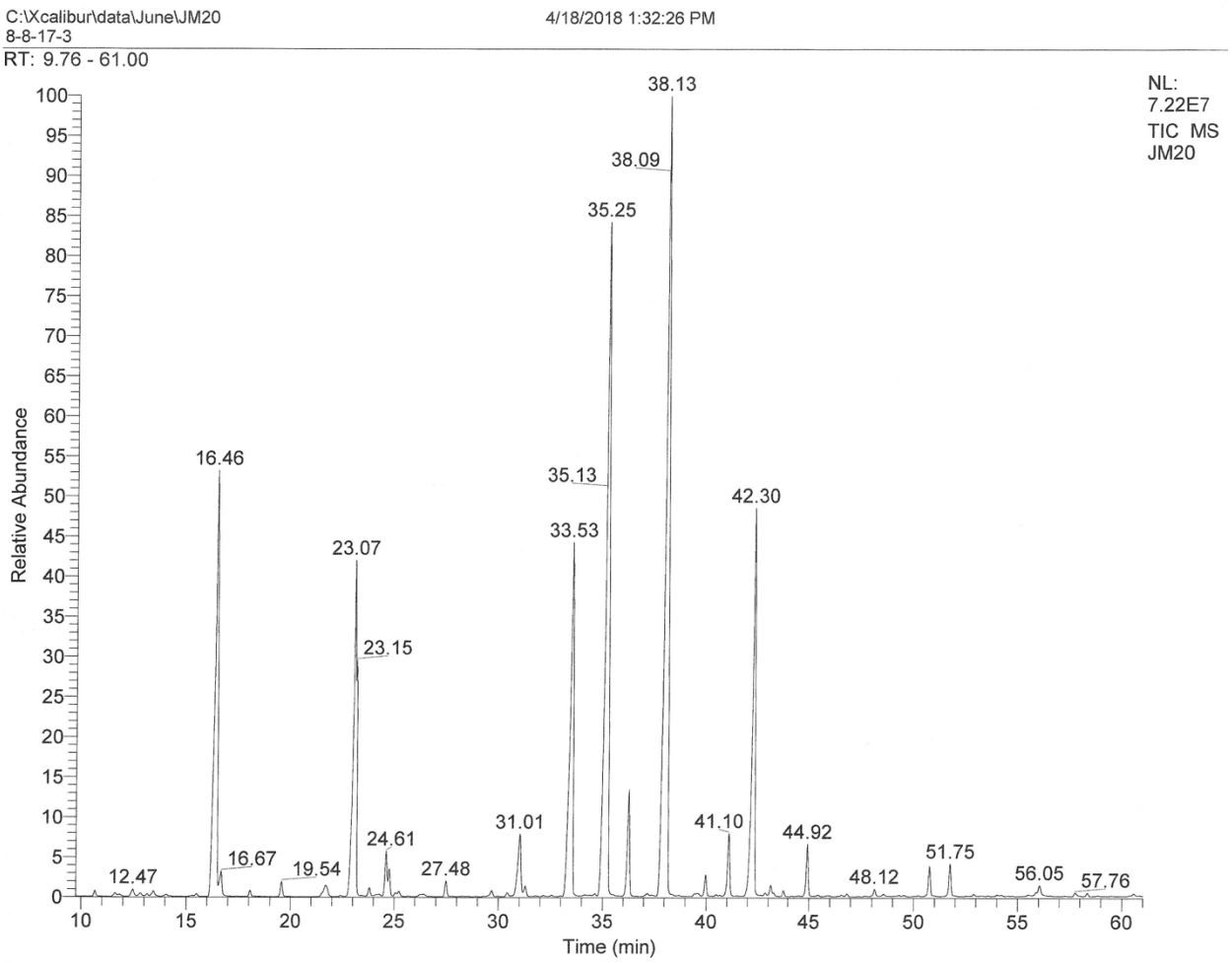

12.3.3.5. Treatment 3, Low Phosphorus, Day 52

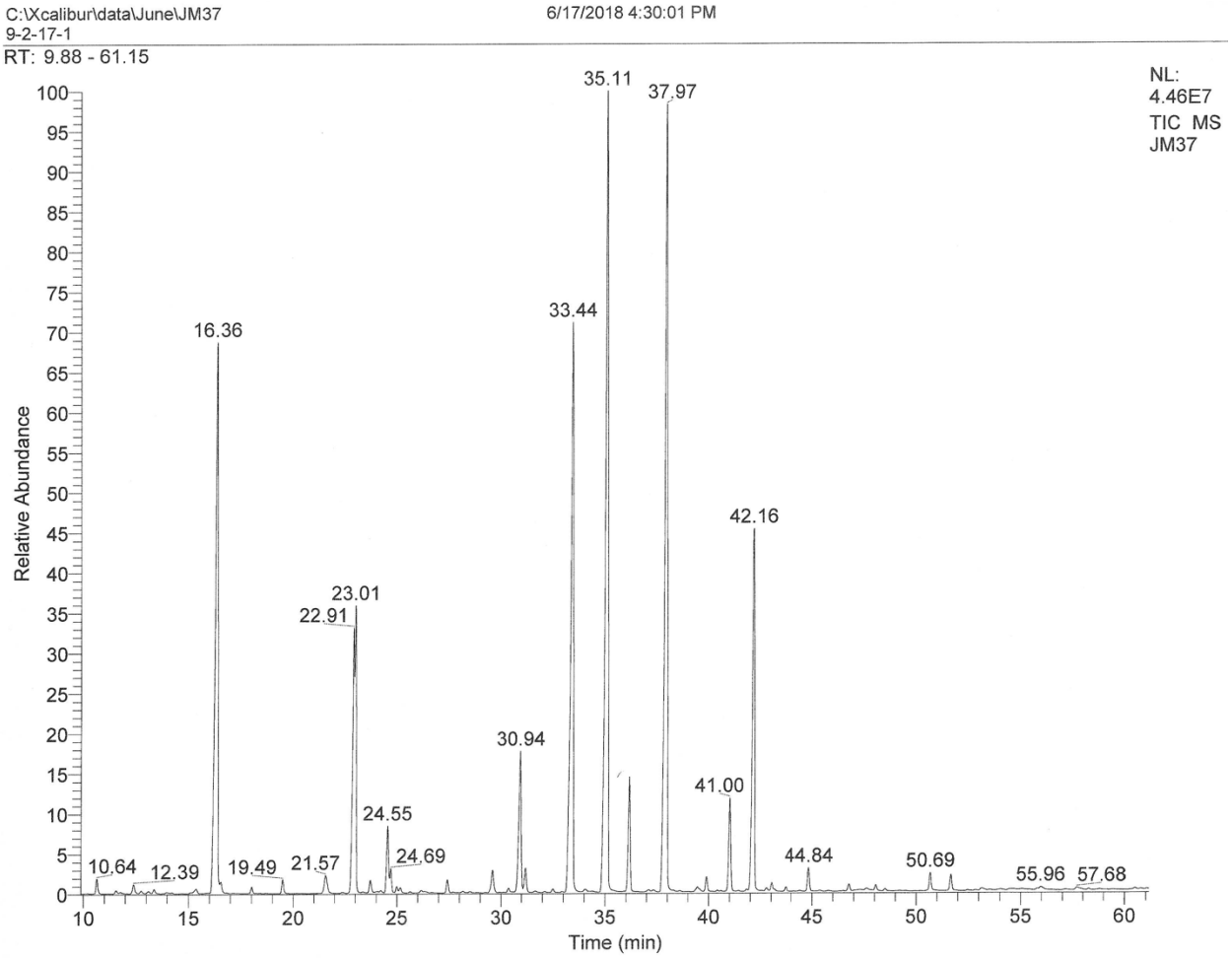

12.3.4. Treatment 4, Low Nitrogen and Low Phosphorus

12.3.4.1. Treatment 4, Low Nitrogen and Low Phosphorus, Day 6

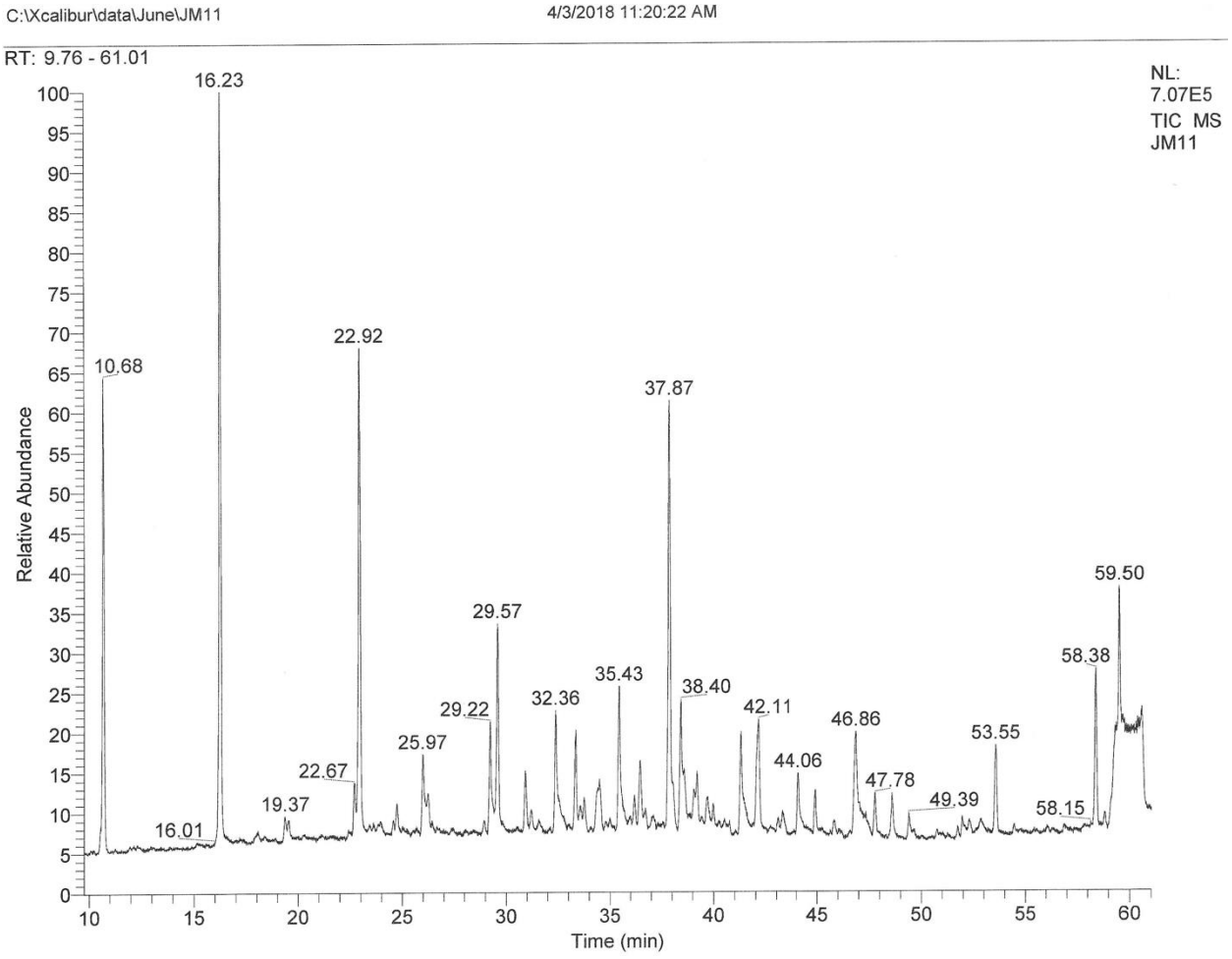

12.3.4.2. Treatment 4, Low Nitrogen and Low Phosphorus, Day 9

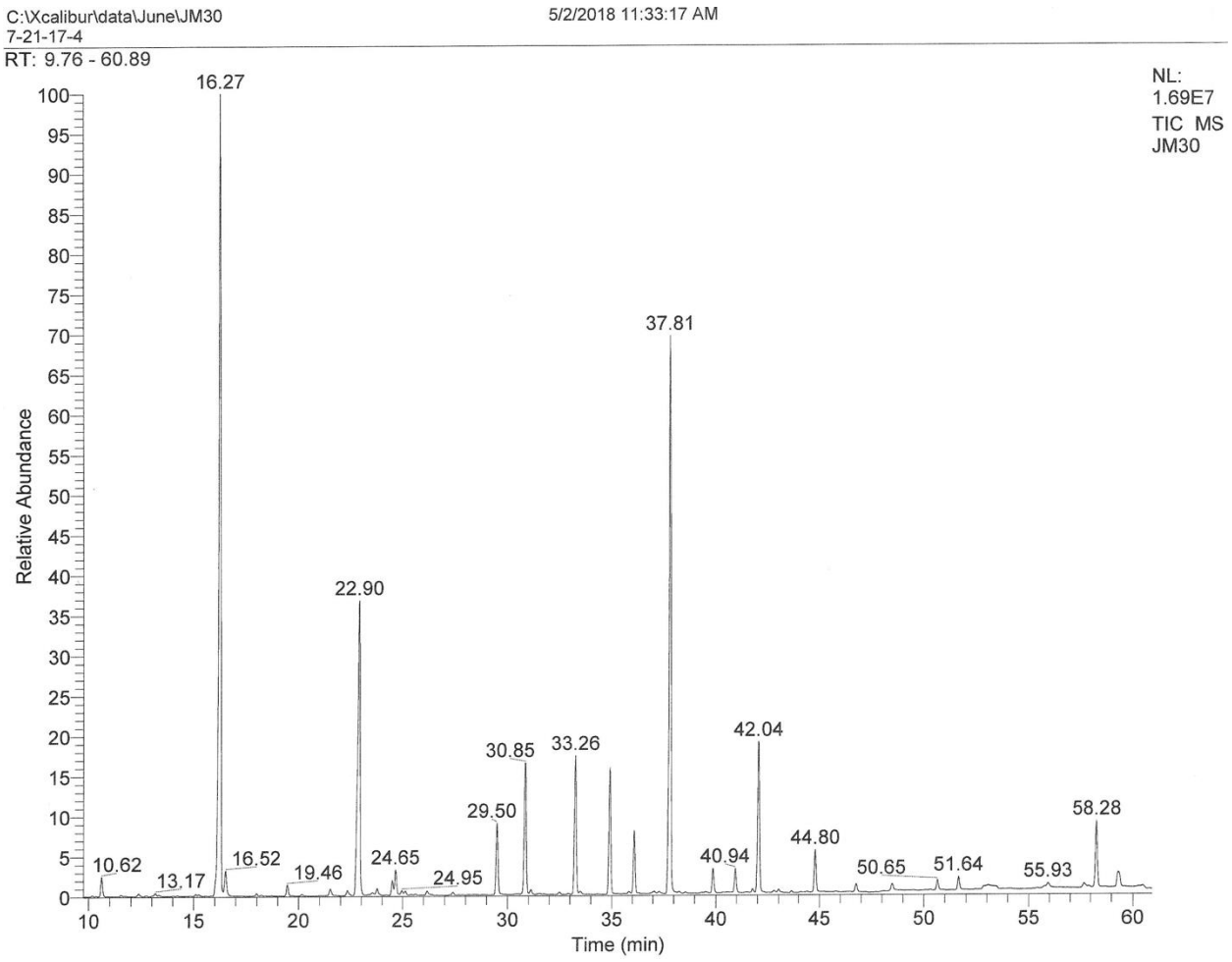

12.3.4.3. Treatment 4, Low Nitrogen and Low Phosphorus, Day 19

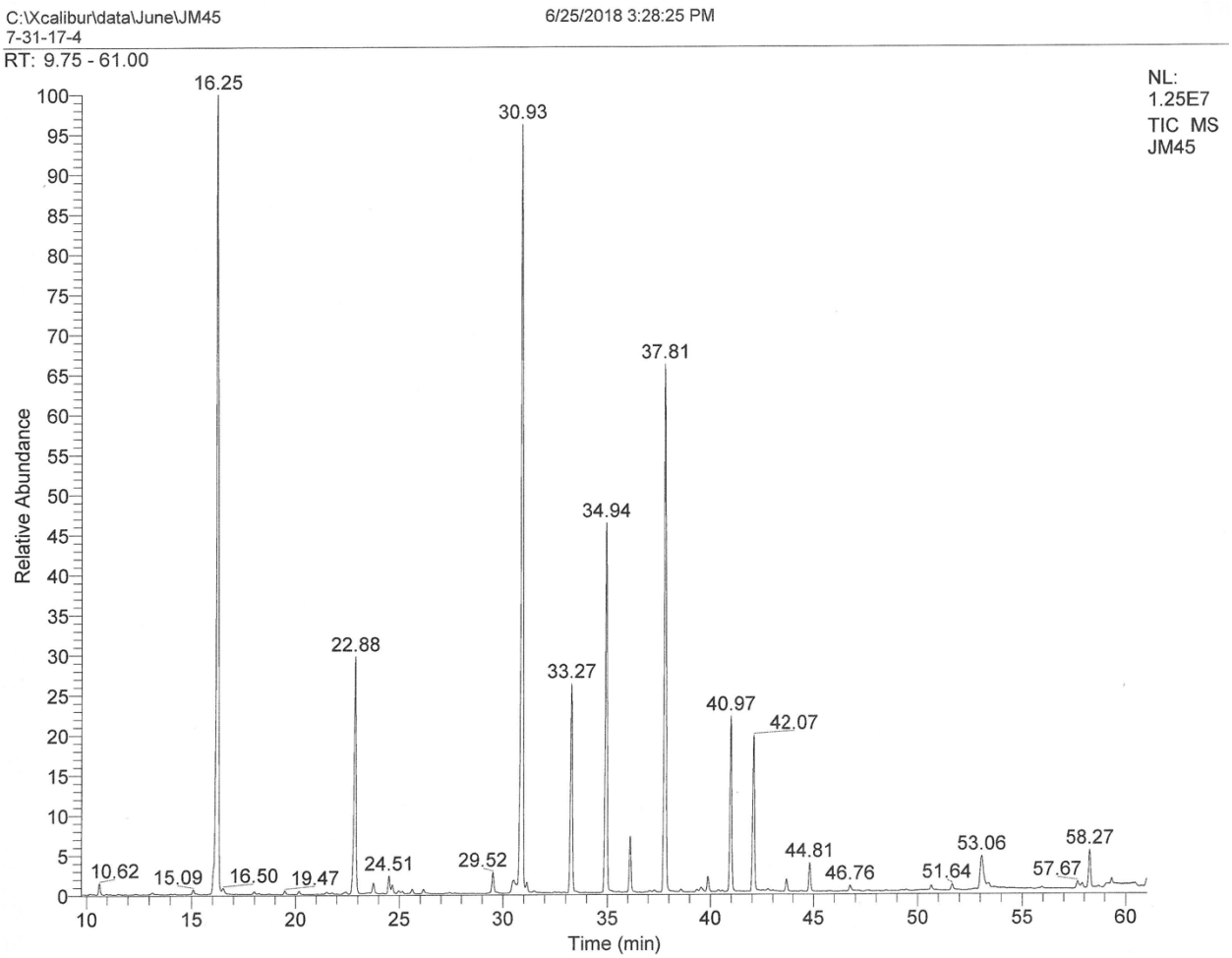

12.3.4.4. Treatment 4, Low Nitrogen and Low Phosphorus, Day 27 A

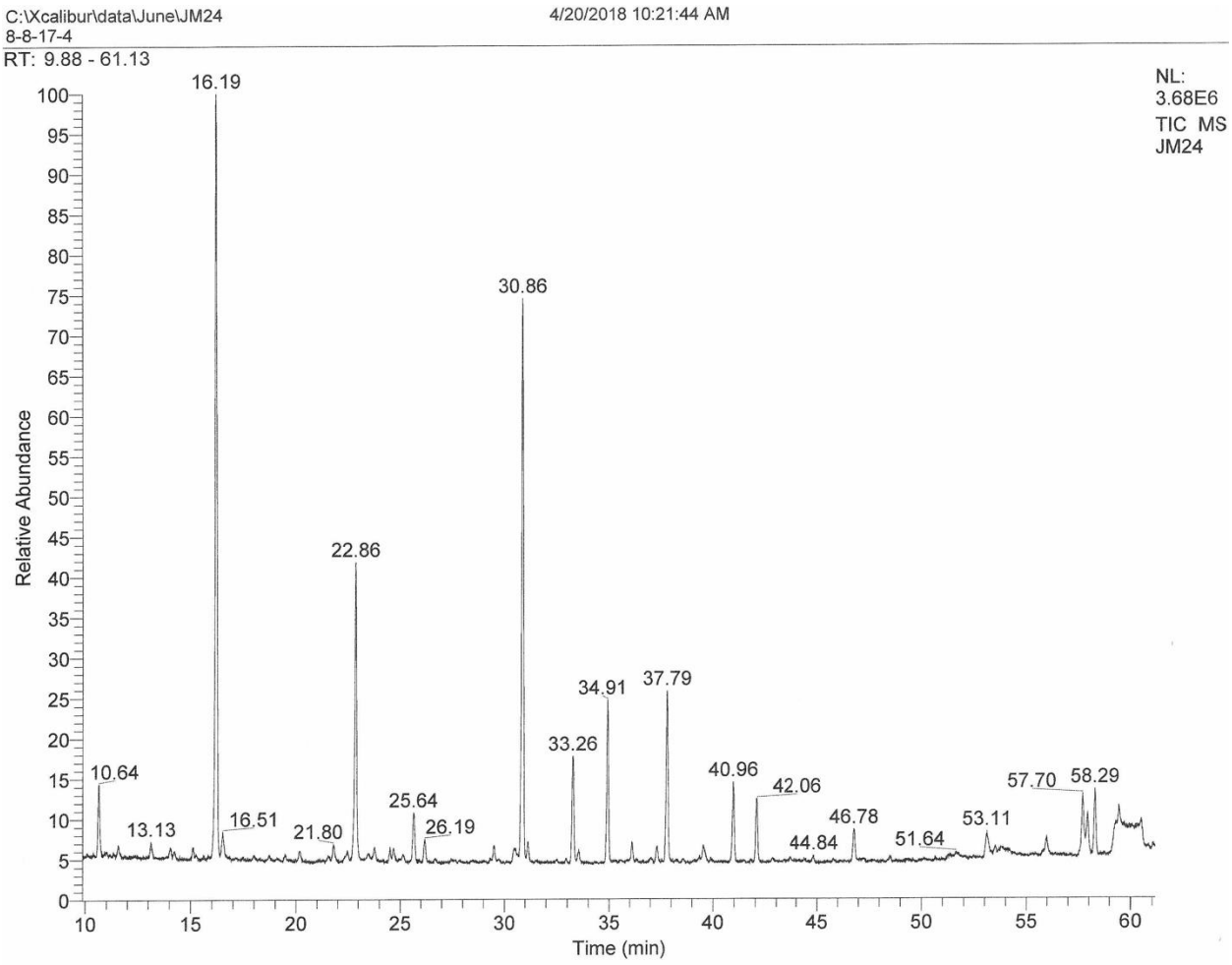

12.3.4.5. Treatment 4, Low Nitrogen and Low Phosphorus, Day 27 B

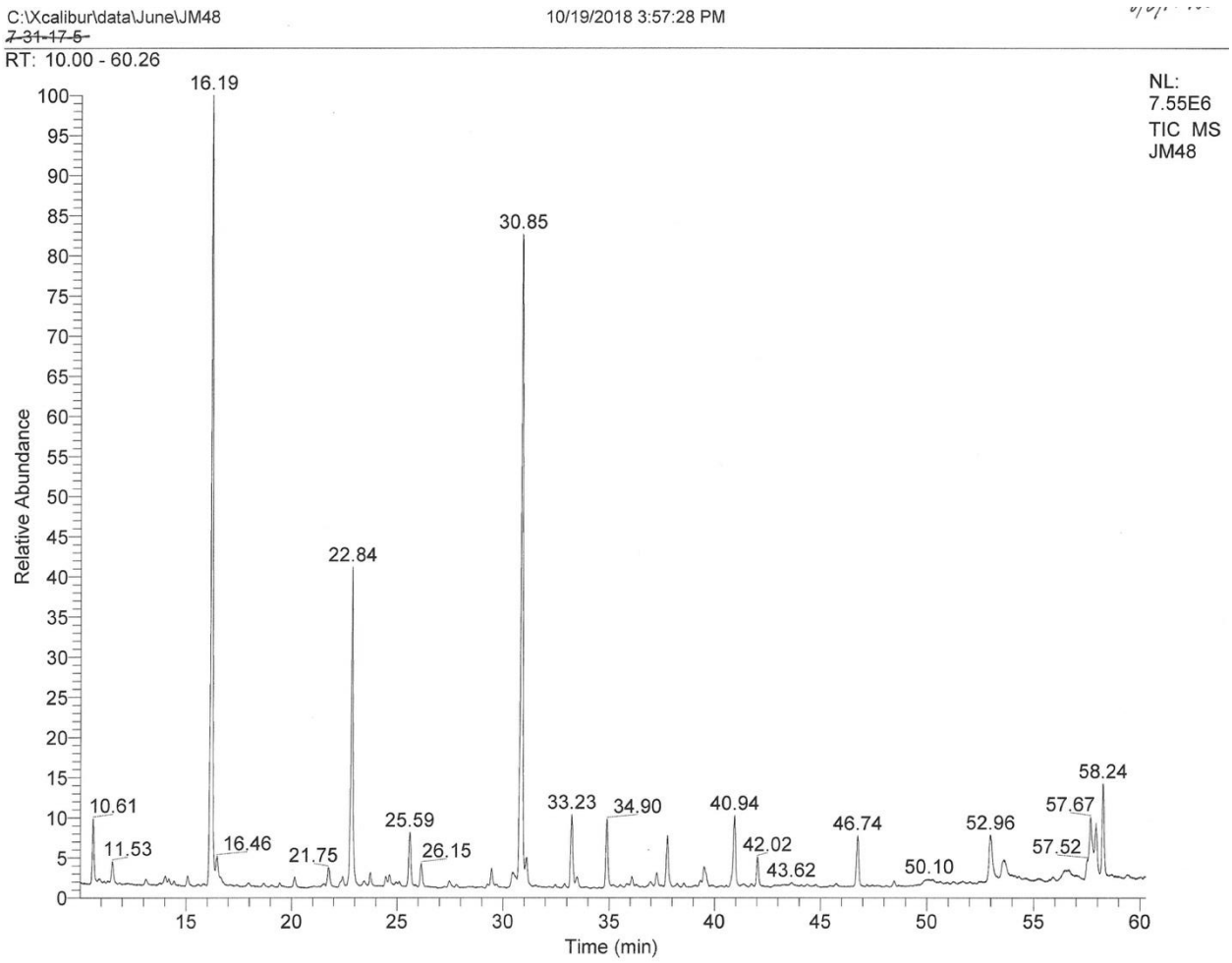

12.3.4.6. Treatment 4, Low Nitrogen and Low Phosphorus, Day 27 C

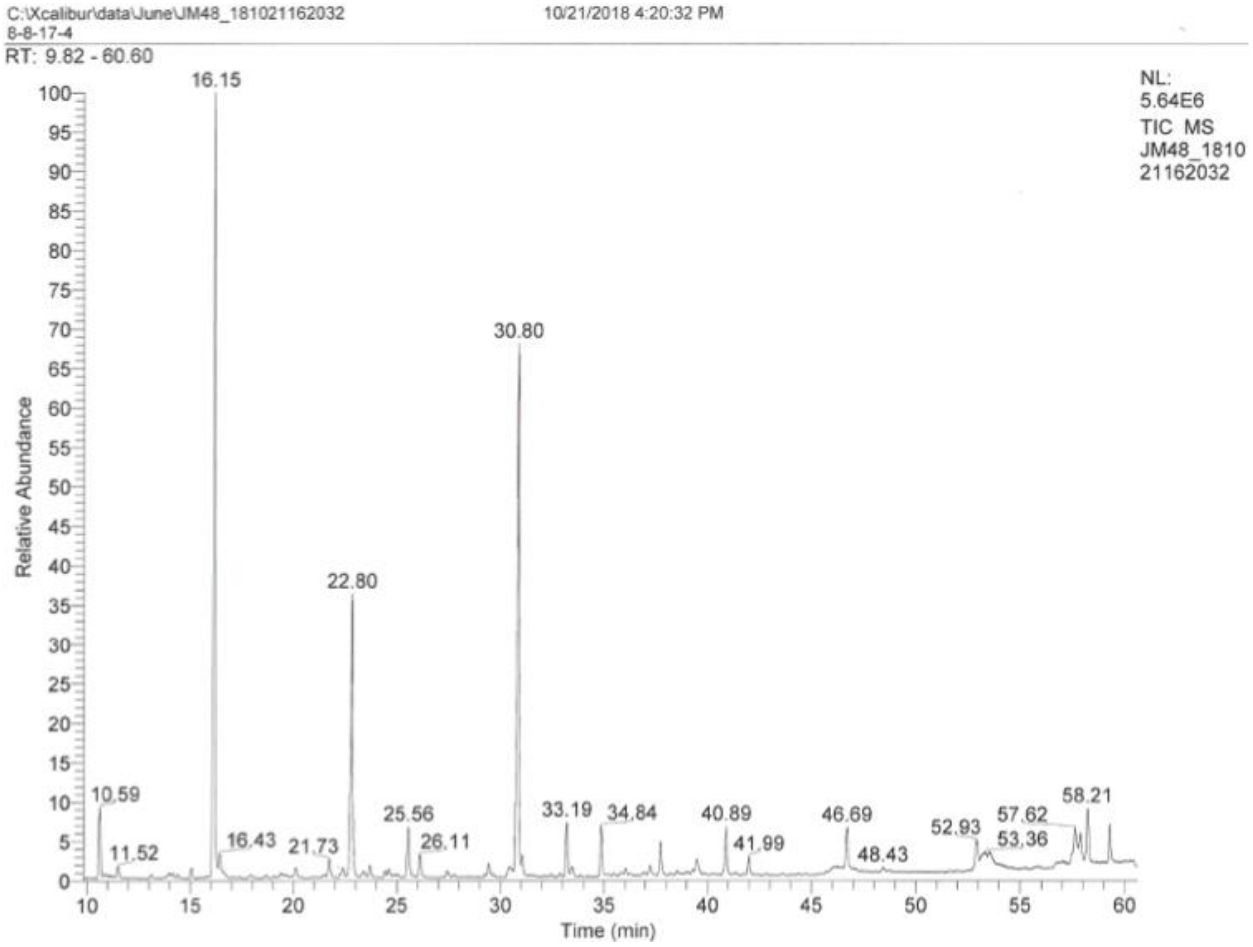

12.3.4.7. Treatment 4, Low Nitrogen and Low Phosphorus, Day 52

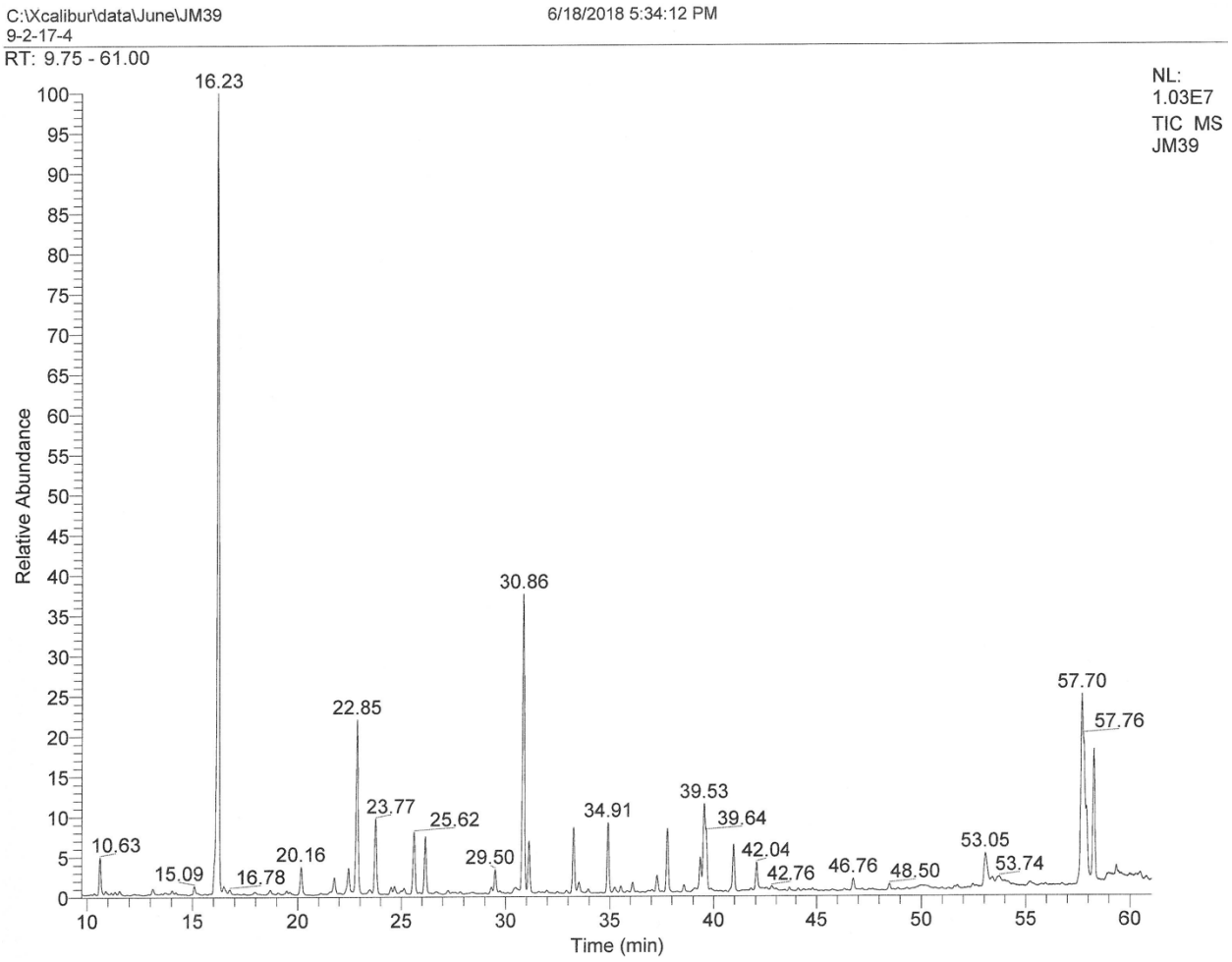

12.3.5. Treatment 5, Low Nitrogen, Low Phosphorus + CO_2

12.3.5.1. Treatment 5, Low Nitrogen, Low Phosphorus + CO_2, Day 6

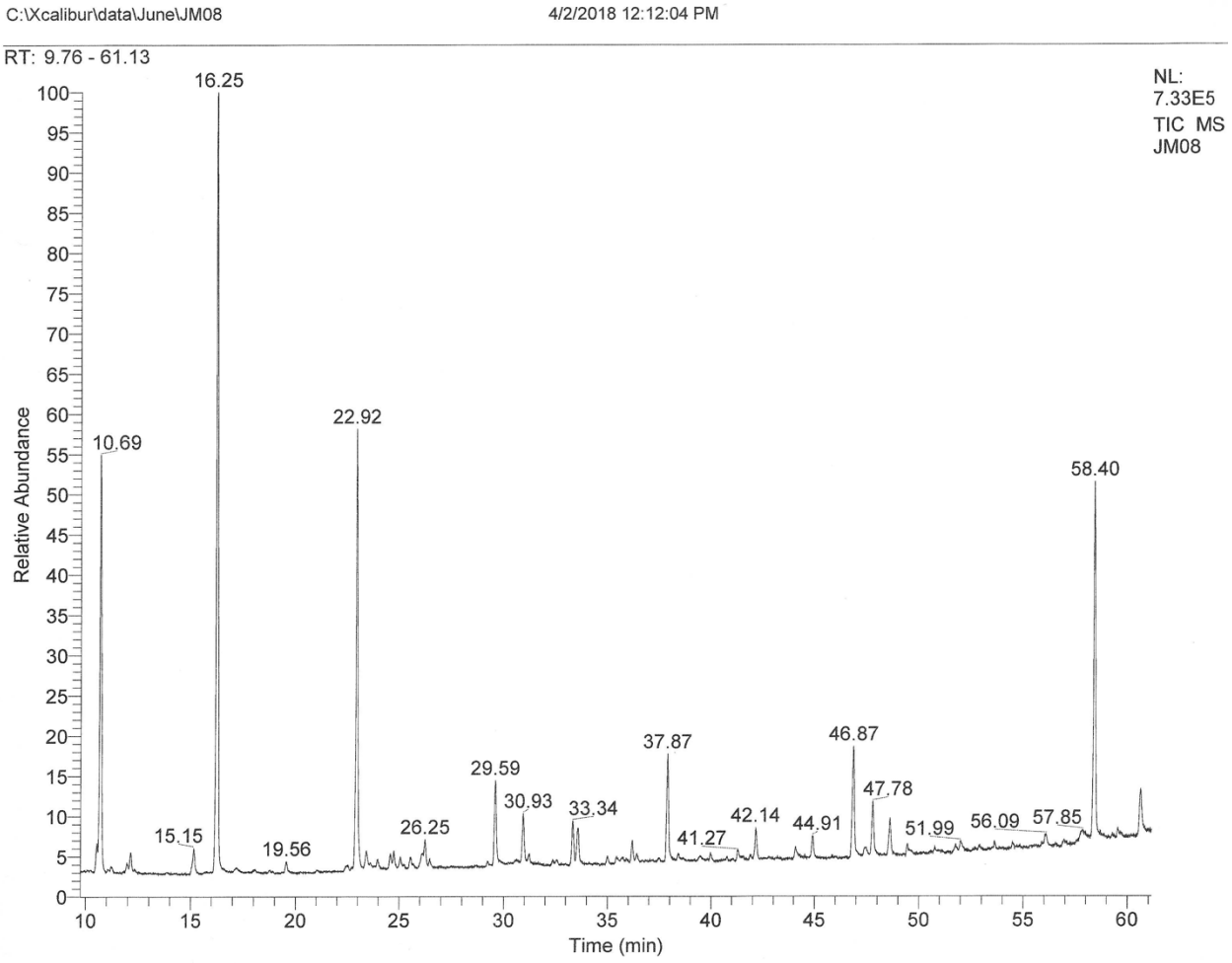

12.3.5.2. Treatment 5, Low Nitrogen, Low Phosphorus + CO_2, Day 9

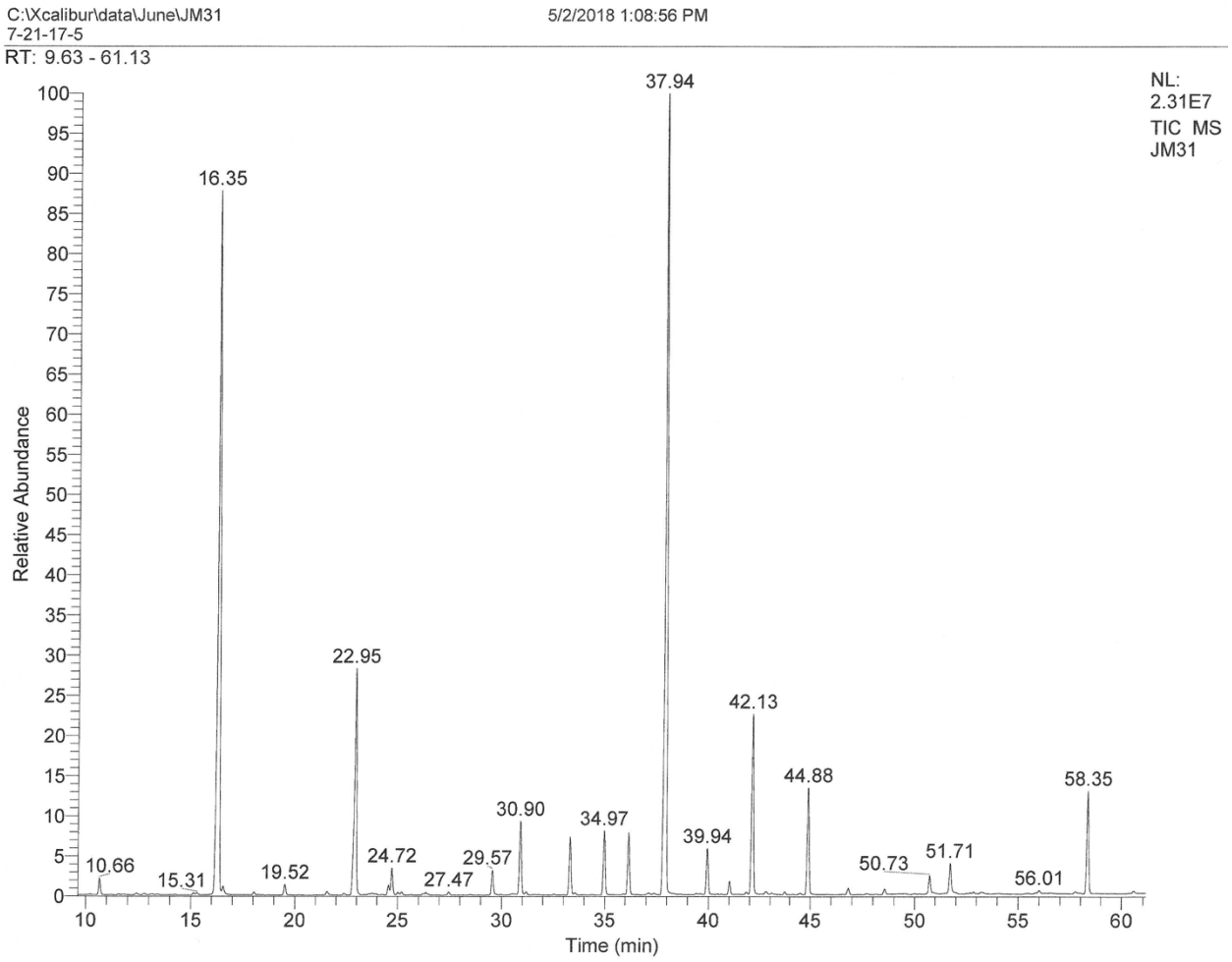

12.3.5.3. Treatment 5, Low Nitrogen, Low Phosphorus + CO_2, Day 15 A

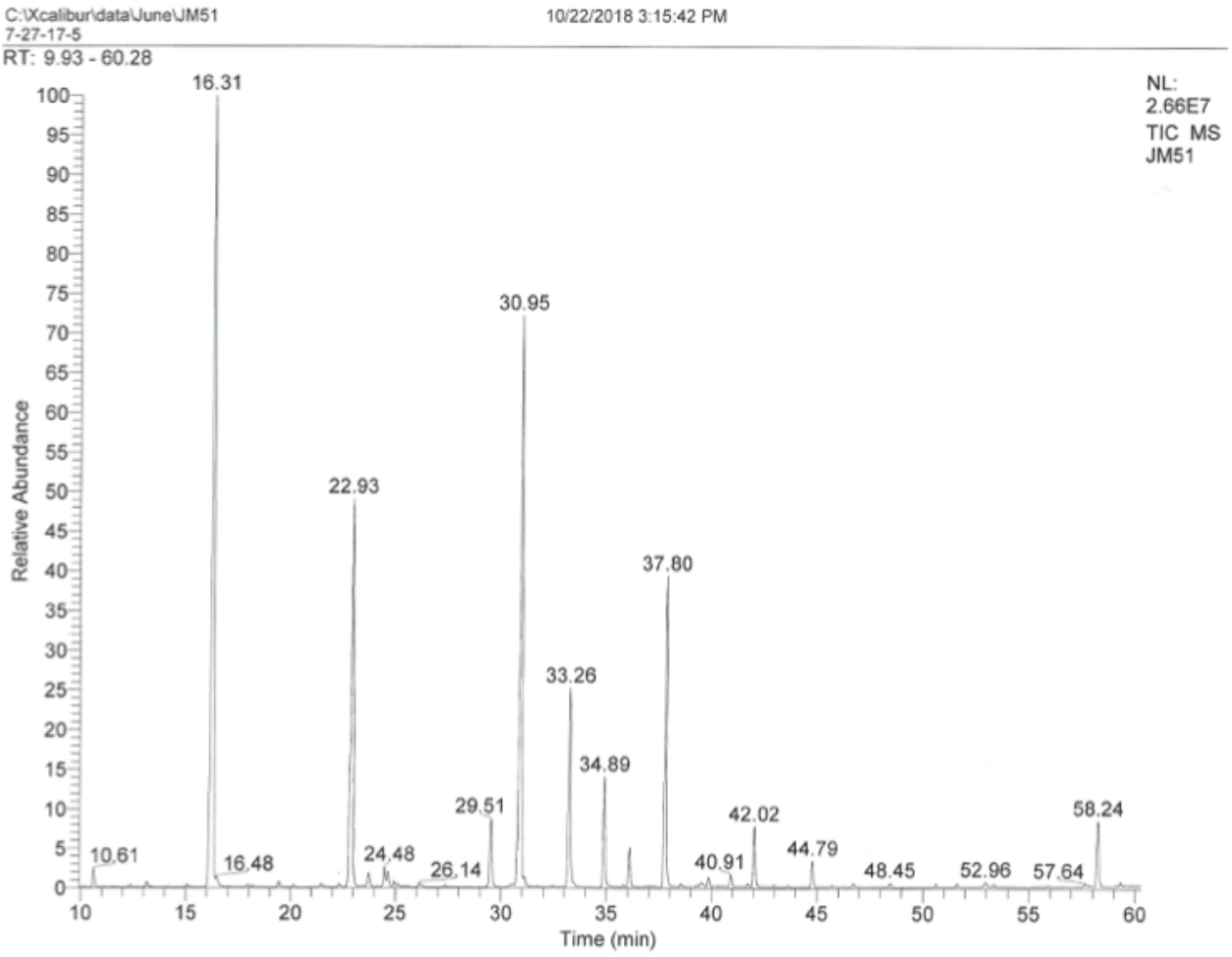

12.3.5.4. Treatment 5, Low Nitrogen, Low Phosphorus + CO_2, Day 15 B

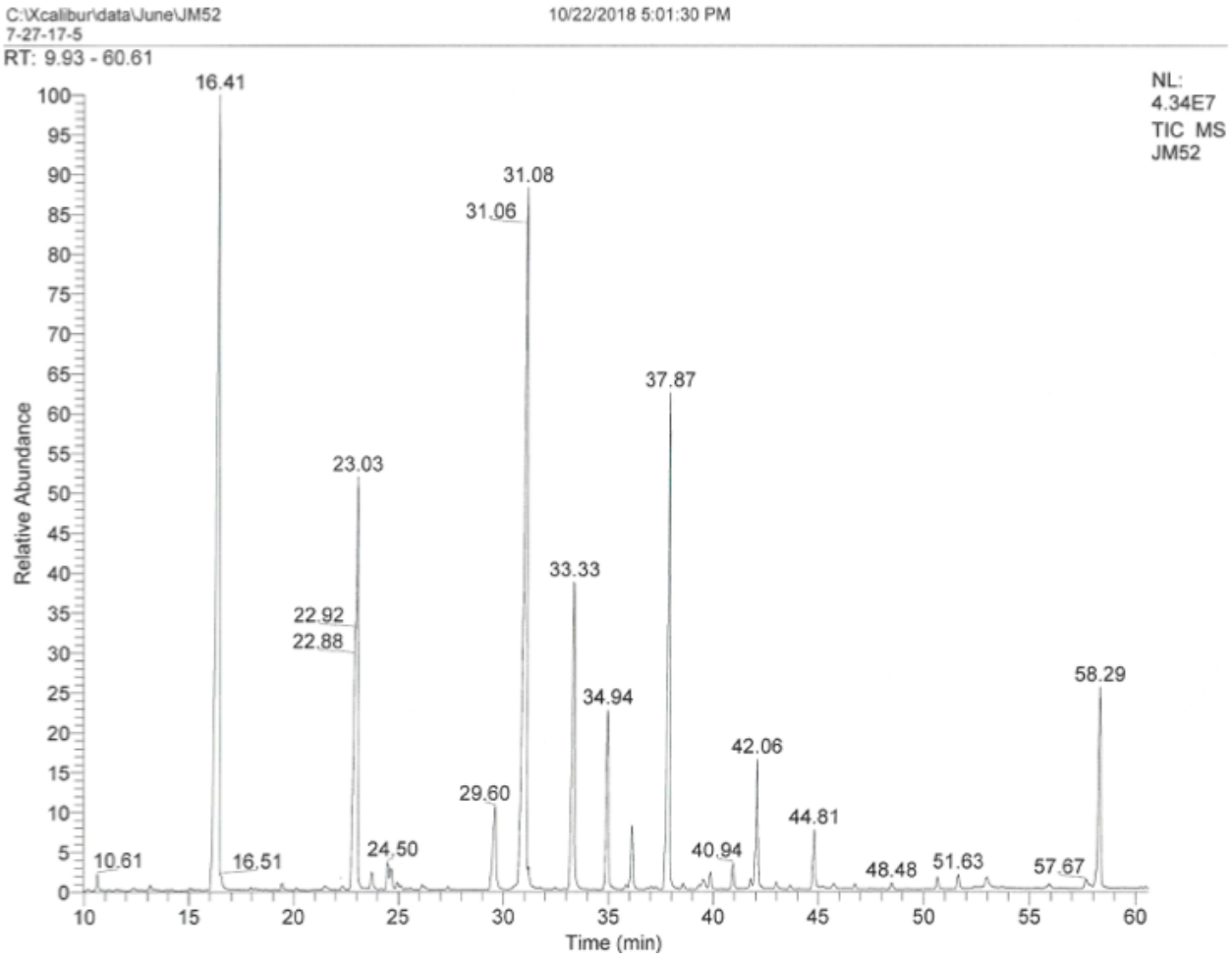

12.3.5.5. Treatment 5, Low Nitrogen, Low Phosphorus + CO_2, Day 15 C

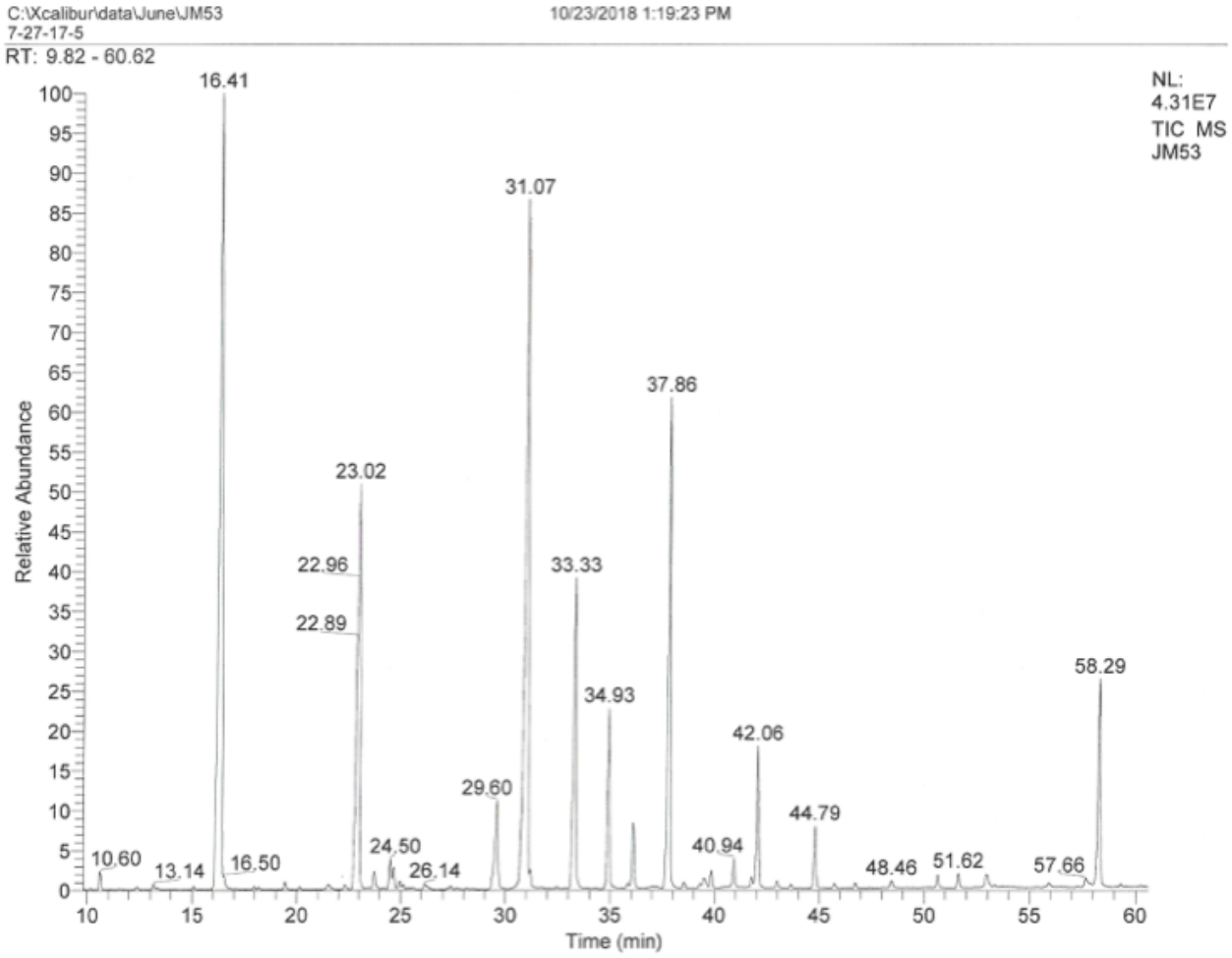

12.3.5.6. Treatment 5, Low Nitrogen, Low Phosphorus + CO_2, Day 19 A

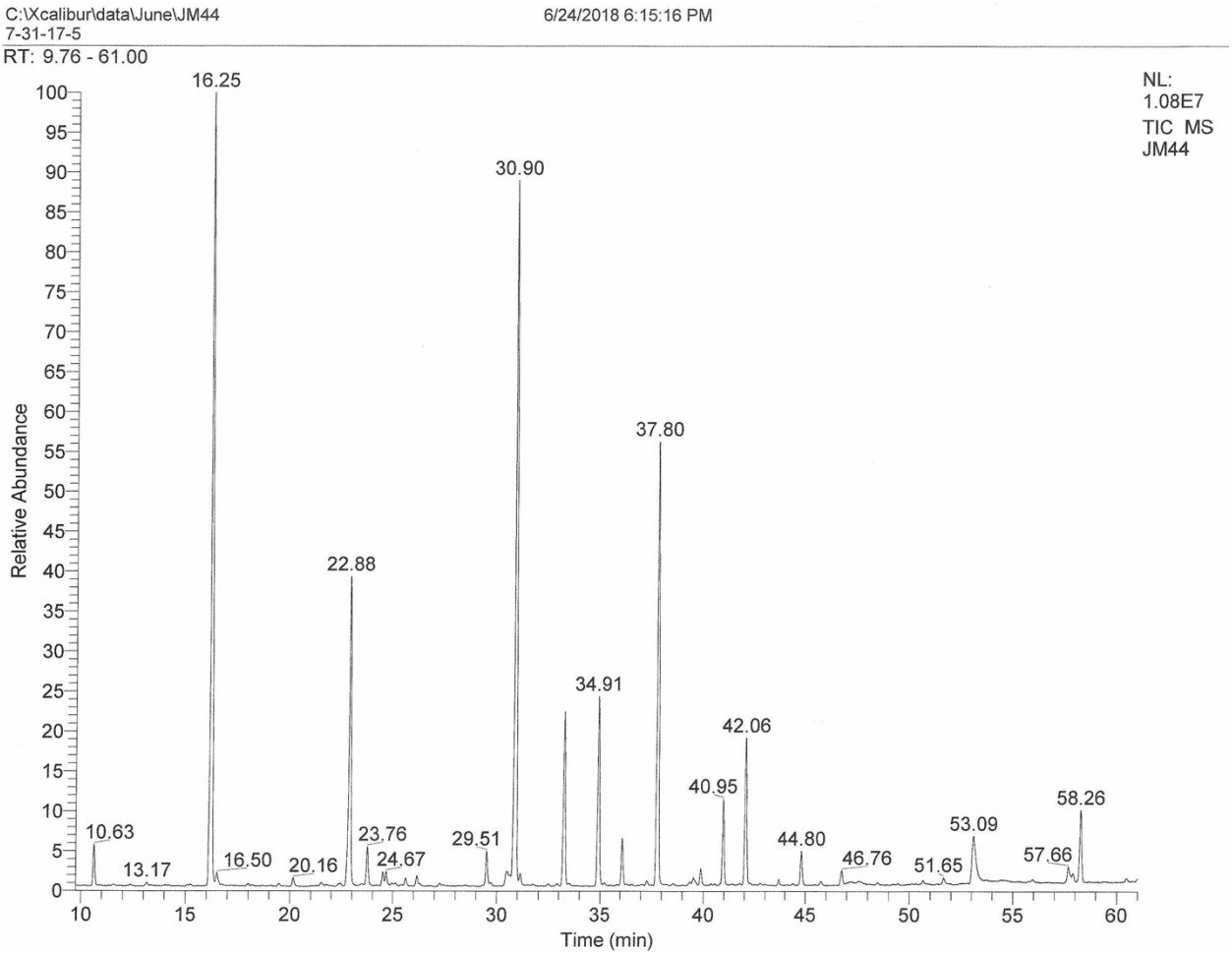

12.3.5.7. Treatment 5, Low Nitrogen, Low Phosphorus + CO_2, Day 19 B

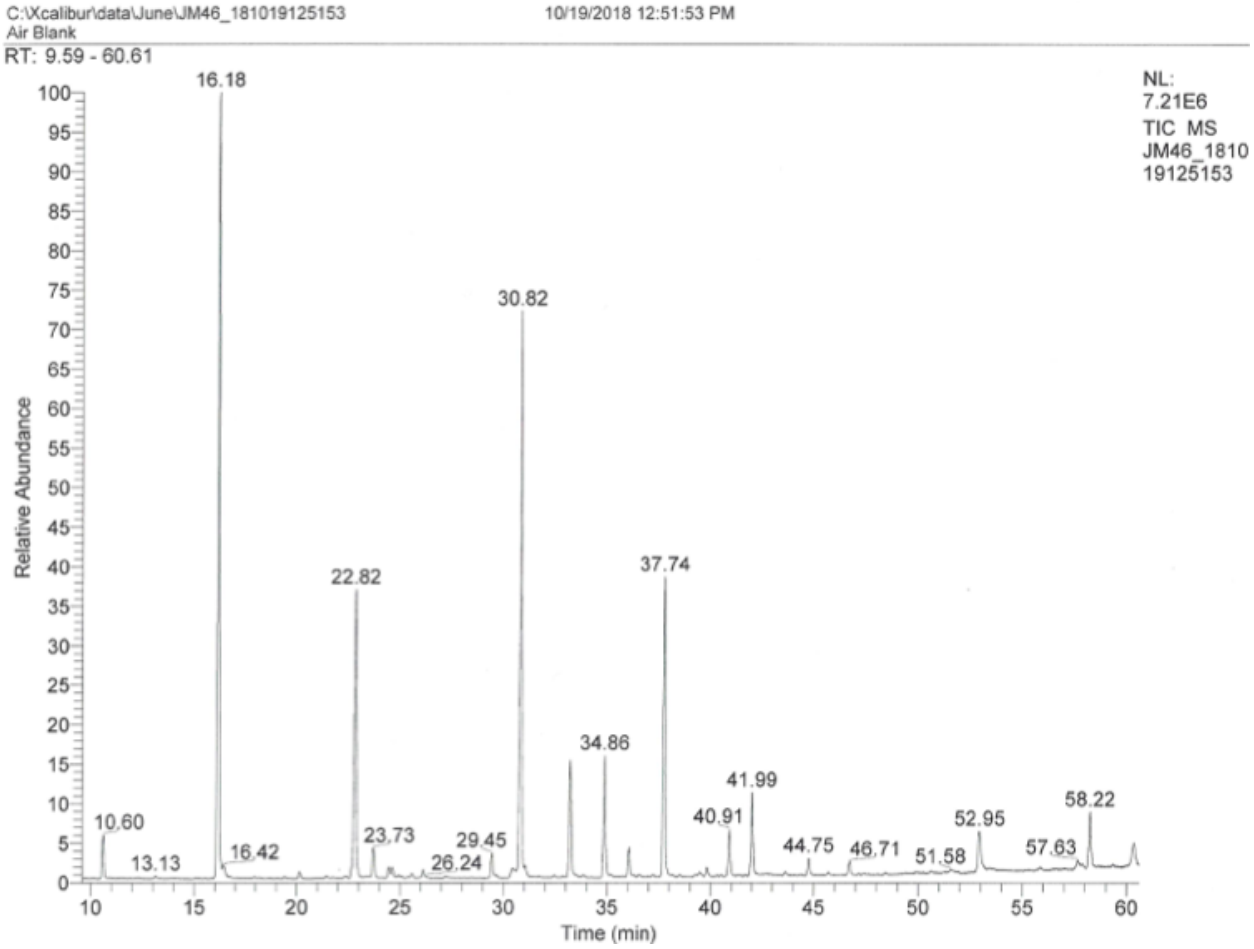

12.3.5.8. Treatment 5, Low Nitrogen, Low Phosphorus + CO_2, Day 19 C

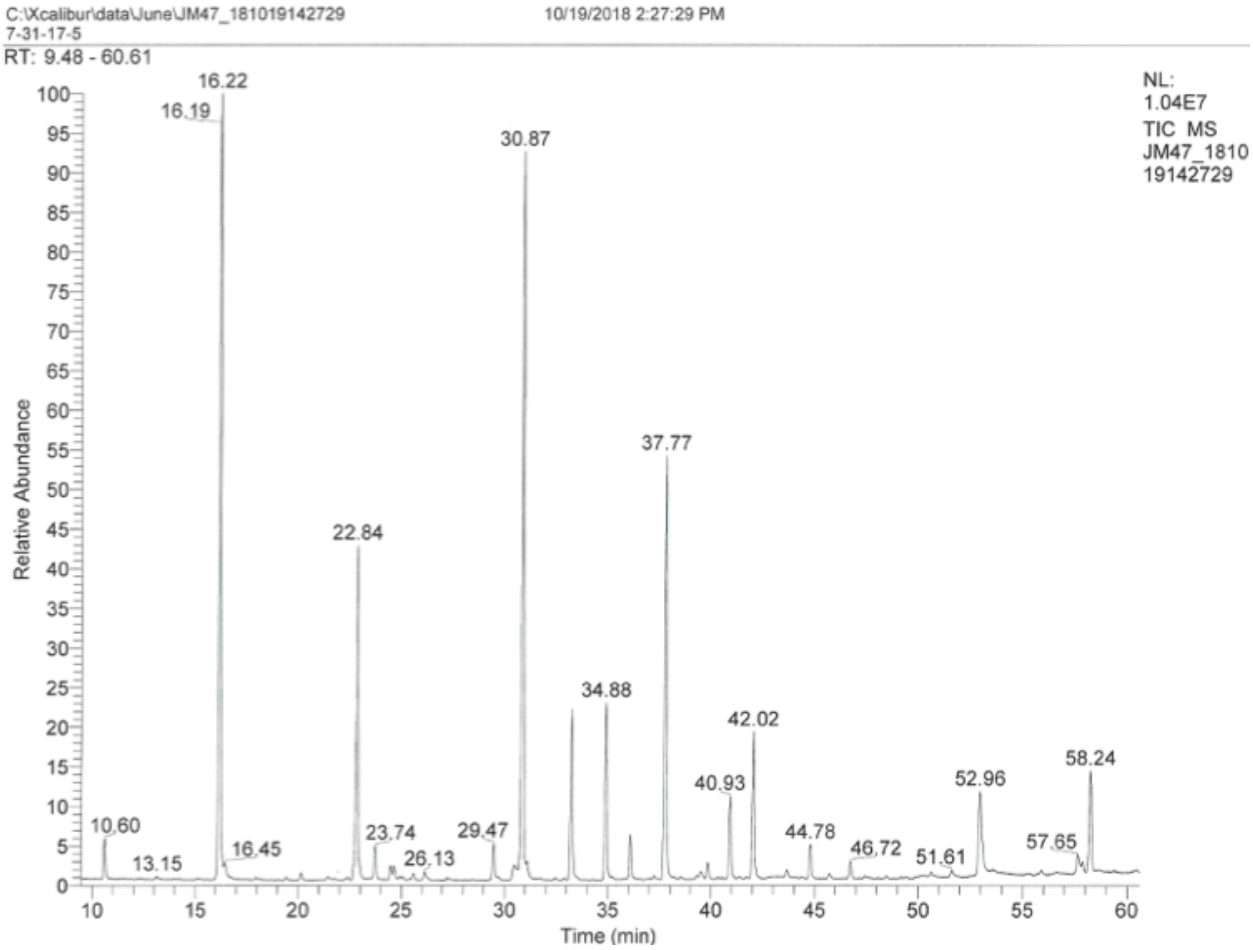

12.3.5.9. Treatment 5, Low Nitrogen, Low Phosphorus + CO_2, Day 19 D

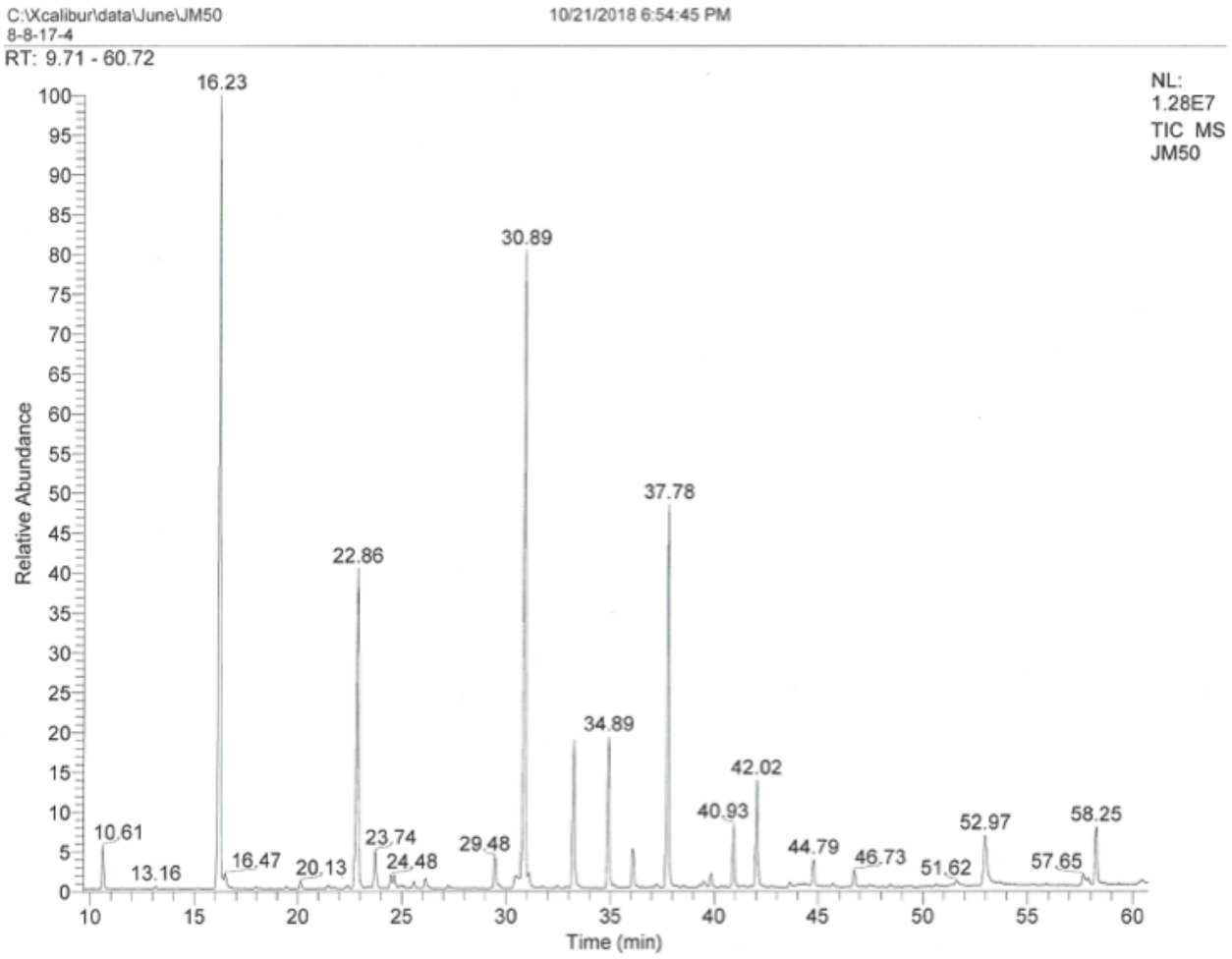

12.3.5.10. Treatment 5, Low Nitrogen, Low Phosphorus + CO_2, Day 27

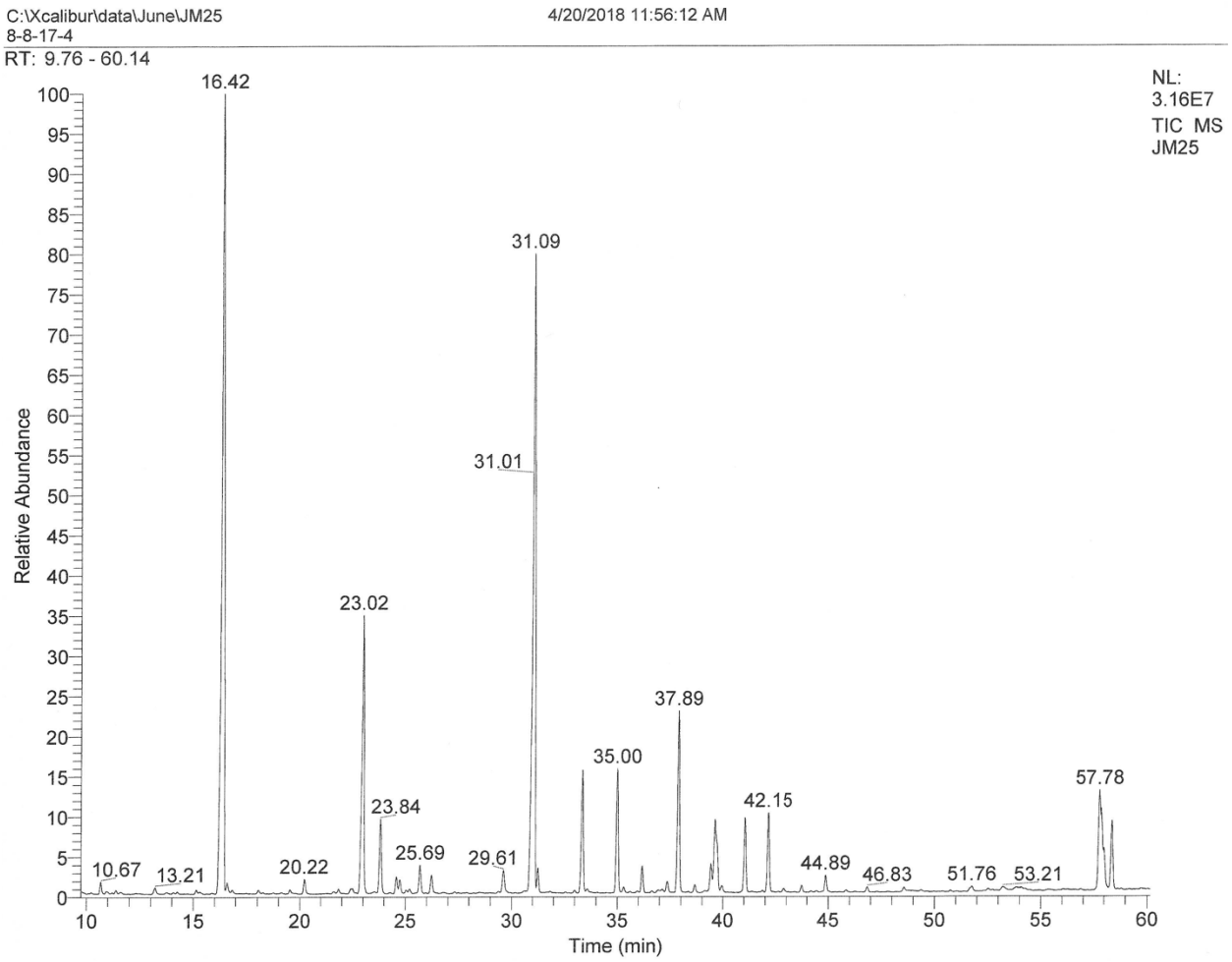

12.3.5.11. Treatment 5, Low Nitrogen, Low Phosphorus + CO_2, Day 52

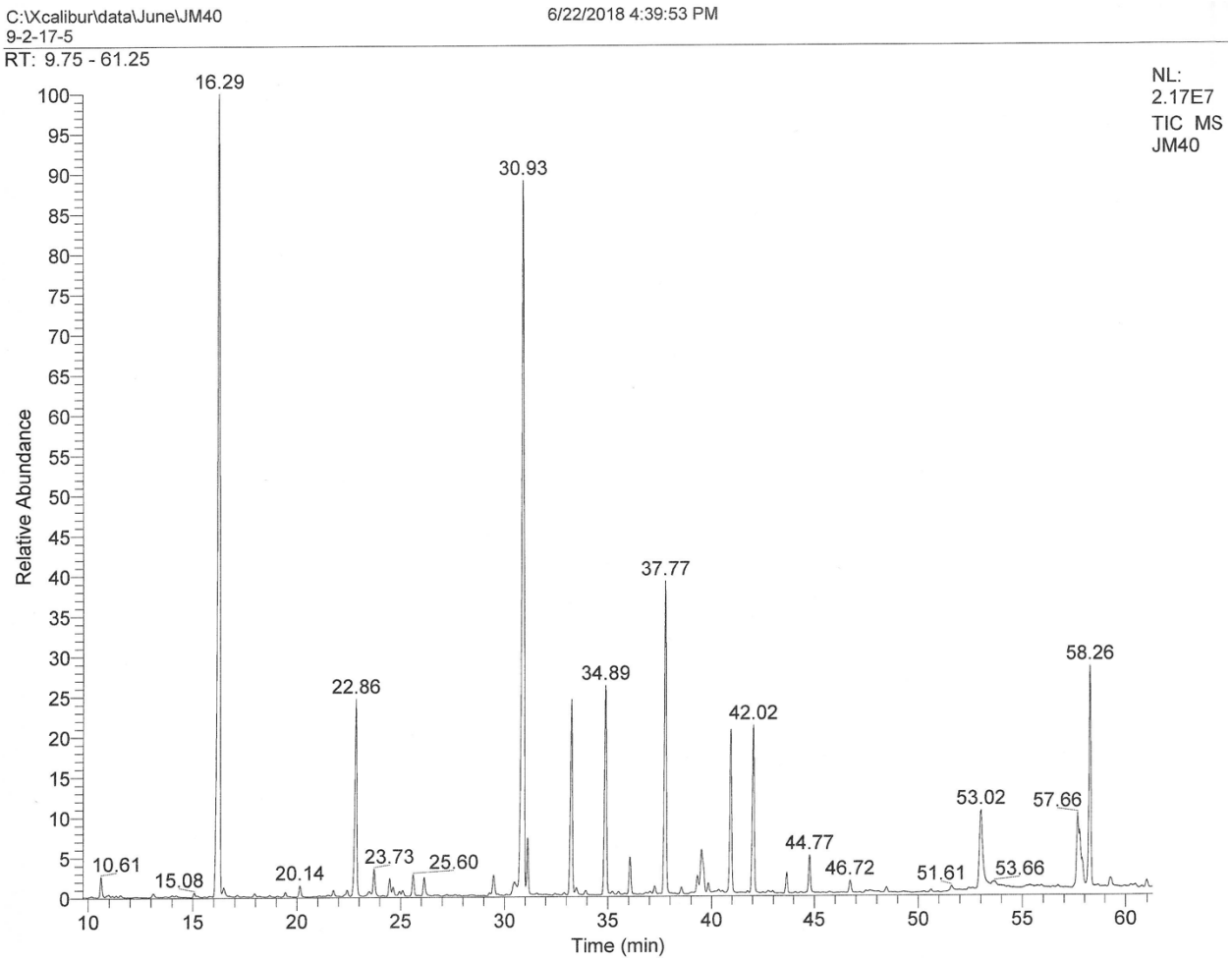

12.3.6. Treatment 6, Intermittent Nitrogen Feeding

12.3.6.1. Treatment 6, Intermittent Nitrogen Feeding, Day 6

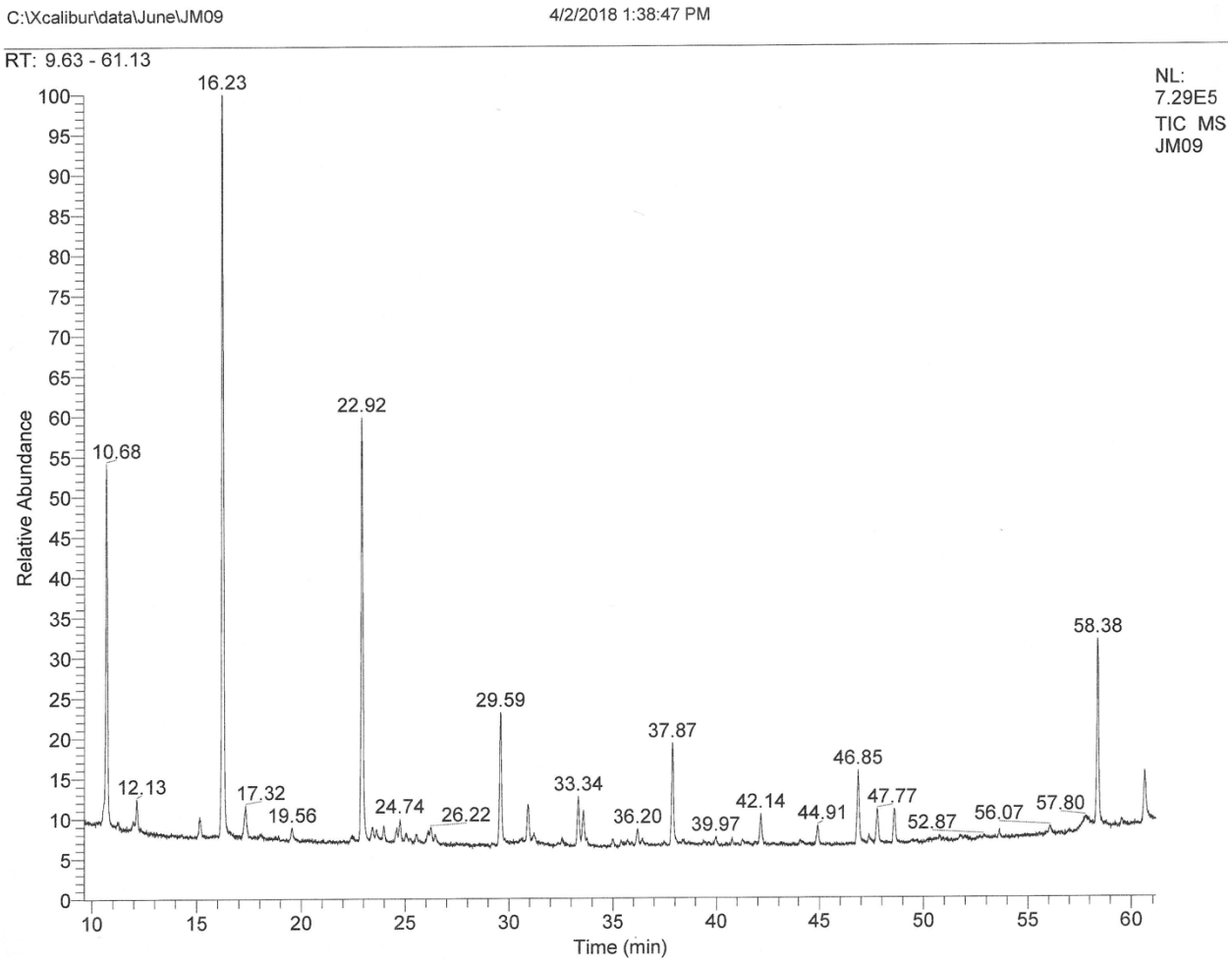

12.3.6.2. Treatment 6, Intermittent Nitrogen Feeding, Day 9

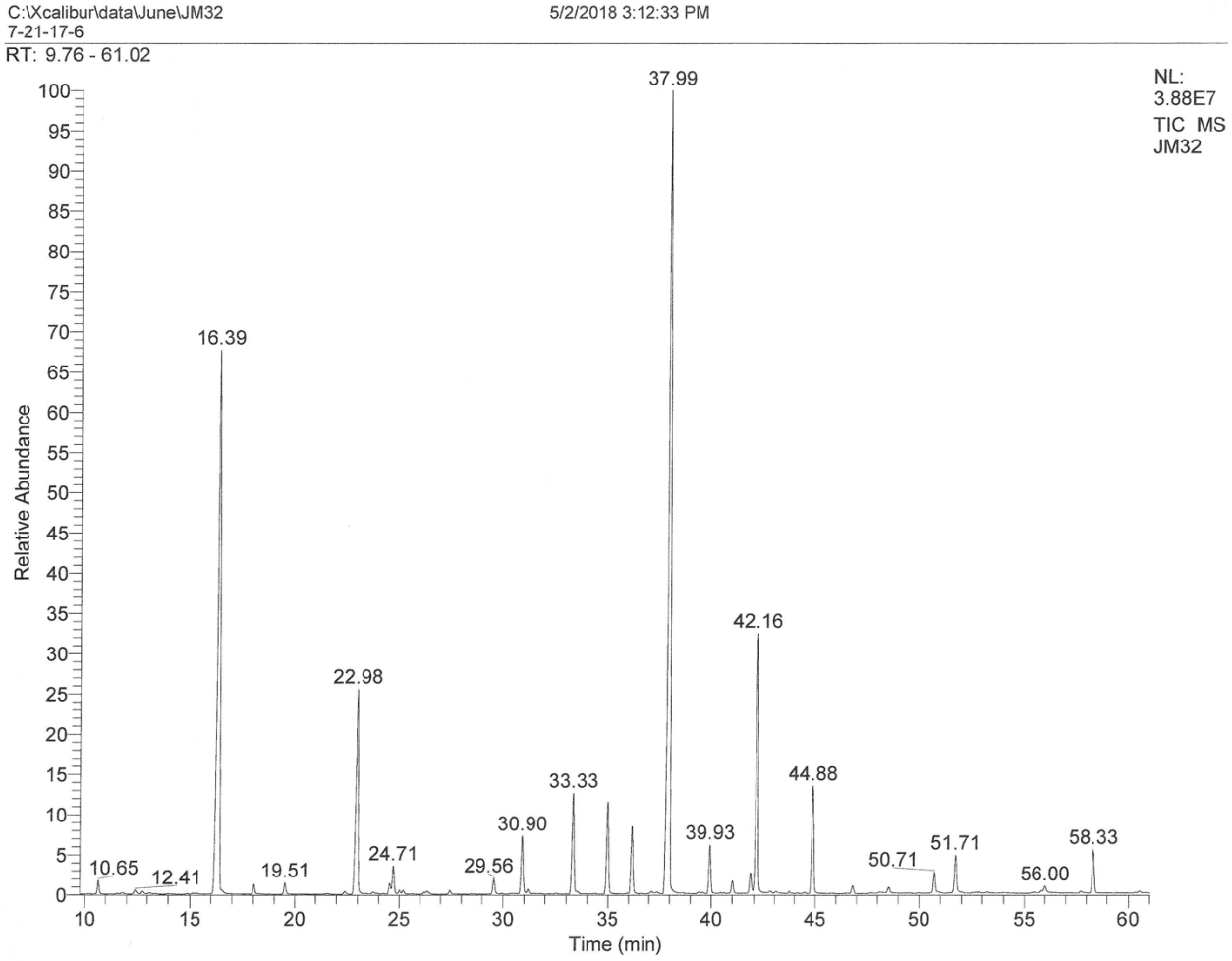

12.3.6.3. Treatment 6, Intermittent Nitrogen Feeding, Day 19

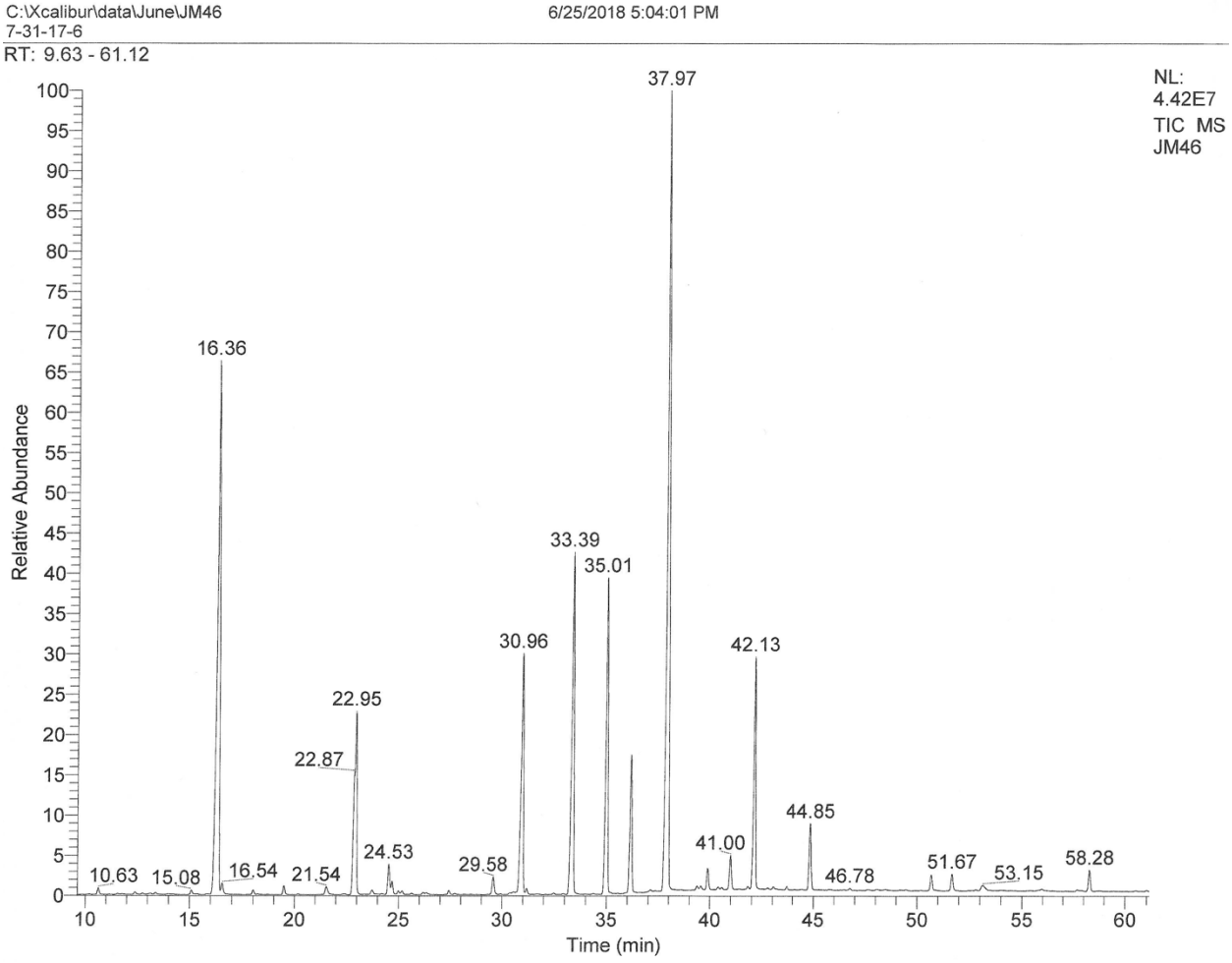

12.3.6.4. Treatment 6, Intermittent Nitrogen Feeding, Day 27

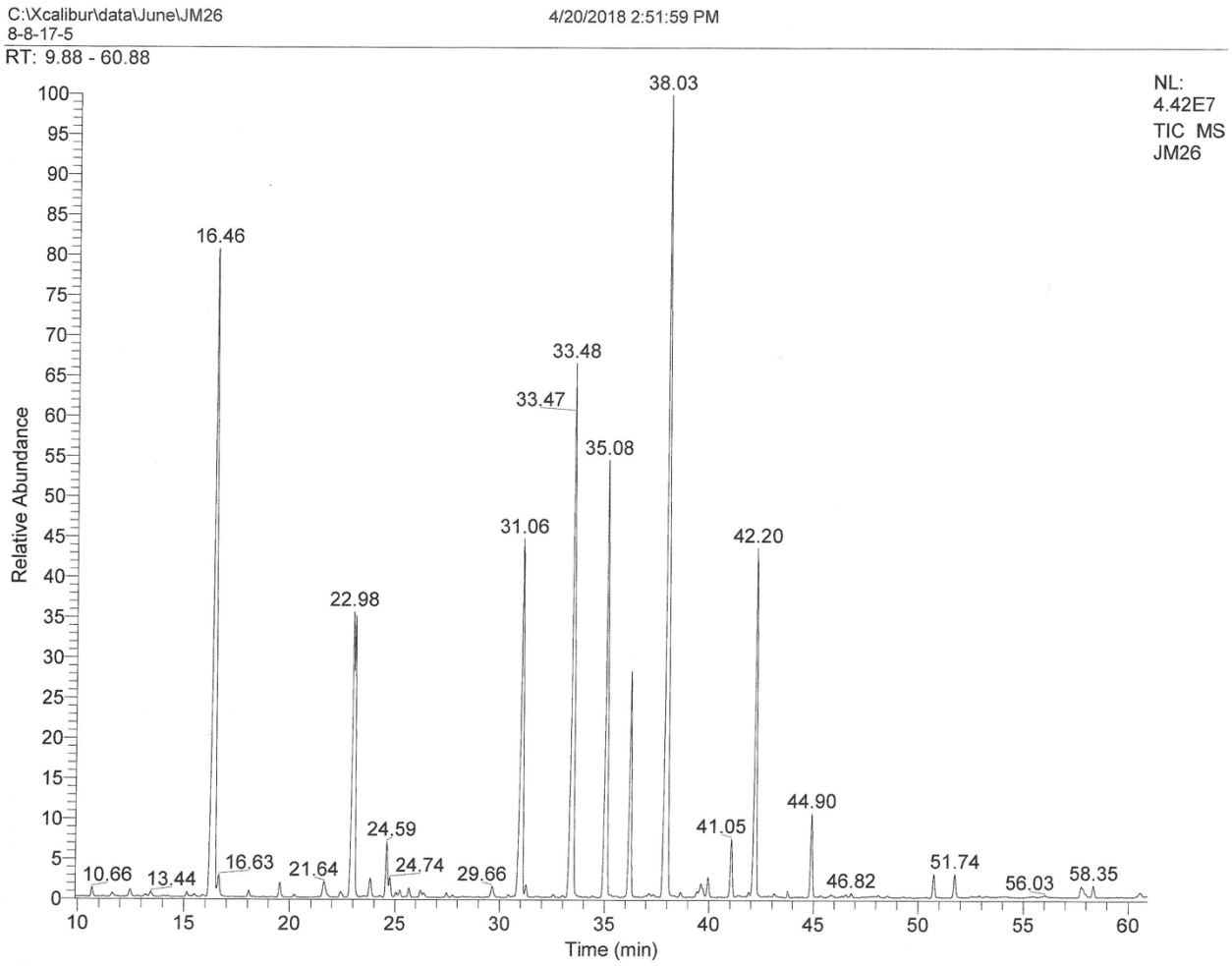

12.3.6.5. Treatment 6, Intermittent Nitrogen Feeding, Day 52

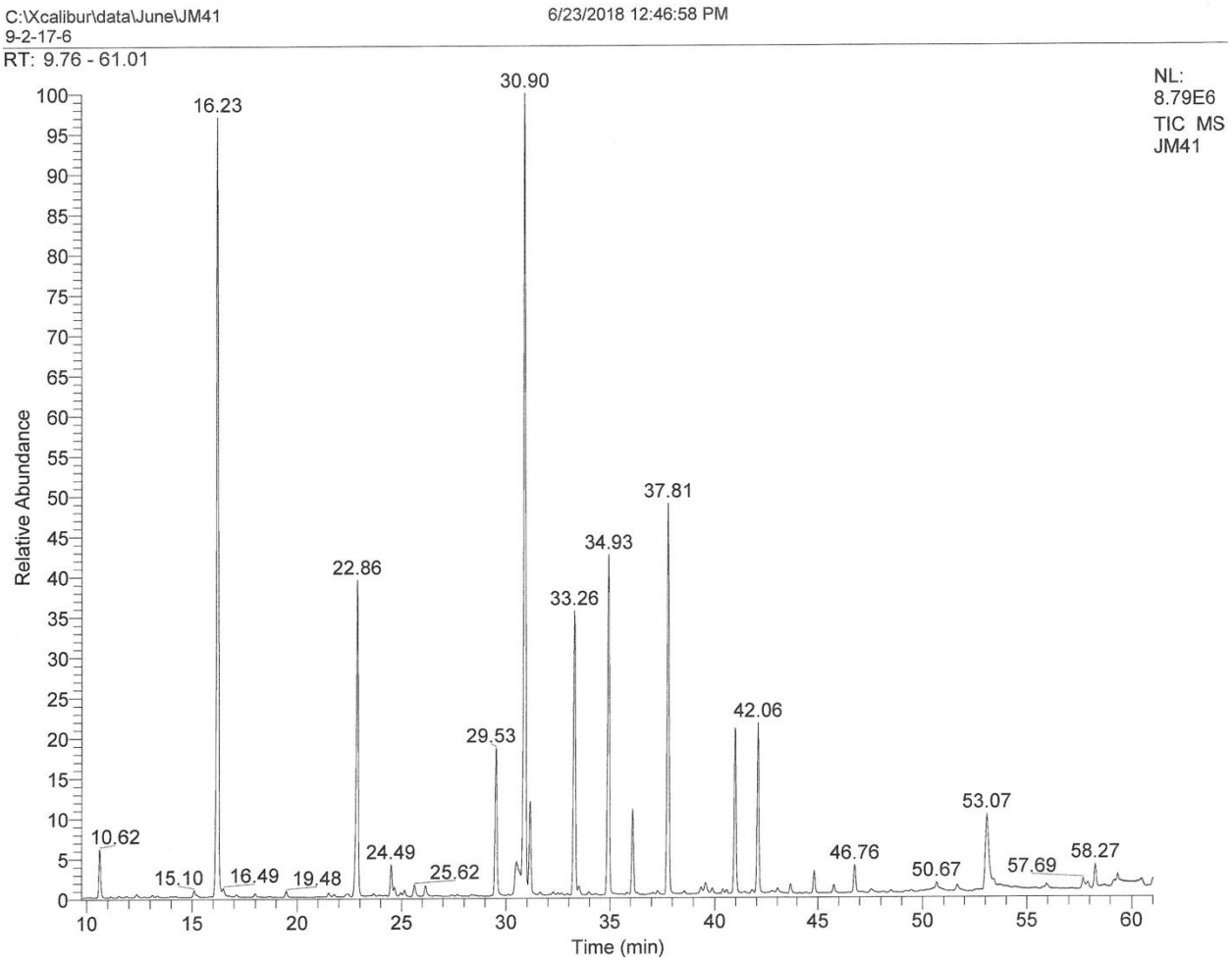

12.4. Appendix H: GC/MS Chemical Ionization Chromatograms

12.4.1. Treatment 1, Standard MAM (Nutrient Replete)

12.4.1.1. Treatment 1, Standard MAM, Day 6

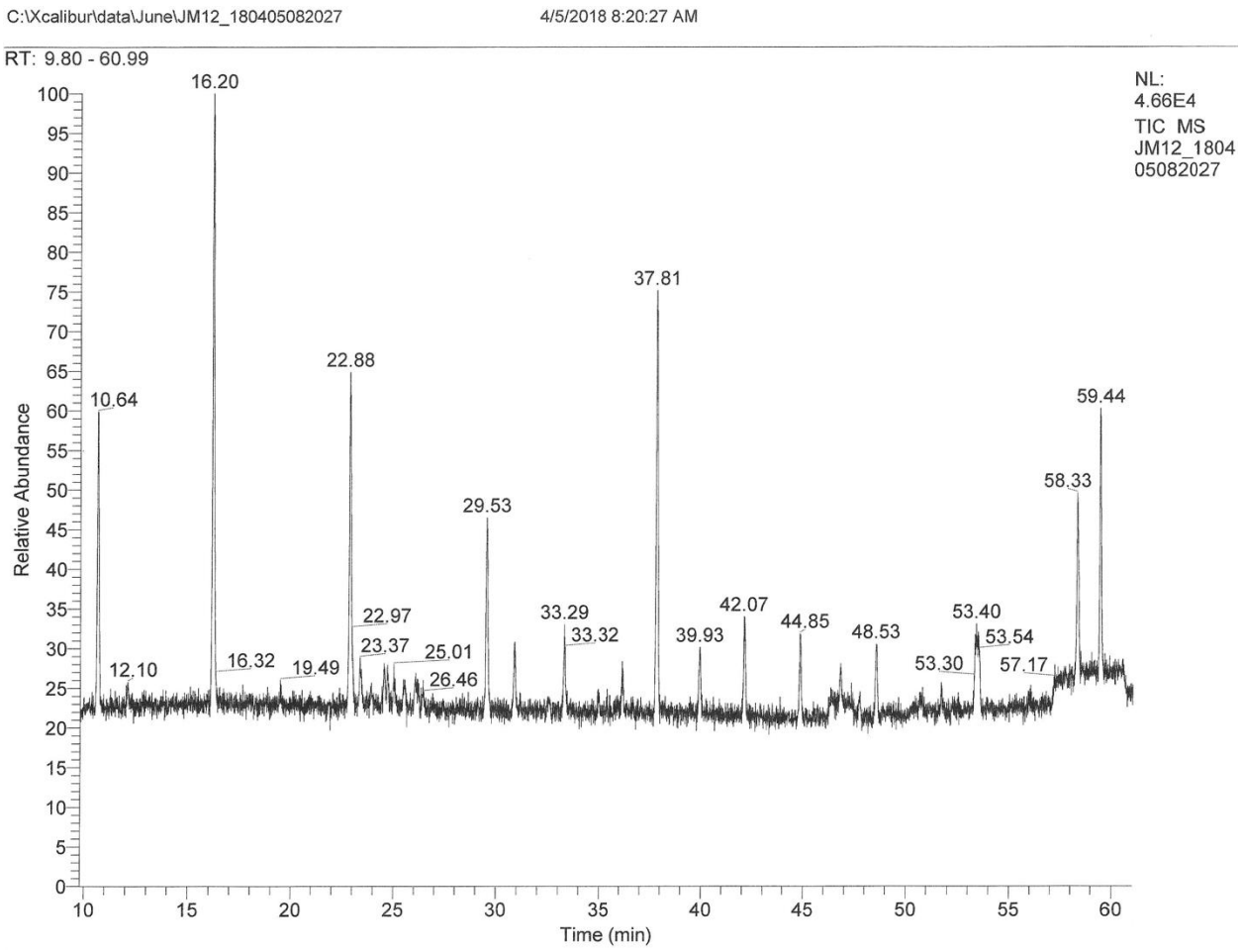

12.4.1.2. Treatment 1, Standard MAM, Day 27

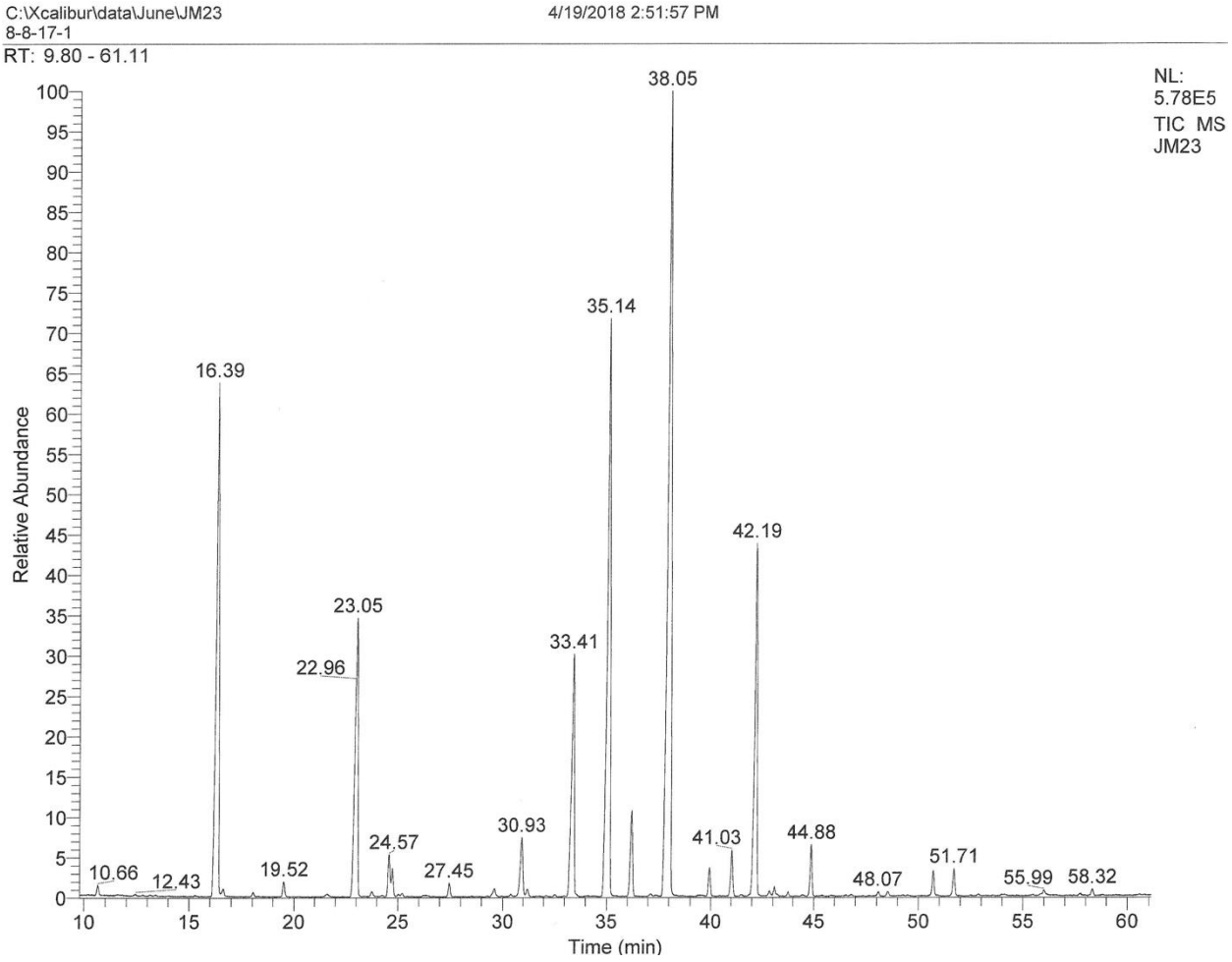

12.4.2. Treatment 2, Low Nitrogen

12.4.2.1. Treatment 2, Low Nitrogen, Day 6

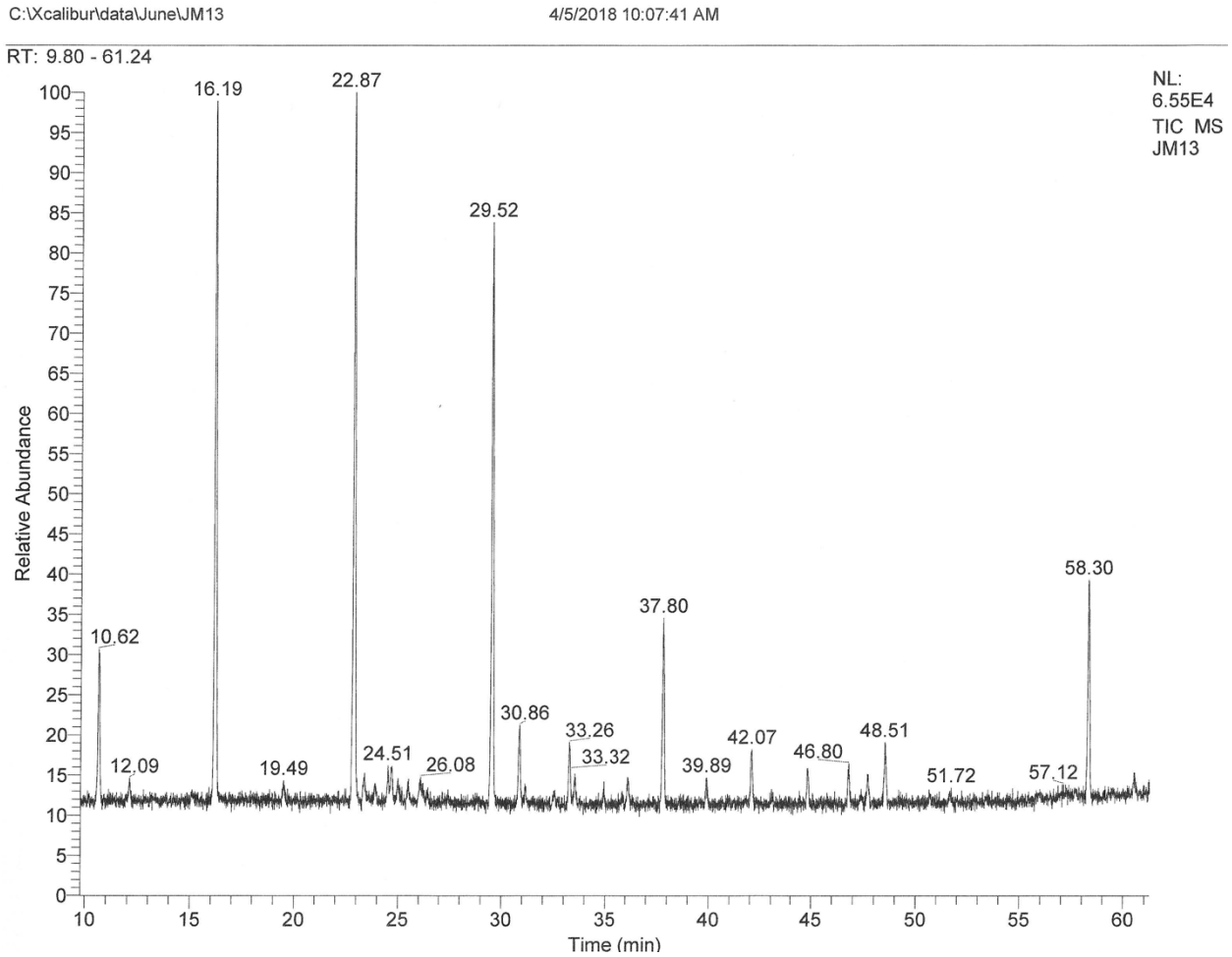

12.4.2.2. Treatment 2, Low Nitrogen, Day 27

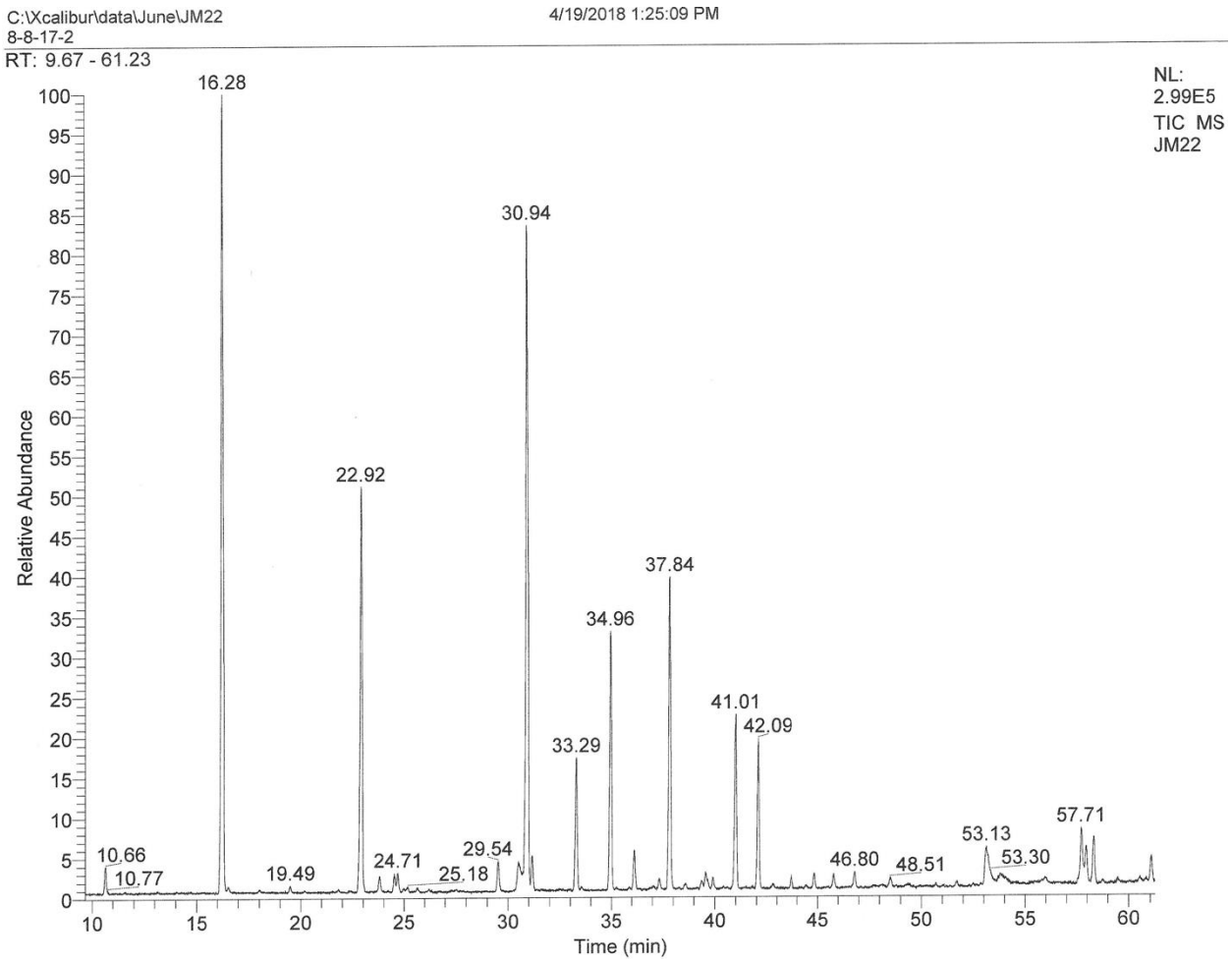

12.4.3. Treatment 3, Low Phosphorus

12.4.3.1. Treatment 3, Low Phosphorus, Day 6

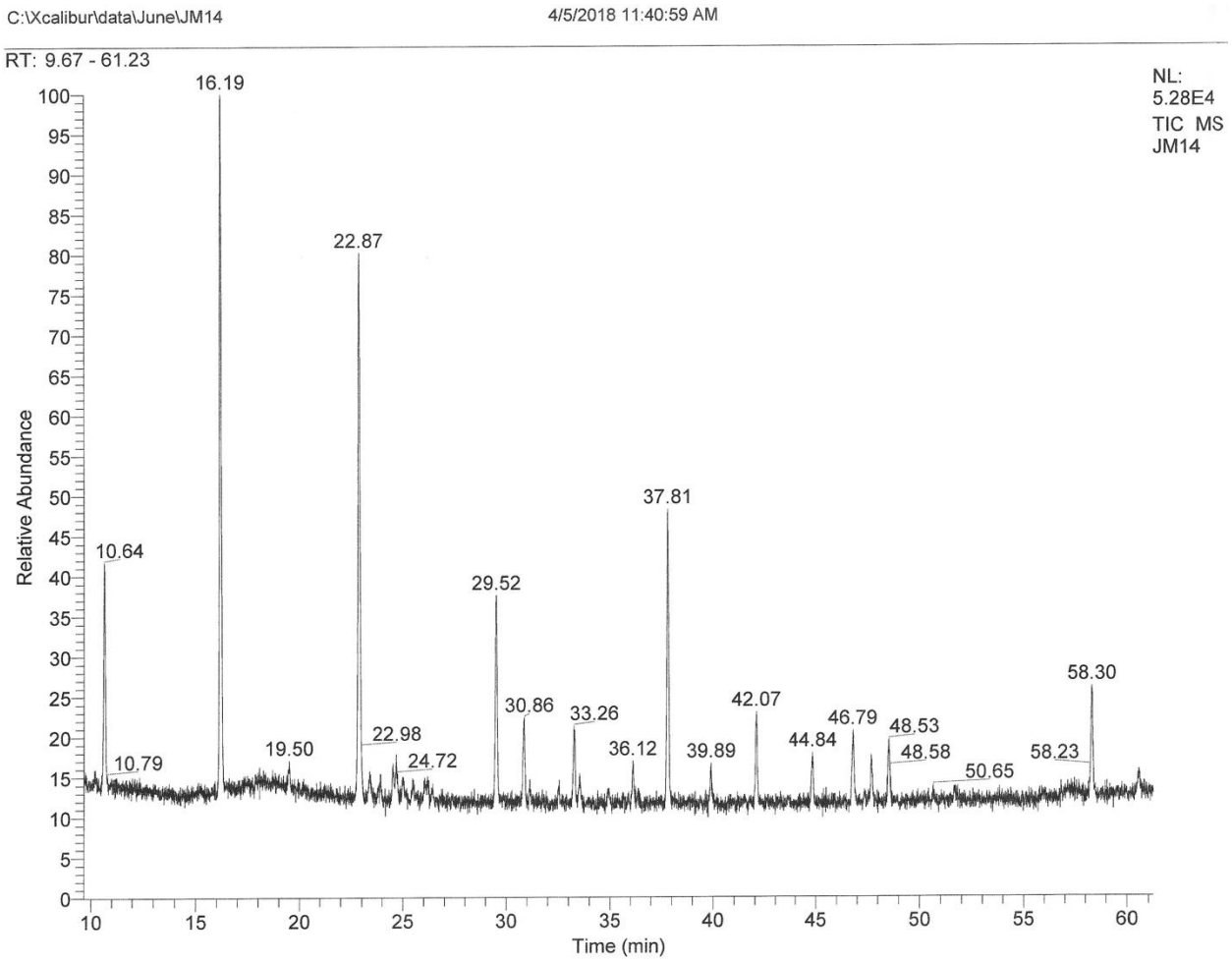

12.4.3.2. Treatment 3, Low Phosphorus, Day 27

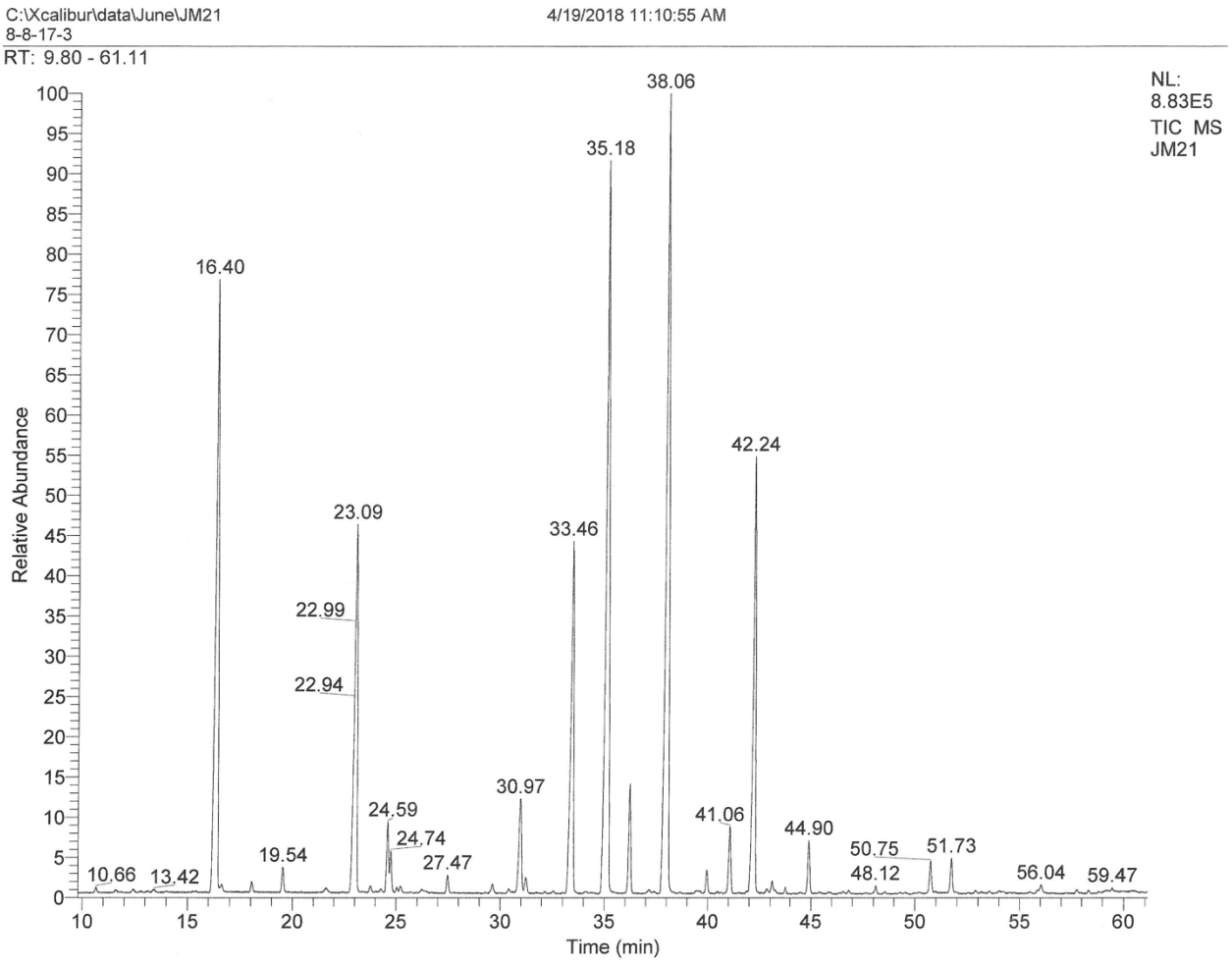

12.4.4. Treatment 4, Low Nitrogen and Low Phosphorus

12.4.4.1. Treatment 4, Low Nitrogen and Low Phosphorus, Day 6

Because of a problem with this run (below), only the retention times between 10.61 minutes and 44.0 minutes were used for FAME identification.

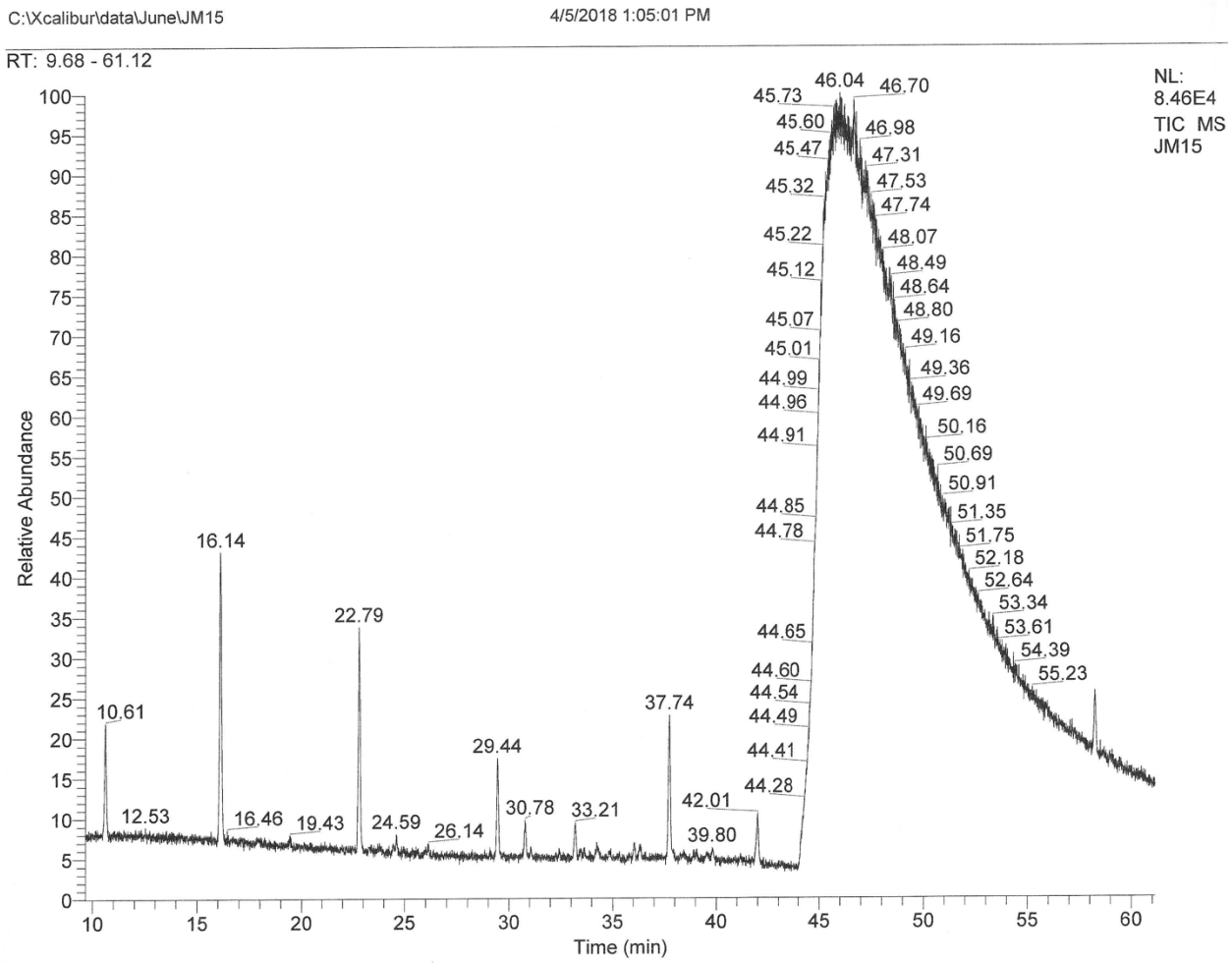

12.4.5. Treatment 5, Low Nitrogen, Low Phosphorus + CO_2

12.4.5.1. Treatment 5, Low Nitrogen, Low Phosphorus + CO_2, Day 6

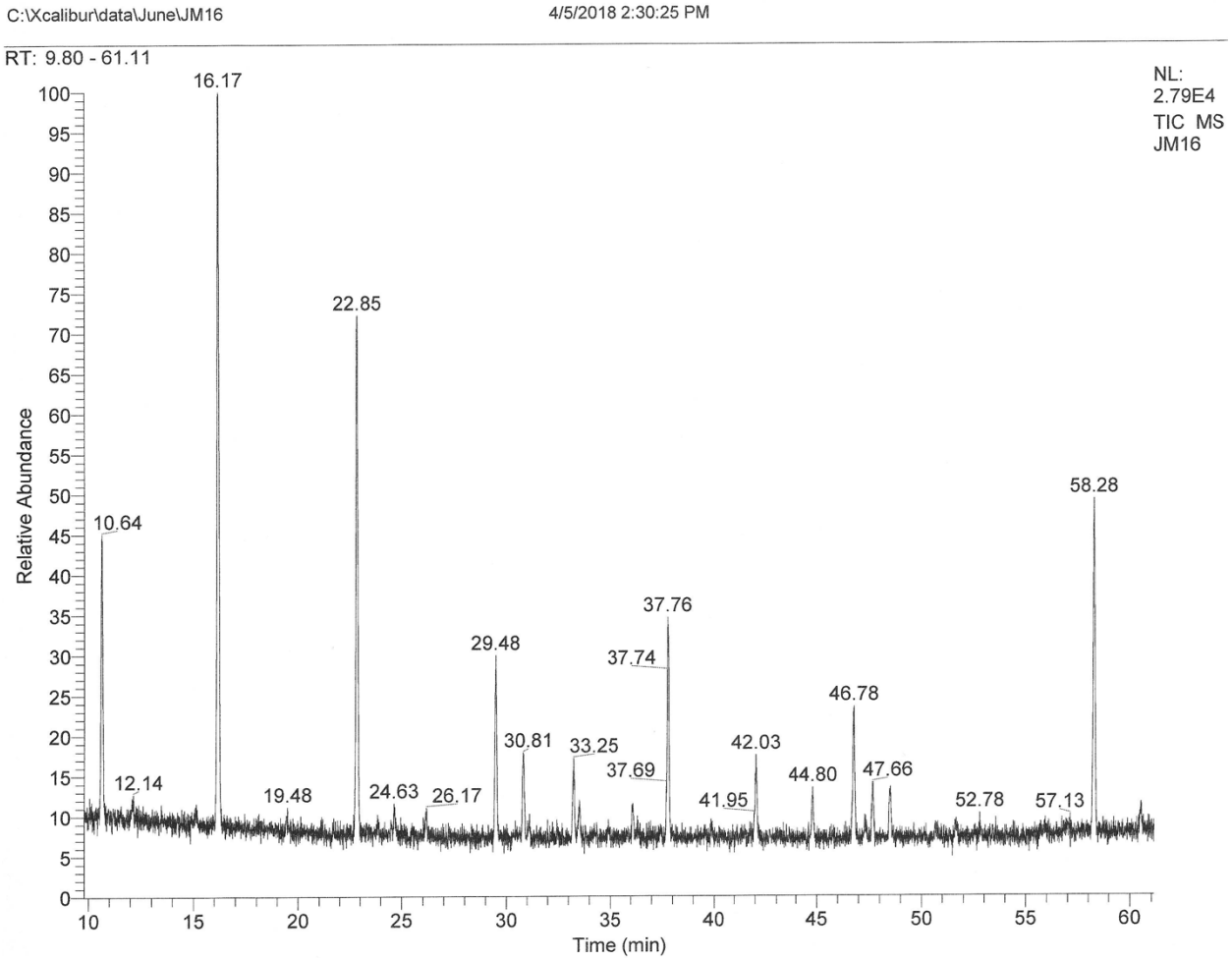

12.4.6. Treatment 6, Intermittent Nitrogen Feeding

12.4.6.1. Treatment 6, Intermittent Nitrogen Feeding, Day 6

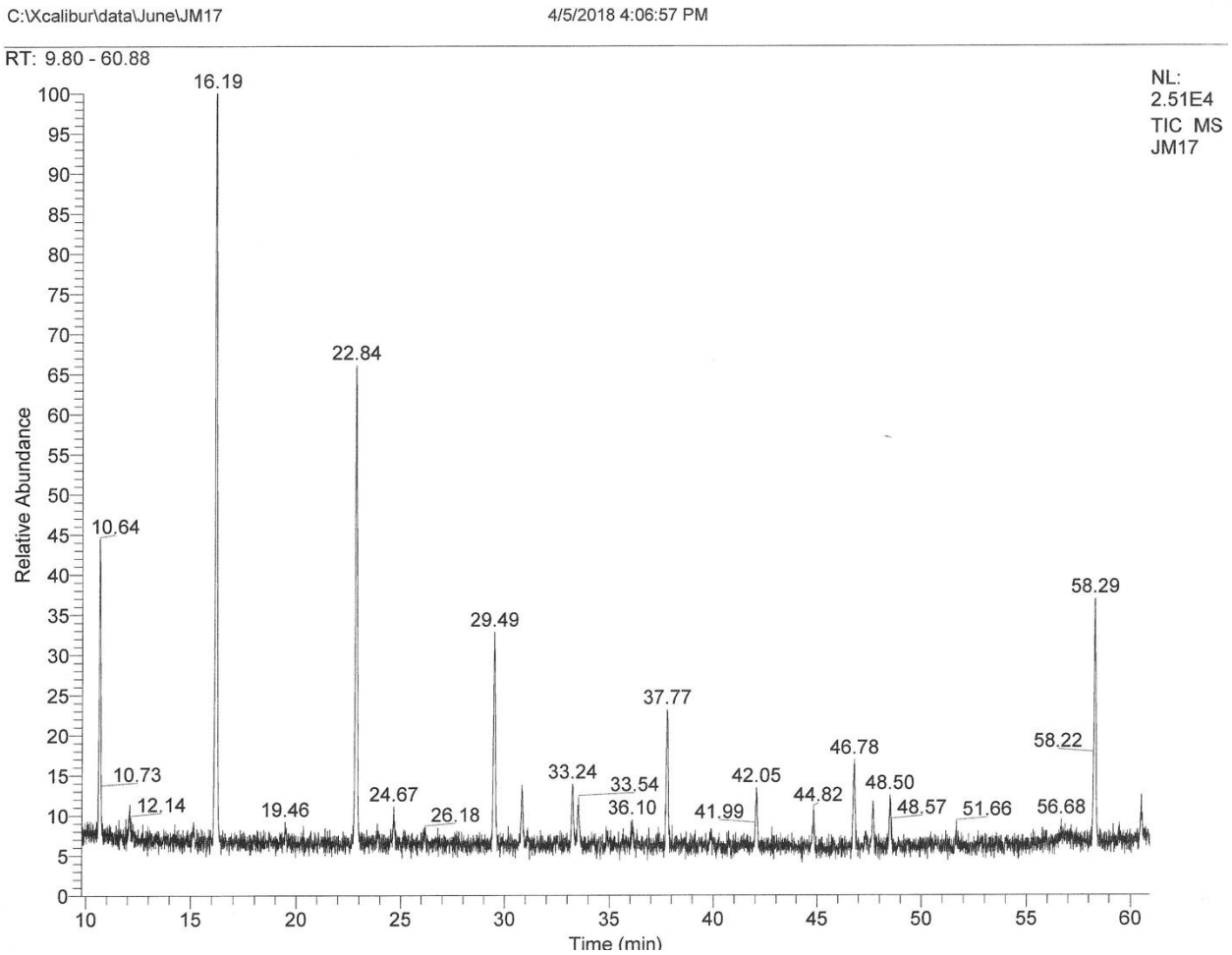

13. Appendix I: Calculations of FAME Concentrations Summary

13.1. Treatment 1. MAM (Nutrient Replete Control)

Treatment	Sample Day	Apex RT - Napthalene RT (RT A)	Peak Areas	Mean RT-Napthalene RT (RT B)	FAME Detected	RT Difference (RT A - RT B)	Mean Response Factors	Peak Areas of Internal Standard	Concentration of I.S. (mg/mL)	Concentrations of FAMEs (mg/mL)	*Area Added Manually
1	**6**	**0.00**	**7480472.08**	**Napthalene**							
1	6	5.62	4252298.17	5.60	C14:0	0.02	1.53	7480472.08	0.020696	0.007712	
1	6	8.93	106198.26	8.86	C15:0	0.07	1.22	7480472.08	0.020696	0.000241	*
1	6	12.28	2719992.81	12.27	C16:0	0.01	1.47	7480472.08	0.020696	0.005123	
1	6	14.08	151290.79	14.05	C16:1	0.03	1.16	7480472.08	0.020696	0.000360	
1	6	15.62	56744.06	15.53	C20:0	0.09	1.38	7480472.08	0.020696	0.000114	
1	6	18.96	1395030.70	18.90	C18:0	0.06	1.56	7480472.08	0.020696	0.002476	
1	6	20.29	410570.40	20.25	C18:1	0.04	1.24	7480472.08	0.020696	0.000915	
1	6	22.69	633490.44	22.68	C18:2	0.01	2.93	7480472.08	0.020696	0.000599	
1	6	24.35	108598.69	24.35	C18:3	0.00	1.44	7480472.08	0.020696	0.000208	
1	6	25.56	429908.73	25.51	C18:3	0.05	1.44	7480472.08	0.020696	0.000824	
1	6	27.23	3824691.55	27.22	C18:4	0.01	1.44	7480472.08	0.020696	0.007332	
1	6	29.31	612441.38	29.28	C18:5	0.03	1.44	7480472.08	0.020696	0.001174	
1	6	31.49	740894.23	31.47	C20:4	0.02	1.38	7480472.08	0.020696	0.001485	
1	6	34.26	741891.18	34.21	C20:5	0.05	0.66	7480472.08	0.020696	0.003093	
1	6	41.08	147011.27	41.06	C22:6	0.02	0.72	7480472.08	0.020696	0.000567	
Total Detected FAME Concentration (mg/mL)										**0.032223**	
1	**9**	**0.00**	**2969845.92**	**Napthalene**							
1	9	5.60	59858187.60	5.60	C14:0	0.00	1.53	2969845.92	0.020696	0.272637	
1	9	8.84	1017090.32	8.86	C15:0	-0.02	1.22	2969845.92	0.020696	0.005818	
1	9	12.23	23010199.54	12.27	C16:0	-0.04	1.47	2969845.92	0.020696	0.109154	
1	9	13.86	784044.21	13.91	C16:1	-0.05	1.16	2969845.92	0.020696	0.004693	
1	9	14.02	3231177.48	14.05	C16:1	-0.03	1.16	2969845.92	0.020696	0.019340	
1	9	14.33	462335.72	14.36	C16:1	-0.03	1.16	2969845.92	0.020696	0.002767	
1	9	14.49	311070.28	14.53	C17:0	-0.04	1.14	2969845.92	0.020696	0.001902	
1	9	15.54	457919.85	15.53	C20:0	0.01	1.38	2969845.92	0.020696	0.002312	
1	9	16.77	381719.20	16.79	C16:2	-0.02	1.16	2969845.92	0.020696	0.002285	
1	9	18.85	2449534.22	18.90	C18:0	-0.05	1.56	2969845.92	0.020696	0.010949	
1	9	20.19	4542318.84	20.25	C18:1	-0.06	1.24	2969845.92	0.020696	0.025497	
1	9	20.48	265252.88	20.53	C18:1	-0.05	2.68	2969845.92	0.020696	0.000691	
1	9	22.61	5992609.46	22.68	C18:2	-0.07	2.93	2969845.92	0.020696	0.014261	
1	9	24.25	5980280.99	24.35	C18:3	-0.10	1.44	2969845.92	0.020696	0.028878	
1	9	25.45	5159564.95	25.51	C18:3	-0.06	1.44	2969845.92	0.020696	0.024915	
1	9	27.18	71525921.19	27.22	C18:4	-0.04	1.44	2969845.92	0.020696	0.345388	

1	9	28.88	189057.26	28.90	C18:4	-0.02	1.44	2969845.92	0.020696	0.000913
1	9	29.22	4704518.43	29.28	C18:5	-0.06	1.44	2969845.92	0.020696	0.022717
1	9	30.30	658170.31	30.37	C20:3	-0.07	1.38	2969845.92	0.020696	0.003323
1	9	31.14	50600.18	31.16	C22:0	-0.02	0.72	2969845.92	0.020696	0.000492
1	9	31.40	12825588.17	31.47	C20:4	-0.07	1.38	2969845.92	0.020696	0.064763
1	9	32.36	187813.64	32.42	C22:1	-0.05	0.72	2969845.92	0.020696	0.001826
1	9	33.01	117510.53	33.08	C20:4	-0.07	1.38	2969845.92	0.020696	0.000593
1	9	34.16	5570344.51	34.21	C20:5	-0.05	0.66	2969845.92	0.020696	0.058493
1	9	37.36	303198.93	37.43	C22:4	-0.06	0.72	2969845.92	0.020696	0.002948
1	9	40.02	983778.60	40.06	C22:5	-0.03	0.72	2969845.92	0.020696	0.009565
1	9	41.01	1266659.01	41.06	C22:6	-0.04	0.72	2969845.92	0.020696	0.012315
Total Detected FAME Concentration (mg/mL)										**1.049434**
1	**19**	**0.00**	**3053569.63**	**Napthalene**						
1	19	5.62	119857154.40	5.60	C14:0	0.02	1.53	3053569.63	0.020696	0.530947
1	19	8.81	2235650.80	8.86	C15:0	-0.05	1.22	3053569.63	0.020696	0.012438
1	19	12.24	58510177.54	12.27	C16:0	-0.03	1.47	3053569.63	0.020696	0.269946
1	19	13.53	141513.60	13.61	C16:1	-0.07	1.16	3053569.63	0.020696	0.000824
1	19	13.85	5015823.06	13.91	C16:1	-0.06	1.16	3053569.63	0.020696	0.029199
1	19	14.01	4009563.66	14.05	C16:1	-0.04	1.16	3053569.63	0.020696	0.023341
1	19	14.34	810234.52	14.36	C16:1	-0.02	1.16	3053569.63	0.020696	0.004717
1	19	14.47	422778.35	14.53	C17:0	-0.06	1.14	3053569.63	0.020696	0.002514
1	19	15.51	253439.62	15.53	C20:0	-0.02	1.38	3053569.63	0.020696	0.001245
1	19	16.75	2193187.67	16.79	C16:2	-0.04	1.16	3053569.63	0.020696	0.012767
1	19	18.84	1191621.75	18.90	C18:0	-0.06	1.56	3053569.63	0.020696	0.005180
1	19	19.68	340127.25	19.82	C17:2 and/or C18:1	-0.13	1.24	3053569.63	0.020696	0.001857
1	19	20.19	9326761.92	20.25	C18:1	-0.06	1.24	3053569.63	0.020696	0.050918
1	19	20.47	1045764.58	20.53	C18:1	-0.06	2.68	3053569.63	0.020696	0.002649
1	19	22.64	46670650.99	22.68	C18:2	-0.04	2.93	3053569.63	0.020696	0.108018
1	19	24.33	126241719.75	24.35	C18:3	-0.02	1.44	3053569.63	0.020696	0.592888
1	19	25.47	18433582.39	25.51	C18:3	-0.04	1.44	3053569.63	0.020696	0.086572
1	19	26.43	738303.40	26.48	C18:4	-0.05	1.44	3053569.63	0.020696	0.003467
1	19	27.27	284814038.72	27.22	C18:4	0.05	1.44	3053569.63	0.020696	1.337616
1	19	29.22	6810895.83	29.28	C18:5	-0.06	1.44	3053569.63	0.020696	0.031987
1	19	30.31	6160597.25	30.37	C20:3	-0.06	1.38	3053569.63	0.020696	0.030255
1	19	31.12	68542.70	31.16	C22:0	-0.04	0.72	3053569.63	0.020696	0.000648
1	19	31.43	55835886.01	31.47	C20:4	-0.04	1.38	3053569.63	0.020696	0.274214
1	19	32.35	947344.45	32.42	C22:1	-0.06	0.72	3053569.63	0.020696	0.008958
1	19	33.01	652402.37	33.08	C20:4	-0.07	1.38	3053569.63	0.020696	0.003204
1	19	34.17	10944287.15	34.21	C20:5	-0.04	0.66	3053569.63	0.020696	0.111772
1	19	37.39	411030.67	37.43	C22:4	-0.03	0.72	3053569.63	0.020696	0.003887
1	19	40.01	3236254.08	40.06	C22:5	-0.05	0.72	3053569.63	0.020696	0.030601
1	19	41.00	3630009.38	41.06	C22:6	-0.05	0.72	3053569.63	0.020696	0.034324
Total Detected FAME Concentration (mg/mL)										**3.606952**

1	**27**	**0.00**	**1905701.30**	**Napthalene**						
1	27	5.65	140964503.73	5.60	C14:0	0.05	1.53	1905701.30	0.020696	1.000576
1	27	8.81	2956405.14	8.86	C15:0	-0.05	1.22	1905701.30	0.020696	0.026354
1	27	12.30	110124529.55	12.27	C16:0	0.03	1.47	1905701.30	0.020696	0.814108
1	27	13.54	257161.56	13.61	C16:1	-0.06	1.16	1905701.30	0.020696	0.002399
1	27	13.87	9145409.92	13.91	C16:1	-0.04	1.16	1905701.30	0.020696	0.085306
1	27	14.01	5164033.37	14.05	C16:1	-0.04	1.16	1905701.30	0.020696	0.048169
1	27	14.35	1237815.30	14.36	C16:1	-0.01	1.16	1905701.30	0.020696	0.011546
1	27	14.48	1163928.09	14.53	C17:0	-0.05	1.14	1905701.30	0.020696	0.011092
1	27	15.39	698321.52	15.53	C20:0	-0.14	1.38	1905701.30	0.020696	0.005495
1	27	16.75	4009024.48	16.79	C16:2	-0.04	1.16	1905701.30	0.020696	0.037395
1	27	18.87	2494847.09	18.90	C18:0	-0.03	1.56	1905701.30	0.020696	0.017379
1	27	19.70	724697.65	19.82	C17:2 and/or C18:1	-0.11	1.24	1905701.30	0.020696	0.006339
1	27	20.21	16464090.74	20.25	C18:1	-0.04	1.24	1905701.30	0.020696	0.144022
1	27	20.50	2277258.24	20.53	C18:1	-0.03	2.68	1905701.30	0.020696	0.009242
1	27	22.68	104605463.80	22.68	C18:2	0.00	2.93	1905701.30	0.020696	0.387934
1	27	24.39	248070792.56	24.35	C18:3	0.04	1.44	1905701.30	0.020696	1.866804
1	27	25.49	26769542.43	25.51	C18:3	-0.02	1.44	1905701.30	0.020696	0.201449
1	27	26.44	991393.50	26.48	C18:4	-0.04	1.44	1905701.30	0.020696	0.007461
1	27	27.31	382585436.09	27.22	C18:4	0.09	1.44	1905701.30	0.020696	2.879066
1	27	29.24	6991762.66	29.28	C18:5	-0.04	1.44	1905701.30	0.020696	0.052615
1	27	30.31	11966336.14	30.37	C20:3	-0.06	1.38	1905701.30	0.020696	0.094165
1	27	31.14	160767.91	31.16	C22:0	-0.02	0.72	1905701.30	0.020696	0.002436
1	27	31.47	102286495.04	31.47	C20:4	0.00	1.38	1905701.30	0.020696	0.804910
1	27	32.36	2568425.86	32.42	C22:1	-0.05	0.72	1905701.30	0.020696	0.038915
1	27	33.04	1203458.20	33.08	C20:4	-0.04	1.38	1905701.30	0.020696	0.009470
1	27	34.17	12864818.26	34.21	C20:5	-0.04	0.66	1905701.30	0.020696	0.210525
1	27	34.70	222956.08	34.75	C21:4	-0.05	0.72	1905701.30	0.020696	0.003378
1	27	37.38	1195338.09	37.43	C22:4	-0.04	0.72	1905701.30	0.020696	0.018111
1	27	40.01	6258599.09	40.06	C22:5	-0.05	0.72	1905701.30	0.020696	0.094825
1	27	41.01	6691790.74	41.06	C22:6	-0.05	0.72	1905701.30	0.020696	0.101388
Total Detected FAME Concentration (mg/mL)										**8.992871**

1	**52**	**0.00**	**4117588.05**	**Napthalene**						
1	52	5.82	525558828.51	5.60	C14:0	0.22	1.53	4117588.05	0.020696	1.726527
1	52	8.87	12521529.95	8.86	C15:0	0.01	1.22	4117588.05	0.020696	0.051660
1	52	12.44	461457692.03	12.27	C16:0	0.17	1.47	4117588.05	0.020696	1.578853
1	52	13.62	907925.01	13.61	C16:1	0.02	1.16	4117588.05	0.020696	0.003920
1	52	13.96	60817071.06	13.91	C16:1	0.05	1.16	4117588.05	0.020696	0.262550
1	52	14.10	17567171.43	14.05	C16:1	0.05	1.16	4117588.05	0.020696	0.075838
1	52	14.39	6056018.79	14.36	C16:1	0.03	1.16	4117588.05	0.020696	0.026144
1	52	14.54	4530269.91	14.53	C17:0	0.01	1.14	4117588.05	0.020696	0.019974
1	52	15.57	2750243.11	15.53	C20:0	0.04	1.38	4117588.05	0.020696	0.010016
1	52	16.81	14034035.51	16.79	C16:2	0.02	1.16	4117588.05	0.020696	0.060585
1	52	18.28	420949.88	18.23	C16:2	0.05	1.16	4117588.05	0.020696	0.001817
1	52	19.08	21418486.83	18.90	C18:0	0.18	1.56	4117588.05	0.020696	0.069051

1	52	19.76	4112964.55	19.82	C17:2 and/or C18:1	-0.05	1.24	4117588.05	0.020696	0.016652
1	52	20.42	116975231.64	20.25	C18:1	0.17	1.24	4117588.05	0.020696	0.473585
1	52	20.66	6023502.36	20.53	C18:1	0.13	2.68	4117588.05	0.020696	0.011314
1	52	22.96	474426462.66	22.68	C18:2	0.28	2.93	4117588.05	0.020696	0.814301
1	52	24.63	778161154.54	24.35	C18:3	0.28	1.44	4117588.05	0.020696	2.710220
1	52	25.62	121447240.06	25.51	C18:3	0.11	1.44	4117588.05	0.020696	0.422983
1	52	26.54	2489712.91	26.48	C18:4	0.06	1.44	4117588.05	0.020696	0.008671
1	52	27.50	808407709.04	27.22	C18:4	0.28	1.44	4117588.05	0.020696	2.815565
1	52	28.89	6129724.79	28.90	C18:4	-0.01	1.44	4117588.05	0.020696	0.021349
1	52	29.30	18480525.92	29.28	C18:5	0.02	1.44	4117588.05	0.020696	0.064365
1	52	30.44	100279374.67	30.37	C20:3	0.07	1.38	4117588.05	0.020696	0.365218
1	52	31.30	6593574.59	31.16	C22:0	0.14	0.72	4117588.05	0.020696	0.046236
1	52	31.66	403658615.20	31.47	C20:4	0.19	1.38	4117588.05	0.020696	1.470128
1	52	32.41	8735996.34	32.42	C22:1	0.00	0.72	4117588.05	0.020696	0.061259
1	52	33.09	5088599.44	33.08	C20:4	0.01	1.38	4117588.05	0.020696	0.018533
1	52	34.23	34093337.79	34.21	C20:5	0.02	0.66	4117588.05	0.020696	0.258214
1	52	34.76	1512073.17	34.75	C21:4	0.01	0.72	4117588.05	0.020696	0.010603
1	52	37.44	8322831.26	37.43	C22:4	0.02	0.72	4117588.05	0.020696	0.058362
1	52	40.08	30768886.47	40.06	C22:5	0.02	0.72	4117588.05	0.020696	0.215759
1	52	41.06	26304430.24	41.06	C22:6	0.01	0.72	4117588.05	0.020696	0.184453
Total Detected FAME Concentration (mg/mL)										**13.934705**

13.1. Treatment 2. Low Nitrogen

Treatment	Sample Day	Apex RT - Napthalene RT (RT A)	Peak Areas	Mean RT-Napthalene RT (RT B)	FAME Detected	RT Difference (RT A - RT B)	Mean Response Factors	Peak Areas of Internal Standard	Concentration of I.S. (mg/mL)	Concentrations of FAMEs (mg/mL)	*Area Added Manually
2	**6**	**0.00**	**2122315.71**	**Napthalene**							
2	6	5.56	7009221.86	5.60	C14:0	-0.04	1.53	2122315.71	0.020696	0.044807	
2	6	8.88	96897.22	8.86	C15:0	0.02	1.22	2122315.71	0.020696	0.000776	
2	6	12.24	7206770.68	12.27	C16:0	-0.03	1.47	2122315.71	0.020696	0.047839	
2	6	14.06	260368.98	14.05	C16:1	0.01	1.16	2122315.71	0.020696	0.002181	
2	6	15.57	172226.72	15.53	C20:0	0.04	1.38	2122315.71	0.020696	0.001217	
2	6	18.91	6134542.45	18.90	C18:0	0.01	1.56	2122315.71	0.020696	0.038370	
2	6	20.25	568946.99	20.25	C18:1	0.00	1.24	2122315.71	0.020696	0.004469	
2	6	20.52	78831.88	20.53	C18:1	-0.01	2.68	2122315.71	0.020696	0.000287	
2	6	22.65	586679.42	22.68	C18:2	-0.03	2.93	2122315.71	0.020696	0.001954	
2	6	24.32	57569.43	24.35	C18:3	-0.03	1.44	2122315.71	0.020696	0.000389	
2	6	25.50	173721.35	25.51	C18:3	-0.01	1.44	2122315.71	0.020696	0.001174	
2	6	27.18	1496347.02	27.22	C18:4	-0.04	1.44	2122315.71	0.020696	0.010111	
2	6	29.28	99927.27	29.28	C18:5	0.00	1.44	2122315.71	0.020696	0.000675	
2	6	31.47	361174.45	31.47	C20:4	0.00	1.38	2122315.71	0.020696	0.002552	
2	6	32.51	178492.26	32.42	C22:1	0.09	0.72	2122315.71	0.020696	0.002428	
2	6	34.21	203928.80	34.21	C20:5	0.00	0.66	2122315.71	0.020696	0.002997	
2	6	40.08	81562.46	40.06	C22:5	0.02	0.72	2122315.71	0.020696	0.001110	
Total Detected FAME Concentration (mg/mL)										**0.163336**	
2	**9**	**0.00**	**2239565.71**	**Napthalene**							
2	9	5.66	106227393.75	5.60	C14:0	0.06	1.53	2239565.71	0.020696	0.641605	
2	9	8.86	1148200.64	8.86	C15:0	0.00	1.22	2239565.71	0.020696	0.008710	
2	9	12.27	38079933.51	12.27	C16:0	0.00	1.47	2239565.71	0.020696	0.239544	
2	9	13.60	58042.50	13.61	C16:1	0.00	1.16	2239565.71	0.020696	0.000461	
2	9	13.90	1753893.75	13.91	C16:1	-0.01	1.16	2239565.71	0.020696	0.013921	
2	9	14.06	3117151.03	14.05	C16:1	0.01	1.16	2239565.71	0.020696	0.024741	
2	9	14.36	582701.87	14.36	C16:1	0.00	1.16	2239565.71	0.020696	0.004625	
2	9	14.53	377100.46	14.53	C17:0	0.00	1.14	2239565.71	0.020696	0.003058	
2	9	15.56	370788.36	15.53	C20:0	0.03	1.38	2239565.71	0.020696	0.002483	
2	9	16.81	457356.93	16.79	C16:2	0.02	1.16	2239565.71	0.020696	0.003630	
2	9	18.92	9224653.42	18.90	C18:0	0.02	1.56	2239565.71	0.020696	0.054678	
2	9	20.26	18219065.66	20.25	C18:1	0.01	1.24	2239565.71	0.020696	0.135615	
2	9	20.53	475018.91	20.53	C18:1	0.00	2.68	2239565.71	0.020696	0.001640	
2	9	22.67	21305114.93	22.68	C18:2	-0.01	2.93	2239565.71	0.020696	0.067232	
2	9	24.32	21703202.64	24.35	C18:3	-0.03	1.44	2239565.71	0.020696	0.138975	
2	9	25.51	12380467.46	25.51	C18:3	0.00	1.44	2239565.71	0.020696	0.079278	
2	9	26.47	450956.15	26.48	C18:4	-0.01	1.44	2239565.71	0.020696	0.002888	
2	9	27.25	124547834.42	27.22	C18:4	0.03	1.44	2239565.71	0.020696	0.797536	
2	9	28.94	219509.16	28.90	C18:4	0.04	1.44	2239565.71	0.020696	0.001406	
2	9	29.28	6048422.58	29.28	C18:5	0.00	1.44	2239565.71	0.020696	0.038731	

2	9	30.37	4140940.95	30.37	C20:3	0.00	1.38	2239565.71	0.020696	0.027728
2	9	31.19	226178.53	31.16	C22:0	0.03	0.72	2239565.71	0.020696	0.002916
2	9	31.47	29909611.90	31.47	C20:4	0.00	1.38	2239565.71	0.020696	0.200277
2	9	32.41	296532.30	32.42	C22:1	-0.01	0.72	2239565.71	0.020696	0.003823
2	9	33.09	378850.05	33.08	C20:4	0.01	1.38	2239565.71	0.020696	0.002537
2	9	34.23	9829868.62	34.21	C20:5	0.02	0.66	2239565.71	0.020696	0.136879
2	9	37.47	71177.45	37.43	C22:4	0.05	0.72	2239565.71	0.020696	0.000918
2	9	40.06	2318406.86	40.06	C22:5	0.01	0.72	2239565.71	0.020696	0.029890
2	9	41.06	2962889.07	41.06	C22:6	0.01	0.72	2239565.71	0.020696	0.038199
Total Detected FAME Concentration (mg/mL)										**2.703923**
2	**19**	**0.00**	**2405731.76**	**Napthalene**						
2	19	5.62	76182860.90	5.60	C14:0	0.02	1.53	2405731.76	0.020696	0.428356
2	19	8.85	288710.26	8.86	C15:0	-0.01	1.22	2405731.76	0.020696	0.002039
2	19	12.26	26348935.16	12.27	C16:0	-0.01	1.47	2405731.76	0.020696	0.154301
2	19	13.86	923819.51	13.91	C16:1	-0.05	1.16	2405731.76	0.020696	0.006826
2	19	14.04	948191.20	14.05	C16:1	-0.01	1.16	2405731.76	0.020696	0.007006
2	19	14.39	290955.62	14.36	C16:1	0.03	1.16	2405731.76	0.020696	0.002150
2	19	14.51	234439.41	14.53	C17:0	-0.02	1.14	2405731.76	0.020696	0.001770
2	19	15.52	159494.77	15.53	C20:0	-0.01	1.38	2405731.76	0.020696	0.000994
2	19	16.76	56608.74	16.79	C16:2	-0.03	1.16	2405731.76	0.020696	0.000418
2	19	18.89	1144123.72	18.90	C18:0	-0.01	1.56	2405731.76	0.020696	0.006313
2	19	19.84	1925576.93	19.82	C17:2 and/or C18:1	0.02	1.24	2405731.76	0.020696	0.013343
2	19	20.26	44212459.98	20.25	C18:1	0.01	1.24	2405731.76	0.020696	0.306369
2	19	20.51	475928.33	20.53	C18:1	-0.02	2.68	2405731.76	0.020696	0.001530
2	19	22.64	16076441.15	22.68	C18:2	-0.04	2.93	2405731.76	0.020696	0.047228
2	19	24.31	31021144.24	24.35	C18:3	-0.04	1.44	2405731.76	0.020696	0.184922
2	19	25.48	7056039.22	25.51	C18:3	-0.03	1.44	2405731.76	0.020696	0.042062
2	19	26.46	145726.65	26.48	C18:4	-0.02	1.44	2405731.76	0.020696	0.000869
2	19	27.21	70748525.63	27.22	C18:4	-0.01	1.44	2405731.76	0.020696	0.421743
2	19	28.91	614934.69	28.90	C18:4	0.01	1.44	2405731.76	0.020696	0.003666
2	19	29.26	2771110.97	29.28	C18:5	-0.02	1.44	2405731.76	0.020696	0.016519
2	19	30.34	15451076.48	30.37	C20:3	-0.03	1.38	2405731.76	0.020696	0.096315
2	19	31.44	16547574.98	31.47	C20:4	-0.03	1.38	2405731.76	0.020696	0.103150
2	19	33.05	975487.42	33.08	C20:4	-0.03	1.38	2405731.76	0.020696	0.006081
2	19	34.19	2732756.91	34.21	C20:5	-0.02	0.66	2405731.76	0.020696	0.035425
2	19	40.04	428982.73	40.06	C22:5	-0.02	0.72	2405731.76	0.020696	0.005149
2	19	41.03	749133.06	41.06	C22:6	-0.03	0.72	2405731.76	0.020696	0.008991
Total Detected FAME Concentration (mg/mL)										**1.903535**
2	**27**	**0.00**	**3788453.85**	**Napthalene**						
2	27	5.65	98998608.66	5.60	C14:0	0.05	1.53	3788453.85	0.020696	0.353478
2	27	8.86	551137.54	8.86	C15:0	0.00	1.22	3788453.85	0.020696	0.002471
2	27	12.29	48767695.40	12.27	C16:0	0.02	1.47	3788453.85	0.020696	0.181352
2	27	13.60	75124.17	13.61	C16:1	0.00	1.16	3788453.85	0.020696	0.000352
2	27	13.89	1545169.99	13.91	C16:1	-0.02	1.16	3788453.85	0.020696	0.007250
2	27	14.06	1978949.14	14.05	C16:1	0.01	1.16	3788453.85	0.020696	0.009285

2	27	14.52	1076550.71	14.53	C17:0	-0.01	1.14	3788453.85	0.020696	0.005159
2	27	15.57	386296.32	15.53	C20:0	0.04	1.38	3788453.85	0.020696	0.001529
2	27	16.86	245855.82	16.79	C16:2	0.07	1.16	3788453.85	0.020696	0.001154
2	27	18.31	59280.92	18.23	C16:2	0.09	1.16	3788453.85	0.020696	0.000278
2	27	18.90	3719636.86	18.90	C18:0	0.00	1.56	3788453.85	0.020696	0.013034
2	27	19.89	3138078.27	19.82	C17:2 and/or C18:1	0.08	1.24	3788453.85	0.020696	0.013809
2	27	20.32	90855735.40	20.25	C18:1	0.07	1.24	3788453.85	0.020696	0.399795
2	27	20.54	2776474.30	20.53	C18:1	0.01	2.68	3788453.85	0.020696	0.005668
2	27	22.66	18547406.89	22.68	C18:2	-0.02	2.93	3788453.85	0.020696	0.034600
2	27	24.33	31121512.67	24.35	C18:3	-0.02	1.44	3788453.85	0.020696	0.117809
2	27	25.50	5254768.30	25.51	C18:3	-0.01	1.44	3788453.85	0.020696	0.019892
2	27	26.41	748685.89	26.48	C18:4	-0.07	1.44	3788453.85	0.020696	0.002834
2	27	27.20	39278577.98	27.22	C18:4	-0.02	1.44	3788453.85	0.020696	0.148687
2	27	28.93	3156707.59	28.90	C18:4	0.03	1.44	3788453.85	0.020696	0.011950
2	27	29.28	1312270.17	29.28	C18:5	0.00	1.44	3788453.85	0.020696	0.004968
2	27	30.38	22800980.31	30.37	C20:3	0.01	1.38	3788453.85	0.020696	0.090256
2	27	31.19	114689.86	31.16	C22:0	0.03	0.72	3788453.85	0.020696	0.000874
2	27	31.46	14804833.16	31.47	C20:4	-0.01	1.38	3788453.85	0.020696	0.058604
2	27	33.09	1256164.63	33.08	C20:4	0.01	1.38	3788453.85	0.020696	0.004972
2	27	34.21	1555945.76	34.21	C20:5	0.00	0.66	3788453.85	0.020696	0.012808
2	27	37.52	113619.37	37.43	C22:4	0.09	0.72	3788453.85	0.020696	0.000866
2	27	40.07	187944.28	40.06	C22:5	0.02	0.72	3788453.85	0.020696	0.001432
2	27	41.05	813653.24	41.06	C22:6	-0.01	0.72	3788453.85	0.020696	0.006201
Total Detected FAME Concentration (mg/mL)										**1.511366**
2	**52**	**0.00**	**1830477.53**	**Napthalene**						
2	52	5.59	60601815.71	5.60	C14:0	-0.01	1.53	1830477.53	0.020696	0.447833
2	52	8.83	383475.32	8.86	C15:0	-0.03	1.22	1830477.53	0.020696	0.003559
2	52	12.20	17603512.84	12.27	C16:0	-0.07	1.47	1830477.53	0.020696	0.135484
2	52	13.84	1317412.86	13.91	C16:1	-0.07	1.16	1830477.53	0.020696	0.012793
2	52	14.01	607195.02	14.05	C16:1	-0.04	1.16	1830477.53	0.020696	0.005896
2	52	14.31	188246.08	14.36	C16:1	-0.05	1.16	1830477.53	0.020696	0.001828
2	52	14.48	481271.60	14.53	C17:0	-0.05	1.14	1830477.53	0.020696	0.004773
2	52	15.52	1533185.15	15.53	C20:0	-0.01	1.38	1830477.53	0.020696	0.012561
2	52	16.82	116267.45	16.79	C16:2	0.03	1.16	1830477.53	0.020696	0.001129
2	52	18.84	4781701.98	18.90	C18:0	-0.06	1.56	1830477.53	0.020696	0.034677
2	52	19.83	2102635.49	19.82	C17:2 and/or C18:1	0.02	1.24	1830477.53	0.020696	0.019149
2	52	20.23	53740226.11	20.25	C18:1	-0.02	1.24	1830477.53	0.020696	0.489420
2	52	20.48	6492961.81	20.53	C18:1	-0.05	2.68	1830477.53	0.020696	0.027433
2	52	22.60	8270612.09	22.68	C18:2	-0.08	2.93	1830477.53	0.020696	0.031932
2	52	24.25	13144846.38	24.35	C18:3	-0.10	1.44	1830477.53	0.020696	0.102984
2	52	25.44	1295115.12	25.51	C18:3	-0.07	1.44	1830477.53	0.020696	0.010147
2	52	26.39	272282.49	26.48	C18:4	-0.09	1.44	1830477.53	0.020696	0.002133
2	52	27.13	12004088.38	27.22	C18:4	-0.09	1.44	1830477.53	0.020696	0.094047
2	52	28.86	7002013.72	28.90	C18:4	-0.04	1.44	1830477.53	0.020696	0.054858

2	52	29.21	252671.05	29.28	C18:5	-0.07	1.44	1830477.53	0.020696	0.001980
2	52	30.30	10979499.10	30.37	C20:3	-0.07	1.38	1830477.53	0.020696	0.089950
2	52	31.09	125167.81	31.16	C22:0	-0.07	0.72	1830477.53	0.020696	0.001974
2	52	31.38	6539192.47	31.47	C20:4	-0.09	1.38	1830477.53	0.020696	0.053573
2	52	32.33	223581.41	32.42	C22:1	-0.09	0.72	1830477.53	0.020696	0.003527
2	52	33.01	862617.12	33.08	C20:4	-0.07	1.38	1830477.53	0.020696	0.007067
2	52	34.14	794702.82	34.21	C20:5	-0.07	0.66	1830477.53	0.020696	0.013539
2	52	41.03	344957.92	41.06	C22:6	-0.02	0.72	1830477.53	0.020696	0.005441
Total Detected FAME Concentration (mg/mL)										**1.669687**

13.1. Treatment 3. Low Phosphorus

Treatment	Sample Day	Apex RT - Napthalene RT (RT A)	Peak Areas	Mean RT-Napthalene RT (RT B)	FAME Detected	RT Difference (RT A - RT B)	Mean Response Factors	Peak Areas of Internal Standard	Concentration of I.S. (mg/mL)	Concentrations of FAMEs (mg/mL)	*Area Added Manually
3	**6**	**0.00**	**3146002.41**	**Napthalene**							
3	6	5.56	6876968.11	5.60	C14:0	-0.04	1.53	3146002.41	0.020696	0.029657	
3	6	8.87	128153.01	8.86	C15:0	0.01	1.22	3146002.41	0.020696	0.000692	
3	6	12.25	5306106.95	12.27	C16:0	-0.02	1.47	3146002.41	0.020696	0.023761	
3	6	13.92	53489.63	13.91	C16:1	0.01	1.16	3146002.41	0.020696	0.000302	
3	6	14.07	350871.51	14.05	C16:1	0.02	1.16	3146002.41	0.020696	0.001983	
3	6	15.57	144323.97	15.53	C20:0	0.04	1.38	3146002.41	0.020696	0.000688	
3	6	18.91	1360154.74	18.90	C18:0	0.01	1.56	3146002.41	0.020696	0.005739	
3	6	20.25	688064.43	20.25	C18:1	0.00	1.24	3146002.41	0.020696	0.003646	
3	6	20.55	111093.19	20.53	C18:1	0.02	2.68	3146002.41	0.020696	0.000273	
3	6	22.67	834616.17	22.68	C18:2	-0.01	2.93	3146002.41	0.020696	0.001875	
3	6	24.30	108716.56	24.35	C18:3	-0.05	1.44	3146002.41	0.020696	0.000496	
3	6	25.51	309850.27	25.51	C18:3	0.00	1.44	3146002.41	0.020696	0.001412	
3	6	27.20	3165530.08	27.22	C18:4	-0.02	1.44	3146002.41	0.020696	0.014430	
3	6	29.29	219235.59	29.28	C18:5	0.01	1.44	3146002.41	0.020696	0.000999	
3	6	31.47	684266.17	31.47	C20:4	0.00	1.38	3146002.41	0.020696	0.003262	
3	6	34.24	427205.46	34.21	C20:5	0.03	0.66	3146002.41	0.020696	0.004235	
3	6	40.11	63240.33	40.06	C22:5	0.05	0.72	3146002.41	0.020696	0.000580	
3	6	41.09	89290.73	41.06	C22:6	0.04	0.72	3146002.41	0.020696	0.000819	
Total Detected FAME Concentration (mg/mL)										**0.094850**	
3	**9**	**0.00**	**3378232.81**	**Napthalene**							
3	9	5.67	118664779.15	5.60	C14:0	0.07	1.53	3378232.81	0.020696	0.475146	
3	9	8.87	1856714.40	8.86	C15:0	0.01	1.22	3378232.81	0.020696	0.009337	
3	9	12.29	45898751.96	12.27	C16:0	0.02	1.47	3378232.81	0.020696	0.191410	
3	9	13.59	65273.07	13.61	C16:1	-0.01	1.16	3378232.81	0.020696	0.000343	
3	9	13.90	2019904.04	13.91	C16:1	-0.01	1.16	3378232.81	0.020696	0.010628	
3	9	14.07	5040397.91	14.05	C16:1	0.02	1.16	3378232.81	0.020696	0.026522	
3	9	14.37	738506.73	14.36	C16:1	0.01	1.16	3378232.81	0.020696	0.003886	
3	9	14.54	437126.20	14.53	C17:0	0.01	1.14	3378232.81	0.020696	0.002350	
3	9	15.57	474742.09	15.53	C20:0	0.04	1.38	3378232.81	0.020696	0.002107	
3	9	16.81	675426.62	16.79	C16:2	0.02	1.16	3378232.81	0.020696	0.003554	
3	9	18.92	4059511.59	18.90	C18:0	0.02	1.56	3378232.81	0.020696	0.015952	
3	9	20.26	8977495.65	20.25	C18:1	0.01	1.24	3378232.81	0.020696	0.044301	
3	9	20.52	705819.45	20.53	C18:1	-0.01	2.68	3378232.81	0.020696	0.001616	
3	9	22.68	17108790.99	22.68	C18:2	0.00	2.93	3378232.81	0.020696	0.035792	
3	9	24.33	21465577.56	24.35	C18:3	-0.02	1.44	3378232.81	0.020696	0.091124	

3	9	25.52	13992774.21	25.51	C18:3	0.01	1.44	3378232.81	0.020696	0.059401
3	9	26.49	1037956.71	26.48	C18:4	0.01	1.44	3378232.81	0.020696	0.004406
3	9	27.30	187918747.18	27.22	C18:4	0.08	1.44	3378232.81	0.020696	0.797735
3	9	28.90	99359.85	28.90	C18:4	0.00	1.44	3378232.81	0.020696	0.000422
3	9	29.30	8769093.53	29.28	C18:5	0.02	1.44	3378232.81	0.020696	0.037226
3	9	30.37	2512757.60	30.37	C20:3	0.00	1.38	3378232.81	0.020696	0.011154
3	9	31.20	166664.69	31.16	C22:0	0.04	0.72	3378232.81	0.020696	0.001424
3	9	31.49	37627990.93	31.47	C20:4	0.02	1.38	3378232.81	0.020696	0.167034
3	9	32.42	573679.20	32.42	C22:1	0.01	0.72	3378232.81	0.020696	0.004903
3	9	33.11	601944.40	33.08	C20:4	0.03	1.38	3378232.81	0.020696	0.002672
3	9	34.23	14714449.40	34.21	C20:5	0.02	0.66	3378232.81	0.020696	0.135834
3	9	34.77	45436.10	34.75	C21:4	0.02	0.72	3378232.81	0.020696	0.000388
3	9	37.45	141730.94	37.43	C22:4	0.02	0.72	3378232.81	0.020696	0.001211
3	9	40.08	3574674.59	40.06	C22:5	0.02	0.72	3378232.81	0.020696	0.030553
3	9	41.07	4439775.62	41.06	C22:6	0.02	0.72	3378232.81	0.020696	0.037947
Total Detected FAME Concentration (mg/mL)										**2.206378**
3	**19**	**0.00**	**2676068.54**	**Napthalene**						
3	19	5.68	161585519.94	5.60	C14:0	0.08	1.53	2676068.54	0.020696	0.816771
3	19	8.85	3157086.00	8.86	C15:0	-0.01	1.22	2676068.54	0.020696	0.020041
3	19	12.32	99278891.48	12.27	C16:0	0.05	1.47	2676068.54	0.020696	0.522652
3	19	13.56	300639.85	13.61	C16:1	-0.04	1.16	2676068.54	0.020696	0.001997
3	19	13.89	7756681.11	13.91	C16:1	-0.02	1.16	2676068.54	0.020696	0.051524
3	19	14.04	5558809.13	14.05	C16:1	-0.01	1.16	2676068.54	0.020696	0.036924
3	19	14.37	861645.55	14.36	C16:1	0.01	1.16	2676068.54	0.020696	0.005723
3	19	14.52	685161.12	14.53	C17:0	-0.01	1.14	2676068.54	0.020696	0.004650
3	19	15.53	674465.72	15.53	C20:0	0.00	1.38	2676068.54	0.020696	0.003780
3	19	16.78	2717656.91	16.79	C16:2	-0.01	1.16	2676068.54	0.020696	0.018052
3	19	18.91	2622010.14	18.90	C18:0	0.01	1.56	2676068.54	0.020696	0.013007
3	19	19.73	575979.95	19.82	C17:2 and/or C18:1	-0.08	1.24	2676068.54	0.020696	0.003588
3	19	20.23	15627037.10	20.25	C18:1	-0.02	1.24	2676068.54	0.020696	0.097348
3	19	20.53	1872490.57	20.53	C18:1	0.00	2.68	2676068.54	0.020696	0.005411
3	19	22.69	79383983.21	22.68	C18:2	0.01	2.93	2676068.54	0.020696	0.209650
3	19	24.40	193925540.26	24.35	C18:3	0.05	1.44	2676068.54	0.020696	1.039240
3	19	25.50	24573389.79	25.51	C18:3	-0.01	1.44	2676068.54	0.020696	0.131688
3	19	26.46	856819.55	26.48	C18:4	-0.02	1.44	2676068.54	0.020696	0.004592
3	19	27.31	321619446.38	27.22	C18:4	0.09	1.44	2676068.54	0.020696	1.723547
3	19	28.90	190052.82	28.90	C18:4	0.00	1.44	2676068.54	0.020696	0.001018
3	19	29.24	6587544.69	29.28	C18:5	-0.04	1.44	2676068.54	0.020696	0.035302
3	19	30.35	10219543.39	30.37	C20:3	-0.02	1.38	2676068.54	0.020696	0.057269
3	19	31.18	168578.93	31.16	C22:0	0.02	0.72	2676068.54	0.020696	0.001819
3	19	31.48	80129372.69	31.47	C20:4	0.01	1.38	2676068.54	0.020696	0.449033
3	19	32.39	1626886.97	32.42	C22:1	-0.02	0.72	2676068.54	0.020696	0.017553
3	19	33.04	953350.35	33.08	C20:4	-0.04	1.38	2676068.54	0.020696	0.005342
3	19	34.17	12526759.03	34.21	C20:5	-0.04	0.66	2676068.54	0.020696	0.145981
3	19	34.71	178856.00	34.75	C21:4	-0.04	0.72	2676068.54	0.020696	0.001930
3	19	37.40	655875.00	37.43	C22:4	-0.02	0.72	2676068.54	0.020696	0.007077

3	19	40.03	4421254.51	40.06	C22:5	-0.02	0.72	2676068.54	0.020696	0.047703
3	19	41.00	5073614.16	41.06	C22:6	-0.05	0.72	2676068.54	0.020696	0.054742
Total Detected FAME Concentration (mg/mL)										**5.534953**
3	**27**	**0.00**	**3254114.83**	**Napthalene**						
3	27	5.79	332676094.26	5.60	C14:0	0.19	1.53	3254114.83	0.020696	1.382877
3	27	8.87	9109859.09	8.86	C15:0	0.01	1.22	3254114.83	0.020696	0.047557
3	27	12.40	285697613.60	12.27	C16:0	0.13	1.47	3254114.83	0.020696	1.236877
3	27	13.62	2241687.44	13.61	C16:1	0.02	1.16	3254114.83	0.020696	0.012245
3	27	13.94	25715338.39	13.91	C16:1	0.03	1.16	3254114.83	0.020696	0.140472
3	27	14.09	13605712.27	14.05	C16:1	0.04	1.16	3254114.83	0.020696	0.074322
3	27	14.38	1896986.55	14.36	C16:1	0.02	1.16	3254114.83	0.020696	0.010362
3	27	14.55	3389000.99	14.53	C17:0	0.02	1.14	3254114.83	0.020696	0.018907
3	27	15.57	1552005.15	15.53	C20:0	0.04	1.38	3254114.83	0.020696	0.007152
3	27	16.81	9617797.92	16.79	C16:2	0.02	1.16	3254114.83	0.020696	0.052538
3	27	18.26	239365.79	18.23	C16:2	0.03	1.16	3254114.83	0.020696	0.001308
3	27	19.02	4780951.74	18.90	C18:0	0.12	1.56	3254114.83	0.020696	0.019503
3	27	19.76	2234572.44	19.82	C17:2 and/or C18:1	-0.05	1.24	3254114.83	0.020696	0.011447
3	27	20.34	49630037.40	20.25	C18:1	0.09	1.24	3254114.83	0.020696	0.254249
3	27	20.61	4775822.83	20.53	C18:1	0.08	2.68	3254114.83	0.020696	0.011350
3	27	22.86	292448564.64	22.68	C18:2	0.18	2.93	3254114.83	0.020696	0.635149
3	27	24.58	608760985.54	24.35	C18:3	0.23	1.44	3254114.83	0.020696	2.682822
3	27	25.60	69210893.91	25.51	C18:3	0.09	1.44	3254114.83	0.020696	0.305014
3	27	26.51	2565131.32	26.48	C18:4	0.03	1.44	3254114.83	0.020696	0.011305
3	27	27.46	693836365.60	27.22	C18:4	0.24	1.44	3254114.83	0.020696	3.057751
3	27	28.90	3864450.75	28.90	C18:4	0.00	1.44	3254114.83	0.020696	0.017031
3	27	29.31	12141039.88	29.28	C18:5	0.03	1.44	3254114.83	0.020696	0.053506
3	27	30.43	41594405.71	30.37	C20:3	0.06	1.38	3254114.83	0.020696	0.191684
3	27	31.63	278358831.86	31.47	C20:4	0.16	1.38	3254114.83	0.020696	1.282791
3	27	32.45	7569150.71	32.42	C22:1	0.03	0.72	3254114.83	0.020696	0.067161
3	27	33.10	3630927.21	33.08	C20:4	0.02	1.38	3254114.83	0.020696	0.016733
3	27	34.25	30555046.43	34.21	C20:5	0.04	0.66	3254114.83	0.020696	0.292822
3	27	34.79	1058282.10	34.75	C21:4	0.04	0.72	3254114.83	0.020696	0.009390
3	27	37.45	4736103.21	37.43	C22:4	0.02	0.72	3254114.83	0.020696	0.042023
3	27	40.07	19081579.65	40.06	C22:5	0.02	0.72	3254114.83	0.020696	0.169310
3	27	41.08	20892304.16	41.06	C22:6	0.02	0.72	3254114.83	0.020696	0.185376
Total Detected FAME Concentration (mg/mL)										**12.301034**
3	**52**	**0.00**	**5040023.35**	**Napthalene**						
3	52	5.72	256066345.18	5.60	C14:0	0.12	1.53	5040023.35	0.020696	0.687250
3	52	8.85	5008594.72	8.86	C15:0	-0.01	1.22	5040023.35	0.020696	0.016882
3	52	12.27	86400259.29	12.27	C16:0	0.00	1.47	5040023.35	0.020696	0.241510
3	52	13.58	865001.61	13.61	C16:1	-0.03	1.16	5040023.35	0.020696	0.003051
3	52	13.91	23155826.68	13.91	C16:1	0.00	1.16	5040023.35	0.020696	0.081669
3	52	14.05	6898201.98	14.05	C16:1	0.00	1.16	5040023.35	0.020696	0.024329
3	52	14.35	2032874.46	14.36	C16:1	-0.01	1.16	5040023.35	0.020696	0.007170

3	52	14.52	1780274.56	14.53	C17:0	-0.01	1.14	5040023.35	0.020696	0.006413
3	52	15.54	1187619.12	15.53	C20:0	0.01	1.38	5040023.35	0.020696	0.003534
3	52	16.79	4778499.06	16.79	C16:2	0.00	1.16	5040023.35	0.020696	0.016853
3	52	18.20	103902.20	18.23	C16:2	-0.03	1.16	5040023.35	0.020696	0.000366
3	52	18.95	10147560.68	18.90	C18:0	0.05	1.56	5040023.35	0.020696	0.026727
3	52	19.73	1548406.54	19.82	C17:2 and/or C18:1	-0.08	1.24	5040023.35	0.020696	0.005122
3	52	20.30	61628569.27	20.25	C18:1	0.05	1.24	5040023.35	0.020696	0.203843
3	52	20.56	9507163.07	20.53	C18:1	0.03	2.68	5040023.35	0.020696	0.014589
3	52	22.80	266382704.80	22.68	C18:2	0.12	2.93	5040023.35	0.020696	0.373536
3	52	24.47	384402829.73	24.35	C18:3	0.12	1.44	5040023.35	0.020696	1.093785
3	52	25.52	40679364.03	25.51	C18:3	0.01	1.44	5040023.35	0.020696	0.115750
3	52	26.48	1047688.40	26.48	C18:4	0.00	1.44	5040023.35	0.020696	0.002981
3	52	27.33	359325227.06	27.22	C18:4	0.11	1.44	5040023.35	0.020696	1.022429
3	52	28.82	2923283.57	28.90	C18:4	-0.08	1.44	5040023.35	0.020696	0.008318
3	52	29.26	5134178.85	29.28	C18:5	-0.02	1.44	5040023.35	0.020696	0.014609
3	52	30.36	34681985.30	30.37	C20:3	-0.01	1.38	5040023.35	0.020696	0.103194
3	52	31.16	356628.78	31.16	C22:0	0.00	0.72	5040023.35	0.020696	0.002043
3	52	31.52	145071327.16	31.47	C20:4	0.05	1.38	5040023.35	0.020696	0.431651
3	52	32.39	3639316.40	32.42	C22:1	-0.02	0.72	5040023.35	0.020696	0.020849
3	52	33.07	1570387.06	33.08	C20:4	-0.01	1.38	5040023.35	0.020696	0.004673
3	52	34.20	8506484.09	34.21	C20:5	-0.01	0.66	5040023.35	0.020696	0.052635
3	52	34.74	496429.08	34.75	C21:4	-0.01	0.72	5040023.35	0.020696	0.002844
3	52	37.42	1973161.79	37.43	C22:4	0.00	0.72	5040023.35	0.020696	0.011304
3	52	40.05	6722408.16	40.06	C22:5	-0.01	0.72	5040023.35	0.020696	0.038512
3	52	41.03	6208857.75	41.06	C22:6	-0.02	0.72	5040023.35	0.020696	0.035570
Total Detected FAME Concentration (mg/mL)										**4.673989**

13.1. Treatment 4. Low Nitrogen & Low Phosphorus

Treatment	Sample Day	Apex RT - Napthalene RT (RT A)	Peak Areas	Mean RT-Napthalene RT (RT B)	FAME Detected	RT Difference (RT A - RT B)	Mean Response Factors	Peak Areas of Internal Standard	Concentration of I.S. (mg/mL)	Concentrations of FAMEs (mg/mL)	*Area Added Manually
4	**6**	**0.00**	**2488334.30**	**Napthalene**							
4	6	5.55	4005217.46	5.60	C14:0	-0.05	1.53	2488334.30	0.020696	0.021838	
4	6	8.85	97180.10	8.86	C15:0	-0.01	1.22	2488334.30	0.020696	0.000663	
4	6	12.24	2810462.13	12.27	C16:0	-0.03	1.47	2488334.30	0.020696	0.015912	
4	6	13.88	46918.47	13.91	C16:1	-0.03	1.16	2488334.30	0.020696	0.000335	
4	6	14.06	142905.23	14.05	C16:1	0.01	1.16	2488334.30	0.020696	0.001021	
4	6	15.54	207528.88	15.53	C20:0	0.01	1.38	2488334.30	0.020696	0.001251	
4	6	18.24	50500.59	18.23	C16:2	0.02	1.16	2488334.30	0.020696	0.000361	
4	6	18.89	1212746.81	18.90	C18:0	-0.01	1.56	2488334.30	0.020696	0.006470	
4	6	20.22	342757.13	20.25	C18:1	-0.03	1.24	2488334.30	0.020696	0.002296	
4	6	20.52	113259.78	20.53	C18:1	-0.01	2.68	2488334.30	0.020696	0.000352	
4	6	22.66	546592.72	22.68	C18:2	-0.02	2.93	2488334.30	0.020696	0.001552	
4	6	24.30	35622.37	24.35	C18:3	-0.05	1.44	2488334.30	0.020696	0.000205	
4	6	25.50	135974.22	25.51	C18:3	-0.01	1.44	2488334.30	0.020696	0.000784	
4	6	26.42	86506.88	26.48	C18:4	-0.05	1.44	2488334.30	0.020696	0.000499	
4	6	27.19	2906612.63	27.22	C18:4	-0.03	1.44	2488334.30	0.020696	0.016752	
4	6	29.28	76101.91	29.28	C18:5	0.00	1.44	2488334.30	0.020696	0.000439	
4	6	31.43	887676.91	31.47	C20:4	-0.04	1.38	2488334.30	0.020696	0.005350	
4	6	32.40	53106.91	32.42	C22:1	-0.02	0.72	2488334.30	0.020696	0.000616	
4	6	34.22	227246.22	34.21	C20:5	0.01	0.66	2488334.30	0.020696	0.002848	
4	6	41.05	33980.09	41.06	C22:6	-0.01	0.72	2488334.30	0.020696	0.000394	
Total Detected FAME Concentration (mg/mL)										**0.079937**	
4	**9**	**0.00**	**2446447.56**	**Napthalene**							
4	9	5.65	116323733.68	5.60	C14:0	0.05	1.53	2446447.56	0.020696	0.643172	
4	9	8.84	1433394.70	8.86	C15:0	-0.02	1.22	2446447.56	0.020696	0.009953	
4	9	12.28	48026170.78	12.27	C16:0	0.01	1.47	2446447.56	0.020696	0.276563	
4	9	13.56	57361.81	13.61	C16:1	-0.04	1.16	2446447.56	0.020696	0.000417	
4	9	13.87	1740444.60	13.91	C16:1	-0.04	1.16	2446447.56	0.020696	0.012646	
4	9	14.03	3162809.73	14.05	C16:1	-0.02	1.16	2446447.56	0.020696	0.022981	
4	9	14.33	487933.59	14.36	C16:1	-0.03	1.16	2446447.56	0.020696	0.003545	
4	9	14.51	466867.95	14.53	C17:0	-0.02	1.14	2446447.56	0.020696	0.003466	
4	9	15.54	722519.43	15.53	C20:0	0.01	1.38	2446447.56	0.020696	0.004429	
4	9	16.78	381300.57	16.79	C16:2	-0.01	1.16	2446447.56	0.020696	0.002771	
4	9	18.88	9509458.84	18.90	C18:0	-0.02	1.56	2446447.56	0.020696	0.051599	
4	9	20.23	17913037.84	20.25	C18:1	-0.02	1.24	2446447.56	0.020696	0.122062	
4	9	20.50	585994.52	20.53	C18:1	-0.03	2.68	2446447.56	0.020696	0.001852	
4	9	22.64	18256247.32	22.68	C18:2	-0.04	2.93	2446447.56	0.020696	0.052739	

4	9	24.29	16247728.07	24.35	C18:3	-0.06	1.44	2446447.56	0.020696	0.095243
4	9	25.47	8167167.07	25.51	C18:3	-0.04	1.44	2446447.56	0.020696	0.047876
4	9	26.44	465887.25	26.48	C18:4	-0.04	1.44	2446447.56	0.020696	0.002731
4	9	27.19	74055231.15	27.22	C18:4	-0.03	1.44	2446447.56	0.020696	0.434108
4	9	28.90	237838.83	28.90	C18:4	0.00	1.44	2446447.56	0.020696	0.001394
4	9	29.24	3131589.47	29.28	C18:5	-0.04	1.44	2446447.56	0.020696	0.018357
4	9	30.32	3040633.82	30.37	C20:3	-0.05	1.38	2446447.56	0.020696	0.018639
4	9	31.15	405269.36	31.16	C22:0	-0.01	0.72	2446447.56	0.020696	0.004783
4	9	31.42	19924518.86	31.47	C20:4	-0.05	1.38	2446447.56	0.020696	0.122134
4	9	32.38	509162.97	32.42	C22:1	-0.03	0.72	2446447.56	0.020696	0.006009
4	9	33.04	213756.45	33.08	C20:4	-0.04	1.38	2446447.56	0.020696	0.001310
4	9	34.18	5488983.45	34.21	C20:5	-0.03	0.66	2446447.56	0.020696	0.069970
4	9	37.44	54929.86	37.43	C22:4	0.02	0.72	2446447.56	0.020696	0.000648
4	9	40.03	1457299.06	40.06	C22:5	-0.02	0.72	2446447.56	0.020696	0.017199
4	9	41.02	1795649.21	41.06	C22:6	-0.03	0.72	2446447.56	0.020696	0.021193
Total Detected FAME Concentration (mg/mL)										**2.069791**
4	**19**	**0.00**	**1044823.75**	**Napthalene**						
4	19	5.63	82324070.57	5.60	C14:0	0.03	1.53	1044823.75	0.020696	1.065808
4	19	8.85	343634.85	8.86	C15:0	-0.01	1.22	1044823.75	0.020696	0.005587
4	19	12.26	24453109.15	12.27	C16:0	-0.01	1.47	1044823.75	0.020696	0.329719
4	19	13.89	1646294.74	13.91	C16:1	-0.02	1.16	1044823.75	0.020696	0.028009
4	19	14.05	751037.18	14.05	C16:1	0.00	1.16	1044823.75	0.020696	0.012778
4	19	14.34	259854.31	14.36	C16:1	-0.02	1.16	1044823.75	0.020696	0.004421
4	19	14.53	220742.07	14.53	C17:0	0.00	1.14	1044823.75	0.020696	0.003837
4	19	15.54	491764.44	15.53	C20:0	0.01	1.38	1044823.75	0.020696	0.007058
4	19	16.79	135893.80	16.79	C16:2	0.00	1.16	1044823.75	0.020696	0.002312
4	19	18.90	2227853.37	18.90	C18:0	0.00	1.56	1044823.75	0.020696	0.028305
4	19	19.88	1253454.62	19.82	C17:2 and/or C18:1	0.07	1.24	1044823.75	0.020696	0.019999
4	19	20.31	80433406.78	20.25	C18:1	0.06	1.24	1044823.75	0.020696	1.283335
4	19	20.53	541516.63	20.53	C18:1	0.00	2.68	1044823.75	0.020696	0.004008
4	19	22.65	20770614.80	22.68	C18:2	-0.03	2.93	1044823.75	0.020696	0.140496
4	19	24.32	35670348.42	24.35	C18:3	-0.03	1.44	1044823.75	0.020696	0.489601
4	19	25.49	5226736.66	25.51	C18:3	-0.02	1.44	1044823.75	0.020696	0.071741
4	19	26.47	197942.50	26.48	C18:4	-0.01	1.44	1044823.75	0.020696	0.002717
4	19	27.19	52395207.96	27.22	C18:4	-0.03	1.44	1044823.75	0.020696	0.719162
4	19	28.93	582663.02	28.90	C18:4	0.03	1.44	1044823.75	0.020696	0.007997
4	19	29.27	1482012.63	29.28	C18:5	-0.01	1.44	1044823.75	0.020696	0.020342
4	19	30.35	16736528.25	30.37	C20:3	-0.02	1.38	1044823.75	0.020696	0.240218
4	19	31.45	15256956.09	31.47	C20:4	-0.02	1.38	1044823.75	0.020696	0.218982
4	19	32.38	54740.84	32.42	C22:1	-0.03	0.72	1044823.75	0.020696	0.001513
4	19	33.06	1159401.66	33.08	C20:4	-0.02	1.38	1044823.75	0.020696	0.016641
4	19	34.19	2786675.36	34.21	C20:5	-0.02	0.66	1044823.75	0.020696	0.083176
4	19	40.03	435547.91	40.06	C22:5	-0.02	0.72	1044823.75	0.020696	0.012036
4	19	41.02	728546.07	41.06	C22:6	-0.03	0.72	1044823.75	0.020696	0.020133
Total Detected FAME Concentration (mg/mL)										**4.839931**

4	27 JM24	**0.00**	**1979452.79**	**Napthalene**							
4	27	5.55	21729448.42	5.60	C14:0	-0.05	1.53	1979452.79	0.020696	0.148490	
4	27	8.83	187665.19	8.86	C15:0	-0.03	1.22	1979452.79	0.020696	0.001611	
4	27	12.22	9169926.23	12.27	C16:0	-0.05	1.47	1979452.79	0.020696	0.065264	
4	27	13.87	322443.94	13.91	C16:1	-0.04	1.16	1979452.79	0.020696	0.002896	
4	27	14.04	403707.30	14.05	C16:1	-0.01	1.16	1979452.79	0.020696	0.003625	
4	27	14.48	276881.48	14.36	C16:1	-0.05	1.16	1979452.79	0.020696	0.002539	
4	27	14.58	36092.76	14.53	C17:0	0.05	1.14	1979452.79	0.020696	0.000273	
4	27	15.55	678044.19	15.53	C20:0	0.02	1.38	1979452.79	0.020696	0.005137	
4	27	16.80	25683.26	16.79	C16:2	0.01	1.16	1979452.79	0.020696	0.000231	*
4	27	18.85	600763.15	18.90	C18:0	-0.05	1.56	1979452.79	0.020696	0.004029	
4	27	19.83	505275.76	19.82	C17:2 and/or C18:1	0.02	1.24	1979452.79	0.020696	0.004255	
4	27	20.22	16081486.18	20.25	C18:1	-0.03	1.24	1979452.79	0.020696	0.135434	
4	27	20.49	409319.51	20.53	C18:1	-0.04	2.68	1979452.79	0.020696	0.001599	
4	27	22.62	3196650.02	22.68	C18:2	-0.06	2.93	1979452.79	0.020696	0.011413	
4	27	24.27	4453967.43	24.35	C18:3	-0.08	1.44	1979452.79	0.020696	0.032269	
4	27	25.46	607959.22	25.51	C18:3	-0.05	1.44	1979452.79	0.020696	0.004405	
4	27	26.39	162856.86	26.48	C18:4	-0.09	1.44	1979452.79	0.020696	0.001180	
4	27	27.15	4854778.33	27.22	C18:4	-0.07	1.44	1979452.79	0.020696	0.035172	
4	27	28.90	662888.90	28.90	C18:4	0.00	1.44	1979452.79	0.020696	0.004803	
4	27	29.24	47745.00	29.28	C18:5	-0.04	1.44	1979452.79	0.020696	0.000346	
4	27	30.32	2262082.82	30.37	C20:3	-0.05	1.38	1979452.79	0.020696	0.017137	
4	27	31.42	1872491.96	31.47	C20:4	-0.05	1.38	1979452.79	0.020696	0.014186	
4	27	33.08	49015.86	33.08	C20:4	0.00	1.38	1979452.79	0.020696	0.000371	
4	27	34.20	158141.17	34.21	C20:5	-0.01	0.66	1979452.79	0.020696	0.002491	
4	27	41.00	389458.44	41.06	C22:6	-0.05	0.72	1979452.79	0.020696	0.005681	
Total Detected FAME Concentration (mg/mL)										**0.504838**	
JM48		**0.00**	**3735031.09**	**Napthalene**							
4	27	5.58	47799067.78	5.60	C14:0	-0.02	1.53	3735031.086	0.020696	0.173626	
4	27	8.83	256504.29	8.86	C15:0	-0.03	1.22	3735031.086	0.020696	0.001167	
4	27	12.23	20304932.29	12.27	C16:0	-0.04	1.47	3735031.086	0.020696	0.076588	
4	27	13.86	534757.44	13.91	C16:1	-0.05	1.16	3735031.086	0.020696	0.002545	
4	27	14.04	656220.99	14.05	C16:1	-0.01	1.16	3735031.086	0.020696	0.003123	
4	27	14.36	135599.10	14.36	C16:1	0.00	1.16	3735031.086	0.020696	0.000645	
4	27	14.50	234253.30	14.53	C17:0	-0.03	1.14	3735031.086	0.020696	0.001139	
4	27	15.54	1552927.99	15.53	C20:0	0.01	1.38	3735031.086	0.020696	0.006235	
4	27	16.86	491248.56	16.79	C16:2	0.07	1.16	3735031.086	0.020696	0.002338	
4	27	18.84	1502018.90	18.90	C18:0	-0.06	1.56	3735031.086	0.020696	0.005338	
4	27	19.84	1076382.08	19.82	C17:2 and/or C18:1	0.03	1.24	3735031.086	0.020696	0.004804	
4	27	20.24	42709051.46	20.25	C18:1	-0.01	1.24	3735031.086	0.020696	0.190622	
4	27	20.49	1585171.09	20.53	C18:1	-0.04	2.68	3735031.086	0.020696	0.003282	
4	27	22.62	4785008.34	22.68	C18:2	-0.06	2.93	3735031.086	0.020696	0.009054	
4	27	24.29	4605334.14	24.35	C18:3	-0.06	1.44	3735031.086	0.020696	0.017683	
4	27	25.45	701439.42	25.51	C18:3	-0.06	1.44	3735031.086	0.020696	0.002693	
4	27	27.15	3366761.01	27.22	C18:4	-0.07	1.44	3735031.086	0.020696	0.012927	

4	27	28.89	2231081.36	28.90	C18:4	-0.01	1.44	3735031.086	0.020696	0.008566	
4	27	30.33	5003152.42	30.37	C20:3	-0.04	1.38	3735031.086	0.020696	0.020088	
4	27	31.12	168336.62	31.16	C22:0	-0.04	0.72	3735031.086	0.020696	0.001301	
4	27	31.41	1981539.51	31.47	C20:4	-0.06	1.38	3735031.086	0.020696	0.007956	
4	27	32.38	12416.88	32.42	C22:1	-0.03	0.72	3735031.086	0.020696	0.000096	*
4	27	33.01	270326.47	33.08	C20:4	-0.07	1.38	3735031.086	0.020696	0.001085	
4	27	34.14	150202.92	34.21	C20:5	-0.07	0.66	3735031.086	0.020696	0.001254	
4	27	41.10	218205.75	41.06	C22:6	0.05	0.72	3735031.086	0.020696	0.001687	
Total Detected FAME Concentration (mg/mL)										**0.555843**	
JM48-181021		**0.00**	**2925455.76**	**Napthalene**							
4	27	5.56	34333252.19	5.60	C14:0	-0.04	1.53	2925455.76	0.020696	0.159224	
4	27	8.82	172978.03	8.86	C15:0	-0.04	1.22	2925455.76	0.020696	0.001004	
4	27	12.21	13150354.90	12.27	C16:0	-0.06	1.47	2925455.76	0.020696	0.063328	
4	27	13.84	256978.57	13.91	C16:1	-0.07	1.16	2925455.76	0.020696	0.001561	
4	27	14.01	321615.04	14.05	C16:1	-0.04	1.16	2925455.76	0.020696	0.001954	
4	27	14.33	79126.61	14.36	C16:1	-0.03	1.16	2925455.76	0.020696	0.000481	
4	27	14.49	97259.90	14.53	C17:0	-0.04	1.14	2925455.76	0.020696	0.000604	
4	27	15.52	1061376.90	15.53	C20:0	-0.01	1.38	2925455.76	0.020696	0.005441	
4	27	16.85	388965.76	16.79	C16:2	0.06	1.16	2925455.76	0.020696	0.002363	
4	27	18.84	708970.40	18.90	C18:0	-0.06	1.56	2925455.76	0.020696	0.003217	
4	27	19.84	568653.01	19.82	C17:2 and/or C18:1	0.03	1.24	2925455.76	0.020696	0.003240	
4	27	20.21	25181100.85	20.25	C18:1	-0.04	1.24	2925455.76	0.020696	0.143492	
4	27	20.46	818698.01	20.53	C18:1	-0.07	2.68	2925455.76	0.020696	0.002164	
4	27	22.60	2591580.64	22.68	C18:2	-0.08	2.93	2925455.76	0.020696	0.006261	
4	27	24.25	2432022.55	24.35	C18:3	-0.10	1.44	2925455.76	0.020696	0.011922	
4	27	25.43	327221.89	25.51	C18:3	-0.08	1.44	2925455.76	0.020696	0.001604	
4	27	27.12	1661348.75	27.22	C18:4	-0.10	1.44	2925455.76	0.020696	0.008144	
4	27	28.87	1019128.55	28.90	C18:4	-0.03	1.44	2925455.76	0.020696	0.004996	
4	27	30.30	2445896.99	30.37	C20:3	-0.07	1.38	2925455.76	0.020696	0.012538	
4	27	31.10	42227.75	31.16	C22:0	-0.06	0.72	2925455.76	0.020696	0.000417	*
4	27	31.40	886329.37	31.47	C20:4	-0.07	1.38	2925455.76	0.020696	0.004543	
4	27	32.21	42520.07	32.42	C22:1	-0.21	0.72	2925455.76	0.020696	0.000420	
4	27	33.00	68084.01	33.08	C20:4	-0.08	1.38	2925455.76	0.020696	0.000349	
4	27	34.14	41894.90	34.21	C20:5	-0.07	0.66	2925455.76	0.020696	0.000447	
4	27	41.09	56870.37	41.06	C22:6	0.04	0.72	2925455.76	0.020696	0.000561	*
Total Detected FAME Concentration (mg/mL)										**0.440277**	
4	**52**	**0.00**	**2855155.31**	**Napthalene**							
4	52	5.60	63828747.81	5.60	C14:0	0.00	1.53	2855155.31	0.020696	0.302400	
4	52	8.84	297928.22	8.86	C15:0	-0.02	1.22	2855155.31	0.020696	0.001773	
4	52	12.22	14370281.65	12.27	C16:0	-0.05	1.47	2855155.31	0.020696	0.070907	
4	52	13.88	500430.84	13.91	C16:1	-0.03	1.16	2855155.31	0.020696	0.003116	
4	52	14.04	636475.61	14.05	C16:1	-0.01	1.16	2855155.31	0.020696	0.003963	
4	52	14.49	641263.33	14.53	C17:0	-0.04	1.14	2855155.31	0.020696	0.004077	
4	52	15.53	4773372.11	15.53	C20:0	0.00	1.38	2855155.31	0.020696	0.025071	
4	52	16.83	168600.97	16.79	C16:2	0.04	1.16	2855155.31	0.020696	0.001050	

4	52	18.87	1944637.55	18.90	C18:0	-0.03	1.56	2855155.31	0.020696	0.009041
4	52	19.84	562427.32	19.82	C17:2 and/or C18:1	0.02	1.24	2855155.31	0.020696	0.003284
4	52	20.23	24630434.88	20.25	C18:1	-0.02	1.24	2855155.31	0.020696	0.143810
4	52	20.49	4021093.99	20.53	C18:1	-0.04	2.68	2855155.31	0.020696	0.010892
4	52	22.62	5413788.58	22.68	C18:2	-0.06	2.93	2855155.31	0.020696	0.013401
4	52	24.28	5667385.63	24.35	C18:3	-0.07	1.44	2855155.31	0.020696	0.028466
4	52	25.47	764650.22	25.51	C18:3	-0.04	1.44	2855155.31	0.020696	0.003841
4	52	26.41	174610.57	26.48	C18:4	-0.07	1.44	2855155.31	0.020696	0.000877
4	52	27.15	5262739.75	27.22	C18:4	-0.07	1.44	2855155.31	0.020696	0.026434
4	52	28.90	11367281.54	28.90	C18:4	0.00	1.44	2855155.31	0.020696	0.057096
4	52	29.25	73963.64	29.28	C18:5	-0.03	1.44	2855155.31	0.020696	0.000372
4	52	30.32	3919940.82	30.37	C20:3	-0.05	1.38	2855155.31	0.020696	0.020589
4	52	31.15	121627.32	31.16	C22:0	-0.01	0.72	2855155.31	0.020696	0.001230
4	52	31.41	2697653.52	31.47	C20:4	-0.06	1.38	2855155.31	0.020696	0.014169
4	52	32.36	138850.43	32.42	C22:1	-0.05	0.72	2855155.31	0.020696	0.001404
4	52	33.03	269877.20	33.08	C20:4	-0.05	1.38	2855155.31	0.020696	0.001417
4	52	34.17	175995.20	34.21	C20:5	-0.04	0.66	2855155.31	0.020696	0.001922
4	52	41.08	359596.45	41.06	C22:6	0.02	0.72	2855155.31	0.020696	0.003637
Total Detected FAME Concentration (mg/mL)										**0.754238**

13.1. Treatment 5. Low Nitrogen & Low Phosphorus + CO_2

Treatment	Sample Day	Apex RT - Napthalene RT (RT A)	Peak Areas	Mean RT-Napthalene RT (RT B)	FAME Detected	RT Difference (RT A - RT B)	Mean Response Factors	Peak Areas of Internal Standard	Concentration of I.S. (mg/mL)	Concentrations of FAMEs (mg/mL)	*Area Added Manually
5	**6**	**0.00**	**2334689.86**	**Napthalene**							
5	6	5.56	4342393.75	5.60	C14:0	-0.04	1.53	2334689.86	0.020696	0.025234	
5	6	8.87	46153.58	8.86	C15:0	0.01	1.22	2334689.86	0.020696	0.000336	
5	6	12.23	2503662.03	12.27	C16:0	-0.04	1.47	2334689.86	0.020696	0.015108	
5	6	13.90	67395.25	13.91	C16:1	-0.01	1.16	2334689.86	0.020696	0.000513	
5	6	14.06	76129.09	14.05	C16:1	0.01	1.16	2334689.86	0.020696	0.000580	
5	6	14.36	34357.22	14.36	C16:1	0.00	1.16	2334689.86	0.020696	0.000262	
5	6	15.56	211550.95	15.53	C20:0	0.03	1.38	2334689.86	0.020696	0.001359	
5	6	18.90	480683.02	18.90	C18:0	0.00	1.56	2334689.86	0.020696	0.002733	
5	6	20.24	266022.33	20.25	C18:1	-0.01	1.24	2334689.86	0.020696	0.001899	
5	6	22.65	243331.65	22.68	C18:2	-0.03	2.93	2334689.86	0.020696	0.000737	
5	6	25.50	93968.01	25.51	C18:3	-0.01	1.44	2334689.86	0.020696	0.000577	
5	6	27.18	619314.12	27.22	C18:4	-0.04	1.44	2334689.86	0.020696	0.003804	
5	6	31.45	163265.84	31.47	C20:4	-0.02	1.38	2334689.86	0.020696	0.001049	
5	6	34.22	111087.40	34.21	C20:5	0.01	0.66	2334689.86	0.020696	0.001484	
Total Detected FAME Concentration (mg/mL)											**0.055674**
5	**9**	**0.00**	**2797883.87**	**Napthalene**							
5	9	5.69	148035233.95	5.60	C14:0	0.09	1.53	2797883.87	0.020696	0.715699	
5	9	8.86	1892928.06	8.86	C15:0	0.00	1.22	2797883.87	0.020696	0.011493	
5	9	12.29	46368575.71	12.27	C16:0	0.02	1.47	2797883.87	0.020696	0.233478	
5	9	13.59	84219.19	13.61	C16:1	-0.01	1.16	2797883.87	0.020696	0.000535	
5	9	13.89	1610557.04	13.91	C16:1	-0.02	1.16	2797883.87	0.020696	0.010232	
5	9	14.06	4669416.71	14.05	C16:1	0.01	1.16	2797883.87	0.020696	0.029666	
5	9	14.36	405212.45	14.36	C16:1	0.00	1.16	2797883.87	0.020696	0.002574	
5	9	14.54	536503.35	14.53	C17:0	0.01	1.14	2797883.87	0.020696	0.003482	
5	9	15.56	231075.35	15.53	C20:0	0.03	1.38	2797883.87	0.020696	0.001239	
5	9	16.81	595568.63	16.79	C16:2	0.02	1.16	2797883.87	0.020696	0.003784	
5	9	18.91	4775878.68	18.90	C18:0	0.01	1.56	2797883.87	0.020696	0.022659	
5	9	19.86	168266.62	19.82	C17:2 and/or C18:1	0.05	1.24	2797883.87	0.020696	0.001003	
5	9	20.24	13676495.96	20.25	C18:1	-0.01	1.24	2797883.87	0.020696	0.081488	
5	9	20.52	554160.99	20.53	C18:1	-0.01	2.68	2797883.87	0.020696	0.001532	
5	9	22.65	10501990.35	22.68	C18:2	-0.03	2.93	2797883.87	0.020696	0.026528	
5	9	24.31	11719121.90	24.35	C18:3	-0.04	1.44	2797883.87	0.020696	0.060068	
5	9	25.51	11073180.64	25.51	C18:3	0.00	1.44	2797883.87	0.020696	0.056757	
5	9	26.47	474335.49	26.48	C18:4	-0.01	1.44	2797883.87	0.020696	0.002431	

5	9	27.28	158258181.20	27.22	C18:4	0.06	1.44	2797883.87	0.020696	0.811175	
5	9	28.92	193357.04	28.90	C18:4	0.02	1.44	2797883.87	0.020696	0.000991	
5	9	29.28	8278153.39	29.28	C18:5	0.00	1.44	2797883.87	0.020696	0.042431	
5	9	30.36	2347125.78	30.37	C20:3	-0.01	1.38	2797883.87	0.020696	0.012580	
5	9	31.18	375511.12	31.16	C22:0	0.02	0.72	2797883.87	0.020696	0.003875	
5	9	31.47	33236871.82	31.47	C20:4	0.00	1.38	2797883.87	0.020696	0.178145	
5	9	32.41	260528.43	32.42	C22:1	-0.01	0.72	2797883.87	0.020696	0.002689	
5	9	33.08	594796.52	33.08	C20:4	0.00	1.38	2797883.87	0.020696	0.003188	
5	9	34.22	19207741.17	34.21	C20:5	0.01	0.66	2797883.87	0.020696	0.214092	
5	9	37.48	89530.38	37.43	C22:4	0.06	0.72	2797883.87	0.020696	0.000924	
5	9	40.07	3842925.14	40.06	C22:5	0.01	0.72	2797883.87	0.020696	0.039658	
5	9	41.05	6312550.42	41.06	C22:6	-0.01	0.72	2797883.87	0.020696	0.065144	
Total Detected FAME Concentration (mg/mL)										**2.639542**	
JM51		**0.00**	**3553467.21**	**Napthalene**							
5	15	5.70	215241432.27	5.60	C14:0	0.10	1.53	3553467.21	0.020696	0.821792	
5	15	8.83	1231860.29	8.86	C15:0	-0.03	1.22	3553467.21	0.020696	0.005889	
5	15	12.32	100818259.21	12.27	C16:0	0.05	1.47	3553467.21	0.020696	0.399705	
5	15	13.57	147105.71	13.61	C16:1	-0.03	1.16	3553467.21	0.020696	0.000736	
5	15	13.87	4097405.98	13.91	C16:1	-0.04	1.16	3553467.21	0.020696	0.020497	
5	15	14.03	3049791.93	14.05	C16:1	-0.02	1.16	3553467.21	0.020696	0.015256	
5	15	14.32	984356.94	14.36	C16:1	-0.04	1.16	3553467.21	0.020696	0.004924	
5	15	14.50	612665.62	14.53	C17:0	-0.03	1.14	3553467.21	0.020696	0.003131	
5	15	15.53	1347425.75	15.53	C20:0	0.00	1.38	3553467.21	0.020696	0.005686	
5	15	16.76	501382.25	16.79	C16:2	-0.03	1.16	3553467.21	0.020696	0.002508	
5	15	18.90	16753279.51	18.90	C18:0	0.00	1.56	3553467.21	0.020696	0.062585	
5	15	19.90	284561.69	19.82	C17:2 and/or C18:1	0.09	1.24	3553467.21	0.020696	0.001335	
5	15	20.34	147221059.40	20.25	C18:1	0.09	1.24	3553467.21	0.020696	0.690660	
5	15	20.52	629085.15	20.53	C18:1	-0.01	2.68	3553467.21	0.020696	0.001369	
5	15	22.65	45977850.12	22.68	C18:2	-0.03	2.93	3553467.21	0.020696	0.091444	
5	15	24.28	24564337.42	24.35	C18:3	-0.07	1.44	3553467.21	0.020696	0.099136	
5	15	25.46	8531246.73	25.51	C18:3	-0.05	1.44	3553467.21	0.020696	0.034430	
5	15	26.42	353291.84	26.48	C18:4	-0.05	1.44	3553467.21	0.020696	0.001426	
5	15	27.19	68481787.25	27.22	C18:4	-0.03	1.44	3553467.21	0.020696	0.276376	
5	15	28.89	1259971.27	28.90	C18:4	-0.01	1.44	3553467.21	0.020696	0.005085	
5	15	29.23	1899058.75	29.28	C18:5	-0.05	1.44	3553467.21	0.020696	0.007664	
5	15	30.30	2706385.37	30.37	C20:3	-0.07	1.38	3553467.21	0.020696	0.011421	
5	15	31.12	486408.02	31.16	C22:0	-0.04	0.72	3553467.21	0.020696	0.003952	
5	15	31.41	13860208.25	31.47	C20:4	-0.06	1.38	3553467.21	0.020696	0.058493	
5	15	32.35	423346.20	32.42	C22:1	-0.06	0.72	3553467.21	0.020696	0.003440	
5	15	33.02	317071.14	33.08	C20:4	-0.06	1.38	3553467.21	0.020696	0.001338	
5	15	34.18	5749754.32	34.21	C20:5	-0.03	0.66	3553467.21	0.020696	0.050460	
5	15	34.81	28199.41	34.75	C21:4	0.06	0.72	3553467.21	0.020696	0.000229	*
5	15	37.42	129018.37	37.43	C22:4	0.00	0.72	3553467.21	0.020696	0.001048	
5	15	40.02	717972.91	40.06	C22:5	-0.03	0.72	3553467.21	0.020696	0.005834	
5	15	41.00	971452.69	41.06	C22:6	-0.05	0.72	3553467.21	0.020696	0.007894	
Total Detected FAME Concentration (mg/mL)										**2.695745**	

JM52		**0.00**	**5436154.59**	**Napthalene**						
5	15	5.81	385874382.74	5.60	C14:0	0.21	1.53	5436154.59	0.020696	0.963036
5	15	8.85	2772089.04	8.86	C15:0	-0.01	1.22	5436154.59	0.020696	0.008663
5	15	12.42	214592980.86	12.27	C16:0	0.15	1.47	5436154.59	0.020696	0.556130
5	15	13.57	342018.06	13.61	C16:1	-0.03	1.16	5436154.59	0.020696	0.001118
5	15	13.89	9279099.57	13.91	C16:1	-0.02	1.16	5436154.59	0.020696	0.030342
5	15	14.04	6830562.88	14.05	C16:1	-0.01	1.16	5436154.59	0.020696	0.022335
5	15	14.33	2294132.35	14.36	C16:1	-0.03	1.16	5436154.59	0.020696	0.007502
5	15	14.51	1463569.71	14.53	C17:0	-0.02	1.14	5436154.59	0.020696	0.004889
5	15	15.54	2868371.35	15.53	C20:0	0.01	1.38	5436154.59	0.020696	0.007913
5	15	16.78	1341894.11	16.79	C16:2	-0.01	1.16	5436154.59	0.020696	0.004388
5	15	18.99	43685083.75	18.90	C18:0	0.09	1.56	5436154.59	0.020696	0.106676
5	15	19.87	104657.83	19.82	C17:2 and/or C18:1	0.06	1.24	5436154.59	0.020696	0.000321
5	15	20.47	346103918.35	20.25	C18:1	0.22	1.24	5436154.59	0.020696	1.061357
5	15	20.59	1466023.06	20.53	C18:1	0.06	2.68	5436154.59	0.020696	0.002086
5	15	22.72	126314906.85	22.68	C18:2	0.04	2.93	5436154.59	0.020696	0.164218
5	15	24.33	69890936.55	24.35	C18:3	-0.02	1.44	5436154.59	0.020696	0.184377
5	15	25.49	25029536.44	25.51	C18:3	-0.02	1.44	5436154.59	0.020696	0.066030
5	15	26.45	1239217.98	26.48	C18:4	-0.02	1.44	5436154.59	0.020696	0.003269
5	15	27.26	201061483.14	27.22	C18:4	0.04	1.44	5436154.59	0.020696	0.530414
5	15	28.90	4963888.65	28.90	C18:4	0.00	1.44	5436154.59	0.020696	0.013095
5	15	29.24	5884541.18	29.28	C18:5	-0.04	1.44	5436154.59	0.020696	0.015524
5	15	30.33	10368212.04	30.37	C20:3	-0.04	1.38	5436154.59	0.020696	0.028602
5	15	31.17	2925663.73	31.16	C22:0	0.01	0.72	5436154.59	0.020696	0.015539
5	15	31.45	50060735.46	31.47	C20:4	-0.02	1.38	5436154.59	0.020696	0.138099
5	15	32.39	2883348.14	32.42	C22:1	-0.02	0.72	5436154.59	0.020696	0.015315
5	15	33.05	1589997.33	33.08	C20:4	-0.03	1.38	5436154.59	0.020696	0.004386
5	15	34.20	23208481.05	34.21	C20:5	-0.01	0.66	5436154.59	0.020696	0.133140
5	15	34.62	286338.61	34.75	C21:4	-0.13	0.72	5436154.59	0.020696	0.001521
5	15	37.43	250864.26	37.43	C22:4	0.01	0.72	5436154.59	0.020696	0.001332
5	15	40.01	5007007.88	40.06	C22:5	-0.05	0.72	5436154.59	0.020696	0.026594
5	15	41.02	5622425.07	41.06	C22:6	-0.03	0.72	5436154.59	0.020696	0.029863
Total Detected FAME Concentration (mg/mL)										**4.148074**

JM53		**0.00**	**5727055.13**	**Napthalene**						
5	15	5.81	385866339.45	5.60	C14:0	0.21	1.53	5727055.13	0.020696	0.914101
5	15	8.85	2782749.65	8.86	C15:0	-0.01	1.22	5727055.13	0.020696	0.008254
5	15	12.42	209127842.42	12.27	C16:0	0.15	1.47	5727055.13	0.020696	0.514438
5	15	13.59	361061.99	13.61	C16:1	-0.01	1.16	5727055.13	0.020696	0.001121
5	15	13.90	9559523.12	13.91	C16:1	-0.01	1.16	5727055.13	0.020696	0.029671
5	15	14.05	7304741.46	14.05	C16:1	0.00	1.16	5727055.13	0.020696	0.022673
5	15	14.34	2372600.16	14.36	C16:1	-0.02	1.16	5727055.13	0.020696	0.007364
5	15	14.53	1515931.86	14.53	C17:0	0.00	1.14	5727055.13	0.020696	0.004807
5	15	15.54	3335882.67	15.53	C20:0	0.01	1.38	5727055.13	0.020696	0.008735
5	15	16.78	1332500.33	16.79	C16:2	-0.01	1.16	5727055.13	0.020696	0.004136
5	15	19.00	42832562.18	18.90	C18:0	0.10	1.56	5727055.13	0.020696	0.099281

					C17:2 and/or						
5	15	19.94	15947.25	19.82	C18:1	0.13	1.24	5727055.13	0.020696	0.000046	*
5	15	20.47	344226570.62	20.25	C18:1	0.22	1.24	5727055.13	0.020696	1.001982	
5	15	20.60	1597254.05	20.53	C18:1	0.07	2.68	5727055.13	0.020696	0.002157	
5	15	22.73	128495094.44	22.68	C18:2	0.05	2.93	5727055.13	0.020696	0.158567	
5	15	24.33	70676900.33	24.35	C18:3	-0.02	1.44	5727055.13	0.020696	0.176980	
5	15	25.51	25633529.45	25.51	C18:3	0.00	1.44	5727055.13	0.020696	0.064188	
5	15	26.45	1345084.28	26.48	C18:4	-0.03	1.44	5727055.13	0.020696	0.003368	
5	15	27.26	201078614.99	27.22	C18:4	0.04	1.44	5727055.13	0.020696	0.503515	
5	15	28.92	5086014.51	28.90	C18:4	0.02	1.44	5727055.13	0.020696	0.012736	
5	15	29.25	5841517.18	29.28	C18:5	-0.03	1.44	5727055.13	0.020696	0.014628	
5	15	30.34	11465070.76	30.37	C20:3	-0.03	1.38	5727055.13	0.020696	0.030021	
5	15	31.17	3304806.62	31.16	C22:0	0.01	0.72	5727055.13	0.020696	0.016662	
5	15	31.46	51690111.39	31.47	C20:4	-0.01	1.38	5727055.13	0.020696	0.135350	
5	15	32.38	2851944.84	32.42	C22:1	-0.04	0.72	5727055.13	0.020696	0.014378	
5	15	33.05	1634290.11	33.08	C20:4	-0.03	1.38	5727055.13	0.020696	0.004279	
5	15	34.19	23980192.66	34.21	C20:5	-0.02	0.66	5727055.13	0.020696	0.130580	
5	15	34.63	162159.27	34.75	C21:4	-0.12	0.72	5727055.13	0.020696	0.000818	
5	15	37.44	545626.08	37.43	C22:4	0.02	0.72	5727055.13	0.020696	0.002751	
5	15	40.03	5142355.99	40.06	C22:5	-0.02	0.72	5727055.13	0.020696	0.025926	
5	15	41.02	5678442.69	41.06	C22:6	-0.04	0.72	5727055.13	0.020696	0.028628	
Total Detected FAME Concentration (mg/mL)										**3.942141**	
JM44		**0.00**	**3262796.71**	**Napthalene**							
5	19	5.62	67517700.14	5.60	C14:0	0.02	1.53	3262796.71	0.020696	0.279913	
5	19	8.83	221311.24	8.86	C15:0	-0.03	1.22	3262796.71	0.020696	0.001152	
5	19	12.25	29272249.99	12.27	C16:0	-0.02	1.47	3262796.71	0.020696	0.126392	
5	19	13.87	1070970.98	13.91	C16:1	-0.04	1.16	3262796.71	0.020696	0.005835	
5	19	14.04	1074074.25	14.05	C16:1	-0.01	1.16	3262796.71	0.020696	0.005852	
5	19	14.35	148446.29	14.36	C16:1	-0.01	1.16	3262796.71	0.020696	0.000809	
5	19	14.50	213103.69	14.53	C17:0	-0.03	1.14	3262796.71	0.020696	0.001186	
5	19	15.54	991687.63	15.53	C20:0	0.01	1.38	3262796.71	0.020696	0.004558	
5	19	16.78	84482.86	16.79	C16:2	-0.01	1.16	3262796.71	0.020696	0.000460	
5	19	18.88	2964901.22	18.90	C18:0	-0.02	1.56	3262796.71	0.020696	0.012063	
					C17:2 and/or						
5	19	19.84	1335061.82	19.82	C18:1	0.02	1.24	3262796.71	0.020696	0.006821	
5	19	20.27	62556213.99	20.25	C18:1	0.02	1.24	3262796.71	0.020696	0.319615	
5	19	20.51	597635.38	20.53	C18:1	-0.02	2.68	3262796.71	0.020696	0.001417	
5	19	22.64	14764834.11	22.68	C18:2	-0.04	2.93	3262796.71	0.020696	0.031981	
5	19	24.28	15716730.23	24.35	C18:3	-0.07	1.44	3262796.71	0.020696	0.069080	
5	19	25.46	3925312.09	25.51	C18:3	-0.05	1.44	3262796.71	0.020696	0.017253	
5	19	26.41	78687.42	26.48	C18:4	-0.07	1.44	3262796.71	0.020696	0.000346	
5	19	27.17	38067731.00	27.22	C18:4	-0.05	1.44	3262796.71	0.020696	0.167319	
5	19	28.90	858628.66	28.90	C18:4	0.00	1.44	3262796.71	0.020696	0.003774	
5	19	29.24	1369387.82	29.28	C18:5	-0.04	1.44	3262796.71	0.020696	0.006019	
5	19	30.32	7267572.85	30.37	C20:3	-0.05	1.38	3262796.71	0.020696	0.033403	
5	19	31.14	81764.70	31.16	C22:0	-0.02	0.72	3262796.71	0.020696	0.000724	
5	19	31.43	12860484.22	31.47	C20:4	-0.04	1.38	3262796.71	0.020696	0.059109	

5	19	32.41	260528.43	32.42	C22:1	-0.01	0.72	3262796.71	0.020696	0.002306	*
5	19	33.05	556304.30	33.08	C20:4	-0.03	1.38	3262796.71	0.020696	0.002557	
5	19	34.17	2834593.36	34.21	C20:5	-0.04	0.66	3262796.71	0.020696	0.027093	
5	19	40.03	421777.07	40.06	C22:5	-0.03	0.72	3262796.71	0.020696	0.003732	
5	19	41.02	756675.16	41.06	C22:6	-0.04	0.72	3262796.71	0.020696	0.006696	
Total Detected FAME Concentration (mg/mL)										**1.197462**	

JM46_18101912										**Small Sample**	
51		**0.00**	**2314250.19**	**Napthalene**						**Volume**	
5	19	5.58	44037646.91	5.60	C14:0	-0.02	1.53	2314250.19	0.020696	0.258168	
5	19	8.82	92869.71	8.86	C15:0	-0.04	1.22	2314250.19	0.020696	0.000682	
5	19	12.22	17790374.48	12.27	C16:0	-0.05	1.47	2314250.19	0.020696	0.108300	
5	19	13.85	597294.59	13.91	C16:1	-0.06	1.16	2314250.19	0.020696	0.004588	
5	19	14.01	536490.63	14.05	C16:1	-0.04	1.16	2314250.19	0.020696	0.004121	
5	19	14.32	84733.97	14.36	C16:1	-0.04	1.16	2314250.19	0.020696	0.000651	
5	19	14.48	80773.55	14.53	C17:0	-0.05	1.14	2314250.19	0.020696	0.000634	
5	19	15.52	518446.71	15.53	C20:0	-0.01	1.38	2314250.19	0.020696	0.003360	
5	19	18.85	1555256.99	18.90	C18:0	-0.05	1.56	2314250.19	0.020696	0.008921	
5	19	19.84	562312.26	19.82	C17:2 and/or C18:1	0.03	1.24	2314250.19	0.020696	0.004051	
5	19	20.22	32596065.20	20.25	C18:1	-0.03	1.24	2314250.19	0.020696	0.234802	
5	19	20.49	210942.02	20.53	C18:1	-0.04	2.68	2314250.19	0.020696	0.000705	
5	19	22.60	6832895.79	22.68	C18:2	-0.08	2.93	2314250.19	0.020696	0.020867	
5	19	24.26	7242387.45	24.35	C18:3	-0.09	1.44	2314250.19	0.020696	0.044880	
5	19	25.46	1731753.42	25.51	C18:3	-0.05	1.44	2314250.19	0.020696	0.010731	
5	19	27.14	17314020.27	27.22	C18:4	-0.08	1.44	2314250.19	0.020696	0.107292	
5	19	28.89	306838.38	28.90	C18:4	-0.01	1.44	2314250.19	0.020696	0.001901	
5	19	29.23	519760.08	29.28	C18:5	-0.05	1.44	2314250.19	0.020696	0.003221	
5	19	30.31	2719088.39	30.37	C20:3	-0.06	1.38	2314250.19	0.020696	0.017620	
5	19	31.39	4941786.03	31.47	C20:4	-0.08	1.38	2314250.19	0.020696	0.032023	
5	19	33.05	201120.73	33.08	C20:4	-0.03	1.38	2314250.19	0.020696	0.001303	
5	19	34.15	1022192.17	34.21	C20:5	-0.06	0.66	2314250.19	0.020696	0.013775	
5	19	40.02	91161.54	40.06	C22:5	-0.04	0.72	2314250.19	0.020696	0.001137	
Total Detected FAME Concentration (mg/mL)										**0.883730**	

JM47_18101914											
27		**0.00**	**3188629.18**	**Napthalene**							
5	19	5.62	67821354.66	5.60	C14:0	0.02	1.53	3188629.18	0.020696	0.288570	
5	19	8.84	188295.52	8.86	C15:0	-0.02	1.22	3188629.18	0.020696	0.001003	
5	19	12.24	31251844.27	12.27	C16:0	-0.03	1.47	3188629.18	0.020696	0.138078	
5	19	13.88	1097333.48	13.91	C16:1	-0.03	1.16	3188629.18	0.020696	0.006117	
5	19	14.03	1017106.24	14.05	C16:1	-0.02	1.16	3188629.18	0.020696	0.005670	
5	19	14.34	170710.31	14.36	C16:1	-0.02	1.16	3188629.18	0.020696	0.000952	
5	19	14.51	192948.14	14.53	C17:0	-0.02	1.14	3188629.18	0.020696	0.001099	
5	19	15.53	900508.81	15.53	C20:0	0.00	1.38	3188629.18	0.020696	0.004235	
5	19	18.87	3562448.68	18.90	C18:0	-0.03	1.56	3188629.18	0.020696	0.014831	

					C17:2 and/or					
5	19	19.85	1356459.45	19.82	C18:1	0.04	1.24	3188629.18	0.020696	0.007092
5	19	20.27	66309545.71	20.25	C18:1	0.02	1.24	3188629.18	0.020696	0.346672
5	19	20.51	484733.47	20.53	C18:1	-0.02	2.68	3188629.18	0.020696	0.001176
5	19	22.63	15246480.72	22.68	C18:2	-0.05	2.93	3188629.18	0.020696	0.033793
5	19	24.28	15529712.39	24.35	C18:3	-0.07	1.44	3188629.18	0.020696	0.069845
5	19	25.46	3994830.65	25.51	C18:3	-0.05	1.44	3188629.18	0.020696	0.017967
5	19	26.44	100943.26	26.48	C18:4	-0.04	1.44	3188629.18	0.020696	0.000454
5	19	27.17	37696985.62	27.22	C18:4	-0.05	1.44	3188629.18	0.020696	0.169543
5	19	28.92	874779.87	28.90	C18:4	0.02	1.44	3188629.18	0.020696	0.003934
5	19	29.25	1331688.80	29.28	C18:5	-0.03	1.44	3188629.18	0.020696	0.005989
5	19	30.33	7734131.42	30.37	C20:3	-0.04	1.38	3188629.18	0.020696	0.036374
5	19	31.13	77463.29	31.16	C22:0	-0.03	0.72	3188629.18	0.020696	0.000701
5	19	31.42	13165277.16	31.47	C20:4	-0.05	1.38	3188629.18	0.020696	0.061917
5	19	32.35	276639.94	32.42	C22:1	-0.06	0.72	3188629.18	0.020696	0.002505
5	19	33.04	694649.14	33.08	C20:4	-0.04	1.38	3188629.18	0.020696	0.003267
5	19	34.18	3062440.38	34.21	C20:5	-0.03	0.66	3188629.18	0.020696	0.029951
5	19	40.03	388309.88	40.06	C22:5	-0.02	0.72	3188629.18	0.020696	0.003516
5	19	41.01	909563.60	41.06	C22:6	-0.05	0.72	3188629.18	0.020696	0.008236
Total Detected FAME Concentration (mg/mL)										**1.263489**
JM50		**0.00**	**4040176.86**	**Napthalene**						
5	19	5.62	84755588.68	5.60	C14:0	0.02	1.53	4040176.86	0.020696	0.283768
5	19	8.85	247436.81	8.86	C15:0	-0.01	1.22	4040176.86	0.020696	0.001039
5	19	12.25	35746534.46	12.27	C16:0	-0.02	1.47	4040176.86	0.020696	0.124567
5	19	13.87	1284191.65	13.91	C16:1	-0.04	1.16	4040176.86	0.020696	0.005671
5	19	14.03	1274558.55	14.05	C16:1	-0.02	1.16	4040176.86	0.020696	0.005628
5	19	14.35	229546.92	14.36	C16:1	-0.01	1.16	4040176.86	0.020696	0.001014
5	19	14.49	188588.83	14.53	C17:0	-0.04	1.14	4040176.86	0.020696	0.000847
5	19	15.52	1230482.94	15.53	C20:0	-0.01	1.38	4040176.86	0.020696	0.004568
5	19	16.78	81395.94	16.79	C16:2	-0.01	1.16	4040176.86	0.020696	0.000359
5	19	18.87	3387495.97	18.90	C18:0	-0.03	1.56	4040176.86	0.020696	0.011123
					C17:2 and/or					
5	19	19.84	1250950.55	19.82	C18:1	0.03	1.24	4040176.86	0.020696	0.005168
5	19	20.28	69152362.17	20.25	C18:1	0.03	1.24	4040176.86	0.020696	0.285674
5	19	20.51	545594.15	20.53	C18:1	-0.02	2.68	4040176.86	0.020696	0.001043
5	19	22.63	16069120.94	22.68	C18:2	-0.05	2.93	4040176.86	0.020696	0.028094
5	19	24.28	16358820.65	24.35	C18:3	-0.07	1.44	4040176.86	0.020696	0.058194
5	19	25.46	4285952.92	25.51	C18:3	-0.05	1.44	4040176.86	0.020696	0.015247
5	19	26.45	82961.51	26.48	C18:4	-0.02	1.44	4040176.86	0.020696	0.000295
5	19	27.17	39539749.69	27.22	C18:4	-0.05	1.44	4040176.86	0.020696	0.140656
5	19	28.91	861498.97	28.90	C18:4	0.01	1.44	4040176.86	0.020696	0.003065
5	19	29.24	1420475.37	29.28	C18:5	-0.04	1.44	4040176.86	0.020696	0.005053
5	19	30.32	6735408.30	30.37	C20:3	-0.05	1.38	4040176.86	0.020696	0.025002
5	19	31.41	12084493.69	31.47	C20:4	-0.06	1.38	4040176.86	0.020696	0.044858
5	19	33.05	521165.19	33.08	C20:4	-0.03	1.38	4040176.86	0.020696	0.001935
5	19	34.18	2779344.57	34.21	C20:5	-0.03	0.66	4040176.86	0.020696	0.021572
5	19	40.02	312131.29	40.06	C22:5	-0.03	0.72	4040176.86	0.020696	0.002221

5	19	41.01	1192454.83	41.06	C22:6	-0.05	0.72	4040176.86	0.020696	0.008484
Total Detected FAME Concentration (mg/mL)										**1.085142**
5	**27**	**0.00**	**2726332.01**	**Napthalene**						
5	27	5.75	267046730.23	5.60	C14:0	0.15	1.53	2726332.01	0.020696	1.324962
5	27	8.86	1137897.88	8.86	C15:0	0.00	1.22	2726332.01	0.020696	0.007090
5	27	12.35	79297052.22	12.27	C16:0	0.08	1.47	2726332.01	0.020696	0.409761
5	27	13.62	249516.84	13.61	C16:1	0.02	1.16	2726332.01	0.020696	0.001627
5	27	13.90	3837898.40	13.91	C16:1	-0.01	1.16	2726332.01	0.020696	0.025023
5	27	14.07	3202765.65	14.05	C16:1	0.02	1.16	2726332.01	0.020696	0.020882
5	27	14.37	776350.20	14.36	C16:1	0.01	1.16	2726332.01	0.020696	0.005062
5	27	14.55	1127931.95	14.53	C17:0	0.02	1.14	2726332.01	0.020696	0.007511
5	27	15.56	4619056.42	15.53	C20:0	0.03	1.38	2726332.01	0.020696	0.025407
5	27	16.80	115775.40	16.79	C16:2	0.01	1.16	2726332.01	0.020696	0.000755
5	27	18.30	50850.29	18.23	C16:2	0.07	1.16	2726332.01	0.020696	0.000332
5	27	18.94	6940185.21	18.90	C18:0	0.04	1.56	2726332.01	0.020696	0.033792
5	27	19.95	178985.90	19.82	C17:2 and/or C18:1	0.14	1.24	2726332.01	0.020696	0.001094
5	27	20.42	210476756.94	20.25	C18:1	0.17	1.24	2726332.01	0.020696	1.286981
5	27	20.59	3952379.65	20.53	C18:1	0.06	2.68	2726332.01	0.020696	0.011212
5	27	22.69	31770610.66	22.68	C18:2	0.01	2.93	2726332.01	0.020696	0.082358
5	27	24.33	31514211.02	24.35	C18:3	-0.02	1.44	2726332.01	0.020696	0.165770
5	27	25.51	6458198.64	25.51	C18:3	0.00	1.44	2726332.01	0.020696	0.033971
5	27	26.45	747957.22	26.48	C18:4	-0.03	1.44	2726332.01	0.020696	0.003934
5	27	27.22	45839235.27	27.22	C18:4	0.00	1.44	2726332.01	0.020696	0.241122
5	27	28.95	28878899.40	28.90	C18:4	0.05	1.44	2726332.01	0.020696	0.151908
5	27	29.28	1286603.25	29.28	C18:5	0.00	1.44	2726332.01	0.020696	0.006768
5	27	30.37	18673929.17	30.37	C20:3	0.00	1.38	2726332.01	0.020696	0.102717
5	27	31.22	523349.14	31.16	C22:0	0.06	0.72	2726332.01	0.020696	0.005543
5	27	31.48	20509399.91	31.47	C20:4	0.01	1.38	2726332.01	0.020696	0.112813
5	27	33.09	1776369.50	33.08	C20:4	0.01	1.38	2726332.01	0.020696	0.009771
5	27	34.22	4388519.56	34.21	C20:5	0.01	0.66	2726332.01	0.020696	0.050199
5	27	40.08	383013.88	40.06	C22:5	0.02	0.72	2726332.01	0.020696	0.004056
5	27	41.09	2235677.26	41.06	C22:6	0.03	0.72	2726332.01	0.020696	0.023677
Total Detected FAME Concentration (mg/mL)										**4.156098**
5	**52**	**0.00**	**3211950.17**	**Napthalene**						
5	52	5.68	165691209.49	5.60	C14:0	0.08	1.53	3211950.17	0.020696	0.697791
5	52	8.84	822105.97	8.86	C15:0	-0.02	1.22	3211950.17	0.020696	0.004348
5	52	12.25	34492120.29	12.27	C16:0	-0.02	1.47	3211950.17	0.020696	0.151288
5	52	13.55	82059.19	13.61	C16:1	-0.05	1.16	3211950.17	0.020696	0.000454
5	52	13.86	2816710.95	13.91	C16:1	-0.05	1.16	3211950.17	0.020696	0.015588
5	52	14.02	1436240.59	14.05	C16:1	-0.03	1.16	3211950.17	0.020696	0.007949
5	52	14.33	655891.83	14.36	C16:1	-0.03	1.16	3211950.17	0.020696	0.003630
5	52	14.49	930637.30	14.53	C17:0	-0.04	1.14	3211950.17	0.020696	0.005260
5	52	15.52	3503676.32	15.53	C20:0	-0.01	1.38	3211950.17	0.020696	0.016358
5	52	18.87	4230765.82	18.90	C18:0	-0.03	1.56	3211950.17	0.020696	0.017485

5	52	19.87	1991459.95	19.82	C17:2 and/or C18:1	0.06	1.24	3211950.17	0.020696	0.010336
5	52	20.32	145324370.66	20.25	C18:1	0.07	1.24	3211950.17	0.020696	0.754252
5	52	20.52	7036695.47	20.53	C18:1	-0.01	2.68	3211950.17	0.020696	0.016943
5	52	22.63	33163101.52	22.68	C18:2	-0.05	2.93	3211950.17	0.020696	0.072970
5	52	24.28	36611142.43	24.35	C18:3	-0.07	1.44	3211950.17	0.020696	0.163464
5	52	25.45	6528180.51	25.51	C18:3	-0.06	1.44	3211950.17	0.020696	0.029147
5	52	26.43	563546.43	26.48	C18:4	-0.05	1.44	3211950.17	0.020696	0.002516
5	52	27.16	53318297.44	27.22	C18:4	-0.06	1.44	3211950.17	0.020696	0.238059
5	52	28.89	11601531.69	28.90	C18:4	-0.01	1.44	3211950.17	0.020696	0.051799
5	52	29.22	1429831.95	29.28	C18:5	-0.06	1.44	3211950.17	0.020696	0.006384
5	52	30.33	29072120.62	30.37	C20:3	-0.04	1.38	3211950.17	0.020696	0.135735
5	52	31.14	224718.02	31.16	C22:0	-0.02	0.72	3211950.17	0.020696	0.002020
5	52	31.41	28251182.98	31.47	C20:4	-0.06	1.38	3211950.17	0.020696	0.131902
5	52	32.35	328748.00	32.42	C22:1	-0.06	0.72	3211950.17	0.020696	0.002955
5	52	33.04	3473795.28	33.08	C20:4	-0.04	1.38	3211950.17	0.020696	0.016219
5	52	34.16	6541123.98	34.21	C20:5	-0.05	0.66	3211950.17	0.020696	0.063509
5	52	34.80	47670.95	34.75	C21:4	0.05	0.72	3211950.17	0.020696	0.000429
5	52	37.46	242376.14	37.43	C22:4	0.04	0.72	3211950.17	0.020696	0.002179
5	52	40.02	511550.32	40.06	C22:5	-0.03	0.72	3211950.17	0.020696	0.004599
5	52	41.00	1211562.28	41.06	C22:6	-0.05	0.72	3211950.17	0.020696	0.010891
Total Detected FAME Concentration (mg/mL)										**2.636461**

13.1. Treatment 6. Low Nitrogen and Phosphorus with Intermittent Nitrogen Feeding

Treatment	Sample Day	Apex RT - Napthalene RT (RT A)	Peak Areas	Mean RT-Napthalene RT (RT B)	FAME Detected	RT Difference (RT A - RT B)	Mean Response Factors	Peak Areas of Internal Standard	Concentration of I.S. (mg/mL)	Concentrations of FAMEs (mg/mL)	*Area Added Manually
6	**6**	**0.00**	**1877949.98**	**Napthalene**							
6	6	5.55	4131344.92	5.60	C14:0	-0.05	1.53	1877949.98	0.020696	0.029847	
6	6	8.88	45050.43	8.86	C15:0	0.02	1.22	1877949.98	0.020696	0.000408	
6	6	12.24	2428816.25	12.27	C16:0	-0.03	1.47	1877949.98	0.020696	0.018221	
6	6	13.92	37424.46	13.91	C16:1	0.01	1.16	1877949.98	0.020696	0.000354	
6	6	14.06	79313.77	14.05	C16:1	0.01	1.16	1877949.98	0.020696	0.000751	
6	6	15.54	126489.67	15.53	C20:0	0.01	1.38	1877949.98	0.020696	0.001010	
6	6	18.91	756205.19	18.90	C18:0	0.01	1.56	1877949.98	0.020696	0.005345	
6	6	20.24	220615.04	20.25	C18:1	-0.01	1.24	1877949.98	0.020696	0.001958	
6	6	22.66	268529.26	22.68	C18:2	-0.02	2.93	1877949.98	0.020696	0.001011	
6	6	25.52	72724.36	25.51	C18:3	0.01	1.44	1877949.98	0.020696	0.000555	
6	6	27.19	565461.68	27.22	C18:4	-0.03	1.44	1877949.98	0.020696	0.004318	
6	6	31.46	168772.23	31.47	C20:4	-0.01	1.38	1877949.98	0.020696	0.001348	
6	6	34.23	80878.51	34.21	C20:5	0.02	0.66	1877949.98	0.020696	0.001343	
Total Detected FAME Concentration (mg/mL)										**0.066469**	
6	**9**	**0.00**	**3951788.98**	**Napthalene**							
6	9	5.74	221425982.70	5.60	C14:0	0.14	1.53	3951788.98	0.020696	0.757931	
6	9	8.86	3570171.18	8.86	C15:0	0.00	1.22	3951788.98	0.020696	0.015347	
6	9	12.33	71594855.57	12.27	C16:0	0.06	1.47	3951788.98	0.020696	0.255235	
6	9	13.59	161678.04	13.61	C16:1	-0.02	1.16	3951788.98	0.020696	0.000727	
6	9	13.90	2873386.45	13.91	C16:1	-0.01	1.16	3951788.98	0.020696	0.012925	
6	9	14.06	8593776.42	14.05	C16:1	0.01	1.16	3951788.98	0.020696	0.038656	
6	9	14.36	934575.62	14.36	C16:1	0.00	1.16	3951788.98	0.020696	0.004204	
6	9	14.53	1121023.19	14.53	C17:0	0.00	1.14	3951788.98	0.020696	0.005152	
6	9	15.55	544083.36	15.53	C20:0	0.02	1.38	3951788.98	0.020696	0.002065	
6	9	16.80	1191749.56	16.79	C16:2	0.01	1.16	3951788.98	0.020696	0.005361	
6	9	18.91	5303239.65	18.90	C18:0	0.01	1.56	3951788.98	0.020696	0.017814	
					C17:2 and/or						
6	9	19.72	248294.05	19.82	C18:1	-0.09	1.24	3951788.98	0.020696	0.001047	
6	9	20.25	18844408.80	20.25	C18:1	0.00	1.24	3951788.98	0.020696	0.079494	
6	9	20.53	1467602.00	20.53	C18:1	0.00	2.68	3951788.98	0.020696	0.002872	
6	9	22.68	33381685.18	22.68	C18:2	0.00	2.93	3951788.98	0.020696	0.059700	
6	9	24.33	28946887.67	24.35	C18:3	-0.02	1.44	3951788.98	0.020696	0.105048	
6	9	25.51	21778427.09	25.51	C18:3	0.00	1.44	3951788.98	0.020696	0.079033	
6	9	26.47	931449.94	26.48	C18:4	-0.01	1.44	3951788.98	0.020696	0.003380	
6	9	27.34	316581049.98	27.22	C18:4	0.12	1.44	3951788.98	0.020696	1.148865	
6	9	28.94	369940.36	28.90	C18:4	0.04	1.44	3951788.98	0.020696	0.001343	
6	9	29.28	14799477.67	29.28	C18:5	0.00	1.44	3951788.98	0.020696	0.053707	

6	9	30.35	4061400.58	30.37	C20:3	-0.02	1.38	3951788.98	0.020696	0.015412
6	9	31.20	6283723.75	31.16	C22:0	0.04	0.72	3951788.98	0.020696	0.045912
6	9	31.51	83785923.43	31.47	C20:4	0.04	1.38	3951788.98	0.020696	0.317952
6	9	32.43	682201.64	32.42	C22:1	0.02	0.72	3951788.98	0.020696	0.004984
6	9	33.09	909369.27	33.08	C20:4	0.01	1.38	3951788.98	0.020696	0.003451
6	9	34.23	33345203.21	34.21	C20:5	0.02	0.66	3951788.98	0.020696	0.263144
6	9	37.46	425963.09	37.43	C22:4	0.04	0.72	3951788.98	0.020696	0.003112
6	9	40.06	6593379.84	40.06	C22:5	0.01	0.72	3951788.98	0.020696	0.048174
6	9	41.06	13162143.16	41.06	C22:6	0.01	0.72	3951788.98	0.020696	0.096169
Total Detected FAME Concentration (mg/mL)										**3.448218**
6	**19**	**0.00**	**2040406.34**	**Napthalene**						
6	19	5.73	240489303.40	5.60	C14:0	0.13	1.53	2040406.34	0.020696	1.594315
6	19	8.86	3033417.78	8.86	C15:0	0.00	1.22	2040406.34	0.020696	0.025255
6	19	12.32	89799231.01	12.27	C16:0	0.05	1.47	2040406.34	0.020696	0.620024
6	19	13.58	212305.22	13.61	C16:1	-0.02	1.16	2040406.34	0.020696	0.001850
6	19	13.90	10148903.39	13.91	C16:1	-0.01	1.16	2040406.34	0.020696	0.088416
6	19	14.05	4066628.87	14.05	C16:1	0.00	1.16	2040406.34	0.020696	0.035428
6	19	14.36	1160844.41	14.36	C16:1	0.00	1.16	2040406.34	0.020696	0.010113
6	19	14.53	1189965.50	14.53	C17:0	0.00	1.14	2040406.34	0.020696	0.010592
6	19	15.55	730749.70	15.53	C20:0	0.02	1.38	2040406.34	0.020696	0.005371
6	19	16.79	1453769.10	16.79	C16:2	0.00	1.16	2040406.34	0.020696	0.012665
6	19	18.95	7150901.84	18.90	C18:0	0.05	1.56	2040406.34	0.020696	0.046523
					C17:2 and/or					
6	19	19.91	377237.46	19.82	C18:1	0.09	1.24	2040406.34	0.020696	0.003082
6	19	20.33	98725601.46	20.25	C18:1	0.08	1.24	2040406.34	0.020696	0.806603
6	19	20.55	1356368.95	20.53	C18:1	0.02	2.68	2040406.34	0.020696	0.005141
6	19	22.76	136358402.36	22.68	C18:2	0.08	2.93	2040406.34	0.020696	0.472307
6	19	24.38	120431104.09	24.35	C18:3	0.03	1.44	2040406.34	0.020696	0.846447
6	19	25.54	50524669.80	25.51	C18:3	0.03	1.44	2040406.34	0.020696	0.355112
6	19	26.48	1164248.66	26.48	C18:4	0.00	1.44	2040406.34	0.020696	0.008183
6	19	27.34	345563826.49	27.22	C18:4	0.12	1.44	2040406.34	0.020696	2.428788
6	19	28.93	1635041.03	28.90	C18:4	0.03	1.44	2040406.34	0.020696	0.011492
6	19	29.27	7689370.24	29.28	C18:5	-0.01	1.44	2040406.34	0.020696	0.054045
6	19	30.37	12193012.50	30.37	C20:3	0.00	1.38	2040406.34	0.020696	0.089614
6	19	31.18	794558.66	31.16	C22:0	0.02	0.72	2040406.34	0.020696	0.011244
6	19	31.50	81815435.90	31.47	C20:4	0.03	1.38	2040406.34	0.020696	0.601315
6	19	32.41	1264121.14	32.42	C22:1	-0.01	0.72	2040406.34	0.020696	0.017888
6	19	33.08	1366492.45	33.08	C20:4	0.00	1.38	2040406.34	0.020696	0.010043
6	19	34.22	23321051.60	34.21	C20:5	0.01	0.66	2040406.34	0.020696	0.356439
6	19	37.44	716496.24	37.43	C22:4	0.02	0.72	2040406.34	0.020696	0.010139
6	19	40.05	6013090.22	40.06	C22:5	-0.01	0.72	2040406.34	0.020696	0.085091
6	19	41.04	6844477.18	41.06	C22:6	-0.02	0.72	2040406.34	0.020696	0.096855
Total Detected FAME Concentration (mg/mL)										**8.720380**
6	**27**	**0.00**	**3034688.85**	**Napthalene**						
6	27	5.80	325298488.72	5.60	C14:0	0.20	1.53	3034688.85	0.020696	1.449983
6	27	8.89	5283753.77	8.86	C15:0	0.03	1.22	3034688.85	0.020696	0.029578
6	27	12.32	97323014.64	12.27	C16:0	0.05	1.47	3034688.85	0.020696	0.451808
6	27	13.61	499949.94	13.61	C16:1	0.01	1.16	3034688.85	0.020696	0.002928
6	27	13.93	18480203.78	13.91	C16:1	0.02	1.16	3034688.85	0.020696	0.108248
6	27	14.08	5741308.41	14.05	C16:1	0.03	1.16	3034688.85	0.020696	0.033630
6	27	14.39	1527603.58	14.36	C16:1	0.03	1.16	3034688.85	0.020696	0.008948

6	27	14.56	2633705.10	14.53	C17:0	0.03	1.14	3034688.85	0.020696	0.015756
6	27	15.57	2620442.91	15.53	C20:0	0.04	1.38	3034688.85	0.020696	0.012949
6	27	16.82	1744024.61	16.79	C16:2	0.03	1.16	3034688.85	0.020696	0.010216
6	27	18.31	262601.85	18.23	C16:2	0.08	1.16	3034688.85	0.020696	0.001538
6	27	19.00	5236750.49	18.90	C18:0	0.10	1.56	3034688.85	0.020696	0.022907
6	27	19.77	839380.66	19.82	C17:2 and/or C18:1	-0.04	1.24	3034688.85	0.020696	0.004611
6	27	20.40	165612282.90	20.25	C18:1	-0.13	1.24	3034688.85	0.020696	0.909756
6	27	20.61	3031803.71	20.53	C18:1	0.08	2.68	3034688.85	0.020696	0.007726
6	27	22.82	242205385.13	22.68	C18:2	0.14	2.93	3034688.85	0.020696	0.564064
6	27	24.42	173704623.13	24.35	C18:3	0.07	1.44	3034688.85	0.020696	0.820871
6	27	25.58	82368972.55	25.51	C18:3	0.07	1.44	3034688.85	0.020696	0.389249
6	27	26.51	2460619.09	26.48	C18:4	0.03	1.44	3034688.85	0.020696	0.011628
6	27	27.37	363106440.02	27.22	C18:4	0.15	1.44	3034688.85	0.020696	1.715923
6	27	28.95	7209576.40	28.90	C18:4	0.05	1.44	3034688.85	0.020696	0.034070
6	27	29.29	6442696.94	29.28	C18:5	0.01	1.44	3034688.85	0.020696	0.030446
6	27	30.39	21731706.96	30.37	C20:3	0.02	1.38	3034688.85	0.020696	0.107390
6	27	31.23	1030338.83	31.16	C22:0	0.07	0.72	3034688.85	0.020696	0.009803
6	27	31.54	132872860.11	31.47	C20:4	0.07	1.38	3034688.85	0.020696	0.656608
6	27	32.43	1162339.88	32.42	C22:1	0.02	0.72	3034688.85	0.020696	0.011059
6	27	33.10	2366978.01	33.08	C20:4	0.02	1.38	3034688.85	0.020696	0.011697
6	27	34.24	29485536.59	34.21	C20:5	0.03	0.66	3034688.85	0.020696	0.303004
6	27	34.69	708069.72	34.75	C21:4	-0.06	0.72	3034688.85	0.020696	0.006737
6	27	37.46	1478000.59	37.43	C22:4	0.03	0.72	3034688.85	0.020696	0.014062
6	27	40.09	8824204.80	40.06	C22:5	0.04	0.72	3034688.85	0.020696	0.083958
6	27	41.08	8516148.85	41.06	C22:6	0.02	0.72	3034688.85	0.020696	0.081027
Total Detected FAME Concentration (mg/mL)										**7.922180**
6	**52**	**0.00**	**3079858.96**	**Napthalene**						
6	52	5.61	52377528.54	5.60	C14:0	0.01	1.53	3079858.96	0.020696	0.230043
6	52	8.86	410774.90	8.86	C15:0	0.00	1.22	3079858.96	0.020696	0.002266
6	52	12.24	22509619.03	12.27	C16:0	-0.03	1.47	3079858.96	0.020696	0.102965
6	52	13.87	2101204.44	13.91	C16:1	-0.04	1.16	3079858.96	0.020696	0.012127
6	52	14.04	545848.58	14.05	C16:1	-0.01	1.16	3079858.96	0.020696	0.003150
6	52	14.34	191549.55	14.36	C16:1	-0.02	1.16	3079858.96	0.020696	0.001106
6	52	14.52	430327.49	14.53	C17:0	-0.01	1.14	3079858.96	0.020696	0.002537
6	52	15.55	831704.27	15.53	C20:0	0.02	1.38	3079858.96	0.020696	0.004050
6	52	16.80	93863.16	16.79	C16:2	0.01	1.16	3079858.96	0.020696	0.000542
6	52	18.91	10623334.68	18.90	C18:0	0.01	1.56	3079858.96	0.020696	0.045788
6	52	19.87	4438773.91	19.82	C17:2 and/or C18:1	0.05	1.24	3079858.96	0.020696	0.024026
6	52	20.28	57076669.05	20.25	C18:1	0.03	1.24	3079858.96	0.020696	0.308940
6	52	20.53	5309921.57	20.53	C18:1	0.00	2.68	3079858.96	0.020696	0.013334
6	52	22.64	19721504.84	22.68	C18:2	-0.04	2.93	3079858.96	0.020696	0.045255
6	52	24.31	23756058.87	24.35	C18:3	-0.04	1.44	3079858.96	0.020696	0.110617
6	52	25.48	5764769.47	25.51	C18:3	-0.03	1.44	3079858.96	0.020696	0.026843
6	52	26.46	209908.20	26.48	C18:4	-0.02	1.44	3079858.96	0.020696	0.000977
6	52	27.19	26700178.71	27.22	C18:4	-0.03	1.44	3079858.96	0.020696	0.124326
6	52	28.92	925943.72	28.90	C18:4	0.02	1.44	3079858.96	0.020696	0.004312
6	52	29.27	302853.75	29.28	C18:5	-0.01	1.44	3079858.96	0.020696	0.001410
6	52	30.34	11473537.90	30.37	C20:3	-0.03	1.38	3079858.96	0.020696	0.055866
6	52	31.17	204129.98	31.16	C22:0	0.01	0.72	3079858.96	0.020696	0.001914
6	52	31.44	11462664.14	31.47	C20:4	-0.03	1.38	3079858.96	0.020696	0.055813

6	52	32.39	413138.48	32.42	C22:1	-0.02	0.72	3079858.96	0.020696	0.003873
6	52	33.07	641784.06	33.08	C20:4	-0.01	1.38	3079858.96	0.020696	0.003125
6	52	34.19	1467831.61	34.21	C20:5	-0.02	0.66	3079858.96	0.020696	0.014863
6	52	37.51	49065.83	37.43	C22:4	0.09	0.72	3079858.96	0.020696	0.000460
6	52	40.05	777803.41	40.06	C22:5	0.00	0.72	3079858.96	0.020696	0.007292
6	52	41.03	670193.37	41.06	C22:6	-0.02	0.72	3079858.96	0.020696	0.006283
Total Detected FAME Concentration (mg/mL)										**1.214102**

14. Appendix J: Description of an Unusual Optical Phenomenon Caused by a Few Species of Golden Algae

Gold on the Heiligenberg? Gold on the Holy Mountain?
by Petra Bauer and Dieter Teufel
Contribution in the Yearbook 1998, of the Handschuhsheim District Association
Translated from German

Complete text and photos can be found at:
http://www.upi-institut.de/_handschuhsheim/goldauf.htm

It was on one of those popular tours of the district club of Handschuhsheim, on a beautiful Sunday morning in August last year. Early on it became clear that the day was going to be hot. It had rained during the night. The forest steamed, it was pleasant to hike through the shady and still cool Mühltal to Heiligenberg. Again and again one stopped. Eugen Holl, as a knowledgeable guide, gave interesting insights into history and stories around our local mountain.

On the summit of Heiligenberg, with the many still visible dwellings of the Celts, who once lived up here, you could feel the touch of past generations. Why did they live in such great numbers on the mountain? Was it the extraction of iron, was it the turmoil of migrations that made life below in the plain too unsafe? Records from this period do not exist. It's too long ago.

Reflecting on such questions, the path led us to Bittersbrunnen, an old waterhole on the outer northwestern edge of the Heiligenberg area, still within the outer ring wall. The water table of the Bittersbrunnens is irregular. It is fed from a trough-shaped, water-impermeable layer in the mountain slope, where the water collects. As the water rises above the edge of this trough, it flows as an overflow source into the Bitters well.

The fountain, which served as a source of water for the former inhabitants of the Heiligenberg beside the Zollstockbrunnen, was redesigned by the Schutzgemeinschaft (protection community) Heiligenberg in 1979 - 1980. The source bottom and the fountain basin, underground were left natural. The origin of the name "Bittersbrunnen" is in the dark. The name certainly does not stem from the fact that the water is "bitter". It is clean and clear spring water. Maybe the name comes from a character called "Bitter": the "Bitter's Well".

It was hot now. We wanted to go down to the well, which looks like a mysterious entrance into the mountain with its tunnel. But what was that? A strange golden glow from the waters of the Bitter Fountain welcomed us. You expect a water hole, spring water, maybe old foliage. But the water was golden, an enigmatic wonder. Is there gold on the Heiligenberg? Does the mountain reveal something inside at the Bittersbrunnen? Are we enchanted, or does the heat of the day play tricks on us?

We moved closer and looked at it from all sides. A golden glow shined out of the water. We wantd to photograph it because we had never seen anything like it. Maybe it would turn out in the photo that it was just an illusion. But later, the photos here on the page show the same thing we saw with our naked eyes: a golden glow on almost the entire water surface of the Bitters Fountain.

When we touched the water with our finger, we saw that the water itself was clear, only on the surface the water had a floating golden dust. Strange, if it stuck to one’s finger, the whole golden glow was gone. Then it was just a brownish material. What's this? Sometimes in late summer you can see puddles of water, especially when it has been raining heavily after a dry heat, with a yellowish powder, pollen from wind-flowering trees like spruce or sweet chestnut. But pollen is yellowish and it does not shine. Here in the Bitters Fountain the color was golden, and one had the feeling that it shined with a bright, golden glow.

We wanted to get to the bottom of it. We collected a little water in a small glass for a closer look under the microscope at home. And then we were really astonished: Tiny, small, golden balls whirled through the drop of water. They were living things, half animal, half plant. With tiny flagella, small little arms, they paddled through the water. Others, of similar shape and also glowing gold, were circular and seated side by side as spheres. We had discovered a unique and very special spectacle of nature: In Bittersbrunnen a colony of rare golden algae had made it their home.

The individual algae were tiny, between eight and ten thousandths of a millimeter in diameter. We calculated 5,000 to 10,000 individuals per square millimeter. This means that about 10 billion gold balls lived in the water of the Bittersbrunnen, more than there are people on earth!

In the microscope, they pulsated and floated, you could watch for hours and not get tired. From time to time you could also see other, "bigger" little creatures, connected to a stalk and with hundreds of small eyelashes on their bell-shaped bodies, the water swirled past their mouths: petite bell animals (Vorticella). If they are startled, e.g. If you bump into the microscope carelessly, they pull themselves together, lightning fast, on their stalk, which curls up like a steel spring. If the water drops remain calm for half to one minute, the stem unrolls and they begin the swirling again. When they caught a delicious golden luster alga, it was swallowed and digested by the bell animal, which also consisted of only one cell.

Since the bell animals were so small, they were transparent in the microscope and you could look through them and see what they had eaten. As you can see on the photo, all the bell animals in the water drop had their belly filled with gold algae. But that's not the end of the chain. Now and then a fidgety rotifer plowed through the water. It also fed on the golden algae. And so the gold algae in Bittersbrunnen were the basis for whole life-chains.

Thus, the view through the microscope revealed a mysterious world in which thousands of lives drifted and wrestled in every drop of the water of the Bittersbrunnen, and struggled to experience light and existence every day anew. These beings were unaware of our world, and we knew nothing of theirs.

The golden algae have long ago made a very special invention in the evolution of life on Earth. As plants with chlorophyll, they can live like other green plants simply from solar energy, with the help of which they convert carbon dioxide and water into food. But unlike normal green plants or algae, they can also live in habitats that are low in light. Namely, they can form a round lens ball, in which they sit on the water surface and align the lens exactly in the direction of the incident light. If they lived in the water just like normal algae, the part of the light that is reflected at an oblique incidence of light on the surface of the water, and therefore does not get into the water at all, would not be usable for them. Due to their place above the water surface, the entire light available in the Bitters fountain is available to them. And in addition, the few rays of light arriving at Bitter’s well are focused by the lens and concentrated directly on the chloroplast, the solar power plant of the cell, where the light is transformed into life energy. The back of the lens acts like a golden mirror, and the rays of light that have not been consumed, are reflected off this mirror and pass through the chloroplast a second time. As a result, weak sunlight is used optimally for photosynthesis, and the golden algae can colonize low-light habitats.

When we come to such a habitat and have the light in our backs, we look with the incoming rays of light at billions of small golden lens balls, which reflect the light and shine it into our eyes as a golden glow. If you look at the water surface from another angle, the golden glow is barely visible, as the picture below shows. This is also the reason why the same golden algae, if we have reached into the water with a finger, those attached to the finger are no longer golden, and only visible as brownish algae. The shining golden glow only appears when millions of lenses are oriented in one direction, in the direction of light, at the astonished observer. It's as if they wanted to call out to us: Do not disturb our order, then we will not destroy the golden glow.

In the following months, the path led us several times to Bittersbrunnen to see how the golden algae were doing. They remained visible until the beginning of October, though not as bright as in August.

Gold luster algae are also magical fellows in other respects. They can easily and relatively quickly turn into several different shapes. When the waters of the Bitters Fountain lie undisturbed and calm, they float to the surface of the water and pierce it, which is not easy given their tiny size and the surface tension of the water. They then lie on the water surface, orient toward the light and catch it.

If the water surface is disturbed, for example, when raindrops reach the water, they are shaken and wetted again. Then they grow a flagellum with which they can row in the water and become mobile. In this way, they can then swim to the best and brightest points of the water to sit again on the water surface. Later, when autumn arrives and the time for hibernation comes, they sink to the bottom of the well, looking for places to hide during winter dormancy.

Mostly, they do this inside the empty cells of dead leaves. In doing so, they transform themselves into a third form, an amoeba-like creeping form which can move into the dead leaves. There they wait for the next spring. When the water becomes warmer and the light brightens again, they wake from their hibernation, become mobile again and strive again for the light.

What can we learn from the tiny gold balls? Even with things that we think we know, you can discover completely new facets if you look closely. You do not need to travel to distant lands to discover miracles, it is sufficient to hike on the Heiligenschuh (Holy Shoe) mountain. And they teach us a second: Even under very adverse living conditions, you can still live well, if you cunningly adapt. Even in a place where only a little light falls, one can live, if one cleverly collects the weak rays of light and transforms them into life energy. In Bittersbrunnen, for example, a whole habitat was created in which bell animals and rotifers are beneficiaries, but without destroying the golden algae.

15. Appendix K: Contact Information, Products and Services

15.1. Algaebase

An online database of microalgae, seaweeds and seagrasses of the world, that includes current taxonomic classification, images, bibliographic information and distributional records.

Guiry, M.D. & Guiry, G.M. 2019. AlgaeBase. World-wide electronic publication, National University of Ireland, Galway. http://www.algaebase.org

15.2. Canadian Phycological Culture Centre

Department of Biology
University of Waterloo
200 University Ave. W
Waterloo ON, Canada N2L 3G1

Modified Acid Medium
https://uwaterloo.ca/canadian-phycological-culture-centre/cultures/culture-media/modified-acid-medium

Original Source: Olaveson, Mary M. and Pamela M. Stokes. 1989. Responses of the acidophilic alga *Euglena mutabilis* (Euglenophyceae) to carbon enrichment at pH 3. Journal of Phycology. 25: 529-539.

15.1. EMtrix, University of Montana

Electron Microscopy Services

University of Montana
Division of Biologocal Science
32 Campus Dr.
Missoula, MT 59812
http://hs.umt.edu/dbs/labs/emtrix/default.php

Dr. Bill Granath, Director and Professor of Microbiology
Dr. Jim Driver, Associate Director

15.2. Ground Water Information Center, MBMG Data Center

Montana Bureau of Mines and Geology
Montana Tech of The University of Montana
1300 West Park Street - Natural Resources Building Room 329
Butte Montana 59701-8997
http://mbmggwic.mtech.edu

Ted Duaime, Hydrogeologist

15.3. Hausser Scientific

35 Horsham Road; Suite C
Horsham, PA 19044

Bright-Line Hemacytometer
http://hausserscientific.com/products/hausser_bright_line.html

15.4. Laboratory for Environmental Analysis

University of Georgia
Center for Applied Isotope Studies
160 Phoenix Rd, Room 134
Athens, GA 30602
https://lea.uga.edu

Dr. Sayed Hassan, Senior Research Scientist

15.5. National Research Council Canada, Conseil national de recherches Canada

1411 Oxford Street
Halifax, Nova Scotia B3H 3Z1
Canada
https://www.nrc-cnrc.gc.ca/eng/solutions/facilities/aquatic_partnership.html

Dr. Stephen J.B. O'Leary, PhD, Team Lead, Algal Genomics & Synthetic Biology
Dr. Fabrice Berrue, Associate Research Officer

SIGNATURE PAGE

This is to certify that the thesis prepared by June E. Mohler Mitman entitled "Growth, Lipid Production and Biodiesel Potential of *Chromulina freiburgensis* Dofl., an Acidophilic Chrysophyte Isolated from Berkeley Pit Lake" has been examined and approved for acceptance by the Department of Chemistry, Montana Technological University, on this 30th day of April, 2019.

Dr. Douglas Cameron, Professor
Department of Chemistry
Chair, Examination Committee

Dr. Martha Apple, Professor
Department of Biological Sciences
Member, Examination Committee

Dr. Pat Munday, Professor
Department of Professional and Technical Communication
Member, Examination Committee

Dr. Kumar Ganesan, Professor
Department of Environmental Engineering
Member, Examination Committee